15 September 2006 | $10

Science

AAAS

Volume 313, Issue 5793

COVER

Moonlit silhouette of the North American black cottonwood *Populus trichocarpa*. Because this tree has a small genome and has long been the subject of commercial and ecological studies, *P. trichocarpa* was selected as the first woody perennial plant to have its genome sequenced. See page 1596.

Photo: David Hiser/Getty Images

DEPARTMENTS

EDITORIAL

NEWS OF THE WEEK

NEWS FOCUS


1560

LETTERS

BOOKS *ET AL.*

POLICY FORUM


1578

PERSPECTIVES

CONTENTS continued >>

Science

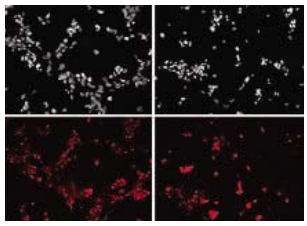

SCIENCE EXPRESS

www.sciencexpress.org

TECHNICAL COMMENT ABSTRACTS

REVIEW

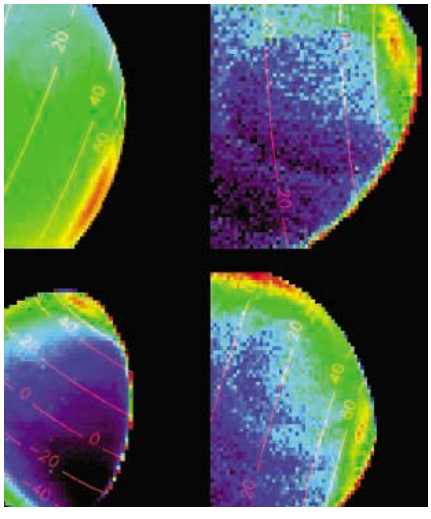

BREVIA

RESEARCH ARTICLES

CONTENTS continued **>>**

REPORTS

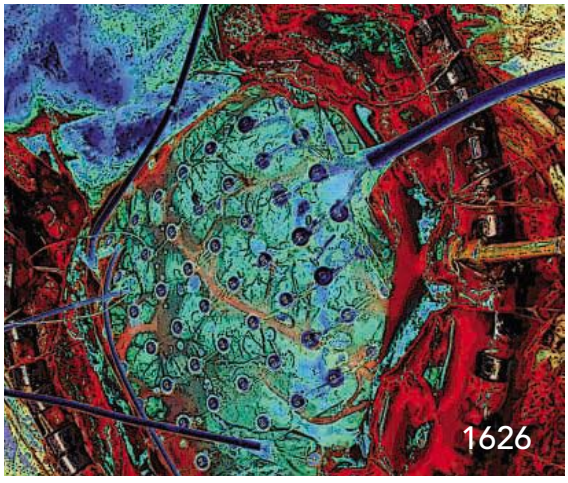

AAAS
ADVANCING SCIENCE, SERVING SOCIETY

SCIENCE (ISSN 0036-8075) is published weekly on Friday, except the last week in December, by the American Association for the Advancement of Science, 1200 New York Avenue, NW, Washington, DC 20005. Periodicals Mail postage (publication No. 484460) paid at Washington, DC, and additional mailing offices. Domestic individual membership and subscription (51 issues): $139 ($74 allocated to subscription). Domestic institutional subscription (51 issues): $650; Foreign postage extra: Mexico, Caribbean (surface mail) $55; other countries (air assist delivery) $85. First class, airmail, student, and emeritus rates on request. Canadian rates with GST available upon request, GST #1254 88122. Publications Mail Agreement Number 1069624. **Printed in the U.S.A.**

Change of address: Allow 4 weeks, giving old and new addresses and 8-digit account number. **Postmaster:** Send change of address to AAAS, P.O. Box 96178, Washington, DC 20090–6178. **Single-copy sales:** $10.00 current issue, $15.00 back issue prepaid includes surface postage; bulk rates on request. **Authorization to photocopy** material for internal or personal use under circumstances not falling within the fair use provisions of the Copyright Act is granted by AAAS to libraries and other users registered with the Copyright Clearance Center (CCC) Transactional Reporting Service, provided that $18.00 per article is paid directly to CCC, 222 Rosewood Drive, Danvers, MA 01923. The identification code for *Science* is 0036-8075. *Science* is indexed in the *Reader's Guide to Periodical Literature* and in several specialized indexes.

CONTENTS continued **>>**

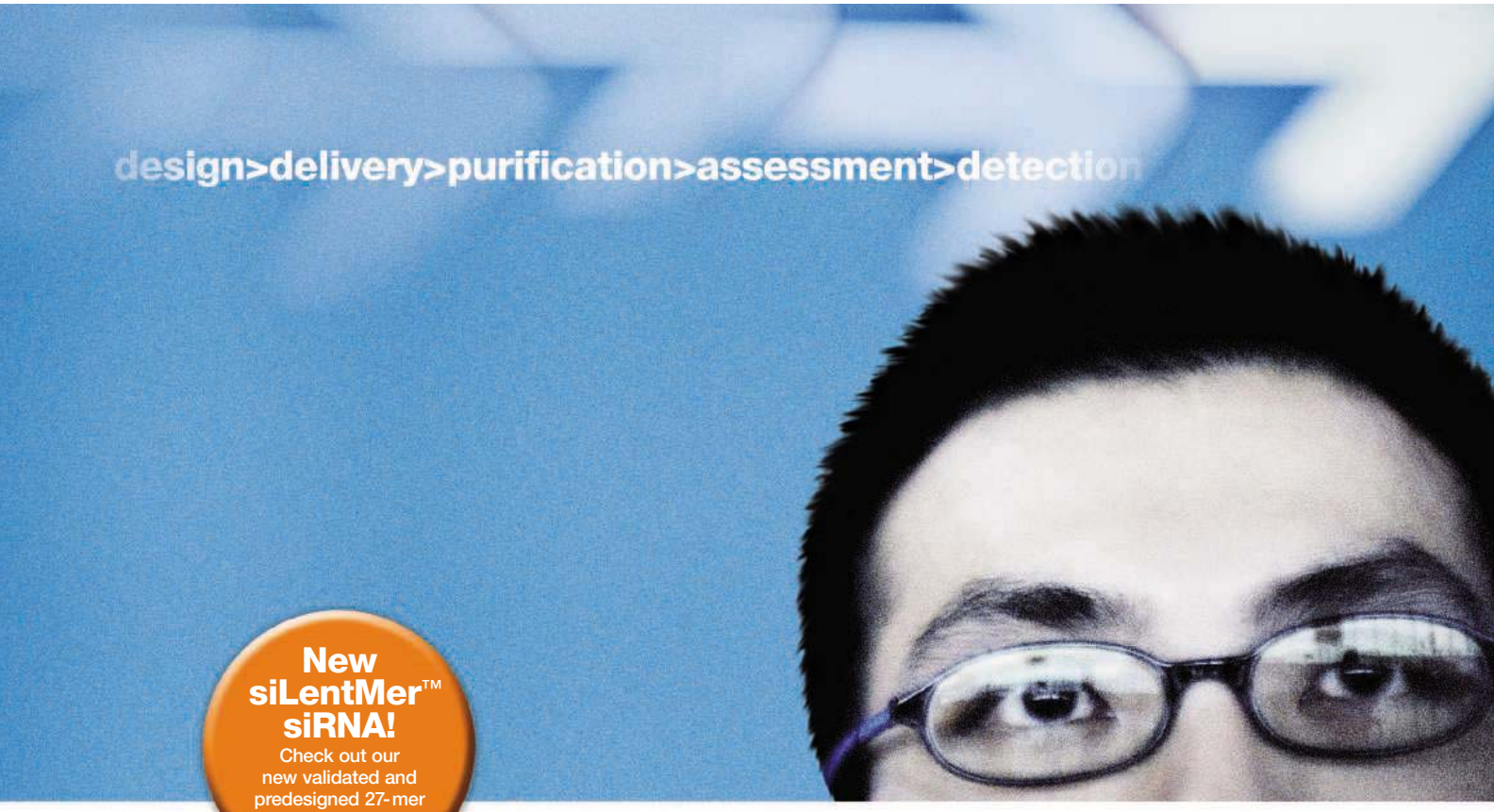

New siLentMer™ siRNA!
Check out our new validated and predesigned 27-mer siRNA duplexes

Bio-Rad and RNAi. Come have a look.

From design to detection, Bio-Rad supports your RNAi research.

With a broad range of proven delivery technologies, award-winning detection systems, and a suite of high-quality support products, it's clear that Bio-Rad has a vision for RNAi.

- High-performing potent siRNA for ≥85% knockdown with as low as 5 nM siRNA
- Greatest choice of delivery technologies
- RNA and protein purification products
- Automated microfluidic RNA analysis
- Sensitive, optimized cDNA synthesis kits
- Systems for protein and mRNA detection

For a close look at Bio-Rad's tools for RNAi, visit us on the Web at **www.bio-rad.com/rnai/**

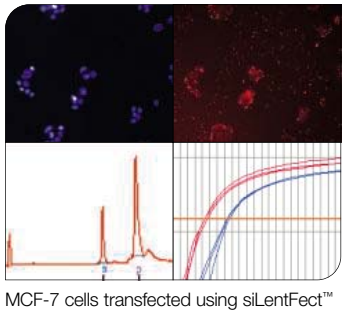

MCF-7 cells transfected using siLentFect™ reagent. RNA purified and analyzed using the Aurum™ total RNA kit and Experion™ system. Real-time PCR detection performed using iScript™ cDNA synthesis kit.

Visit us on the Web at **discover.bio-rad.com**
Call toll free at 1-800-4BIORAD (1-800-424-6723);
outside the US, contact your local sales office.

BIO-RAD

SCIENCE**NOW**

www.sciencenow.org DAILY NEWS COVERAGE

A Human Spin on Hurricanes
Human-induced climate change linked to hurricane severity.

Hey Honey, I'm No Bee
Beetle larvae fool male bees by mimicking a female's scent.

A Plethora of Alien Seas
New models predict that Earth-like worlds may not be needles in a haystack.

Job searching for real.

SCIENCE **CAREERS**

www.sciencecareers.org CAREER RESOURCES FOR SCIENTISTS

US: Tooling Up—Conducting an Authentic Job Search
D. Jensen
Technical professionals don't have to be insincere when hunting for jobs.

US: How to Get Hired in Academia
A. Fazekas
What are hiring committees at colleges and universities looking for in faculty-job applicants?

UK: Careers in Forensics Research
N. Anscombe
Forensics caseworkers have a high profile these days, but some forensic scientists work behind the scenes.

MISCINET: Dissecting Dialects
R. Arnette
Jennifer Bloomquist studies linguistic variation among residents of the Appalachian Mountains.

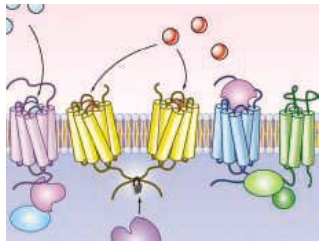

Transglutaminases and GPCR signaling.

SCIENCE'S **STKE**

www.stke.org SIGNAL TRANSDUCTION KNOWLEDGE ENVIRONMENT

PERSPECTIVE: Crosslinking Transglutaminases with G Protein–Coupled Receptor Signaling
S. E. Iismaa, G. E. Begg, R. M. Graham
Transglutaminases use multiple mechanisms to regulate G protein–coupled receptors.

PROTOCOL: Simultaneous Optical Measurements of Cytosolic Ca^{2+} and cAMP in Single Cells
M. C. Harbeck, O. Chepurny, V. O. Nikolaev, M. J. Lohse, G. G. Holz, M. W. Roe
FRET biosensors can be combined with Fura-2 to investigate interactions between Ca^{2+} and cAMP signaling.

E-LETTER: Improved PRMT Substrate Detection
R. B. Denman
Read this modification to the STKE Protocol on methods for the analysis of protein arginine methylation.

SCIENCE**PODCAST**

Listen to the 15 September *Science* Podcast to hear about the oldest writing in the New World, testing general relativity, the first tree genome, and more.
www.sciencemag.org/about/podcast.dtl

Separate individual or institutional subscriptions to these products may be required for full-text access.

K. lactis Protein Expression Kit from New England Biolabs

YEAST PROTEIN EXPRESSION MADE EASY

The *K. lactis* Protein Expression Kit provides a simple method to clone and express your gene of interest in the yeast *Kluyveromyces lactis*. This system offers many advantages over bacterial systems and eliminates the methanol containing medium and antibiotic requirements of *Pichia pastoris*. With easy-to-use protocols and highly competent *K. lactis* cells included, this system can take you from bench top to large scale production with ease.

Advantages:

- High yield protein expression
- Rapid high cell density growth
- Methanol-free growth media
- Plasmid integration enhances stability
- Acetamide selection enriches for multi-copy integrants, enhancing yield
- Tight control of gene expression enables expression of toxic genes
- Access to eukaryotic protein folding and glycosylation machinery
- Simultaneous expression of multiple proteins
- Ease-of-use for those inexperienced with yeast systems
- Yeast competent cells included
- No license required for research use

***K. lactis* Protein Expression Kit** **E1000**

Kit components sold separately

***K. lactis* GG799 Competent Cells** **C1001**

pKLAC1 Vector **N3740**

	K. lactis	*P. pastoris*
High yield expression	✓	✓
Rapid high cell density growth	✓	✓
Yeast Competent Cells Included	✓	
Methanol-free growth media	✓	
Antibiotic-free Selection	✓	
Enhanced multi-copy integration	✓	
Protein folding and glycosylation	✓	✓
Expression of genes toxic to *E. coli*	✓	✓

Quick comparison of *K. lactis* and *P. pastoris* expression systems.

For more information and international distribution network, please visit www.neb.com

- **New England Biolabs Inc.** 240 County Road, Ipswich, MA 01938 USA 1-800-NEB-LABS Tel. (978) 927-5054 Fax (978) 921-1350 info@neb.com
- **Canada** Tel. (800) 387-1095 info@ca.neb.com
- **Germany** Tel. 0800/246 5227 info@de.neb.com
- **UK** Tel. (0800) 318486 info@uk.neb.com
- **China** Tel. 010-82378266 beijing@neb-china.com

NEW ENGLAND BioLabs® Inc.
the leader in enzyme technology

EDITED BY STELLA HURTLEY AND PHIL SZUROMI

<< Old Olmec Writing

The Olmec civilization of Central America [~1200 to 400 years before the common era (BCE)] may have been the precursor to later complex societies such as the Maya (100 to 600 CE) and Aztec (1200 to 1500 CE), yet unambiguous evidence of earliest Olmec writing is lacking. **Rodríguez Martínez *et al.*** (p. 1610; see the news story by **Lawler**) report the discovery of a stone block from Veracruz, Mexico, inscribed with an unknown system of writing. Taken from a gravel quarry, the block has been dated to the first millennium CE, which is earlier than previous finds. The glyphs, still undeciphered, bear similarity to other Olmec imagery, and the pattern is consistent with a system of writing.

Ethereal Ethane

Scientists predicted that Titan's surface should be awash with liquid ethane, but the low and mid-latitudes of this saturnian moon are merely moist, and dunes prevail rather than seas. **Griffith *et al.*** (p. 1620; see the Perspective by **Flasar**) argue that a large cloud near the north pole of Titan spotted by Cassini's Visual Infrared Mapping Spectrometer may harbor the missing ethane. Similar to Earth, cold air downwells near the winter pole and causes the formation of stratospheric polar clouds. Solid ethane snow may frost the surface at the pole if the conditions are cold enough.

Themes and Variations in Secretion and Endocytosis

Cells need to secrete a variety of proteins from the cell surface and also need to internalize some of these surface proteins, as well as other external proteins. **McNiven and Thompson** (p. 1591) review the mechanisms involved in the formation of coated exocytic transport vesicles as they are exported from the Golgi complex en route to the plasma membrane and compare and contrast them with the formation of coated endocytic vesicles.

European Meltwaters

At the height of the last glaciation, a combination of low sea level and the position of the Fennoscandian and British ice sheets caused much of the runoff from continental Europe to flow through an enormous river that flowed into the Atlantic Ocean through what now is the English Channel, called the Channel River. **Ménot *et al.*** (p. 1623) present a record of Channel River activity between about 30,000 and 5,000 years before the present. Its flow began to swell around 22,000 years ago, reached a peak between 19,000 and 17,000 years ago, and ended abruptly then at the start of Heinrich Event 1. This record should help allow models to determine what effect the melting of European glaciers at the end of the Last Glacial Maximum had on ocean circulation, as has been done for the melting of the Laurentide Ice Sheet on the other side of the Atlantic Ocean.

Seeking the Genome for the Trees

Although the genomes of some model plants such as *Arabidopsis* and rice have been sequenced, they are different in many key ways from their long-lived, woody relatives, the trees. **Tuskan *et al.*** (p. 1596; see the cover and the news story by **Stokstad**) present the genome sequence of the black cottonwood, *Populus trichocarpa*, which has undergone two whole genome duplication events, one of which occurred at the same time as in *Arabidopsis*. The *Populus* genome has evolved more slowly than *Arabidopsis*, with reduced rates of nucleotide substitution, tandem gene duplication, and gross structural rearrangements of chromosomes. Comparisons of the gene families between *Populus* and *Arabidopsis* reveal a complex pattern, with *Populus* expansions in disease resistance, meristem development, metabolite transport, and cellulose and lignin biosynthesis.

Reducing Crashes to Taps

During the past 30 years, molecular beam techniques have uncovered numerous details of molecular collisions and reactions. A major limitation, however, has been the inherent velocity spread in these beams, which hinders the study of collisions at very low energy. This regime is of interest because of the complexes that can form when weakly attractive forces are not overwhelmed by translational momentum. **Gilijamse *et al.*** (p. 1617) use inhomogeneous electric fields to slow down a beam of OH radicals through Stark deceleration, while maintaining a very narrow velocity spread. The rotational-state dependence of OH scattering events with a beam of xenon atoms was determined for a collision-energy range extending below 1 kilocalorie per mole.

Of Aging and Aggregation

Protein aggregation that is associated with late age-onset diseases such as Alzheimer's and

Continued on page 1539

CREDITS (TOP TO BOTTOM): RODRÍGUEZ MARTÍNEZ *ET AL.*; GILIJAMSE *ET AL.*

www.roche-applied-science.com

Innovative Genomic Analysis

Searching for Innovation?

Look no further

For more information about these and other innovative products, visit us at **www.roche-applied-science.com** today.

Leap ahead of your competition with cutting-edge genomics instruments and reagents from Roche Applied Science. Generate data faster and easier than ever before with innovative products for innovative research.

Genome Sequencer 20 – Real Technology, Real Results
Accelerate genetic analysis of *de novo* genomes, complex populations, SNPs, tags, miRNA, and more. Generate data in days – not months or years – with the newest revolution in sequencing technology.

LightCycler® 480 Plate-Based Real-Time PCR System – The Versatile Alternative
Count on the speed and accuracy you have come to expect from the leader in rapid real-time PCR – in a more convenient and versatile 96- or 384-well plate format.

Universal ProbeLibrary – Simplifying and Improving qPCR with Novel Technologies
Design a new gene expression qPCR assay in seconds and run it tomorrow. Obtain the benefits of hydrolysis probe assays at a fraction of the cost.

Roche Diagnostics

Roche Diagnostics GmbH
Roche Applied Science
68298 Mannheim
Germany

Continued from page 1537

Parkinson's has toxic effects. **Cohen *et al.*** (p. 1604) show, in a worm model of amyloidosis, that the aging process is linked to toxic protein aggregation. Molecules associated with the insulin signaling pathway—a cascade that is linked to aging—also influence aggregation and toxicity. The transcription factor DAF-16 and heat shock protein HSF-1 function to promote aggregation or disaggregation, respectively, of β-amyloid peptides. The authors propose a cellular mechanism hinging on these two factors whereby toxic aggregates are identified and prepared for disaggregation and degradation.

The Rhythm in the Brain

Spontaneous cortical oscillations facilitate synaptic plasticity; correlate with attention and perceptual binding; and may play a role in transient, long-range coordination of distinct brain regions. Exactly how these transient oscillations influence each other and coordinate processing at both the single neuron and population levels is still not understood. **Canolty *et al.*** (p. 1626) show that the amplitude and phase of cortical theta rhythms modulate the power of high gamma band neuronal oscillations in the human electrocorticogram. High gamma activity directly reflects the activation of a local cortical area and is correlated with the functional magnetic resonance imaging blood oxygen level dependent–signal. The much slower theta rhythm is more distributed across the cortex and is associated with novelty, attention, working memory, and exploratory behavior. Importantly, the strength of this theta-gamma coupling is correlated with variations in a battery of cognitive tasks.

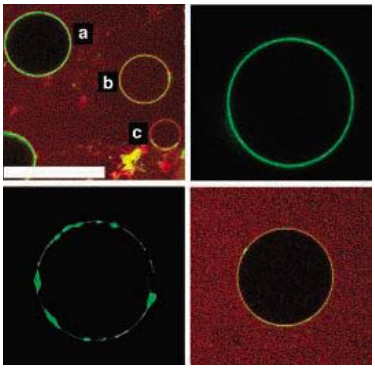

CREDIT: HASPER ET AL.

Two Ways to Kill a Bacterium

In bacterial peptidoglycan synthesis, lipid II is required for the transport of cell-wall subunits across the bacterial cytoplasmic membrane. Lipid II is a target for antibiotics like vancomycin and lantibiotics, such as nisin and mutacin, which are small peptides bearing lanthionine rings. These drugs act by contrasting mechanisms. Vancomycin binds to the pentapeptide of lipid II, whereas lantibiotics bind to the pyrophosphate of lipid II via the lanthionine rings. **Hasper *et al.*** (p. 1636) have discovered that although some lantibiotics aggregate to form pores in membranes, others kill bacterial cells without forming pores. Instead, immobilization of lipid II prevents it from reaching sites where peptidoglycan synthesis occurs, such as at the septum of dividing cells, and blocking cell-wall synthesis.

Caveolin and Liver Regeneration

Caveolin is a key component of caveolae, cell surface invaginations involved in the internalization of a variety of signaling molecules and the uptake of certain viruses. Surprisingly enough, when caveolin knockout mice were generated a few years ago, they appeared to be healthy. **Fernández *et al.*** (p. 1628; see the Perspective by **Brasaemle**) have now examined these mice in more detail and discovered a phenotype in these animals—a profound defect in liver regeneration leading to reduced survival after partial hepatectomy. Problems uncovered included changes in lipid metabolism and cell cycle progression. Treating mutant mice with glucose could circumvent the defect and improve survival after liver damage.

Perfecting Pathogenic Potential

The human pathogen *Mycobacterium tuberculosis* does not have recognizable homologs of secretion machines that are essential for the virulence of many bacterial pathogens. Instead, the ESX-1 system is required for growth of *M. tuberculosis* in macrophages and for controlling host cell response to infection. This system secretes a pair of virulence factors, ESAT-6 and CFP-10, that are essential for *M. tuberculosis* virulence. **DiGiuseppe Champion *et al.*** (p. 1632; see the Perspective by **Ize and Palmer**) identified a C-terminal signal sequence required for directing the ESAT-6/CFP-10 virulence factor complex for secretion from *M. tuberculosis*. Mutations in this signal sequence that prevented interaction with the secretion machine also prevented secretion. The CFP-10 signal sequence also drove secretion of an unrelated protein.

Optimize your microarray assays

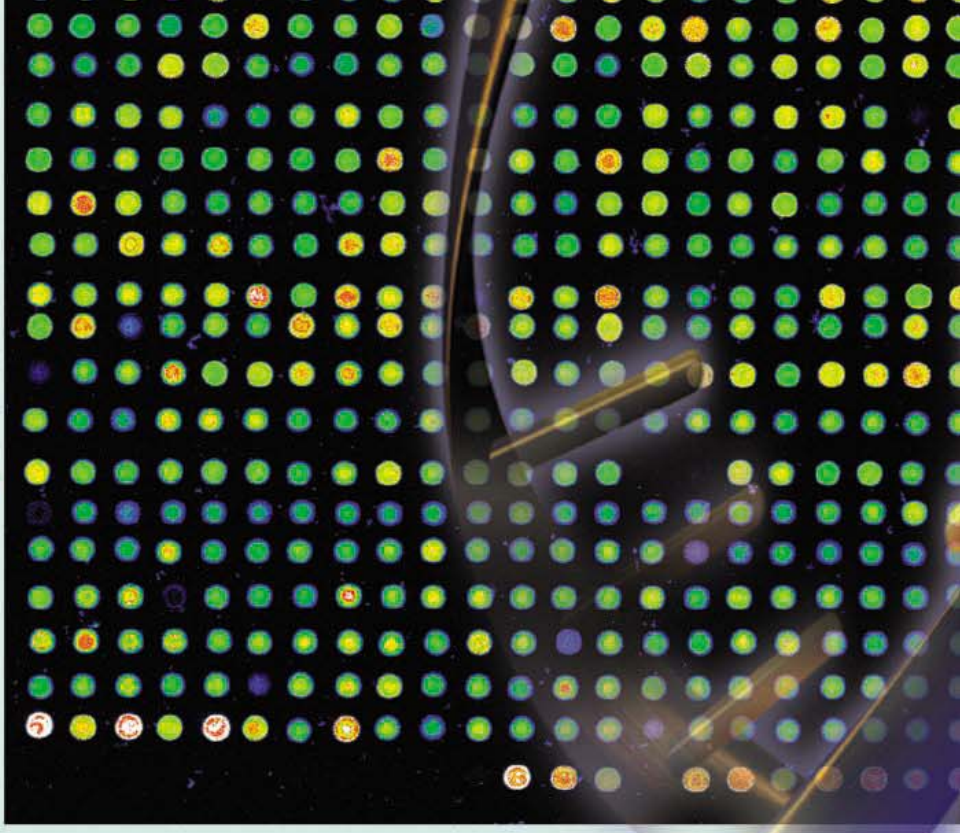

You rely on IDT for top quality oligos, so trust IDT with your microarrays. We offer an assortment of products to support researchers who print their own microarrays.

Epoxide Spotting Buffer (ESB)

- Optimized for spotting amine-modified or I-Linker™ modified oligos on epoxy surface slides
- Designed to reduce evaporation and deliver ~85 micron spots with uniform hybridization signals
- Suitable for both short and overnight microarray print runs

SpotQC

Detector oligos have improved thermodynamics allowing greater hybridization uniformity over a wider variety of sequence compositions.

- Cy3™-labeled detector oligo developed for direct hybridization fluorescence detection.
- Biotin-labeled detector oligo developed for secondary fluorescent, chemiluminescent, or colorimetric hybridization detection assays.

SpotQC Hybridization Buffer

Optimized hybridization solution specifically formulated for use with IDT's SpotQC oligos. It allows for the dilution of the SpotQC detector oligo up to 20fold while maintaining the superior detection of a broader range of oligo-probe lengths and GC compositions with our proprietary detector oligo.

Learn more at www.idtdna.com/microarrays

Innovation and Precision in Nucleic Acid Synthesis **www.idtdna.com** **800.328.2661**

IDT
INTEGRATED DNA TECHNOLOGIES, INC.

Corporate Headquarters
Integrated DNA Technologies, Inc.
1710 Commercial Park
Coralville, IA 52241 USA

West Coast Operations
Integrated DNA Technologies, Inc.
6868 Nancy Ridge Drive
San Diego, CA 92121 USA

BSI REGISTERED
ISO 9001:2000
FM88954

Don Kennedy is Editor-in-Chief of *Science*.

Animal Activism: Out of Control

THE SCIENTIFIC COMMUNITY HAS RESPONDED TO SEVERAL IMPORTANT SCIENCE POLICY issues this year and is getting a little public traction on some, including stem cell research policies and global climate change. We have mostly ignored another, however, and it's a big one. Scientific progress depends on experiment, and in the life sciences that usually entails the use of live animals. But in many countries, animal rights organizations have successfully used extreme tactics to intimidate scientists and their institutions.

Scientists in the United Kingdom have been engaged in this struggle longer than those in the United States, and they appear to have been vigilant enough to secure at least some moderation of the problem. In the United States, however, if you conduct experiments on primate nervous systems, you might have the following experience. Photographs, allegedly of your subjects wearing expressions of extreme pain, are circulated to media outlets. Crowds with bullhorns picket your residence, and leaflets declaring that you commit "atrocities" are distributed to your neighbors. Your colleague who works on monkey behavior is the target of a firebomb. It is mistakenly placed on a neighbor's porch; the good news is that the fuse timer failed, but the Federal Bureau of Investigation (FBI) says the blast might well have killed those inside.

Am I making this up? Well, it happened to Dr. Dario Ringach, a member of the neurobiology faculty at the University of California, Los Angeles (UCLA). The work he did on higher-order information processing in visual systems had been published in good journals, including this one. The dénouement of the assault he weathered for 4 years is described in a triumphal press release from the Animal Liberation Front (ALF): "You Win" it said, quoting Ringach. The subhead read, "UCLA Vivisector Dario Ringach Quits Animal Experimentation." The release boasts about the reason for this outcome: He "asked that his family be left alone," it says. Well, in the absence of timely help from his institution, he made the best decision he could, as you or I probably would have. Meanwhile, the ALF has taken credit for both this victory and the firebombing.

During the long spell of Ringach's harassment and the run-up to the firebombing, UCLA was mostly silent, just when the faculty might have expected some high-level encouragement and protection. The UCLA News Office had labeled the firebombing as terrorism and said: "UCLA condemns that." Fine as far as it went, but a firm statement from the top was needed, and one was finally forthcoming on 27 August, weeks after these troubling incidents. It came from Acting Chancellor Norman Abrams, who condemns the harassers as terrorists (thereby choosing exactly the right word), promises more security to protect the faculty members who do animal research, and doubles the $30,000 FBI reward for apprehension of the firebomber. That will help, but more remains to be done. It turns out that the folks who are promoting the harassment of faculty have had inside help and participation from students. Yet appeals by researchers for disciplinary action have gone unanswered, even though harassment is a listed violation under the UCLA Student Code.

Meanwhile, there's more on tap. The ALF has announced its own reward: $10,000 for anyone who supplies information that "leads to the end of an animal experiment or the arrest and final conviction of any vivisector at UCLA." It's good that the university is now moving on the problem. But the terrorists, equipped with a kind of moral certainty that cannot distinguish righteous from right, are likely to continue this campaign unless the law of the land makes it clearly illegal and punishable. Fortunately, there is an opportunity for effective congressional action in this area. H.R. 4239 (the Senate companion is S. 1926) has already been heard by the House Judiciary Committee. Entitled the Animal Enterprise Terrorism Act, it would prohibit threats against researchers and their families and establish penalties for economic damage or for placing a researcher in reasonable fear of death or bodily injury. It also specifically prohibits "tertiary" targeting: actions against those who have a relationship or transactions with animal enterprises, including researchers. The House Judiciary Committee should get this bill out for a vote as soon as possible, before somebody gets killed.

– Donald Kennedy

10.1126/science.1134384

EDITED BY STELLA HURTLEY AND JAKE YESTON

ECOLOGY

Single Symbionts for Corals

Tropical coral reefs are stressed by sea-level rise and higher water temperatures brought on by climate change. Stress prompts corals to shed their photosynthetic symbionts, or zooxanthellae, and large areas of reefs can "bleach," sometimes killing the coral. Controversy has centered on whether bleaching is adaptive to enable bleached corals to acquire different symbionts that could endow their hosts with different physiologies to cope with different conditions, in particular greater temperature tolerance. Symbiont shuffling could happen only if the host coral can naturally tolerate a variety of symbionts. Goulet has undertaken a meta-analysis and review of 43 papers containing genotype data for 442 coral-zooxanthellae associations. It seems that most mature hard coral individuals harbor only one strain of symbiont and will retain the same genotype for decades, even after transplantation from one site to another. It remains unclear how the remaining 23% of corals that can host several symbionts respond to bleaching conditions. — CA

Mar. Ecol. Prog. Ser. **321**, 1 (2006).

CHEMISTRY

Flowing Precious Metals

With the exception of mercury, metals tend to require substantial heating before flowing as liquids; even alloys expressly designed for use as soldering fluxes generally melt well above room temperature. Warren *et al.* show that a particular ligand and counter-ion combination confers flowing properties to a range of precious metal nanoparticles ~2 nm in diameter. Crystalline particles of platinum and gold, and predominantly amorphous palladium and rhodium particles, were prepared with *N,N*-dioctyl-*N*-(3-mercaptopropyl)-*N*-methyl ammonium capping ligands (bound to the metal through sulfur) by reduction of metal salts in tetrahydrofuran solution. Exchange of bromide counter-ions with sulfonates bearing long hydrophobic tails yielded a substance that, after thorough drying under vacuum, exhibited highly viscous liquid-like flow at room temperature; a 50-mg droplet moved at a rate of just over 2 cm/hour down an inclined glass plane. The authors envision that these flowing nanoparticles may offer convenient routes to self-assembled materials, as well as applications in heat-transfer media. — MSL

J. Am. Chem. Soc. **128**, 10.1021/ja064469r (2006).

GEOLOGY

Tales of Wander

True polar wander describes relative motion between Earth's spin vector and the solid Earth. One class of this phenomenon, inertial interchange true polar wander, occurs when normal advection of mantle density heterogeneities produces changes in the relative magnitudes of the principal inertia axes, causing Earth to rotate quickly by as much as 90°, until the new major rotational axis is aligned with the spin vector. In addition to the paleomagnetic variations that would accompany such a rapid change of Earth's orientation, another observable consequence could be transient sea-level variations resulting from the differential response of the slowly re-equilibrating mantle/lithosphere and the rapidly re-equilibrating world ocean. A third potential but indirect effect, arising from sea-level change, is perturbation of the carbon cycle, as marine biological productivity is affected by water depth variations.

Svalbard stone.

In an investigation of possible true polar wander, Maloof *et al.* present paleomagnetic data from three Middle Neoproterozoic carbonate units in Svalbard, Norway, which show large shifts in paleomagnetic orientation coincident with abrupt changes in $\delta^{13}C$ and relative sea level. They conclude that the best explanation for the data is that this area experienced rapid shifts of paleogeography during a pair of true polar wander events. Their hypothesis can be further tested by analyzing sediments of the same age from other basins for predictable related changes. — HJS

Geol. Soc. Am. Bull. **118**, 1099 (2006).

MOLECULAR BIOLOGY

Circle of One

All living things must maintain and repair their genomes, and nonhomologous end joining (NHEJ) is one of the most important pathways for patching up potentially disastrous double-strand (ds) breaks in DNA; so-called Ku proteins play a central role in the process. But viruses, so it was thought, don't seem to use NHEJ in this way.

Corndog and Omega are dsDNA viruses or, more precisely, bacteriophages that infect bacteria, in this case, *Mycobacterium* species. Oddly enough, as Pitcher *et al*. now show, Corndog and Omega both contain Ku homologs in their genomes. The viral Ku proteins can work together with the bacterial ligase LigD to repair ds breaks in a yeast system. This suggests that NHEJ is somehow involved in the viral life cycle, where previously there was no indication of such a requirement.

Corndog and Omega enter bacterial cells as linear viruses that must circularize to allow rolling circle replication—an essential part of

CREDITS (TOP TO BOTTOM): GOULET, *MAR. ECOL. PROG. SER.* **321**, 1 (2006); MALOOF *ET AL., GEOL. SOC. AM. BULL.* **118**, 1099 (2006)

the viral life cycle. Related viruses, such as Lambda, have long 9–nucleotide (nt) cohesive (*cos*) ends that provide a favorable equilibrium for self-association. Corndog and Omega have very short *cos* ends, of only 4 nt, which are too short to self-associate efficiently and promote genome circularization. Thus the viral Ku, working together with the host LigD, may help to bring the *cos* ends together, paralleling their function in dsDNA break repair. — GR

Mol. Cell **23**, 743 (2006).

ECOLOGY/EVOLUTION

In Perfect Symmetry

Bilaterally symmetric flowers have evolved from radially symmetric flowers in a range of plant families, and this transition is usually correlated with a switch from generalist to specialist pollinators. Although the developmental changes involved in the transition are relatively well understood at the molecular genetic level, the selective forces behind it are less clear. Gomez *et al*. monitored the pollination rates of *Erysimum mediohispanicum*, a herbaceous plant of the southern Spanish mountains, which shows intraspecific variation in flower shape and is pollinated by beetles, bees, and hoverflies. The more bilaterally symmetric flowers were favored by the most abundant pollinating insect, the generalist beetle *Meligethes maurus*, and these flowers also produced the highest number of offspring. The significant fitness differences between flowers of differing shape suggest the adaptive route by which bilateral symmetry can evolve, even if the pollinators are generalists like most beetles. — AMS

***Erysimum mediohispanicum* variants.**

CREDIT: GOMEZ *ET AL., AM. NAT.* **168**, 10.1086/507048 (2006)

Am. Nat. **168**, 10.1086/507048 (2006).

CLIMATE SCIENCE

Shedding Light on the Sun

Satellite measurements show that solar irradiance, essentially the amount of energy that reaches Earth, varies over the 11-year solar cycle by ~0.1%, too small a change to have a noticeable impact on Earth's average temperature. However, a long-standing question in climate science is whether larger solar changes have occurred that might have caused warming over the past century or climate change at some stage of the Holocene (or an even longer span of time).

Bard and Frank provide a thorough critical review of both the problematic evidence for longer changes in solar irradiance and the possible climatic effects these changes could have induced. The authors point out that many proposed connections, for example between the records of cosmogenic nuclides such as ^{14}C and ^{10}Be and records of climate change, are based on correlations—some of which have large and perhaps unappreciated uncertainties—and on imperfect and indirect records. They conclude that there might still be a connection between solar changes and the Medieval Warm Period and Little Ice Age, but that overall solar changes, most of which remain unproven, probably represent a second-order influence on the behavior of Earth's recent climate. — BH

Earth Planet. Sci. Lett. **248**, 1 (2006).

IMMUNOLOGY

Vascular Origins

During the development of an embryo, cells of the hematopoietic system and endothelium have a common origin. Bone marrow–derived cells may even contribute to vessel growth in some settings. It has not been clear, however, whether hematopoietic cells normally contribute to vascular development.

Sebza *et al*. extend previous work in which the hematopoietic immune signaling proteins Syk and SLP-76 were found to regulate the developmental separation of lymphatic and blood vessel systems [*Science* **299**, 247 (2003)]. Directed transgenic reexpression of SLP-76 in a subset of hematopoietic cells was sufficient to correct the defect in lymphatic-vascular connection apparent in mice that lack Syk and SLP-76. By generating chimeric animals bearing both wild-type and Syk/SLP-76–deficient cells, it was also possible to establish this phenomenon as an endothelial cell-autonomous effect. Thus, the study demonstrates that under steady-state conditions, cells of hematopoietic origin can contribute directly to blood lymphatic-vascular separation as precursors of endothelial cells. It will now be interesting to pursue experiments that more precisely characterize the progenitor cells and their relationship with endothelium during the processes of blood and lymphatic vessel growth and repair. — SJS

Dev. Cell **11**, 349 (2006).

you've got
better
things
to do...

better consistency

better purification

better results

Introducing
Personal Automation

Meet Maxwell

Maxwell™ 16 gives you consistent purification results — processing up to 16 samples in 30 minutes. It's personal automation, right at your lab bench. DNA, RNA or protein purification, your choice. Finally reagents, instrumentation, service and support from one reliable source. You'd better visit: **www.MeetMaxwell.com**

Promega

www.sciencemag.org

Science

1200 New York Avenue, NW
Washington, DC 20005
Editorial: 202-326-6550, FAX 202-289-7562
News: 202-326-6500, FAX 202-371-9227

Bateman House, 82-88 Hills Road
Cambridge, UK CB2 1LQ
+44 (0) 1223 326500, FAX +44 (0) 1223 326501

Subscription Services For change of address, missing issues, new orders and renewals, and payment questions: 866-434-AAAS (2227) or 202-326-6417, FAX 202-842-1065. Mailing addresses: AAAS, P.O. Box 96178, Washington, DC 20090-6178 or AAAS Member Services, 1200 New York Avenue, NW, Washington, DC 20005

Institutional Site Licenses please call 202-326-6755 for any questions or information

Reprints: Author Inquiries 800-635-7181
Commercial Inquiries 803-359-4578
Corrections 202-326-6501

Permissions 202-326-7074, FAX 202-682-0816

Member Benefits Bookstore: AAAS/BarnesandNoble.com bookstore www.aaas.org/bn; Car purchase discount: Subaru VIP Program 202-326-6417; Credit Card: MBNA 800-847-7378; Car Rentals: Hertz 800-654-2200 CDP#343457, Dollar 800-800-4000 #AA1115; AAAS Travels: Betchart Expeditions 800-252-4910; Life Insurance: Seabury & Smith 800-424-9883; Other Benefits: AAAS Member Services 202-326-6417 or www.aaasmember.org.

science_editors@aaas.org	(for general editorial queries)
science_letters@aaas.org	(for queries about letters)
science_reviews@aaas.org	(for returning manuscript reviews)
science_bookrevs@aaas.org	(for book review queries)

Published by the American Association for the Advancement of Science (AAAS), *Science* serves its readers as a forum for the presentation and discussion of important issues related to the advancement of science, including the presentation of minority or conflicting points of view, rather than by publishing only material on which a consensus has been reached. Accordingly, all articles published in *Science*—including editorials, news and comment, and book reviews—are signed and reflect the individual views of the authors and not official points of view adopted by the AAAS or the institutions with which the authors are affiliated.

AAAS was founded in 1848 and incorporated in 1874. Its mission is to advance science and innovation throughout the world for the benefit of all people. The goals of the association are to: foster communication among scientists, engineers and the public; enhance international cooperation in science and its applications; promote the responsible conduct and use of science and technology; foster education in science and technology for everyone; enhance the science and technology workforce and infrastructure; increase public understanding and appreciation of science and technology; and strengthen support for the science and technology enterprise.

Information for Contributors

See pages 102 and 103 of the 6 January 2006 issue or access www.sciencemag.org/feature/contribinfo/home.shtml

DATABASES

TROPICAL TROVE

Last year, the Smithsonian Tropical Research Institute in Panama posted its 20-year archive of tree census data (NetWatch, 22 April 2005, p. 475). Now, the institute has launched a bioinformatics clearinghouse that provides access to more researchers' data sets, photos, and other resources. If you're curious about plants such as *Tabebuia*, a genus of hardy tropical trees, the site's herbarium offers a taxonomic database; an identification key and photo gallery are in the works. The physical monitoring page connects to meteorological and hydrological measurements for eight sites in the country. Browse the species list for the Bocas del Toro station on the Caribbean coast to see photos of creatures such as the iridescent queen angelfish (*Angel reina*; above). >> biogeodb.stri.si.edu/bioinformatics

AUDIO

Sounds of Silence >>

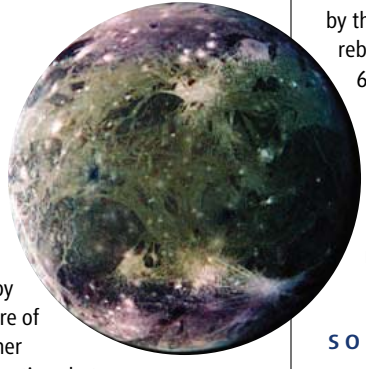

Lightning in Saturn's atmosphere sounds like raindrops pattering on leaves, and the microwave radiation left over from the big bang is reminiscent of a vacuum cleaner running in the next room. These two sites let you listen to space, offering recordings of unearthly noises and various types of energy translated into frequencies we can hear. At Spacesounds,* a commercial site created by artists and scientists, you can tune in to the magnetosphere of Jupiter's moon Ganymede (right), the Vela pulsar, and other objects. Space-flight devotees can play hours of communications between ground control and the crews of the Apollo, Gemini, Mercury, and space-shuttle missions. The squeaks, chirps, roars, and other noises at Space Audio† from the University of Iowa in Iowa City sound like they came from a David Lynch movie. >>

* spacesounds.com/home/index.html
† www-pw.physics.uiowa.edu/space-audio

FUN

Nobel Prize Handicapping

The first of this year's Nobel prizes won't be announced until 2 October, but the prognosticating has already begun. This site from the publisher Thomson Scientific predicts contenders for the science awards. The company's experts factor in variables such as the number of highly cited papers and whether the candidate has already nabbed another significant prize. Of Thomson's 27 picks since 2002, four have won the Nobel. An online poll lets visitors vote for their favorites. In the chemistry category, for instance, three researchers who probed the roles of nuclear hormone receptors had the edge last week. >> www.scientific.thomson.com/nobel

RESOURCES

A Marsh Reborn

The Middle East's largest wetlands, the sprawling marshes near the junction of the Tigris and Euphrates rivers in Iraq were once home to about 500,000 people. But the ecosystem withered because of upstream water diversions and Saddam Hussein, who ordered the wetlands drained to suppress dissent in southern Iraq (*Science*, 25 February 2005, p. 1186). This site from the U.N. Environment Programme follows the progress of a project to restore the parched area begun after the U.S.–led invasion in 2003. At the time, the wetlands' original 20,000 square kilometers had dwindled by more than 90%. But by this June, they had rebounded to about 60% of their previous size. The site offers satellite land cover maps and progress reports that track water extent and vegetation regrowth. In these satellite images from 2003 (top) and 2005, dark blue denotes newly inundated areas. >> imos.grid.unep.ch

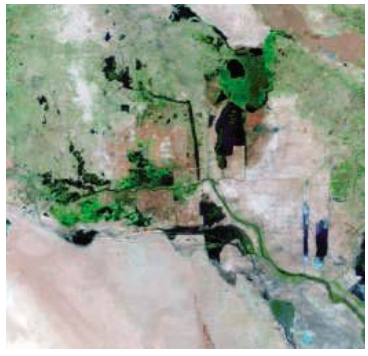

SOFTWARE

Metabolic Networking

Molecular biologists can turn their genomic or proteomic data into maps of metabolic pathways with this program from SRI International of Menlo Park, California. The nonprofit institute's BioCyc Web site (NetWatch, 30 January 2004, p. 601) houses metabolic diagrams for more than 200 species. Researchers can download a software bundle that creates similar figures for their own organisms, using gene-expression results and other types of data. You can animate the diagrams to reflect changes over time. The program is free to academic researchers who request it. >> biocyc.org/download.shtml

Send site suggestions to >> netwatch@aaas.org
Archive: www.sciencemag.org/netwatch

CREDITS (TOP TO BOTTOM): MARY HART/UNIVERSITY OF KENTUCKY; U.N. ENVIRONMENT PROGRAMME; NASA

THE DR. PAUL JANSSEN AWARD FOR BIOMEDICAL RESEARCH

CONGRATULATIONS TO
DR. CRAIG C. MELLO

Winner of The Dr. Paul Janssen Award for Biomedical Research, 2006

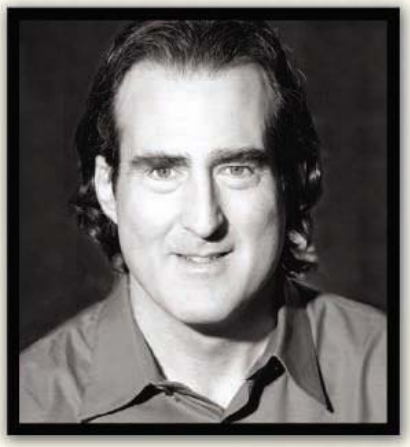

DR. CRAIG MELLO
University of Massachusetts Medical School
and the Howard Hughes Medical Institute

Dr. Craig Mello has been selected as the recipient of the Award for his role in the discovery of RNA interference (RNAi) and the elucidation of its biological functions.

The Dr. Paul Janssen Award for Biomedical Research biannually honors the work of an active scientist in academia, industry or a scientific institute who exhibits the standards of innovation, insight and leadership that Dr. Paul Janssen showed while moving the boundaries of medical science and touching the lives of patients.

Visit **www.pauljanssenaward.com** for more information.

2006 Selection Committee

Dr. Arvid Carlsson
Dr. Jean-Marie Lehn
Dr. Hartmut Michel
Dr. Edward Scolnick
Dr. Solomon Snyder
Sir Richard Sykes

Johnson & Johnson

Leading Gas Spewers

In 2000, the last year for which comprehensive data are available, the United States emitted a fifth of the world's greenhouse gases, or 6928 million tons equivalent CO_2. China's output almost equals those of India, Canada, Russia, and South Korea combined. The World Resources Institute created this map to show how different U.S. regions compare with top world emitters, with total emissions shown in millions of tons equivalent CO_2.

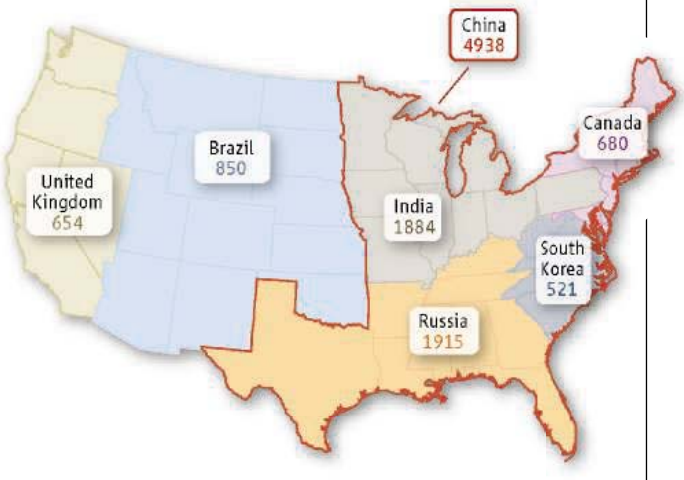

They Said It . . .

"In retrospect, the choice of entertainment was inappropriate for the occasion."

—A statement from Australian National University in response to complaints about balloon- and lingerie-clad burlesque dancers who put on a show at the Australia New Zealand Climate Forum in Canberra, 5–7 September.

MOVE OVER, FIRE ANTS

A mysterious species of ant has invaded Houston, Texas, and no one knows where the creatures came from. The insects, of the genus *Paratrechina*, are known as "crazy ants" because of their frenzied movements. They are so numerous and aggressive that they're driving away the notorious imported red fire ant. The crazy ants are a major headache for homeowners, and researchers fear they could also harm wildlife and endanger electrical equipment.

Ants getting ready to short out Houston.

An exterminator first noticed the ants in 2002 and contacted Roger Gold, an urban entomologist at Texas A&M University in College Station. He and graduate student Jason Meyers are studying ways to control the ants but without much luck. "You can kill hundreds of thousands of ants, and the remaining ones walk over the cadavers and continue on their way," Gold says.

The ants raised worries this summer when they crawled into circuit boards and shorted out a radiation scanner at the Port of Houston. They are now about 20 kilometers from NASA's Johnson Space Center. Research on control is hampered by the fact that the Houston species hasn't been identified yet. And it's not clear whether the ants are agricultural pests, so the U.S. Department of Agriculture isn't taking action.

TALLYING MIDEAST DAMAGE >>

Now that the bullets and bombs have largely stopped flying, the job of assessing the damage in Lebanon and Israel has begun. By comparing before-and-after satellite views, scientists at the European Union Satellite Centre in Madrid, Spain, and the Joint Research Centre in Ispra, Italy, have produced a tally of Lebanon's destruction. More than 1500 buildings, 500 road sections, 500 cultivated fields, and 21 bridges were hit in southern Lebanon and Beirut. The scientists note that this is an underestimate because it only covers damage visible from space.

The environment was also a casualty. A major oil spill (right) has coated at least 150 kilometers of Lebanon's beaches as a result of an Israeli attack on a coastal power plant in July. According to the World Conservation Union, samples of the 15,000 tons of oil that have washed ashore reveal a high concentration of cancer-causing aromatic hydrocarbons. Much oil has also sunk below the surface, posing further risks to the food chain and difficulties for the cleanup.

The Israelis' assessment, reported on 30 August by the Ministry of Environmental Protection, says that Hezbollah rockets damaged 12,000 buildings or apartments, destroying 2000. Fires sparked by the rockets wiped out 1200 square kilometers of forest, including 70% of the Naftali mountain range, according to the ministry, which also cites damage to a wastewater treatment plant and the release of hazardous substances from storage facilities.

CREDITS (TOP TO BOTTOM): SOURCE: WORLD RESOURCES INSTITUTE; JASON MEYERS/TEXAS A&M UNIVERSITY; J. BOHANNON/*SCIENCE*

The first tree genome
1556

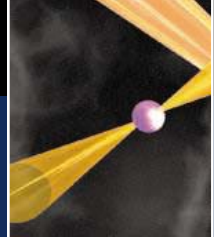

Testing Einstein
1556

NONPROLIFERATION

Endgame for the U.S.–Russian Nuclear Cities Program

The United States and Russia seem ready to pull the plug on an 8-year-old effort to help steer Russian nuclear weapons scientists into civilian work. The joint Nuclear Cities Initiative (NCI) has been on life support for 3 years. It's likely to die next week, NCI proponents say—undercutting efforts to help Russia shrink its massive nuclear complex and bottle up its expertise.

Other U.S.-funded programs employing Russian weapons scientists will continue, but they "are grossly insufficient" to help Russia deal with the problems ahead, says Matthew Bunn, a nonproliferation expert at Harvard University's Belfer Center for Science and International Affairs. And while NCI appears to be out of steam, a much-discussed European NCI has never even left the depot. "The real issue is the slow abandonment of [weapons] scientist programs by the U.S. and Europe," says Kenneth Luongo, executive director of the Russian-American Nuclear Security Advisory Council, a think tank in Washington, D.C., and Moscow. NCI "bought the United States a seat at the table for discussions of these cities' futures," adds Bunn. But getting dramatic results would require a "significantly bigger effort."

Russia's design labs and factories for fabricating nuclear fuel and warheads are dispersed in 10 closed cities that employ some 75,000 people on weapons-related work (see map). After the collapse of the Soviet Union in 1991, several U.S. agencies began assisting Russia with money for specific projects, including safeguarding uranium and plutonium stockpiles from nuclear traffickers and providing grants to reduce the temptation for scientists to work in countries such as Iran or North Korea. The U.S. Department of Energy (DOE) augmented these efforts with NCI after the ruble's collapse in 1998, when scientists were in dire straits. It was the first U.S. program specifically aimed at helping Russia downsize its nuclear complex.

NCI was controversial from the start, however. Critics in Congress and in the Bush Administration argued that it bankrolled middling scientists, freeing Russia to focus resources on the best weapons designers. Proponents responded that because Russia's reservoir of nuclear talent runs so deep, it's worth engaging even second- and third-tier scientists. Russia has 2000 to 3000 scientists with nuclear bomb–making skills and as many as 15,000 more who could aid a hostile weapons program, the nonprofit Nuclear Threat Initiative estimated in a report, *Securing the Bomb 2005: The New Global Imperatives.*

Scratching the surface. NCI created hundreds of jobs for scientists in three of Russia's 10 nuclear cities, but thousands may soon be out of work.

By helping Russia "ease its nuclear cities on the path to sustainable civilian work," says Bunn, NCI has "reduced the danger that experts from some of these cities would … sell their weapons-related knowledge." All told, DOE claims that NCI's roughly $110 million war chest over 8 years created 1600 civilian jobs in three cities—Sarov and Snezhinsk, which specialize in nuclear weapons design, and Zheleznogorsk, a plutonium production town in southern Siberia—and drew in $63 million from outside sources.

Even if NCI disappears, some of its projects will continue under allied programs, such as DOE's Initiatives for Proliferation Prevention and the multilateral International Science and Technology Center. Bryan Wilkes, a spokesperson for DOE's National Nuclear Security Administration, which oversees NCI, said work with Russian scientists will continue; another NNSA official notes, however, that total assistance will decrease by about $10 million per year. But a number of projects have already ended. One casualty is a trove of data on everything in the nuclear cities from joint ventures to crime rates. The information, published in a quarterly bulletin by Sarov's Analytical Center for Nonproliferation, is "invaluable," says Luongo. "In the Cold War, we would have paid billions for it." NCI ended support for the bulletin last February.

Analysts blame both governments for NCI's slow death. The Russia–U.S. NCI pact lapsed in 2003 after the two countries failed to agree on liability and tax issues. A provision gave NCI a 3-year grace period to wind down projects while negotiations on resurrecting it went on. "It was a good program. We wished it to continue, but the bureaucrats killed it," says one scientist at Sarov who was not authorized to speak to the press and asked to remain anonymous.

NCI's threatened termination comes at a critical time for people who live and work in the once-top-secret nuclear enclaves. Earlier this year, Russia's federal government ended subsidies to the closed cities, leaving gaping budgetary holes. According to *Securing the Bomb*, the mayor of Zheleznogorsk recently warned: "We have no idea at all how the budget will be filled. … A starving operator of a nuclear power unit is more dangerous than any terrorist." Layoffs of "many thousands of people" are expected in the coming decade with the closure of plutonium production and reprocessing facilities in Zheleznogorsk and Seversk, Bunn says. In its final months, NCI had stepped up activities in those two cities to help cushion the blow for unemployed scientists. Now it too finds itself out of a job.

–RICHARD STONE AND ELI KINTISCH

SOURCE: DOE

ARCHAEOLOGY

Claim of Oldest New World Writing Excites Archaeologists

A stone block uncovered in a Mexican quarry provides dramatic evidence that the ancient Olmec people developed a writing system as early as 900 B.C.E., according to seven Mesoamerican scholars writing in this week's issue of *Science* (p. 1610). That makes the block's 62-sign inscription by far the oldest writing discovered in the New World and hints at surprising complexity in a culture that may have laid the foundation for the Mayan and Aztec empires encountered by the Spanish a millennium and a half later. "It's a jaw-dropping find," says Brown University anthropologist and co-author Stephen Houston. "It takes this civilization to a different level."

Other specialists agree. "This is an exciting discovery of great significance," says anthropologist Mary Pohl of Florida State University in Tallahassee. Even skeptics say they are convinced that the signs represent true script. But controversy remains over the block's dating and implications. And the inscription—which can't yet be read and seems unrelated to later Mesoamerican scripts—is unlikely to resolve the heated debate over whether the Olmec were the dominant culture of their time or one of many societies that shaped Mesoamerica.

The Olmec civilization appeared on the coast of the Gulf of Mexico around 1200 B.C.E. and quickly flourished thanks to rich soils and high rainfall that allowed intensive maize production. The first center, San Lorenzo Tenochtitlán, was abandoned about 900 B.C.E. just as another one at nearby La Venta arose. By 400 B.C.E., the Olmec culture had largely vanished. During that half-millennium, Olmec fashions spread around Mesoamerica, although the extent of their influence remains contentious. Along with creating a sophisticated calendar, the Olmec carved glyphs as early as the San Lorenzo phase. Later glyphs found during the La Venta period provide more extensive evidence of iconography, but scholars are divided over whether those could be classified as writing (*Science*, 6 December 2002, p. 1872).

Road builders quarrying fill from an ancient mound at Cascajal, outside San Lorenzo, found the new block with pottery fragments and figurines. The local authority on cultural materials stored the objects in his home and alerted the paper's first two authors, anthropologists Maria del Carmen Rodriguez Martinez and Ponciano Ortiz Ceballos of the Centro del Instituto Nacional de Antropología e Historia. The block was then examined by the entire team this spring. Chemical analysis shows an ancient patina in the stone's incisions, which were made with a blunted blade to make outlines and a sharper one to make cuts within the signs.

The authors argue that the block is roughly the same age as the artifacts found with it, which they say date to the latter part of the San Lorenzo phase; they also note that the site is close to San Lorenzo itself. "There is quite a good deal of evidence on the probable context," says Pohl, who accepts the conclusion. But those claims don't wash for some other researchers, who note that all of the artifacts were found out of context. "Once I owned a home near to Lincoln's log cabin, but that proximity didn't date my house to the same period," says David Grove, an emeritus anthropologist at the University of Florida, Gainesville. "Likewise, the literally mixed bag of shards kept by village authorities doesn't help at all to date the piece."

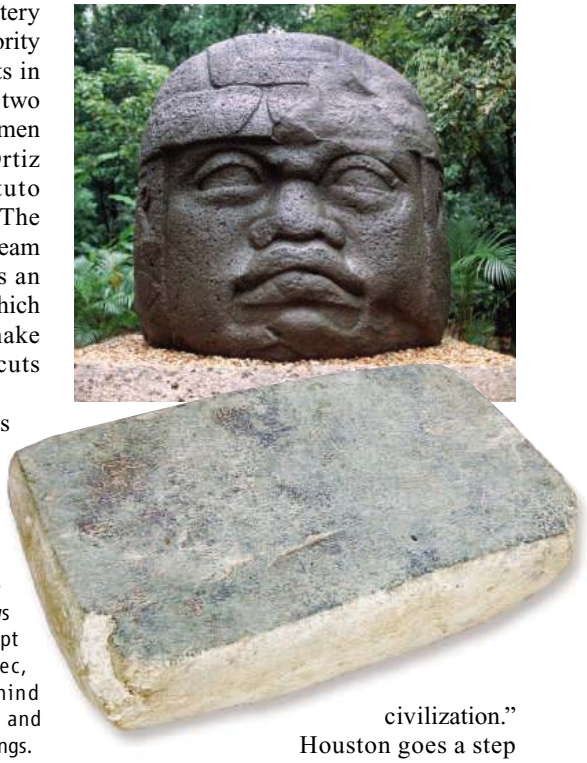

Heady find. The Cascajal block shows signs of early script among the Olmec, who also left behind large stone heads and monumental buildings.

Adds John Clark, an anthropologist at Brigham Young University in Salt Lake City, Utah: "Is the block associated with San Lorenzo or La Venta? We can't answer that definitively." Like Grove, he favors a later date, when Olmec glyphs became more common.

Whatever the date, he and Grove agree that the inscription qualifies as writing and so is a dramatic find. A few of the signs are repeated, and there is a pattern of variable as well as short and repeated sequences. "The Cascajal block conforms to all expectations of writing," the authors say. They argue that such sophistication reveals "a new complexity to this civilization."

Houston goes a step further, saying, "We're looking, possibly, at the glimmerings of an early empire."

The script's influence on later systems is unclear, however. The text runs horizontally rather than vertically as in later Mesoamerican scripts. Nor can the writing be linked with a later writing system, Isthmian, which emerged around 500 B.C.E. and has radically different signs. Nevertheless, the authors conclude that "the clear linkage of the script to the widely diffused signs of Olmec iconography" argues in favor of a widespread system that died out before others appeared in succeeding centuries—perhaps as happened to one of the world's first writing systems, the Indus script, which vanished shortly after 2000 B.C.E.

Like Indus script, the newly discovered Olmec writing remains undeciphered. "We would need a Rosetta stone," says Houston. Clark hopes that the Cascajal block will encourage researchers to go back to the site. "Now we need to dig some control pits and do some real archaeology," he says.

–ANDREW LAWLER

CREDITS (TOP TO BOTTOM): DANNY LEHMAN/CORBIS; C. RODRIGUEZ MARTINEZ *ET AL.*, *SCIENCE*

We can't change our genes to fit our medicines,

but we can change our medicines to fit our genes.

Not someday. Now.

Working with you, we can comprehensively analyze the DNA from thousands of patients taking your drug. Out of the millions of genetic variations between patients, we may be able to help you identify the ones that are associated with strong efficacy, poor efficacy, or side effects. Perlegen's exceptional coverage of the genome and experienced team of analysts could help you get clinically relevant answers, not just data, in a matter of months.

We partner with the top pharmaceutical companies around the world. We also license late-stage drugs. If you have a drug that can benefit from our approach, please contact us.

Patients are waiting.

genetics@perlegen.com
Mountain View, California • 650-625-4500
Tokyo, Japan • 81 (0)3 3444-6080
www.perlegen.com

Targeting today's drugs.
Discovering tomorrow's.™

PERLEGEN SCIENCES®

ASTROPHYSICS

Space Mission to Shine a Light on Solar Flares

TOKYO—Solar flares and coronal mass ejections, the most powerful explosions in our solar system, periodically blitz Earth with charged particles that can disrupt radio signals, fry satellite electronics, and threaten the health of astronauts who find themselves outside our planet's sheltering ionosphere. Yet these phenomena are little understood. Scientists don't know, for example, what generates the magnetic energy thought to power solar flares, what triggers the energy's release, or even whether solar flares pop up all over the sun's surface or just in certain regions.

Solar-B, a spacecraft set for launch from Japan's Uchinoura Space Center on 23 September, "is designed to answer these questions," says John Davis, a Solar-B project scientist at NASA's Marshall Space Flight Center in Huntsville, Alabama. A better understanding of solar processes, he says, "could have a broad impact on physics."

Solar-B is an encore to Yohkoh, the first spacecraft to observe a solar flare's highly energetic x-rays, which are obscured from land-based telescopes by Earth's atmosphere. Spiro Antiochos, an astrophysicist at the U.S. Naval Research Laboratory in Washington, D.C., says that Yohkoh, launched in 1991, provided "the first definitive observations" connecting solar flares to magnetic reconnection, in which magnetic fields generated deep within the sun suddenly break apart and reform, releasing massive amounts of energy. This energy heats the corona and accelerates electrons, protons, and heavier ions into space, forming solar flares. Yohkoh, however, was unable to link specific magnetic field structures to solar flares.

Solar-B should fill in the gaps. "What we expect from Solar-B is to clearly identify a specific magnetic field motion and a specific type of magnetic field appearing on the sun's surface and the coronal response," says Takeo Kosugi, project manager for the Institute of Space and Astronautical Science in Sagamihara, which is reprising its Yohkoh partnership with NASA and the U.K.'s Particle Physics and Astronomy Research Council on the mission.

Three telescopes onboard the $210 million spacecraft will help achieve this precision. Its optical scope, with a 0.5-meter mirror—the largest of its kind put in space to observe the sun—will be able to resolve solar features as small as 150 kilometers across and will have a vector magnetograph that determines the polarization of magnetic fields. An improved x-ray telescope will provide higher resolution images of flares and other phenomena than Yohkoh could manage and will measure temperatures exceeding 10 million kelvin—a first. And an extreme ultraviolet imaging spectrometer will observe solar plasma, helping relate the movement of hot gases in the corona to the underlying magnetic fields. Solar-B will provide round-the-clock observations for 8 months a year over a planned mission lifetime of 3 years.

Sun spotter. Solar-B promises the finest look yet at magnetic processes that produce flares and coronal mass ejections.

CREDIT: JAXA/ISAS

Although Solar-B's primary objective is to unravel basic solar processes, there could be practical payoffs as well. Davis says that NASA hopes to develop an ability to predict flares and coronal mass ejections before they occur—and even better, when they won't occur. The latter knowledge would allow the agency to designate "safe periods" of hours or days for astronauts to venture out on spacewalks. And that could take the sting out of a very nasty solar punch.

–DENNIS NORMILE

Interest in Conflicts

The influential officials who oversee conflict-of-interest policies for their institutions think that a little disclosure goes a long way. A survey of 45 senior U.S. researchers in the *Journal of Law, Medicine & Ethics* has found that although all believe conflicts should be disclosed to volunteers participating in clinical research, few thought that the details of those conflicts were worth sharing. "I do not really think that there is a lot of need for saying Company XYZ is paying me $6000 for every patient we enroll in this" if the money funds research, one of those surveyed explained. Thirty-four researchers believed the funding source should be disclosed, but many feared that given dollar amounts, research participants would overestimate the influence of the payment on the investigator's behavior. An earlier study by the researchers who did the survey, led by scientists at Johns Hopkins University, found that both healthy and chronically ill people rated disclosure more important as the risk of research rose. **–JENNIFER COUZIN**

Conferences to Get Less Perky

BEIJING—Members of the Chinese Academy of Sciences and the Chinese Academy of Engineering enjoy privileges including easy grant money, housing subsidies, and personal drivers. But organizers of the Xiangshan Science Conferences have decided to bar academy members from using their titles when registering for conferences or in proceedings publications. Held every 2 weeks throughout the year on topics as diverse as neurobiology and robotics, the meetings influence the government's research priorities. The new rules send a message that "every conferee is equal," says Xiangshan staffer Liu Yuchen.

The change "emphasizes that equality among scientists … determines the development of science," says Zhu Pengcheng, a molecular biologist at Harvard Medical School in Boston who attended a recent Xiangshan meeting in Beijing. **–YAN ZHAO**

Tumor Gene Troika

Three types of cancer—lung, brain, and ovarian—have been chosen for a pilot run of The Cancer Genome Atlas, a $1.5 billion plan to search for all mutations involved in cancer (*Science*, 8 September, p. 1370). The cancers were chosen because the tissue banks supplying them met ethical and scientific standards, say the National Institutes of Health's cancer and genome institutes, which are sponsoring the $100 million, 3-year pilot. **–JOCELYN KAISER**

INFECTIOUS DISEASE

Extensively Drug-Resistant TB Gets Foothold in South Africa

An outbreak of what's called "extensively drug-resistant tuberculosis," or XDR TB, in KwaZulu-Natal Province, South Africa, appears to be nearly twice as large as originally reported. At a meeting of international public health officials held in Johannesburg last week to discuss what were then 53 cases of the highly lethal tuberculosis at one health-care center, South African researchers reported that they now had identified a total of 102 cases at 28 hospitals. "It is extremely worrying, and WHO [the World Health Organization] is responding very proactively," says Paul Nunn, who coordinates the TB/HIV and Drug Resistance Unit for the Stop TB Department at WHO, one of the meeting's co-organizers. "XDR threatens the significant gains made in the last 15 years in TB control globally."

Widespread. New analyses have discovered XDR TB cases at 28 hospitals in KwaZulu-Natal.

The South African outbreak of XDR TB is the largest ever reported. WHO and the U.S. Centers for Disease Control and Prevention, another meeting co-organizer, first described XDR TB in the 24 March *Morbidity and Mortality Weekly Report* (*MMWR*). The researchers defined XDR TB as being resistant to the two widely used first-line drugs and three of the six main classes of second-line treatment. (Multidrug-resistant TB, by contrast, does not respond to first-line drugs.) At the time, the researchers had identified 347 XDR TB cases worldwide, and only one was in Africa. In the 53 cases in KwaZulu-Natal, first reported publicly in August at the international AIDS conference (*Science*, 25 August, p. 1030), the average time to death was 16 days after a sputum sample was taken. "This is about as fatal as you can get," says Nunn.

In every one of the 102 cases that has been checked, the patients have also been infected with HIV. TB is a leading killer of people with AIDS, and some evidence suggests that TB transmits more easily in HIV-infected people. TB also complicates treatment of HIV.

Resistance to TB drugs typically develops when people do not finish their full course of medication or receive drugs that have limited potency. Preliminary data suggest that many of the XDR TB patients are infected with the KZN strain that first surfaced in KwaZulu-Natal in 1995 as a major source of multidrug resistance. Says WHO epidemiologist Abigail Wright: "It's very worrying when you see dominant families [of *Mycobacterium tuberculosis*] becoming extensively resistant."

Wright, who co-authored the *MMWR* report, stresses that no one yet has a good handle on the global prevalence of XDR TB. Nunn notes that South Africa is more developed than many of its neighbors and has a better detection system. "The same kind of outbreaks in more isolated conditions might pertain," says Nunn. "What's going on in Zambia and Zimbabwe? We really need to know." **–JON COHEN**

SCIENTIFIC COMMUNITY

Campaign Heats Up for WHO Director-General

In what promises to be an unusually hard-fought and public race, 13 candidates are competing to be the next director-general of the World Health Organization (WHO). The surfeit of contenders means that the process will be even less predictable than usual, say observers, but early signs are that it also may be more open than previous campaigns.

In November, the WHO executive board will choose a successor to Director-General Jong Wook Lee, who died suddenly of a stroke in May, only 3 years into his 5-year term. After a flurry of last-minute nominations before the 5 September deadline, the list includes four candidates from Europe, three from the Middle East, three from Asia, one from Africa, and two from Latin America. Early front-runners include Mexican health minister Julio Frenk and two insiders: bird flu czar Margaret Chan of Hong Kong, WHO's assistant director-general for communicable diseases, and Shigeru Omi, the Japanese head of WHO's Western Pacific Division. Pascoal Mocumbi, former prime minister of Mozambique, and Bernard Kouchner of France, co-founder of Doctors Without Borders, may also gather strong support.

The campaign is already intense. Frenk has already launched a Web site outlining his goals and priorities. He told *Science* that his experience reforming Mexico's health system makes him the strongest candidate. "Being minister of health of a large developing country is probably the best hands-on training you can have," he said. Chan told journalists last week that she was confident she would win the nomination. Some WHO watchers speculate that Mocumbi will be a strong candidate among countries advocating for WHO's first African leader.

Such posturing is a healthy sign, says Christopher Murray of Harvard School of Public Health in Boston. WHO's selection process is frequently criticized for being too influenced by behind-the-scenes diplomatic deals. The Web sites and statements are aimed at the broader public health community instead of the politicians and diplomats, Murray says. "If it does influence the race, that's a very good thing," he says.

One of the key questions facing the next director is where the organization fits among the other new influences in global health, says international health expert Gerald Keusch of Boston University. "Can WHO play in the same sandbox with the Gates Foundation? It's not going to have a $60 billion endowment to work with, so it's got to have something on the intellectual, political, and ethical scene to contribute—and be willing to be a partner." **–GRETCHEN VOGEL**

With reporting by Jon Cohen, Martin Enserink, and Eliot Marshall.

INFLUENZA

Ground the Planes During a Flu Pandemic? Studies Disagree

By scouring mortality data from 121 cities across the United States, Harvard researchers have found footprints of 9/11 that they say should guide policy during an influenza pandemic. The decline in air travel in the months after the terrorist attacks delayed the annual flu season in the United States by almost 2 weeks, they conclude—a finding that suggests that a flu pandemic, too, could be slowed down, perhaps by months. But researchers who have studied the same question using computer models—and found closing down airports to be less useful—are skeptical.

The 2003 outbreak of SARS drove home the widely held belief that global mobility helps spread infections; indeed, it's almost a cliché among researchers to say that the most important disease vector today is the Boeing 747. But air-travel restriction won't help slow a flu pandemic much, three model studies concluded earlier this year—especially when compared to the judicious use of vaccines, antiviral drugs, isolation, and quarantine.

In a paper published in July in *Nature*, for instance, Neil Ferguson of Imperial College London and his colleagues tested how the United States and the United Kingdom might best mitigate a pandemic's ravages. They found that unless they are 99% effective, border controls and internal travel restrictions won't slow viral spread by more than 2 or 3 weeks. Ben Cooper and his colleagues at the U.K. Health Protection Agency, who modeled air travel around the world in a June paper in *PLoS Medicine*, also found limits "of surprisingly little value." The reason, says Ferguson, is that flu spreads extraordinarily rapidly.

But in the real world, the 27% reduction in international air-travel volume after 9/11 appears to have caused a 13-day delay in the 2001–02 influenza season—considerably more than the models would predict, say John Brownstein and Kenneth Mandl of Children's Hospital Boston and Harvard Medical School in a paper released on 11 September by *PLoS Medicine*. Analyzing data from 1996 to 2005, they also found a correlation between higher air-travel volumes in the fall and a slightly earlier flu season. Extrapolations suggest that a full-blown travel ban, as opposed to the post-9/11 slump, might delay a flu pandemic by as much as 2 months, says Brownstein—precious time to activate countermeasures and work on a vaccine.

The modelers aren't convinced, however. Ferguson says there is no proof that the relation between travel and timing of the flu season is causal, and he questions the team's use of a complex statistical measure to determine the timing of the peak. Although the study is "very nice," the 9/11 effect "is an *n* of 1; it's intriguing, but you can't draw any conclusions," says Ira Longini of the University of Washington, Seattle, who co-authored a paper in the *Proceedings of the National Academy of Sciences* in April that also concluded that travel bans had little value.

Brownstein suspects that some of the criticism may stem from the contradiction between his data and the models. "They are making assumptions about the relationship between air travel and the spread of influenza," he says. "But this is empirical evidence."

Although some countries' pandemic preparedness plans list travel bans as an option, Ferguson says most governments that have studied the idea seriously have rejected it. The World Health Organization's (WHO's) Global Influenza Preparedness Plan does not recommend travel bans because enforcement "is considered impractical," but a footnote adds that they "could be considered as an emergency measure to avert or delay a pandemic." WHO spokesperson Gregory Hartl says the new study is "very interesting" and "opens up the debate again."

–MARTIN ENSERINK

CREDIT: JASON WISE/AP PHOTO

Delayed. The decline in air travel after 9/11 delayed the U.S. flu season by almost 2 weeks, a new study says.

NASA Science Chief Calls It Quits

One year after taking the job, NASA's science chief last week told her staff she will resign this spring. A biologist and former astronaut, Mary Cleave oversees the agency's space, planetary, and earth sciences research—programs in turmoil over budget overrun pressures. Cleave, who was unavailable for comment, alienated many scientists during her brief tenure by backing the elimination of a host of projects and reduced research funding. Meanwhile, NASA Administrator Michael Griffin told key senators in a letter that a plan to eliminate space-station research funding was simply "intended to prepare for potential budget reductions." The senators had complained that cutting research made no sense given the investment in building the orbiting lab.

–ANDREW LAWLER

Cancer Watch at Ground Zero

Public health researchers in New York will begin a long-term surveillance program next month of workers exposed to dust during rescue and recovery efforts after the 2001 World Trade Center attacks. Some 40,000 workers combed through the rubble, breathing dust laced with toxics such as dioxin or asbestos. According to a paper published in *Environmental Health Perspectives* last week, 61% of 9442 workers surveyed have developed acute respiratory problems such as labored breathing.

The new effort will receive $26 million in federal funds until 2009 and track some 30,000 workers for long-term lung problems as well as cancers. Society owes answers to the "volunteers who leapt into the fray," says co-leader Philip Landrigan of Mount Sinai Medical Center in New York City, one of five clinical centers on the effort. **–ERIK STOKSTAD**

Academic Demotion

MOSCOW—The Russian Academy of Sciences could be stripped of authority to select a president and control its own finances if proposed changes in Russia's law on science take effect. A closed Cabinet meeting last week endorsed legal changes that could clear parliament in a matter of weeks, observers say. Critics of the move say that the new scheme will give the government new authority to set the nation's basic research agenda and that the academy will be turned into a club. Many scientists fear that the government will sell off the academy's valuable property assets. Putting a good face on the situation, academy spokesperson Irina Presnyakova said that the pending changes will bring the academy prestige and fiscal certitude.

–BRYON MACWILLIAMS

GENOMICS

Poplar Tree Sequence Yields Genome Double Take

Black cottonwoods are the lab rats of the tree world. It's relatively easy to add or knock out genes, and like other members of the poplar genus, they grow quickly enough that researchers can check the outcome of some experiments in less than a year. Foresters love poplars too: Their fast growth rate makes them a good source of fiber for paper, lumber, plywood—and a possible source of biofuels. All these reasons motivated more than 100 researchers to sequence the tree's genome.

Unveiled. The genome of black cottonwood should provide insights into how to improve commercial varieties of it and other poplars.

On page 1596, the team, led by Gerald Tuskan of Oak Ridge National Laboratory (ORNL) in Tennessee and Daniel Rokhsar of the Joint Genome Institute (JGI) in Walnut Creek, California, describes its first analysis of the more than 45,000 likely genes in black cottonwoods (*Populus trichocarpa*). The group has begun to sketch out the evolutionary history of *Populus*, finding, for example, that a doubling of the genome about 65 million years ago freed up many genes to acquire functions important for trees, such as wood formation.

Cottonwood is the first tree and the third plant genome to be sequenced, coming after the herbaceous annual *Arabidopsis* and rice. The bulk of the sequencing was done at JGI and ORNL, with researchers around the world contributing genetic markers—such as 324,000 expressed sequence tags—which aided in the search for genes. Four groups then independently trained computer algorithms to search for coding sequences, and they all agreed on 45,555 likely nuclear genes.

By comparing the new sequence to that of *Arabidopsis* and sections from other plants, the team determined that the ancestral genome of poplars had been duplicated at least three times: first, at the base of all angiosperms, then about 100 million to 120 million years ago, and most recently 60 million to 65 million years ago. "The genome sequence shows this incredibly complicated evolution, full of diversity," says Gail Taylor of the University of Southampton, U.K., who is not an author. "It's like an Aladdin's cave." Similar doublings also occurred in rice and *Arabidopsis*, so they appear to be widespread among plants, Tuskan says.

Genome duplications offer new grist for natural selection because a second copy of a gene can evolve a new function. Although the *Populus* genome has lost some of its extra copies, it retained others that might be particularly useful for fending off pathogens, synthesizing lignin and cellulose, transporting metabolites, and bringing about programmed cell death (which may be important for seasonal growth and autumnal senescence).

The next step is to figure out what more of the genes do—half have no known function—by creating mutants with genes that are under- or overexpressed. "There will be thousands of new functions that were not known or fully appreciated in other species," predicts Steven Strauss of Oregon State University in Corvallis. This will help lead to the development of new varieties of poplars that might have longer growing seasons or pack on more biomass. It could also have payoffs for ecologists, clarifying the keystone role of poplars in riparian and other ecosystems. "There's a whole new area of science opening up," Taylor says.

–ERIK STOKSTAD

ASTROPHYSICS

Pulsars' Gyrations Confirm Einstein's Theory

Comparing a pair of massive stellar clocks known as pulsars, an international team of astronomers has put Einstein's theory of gravity to its toughest test yet. Published online by *Science* this week (www.sciencemag.org/cgi/content/abstract/1132305), the results show that the theory of general relativity (GR) is accurate to within 0.05%, even in the ultrastrong gravity of a pulsar, a spinning neutron star measuring roughly 20 kilometers wide but weighing more than the sun. Further observations could enable researchers to peek into the structure of neutron stars, the hearts of which may contain a bizarre form of nuclear matter that flows without resistance.

Most physicists agree that GR cannot be the last word on gravity because it clashes with quantum mechanics. The new observation limits the possibilities for tinkering with GR, says Joseph Taylor, a physicist at Princeton University. "They're tightening the constraints on any alternative to Einstein's theory," he says.

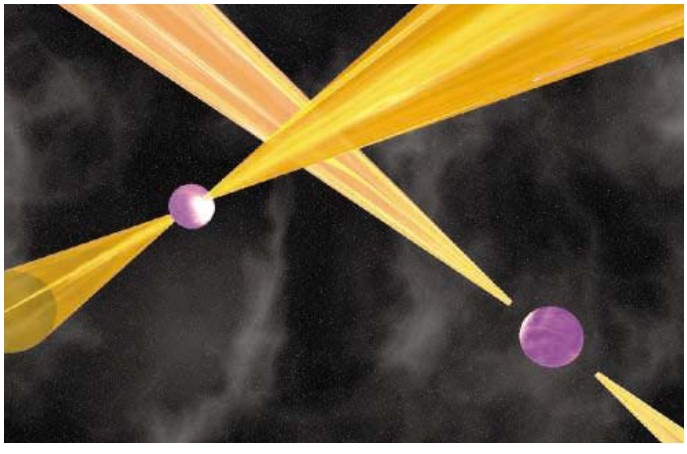

Timepieces. Taking the pulses of two pulsars as they whiz around each other, astronomers have determined their orbit and tested general relativity.

According to GR, matter and energy warp space and time, making free-falling objects travel along curved paths and producing the effects ▶

CREDITS (TOP TO BOTTOM): MICHAEL BOYS/CORBIS; MICHAEL KRAMER/JODRELL BANK OBSERVATORY, UNIVERSITY OF MANCHESTER

we call gravity. Einstein specified a particular mathematical connection between the density of matter and energy and the curving of spacetime. To test the theory, a team led by astronomer Michael Kramer of the Jodrell Bank Observatory in Macclesfield, U.K., studied a unique astronomical object: a pair of pulsars 2000 light-years away that orbit each other at a distance of just a million kilometers (*Science*, 9 January 2004, p. 153).

Spinning like a lighthouse beacon, a pulsar beams radio waves into space, creating a pulsing signal that's nearly as steady as an atomic clock. If a pulsar orbits another object, the rate of pulsing rises and falls repeatedly as the pulsar speeds alternately toward and then away from Earth. By tracking the variations in the rates of both pulsars from April 2003 to January 2006, the researchers deduced the details of their orbit, such as the length of its elliptical shape, the rate at which the ellipse rotates, and how the orbit is tilted relative to the line from the pulsar to Earth.

They quantified the details in several so-called post-Keplerian parameters and found that all the parameters were consistent with one another and with GR to within the uncertainties. "General relativity does a perfect job of describing what we know of the system so far," says Ingrid Stairs, an astronomer and team member from the University of British Columbia in Vancouver, Canada.

Taylor and others had tested GR by studying single pulsars orbiting other objects. But with just one pulsar, researchers cannot directly determine certain details, such as the relative masses of the orbiting objects, says Taylor, who won the Nobel Prize in physics in 1993. Moreover, the pulsars in the double pulsar are moving faster than those in the other systems, he says, which accentuates relativistic effects.

As well as testing GR, further observations might reveal a subtle interplay between the rate at which the pulsars orbit and the rate at which each spins on its axis. That would give scientists a direct measurement of the distribution of mass within a neutron star and a first real glimpse into its mysterious insides, says Thibault Damour, a theoretical physicist at the Institut des Hautes Études Scientifiques in Bures-sur-Yvette, France. "This is not for today," he says, "but it shows that high-accuracy measurements might open a new window on nuclear physics." It might take more than a decade to see the effect, but all say it will be worth the wait.

–ADRIAN CHO

CREDIT: PHILIPPE PLAILLY/EURELIOS, RECONSTRUCTION ATELIER DAYNES

PALEOANTHROPOLOGY

Mild Climate, Lack of Moderns Let Last Neandertals Linger in Gibraltar

One of the few things researchers agree on regarding the Neandertals is that the story of these European hominids ends in extinction. But just when the last Neandertal died, and whether modern humans or a changing climate sealed their fate, are matters of lively debate (*Science*, 14 September 2001, p. 1980). Now a team working at Gibraltar, at the southern tip of Spain, reports radiocarbon dates suggesting that some Neandertals survived thousands of years longer than previously thought, taking refuge in southern Europe where the climate and environment were favorable, and where moderns were still fairly thin on the ground. "While pioneer modern humans were staking tenuous footholds" in the region, says team leader Clive Finlayson, a biologist at the Gibraltar Museum, the last Neandertals "were hanging on."

The good life. Did Neandertals find refuge from a harsh climate and modern humans along Gibraltar's lush coast?

Anthropologist Eric Delson of the City University of New York says that "the dates appear fully supported," and that the notion of Neandertal refugia is "quite reasonable." But some archaeologists believe contamination from younger material might have skewed the dates. "I have considerable reservations," says archaeologist Paul Mellars of the University of Cambridge in the United Kingdom.

The new dates come from Gorham's Cave in Gibraltar, where Neandertals left their characteristic Mousterian stone tools, although no fossils have been found. The international team obtained 22 radiocarbon dates from small pieces of charcoal in Mousterian layers dug between 1999 and 2005. The dates, reported online this week in *Nature*, range from 23,000 to 33,000 with a cluster at about 28,000 raw "radiocarbon years"; these must be calibrated to provide true calendar years. Although the calendar age is probably at least several thousand years older than the radiocarbon years, the calibration is uncertain (see p. 1560), and the team has stuck to uncalibrated dates. Reconstructions suggest that Gibraltar was surrounded by coastal wetlands and woodlands and blessed with mild temperatures at this time, Finlayson says, and the Neandertals enjoyed a rich cornucopia of resources including shrubs, birds, reptiles, and mollusks.

The Gibraltar dates appear to be the youngest accepted for a Neandertal site, although sites in Spain and Portugal have been dated as late as 32,000 radiocarbon years ago. But the Gibraltar Neandertals were not entirely alone: Although there are very few modern human sites in the region older than 30,000 years, one site about 100 kilometers east at Bajondillo, Spain, has been dated to about 32,000 uncalibrated years ago. The team concludes that Neandertals did not rapidly disappear as moderns advanced but rather co-existed with them in a "mosaic" of separate, low-density populations over thousands of years.

Mellars counters that many of the new dates actually cluster around 30,000 to 31,500 years ago, and the later ones could be contaminated. And archaeologist João Zilhão of the University of Bristol in the U.K. dismisses the idea that Neandertals and moderns lived near each other but had only limited contact. "This really stretches the bounds of credulity," Zilhao says.

But the Gibraltar Neandertals used only Mousterian technology rather than copying some modern techniques as late Neandertals did elsewhere in Europe, notes Katerina Harvati of the Max Planck Institute for Evolutionary Anthropology in Leipzig, Germany. In the end, Harvati says, the Neandertal groups who stuck to their own traditions might have had the better strategy, and survived longer.

–MICHAEL BALTER

BIBLIOGRAPHY CENTRAL

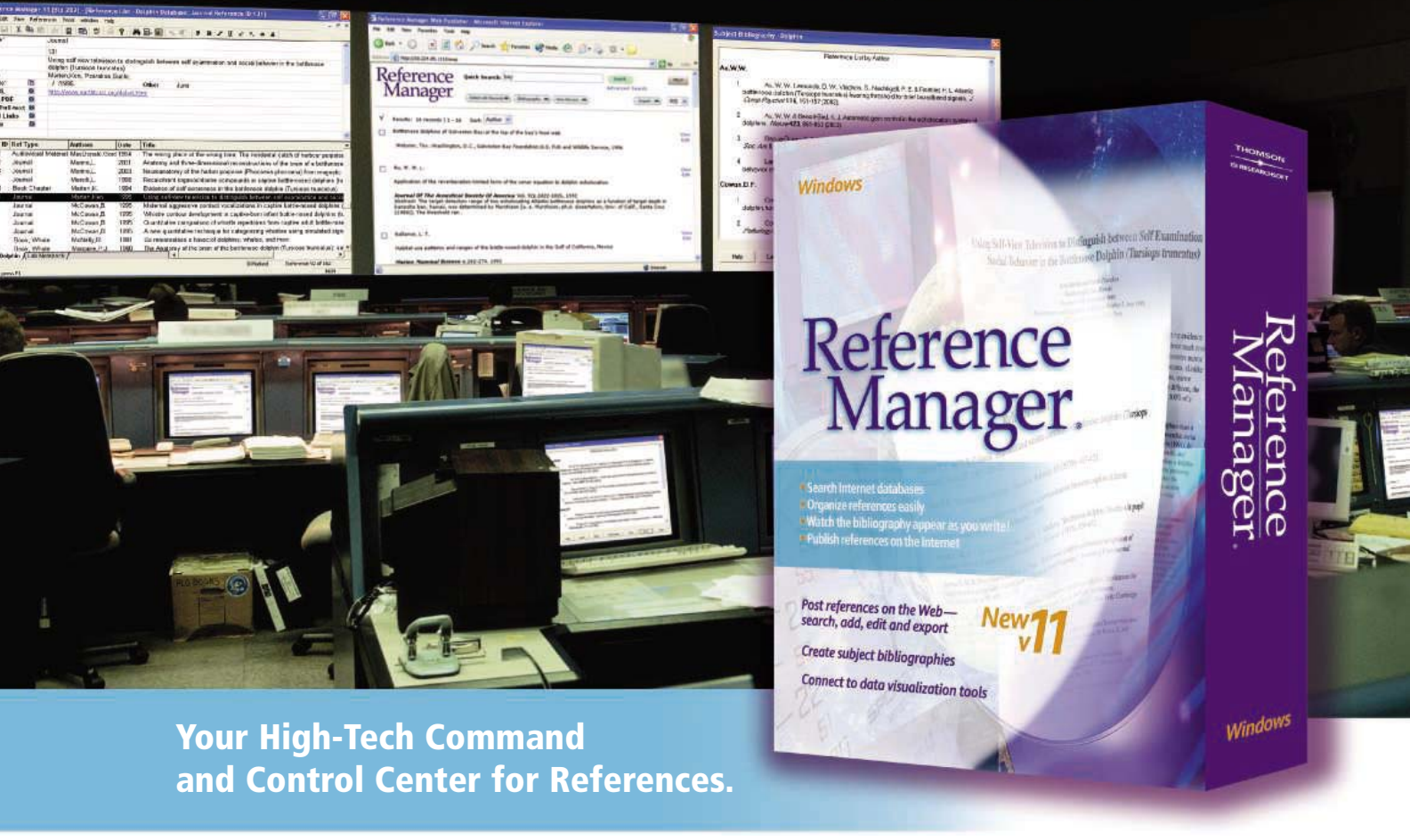

Your High-Tech Command and Control Center for References.

Introducing Reference Manager 11—a powerful upgrade to the bibliographic software that streamlines research, writing and publishing.

Reference Manager has served corporate, government and academic researchers worldwide for over 20 years. And now version 11 delivers new ways to share and view your reference collections: Post your databases to the Web. Collaborate with colleagues over a network. Link to full text pdf files.

These are just some of the powerful features that await you. Reference Manager is your command and control center for all things reference related.

What's new in v11:

- Publish Reference Manager databases to the Web or intranet
- Create subject bibliographies instantly
- Access new and updated content files at www.refman.com
- Share traveling libraries with colleagues
- Connect to data visualization tools

Put innovation into action. Order or upgrade today.
Available for Windows in a single-user and network edition.
Phone: 800-722-1227 • 760-438-5526 • info@isiresearchsoft.com

Download a Free Demo Today
www.refman.com

THOMSON
ISI RESEARCHSOFT

GENOMICS

Microarray Data Reproduced, But Some Concerns Remain

Over the past several years, debate has raged in the microarray community over how reliably these microchip-sized tools measure gene expression. Now, in a clutch of six papers published online last week by *Nature Biotechnology*, a consortium of 137 researchers from 51 different organizations concludes that the technology works better than expected and that results can usually be reproduced across labs. But some caution that the findings, although a technical feat, do not mark the end of microarray worries, nor do they necessarily speed the entry of the devices into patient care.

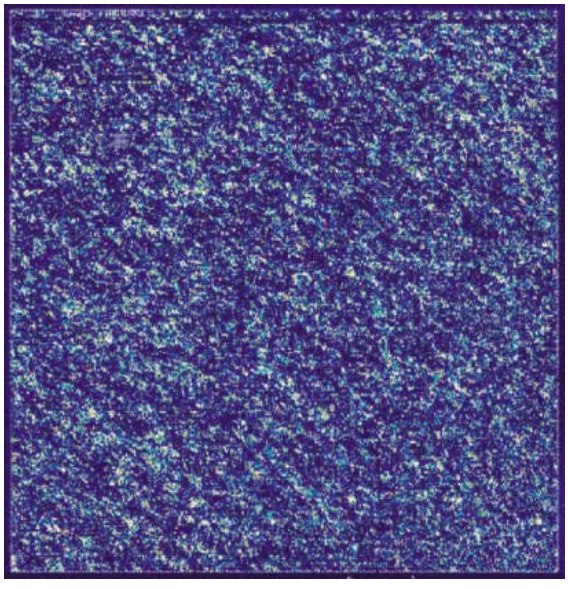

Replicable. Certain gene-expression patterns, such as those shown here, can be reproduced across labs more reliably than thought.

The MicroArray Quality Control (MAQC) project was initiated in 2005 by the U.S. Food and Drug Administration (FDA), which has a keen interest in seeing the technology aid drug development. If reliable, microarrays could be used for everything from testing a drug's effects to identifying patients most likely to benefit from a particular treatment. The MAQC venture came about after a controversial 2003 paper by Margaret Cam of the National Institute of Diabetes and Digestive and Kidney Diseases in Bethesda, Maryland. Cam worked with pancreatic cells and reported that three different microarray platforms revealed similar expression levels for only four of 185 genes tested (*Science*, 22 October 2004, p. 630). The inconsistent results likely stemmed, at least in part, from some microarray probes responding to the RNA of untargeted genes.

The MAQC project was far more expansive. It put 20 microarray products and three alternative technologies through more than 1300 tests at different labs. The project investigator repeatedly tested expression levels of more than 12,000 genes using messenger RNA (mRNA) samples drawn from a composite of human tumor cell lines and from the human brain. The expression results overlapped—meaning that a gene's expression was recorded the same way by each microarray—from 70% of the time to more than 90%.

"This can bring a complete change in mindset in analyzing microarray data," says Leming Shi, a computational chemist with FDA, who led the consortium. He attributes many of the problems in previous studies to faulty statistics or unfamiliarity with the technology.

Others say the concern about microarrays isn't over yet. "I would counsel caution" in interpreting these results, says Marc Salit, a chemist at the National Institute of Standards and Technology, who consulted with the authors on the project. He notes that the RNA samples MAQC compared are far more distinct from one another than are biological samples commonly compared in microarray studies—such as normal and cancerous cells from the same organ. Salit says this level of agreement would be unlikely in such cases, "because you'd be looking at more subtle differences." Still, he notes that scientists can now test their own microarray technologies against the MAQC samples and gauge their reliability.

"Here's the industrial standard," agrees Hanlee Ji, an oncologist and clinical geneticist at Stanford University in Palo Alto, California, who was part of the MAQC consortium. "Is your performance comparable to theirs, or is it so askew that that makes you concerned about your data?" FDA, says Ji, could hold microarray data supplied in drug applications to this new standard.

But microarray technology still has a way to go before it can be broadly used to predict cancer prognosis or diagnose disease. MAQC project members will gather in Arkansas on 21 September to determine what criteria should be used when applying microarray data to disease, and which illnesses are worth focusing on first. **–JENNIFER COUZIN**

CREDIT: COURTESY OF AFFYMETRIX

U.S. GRADUATE EDUCATION

Foreign Enrollment Rebounds After 3-Year Slump

Foreign-born students have rediscovered U.S. graduate schools. After a 3-year decline, the number of foreign students starting graduate studies in the United States rose 4% last year. And, continuing the upswing, the number of international graduate applications to U.S. universities shot up 12% this year, suggesting that the country may be regaining its positive image among foreign students.

Observers credit the rebound, documented in a 643-institution survey released this week by the Council of Graduate Schools (CGS), to speedier processing of visa applications and increased international outreach. "The U.S. government has clearly made efforts" to modify some of the restrictive visa policies that were put in place after the 2001 terrorist attacks, says CGS President Debra Stewart. "The visa situation is still not perfect, but it is much better than it was in 2004." A majority of foreign-born graduate students pursue degrees in the sciences and engineering.

Iowa State University (ISU) in Ames last year began paying the $100 fee charged every foreign student to register in the U.S. government's Student and Exchange Visitor Information System. "We're seeing some rewards," says admissions officer Patricia Parker, citing an increase of 400 international graduate applications this year. The U.S. State Department has helped too, Parker says, by sending embassy officials to local universities to explain visa application procedures.

Stewart says the rapidly expanding pool of college graduates in countries such as India and China should be a boon to U.S. graduate programs. But she warns her colleagues against complacency: "Given the increased global competition for talent, the U.S. government must turn its visa policy from an impediment against foreign students to an instrument of recruitment."

–YUDHIJIT BHATTACHARJEE

In a heroic and sometimes contentious effort, researchers push to extend accurate radiocarbon dating back to 50,000 years ago

Radiocarbon Dating's Final Frontier

The 1994 discovery of France's Grotte Chauvet revolutionized ideas about symbolic expression in early modern humans. The breathtaking drawings of horses, lions, and bears that adorned the cave walls were executed with perspective and shading and rivaled the virtuosity of all other known cave art. But when were those drawings made? Early radiocarbon dates suggested 32,000 years ago, right after a major cold spell hit Europe. This implied that modern humans blossomed under frigid conditions while their Neandertal cousins were going extinct. But improved radiocarbon dating now suggests that the oldest paintings at Chauvet could be at least 36,000 years old. That's smack in the middle of a period of relative warmth and challenges speculation about modern humans' adaptability to a cold climate.

Getting the dating right is "crucial," says archaeologist Clive Gamble of the University of London's Royal Holloway campus. "It is not just a case of winning a trophy by being the oldest. The model up to now has been that modern humans could go anywhere and do anything, and … it didn't matter what the climate was." Thanks to more accurate dating, says Gamble, "that model is now showing signs of cracking."

Indeed, as radiocarbon experts revise their estimates, all researchers working in the eventful period from about 50,000 to 25,000 years ago are facing an across-the-board realignment of dates. That's when both Neandertals and modern humans lived in Europe and when wildly fluctuating temperatures culminated in the spread of glaciers across much of the Northern Hemisphere.

Push 'em back. These fighting rhinos in France's Grotte Chauvet could be more than 4000 years older than originally thought.

There's no question about the basic principles of the radiocarbon method: Plants and animals absorb trace amounts of radioactive carbon-14 (^{14}C) from CO_2 in the atmosphere while alive but cease to do so when they die. So the steady decay of ^{14}C in their tissues ticks away over the years. But the amount of ^{14}C produced in the atmosphere varies with the sun's solar activity and fluctuations in Earth's magnetic field. This means that the radiocarbon clock can race ahead or seemingly stop for up to 5 centuries. As a result, raw radiocarbon dates sometimes diverge from real calendar years by hundreds or even thousands of years. Thus researchers must calibrate the clock to account for these fluctuations, and that can be a challenge. For example, the start of the Holocene, the period when the last ice age ended, is usually dated to 10,000 uncalibrated radiocarbon years ago. But the radiocarbon clock stopped for several hundred years right at that point, so that the start of the Holocene—when agriculture began—can't be pinned down any more pre-

PHOTO COLLAGE: K. BUCKHEIT KRAUSE/*SCIENCE* (IMAGES: JUPITER IMAGES; GETTY IMAGES; DK LIMITED/CORBIS); (BOTTOM) JEAN CLOTTES

By land and by sea. Corals and foraminifers from the oceans, and trees from the land, are used to craft the radiocarbon calibration curve.

cisely than somewhere between 11,200 and 11,800 years ago (see graph). Because the best estimate of the calibration keeps changing, many scientists avoid reporting calendar years and simply cite "radiocarbon years" as a universal measuring stick when announcing new finds (see News of the Week story by Balter).

Yet recent progress in radiocarbon dating may finally give researchers the accuracy they seek. In 2004, after 25 years of painstaking labor, an international group of radiocarbon experts extended the calibration curve back to 26,000 years by using data from tree rings, corals, lake sediments, ice cores, and other sources to create a detailed record of ^{14}C variations over the millennia. The final frontier, which the group hopes to reach by the end of this decade, will be to push calibration to the 50,000-year mark; beyond that, there is too little residual ^{14}C to measure precisely.

Refinement of existing data, plus some promising new data sources, including ancient trees from the swamps of New Zealand, may help close the final gap. "These are very exciting times," says nuclear physicist Johannes van der Plicht, director of the radiocarbon laboratory at the University of Gröningen in the Netherlands. He adds that a final calibration curve "will answer so many questions in archaeology," in large part because the 50,000-year limit coincides with a major migration of modern humans from Africa to Europe and Asia.

Earth scientists, many of whom use radiocarbon dating to study the movement of glaciers and ocean currents, are equally enthusiastic, in part because of the unprecedented climate variability that occurred between 30,000 and 50,000 years ago. Those who study sea-level fluctuations during and after the last ice age—data used to model patterns of global warming—rely "almost entirely" on radiocarbon dating, adds geophysicist Richard Peltier of the University of Toronto in Canada.

Yet the eagerly awaited calibration is complicated by dissent in the ranks. One U.S. scientist has bypassed the international working group and published his own calibration curve, to the annoyance of many colleagues, while a British archaeologist is using provisional calibration data—prematurely, in the view of some radiocarbon experts—as evidence that *Homo sapiens* spread across Europe more rapidly than previously thought. Both researchers argue that science can't wait for an international agreed-upon calibration curve. The question at issue, says archaeologist Sturt Manning of Cornell University, is "who actually owns time": the experts working to calibrate radiocarbon, or the research community at large.

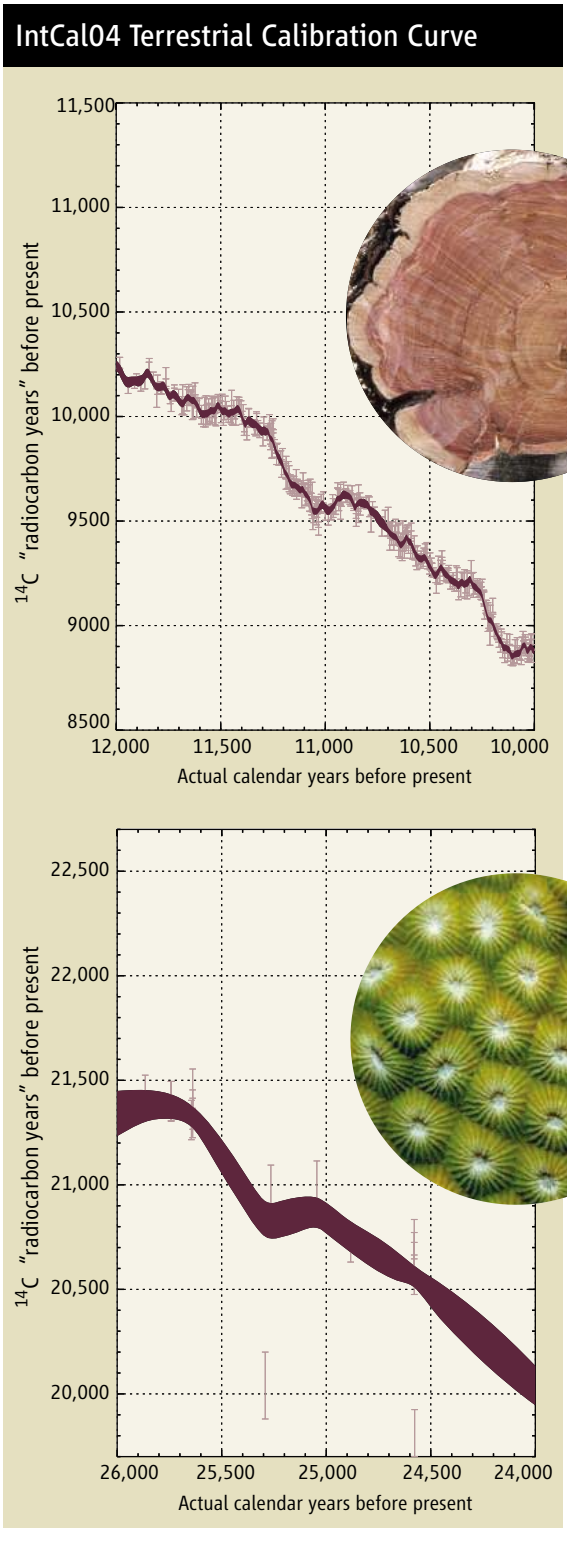

Ribbons of time. The thickness of the curves shows that calibration of very old dates, based on deep-sea corals (*bottom graph*), is less precise than younger dates based on tree rings (*top*).

CREDITS: ADAPTED FROM P. J. REIMER *ET AL.*, *RADIOCARBON* **46**, 3 (2004); (INSETS, TOP TO BOTTOM) AEGEAN DENDROCHRONOLOGY PROJECT, CORNELL UNIVERSITY; JEAN JAUBERT

Science from the sewer

The radiocarbon revolution that gave such a huge boost to archaeology and other fields had somewhat inauspicious origins: the sewers of Baltimore, Maryland. In 1947, chemist Willard Libby and his colleagues demonstrated that methane gas produced by Baltimore's Patapsco Sewage Plant contained trace amounts of radioactive ^{14}C, thus proving that living organisms harbored the isotope (*Science*, 30 May 1947, p. 576). On the other hand, methane from much older sources, such as petroleum deposits millions of years old, did not contain ^{14}C. From that point on, as Libby put it in his 1960 Nobel Lecture, "we [were] in the radiocarbon-dating business."

The revolution's early days were heady times. Libby wowed archaeologists when he accurately dated a number of samples whose ages were already known, including the 2750 B.C.E. coffin of the Egyptian pharaoh Zoser (*Science*, 23 December 1949, p. 678). Most archaeologists, who had previously relied on relative dating methods based on pottery styles, inscriptions, and guesswork, were thrilled to finally have a method for absolute dating, although a few attacked the method when it contradicted their pet theories.

Some other dating methods, including thermoluminescence and uranium-series dating, overlap with the period covered by radiocarbon. But these techniques cannot be applied to bones, seeds, and other organic materials found in abundance on most archaeological sites. Yet as early as 1960, when Libby was

awarded the Nobel Prize for his work, dating experts realized that past fluctuations in ^{14}C levels were leading to erroneous and inconsistent results. Thus, although Libby had good luck with Zoser's coffin, radiocarbon dating of some earlier Egyptian artifacts contradicted dates from reliable historical sources. As the number of such troublesome discrepancies rose, it became clear that a calibration curve to correct for ^{14}C variations, based on an independent data source, would be needed.

Fortunately, just such a source was at hand: the sequences of annual tree rings, which dendrochronologists had been accumulating for decades. Long-lived trees such as the California bristlecone pine and European oaks and pines, which are often preserved in peat bogs, provide sections of ring width patterns that dendrochronologists use as bar codes to line up sequences of increasingly greater ages. By radiocarbon dating the rings, researchers began to construct calibration curves that could convert raw radiocarbon dates into real calendar years going back thousands of years.

Since then, the story has been one of continuously improving accuracy, as researchers have worked to pin down the curve. Starting in the late 1970s, radiocarbon labs began using accelerator mass spectrometry to directly count ^{14}C atoms rather than estimating them indirectly; this allowed tiny samples such as small seeds and grains to be dated with much greater precision. And the early 1980s saw "a movement to have a consistent calibration," says Timothy Jull, head of the radiocarbon lab at the University of Arizona in Tucson and editor of the flagship journal *Radiocarbon*. An international group has since met regularly on the issue, and new curves have been published approximately every 6 years.

The most recent calibrations, unveiled in *Radiocarbon* in 2004, consist of three different curves: one to date marine samples and one each for terrestrial samples in the northern and southern hemispheres. The effort involved in each is tremendous. For example, IntCal04 is based in part on the overlapping alignment of many thousands of tree-ring segments from the Northern Hemisphere dating back to 12,400 years ago. "This is a phenomenal achievement," says Richard Fairbanks, an isotope chemist at Columbia University's Lamont-Doherty Earth Observatory in Palisades, New York, and a former member of the IntCal04 group.

Beyond the limits of the dendrochronology record, however, radiocarbon experts have had to rely on other, considerably less precise sources of data. Between 12,400 and 26,000 years ago, the IntCal04 curve is based on two types of marine deposits: foraminifers (single-celled organisms that secrete calcium carbonate) from the Cariaco Basin of northern Venezuela up to 14,700 years ago (*Science*, 9 January 2004, p. 202), and several fossil coral records, including samples collected by Fairbanks and colleagues from the Atlantic and Pacific oceans, that cover this entire period.

The new curve also introduces statistical methods to reduce uncertainties. Researchers applied a complex probabilistic approach called Bayesian statistics to make educated estimates of what the calibration curve should look like. When each data point was weighted according to how certain researchers were about it, "a more robust estimate of the curve resulted," says Caitlin Buck, an archaeological statistician at the University of Sheffield in the U.K. and member of the IntCal group. Statistics can also improve the dates at specific sites, as in the case of the volcanic eruption of the Greek island of Thera, which destroyed a Minoan town and was recently dated to about 1600 B.C.E.—at least 100 years earlier than other estimates (*Science*, 28 April, p. 508).

The field's progress can be viewed graphically, points out Cornell's Manning. The calibration curve is actually a ribbon rather than a line (see graphs, p. 1561), in which the width of the ribbon represents the remaining uncertainties in translating radiocarbon dates to calendar years. "If you plot all the calibration curves over the last 20 years, you will find that the ribbon is getting much narrower," Manning says.

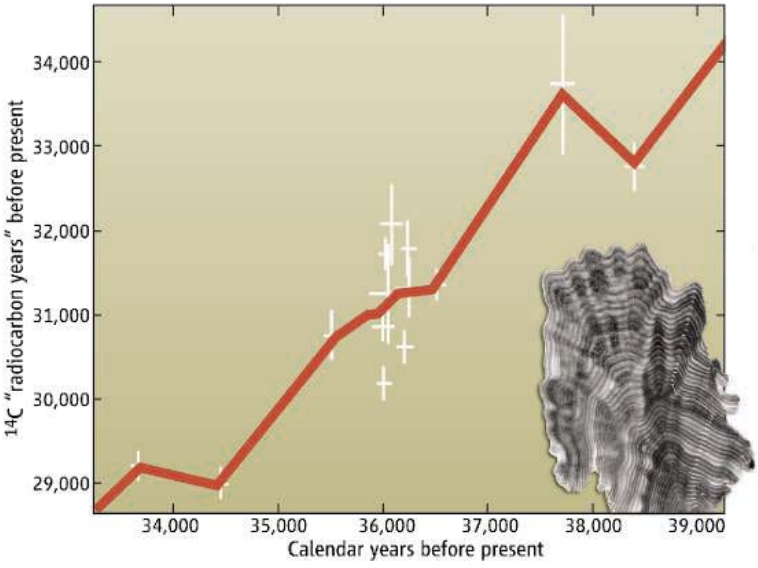

Going it alone. Richard Fairbanks's curve, based on corals (*inset*), extends the radiocarbon calibration to critical periods in human evolution.

All the way back?

Encouraged by their recent successes, radiocarbon researchers now have their eyes on the bigger prize of the 50,000-year limit. Indeed, when the IntCal group began work on the 2004 curve, it had high hopes of extending it back to this final barrier. Yet it was not to be. Although the marine data sets were reasonably consistent with each other up to 26,000 years ago, after that they began to scatter and diverge, in some cases by up to several millennia. Geochronologist Paula Reimer of Queen's University in Belfast, Northern Ireland, who coordinates the working group, says that the differences—among the raw data as well as among the researchers—were just too great: "We had four or five people, all of whom thought their records were right." So the group settled for publishing in *Radiocarbon* a comparison of the data sets earlier than 26,000 years, which they ironically called "NotCal"—meaning, Reimer and other members say, that it was *not* intended to be used as a calibration curve.

But archaeologist Paul Mellars of the University of Cambridge in the U.K. used the published data to essentially do just that. Mellars was eager to get the most accurate dates for possibly contemporaneous Neandertal and modern human sites in Europe. So he used the midpoint of the differing "NotCal" curves to approximately calibrate the radiocarbon ages of 19 hominid sites ranging from Israel in the East to Spain in the West. Using this best-guess method, Mellars found that modern humans had not only spread across Europe faster than previously thought, but that they had overlapped with Neandertals during a shorter interval: only about 6000 years rather than 10,000 years in Europe as a whole, and as little as 1000 years in some parts of the continent. Mellars concluded in the 23 February 2006 issue of *Nature* that Neandertals must

CREDITS: ADAPTED FROM RICHARD FAIRBANKS/LAMONT-DOHERTY EARTH OBSERVATORY; (INSET) KEVIN HELMLE/NATIONAL CORAL REEF INSTITUTE/NSUOC

have "succumbed much more rapidly to competition" from modern humans than many had assumed.

But Reimer and others say Mellars should not have used the NotCal data as he did. "It is dangerous to draw too fine conclusions using these data sets," says Reimer, because they have not been finalized and the divergences between them have yet to be reconciled. Other researchers have started asking van der Plicht whether they can use the "Mellars curve" for calibration. "This is a bad thing," says van der Plicht.

Mellars insists that archaeologists can't wait for a final calibration curve. "Are we all really expected to keep studies of modern human origins on hold for the next 5 years, until they decide they've finally got the calibration act together?" he asks. The working group, he argues, "has hijacked the term 'calibration' to mean an absolutely agreed, rubber stamped, legalistic, signed, sealed, and delivered curve." And even when the experts agree on a curve, Mellars says, it will not be "final and absolute" but "simply the best estimate from the data at the time."

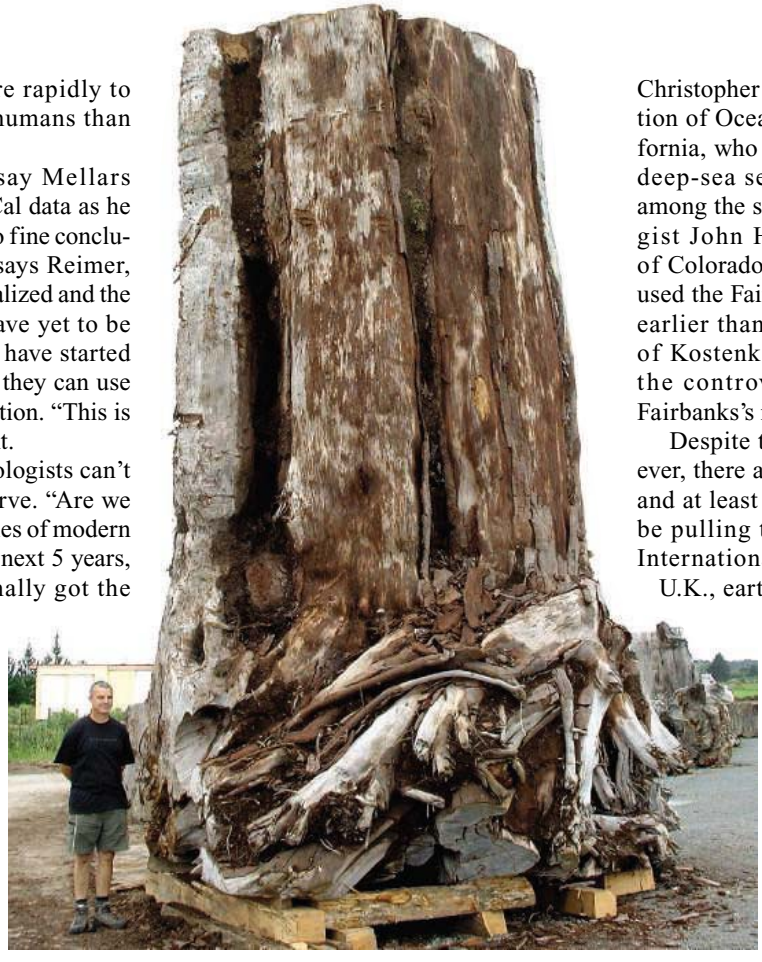

Tall order. Researchers hope ancient kauri trees buried in New Zealand swamps may extend tree-ring records back to at least 50,000 years ago.

CREDIT: CHRIS TURNEY

Fairbanks is equally impatient. Last year, he and his co-workers decided to strike out on their own rather than wait for the consensus curve. In the September 2005 issue of *Quaternary Science Reviews* (*QSR*), the team published its own version of a calibration curve spanning the entire period from 50,000 years ago to today, based on its dating of fossil corals from the Atlantic and Pacific oceans. The team dated the corals using both radiocarbon and uranium-thorium dating. And the authors made it clear that they intended their curve to be used as a "stand-alone" radiocarbon calibration, arguing that their screening criteria for coral data were more rigorous than those of other coral data sets as well as the Cariaco Basin foraminifers.

The more than 20 members of the IntCal04 working group, however, did not take this affront lying down. In the April 2006 issue of *QSR*, they contended in a letter that the Fairbanks paper was "extremely misleading" about the efforts of other groups and argued that stand-alone curves would lead to "confusion" among archaeologists and other researchers who had to use them. "The question is whether we maintain a common calibration curve or have different calibrations, as we did in the past," says Jull. And Reimer maintains that the Fairbanks curve does not sufficiently take into account uncertainties from using a marine data set to estimate a terrestrial curve, because the oceans contain less ^{14}C than the atmosphere and researchers must try to correct for the difference.

Fairbanks, however, defends his decision to go it alone. "There is a critical need to have at least the skeleton of a precise and accurate radiocarbon calibration curve spanning the useful limits of radiocarbon dating now," he says. "No international commission will stop scientific progress under the guise of consensus science." Fairbanks adds that the IntCal04 group relied heavily on his team's coral data to extend its curve to 26,000 years. And he notes that he apparently has a growing number of customers. When his calibration Web site* debuted in August 2005, it received 900 visitors per month; by July 2006, it was getting about 1900. "Rick's curve is simply the most objective, because it involves the fewest assumptions," says Christopher Charles of the Scripps Institution of Oceanography in San Diego, California, who used Fairbanks's curve to date deep-sea sediments and counts himself among the satisfied customers. Archaeologist John Hoffecker of the University of Colorado, Boulder, whose team recently used the Fairbanks curve to calibrate dates earlier than 40,000 years ago at the site of Kostenki in Russia, says that despite the controversy he was "reassured by Fairbanks's reputation."

Despite this acrimonious debate, however, there are signs that the community—and at least some of the data—might now be pulling together. At last April's 19th International ^{14}C Conference in Oxford, U.K., earth scientist Konrad Hughen of Woods Hole Oceanographic Institution in Massachusetts, leader of the Cariaco Basin team, presented revised data that seemed to close much of the gap with Fairbanks's coral dates. "They are now getting very close," says Manning, although Fairbanks points out that "Hughen's Cariaco Basin data set shifted closer to our coral data … and not the other way around."

And whereas the European tree-ring record goes back only 12,400 years, a paper presented at Oxford by Chris Turney of the University of Wollongong in Australia suggests that such records may be pushed back even to the 50,000-year limit. Turney and colleagues have been radiocarbon-dating fossil kauri trees—which can live up to 1000 years—from swamps in New Zealand. The dates stretch back 55,000 years and hold out the promise of a new terrestrial calibration source that could help reconcile some of the uncertainties in the marine records. "This would resolve a lot of issues," Reimer says, "although it will take a lot of work." Nevertheless, radiocarbon experts are optimistic that the 50,000-year barrier will soon be reached. "I foresee that in 10 years it will all be solved," says van der Plicht.

If so, the revolutionary promise that Libby and his colleagues first glimpsed in the sewers of Baltimore may soon become reality. And we may end up with a much better idea of when and why the creators of the Grotte Chauvet's glorious artworks came to France—and what the weather was really like when they ventured outside.

–MICHAEL BALTER

* www.radiocarbon.LDEO.columbia.edu

A Stressful Situation

When unfolded proteins amass, they stress the cell's endoplasmic reticulum. This ER stress is now being linked to diabetes, cancer, neurodegeneration, and other ills

Even the most quality-conscious automaker occasionally rolls a defective car off the assembly line. Cells have a similar problem when it comes to manufacturing proteins. It's a complicated task and things can go wrong. Protein synthesis involves a lot more than stringing amino acids together in the right order. To function correctly, each linear strand of amino acids has to fold into just the right three-dimensional shape and may also have to be modified by addition of sugars or other accessory molecules.

Like any good automaker, cells synthesizing proteins have mechanisms to maintain quality. Recently, cell biologists have learned a great deal about how the cell manages this quality control for the protein assembly line located within a convoluted network of membranous tubes known as the endoplasmic reticulum (ER). Roughly one-third of the cell's proteins, mainly those that end up in cellular membranes or are secreted to the outside, are made in the ER.

Researchers have shown that the ER membrane contains three separate sensor molecules that respond when excessive amounts of unfolded proteins build up inside. This can happen with mutant proteins, such as the ones that cause hereditary Alzheimer's and Parkinson's disease. But it can also occur under more normal conditions if for some reason proteins are synthesized faster than they can fold and be modified. To alleviate this "ER stress," the sensors trigger a series of signaling pathways that shut down the synthesis of most proteins while turning up the production of those needed for protein folding and degradation.

This so-called unfolded protein response (UPR) is intended to protect the cell, but it's not foolproof. Sometimes, for example, the UPR can't eliminate the abnormal protein buildup in the ER. In that event, prolonged activity of the UPR may trigger cell death and may thus contribute to the neuronal loss of Alzheimer's, Parkinson's, and other neurodegenerative diseases. And the UPR may even backfire by protecting the cells of cancerous tumors from the lack of oxygen and nutrients they experience as tumors grow.

In addition to cancer and neurodegeneration, ER stress and the UPR have been linked to several other common human ills, including diabetes and heart disease. In fact, the research has already suggested a new way to guide breast cancer therapy and hinted at a novel drug treatment for diabetes. "The field is expanding so much in terms of mechanism and relevance to disease. … It's just popping up everywhere," says cell biologist Randal Kaufman of the University of Michigan Medical Center in Ann Arbor.

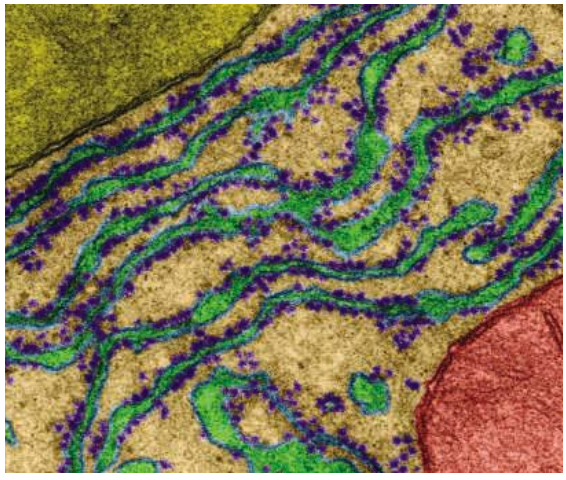

Double-edged sword. Buildup of unfolded proteins in the ER, shown here in green with blue ribosomes, triggers a series of responses that are intended to protect cells but which can misfire and cause disease.

"The field is expanding so much in terms of mechanism and relevance to disease. … It's just popping up everywhere."

—Randal Kaufman, University of Michigan Medical Center

Identifying the players

Researchers are starting to find so many disease links at least partly because they now have a solid understanding of the molecular underpinnings of the ER stress system. "Most of the major components of the signaling apparatus have been ironed out," says Linda Hendershot of St. Jude Children's Research Hospital in Memphis, Tennessee.

Cell biologists got their first glimpse of ER stress and the UPR in the late 1980s when a group led by Kaufman and another led by Joseph Sambrook of Cold Spring Harbor Laboratory on New York's Long Island independently noticed that accumulation of unfolded proteins in the ER led to increased activity of a group of genes already known to turn on when glucose concentrations are high. The products of some of these so-called glucose regulated protein (GRP) genes are involved in protein folding, so it seemed as though the ER was trying to resolve its backup by turning up their synthesis.

The researchers then wanted to know how unfolded proteins in the ER signal to the genes in the nucleus. In the early to mid-1990s, three proteins located in the ER membrane were found to be the key sensors. The first to be identified was a protein called IRE1 that was linked to the UPR in yeast by Peter Walter of the University of California, San Francisco (UCSF), and by Kazutoshi Mori, who was then working in Sambrook's lab. This protein is an enzyme that can cut RNAs—an activity that turned out to be crucial to its gene-regulating function.

The researchers found that when unfolded proteins clutter the ER, IRE1 cuts a segment out of the messenger RNA (mRNA) that directs the synthesis of a yeast protein called HAC. Another enzyme then rejoins the two end pieces, producing a shorter mRNA but a longer HAC protein due to a shift in the way the mRNA is translated. HAC is a transcription factor that activates GRP genes and others involved in protein folding, and the longer version does this much more effectively than the original one.

Altering the splicing of a transcription factor's mRNA was a novel way of regulating gene expression. "We had an absolutely wonderful time," Walter recalls. "Every leaf we turned over revealed something new." The mechanism wasn't unique to yeast. A few years later, Kaufman's team and also that of David Ron at New York University School of Medicine in New York City showed that mammalian cells have their own versions of IRE that work on the mRNA for a transcription factor called Xbp1.

At about the same time, Ron's group and other researchers identified a protein called PERK as a second ER stress sensor. PERK is one of the cell's many kinase enzymes. Once activated, it adds a phosphate group to a protein called eIF2α, which normally helps initiate the translation of mRNAs into proteins.

PERK's phosphorylation blocks eIF2α's function, thus helping alleviate ER stress by shutting down the production of most proteins.

Finally, Mori's group, now at the University of Kyoto, Japan, identified ATF6 as the third ER stress sensor. When unfolded proteins amass, protease enzymes split off a segment of ATF6, and this fragment travels to the nucleus, where it helps activate protein-folding genes.

PERK, IRE, and ATF6 may be able to sense unfolded proteins both indirectly and directly. In the absence of ER stress, binding of a regulator protein called BiP/GRP78 keeps them in check. Unfolded proteins can essentially pull off the BiP/GRP78, freeing the three sensors to trigger the UPR. In addition, recent structural studies of IRE1 by Walter and Robert Stroud, also at UCSF, suggest that this protein has a deep groove that may enable it to bind unfolded proteins directly.

Diabetes culprit?

Once researchers identified the major genes for the ER stress sensors and other components of the UPR, they could manipulate the genes to see how they affect development and health in animals. A possible diabetes connection quickly became apparent. The first indication came in 2000 when Cécile Julier's team at the Pasteur Institute in Paris found that Wolcott-Rallison syndrome, a rare human hereditary disease whose symptoms include infancy-onset diabetes, is caused by mutations that inactivate *PERK*. When Ron and his colleagues subsequently knocked out the gene in mice, the animals also became diabetic shortly after birth because their insulin-producing beta cells malfunctioned and died.

Further evidence that the PERK arm of the UPR is needed for normal beta-cell function came from Kaufman and his colleagues. They produced mice with a mutation in one copy of the gene for PERK's target. The defect prevents eIF2α from being phosphorylated by the kinase.

The Michigan team showed that on a high-fat diet, the mutant mice became much more obese than did normal animals. The mutants also developed diabetes. Examination of the animals' beta cells revealed a swollen ER, apparently full of unfolded proteins including insulin, which the cells no longer secrete normally. "Compromise of the protein-folding environment is especially detrimental to the survival and function of beta cells," Ron concludes.

Whether mutations in PERK pathway constituents are a common cause of diabetes in humans is currently unclear, but the beta-cell failure in Wolcott-Rallison syndrome as well as the diabetes of mice with PERK pathway defects is reminiscent of type 1 diabetes, which usually occurs in childhood as a result of the death of the beta cells and the consequent loss of insulin production.

Recent evidence from Gökhan Hotamisligil, Umut Özcan, and their colleagues at Harvard School of Public Health in Boston has also linked ER stress and the UPR to type 2 diabetes, which develops because the patients' cells become unable to respond to insulin. Obesity is a major risk factor for type 2 diabetes, although how it leads to the disease has been a mystery. But Hotamisligil says he realized a few years ago that a variety of conditions linked to obesity, including lipid accumulation, high demand for protein synthesis, and glucose deprivation, can trigger ER stress.

To find out whether such stress might be involved in type 2 diabetes, the Harvard workers turned to the *ob/ob* strain of mice. The animals, which are genetically obese because they lack an appetite-regulating hormone called leptin, develop an insulin-resistant form of the disease. In work published about 2 years ago, Hotamisligil and his colleagues found that fat and liver cells from the animals produce increased amounts of several proteins involved in ER stress responses (*Science*, 15 October 2004, p. 457). "All branches of the UPR are activated," Hotamisligil says.

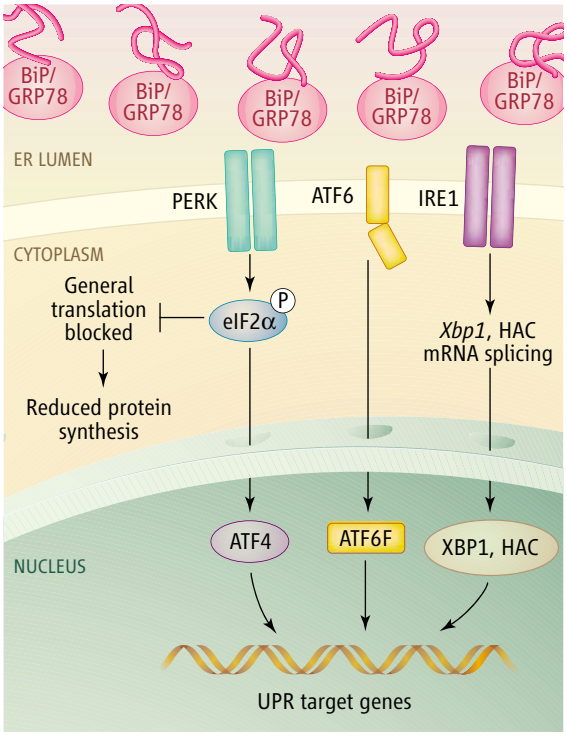

The three sensors. When unfolded proteins in the ER pull the regulator BiP/GRP78 off the sensor proteins PERK, IRE1, and ATF6, they send signals into the nucleus that trigger the unfolded protein response. As a result, synthesis of most proteins gets turned off, while the cell makes more of those proteins needed for protein folding and destruction.

Ron and his colleagues had previously shown that one result of IRE1 activation is increased activity of a kinase called JNK. And JNK, the Harvard team found, phosphorylates one of the cell's insulin receptors, rendering it unresponsive to the hormone—a change that could account for the development of insulin insensitivity in *ob/ob* mice. Consistent with that, the researchers found that they could prevent development of insulin resistance in both *ob/ob* cells and in living mice by blocking IRE1 or JNK action.

More recently, Hotamisligil and his colleagues showed that treatments that relieve ER stress can even reverse already-established diabetic changes in the mutant mice (*Science*, 25 August, p. 1137). For these experiments, they gave the animals either of two small-molecule drugs that were developed for treating other conditions but which can promote protein folding in the ER. Within 4 days, insulin sensitivity in the animals returned, and their previously high blood glucose concentrations dropped to normal. "The results were quite spectacular—more than we expected," Hotamisligil says.

Although the drugs are not widely used, the U.S. Food and Drug Administration has already approved both for certain liver diseases and hereditary disorders of the urea cycle, the cell's waste-management system. Thus, they are candidates for clinical testing as diabetes therapies. Christopher Newgard, a diabetes expert at Duke University School of Medicine in Durham, North Carolina, describes the Hotamisligil team's results as "compelling and exciting." It's too soon to tell, however, whether the drugs will have unwanted side effects if given to the large population of diabetes patients.

Cancers' friend

Type 2 diabetes is not the only disease that may be fostered by the cell's efforts to protect itself against ER stress. Recent results also put cancer in that category.

Cancer cells are subject to ER stress because a tumor can grow faster than its blood supply, thus leaving its cells short of oxygen and nutrients. Exactly how that leads to ER stress is unclear, but the nutrient deficiency may rob tumor cells of the energy they need for protein folding and the glucose needed to add the sugars to their

ILLUSTRATION: PRESTON HUEY/*SCIENCE*, ADAPTED FROM ZHAO AND ACKERMAN, *CURRENT OPINION IN CELL BIOLOGY* 18 (2006)

proteins. But whatever the cause, Hendershot says, "the UPR seems to kick in. It's protective to the [cancer] cell—but detrimental to the host."

Some of the results linking cancer progression to the UPR come from Constantinos Koumenis and his colleagues at Wake Forest University School of Medicine in Winston-Salem, North Carolina. Working with Bradley Wouters of the University of Maastricht in the Netherlands, they found that activation of the PERK branch of the UPR fosters tumor growth. For example, tumor cells in which the *PERK* gene had been knocked out grew very poorly, compared to cells that still contained the gene, when transplanted into mice.

Similarly, Albert Koong and Lorenzo Romero-Ramirez of Stanford University in Palo Alto, California, and their colleagues showed that activity of the IRE1-XBP1 branch of the UPR is required for tumor growth. "If you block the UPR in any of these tumor systems, the tumors grow slower and smaller," says Koumenis, who recently moved to the University of Pennsylvania. And the effects are apparently not limited to experimental tumors in animals: Human tumors show increased expression of UPR system components, particularly in oxygen-starved areas.

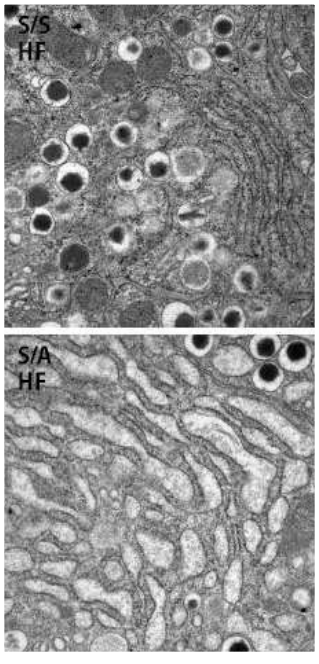

At least one of these components may help assess how breast cancers will respond to chemotherapy. About 10 years ago, Amy Lee's team at the University of Southern California Keck School of Medicine in Los Angeles found that the UPR regulator BiP/GRP78 is needed for the growth of fibrosarcoma tumors implanted in mice. Further work by her group and others has shown that BiP/GRP78 levels increase as tumors, including human breast and lung cancers, grow.

The protein may help cancer cells survive, Lee says, by inhibiting programmed cell death or apoptosis. Although a prolonged UPR can promote apoptosis, several groups, including Lee's, have found that BiP itself is anti-apoptotic. They've shown that it interferes with caspase enzymes and other components of cell death pathways.

This mode of operation may also help explain another cancer-friendly aspect of UPR activation. Cancers often develop resistance to the drugs and radiation used to treat them, and researchers, including Lee and Hendershot, have found that the UPR contributes to this resistance for some drugs, particularly those that work by triggering apoptosis.

In the 15 August issue of *Cancer Research*, Lee and her colleagues report that it may be possible to use the BiP/GRP78 status of a patient's breast cancer cells to guide her therapy. As expected from their previous results, the researchers found that about two-thirds of tumor samples obtained before the initiation of chemotherapy exhibited overexpression of the protein.

Patients who had BiP/GRP78-positive tumors and were treated only with the drug adriamycin, an apoptosis inducer, had a higher risk of relapsing than patients with negative tumors. "We found that we can use this marker as a predictor of chemotherapy resistance in breast cancer," says Lee.

The situation is complicated, however, because in other cases the UPR may actually increase sensitivity to chemotherapeutic drugs. For example, Lee and her colleagues found that patients who took both taxane and adriamycin and had BiP/GRP78-positive tumors fared better than those whose tumors did not overexpress the protein. "We need some hard research to understand when UPR activation is good and when it is bad," Hendershot says.

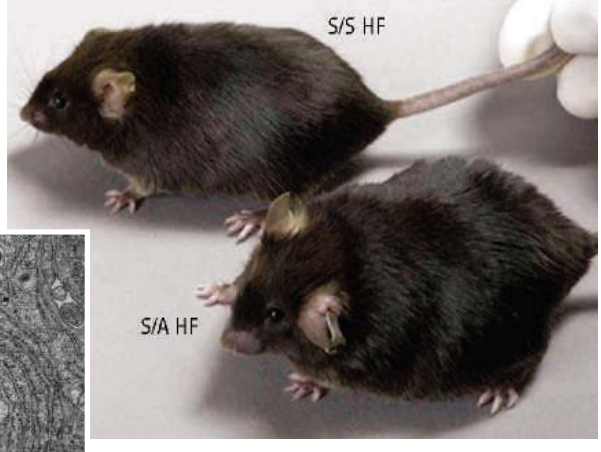

Path to diabetes. A mouse (*bottom*) with a mutation affecting the PERK pathway becomes much fatter when fed a high-fat diet than a normal mouse (*top*) does and also develops diabetes. The greatly enlarged ER of the mutant animal's beta cells (*bottom micrograph*), compared to that of normal beta cells (*top*), suggests that this is related to ER stress.

A stressed brain

Neurobiologists are facing a similar issue. Many of the most common and devastating neurodegenerative diseases, including Alzheimer's, Parkinson's, and Huntington's, are characterized by the accumulation and aggregation of misfolded proteins. Not surprisingly then, numerous researchers have found evidence that the UPR is turned on in these conditions.

Studies of both human brain samples taken at autopsy and the brains of mice that have been genetically engineered to mimic the diseases have revealed increased expression of various components of the UPR pathways. "Everyone pretty much agrees that [the UPR] is activated" in Alzheimer's and other neurodegenerative diseases, says neurobiologist Dale Bredesen of the Buck Institute for Age Research in Novato, California, whose group is among those doing the work.

But that activation may ultimately do more harm than good. If the UPR fails to resolve the ER stress that the patients' brain neurons are experiencing, its sustained attempts may contribute to the progression of the diseases by triggering apoptosis in the cells. "The initial response is protective, but the late response is destructive," Bredesen says.

Exactly how the UPR sets the cell on the road to apoptosis remains one of the big mysteries of the field, however. Neurobiologists have come up with some leads. For example, Bredesen's team and others have fingered caspase 12 as a possible link. Treatments that induce ER stress lead to increased activity of this enzyme, which is among those that bring about the final destruction of cells undergoing apoptosis. The work was done with mouse models, however, and it's unclear whether something similar occurs in the human diseases.

Researchers would like to get a better handle on how the UPR triggers apoptosis, as that might provide new targets for drug therapies. The fact that the UPR can be helpful in some situations and harmful in others could complicate such a drug development effort, however. Maintaining quality control on the cell's protein assembly line looks to be a great deal more difficult than the problems car manufacturers face.

–JEAN MARX

CREDITS: DONALYN SCHEUNER *ET AL.*, *NATURE MEDICINE* 11, 7 (JULY 2005)

Buzz cut. As feral goats turned Isabela's brush and cloud forests into patchy grassland, tortoises suffered.

CREDIT: TUI DE ROY/ROVING TORTOISE

INVASIVE SPECIES

The Galápagos Islands Kiss Their Goat Problem Goodbye

The world's largest eradication campaign has virtually rid an ecological wonderland of feral goats, a devastating invader. Next in the crosshairs: cats and rats

SANTA CRUZ, GALÁPAGOS ISLANDS—Rachel Atkinson hops like a Darwin finch from one volcanic outcropping to the next, then plunges into ankle-deep mud. Squishing as she walks, the botanist with the Charles Darwin Research Station homes in on the ailing invaders: blackberry, passion fruit, and quinine bushes clustered near Santa Cruz Island's last shrubby stands of *Scalesia* trees. Atkinson smiles in approval. One more blast of herbicide ought to prevent the aliens from regrowing and give the *Scalesia* a shot at survival after all.

Atkinson's search-and-destroy mission is part of an ambitious 6-year, $18 million Global Environment Facility (GEF) effort by the station and Galápagos National Park to turn the tide against invasive species in the Galápagos Islands, the fragile crucible of life that inspired Charles Darwin to formulate his theory of evolution 150 years ago. The GEF grant runs until next year, but the results so far are stunning. A survey here last month has confirmed that enemy number one—the feral goat—has been virtually wiped off Isabela, Santiago, and Pinta islands. All told, some 140,000 feral goats were slain in 5 years of the GEF-funded Project Isabela, the largest eradication project ever undertaken. "A great battle has been won here," says Victor Carrion, subdirector of the park.

Although one bane has been eliminated, others are at large. In northern Isabela, rats have ravaged the last two nesting sites of mangrove finches, estimated at fewer than 100. And both rats and feral cats have decimated a subspecies of marine iguana (*Amblyrhynchus cristatus albemarlensis*) endemic to Isabela, prompting the World Conservation Union to add it to its vulnerable list in 2004. Rangers have set out traps and poison for Isabela's rats and are plotting eradication campaigns on Floreana and Santiago islands. An effort to poison feral cats will commence next year.

The Galápagos have been under siege ever since pirates and whalers began visiting the archipelago in the 1700s and leaving behind goats, pigs, and other animals as a living larder for future visits. But it wasn't until the late 1980s that the goat population suddenly started booming, possibly due to El Niño–driven changes in vegetation patterns. Godfrey Merlen, a Galápagos native and director of WildAid, says he saw "two or three" goats on the upper flanks of Isabela's Alcedo volcano in 1992. When he returned 3 years later, he saw hundreds. "It was total chaos," Merlen says. The goats had denuded the once-lush terrain, transforming brush and cloud forests into patchy grassland.

Ecological shock waves rippled across Isabela. The highlands had served as a safe haven for species such as the giant tortoise. "We saw many more tortoises falling into the volcanic craters," trying to reach feeding grounds or because of erosion, says Carrion. "Being a baby tortoise is hard enough," adds Thomas Fritts, past president of the Charles Darwin Foundation. "Competing with voracious herbivores is an extra challenge."

Park rangers quickly cottoned on and started slaying the goats in 1995. They had eradicated a much smaller population from Española Island in the 1970s. But with tens of thousands of goats on northern Isabela alone, officials knew they needed a novel approach. In 2000, GEF agreed to bankroll an antigoat operation as long as it was part of an effort to tackle invasive species across the board (*Science*, 27 July 2001, p. 590).

Goats were still top priority. The park imported hunting dogs from New Zealand and trained them to track and kill goats. Helicopters were pressed into service for sharpshooters to reach rugged highlands. To flush out the last feral holdouts, the park released "Judas" goats, including sterilized females plied with hormones to keep them in heat and attract males. The last feral goat in northern Isabela was shot in March. Hunters have also purged pigs from Santiago and donkeys from both islands.

Local scientists say native plants are already bouncing back. Seedlings of *Scalesia* and soldierbush are sprouting on Alcedo. And on Santiago, cat's claw and Galápagos guava are thriving, providing nesting grounds for the secretive Galápagos rail.

One looming threat is microbial invaders. "What can cause far greater and permanent damage are the small introduced species [such as] West Nile virus, now in Colombia, a stone's throw away from Galápagos," says Merlen. In a paper in the August issue of *Conservation Biology*, Marm Kilpatrick of the Consortium for Conservation Medicine in New York City and colleagues concluded that West Nile virus–ridden mosquitoes could easily hitch a ride on a commercial jet from mainland Ecuador. "The Galápagos has been very lucky so far, but it's just a matter of time," says Simon Goodman of the University of Leeds in the U.K., an author of the paper. He says that West Nile virus could inflict the sort of damage in the Galápagos that avian malaria did in Hawaii in 2004, when it drove a honeycreeper (*Melamprosops phaeosoma*) to extinction. Galápagos officials pledge to remain vigilant and point to the establishment in 2003 of a molecular pathology lab on Santa Cruz funded by the U.K.'s Darwin Initiative.

To avoid ceding hard-won breathing room for native species, the park and research station plan to set up a $15 million fund for ongoing eradication efforts. In the meantime, they are stepping up efforts against invasive plants and gearing up for the cat-and-rat blitzkrieg. Unless these and other unwelcome visitors go the way of the goats, warns Carrion, "the worst may be yet to come."

–JERRY GUO

Jerry Guo is a freelance writer in New Haven, Connecticut.

* this drug knows everything about Mr. Holliday.

It's tailor-made for his DNA. IBM and IBM Business Partners are working to support research that is making personalized medicine a reality. From data-mining algorithms and vast supercomputing power to secure genomic information warehouses, we're helping pharma and biotech companies shorten drug development cycles, streamline clinical trials, and bring new targeted treatments to market. Want innovation for growth? Talk to the innovator's innovator. Call on IBM. To learn more, visit ibm.com/healthcare/personalized

what makes you special?

IBM

EDITED BY YUDHIJIT BHATTACHARJEE

Two Cultures

COUNT THOSE BEATS. Modern jazz can be as complex as an exotic mathematical problem. But saxophonist Rudresh Mahanthappa's music is inspired by math itself.

The New York–based jazz composer's latest album, *Codebook*, conveys elements of number theory and cryptography in musical form. In some pieces, concepts such as the Fibonacci sequence—an infinite set of integers created by adding the last two numbers in the series—serve as the basis of the rhythm and melodies. In others, mathematical ideas dictate the evolution of the score. Encoded throughout the music are the names of the band members and famous jazz melodies.

"Math has always been at the core of what I do," says Mahanthappa, 35, who has been fascinated by math from an early age. He has made a name for himself by blending jazz with the complex rhythms of Indian classical music. Adding a mathematical component was an even bigger challenge. "Translating an idea from number theory or cryptography to music doesn't automatically yield anything that's playable or that sounds good," says Mahanthappa.

"He proves, by using musical notes, what mathematicians have always believed: that math is beautiful," says Princeton University mathematician Manjul Barghava, himself an acclaimed player of the tabla, an Indian percussion instrument. *Codebook* will be available from Pi Recordings on 26 September.

Got a tip for this page? E-mail people@aaas.org

SIDELINES

CULTURAL VALUES. Carla Ellis hadn't cartooned regularly since her undergraduate days in the 1960s. But a contest put on by the Union of Concerned Scientists to highlight what the advocacy group sees as the increasing U.S. government manipulation of research inspired the Duke University computer scientist to sharpen her pencil. "My cartooning is kind of a secret," says Ellis, who is especially concerned about "censorship" at the Environmental Protection Agency and Food and Drug Administration. Ellis is one of 12 finalists vying for the $500 prize. The White House Office of Science and Technology Policy had no comment on the contest.

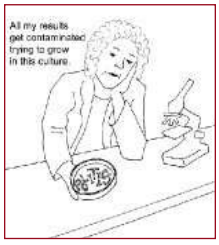

DEATHS

DEVOTED. Mental health researchers and practitioners are in shock over the murder of Washington, D.C.–area psychiatrist Wayne Fenton on 3 September. Fenton, 53, was allegedly beaten to death in his office by a patient, 19-year-old Vitali A. Davydov, who was suffering from symptoms of both bipolar disorder and schizophrenia.

Fenton was director of the division of adult translational research and treatment at the National Institute of Mental Health (NIMH) and associate director of clinical affairs. NIMH psychiatrist Husseini Manji says Fenton was "very instrumental in trying to get treatment studies under way" for both schizophrenia and bipolar disorder, which "he viewed as the cancers of mental illness." In addition to his full-time job, Fenton spent evenings and weekends seeing patients, most of whom were "very ill," Manji says. "Everyone's absolutely devastated. Wayne was one of those decent, decent good guys who goes out of his way to help people. … Maybe [the murder] will raise awareness of how bad these illnesses are."

Awards >>

FACE OF SCIENCE. It's not quite a labs-to-riches story, but physicist Kathy Sykes has gone from being a Bristol University postdoc to being one of the U.K.'s best known advocates of science. Last week Sykes, now professor of public engagement in science and technology and part-time TV personality, won the $19,000 Kohn Prize from the Royal Society for enhancing public understanding of science.

After earning a Ph.D. studying biodegradable plastics, Sykes cut her popularizing teeth as head of science at Explore@Bristol, a hands-on science museum. She appeared on the BBC's *Rough Science* and initiated the Cheltenham Science Festival and FameLab, a nationwide talent competition in which researchers have 3 minutes to talk about science. In 2002, her alma mater made her the youngest university professor in the United Kingdom.

As a pillar of academic life, Sykes is trying to improve how the university relates to the city around it. She's organized community events to discuss the impact of drugs on the brain and behavior and an interactive science exhibit in a local shopping mall.

BIG MONEY. Researchers in plant science and astronomy are among the winners of this year's prizes awarded by the International Balzan Foundation in Milan, Italy.

Elliot Meyerowitz of the California Institute of Technology and Chris Somerville of Stanford University share $800,000 for their work on establishing *Arabidopsis* as a model organism. Paolo de Bernardis of the University of Rome "La Sapienza" and Andrew Lange of the California Institute of Technology share another $800,000 for their role in the Boomerang Antarctic Balloon experiment, which mapped background cosmic radiation left over from the big bang. The foundation has also awarded humanities prizes to musicologist Ludwig Finscher of the University of Heidelberg in Germany and to political scientist Quentin Skinner of the University of Cambridge in the U.K.

Open to

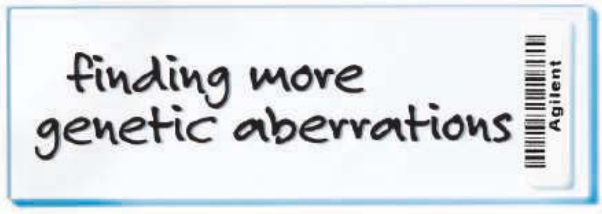

Pinpoint novel copy number changes with Agilent oligo aCGH microarrays

Open your imagination to what a single chip can show you. Agilent's high-resolution array-based comparative genomic hybridization (aCGH) platform provides the flexibility and sensitivity you need to study chromosomal abnormalities. From genome-wide arrays featuring CGH-optimized 60-mer probe sets to high-definition arrays that zoom in to pinpoint more microaberrations than any other method, Agilent delivers the tools you need to find the genetic changes you're searching for.

To hear from researchers who are charting their own course in CGH, visit www.OpenGenomics.com

Agilent Technologies

LETTERS

edited by Etta Kavanagh

Cuts in Homeland Security Research

IS IT TIME FOR CONGRESS TO REDUCE ITS COMMITMENT TO RESEARCH related to the U.S. Department of Homeland Security (DHS)? Your article "Congress dials back research on understanding terrorism" (Y. Bhattacharjee, News Focus, 4 Aug., p. 610) states, "senators would prohibit DHS from funding any center for more than 3 years." Such a mandate is unprecedented, and we are concerned that this provision could result in the arbitrary termination of valuable and productive research centers.

The nation is threatened not only by terrorism but also by natural disasters such as major hurricanes and earthquakes, as well as intentional or naturally occurring disease outbreaks. The DHS-sponsored University Centers were selected through a competitive, merit-based process to meet specific needs for long-term research capabilities. The centers—with their network of university, industry, and government partners throughout the country—are a mechanism to ensure that fundamental research relevant to DHS is conducted and that the knowledge gained rapidly reaches policy-makers and first responders.

> "[T]his provision could result in **the arbitrary termination** of valuable and productive research centers."
>
> —Busta *et al.*

The federal effort has been modest: $62 million in fiscal year (FY) 2006 and only $52 million requested for FY 2007. That is about what the United States spends on the space program in just 2 weeks each year. The "oldest" DHS University Center is just over 2 years old. It is unreasonable to expect that in 3 years, we would be able to walk away from this mission, just as we would not expect success in such a short period of time for the fundamental research required to develop a new vaccine or any other new technology.

Moreover, any university participating in the DHS Centers program would be unable to receive support beyond the 3-year limitation, prohibiting future participation in the program by nearly 80 partner universities in 30 states. The Senate's language on this issue would undermine a key portion of the nation's research and education enterprise related to the nation's homeland security interests and should be reversed.

FRANCIS BUSTA,[1] NEVILLE CLARKE,[2] LYNN R. GOLDMAN,[3] CHARLES HAAS,[4] GABOR KELEN,[3] GARY LAFREE,[5] JOAN ROSE,[6] DETLOF VON WINTERFELDT[7]

[1]Director, National Center for Food Protection and Defense (NCFPD), University of Minnesota, 925 Delaware Street SE, Suite 200, Minneapolis, MN 55455, USA. [2]Director, National Center for Foreign Animal and Zoonotic Disease Defense (FAZD), Texas A&M University, 1500 Research Parkway, Suite 100 A, College Station, TX 77843, USA. [3]Co-Director, National Center for the Study of Preparedness and Catastrophic Event Response (PACER), Johns Hopkins University, Davis Building, Suite 3220, 5801 Smith Avenue, Baltimore, MD 21209, USA. [4]Co-Director, Cooperative Center: Center for Advancing Microbial Risk Assessment (CAMRA), Drexel University, Department of Civil, Architectural and Environmental Engineering, Philadelphia, PA 19104, USA. [5]Director, National Center for the Study of Terrorism and Responses to Terrorism (START), University of Maryland, 3300 Symons Hall, College Park, MD 20742, USA. [6]Co-Director, Cooperative Center: Center for Advancing Microbial Risk Assessment (CAMRA), Michigan State University, 301 Manly Miles Building, 1405 South Harrison Road, East Lansing, MI 48823, USA. [7]Director, Center for Risk and Economic Analysis of Terrorism Events (CREATE), University of Southern California, RGL 313 University Park, Los Angeles, CA 90089, USA.

Public Access Success at PubMed

IN THEIR LETTER "PUBLIC ACCESS FAILURE AT PubMed" (7 July, p. 43), M. Stebbins *et al.* chronicled the failure of the voluntary NIH policy to provide open access copies of primary research articles at PubMed Central (PMC).

The value of open access publishing has been touted as providing access to articles for the general public, whose tax dollars often pay much of the cost of the research. Stebbins *et al.* suggest that there has been a "lack [of] a demonstrated desire by the general public for access to primary research papers." If this is correct, one might ask from where the "push" for open access is coming. In my opinion, this conflict has largely been between scientists and librarians, who feel that publishers are reaping large, unjustified profits from publicly funded research, and publishers (both for-profit and not-for-profit), who argue that the "value added" by the peer review system justifies their charges.

Largely overlooked in this conflict is the longstanding success and enduring value of PubMed. Distinct from PMC, PubMed (www.pubmed.gov) is a database of the abstracts of millions of scientific publications. Abstracts are posted at the time of publication. Virtually all biomedical research, whether publicly or privately funded, is included. Members of the general public who have an interest in a disease or any other biomedical issue can easily search PubMed to read synopses of cutting-edge research.

I suggest that one reason for the public's "lack of demonstrated desire" for primary research articles is their ready access to research information at PubMed and other authoritative sources on the Internet. Before mandating a costly and confusing parallel publication system at PMC, we should be sure that the resource already provided by U.S. taxpayer dollars at PubMed is not meeting the public's need for information.

DAVID C. BEEBE

Janet and Bernard Becker Professor of Ophthalmology and

Visual Sciences, Professor of Cell Biology and Physiology, Campus Box 8096, Washington University, St. Louis, MO 63110, USA. E-mail: beebe@wustl.edu

Support for the NIH Public Access Policy

IN THEIR LETTER "PUBLIC ACCESS FAILURE AT PubMed" (7 July, p. 43), M. Stebbins *et al.* express a skeptical view of the NIH public access policy, basing their critique on several misconceptions that deserve comment.

1) Is the policy too costly? The current NIH appropriation is $27.9 billion. The $3 million anticipated yearly cost of the public access policy represents 0.011% of the appropriation. In fact, the expenditure on public access is dwarfed by the $30 million annually that NIH reports it provides its funded investigators for page charges and other costs of publishing in subscription journals (*1*).

2) Stebbins *et al.* claim that there is a lack of "a demonstrated desire by the general public for access to primary research papers." Usage statistics for PubMed Central (PMC)—the NIH database that provides full-text research articles to the public for free and serves as the repository for articles submitted under the public access policy—suggest otherwise. There were more than 5 million users of PMC in April. That level of use suggests that not only are working scientists taking advantage of the resource, students and the lay public are as well. There is surely usage from junior colleges, research institutes, small companies, and many other organizations that do not have large budgets for biomedical research journal subscriptions.

3) The public access policy is criticized because there is "no dedicated system to guarantee that corrections" can be made after publication. Substantive author corrections or retractions are often made by the subsequent publication of errata or retraction notices. The National Library of Medicine has an established system that ensures that any published errata or retractions are noted in the PubMed citation and PMC full-text articles include a link (*2*).

4) Stebbins *et al.* claim that many reviews and commentaries are found in PMC, in apparent violation of the public access policy, which applies to "final, peer-reviewed manuscripts and publications that result from research supported, in whole or in part, with direct costs from NIH" (*3*). Since articles that appear to be reviews or commentaries are often peer-reviewed and include descriptions of original research, NIH has wisely left the decision of what falls within the scope of the policy to the grantee.

5) Articles made available through PMC would not represent "prior art" for purposes of patenting, since NIH only posts the author manuscripts after the articles have been released by the journals in which they are published.

6) Stebbins *et al.* claim that the proposed Federal Research Public Access Act (S.2695) requiring federal agencies to implement a public access policy has drawn criticism because it "unfairly places scientists between funding agencies and publishers." Actually, organizations that have a financial stake in publishing are the main source of opposition to the policy and to S.2695. Scientists submit articles without compensation, they carry out peer review usually without compensation, and they often serve as editors for little or no compensation. Publishers make huge profits from this business model based on free labor. Because of the unsupported concern that the public access policy would adversely affect their business interests, they use their political and economic clout to lobby for restricted access, which is detrimental to the professional interests of the scientists that they claim to be serving.

One of us has submitted several articles to PMC under the public access policy. The process was quick and painless and allowed the articles to achieve greater readership. If participation by NIH grantees becomes mandatory, the policy will have a significant beneficial impact on biomedical science by making a large body of the research literature available without access barriers.

MICHAEL A. ROGAWSKI[1]*† AND PETER SUBER[2]†

[1]National Institute of Neurological Disorders and Stroke, National Institutes of Health, Bethesda, MD 20892, USA. [2]Public Knowledge, 1875 Connecticut Avenue, NW, Suite 650, Washington, DC 20009, USA.

*To whom correspondence should be addressed. E-mail: michael.rogawski@nih.gov

†The views expressed do not necessarily represent those of the authors' employers.

References

1. See footnote 8 in http://grants.nih.gov/grants/guide/notice-files/NOT-OD-05-022.html#ftn8.
2. See www.nlm.nih.gov/pubs/factsheets/errata.html.
3. See http://grants.nih.gov/grants/guide/notice-files/NOT-OD-05-045.html.

Ongoing Controversy over Debye's WWII Role

IN AN ARTICLE ENTITLED "BLOCKING A BOOK, Dutch university rekindles furor over Nobelist Debye" (News of the Week, 30 June, p. 1858), M. Enserink reports on a controversy over the name of a research institute at Utrecht University. Blocking a book is a serious matter, so it is fortunate that this is not correct.

Earlier this year, Utrecht University decided to remove the name of Peter Debye from a research institute. This decision was prompted by a publication on Debye's role before and during World War II (*1*) ("Fallen from grace," Newsmakers, 3 Mar., p. 1239). One of the facts is that Debye, as president of the German Physical Society, asked Jewish members to resign in a 1938 letter signed "Heil Hitler." Utrecht University felt that the new facts were incompatible with the continued use of the Debye name. The research institute in question gathered information for independent scientific research on Debye's role, to be conducted by an agency such as the Netherlands Institute for War Documentation (NIOD). The managing director of the former Debye Institute, Gijs van Ginkel, who is not a historian, added a personal judgment to the gathered information about Debye and the university's decision, without hearing both sides of the case. As a result, the text contained factual inaccuracies.

The Executive Board of the university and the management of the research institute then decided to separate the information that had been gathered by the research institute from van Ginkel's remarks. So this is not a case of the university blocking the publication of a book.

THE EXECUTIVE BOARD OF UTRECHT UNIVERSITY

Utrecht University, 3508 TC Utrecht, the Netherlands.

Reference

1. S. Rispens, *Einstein in Nederland: Een intellectuele biografie* (Ambo, Amsterdam, 2006).

Response

THE EXECUTIVE BOARD SEEMS TO SUGGEST that Debye's 1938 "Heil Hitler!" letter is a

Letters to the Editor

Letters (~300 words) discuss material published in *Science* in the previous 6 months or issues of general interest. They can be submitted through the Web (www.submit2science.org) or by regular mail (1200 New York Ave., NW, Washington, DC 20005, USA). Letters are not acknowledged upon receipt, nor are authors generally consulted before publication. Whether published in full or in part, letters are subject to editing for clarity and space.

new fact upon which it based the decision to remove Debye's name from the institute. However, the letter has been reproduced and discussed for many years, including in a paper published in 1988 (*1*–*3*). The term "blocking" seems justified in this case. Staff at the former Debye Institute had planned to publish a book in defense of Debye, but decided not to after what a university spokesman described as a "pithy" conversation with the Executive Board. Institute staff have been banned from discussing the issue with the press.

MARTIN ENSERINK

References

1. H. Rechenberg, *Phys. Bl.* **44** (no. 11), 418 (1988).
2. V. R. Remmert, *DMV-Mitteilungen* **12-4/2004**, 223 (2004).
3. D. Hoffmann, M. Walker, *Phys. Today*, p. 52, Dec. 2004.

Bias About Climate Change

SCIENCE'S BRITTLE AVERSION TO POLICYmakers who want to know more about climate change was on full display in the 28 July account of the U.S. House of Representatives hearing on the hockey stick theory ("Politicians attack, but evidence for global warming doesn't wilt," R. A. Kerr, News of the Week, p. 421).

Kerr refers to Committee Chairman Joe Barton's request for independent statistical analysis of the hockey stick theory not as a logical step, but as "a highly unusual move." And didn't everybody just hate how he "bore down" on the National Academies' panel's chairman? Thank goodness Gerald North "deflected the charge like an all-star hockey goalie."

The best that can be said of Kerr and his publisher, Alan Leshner, is that they don't hide their biases. And they will have further opportunities for public display now that Congressman Barton has broached the idea of inviting experts at the National Research Council and the Government Accountability Office to get involved in the evaluation process.

Lord only knows how *Science* will fault that, but in a place where the mere asking of questions is deemed a threat, you just know they will.

LARRY NEAL

Deputy Staff Director, House Energy and Commerce Committee, 2125 Rayburn House Office Building, Washington, DC 20515, USA.

TECHNICAL COMMENT ABSTRACTS

Comment on "Large-Scale Sequence Analysis of Avian Influenza Isolates"

Edward C. Holmes, David J. Lipman, Dmitriy Zamarin, Jonathan W. Yewdell

Obenauer *et al.* (Research Articles, 17 March 2006, p. 1576) reported that the influenza A virus PB1-F2 gene is evolving under strong positive selection, as documented by an extremely high ratio of the number of nonsynonymous nucleotide substitutions to the number of synonymous substitutions (dN/dS). However, we show that this observation is likely to be an artifact related to the location of PB1-F2 in the +1 reading frame of the PB1 gene.

Full text at www.sciencemag.org/cgi/content/full/313/5793/1573b

Response to Comment on "Large-Scale Sequence Analysis of Avian Influenza Isolates"

John C. Obenauer, Yiping Fan, Clayton W. Naeve

We repeated the dN/dS analysis as described by Holmes *et al.* using the methods and data as described in our original report. We obtained essentially the same results and agree that it cannot be concluded from dN/dS calculations whether PB1-F2 is under positive, negative, or neutral selection.

Full text at www.sciencemag.org/cgi/content/full/313/5793/1573c

A New Era in Laboratory Leadership.

The University of Chicago announces a new partnership to manage the Argonne National Laboratory.

Committed to producing outstanding science for the benefit of our nation.

Under the University of Chicago's leadership, Argonne has been a pioneer in scientific and technological achievement in the energy, physical, biological and computational sciences.

Beginning October 1, 2006, the University of Chicago will manage the Laboratory through UChicago Argonne, LLC, a new entity created to meet the Department of Energy's needs and advance its mission.

Together with its new partners, Jacobs Engineering Group, Inc. and BWX Technologies, Inc., and through important alliances with Northwestern University, the University of Illinois at Urbana – Champaign and the University of Illinois at Chicago, the UChicago Argonne, LLC will combine the finest scientific leadership with best practice management methods to ensure safety and efficiency.

The UChicago Argonne LLC stands ready to address some of the most pressing scientific and technological problems facing our nation.

UChicago ▶
Argonne LLC

For more information visit www.uchicagoargonnellc.org

SOCIOLOGY

Through Art to Association in Japanese Politics

Christena Turner

Japan is often perplexing—even the stereotypes contradict one another. Which is it: open, friendly, and welcoming or closed, distant, and restrained? Because it is so easy to get lost in a country where streets aren't usually named and houses are numbered in the order in which they are built, it is common to be rescued by strangers. The stranger who helped me find my way to Nagasaki invited me to lunch and introduced me to a family whose home I finally departed nearly two weeks later. In contrast, however, there is the feeling of many foreigners who live and work in Japan for extended periods of time that, as a crestfallen colleague of mine once remarked, one does not "really belong."

Bonds of Civility
Aesthetic Networks and the Political Origins of Japanese Culture

by Eiko Ikegami

Cambridge University Press, New York, 2005. 475 pp. $80, £45. ISBN 0-521-80942-8. Paper, $36.99, £20.99. ISBN 0-521-60115-0.

Eiko Ikegami's fascinating *Bonds of Civility*: *Aesthetic Networks and the Political Origins of Japanese Culture* argues that Japanese sociability is characterized by an extensive repertoire of practices for handling the problem of how to interact with strangers. Somewhere between friends and enemies lies the domain of strangers. Somewhere between intimacy and danger lies the domain of civility. "The degree of 'strangership' may be an indication of the degree of civility in a given society," she claims. Civility permits ordinary people to be confident in interactions with those of unknown or different backgrounds, making it possible to form social bonds in the absence of friendship or kinship. Why does this matter so much?

A central issue for social scientists concerned with the conditions necessary for modern democracies is the emergence of voluntary associations of individuals formed outside the realms of both the political institutions of the state and the intimate ties of the family. This realm of civil society has intrigued researchers for more than a century, and the difficulty of locating Western-style civil society in non-Western states has perplexed all who take the concept to be universal rather than culturally bounded. Ikegami (a sociologist at the New School for Social Research) joins others who have argued that civil society is inadequate to the task of understanding non-Western experience and suggests that we look at networks of civility instead (*1*, *2*).

Ikegami's most original contribution here is her argument that networks of people engaged in interactive artistic and cultural pursuits created the bonds of "civility without civil society" that prepared the population of pre-modern Japan for its strikingly rapid transformation into one of the first and most successful modern nations outside of the West. Art created politics when participation in aesthetic networks taught people technologies of association among strangers that eased the transition toward institutions of a modern political economy.

Aesthetic activities demand that people share sentiments as well as ideas and idioms as well as arguments. Participation in networks of artistic hobbyists taught people how to moderate closeness and distance, form associations, and interact in emerging public activities. The civility nurtured in these extensive networks of strangers provided patterns for relating to people with whom one shared only "weak ties." Relying on the classic work of Mark Granovetter (*3*), Ikegami argues that weak ties are the strong force behind an emerging modern polity, commercial economy, and national society.

Many outside of Japan have written poems in the five syllable–seven syllable–five syllable form of haiku, the most recognizable form of Japanese poetry. Few, however, realize that haiku was originally only the first of many stanzas in a lengthy "linked verse" poem, composed by numerous amateur poets sitting together enjoying a session of shared artistic production. These voluntary networks cut across social classes and endured beyond a single session. They even inspired long-distance composition and poetry contests that were carried on through regionally and nationally distributed commercial publication networks. A well-known poet might write the first stanza; in response, the next member would add a second that was linked to the previous themes and images. Repeated innumerable times, the result was a linked verse poem, sometimes as long as 100 stanzas, composed by many authors. So important was the process of sitting, communicating, and interacting with others in shared creative practice that the famous Japanese poet Bashō remarked that the poem itself was mere "garbage" if removed from this interactive context. The rules of cultural production in cultural network activities like these became rules of social relationships among equals—a rehearsal of sorts for civility among strangers.

Drinking contest. During the Tokugawa period, aesthetic networks were used "to organize fun events as well as serious literary and artistic activities." Ikegami describes the "Sake Drinking Battle" held in 1815 at Senju, and includes this section from *Tōin Zukan.*

The reviewer is at the Department of Sociology, University of California, San Diego, La Jolla, CA 92093, USA. E-mail: chturner@ucsd.edu

Thus, in pre-modern Japan, people knew how to gather together, communicate with one another, organize public events, and maintain weak ties. Ikegami maintains that these cultural networks and activities subtly but successfully undermined the feudal status system and paved the way for modern forms of civic relationships.

The power of frivolity in a society of strict hierarchy and control lies in its seeming irrelevance combined with the subversive nature of pleasure. The popularity of sake drinking contests reminds us of the importance of irrelevance and the power of play in creating social bonds. As shogunate control became stronger and explicitly political associations were abolished, flourishing cultural networks took on increased importance. A pictorial scroll by a famous Edo period painter, Sakai Hoitsū, depicts an early 19th-century sake drinking contest (see the figure) held in Senju, a suburb of Edo. With the offer of free sake to all participants, people of any social status were invited to show off their ability to hold liquor and compete for a top spot in the rankings that were printed and widely distributed afterward. A prominent sign hung over the event read "No Admission for Bad Guests—Teetotalers and Logical Minds." This playful event was graced with the presence of famous writers, poets, and painters who served as judges of the competition, and whose own artistic works vividly depicted its "state of anarchy."

Free association in cultural activities of various kinds, including foolishness, constitutes an important alternative to characterizations of emerging civil society in Western societies and suggests the importance of sense and sensibility as well as logic and rationality in social life. Prior to modernization, Japan had established forms for interaction across social classes and formal categories of identity that emphasized shared appreciation for arts and collective experience of moments of beauty, joy, humor, and pleasure. Social networks based on these activities later served as important models for creating communities of shared heritage, orientations, and meanings—what Benedict Anderson has termed "imagined communities" (*4*)—that constituted an emerging national culture.

Ikegami's history reminds us that strangers emerge in a historical context and that frequency, density, and complexity of contact change over time. Haiku and sake may seem unlikely objects around which to build networks that come to resemble "an educational program for developing civility in public space," but the author's elegant conceptualization of a wide field of arts, contests, hobbies, and pleasures as "sites of social interaction" between otherwise unrelated individuals is persuasive.

As a network theorist, Ikegami is better at analyzing relationships between those within networks than at accounting for those who are left out. Her book is likely to provoke contests of its own within sociology. Networks, she precariously claims, matter more than the revered "hard categories" of class, status, and gender. It is, however, her more modest claim that "in real life, the boundaries of hard social categories are often not as unyielding as we expect" that resonates with research on overlapping identities and the problem with locating clear lines of demarcation.

One of the excesses of our characterization of civil society is the dominance of rational debate and interest-based activities. Ikegami takes exception to this emphasis, suggesting that a wider range of activities in public space matter to political life. If political culture and the analysis of power can incorporate shared practices, aesthetics, sensuality, tacit forms of communication, and embodied forms of knowledge, we might begin to understand why people are moved to act and not just how they decide to do so.

Unable to rest comfortably with either the West or "the rest" in our new world order, Japan makes us dimly aware that something is amiss in the dichotomous topography of our times (*5*). Ikegami is right in noting that we may need a "new form of global civility" to deal with our own network revolution. Traveling outside one's own national culture is often said to improve self-knowledge. Reading Ikegami is like taking a trip through time, across social classes, and beyond the boundaries of nations. One returns convinced that art and politics, aesthetics and economics, the rational and the sensual are so deeply interwoven that we should reconsider not only our notions of pre-modern Japan but also our notions of contemporary social life—in Japan and in "the rest" as well.

References and Notes

1. C. Gluck, in *Mirror of Modernity: Invented Traditions of Modern Japan*, S. Vlastos, Ed. (Univ. California Press, Berkeley, 1998), pp. 262–284.
2. A. Barshay, in *Mirror of Modernity: Invented Traditions of Modern Japan*, S. Vlastos, Ed. (Univ. California Press, Berkeley, 1998), pp. 243–261.
3. M. S. Granovetter, *Am. J. Sociol.* **78**, 1360 (1973).
4. B. Anderson, *Imagined Communities: Reflections on the Origin and Spread of Nationalism* (Verso, London, 1983).
5. Now widely used, the framework of "the west and the rest" was developed by the political scientist Samuel P. Huntington in *The Clash of Civilizations and the Remaking of World Order* (Simon and Schuster, New York, 1996). In that work, he labels Japan a "lone country."

10.1126/science.1130749

POLITICAL SCIENCE

Determinants of Democratization

Romain Wacziarg

Economic Origins of Dictatorship and Democracy is the latest salvo in a methodological debate that promises to change the face of political science. In this superb volume, Daron Acemoglu and James A. Robinson seek to answer age-old questions in political economy: What factors, particularly economic factors, explain why some countries pass from dictatorship to democracy? What determines whether such transitions will be consolidated or whether a country will revert to rule by a small elite? Their answers, and the manner in which these were obtained, are refreshingly new.

Economic Origins of Dictatorship and Democracy

by Daron Acemoglu and James A. Robinson

Cambridge University Press, New York, 2006. 431 pp. $35, £25. ISBN 0-521-85526-8.

The book's main argument is subtle and complex, so a short summary cannot do it justice. Let me attempt one nonetheless. Suppose that a country is initially ruled by a wealthy elite that faces demands from the majority for policies that benefit the latter. The elite can respond in three basic ways: They can repress the revolutionary tendencies of the majority through violence and coercion. They can implement policies beneficial to the majority, for instance by enacting monetary transfers from the elite to the populace. Lastly, they can transfer political power to the masses by expanding the franchise, so that the majority can itself determine public policy. Which outcome will result from the struggle played out through time between the elite and the masses?

The authors being trained as economists (*1*), their answer (not surprisingly) involves consideration of the relative costs and benefits of each of the three possible outcomes.

The reviewer is at the Stanford Graduate School of Business, 518 Memorial Way, Stanford, CA 94305, USA. E-mail: wacziarg@stanford.edu

Le 28 Juillet. La Liberté guidant le peuple. Eugène Delacroix's painting (1831 Salon) celebrates the unsuccessful 28 July 1830 attempt by the people of Paris to reestablish the Republic.

CREDIT: ERICH LESSING/ART RESOURCE, NY

If repression is costly in terms of social upheaval and disruption of production, concessions will tend to be the elite's preferred option. But why not always concede to the demands of the masses by simply enacting policies that benefit them rather than by transferring political power to the majority (that is, democratizing)? The answer is that when the elite concedes on policies but not on political institutions, there is no guarantee that the policy favored by the masses won't be overturned at a later date, when pressures for social change have eased. Only by transferring de jure political power, which is much harder to reverse, can the elite demonstrate a credible commitment to a regime that delivers policies favored by the masses.

In some ways, this basic model is a formalization of Marx's dialectical materialism: Institutional change results from distributional struggles between two distinct social groups, a rich ruling class and a poor majority, each of whose interests are shaped primarily by economic forces (*2*). It goes beyond this by drawing on more recent ideas of Douglass North and Barry Weingast, who argued that institutional reform can be a way for the elite to credibly commit to future policies by delegating their enactment to interests that will not wish to reverse them (*3*). The book's substantive contribution is to bring these intellectual traditions together under a consistent theoretical framework, delivering rich empirical predictions on the factors leading to democratization and institutional stability. These factors are the economic, social, and institutional determinants of the costs and benefits of repressing versus conceding, such as the size of the middle class, the structure of production, economic inequality, the prevalence of economic shocks and crises, and the degree of globalization. Each is found to have sometimes complex, but always empirically testable, relationships with the political regime.

The next step in this research agenda is to carry out an empirical evaluation of the many hypotheses formulated by Acemoglu and Robinson. Since the early 1980s, numerous developing countries have undergone a wave of democratization, and some of them have subsequently reversed course. These changes provide fertile ground for evaluating the book's claims. Is it true, for instance, that high degrees of income inequality are not conducive to democratization? Are agricultural and resource-based countries really less likely to sustain democratization? What is the impact of globalization on the likelihood and persistence of political reforms?

The book addresses such questions primarily from a theoretical perspective, leaving the reader hungry for empirical evidence. A critical reader might also take issue with a basic premise of the authors' model: Acemoglu and Robinson assume that democratic institutions deliver policies beneficial to the masses. However, as the authors recognize, populist dictators have also been known to deliver policies beneficial to the majority, and in democracies the will of the majority can be subverted (through, e.g., corruption or vote buying) to the benefit of the elite. In fact, perhaps surprisingly, there is scant empirical evidence that greater income inequality leads to more redistribution in democratic systems. This is illustrated by the recent example of the United States, but holds more broadly across countries. A rigorous empirical evaluation of the link between democracy and redistribution therefore seems essential to evaluate the theory's relevance for real-world phenomena.

Yet providing testable theories is not the book's only contribution to scientific knowledge. Another, perhaps more important, contribution is the manner in which its central questions are approached. *Economic Origins of Dictatorship and Democracy* contributes to social science by addressing issues traditionally studied by political scientists with the rigorous tools of economic analysis. Acemoglu and Robinson use formal game theoretic models, proceeding from assumptions to empirically falsifiable predictions, in keeping with the Popperian tradition. Such an approach is relatively new to political science, in spite of that discipline's name. This is particularly true for the subdiscipline of comparative politics, which still largely relies on rhetoric and anecdotes—rather than mathematically rigorous proofs and large-sample statistical evidence—to explain social phenomena. The authors' work is an admirable illustration of a growing trend toward formal reasoning and the derivation of empirically testable propositions from internally consistent, stylized models. This is a trend that revolutionized economics starting in the middle of the last century. It is now sweeping political science, and the experience of economics suggests it is the way of the future. As it takes hold, the social sciences are bound toward greater and greater consilience.

References and Notes

1. Acemoglu is a professor of applied economics at the Massachusetts Institute of Technology; Robinson, a professor of government at Harvard University.
2. K. Marx, *A Contribution to the Critique of Political Economy* (Berlin, 1859), preface.
3. D. C. North, B. R. Weingast, *J. Econ. Hist.* **49**, 803 (1989).

10.1126/science.1131936

SOCIAL SCIENCE

Death in Darfur

Analysis of factors confounding previous estimates leads to the conclusion that hundreds of thousand of people rather than tens of thousands have died as a result of the conflict in Darfur.

John Hagan* and Alberto Palloni

The crisis of death and displacement in western Sudan began in February of 2003 and soon engulfed all three states of North, West, and South Darfur. To begin to comprehend the tragedy of the conflict and the extent of the genocide (*1*, *2*), it is necessary to have an accurate estimate of the number of deaths that occurred. Yet current estimates differ by more than an order of magnitude.

This uncertainty results from difficulties inherent in surveying a war-torn region in Africa, as well as assumptions made by agencies trying to generate estimates. There is no way, as might happen in a natural disaster, to get an accurate body count; estimates must rely on interviews. Surveys from displacement camp samples must be substituted for unavailable population-based census data; extrapolating from limited samples to an entire population at risk is problematic. A quarter-century of famine and war has reconfigured nuclear families, making sampling units in surveys problematic. Current surveys also vary in recall periods and coverage. Finally, past estimates of Darfur mortality have been based on the dubious assumption of constant numbers of deaths per month.

The initial World Health Organization (WHO) study, conducted with cooperation of the Sudanese Ministry of Health, presented crude mortality rates (CMRs) developed from sample surveys conducted in "internally displaced person" (IDP) camps (*3*). The CMRs were calculated for 2 months when respondents were mostly in the camps and past the risk of violent attacks that led to their displacement (*4*). In fall 2004, WHO based a projection that 70,000 had died in 7 months (*5*) on extrapolation of the earlier, 2-month data, under the assumption of a constant death rate. This assumption is doubtful and the underestimation of precamp violent deaths was emphasized in a British parliamentary committee report (*4*).

Early in 2005, a United Nations (U.N.) humanitarian coordinator reported that 180,000 died over 18 months (*6*)—on the basis of extrapolation from the WHO estimate (*7*). Other estimates doubled the 180,000 figure (*8*–*10*), and Kofi Annan suggested there were 300,000 deaths (*11*). Then in spring of 2005, U. S. Deputy Secretary of State Robert Zoellick reported a lower estimate of 63,000 to 146,000 "excess" deaths (*12*). Following the State Department estimate, the press largely reverted to reporting a Darfur death toll in the tens of thousands and underestimated hundreds of thousands of lost lives (*13*, *14*).

Disruption of family structures and loss of kinship boundaries make counting the dead more difficult. Refugees in an IDP camp school, Nyala, South Darfur, Sudan.

CREDIT: ZOHRA BENSEMRA/REUTERS

The State Department estimate remedied the assumption of constant monthly mortality, but introduced new issues (*15*, *16*). It drew on health surveys that were not fully identified and for which primary sources are uncertain. Monthly CMRs and risk populations were not specified. It focused on camp health problems rather than precamp violence.

The State Department estimate draws a further distinction between "excess" and "normal" or "expected" mortality under a hypothetical situation without the conflict. This generates opportunities for additional errors. The Darfur conflict has lasted more than 3 years, and in an actuarial sense, some deaths would be expected. Yet there are legal and moral difficulties in equating deaths expected in a settled population with deaths in "displacement" camps.

To address these issues, we have built an estimate from the best of the primary surveys from the West Darfur camps. All use systematic sampling, report age-specific mortality rates, and provide some information on violence. We first focus on the 19-month period when we could combine the wide coverage of the surveys by WHO in 43 West Darfur camp sites with the more detailed information gathered by Médecins Sans Frontières (MSF) in five West Darfur camps (*17*). The MSF Surveys detailed pre- and in-camp mortality. They could only ask explicit questions about precamp violence in five camps. The WHO surveys focused on in-camp mortality with limited representation of precamp violence, but with coverage of the entire state of West Darfur (*3*, *18*).

The U.N. generates humanitarian profiles of people counted in the camps and people surrounding the camps who together constitute conflict-affected people who are also in need of assistance. These counts are important to the United Nations as the basis of planning and support. The United Nations does not ask specific questions about violence, but the numbers generated are essential in calculating the population at risk, which we used to estimate the actual numbers of deaths in West Darfur. West Darfur refugees in Chad are not included in these profiles. We used a State

J. Hagan is in the Department of Sociology, Northwestern University, Evanston, IL 60208, and with the American Bar Foundation, Chicago, IL 60611, USA. A. Palloni is in the Department of Sociology, University of Wisconsin, Madison, WI 53706, USA.

*Author for correspondence. E-mail: j-hagan@northwestern.edu

Department survey and U.N. refugee camp counts to complete the estimate of the West Darfur population at risk (*1*).

We used the WHO and MSF surveys to obtain direct and indirect monthly estimates of CMRs, which respectively over- and underestimate mortality and thus are best used in combination (*19*). (Methodological details are presented in the supporting online material.) The direct method is based on CMRs calculated for all age groups in the surveys. These rates are likely upwardly biased by reports of deaths of extended, as well as nuclear family, members, because kinship boundaries often expand and become more inclusive in response to war. The indirect method counters this by relying on under-age-5 mortality rates (M5) reported in the surveys. These rates are likely downwardly biased by missing children whose entire unrepresented families have died. The indirect method uses Coale-Demeny North life tables for sub-Saharan Africa to estimate the full age distribution of mortality in the absence of wartime violence. Violence is reincorporated on the basis of the proportion of violence reported in the surveys, but the overrepresentation of young adults with low mortality outside of war is also a downward bias in the indirect method.

The figure below displays (on the left side) the upper and lower 95% bound CMRs for the direct and indirect estimates (*19*). The right side displays the upper and lower bound and midpoint number of deaths associated with these methods. The peak in the death estimates occurs later than the peak CMRs side because of the ongoing growth of the conflict-affected population associated with the expanding conflict.

We conservatively estimate 19 months of mortality in West Darfur as 49,288 (with a range from 40,850 to 67,598) by summing the means for estimated deaths between the high and low monthly figures in the right side of the figure. When the right tail of this distribution is extended to May 2006 (*18*), the total number of deaths is 65,296 in West Darfur alone, with a range from 57,506 to 85,346. This estimate covers 31 months of conflict that, as of August 2006, has been under way for 43 months. If the further 12 months of conflict were well estimated, and/or if all or most missing or disappeared persons were presumed dead, the death estimate would be much higher.

Largely as a result of this killing, more than one million individuals are now displaced or affected in West Darfur (*20*). About one million people are similarly displaced in each of the adjoining Sudanese states of North and South Darfur. If the same ratio of death to displacement applies across states, this implies that close to 200,000 deaths have occurred over 31 months in Greater Darfur. This calculation divides the difference between potential upward and downward biases of direct and indirect methods. If the high direct and low indirect bands of estimates are extended across the three Darfur states for 31 months, the range is between ~170,000 and ~255,000 estimated deaths. It is likely that the number of deaths for this conflict in Greater Darfur is higher than 200,000 individuals, and it is possible that the death toll is much higher.

Our awareness of the humanitarian catastrophe in Darfur and others like it would be much improved by regular systematic surveys in IDP camps of age-specific, pre- and in-camp mortality. Nongovernmental organizations have had great difficulty undertaking this survey work because of the conflict conditions in Darfur. Although we cannot overcome the limitations in the basic information, on the basis of the surveys available, we conclude that the death toll in Darfur is conservatively estimated to be in the hundreds of thousands rather than tens of thousands of people.

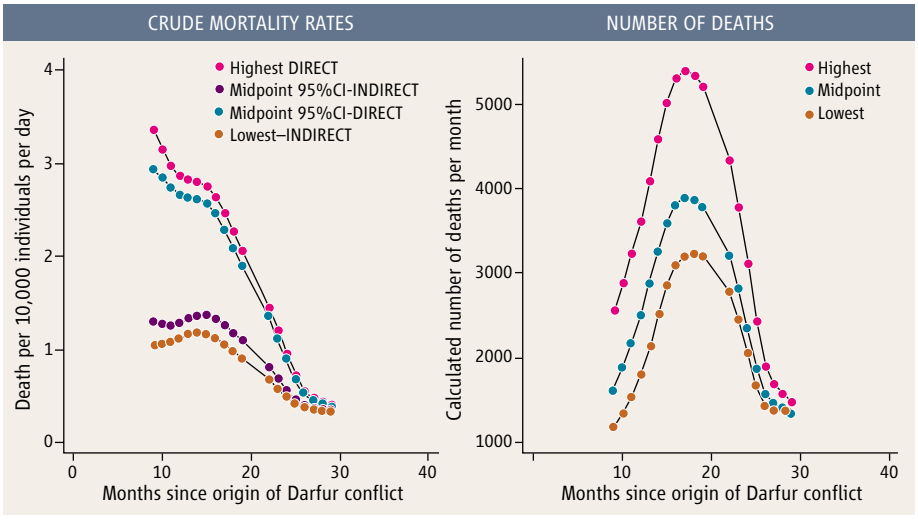

Estimated deaths during Darfur conflict. Estimated ranges for CMR and number of deaths. Direct estimates of CMR were derived from the survey material; indirect estimates were based on child mortality rates. It is likely that direct estimates of CMR are overestimates, whereas indirect estimates are underestimates; they were used in combination to produce upper and lower bounds. Numbers of deaths were calculated from the CMRs and estimates of the affected populations. For details, see text and SOM.

References and Notes

1. *Documenting Atrocities in Darfur* (U.S. Department of State Publication 11182, Bureau of Democracy, Human Rights, and Labor and Bureau of Intelligence and Research, Washington, DC, September 2004).
2. News "Excerpts: U.S. Congress resolution on Darfur," BBC News, 23 July 2004; www.cnn.com/2004/WORLD/africa/09/09/sudan.powell (accessed 11 September 2006).
3. World Health Organization (WHO), *Retrospective Mortality Survey Among the Internally Displaced Population, Greater Darfur, Sudan, August 2004* (WHO, Geneva, 15 September 2004).
4. See the conclusion of *Darfur, Sudan: The Responsibility to Protect*, in *Fifth Report of Session 2004–05* (International Development Committee, U.K. House of Commons), vol. 1, p. 11.
5. WHO Media Centre, "Mortality projections for Darfur," presented by D. Nabarro (WHO, Geneva, 15 October 2004); www.who.int/mediacentre/news/briefings/2004/mb5/en/ (accessed 6 April 2005).
6. Associated Press, "U.N. now estimates 180,000 dead in Sudan," *New York Times,* 16 March 2005.
7. WHO media briefing notes, U.N. Palais press corps, Geneva, "Mortality projections for Darfur, 15 October 2004," presented by D. Nabarro (WHO, Geneva, 2004).
8. E. Reeves, "Darfur mortality update: June 30, 2005," *Sudan Tribune*, 1 July 2005, www.sudantribune.com.
9. J. Coebergh, *Sudan: Genocide Has Killed More than Tsunami*, Parliamentary brief, February 2005, vol. 5, no. 7, p. 5.
10. J. Hagan, W. Rymond-Richmond, P. Parker, *Criminology* **43**, 525 (2005).
11. K. Annan, "Billions of promises to keep," 13 April 2005, *New York Times*, p. A29.
12. U.S. Department of State, *Sudan: Death Toll in Darfur* (Fact sheet, Bureau of Intelligence and Research, Washington, DC, March 25, 2005); www.state.gov/s/inr/rls/fs/2005/45105.htm (accessed April 26, 2005).
13. *Chronology of Reporting on Events Concerning the Conflict in Darfur, Sudan* (Coalition for International Justice, Washington, DC, and The Hague, 2006).
14. "Sudan to make its case against a U.S. force in Darfur," *New York Times*, 23 August 2006, p. A12.
15. "Darfur's real death toll," Editorial, *Washington Post*, 24 April 2005, p. B6.
16. R. Zoellick, "On Darfur, a call for the wrong action," Letter to the editor, *Washington Post*, 27 April 2005, p. A22.
17. E. Depoortere *et al.*, *Lancet* **364**, 1315 (2004).
18. WHO, Sudan Federal Ministry of Health, *Mortality Survey Among Internally Displaced Persons and Other Affected Populations in Greater Darfur, Sudan* (WHO, Geneva, September 2005).
19. We linked a bootstrapping procedure to construct 95% confidence intervals with a LOWESS regression analysis (that minimizes the impact of deviant observations) to construct the direct and indirect estimates.
20. *U.N. Darfur Humanitarian Profile No. 22*, 1 January 2006.

21. Supported by NSF grant LSS 0550299 and the American Bar Foundation. We thank G. Ferrales, P. Parker, W. Rymond-Richmond, and H. Schoenfeld for their assistance.

Supporting Online Material

www.sciencemag.org/cgi/content/full/313/5793/1578/DC1

10.1126/science.1127397

CELL BIOLOGY

A Metabolic Push to Proliferate

Liver regeneration requires a membrane protein that is involved in lipid uptake, storage, and metabolism by hepatocytes.

Dawn L. Brasaemle

Animals have remarkable abilities to respond to injuries. Within 1 week after the surgical removal of 70% of a rodent's liver, the organ can regenerate its original mass and function normally. The remaining cells of an injured liver need to obtain enough energy and building materials to support rapid cell division and tissue regrowth. This process depends on the cell's ability to metabolize fatty acids that are released from adipose tissue. On page 1628 of this issue, Fernández *et al.* (*1*) report that a common cellular protein plays a critical role in the liver's metabolic push to proliferate and regenerate.

Enhanced online at www.sciencemag.org/cgi/content/full/313/5793/1581

An injured liver produces cytokine signals that trigger the release of fatty acids from adipose tissue into circulation. These fatty acids are taken up by hepatocytes where they are esterified and stored as triacylglycerols in large lipid droplets before ultimately being metabolized (*2*). Fernández *et al.* show that mice genetically altered to lack the protein caveolin-1 had impaired liver regeneration (after a partial hepatectomy) and reduced survival under normal diet conditions. Residual hepatocytes failed to accumulate large lipid droplets and cell division stalled, leading to the death of most animals within 72 hours. By contrast, when caveolin-1 null mice were fed large amounts of dietary glucose before and after hepatectomy, the animals displayed nearly normal liver regeneration and survival.

Caveolins have been extensively characterized as major protein components of caveolae, flask-shaped invaginations of animal cell plasma membranes. Caveolin-1 and -2 are expressed in most cell types, whereas caveolin-3 is expressed primarily in cardiac, skeletal, and smooth muscle (*3*). Several functions have been ascribed to caveolins, including maintenance of caveolar structure, mediation of endocytosis and transcytosis of molecules attached to the cell surface, organization of signaling proteins, and less well understood roles in cellular cholesterol homeostasis and fatty acid transport.

How does caveolin-1 regulate lipid metabolism in hepatocytes? Fatty acids likely transit across the hepatocyte plasma membrane both by simple diffusion and with the assistance of putative membrane-associated fatty acid transporters, one of which is caveolin-1. Another putative fatty acid transporter, CD36/FAT, also localizes to caveolae (*4*). Furthermore, the disruption of caveolae by depleting membrane cholesterol or by inhibiting caveolin expression or function reduces the uptake of fatty acids into cells (*4*) Conversely, overexpression of caveolin-1 increases the cholesterol content of the plasma membrane and fatty acid uptake into cultured cells (*5*), although it is not clear whether caveolin-1 is directly involved in fatty acid transport in this case.

The precise molecular mechanisms of fatty acid uptake remain controversial. However, it is generally accepted that net uptake is coupled to intracellular metabolism of fatty acids (see the figure). The rapid synthesis of fatty acyl–coenzyme A (CoA) traps fatty acids inside the cell and creates a "sink," thereby increasing subsequent uptake of free fatty acids (*6*). The fatty acyl-CoAs are used to synthesize phospholipids and triacylglycerols, further promoting uptake of fatty acids. Interestingly, overexpression of enzymes in these biosynthetic pathways increases net uptake by promoting metabolism of fatty acids (*6*). Fernández *et al.* show that the livers of caveolin-1 null mice fail to store triacylglycerol in lipid droplets after partial hepatectomy. When fatty acids were provided as the major carbon source in the absence of glucose, caveolin-1 null hepatocytes failed to accumulate lipid droplets or divide, whereas wild-type hepatocytes displayed normal cell division. The short-term uptake of a fluorescent fatty acid analog was comparable in caveolin-1 null and wild-type hepatocytes (*1*). However, this analog is poorly metabolized and does not accurately measure prolonged fatty acid import that is coupled to metabolism (*6*). Thus, although the initial fatty acid import step may be intact, caveolin-1 null hepatocytes have impaired fatty acid metabolism.

Most studies to date have focused on functions of caveolins localized to plasma membrane or endosomes. But caveolins also associate with cytoplasmic lipid droplets under a variety of conditions, including treatment of cultured cells with fatty acids (*7*) and partial hepatectomy (*8*). The transient increase in caveolin-1 content of lipid droplets in hepatocytes may alter triacylglycerol catabolism. These triacylglycerol stores play an important role in liver regeneration (*9*). Their hydrolysis by cytosolic lipases releases fatty acids for mitochondrial β-oxidation, which is coupled to the production of adenosine 5′-triphosphate (ATP). Additionally, fatty acids and partially hydrolyzed lipids are ready substrates for the biosynthesis of membrane phospholipids that are required to support rapid cell division. The reduced triacylglycerol accumulation in caveolin-1 null hepatocytes after partial hepatectomy (*1*) may imply more rapid turnover of triacylglycerols in the absence of lipid

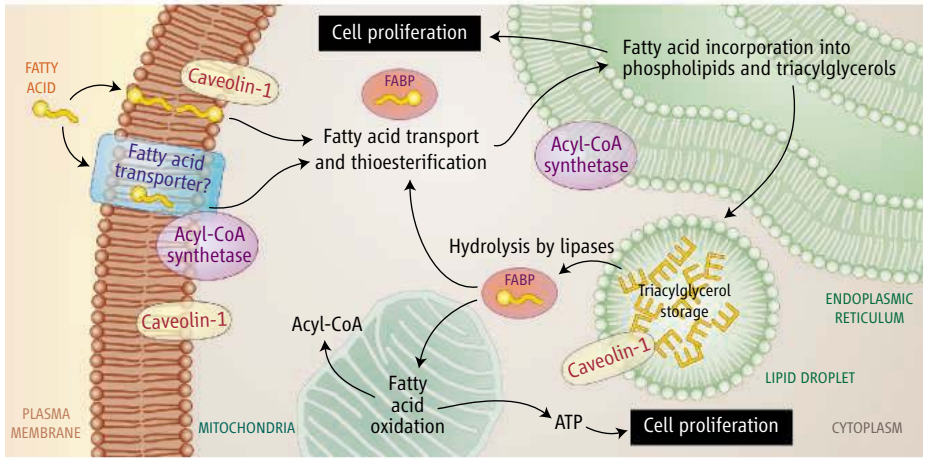

CREDIT: P. HUEY/*SCIENCE*

Lipid metabolism during liver regeneration. Fatty acids released from adipose tissue are delivered to hepatocytes, where they are stored and metabolized to support membrane synthesis and cell proliferation. Caveolin-1 may be involved in one or more stages of this process. FABP, fatty acid binding protein.

The author is in the Department of Nutritional Sciences, Rutgers, The State University of New Jersey, New Brunswick, NJ 08901, USA E-mail: brasaemle@aesop.rutgers.edu

droplet–associated caveolin-1. Increased triacylglycerol hydrolysis would likely restrict further uptake of fatty acids into the cell, but would also produce larger amounts of fatty acids available for β-oxidation and energy production. Importantly, a transient increase in liver triacylglycerol levels in glucose-fed caveolin-1 null mice suggests that metabolic pathways for the synthesis and catabolism of triacylglycerols are intact. Furthermore, phospholipid biosynthesis was sufficient to support membrane synthesis required for cell division and liver regeneration when glucose was provided. Thus, the current data best support a role for caveolin-1 in the accumulation, but not the hydrolysis, of triacylglycerols.

Clearly, the hepatocytes of caveolin-1 null mice display a major disruption in the utilization of circulating fatty acids. Further experimentation is required to understand the role that caveolin-1 plays in the uptake or metabolism of fatty acids, and whether the site of action is at the plasma membrane or the lipid droplet. An additional contributing factor may be the role that caveolins play in modulating cell signaling processes such as the response to insulin that controls carbohydrate and lipid metabolism in the liver, and throughout the body.

References and Notes

1. M. A. Fernández *et al.*, *Science* **313**, 1628 (2006).
2. G. C. Farrell, *Hepatology* **40**, 1252 (2004).
3. A. W. Cohen *et al.*, *Physiol. Rev.* **84**, 1341 (2004).
4. R. Ehehalt *et al.*, *Mol. Cell. Biochem.* **284**, 135 (2006).
5. T. Meshulam *et al.*, *Biochemistry* **45**, 2882 (2006).
6. D. G. Mashek, R. A. Coleman, *Curr. Opin. Lipidol.* **17**, 274 (2006).
7. S. Martin, R.G. Parton, *Semin. Cell Dev. Biol.* **16**, 163 (2005).
8. A. Pol *et al.*, *Mol. Biol. Cell* **15**, 99 (2004).
9. E. Shteyer *et al.*, *Hepatology* **40**, 1322 (2004).
10. I thank J. Storch and N. Wolins for useful discussions and critical review. Supported by the American Heart Association and the NIH.

10.1126/science.1133253

PLANETARY SCIENCE

Titan's Polar Weather

The discovery of ethane clouds on Saturn's moon Titan provides insight into complex planetary atmospheres.

F. M. Flasar

To the eye, Saturn's largest moon is enshrouded in a thick, reddish-brown photochemical smog. Like Earth, Titan's atmosphere is primarily nitrogen, but its second most abundant constituent is methane, not oxygen. Ultraviolet sunlight and energetic electrons streaming in from Saturn's magnetosphere act directly and indirectly to dissociate methane and nitrogen and form a suite of organic molecules, both hydrocarbons (molecules composed of hydrogen and carbon) and nitriles (molecules containing carbon and nitrogen linked by a triple bond). These organic molecules react to produce more complex and heavier molecules and ultimately the photochemical hazes that envelop the moon, although much of the detail remains obscure. As Griffith *et al*. report on page 1620 of this issue (*1*), detection of a vast ethane cloud in Titan's arctic region is another step in unraveling the complex nature of its atmosphere.

Titan's temperatures are cold, as low as 70 K at the tropopause, which marks the boundary between the troposphere and stratosphere. Many of the organic molecules condense at these temperatures, but only a few have been directly identified. Sporadic brightenings, seen in near-infrared images from ground-based telescopes and the Cassini orbiter (*2*–*4*), have been interpreted as methane itself condensing in the troposphere. These clouds form where there is convective activity under summertime conditions. Most other types of condensates, however, have been observed in Titan's north polar stratosphere when temperatures there have been coldest. They have been identified in far-infrared spectra obtained with the Voyager and Cassini spacecraft. The Voyagers flew past Titan in 1980–1981, when it was early northern spring, and Cassini is currently orbiting in northern winter. So far, the nitriles C_4N_2 (dicyanoacetylene) and HC_3N (cyanoacetylene) have been identified as condensed ices (*5*, *6*), and tentative identifications of solid C_2H_2 (acetylene) and C_2H_5CN (propionitrile) have been made (*6*, *7*).

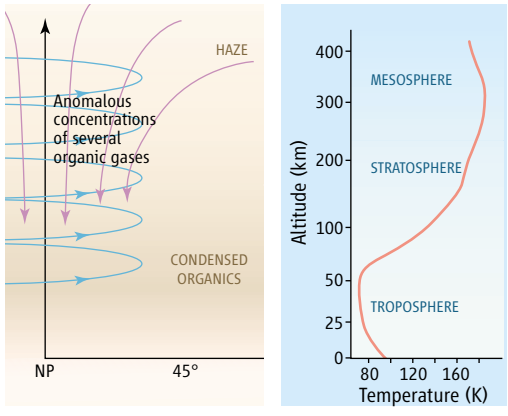

Smog patterns. (**Left**) Schematic of atmospheric circulation and (**right**) thermal structure in Titan's north polar region in winter and early spring. The sinking flow pattern at the pole may explain the enhanced abundance of organic species in Titan's stratosphere.

What occurs at high-northern latitudes is more complicated than just seasonal cooling, and it likely involves both chemistry and atmospheric transports. The cold polar temperatures in winter and early spring imply that strong winds blow around the pole (*8*). In addition, infrared measurements from both Voyager and Cassini show that the abundances of several organic gases in the stratosphere are greater at high northern latitudes than elsewhere (*8*, *9*). Because much of the formation of nitriles and hydrocarbons (other than methane) occurs higher in Titan's atmosphere, the concentration of many of these gases increases with altitude. Thus, subsiding air above the north pole could explain the enhancement observed in the data (see the figure). On Earth, the meridional circulation in the stratosphere and mesosphere subsides over the winter pole (*10*–*12*). In fact, global circulation models of Titan (*13*, *14*), based on terrestrial codes, also predict subsidence over its winter pole.

The situation on Earth may help elucidate the complex situation that seems to exist on Titan. The mean meridional winds in Earth's stratosphere and overlying mesosphere are slow, and they do not transport heat and constituents very efficiently. Normally, this transport is effected by planetary-scale waves. The stratosphere over the winter poles is in darkness and cold. As a consequence of the strong circumpolar winds that are associated with the low polar temperatures, the polar airmass is isolated. The strong winds about the winter pole inhibit the rapid mixing of cold polar air with warmer air at lower latitudes by planetary waves (*10*). This allows the radiative cooling of the polar stratosphere to continue unabated and polar stratospheric clouds to form in a normally dry environment. There is a slow cross-equatorial global circulation,

The author is in the Planetary Systems Laboratory, NASA Goddard Spaceflight Center, Greenbelt, MD 20771, USA. E-mail: f.m.flasar@nasa.gov

with a sinking motion over the winter pole. This descent causes the concentration of several species, such as N_2O (nitrous oxide), methane, and HF (hydrogen fluoride) to be more nearly that of the mesosphere instead of the stratosphere outside the vortex (*11*, *12*).

The terrestrial polar stratospheric clouds are an essential ingredient for the ozone hole. Normally, chlorine in the stratosphere (from chlorofluorocarbons) is locked in stable reservoirs, such as $ClONO_2$ and HF. However, in the presence of cloud particles, these react to form HNO_3 (nitric acid) and Cl_2. The cloud particles remove the nitric acid by embedding it in trihydrate particles—$HNO_3 \cdot 3H_2O$—thereby denitrifying the polar atmosphere and preventing the stable reservoirs of chlorine from re-forming. When the sun returns with spring to the poles, the Cl_2 dissociates and atomic chlorine readily destroys ozone (*10*). None of this could have happened except for the strong circumpolar vortex, which isolates the polar air, allowing it to become cold enough for the stratospheric clouds to form. As spring progresses and sunlight warms the pole, the circumpolar winds weaken and planetary-scale waves erode and finally disrupt the vortex.

Titan has a moderately reducing atmosphere and different chemistry from Earth, but the question of whether a similarly complex phenomenon occurs is intriguing. Certainly there are several similarities: cold polar temperatures, strong circumpolar winds, concentration differences in several organic compounds that seem consistent with isolation, and condensates. Yet, the importance of surface chemistry involving organic gases and cloud and haze particles in the polar regions is not well understood. Moreover, planetary waves have not yet been detected. In fact, on a slowly rotating body such as Titan with its 16-day period, the natural scale of these waves may be too large to fit into an atmosphere on a body with only a 2575-km radius (*15*). However, other classes of waves, such as smaller scale internal gravity waves, may play a role similar to planetary waves on Earth. Questions like these need to be examined, with data and modeling.

Until now, clouds of the most abundant product of methane dissociation, ethane, have eluded detection. The Griffith *et al.* identification of polar ethane clouds is reassuring, in that it validates the basic ideas we have about Titan's meteorology and chemistry: first, that condensation does occur, as expected, in the lower stratosphere, and second, that the inferred altitudes of the ethane cloud (30 to 50 km) are consistent with subsidence in the winter polar region. This and other clues that we will obtain will help us to sort out the things we still puzzle over.

References

1. C. A. Griffith *et al.*, *Science* **313**, 1620 (2006).
2. M. E. Brown, A. H. Bouchez, C. A. Griffith, *Nature* **420**, 795 (2002).
3. H. G. Roe *et al.*, *Astrophys. J.* **581**, 1399 (2002).
4. C. A. Griffith *et al.*, *Science* **310**, 474 (2005).
5. R. E. Samuelson *et al.*, *Planet. Space Sci.* **45**, 941 (1997).
6. R. K. Khanna, *Icarus* **178**, 165 (2005).
7. R. K. Khanna, *Icarus* **177**, 116 (2005).
8. F. M. Flasar *et al.*, *Science* **308**, 975 (2005).
9. A. C. Coustenis, B. Bézard, *Icarus* **115**, 126 (1995).
10. M. R. Schoeberl, D. L. Hartmann, *Science* **251**, 46 (1991).
11. M. C. Abrams *et al.*, *Geophys. Res. Lett.* **23**, 2341 (1996).
12. M. C. Abrams *et al.*, *Geophys. Res. Lett.* **23**, 2345 (1996).
13. S. Lebonnois *et al.*, *Icarus* **152**, 384 (2001).
14. F. Hourdin *et al.*, *J. Geophys. Res.* **109**, E12005, 10.1029/2004JE002282 (2004).
15. C. B. Leovy, J. B. Pollack, *Icarus* **19**, 195 (1973).

10.1126/science.1130698

MICROBIOLOGY

Mycobacteria's Export Strategy

Identification of targeting sequences needed for secretion of the virulence proteins encoded by mycobacteria has potential applications for the design of live, attenuated vaccines.

Bérengère Ize and Tracy Palmer

Tuberculosis has probably killed more humans than any other disease in history, and on average four people die of this disease every minute around the world (*1*). The causative agent, *Mycobacterium tuberculosis*, is a Gram-positive bacterium that can lie dormant in the body for decades before reawakening to cause acute disease. One of the major ways that bacteria subvert host defenses is by secreting virulence proteins. Indeed, pathogenic bacteria have evolved a number of elaborate transport machines whose sole function is to deliver such factors into the host, often carefully timed to hit the right place at the right time. Recently, a new protein secretion pathway, ESX-1 (ESAT-6 system-1) or Snm (secretion in mycobacteria), was discovered in *M. tuberculosis* (*2*–*5*), and is present in many other Gram-positive bacteria (*6*). This discovery has challenged our knowledge of the organism and more generally of protein secretion in prokaryotes. On page 1632 of this issue, DiGiuseppe Champion *et al.* (*7*) identify the first targeting signal that promotes protein secretion by this pathway.

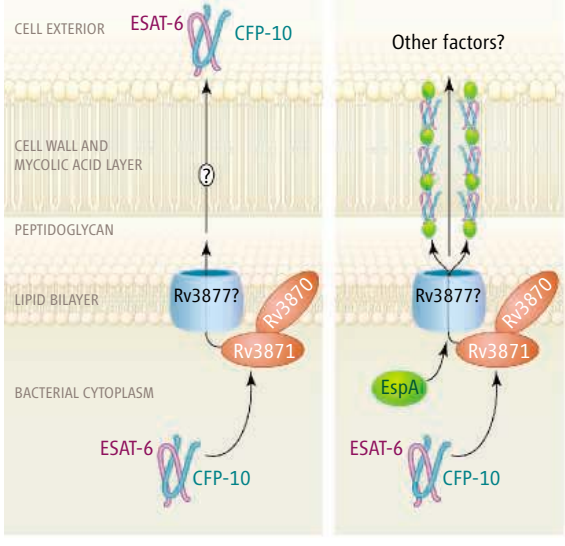

Exporting virulence factors. (Left) In one model, the ESAT-6–CFP-10 dimer of virulence factors binds to the Rv3871 component of the secretion machinery by means of the carboxyl-terminal peptide on CFP-10. The complex moves to the transport channel, presumably Rv3877. Functions of the other essential secretion components [Rv3870; Rv3868 and Rv3869 (not shown)] are not known. **(Right)** Alternatively, ESAT-6, CFP-10, and the bacterial protein EspA may form a conduit to the cell surface, allowing the passage of other bacterial proteins (*15*).

Protein delivery during infection is relatively well understood for Gram-negative bacterial pathogens, which possess one or more specialized protein transport systems (numbered Type I to Type VI). These types of export pathways are encoded on so-called pathogenicity islands, regions of the genome that are associated with virulence. Protein secretion in Gram-negative bacteria is partic-

The authors are with the School of Biological Sciences, University of East Anglia, Norwich NR4 7TJ, UK and the Department of Molecular Microbiology, John Innes Centre, Norwich NR4 7UH, UK. E-mail: tracy.palmer@bbsrc.ac.uk

ularly complex because they are bounded by two lipid bilayers, and their proteins must pass through both of these hydrophobic barriers to reach host cells. Gram-positive bacteria are generally simpler in structure in that they lack the second lipid bilayer, yet surprisingly, our understanding of virulence factor secretion in these organisms is rudimentary. Although they have been known to lack the canonical Type I to Type VI systems of Gram-negative bacteria, it was only recently that the ESX-1 system was discovered.

A large number of low molecular weight proteins are secreted by *M. tuberculosis* when the bacteria are cultured in vitro. Two of these are potent immune response elicitors—early secreted antigenic target–6 (ESAT-6) and culture filtrate antigen 10 kD (CFP-10). These proteins form a heterodimer and secretion of ESAT-6 depends on the presence of CFP-10 (*4*, *8*, *9*). The genes encoding both antigens are localized on the region of difference 1 (RD1). RD1 encompasses most of a 15-gene cluster called ESX-1, which is duplicated a number of times in the *M. tuberculosis* genome (*10*). It is also a part of the *M. tuberculosis* genome that is absent from the attenuated *M. bovis* bacillus Calmette-Guérin (BCG) or the avirulent *M. microtii* strains (*11*, *12*).

At least five genes encoded within the ESX-1 cluster, *Rv3868* through *Rv3871* and *Rv3877*, are required for secretion of ESAT-6 and CFP-10 (*3*–*5*, *13*). *Rv3877* encodes a transmembrane protein that may form all or part of a channel. *Rv3869* also encodes a membrane-associated protein (see the figure). *Rv3868*, *Rv3870*, and *Rv3871* encode ATPases (adenosine triphosphatases) that may transduce the energy of ATP hydrolysis into mechanical work. CFP-10, but not ESAT-6, interacts with the ATPase Rv3871 (*4*).

The study by DiGiuseppe Champion *et al*. takes a large step toward elucidating the means by which CFP-10 and ESAT-6 are targeted for secretion. The authors constructed truncations and single–amino acid variants in the CFP-10 protein to define the regions important for associating with ESAT-6 and Rv3871. Interaction with Rv3871 is mediated by the carboxyl-terminal seven amino acids of CFP-10. Specific substitution of residues in this region abolished this association, but did not affect complex formation with ESAT-6, showing that these interactions are separable. The same substitutions also abolished secretion of CFP-10, suggesting that its interaction with Rv3871 is a prerequisite for export. Remarkably, mutations in CFP-10 that abolished its secretion also completely blocked export of ESAT-6, implying that both proteins are targeted to the secretion machinery as a complex. Moreover, the nuclear magnetic resonance solution structure of the ESAT-6–CFP-10 complex reveals extensive contacts between the two proteins, but that the carboxyl-terminal 15 amino acids of CFP-10 extend from the complex and adopt an α-helical structure (*14*). An open question that arises from the DiGiuseppe Champion *et al.* study is whether ESAT-6 and CFP-10 are secreted as a folded protein complex or whether one or more of the essential ATPases is required to tear the complex apart before export, allowing each protein to be secreted separately.

DiGiuseppe Champion *et al*. further demonstrate that when the key seven amino acids of CFP-10 are amended to another protein, the protein is exported from bacteria. Thus, the signal is portable and can target the secretion of heterologous proteins. This is of particular interest because it may provide a means to engineer more effective live attenuated vaccines. It has long been known that vaccination with BCG is effective only when administered live, suggesting that active secretion is necessary to generate an effective immune response. Enhanced secretion of antigens by engineering of the ESX-1 secretion system may therefore ultimately provide a mechanism for boosting protection against tuberculosis.

References

1. World Health Organization Fact Sheet (www.wpro.who.int/media_centre/fact_sheets/fs_20050324.htm).
2. A. S. Pym *et al.*, *Nat. Med.* **9**, 533 (2003).
3. T. Hsu *et al.*, *Proc. Natl. Acad. Sci. U.S.A.* **100**, 12420 (2003).
4. S. A. Stanley, S. Raghavan, W. W. Hwang, J. S. Cox, *Proc. Natl. Acad. Sci. U.S.A.* **100**, 13001 (2003).
5. K. M. Guinn *et al.*, *Mol. Microbiol.* **51**, 359 (2004).
6. M. J. Pallen, *Trends Microbiol.* **10**, 209 (2002).
7. P. A. DiGiuseppe Champion, S. A. Stanley, M. M. Champion, E. J. Brown, J. S. Cox, *Science* **313**, 1632 (2006).
8. P. S. Renshaw *et al.*, *J. Biol. Chem.* **277**, 21598 (2002).
9. P. Brodin *et al.*, *J. Biol. Chem.* **280**, 33953 (2005).
10. S. T. Cole *et al.*, *Nature* **393**, 537 (1998).
11. G. G. Mahairas *et al.*, *J. Bacteriol.* **178**, 1274 (1996).
12. A. S. Pym *et al.*, *Mol. Microbiol.* **46**, 709 (2002).
13. P. Brodin *et al.*, *Infect. Immun.* **74**, 88 (2006).
14. P. S. Renshaw *et al.*, *EMBO J.* **24**, 2491 (2005).
15. S. M. Fortune *et al.*, *Proc. Natl. Acad. Sci. U.S.A.* **102**, 10676 (2005).

10.1126/science.1132537

CHEMISTRY

The Organic Approach to Asymmetric Catalysis

Benjamin List and Jung Woon Yang

Small organic molecules are increasingly used as asymmetric catalysts, complementing the enzymes and metal complexes traditionally used to make chiral products.

When chemists make chiral compounds—molecules that behave like object and mirror image, such as amino acids, sugars, drugs, or nucleic acids—they like to use asymmetric catalysis, in which a chiral catalyst selectively accelerates the reaction that leads to one mirror-image isomer, also called enantiomer. For example, the "Monsanto process" uses a chiral rhodium catalyst to synthesize the drug L-dopa, used to treat Parkinson's disease (*1*).

For decades, the generally accepted view has been that there are two classes of efficient asymmetric catalysts: enzymes and synthetic metal complexes (*2*). However, this view is currently being challenged, with purely organic catalysts emerging as a third class of powerful asymmetric catalysts.

Most biological molecules are chiral and are synthesized in living cells by enzymes using asymmetric catalysis. Chemists also use enzymes or even whole cells to synthesize chiral compounds. Such biological catalysis is increasingly used on an industrial scale and is particularly preferred in hydrolytic reactions. The other class of accepted and efficient chiral catalysts, metal complexes, are reagents based on inorganic chemistry. Transition metal catalysts are particularly useful for asymmetric hydrogenations, but may leave possibly toxic traces of heavy metals in the product.

In contrast, in organocatalysis, a purely organic and metal-free small molecule is used to catalyze a chemical reaction. In

The authors are at the Max-Planck Institut für Kohlenforschung, 45470 Mülheim an der Ruhr, Germany. E-mail: list@mpi-muelheim.mpg.de

addition to enriching chemistry with another useful strategy for catalysis, this approach has some important advantages. Small organic molecule catalysts are generally stable and fairly easy to design and synthesize. They are often based on nontoxic compounds, such as sugars, peptides, or even amino acids, and can easily be linked to a solid support, making them useful for industrial applications. However, the property of organocatalysts most attractive to organic chemists may be the simple fact that they are organic molecules.

Organocatalysts have been used sporadically throughout the last century; indeed, an organic catalyst was used in one of the very first examples of a nonenzymatic asymmetric catalytic reaction (*3*). But recently, this area has grown at a breathtaking pace. Within a few years, powerful organocatalysts for a wide range of reactions have been designed and developed (*4*–*6*).

A particularly appealing discovery of great potential is the use of chiral Brønsted acids as organocatalysts. Organic Brønsted acids function by donating a proton to the substrate. They have been used as catalysts for a variety of reactions since the beginnings of modern chemistry, but applications in asymmetric catalysis have been extremely rare. A breakthrough in this area came when Jacobsen *et al.* developed highly active Brønsted acid organocatalysts that incorporate a urea motif as the active principle (*7*).

One powerful application of these catalysts is in the Strecker reaction (*7*, *8*), one of the most general and useful ways to make enantiomerically pure amino acids (see the figure, top). In this transformation, hydrogen cyanide reacts with imines (which contain a carbon-nitrogen double bond). In the presence of the Jacobsen urea catalyst, amino nitriles are obtained in high enantiomeric ratios (er; this is the ratio of the two mirror image isomers); hydrolysis of these compounds yields valuable amino acids. This type of catalysis, in which the catalyst donates a hydrogen bond to a reactive intermediate, is very common in enzymes, but only became a powerful tool for asymmetric organocatalysis through the work of Jacobsen and co-workers (*7*, *8*).

Akiyama *et al.* recently developed even stronger Brønsted acids based on the phosphoric acid motif. These acids catalyze reactions such as the hetero-Diels-Alder reaction between imines and dienes (the latter contain two carbon-carbon double bonds) (see the figure, middle) (*9*). The resulting cyclic molecules are of interest in drug development. Independently, Terada *et al.* have recently shown that such phosphoric acid catalysts are highly active and have the potential of becoming as efficient as even the most active metal- or biocatalysts (*10*).

Yet, there is more to organocatalysis than Brønsted acids. Lewis base organocatalysis, in which the catalyst donates not protons but electrons to the substrate, is another very actively researched area. Catalysts include amines, phosphines, and even carbenes. The amino acid proline is an exceptionally simple yet versatile amine catalyst and has attracted a lot of attention (*11*, *12*). Another useful example of amine-catalyzed reactions was recently published by Maruoka and co-workers. (*13*). This group has designed a highly active and selective catalyst for the Mannich reaction, which also involves imines (see the figure, bottom). The catalyst activates aldehydes (widely used organic substrates that contain a carbon-oxygen double bond) to react with imines to give useful intermediates for the synthesis of biologically active compounds.

The reactions discussed here are just a small subset of the increasing number of highly selective and efficient organocatalytic transformations. Finally, an organic approach to asymmetric catalysis that allows organic chemists to design and to understand their catalysts themselves is at hand. Organocatalysis complements the traditional and highly developed inorganic and biological approaches to asymmetric catalysis. Because of its many attractive features, applications in the pharma-

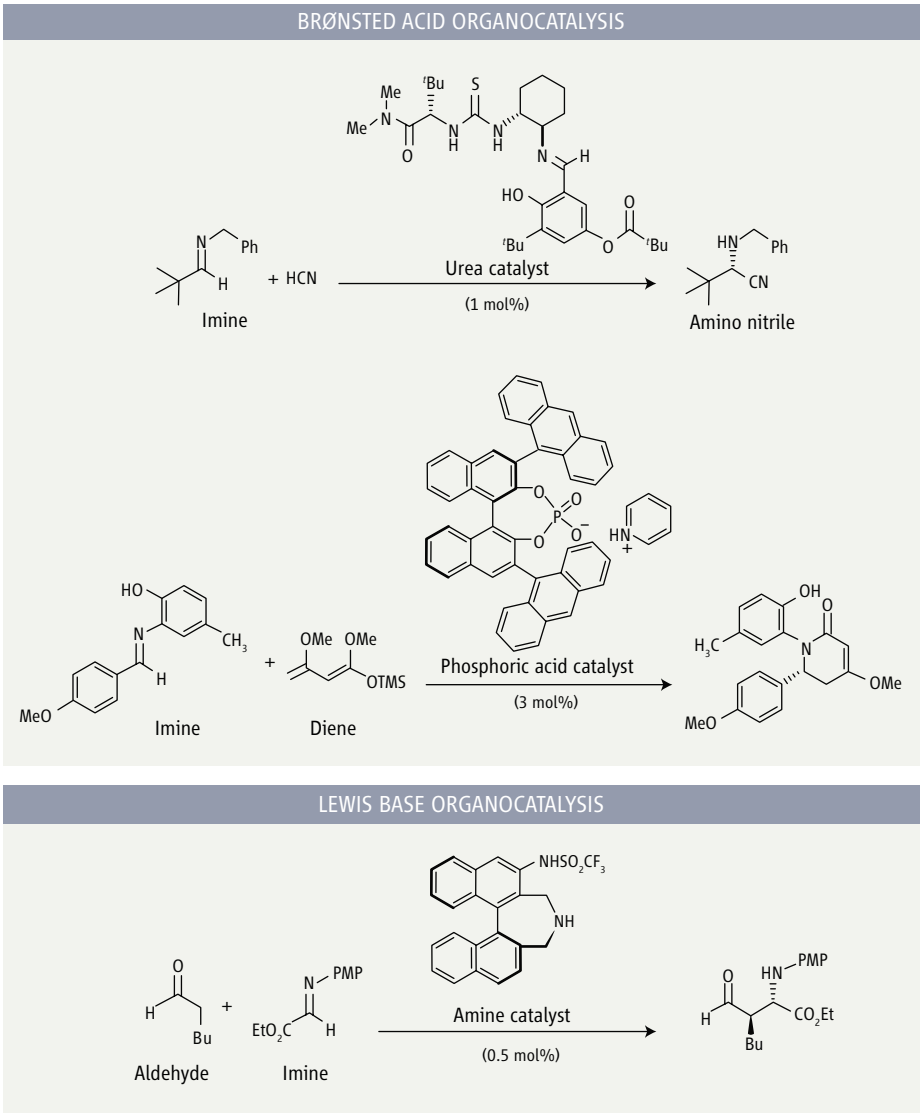

Powerful organocatalysts. In the emerging field of organocatalysis, Brønsted acid organocatalysts (**top**, **middle**) and Lewis base organocatalysts (**bottom**) have received particular attention. The reactions shown have enantiomeric ratios of at least 98.5:1.5.

ceutical industry can be expected. There is little doubt that organocatalysis is here to stay.

References and Notes

1. W. S. Knowles, *Adv. Synth. Cat.* **345**, 3 (2003).
2. K. C. Nicolaou, E. J. Sorensen, *Classics in Total Synthesis* (Wiley-VCH, Weinheim, 1996), p. 344.
3. G. Bredig, P. S. Fiske, *Biochem. Z.* **46**, 7 (1912).
4. A. Berkessel, H. Gröger, *Asymmetric Organocatalysis* (VCH, Weinheim, Germany, 2005).
5. A. B. Northrup, D. W. C. MacMillan, *Science* **305**, 1752 (2004).
6. D. Enders, M. R. M. Hüttl, C. Grondal, G. Raabe, *Nature* **441**, 861 (2006).
7. M. S. Taylor, E. N. Jacobsen, *Angew. Chem. Int. Ed.* **45**, 1520 (2006).
8. P. Vachal, E. N. Jacobsen, *J. Am. Chem. Soc.* **124**, 10012 (2002).
9. J. Itoh, K. Fuchibe, T. Akiyama, *Angew. Chem. Int. Ed.* **45**, 4796 (2006).
10. M. Terada, K. Machioka, K. Sorimachi, *Angew. Chem. Int. Ed.* **45**, 2254 (2006).
11. B. List, R. A. Lerner, C. F. Barbas III, *J. Am. Chem. Soc.* **122**, 2395 (2000).
12. M. Movassaghi, E. N. Jacobsen, *Science* **298**, 1904 (2002).
13. T. Kano, Y. Yamaguchi, O. Tokuda, K. Maruoka, *J. Am. Chem. Soc.* **127**, 16408 (2005).

10.1126/science.1131945

STRUCTURAL BIOLOGY

Dynamic Visions of Enzymatic Reactions

Experimental evidence is provoking further discussion of a stochastic view of protein behavior.

Michele Vendruscolo and Christopher M. Dobson

The action of many proteins involves large-scale conformational changes that typically take place on the millisecond time scale. Examples include the cooperative transitions that enable efficient oxygen transport by hemoglobin in the blood, and the series of motions involved in muscle contraction (*1*). But even proteins that do not undergo such dramatic conformational excursions are not the rigid objects that structural models often imply. The conformations of all proteins constantly fluctuate, with some motions taking place on time scales of a picosecond or less and involving displacements in atomic positions of ~0.1 nm (*1*–*6*) .

Are these motions simply inherent properties of molecules held together by relatively weak interactions, or have they evolved to enhance their functional efficiency? There is increasing evidence that both views may in fact have validity and that biology has channeled the inherent motions of proteins into directions that enhance their effectiveness. For example, structural fluctuations of enzymes appear to increase the probability of binding certain ligands, although more studies are needed to establish their effects on the catalytic rates themselves. On page 1638 of this issue, Boehr *et al*. (*7*) report experimental evidence that is interpreted in terms of this view of enzymology. They also indicate that many fluctuations can be linked together into whole reaction cycles that carry out a complex chemical process with great efficacy.

In recent years, the idea that random conformational fluctuations of proteins are channeled into productive events has gained popularity. This concept is rooted in a statistical view that has revolutionized, for example, our understanding of protein folding (*1*, *2*, *8*–*10*), a process now perceived not as a deterministic sequence of well-defined conformations, but rather in terms of stochastic events along free-energy landscapes that funnel the molecular fluctuations toward their native structures. The "jigglings and wigglings" of protein molecules anticipated by Feynman (*11*) appear therefore to have been harnessed for specific purposes during molecular evolution.

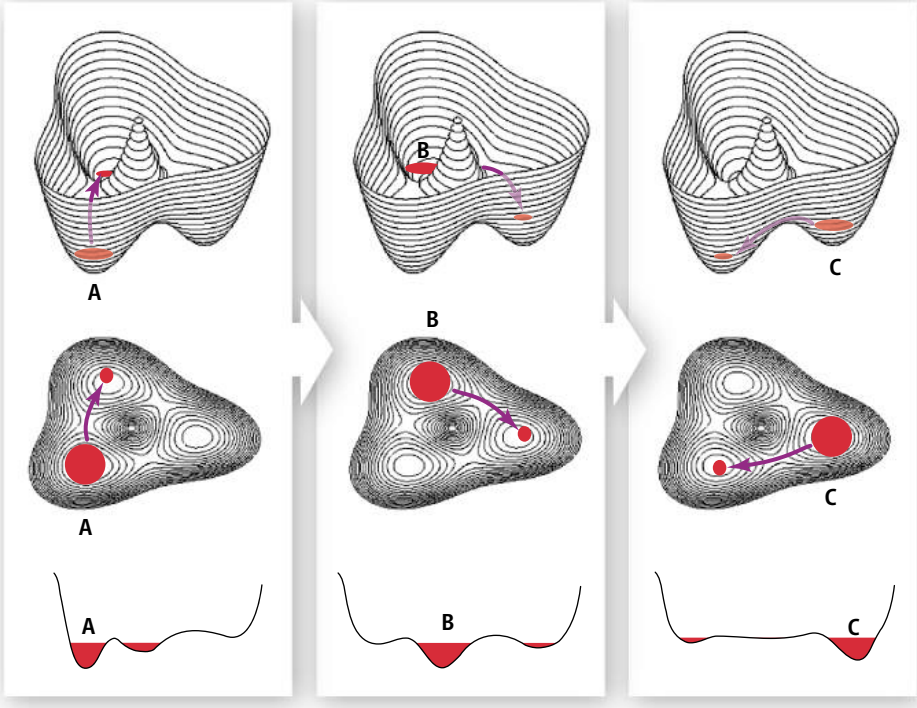

A free-energy channel model for enzymatic behavior. The binding of a ligand shifts the predominant population of enzyme molecules from the free state (**A**) to a bound state (**B**) that was previously sampled transiently through stochastic fluctuations. Further conformational fluctuations from **B** enable the catalytic state (**C**) to be accessed. When the enzyme returns to state **A**, the cycle can begin again.

Application of this statistical view to enzyme behavior suggests that conformational fluctuations resulting from the concerted motions of many atoms can push the unbound states of enzymes into conformations closely resembling the bound states, thereby priming them to form complexes with specific ligands (*5*, *12*, *13*). Thus, although the unbound state of a protein is inherently flexible, fluctuations are not random. Rather, they take place preferentially in a way that prepares the protein to bind to its cofactors and substrates. The free-energy landscapes of the free and the bound states differ just enough to cause changes in the relative populations of their principal states. After binding, the free-energy landscape (*7*) is plastically deformed just enough to make a slightly different state of the protein become the most populated (see the figure).

Boehr *et al*. suggest that certain enzymes can combine flexibility with plasticity to

The authors are in the Department of Chemistry, University of Cambridge, Lensfield Road, Cambridge CB2 1EW, UK

achieve a sophisticated series of changes in structure and dynamics. According to this view, for each state along the enzymatic cycle of dihydrofolate reductase (DHFR) (*14*), a binding event can cause a protein molecule to occupy a new free-energy minimum (see the figure), stabilized by a ligand and geared to fluctuate toward another state that binds the next ligand in the catalytic cycle. The five successive steps of such transitions that exist in DHFR would thus show just how effectively evolution can coordinate the thermal motion of hundreds of atoms to perform biological functions.

If this view turns out to be correct, then the free-energy landscapes of enzymes would not just be funnels; rather, they would appear more as a set of coupled low-energy states. In the case of catalytic cycles, these free-energy landscapes could be merged into rings that resemble perhaps rather battered sombreros (see the figure). Such a shape can be created by stringing together several free-energy funnels, one for each of the structurally quite similar states along the catalytic cycle. The alignment of these funnels could result in a channeling mechanism that generates the complex motions required for enzymatic activity by breaking them down into simpler ones that are closely coupled to each other.

Although much remains to be learned, this free-energy channel model may be the result of a general type of free-energy surface characterized by statistical pathways that enable the performance and regulation of catalytic reactions by a succession of binding events. Increasingly complex reactions could be realized by generating further funnels along the channel. Exploration of these concepts will be particularly relevant in view of the increasing realization that enzymes—and other proteins—act as part of complex networks of interconnected processes.

Boehr *et al.* infer the structural similarity of an excited state with the ground state of the following step of the enzymatic cycle from the correlations between the chemical shifts of these states. Recent advances in protein structure determination (*5, 15*) using the same sort of nuclear magnetic resonance data that can be extracted from the type of experiments carried out by Boehr *et al*., suggest that detailed structures of the excited states themselves could be just around the corner. Examination of such structures would undoubtedly enable these interesting concepts to be tested further and could also shed light on the role of the multiple protein-protein interactions now being discovered through proteomic techniques, and be of great practical value for rational drug design.

References

1. A. R. Fersht, *Structure and Mechanism in Protein Science: A Guide to Enzyme Catalysis and Protein Folding* (Freeman, New York, 1999).
2. H. Frauenfelder, S. G. Sligar, P. G. Wolynes, *Science* **254**, 1598 (1991).
3. M. Karplus, J. A. McCammon, *Nat. Struct. Biol.* **9**, 646 (2002).
4. M. M. G. Krishna, L. Hoang, Y. Lin, S. W. Englander, *Methods* **34**, 51 (2004).
5. A. Mittermaier, L. E. Kay, *Science* **312**, 224 (2006).
6. K. Lindorff-Larsen, R. B. Best, M. A. DePristo, C. M. Dobson, M. Vendruscolo, *Nature* **433**, 128 (2005).
7. D. D. Boehr, D. McElheny, H. J. Dyson, P. E. Wright, *Science* **313**, 1638 (2006).
8. K. A. Dill, H. S. Chan, *Nat. Struct. Biol*. **4**, 10 (1997).
9. C. M. Dobson, A. Sali, M. Karplus, *Angew. Chem. Int. Ed*. **37**, 868 (1998).
10. P. G. Wolynes, J. N. Onuchic, D. Thirumalai, *Science* **267**, 1619 (1995).
11. R. P. Feynman, R. B. Leighton, M. Sands, *The Feynman Lectures on Physics* (Addison-Wesley, Reading, MA, 1963).
12. E. Z. Eisenmesser *et al.*, *Nature* **438**, 117 (2005).
13. D. Kern, E. R. P. Zuiderweg, *Curr. Opin. Struct. Biol*. **13**, 748 (2003).
14. S. Hammes-Schiffer, S. J. Benkovic, *Annu. Rev. Biochem.* **75**, 519 (2006).
15. D. M. Korzhnev *et al.*, *Nature* **430**, 586 (2004).

10.1126/science.1132851

PHYSICS

Detecting and Controlling Electron Correlations

Measurement and control of fluctuations in circuits may lead to devices for quantum computation.

Markus Büttiker

As electronic devices shrink to nanometer dimensions, their properties are increasingly governed by quantum effects rather than by classical physics. Electron motion is no longer a simple matter of electrical currents flowing in circuits, but is instead highly influenced by the diffraction and interference of the particle wave functions as described by quantum mechanics. In this case, the fluctuations exhibited by electron currents may contain information that is fundamental to understanding physics at nanometer scales. The ways in which such fluctuations are correlated in a nanostructure are interesting, especially for the possible construction of quantum information-processing elements. A recent experiment by Oberholzer *et al*. (*1*) shows how the quantum correlations between current fluctuations at two contacts of a normal conductor can be controlled simply by tuning an electrode voltage.

The physics of current fluctuations has been the subject of much experimental and theoretical exploration. The findings of Oberholzer *et al.* in particular confirm a theoretical prediction about current correlations made by Texier and Büttiker in 2000 (*2*). Previously, the sign of the current-current correlation measured between contacts in a device has always been connected to the statistical properties of the carriers (*3*). Electrons are fermions and the Pauli principle dictates that each state can only be singly occupied; as a consequence, current-current correlations in normal conductors are negative. Conversely, for current carriers that obey Bose-Einstein statistics (in which a given state can be occupied by multiple quanta), positive correlations are observed. To reverse the sign of these correlations, the experiment brings another effect into play: Electrons are carriers with charge. A charge imbalance leads to an electric field that in turn acts on all electrons in the same way within its range, leading to additional correlations. These correlations can dominate the antibunching effect of the Pauli principle and lead to positive correlations even in a purely normal conductor.

The geometry analyzed theoretically (*2*) and used in the experiment (*1*) is shown in the figure. The conductor consists of a high-mobility two-dimensional electron gas with a geometry determined by top gates (A, B, C in the figure). If a voltage is applied to the gates, they deplete the electron gas underneath them, thus generating the desired geometry. The conductor consists of two narrow orifices called quantum point contacts (QPCs), labeled A and B. Electron current is incident at contact 1, and the current

The author is in the Département de Physique Théorique, Université de Genève, CH-1211 Geneva 4, Switzerland. E-mail: markus.buttiker@physics.unige.ch

correlations are measured between contacts 2 and 3. In addition, there is a fourth contact, which can be opened or closed with the help of a side gate C. The conductor is subject to a high magnetic field such that it is in an integer quantum Hall state. This allows the creation of states in which carriers skip in one direction along the edges ("edge states") that form the equivalent of controlled electron "beams," like the beams in an interferometer. The experiment is carried out for a magnetic field for which there are only two edge states. The two edge states are depicted in the figure with fine red and blue lines.

At low temperatures, if scattering events are purely elastic, noise is generated whenever there exists more than one final state for a given initial state. In the experiment, noise is generated at QPC A by adjusting the gates such that the inner edge state is only partially transmitted. A carrier incident in this state is reflected with some probability back into contact 1 or transmitted with some probability into contact 4 (if the gate to this contact is open). Therefore, this process creates an inner edge state leading away from the QPC with a carrier population that fluctuates in time. In contrast, the outer edge state transmits perfectly through the QPC and is noiseless.

If the gate at contact 4 is closed, both the outer noiseless edge state and the inner edge state approach the second QPC (denoted B in the figure). If QPC B is configured such that the noiseless edge state is fully transmitted and the inner edge state is fully reflected, then the current at contact 2 is noiseless, and its correlation with current at contact 3 is zero. If QPC B is opened a bit such that the noisy edge state is partially transmitted, then both the current in contact 2 and that in contact 3 will fluctuate. The Pauli principle is dominant, and the correlation is negative. In fact, this configuration was examined in an earlier experiment by the same group (*4*) to demonstrate negative correlations (*4*–*6*). With both QPCs partially transmitting an edge state, the role of the first contact is simply to regulate the occupation of the edge state incident on the second QPC. If the transmission through QPC A is reduced, the population of the noisy edge state is more and more diluted and, consequently, the negative correlation becomes smaller and smaller.

The crucial addition in the new experiment is the fourth contact. It comes into play when gate C to this contact is opened. The fourth contact is now not simply a current sink but a voltage probe. Ideally a voltage probe draws no net current. Because the current incident on the probe is noisy, the voltage in this contact must fluctuate. The fluctuating voltage acts on all carriers in the probe equally, and therefore it will reemit carriers in the two outgoing edge states in synchronism. If QPC B is now set to reflect the inner edge state completely, even the outer fully transmitted edge state is noisy. The collective response due to the fluctuating voltage of the probe leads to positive correlations, as predicted (*2*) and observed in the experiment of Oberholzer *et al*. (*1*). Note that there is no violation of the Pauli principle: Both edge states emerging from the voltage probe remain at all times singly occupied.

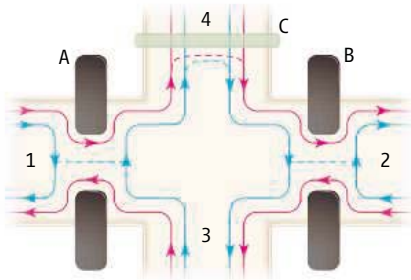

An electron beam splitter. Experimental configuration for the detection of negative, zero, or positive current correlations.

The collective emission of carriers described here is not the only effect that can generate positive correlations in electrical conductors. Emission of a Cooper pair from a superconductor into the normal metal leads to a pair of electrons that can generate positive correlations (*7*, *8*). Similarly, normal conductors with ferromagnetic contacts can show positive correlations due to "spin" bunching or dynamical spin blockade (*9*, *10*). It is also known that high-frequency current correlations can be positive in purely normal conductors due to collective voltage fluctuations (*11*). Yet the experiment by Oberholzer *et al*. (*1*) is the first one to report positive fluctuations. Moreover, in this experiment, the sign of the correlations can be changed simply by turning on and off a gate voltage (the connection to the voltage probe).

The collective emission of carriers from a voltage probe is at its core a classical effect. It is only the noise of the incident channel that is generated quantum mechanically (through transmission and reflection at QPC A). One might therefore ask whether there are other geometries that will also show positive correlations in normal conductors. The answer is yes: Wu and Yip (*12*) analyzed geometries in which a quantum coherent conductor is connected to macroscopic resistors at its contacts. As in the effect described above, voltage fluctuations at the connection of the mesoscopic conductor and the macroscopic classical resistors generate a feedback effect (a collective response) that leads to positive correlations. Still another set of geometries have been investigated by Rychkov and Büttiker (*13*): If noise is fed into a conductor that is made to behave classically through increased inelastic scattering, the current correlations are predicted to become positive. This leads to a picture in which a quantum coherent conductor exhibits negative correlations but a macroscopic conductor divides the incident noise in a collective manner and as a result exhibits positive correlations. A recent experiment by Chen and Webb (*14*) in which a noise source feeds current fluctuations into a beam splitter confirms this picture. And recently, McClure *et al.* (*15*) have demonstrated that the sign of current correlations of two capacitively coupled quantum dots can be changed simply by tuning gate voltages.

There is much interest in generating, manipulating, and detecting entangled states in electrical conductors. Of particular interest are proposals for accomplishing this with purely normal conductors (*16*). My colleagues and I have also made predictions that link entanglement to a two-particle Aharonov-Bohm effect in which no individual particle encircles the flux but two-particle states are sensitive to the flux (*17*). Observation of such quasiparticle entanglement requires that voltage fluctuations that generate collective effects are largely absent. Experiments such as those carried out by Oberholzer *et al*. will help us to understand the necessary conditions.

References

1. S. Oberholzer *et al*., *Phys. Rev. Lett*. **96**, 046804 (2006).
2. C. Texier, M. Büttiker, *Phys. Rev. B* **62**, 7454 (2000).
3. Y. M. Blanter, M. Büttiker, *Phys. Rep*. **336**, 2 (2000).
4. S. Oberholzer *et al*., *Physica E* **6**, 314 (2000).
5. M. Henny *et al*., *Science* **284**, 296 (1999).
6. W. D. Oliver, J. Kim, R. C. Liu, Y. Yamamoto, *Science* **284**, 299 (1999).
7. M. P. Anantram, S. Datta, *Phys. Rev. B* **53**, 16390 (1996).
8. T. Martin, *Phys. Lett. A* **220**, 137 (1996).
9. O. Sauret, D. Feinberg, *Phys. Rev. Lett*. **92**, 106601 (2004).
10. A. Cottet, W. Belzig, C. Bruder, *Phys. Rev. Lett*. **92**, 206801 (2004).
11. A. M. Martin, M. Büttiker, *Phys. Rev. Lett*. **84**, 3386 (2000).
12. S.-T. Wu, S. Yip, *Phys. Rev. B* **72**, 153101 (2005).
13. V. S. Rychkov, M. Büttiker, *Phys. Rev. Lett.* **96**, 166806 (2006).
14. Y. Chen, R. A. Webb, *Phys. Rev. Lett.* **97**, 066604 (2006).
15. D. McClure *et al.*, preprint available at http://arxiv.org/abs/cond-mat/0607280.
16. C. W. J. Beenakker, preprint available at http://arxiv.org/abs/cond-mat/0508488.
17. P. Samuelsson, E. V. Sukhorukov, M. Büttiker, *Phys. Rev. Lett*. **92**, 026805 (2004).

10.1126/science.1127386

PICTURE YOURSELF AS A AAAS SCIENCE & TECHNOLOGY POLICY FELLOW!

Advance your career and serve society by plugging the power of science into public policy. Year-long Science & Technology Policy Fellowships offer opportunities in six thematic areas: Congressional • Diplomacy • Energy, Environment, Agriculture & Natural Resources • Global Stewardship • Health, Education, & Human Services • National Defense & Global Security.

Work in Dynamic Washington, D.C.
Since 1973, AAAS Fellows have been applying their expertise to federal decision-making processes that affect people in the U.S. and around the world. A broad range of assignments are available in the U.S. Congress and executive branch agencies.

Join a Network of Nearly 2,000 Fellows.
AAAS Fellows benefit from a growing and diverse network of colleagues. Applicants must hold a PhD or equivalent doctoral-level degree in any physical, biological, medical/health, or social science, or any engineering discipline. Individuals with a master's degree in engineering and three years of post-degree professional experience also may apply. Federal employees are not eligible and U.S. citizenship is required.

Apply Now!
The application deadline for the 2007-2008 Fellowships is 20 December 2006. Fellowships are awarded in the spring and begin in September. Stipends range from $67,000 to $87,000, depending on experience.
To apply: fellowships.aaas.org

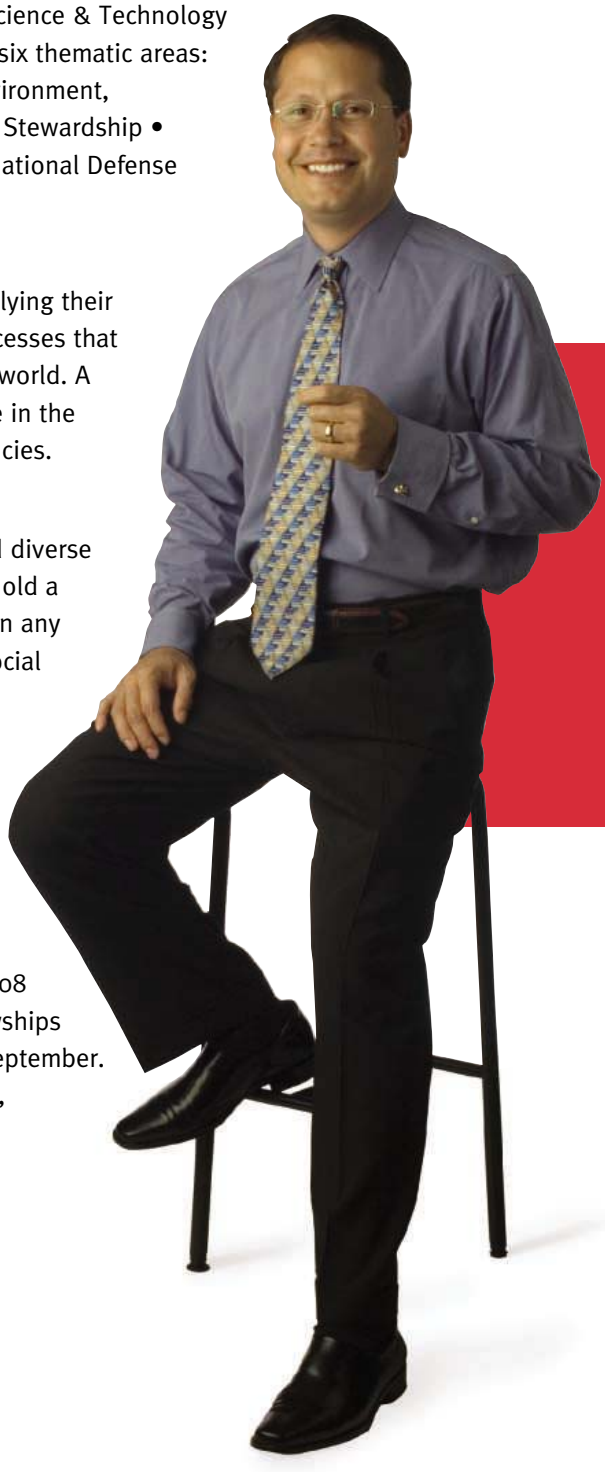

Enhancing Public Policy, Advancing Science Careers

Horacio Murillo, MD, PhD

Mayo Medical School; Molecular Pharmacology, Mayo Graduate School.

2005-2006 AAAS Congressional Fellow in the U.S. Senate Committee on Health, Education, Labor and Pensions.

Now completing a second residency in diagnostic radiology at the University of Texas Health Science Center at San Antonio.

AAAS
ADVANCING SCIENCE, SERVING SOCIETY

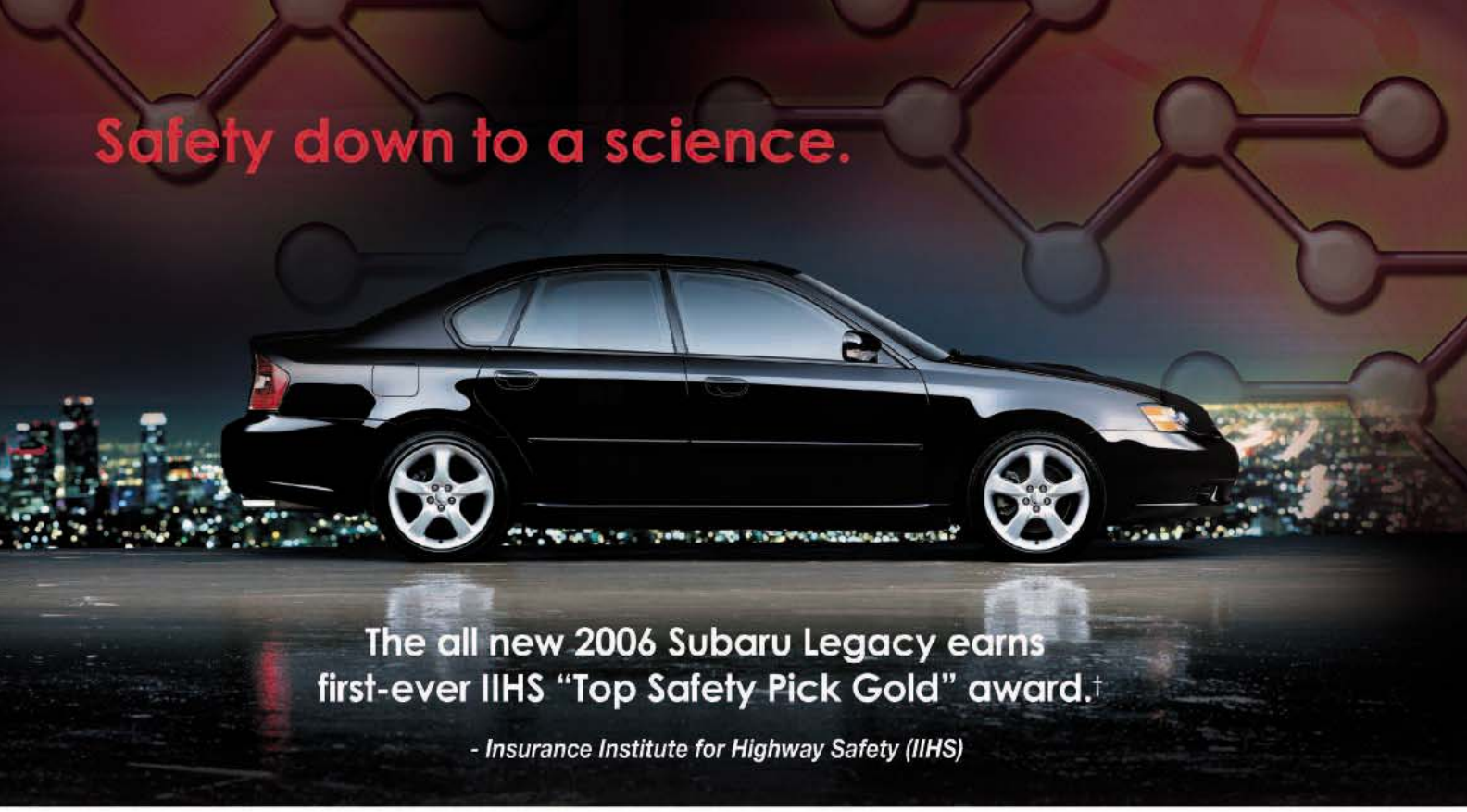

Subaru's sponsorship of the American Association for the Advancement of Science (AAAS) highlights our advanced design of symmetrical all-wheel drive technology to our target markets and underscores Subaru's commitment to further science, engineering and technology education both at the annual meeting and programs throughout the year. Subaru is proud to be the Premier Automotive Sponsor of the AAAS.

In a continuing effort to offer our partners unique and valuable benefits, we provide special offers for AAAS Members, the Subaru VIP Partners Program. AAAS Members can **save up to $3,000*** off the manufacturer's suggested retail price (depending on model and accessories) on the purchase or lease of a new Subaru from participating dealers. To qualify, you must be a AAAS member in good standing for at least six consecutive months prior to participation in this program. Please contact AAAS Member Services at 202.326.6417 or e-mail membership@aaas.org **BEFORE** visiting your local Subaru dealer. Access subaru.com to find a nearby dealer or learn more about Subaru vehicles.

Science
AAAS

Think. Feel. Drive.™

SUBARU

*From MSRP to dealer invoice. MSRP does not include tax, title, and registration fees. Limited time offer subject to change without notice. Terms and conditions apply. This offer replaces all other existing offers, cannot be redeemed for cash and is not applicable in Canada and Hawaii. † Based on Insurance Institute for Highway Safety 40 mph offset frontal crash test, 31 mph side impact test, and 20 mph rear impact test.

Vesicle Formation at the Plasma Membrane and Trans-Golgi Network: The Same but Different

Mark A. McNiven* and Heather M. Thompson

An elaborate vesicle transport system supports the active exchange of membranes and protein cargo between the plasma membrane and the trans-Golgi network. Many observations suggest that highly conserved mechanisms are used in vesicle formation and scission. Such similarity is found both at the level of the receptor-ligand sequestration process that uses clathrin and associated polymeric and monomeric adaptor proteins, and in the machinery used to deform and vesiculate lipid membranes.

The plasma membrane (PM) and the Golgi apparatus exhibit a yin and yang relationship centered on the sorting, packaging, vesiculation, and transport of membranes and protein cargo, either into (the PM) or out of (the Golgi apparatus) the cell. Rather than being antagonistic in function, these sister sites actually represent a "membrane continuum" that shares and exchanges a related functional machinery to support its complex tasks (Fig. 1 and table S1). Situated along this continuum are sorting stations, including several types of sorting and recycling endosomal compartments on one side and the trans-Golgi network (TGN) on the other. All of these compartments are in continuous communication with each other and share many similar structures and components. Here we focus on the similarities, while also indicating some differences, of this sorting and transport continuum.

Similarities in Protein-Sorting Mechanisms at the PM and TGN

The selective sequestration and packaging of protein cargo are key functions performed at both the PM and TGN. Clathrin and its associated coat proteins provide the central scaffold on which many of these processes are organized and are very similar at both sites (Fig. 1 and table S1). Although most studies have focused on clathrin-coated vesicle (CCV) formation at the PM during endocytosis, marked similarities have been noted at the TGN (*1*–*3*).

Of the clathrin-associated accessory proteins, the heterotetrameric adaptor proteins (APs), as well as the more recently identified monomeric clathrin-associated sorting proteins, provide the "first line" of cargo-sequestration specificity on a widely distributed clathrin cage (*4*–*6*). Four AP complexes have been identified, and they all exhibit a similar organization, consisting of two large subunits (γ/β1, α/β2, δ/β3, and ε/β4), a medium subunit (μ1-4), and a small subunit (σ1-4). Despite the modest identity among analogous subunits (20 to 40%), they appear to be structurally similar and to assemble into their respective AP complexes in a similar manner. The AP complexes do, however, display differences in cellular localization patterns and mediate distinct vesicle-formation processes. AP-1, AP-3, and AP-4 are generally believed to function at the TGN and/or endosomes, whereas AP-2 functions at the PM (*7*). Both functional and structural studies have firmly established a role for AP-2 in protein sorting and CCV formation at the PM; in comparison, the roles of the other AP complexes in vesicle formation are somewhat less clear (*8*, *9*).

AP-mediated protein sorting depends on the recognition of sorting motifs that are present in the cytosolic domains of transmembrane proteins (*7*, *10*). There are at least three classes of sorting motifs recognized by AP complexes. The Asn-Pro-X-Tyr motif, which is found in the cytosolic tails of the insulin receptor, epidermal growth factor (EGF) receptor, and low-density lipoprotein receptor, appears to be recognized by AP-2 at the PM; however, this motif also interacts with non–AP-2 clathrin adaptors to mediate internalization (*4*). Another tyrosine-based motif, Tyr-X-X-∅ (where ∅ is a bulky hydrophobic amino acid), found in transmembrane proteins such as the transferrin receptor and mannose-6-phosphate receptor, is recognized by the μ subunit of all four AP complexes, and this motif can thus mediate receptor cargo sorting at the PM, TGN, and endosomes. A third motif, [Asp-Glu]X-X-X-Leu[Leu-Ile] ([DE]XXXL[LI]), is dileucine-based and resides in the cytosolic tails of proteins targeted to endosomal and lysosomal compartments. In addition, this motif has been implicated in basolateral targeting in polarized epithelial cells. Dileucine-based motifs are recognized by AP-1, AP-2, and AP-3; however, each AP complex exhibits distinct preferences for certain [DE]XXXL[LI] motifs. The affinity of interactions between the AP complexes and a specific binding motif might differ, depending on the context of the motif within the protein, the membrane-organelle environment, and the phosphorylation state of the AP complex. Thus, a nascent receptor may exhibit a distinct affinity for one AP complex when leaving the TGN but demonstrate other affinities for different AP complexes when being internalized from the PM or recycled from endosomes.

Variations of a Common Sorting Machine

There is substantial homology between the protein-sequestration and -sorting machinery at the PM and TGN. Superimposed on this conserved process are several layers of regulation and targeting that provide specificity. Because clathrin, adaptor proteins, and many additional linker proteins are widely used, what variations then might provide distinction between the two sites? It appears that different lipids and phosphoinositides (*11*–*13*); small guanosine triphosphatases (GTPases) (*14*, *15*); and a second family of adaptors, the GGAs [Golgi-localized, γ-ear–containing, adenosine diphosphate ribosylation factor (ARF)–binding proteins] (*16*, *17*), work together toward this end.

The classes of lipids that make up the lipid environments at the PM and TGN are similar in many respects, containing cholesterol, sphingolipids, and phosphoinositides (*11*–*13*, *18*, *19*). In addition, lipid microdomains or rafts are present at both sites [for site differences, see (*20*)]. Lipid rafts are thought to mediate clathrin-independent vesicle formation and have been proposed to participate in sorting at the TGN in polarized epithelial cells for the transport of apically localized proteins (*8*, *21*). Thus, although the ratio of these lipids may differ to some degree at the two sites, with cholesterol and sphingolipids being more enriched at the PM than the TGN, the participation of membrane microdomains is maintained.

The use of inositol phospholipids during vesicle formation also seems to be conserved; however, phosphoinositides containing different combinations of phospho-modifications on the inositol ring appear to be preferentially generated at certain membranous sites, where they can then participate in distinct vesicle-trafficking pathways (*11*, *12*). Whereas phosphatidylinositol 4,5-bisphosphate (PIP_2) is more prominent at the PM and binds to AP-2, phosphatidylinositol 4-monophosphate (PI4P) is more prominent at the TGN and binds to AP-1. The delegation of PI4P to the Golgi and PIP_2 to the cell surface is less tidy than it may first appear, because PIP_2 has been implicated not only in clathrin-dependent and -independent vesicle formation from the PM but also in the early formation of the phagocytic cup, Golgi intracisternal transport, and "comet"-based vesicle formation from the TGN. Thus, the same phosphoinositide appears to be

Department of Biochemistry and Molecular Biology and the Miles and Shirley Fiterman Center for Digestive Diseases, Mayo Clinic College of Medicine, Rochester, MN 55905, USA.

*To whom correspondence should be addressed. E-mail: mcniven.mark@mayo.edu

essential in multiple distinct vesicle-formation processes at the PM and the Golgi. The lipid environment, therefore, seems to be similar in some aspects between these two sites, although the exact lipid composition of vesicles (formed from the PM and TGN) most likely exhibits differences. Although they are important, lipids alone do not provide for complete specificity; some additional identity is provided by small GTPases.

The ARF family of small GTPases plays an important role in regulating vesicle formation in the secretory as well as endocytic pathways (*22*). When active in the GTP-bound state, ARF1 recruits the Golgi-associated adaptor AP-1 to the TGN. Thus, TGN targeting of AP-1 is achieved by interaction with both the Golgi-enriched PI4P and active ARF1. A similar dependence on ARF family members for CCV formation also exists at the PM in some instances. For example, the ARF family member ARF6, which resides primarily at the PM, participates in clathrin-mediated endocytosis in polarized epithelial cells and interacts with the PM adaptor AP-2 to modulate CCV formation (*23*). A general function for ARF6 in CCV formation, however, is not present in all cell types.

At the TGN, another family of adaptor proteins, the GGAs, functions along with the AP-based sorting system (*16*, *17*). Like AP-1, the recruitment of GGAs to the Golgi is dependent on ARF1 (*24*). In addition, GGAs may function along with AP-1 in the generation of a subset of CCVs targeted to lysosomes. In this regard, it is noteworthy that the GGAs mediate the sorting of lysosome-targeted proteins through binding to dileucine motifs distinct from those recognized by AP-1. Whereas AP-1 binds to [DE]XXXL[LI] motifs, GGAs bind to Asp-X-X-Leu-Leu motifs.

The GGAs also contain a protein domain that binds ubiquitin (*25*, *26*). The ubiquitin modification appears to be used as a mechanism to initiate the sorting of nascent proteins at the TGN that are to be targeted to the vacuole in yeast (*27*, *28*). Although such a mechanism has not been demonstrated in mammalian cells, ubiquitin modification is used by the endocytic machinery at the PM to sort endocytosed proteins to endosomes and subsequently lysosomes for degradation (*27*, *29*, *30*). Thus, ubiquitin sorting signals may be used at both vesicle-formation sites but are recognized by different ubiquitin-binding proteins: GGAs at the TGN and adaptor proteins, such as Eps15 and Epsin, at the PM. Eps15 was first identified in a search for EGF receptor substrates (*31*) and functions in CCV formation at the PM (*32*). Epsin, on the other hand, was identified as a result of its binding to Eps15 through Asn-Pro-Phe motifs present in the C terminus of Epsin and Eps15 homology domains present in the N terminus of Eps15 (*33*). In addition to binding to each other, both Eps15 and Epsin also bind to AP-2 (*33*–*35*) and contain ubiquitin interacting motifs (UIMs) (*25*). These UIMs mediate the binding of Eps15 and Epsin to ubiquitinated EGF receptors after ligand stimulation and are also necessary for the ubiquitination of the proteins themselves. Because Eps15 and Epsin interact with each other, with the components of the CCV-formation machinery, and with ubiquitinated EGF receptors, these attributes may provide a means to sequester and sort activated EGF receptors for internalization and degradation (*29*, *30*). In addition to functioning at the PM, Eps15 has also been localized to the TGN, where it binds to AP-1 through the γ-adaptin appendage domain (*36*). Thus, Eps15 and GGAs, in conjunction with AP-1, might mediate the sorting of ubiquitinated cargo at the TGN.

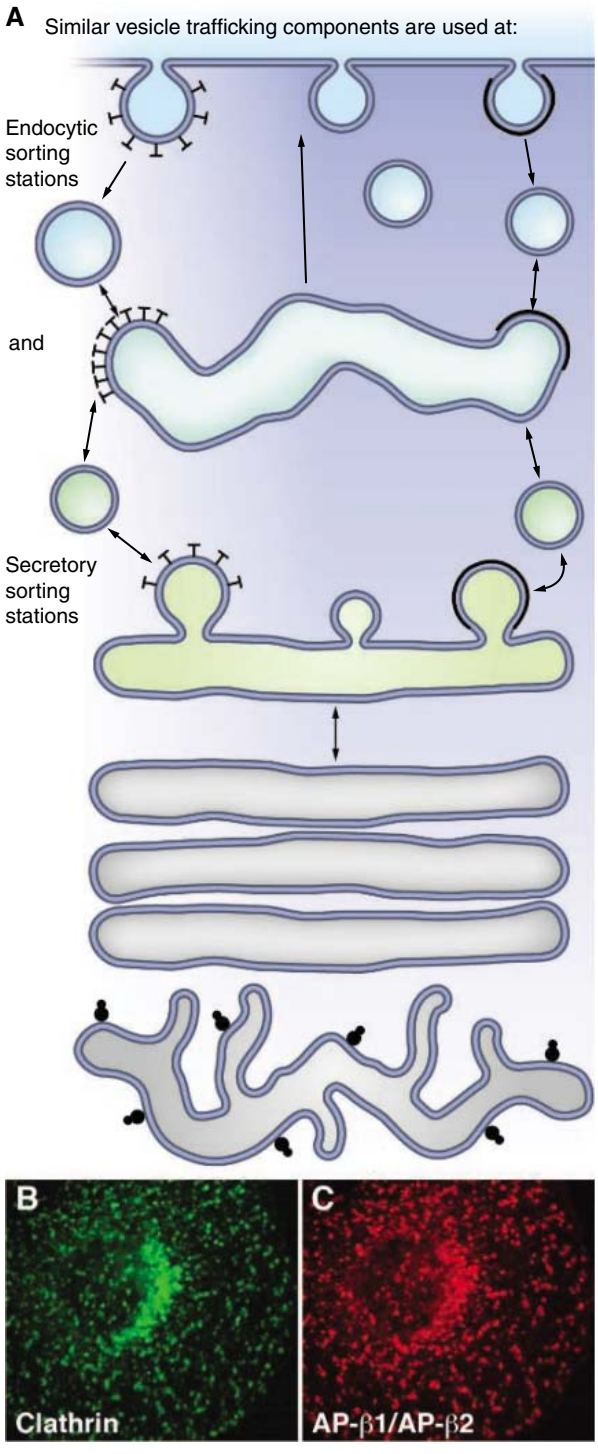

Fig. 1. The PM and Golgi apparatus as sister sites that communicate via a tubular-vesicular membrane continuum. (**A**) Vesicle trafficking between the PM (blue) and TGN (green) is shown as a continuum indicated by the shift between blue and green and designed to represent the communication of membranes and vesiculation machinery between the two sister sites. The "T" symbols and solid black lines along the outside of vesicles and organelles represent clathrin and nonclathrin coats, respectively. The gray coloration of the endoplasmic reticulum, cis-Golgi, and medial-Golgi is meant to indicate a sorting and vesiculation machinery distinct from that used by the TGN and PM. (**B** and **C**) Fluorescence micrograph of a cell costained for clathrin (B) and the β subunits of AP-1 and AP-2 (C), indicating similarities in coat-protein components present at the PM and TGN.

Lipid-Membrane Binding, Bending, and Pinching

Membrane curvature and severing at the PM and TGN after cargo sequestration are essential aspects of vesicle formation and are dependent on the cumulative contribution of lipids, proteins, and lipid-protein interactions (*37*–*39*). As for the coat-cargo sorting scaffold, the vesiculation machinery is highly redundant at both sites and uses many of the same types of lipid-binding scaffold proteins and classes of lipid-modifying enzymes (Fig. 2 and table S1). Many of these lipid-binding proteins contain one of two motifs that are present from yeast to mammals: the Epsin N-terminal homology/AP180 N-terminal homology (ENTH/ANTH) domain (*40*–*42*) and the Bin-amphiphysin-Rvs161/167p (BAR) domain (*43*, *44*).

As the name implies, the ENTH domain was originally identified as a protein module present in Epsin. Subsequently, the ANTH domain was identified in the brain-specific AP180 protein, which mediates CCV formation. A nonneuronal homolog of AP180, termed clathrin-assembly lymphoid myeloid leukemia protein, that contains an ANTH domain and is involved in CCV formation also exists. Both the ENTH and ANTH domains bind to inositol phos-

pholipids, exhibiting a preference for PIP_2, but through somewhat different mechanisms (*41*, *42*). Outside of the ENTH/ANTH domains, these proteins are divergent, but all contain motifs supportive of a role in endocytic CCV formation (*42*). Although the mechanism by which ANTH domain–containing proteins deform membranes is not totally clear, more information is known about ENTH proteins. The ENTH domain of Epsin is thought to bind to PM regions rich in PIP_2 and, through membrane insertion, to support membrane deformation in synergy with other effector proteins, such as AP-2 and clathrin (*39*, *45*).

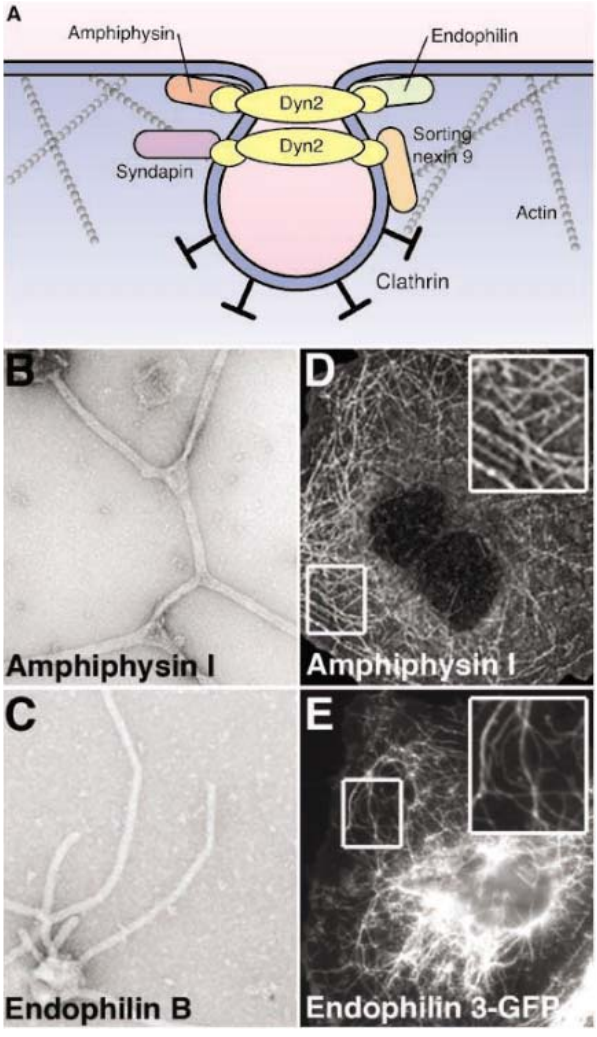

Fig. 2. Common membrane-tubulating proteins at the PM and TGN. (**A**) Similar protein players are used to bind and deform lipids at both the PM and TGN. Along with conventional clathrin coats and adaptors, a variety of BAR and F-BAR/EFC domain–containing proteins bind and deform membranes into tubules, in preparation for vesiculation in concert with the large GTPase Dyn and the actin cytoskeleton. (**B** and **C**) Electron micrographs of negative-stained liposomes tubulated in vitro by the addition of purified BAR domain–containing proteins present at the PM [amphiphysin I in (B)] and TGN [endophilin B in (C)]. (**D** and **E**) Fluorescence micrographs indicating the tubulating action of the BAR domain–containing proteins amphiphysin I (D) and endophilin 3 (E) within the confines of living cells upon their overexpression. Insets show higher magnifications of the boxed regions, emphasizing the massive membrane tubulation induced by these proteins. Different family members of both of these tubulating proteins have been localized to either the PM or TGN. [(B) and (C) are reproduced from (*52*) with permission from The Rockefeller University Press; (D) is reproduced from (*44*) with permission from the American Association for the Advancement of Science; and (E) is reproduced from (*57*) with permission from Elsevier.]

Some proteins containing ENTH/ANTH domains support clathrin-mediated endocytosis, whereas other ENTH/ANTH domain–containing proteins, such as Epsin-related (EpsinR) and HIP1/HIP1-related (HIP1R), are involved in CCV formation at the TGN or TGN and PM, respectively (*40*, *42*, *46*). EpsinR, also known as Enthoprotin and Clint, has a clathrin-binding motif, like Epsin; but rather than an AP-2–binding motif, EpsinR contains an AP-1/GGA2-binding motif and exhibits a slight preference for the TGN-enriched PI4P, making this modified Epsin well suited for TGN function. HIP1/HIP1R, on the other hand, is involved in CCV formation (both at the PM and TGN) and provides a link between CCV formation and actin dynamics (*47*).

A second recently identified protein domain with membrane-binding properties is the BAR domain (*43*, *44*). This domain is present in many proteins with roles in membrane dynamics, including membrane tubulation and ruffling. In its simplest form, the BAR domain functions as a membrane curvature–sensing module, meaning that the exact curvature of a membrane affects the binding of proteins with this type of BAR domain (*44*). However, some proteins contain an N-BAR domain, where an unstructured amphipathic helix is also present N-terminal to the BAR domain. The presence of this amphipathic helix in addition to the BAR domain seems to allow these proteins to both sense and induce membrane curvature, presumably toward vesicle formation and scission. Amphiphysin, which contains an N-BAR domain, is able to bind and tubulate membranes both in vitro and in vivo (Fig. 2, B and D) and is involved in CCV formation during endocytosis. Amphiphysin may function at late stages of vesicle formation, when a membrane tubule or neck would be generated just before severing of the vesicle from its donor membrane (*37*). Other proteins containing BAR domains have been identified that also play a role in endocytosis, including endophilin and sorting nexin 9 (*43*, *44*, *48*–*50*). At the TGN, variants of amphiphysin and endophilin are present and exhibit functions independent of endocytosis (*51*–*53*). Sorting nexin 9, in contrast, has been demonstrated to bind to both the α subunit of AP-2 (*48*, *49*, *54*) and the γ subunit of AP-1 (*49*, *55*). Thus, a series of related ENTH/ANTH and BAR domain–containing proteins with membrane-deforming properties has been superimposed on the clathrin-adaptor sorting machinery to initiate the tubulation and vesiculation of sequestered cargo from both the PM and the TGN.

Vesicle Scission

The actin cytoskeleton, in tandem with an extended family of membrane-tubulating and -severing proteins, may provide the final mechanical action to liberate nascent vesicles from both sister sites (Fig. 3 and table S1) (*46*, *47*, *56*–*61*). Several actin-binding proteins, some of which also have lipid-binding properties, participate in the act of deforming both the PM and TGN donor membranes in concert with the large GTPase dynamin (Dyn) (*56*–*59*, *61*, *62*). Dyn is well known for its role as a molecular pinchase that assembles as an oligomeric complex in the form of spirals on lipid tubules and at the neck of nascent vesicle buds to help mediate the scission process upon GTP hydrolysis (*63*–*65*). Once thought to function exclusively in clathrin-mediated endocytosis at the PM, Dyn has since been found to mediate multiple forms of vesicle formation and to function at many cellular organelles, including the TGN (*66*). Conserved Dyn-independent fission mechanisms also exist at the PM and TGN, one example of which is vesicle formation mediated by C-terminal binding protein 3/brefeldin A–ribosylated substrate (CtBP3/BARS) (*67*). In epithelial cells, CtBP3/BARS mediates the Dyn-independent fission of basolateral transport carriers from the TGN and fluid-phase endocytosis; however, the exact mechanism of fission is unclear.

A subset of actin-regulatory proteins bind the proline-rich domain (PRD) of Dyn and also have membrane-deforming properties (*56*, *57*). These proteins contain a Fes/CIP4 homology (FCH) domain adjacent to a region that shares some homology with the C-terminal half of the BAR domain; thus, this domain was termed F-BAR for FCH and BAR (*57*) and EFC for extended FC (*56*). As for BAR domain–containing proteins, F-BAR/EFC domain–containing proteins exhibit membrane tubulation activity both in vitro and in vivo. Further, many of these proteins bind to Dyn through a Src-homology 3 (SH3) domain–PRD–based interaction to support membrane tubulation and vesiculation (*57*). Just as some BAR domain–containing proteins are

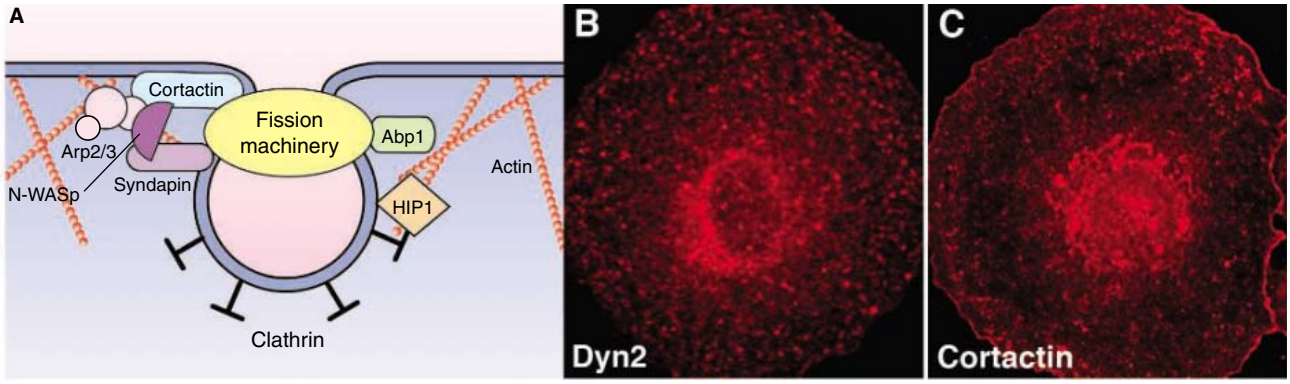

Fig. 3. The vesicle fission machinery and an associated actin cytoskeleton act in concert to liberate nascent vesicles from both the PM and TGN. (**A**) A complex actin cytoskeletal network centered around proteins involved in membrane fission functions together with the clathrin-based sorting and budding machinery to complete the process of cargo sequestration, vesicle formation, and membrane scission. (**B** and **C**) Fluorescence micrographs of cells stained for Dyn2 (B) and cortactin (C) as examples of components of the fission machinery and actin cytoskeleton that are present at both the PM and TGN.

present at the PM and TGN, the F-BAR/EFC domain–containing protein syndapin, also called PACSIN, has been implicated in vesicle formation from both the PM and TGN (*61*, *68*). Thus, these studies implicate a synergistic action among Dyn, actin, and F-BAR/EFC domain–containing proteins during vesicle formation from both of these sister sites.

Vesicle formation at either the PM or TGN might include a dynamic structural scaffold on which the membrane can be tubulated and vesiculated by a protein complex containing several actin- and lipid-binding proteins. Thermodynamically, this scission process is no small task. Thus, it is not surprising that a tag team approach that uses multiple structural and lipid-deforming proteins, as well as force-generating enzymes, would be required to work together in concert to liberate nascent vesicles from a stable membrane bilayer.

Future Directions

The similarities between the clathrin-based vesiculation machinery at both the PM and TGN are strong. Although differences do exist, it is clear that a central theme of vesicle formation has evolved within the continuum of the two related but distinct sorting stations. With the rapid and overwhelming identification of many previously unrecognized adaptors, lipid-binding and -modifying enzymes, and cytoskeletal components, the task is now to define how all of these players interact with each other within the confines of a living cell, how they are regulated during the endocytic and secretory processes, and how they malfunction during human disease.

References and Notes

1. S. A. Mousavi, L. Malerod, T. Berg, R. Kjeken, *Biochem. J.* **377**, 1 (2004).
2. F. M. Brodsky, C. Y. Chen, C. Knuehl, M. C. Towler, D. E. Wakeham, *Annu. Rev. Cell Dev. Biol.* **17**, 517 (2001).
3. L. M. Traub, *Biochim. Biophys. Acta* **1744**, 415 (2005).
4. M. S. Robinson, *Trends Cell Biol.* **14**, 167 (2004).
5. M. A. Edeling, C. Smith, D. J. Owen, *Nat. Rev. Mol. Cell Biol.* **7**, 32 (2006).
6. T. J. Brett, L. M. Traub, *Curr. Opin. Cell Biol.* **18**, 395 (2006).
7. J. S. Bonifacino, L. M. Traub, *Annu. Rev. Biochem.* **72**, 395 (2003).
8. E. Rodriguez-Boulan, G. Kreitzer, A. Musch, *Nat. Rev. Mol. Cell Biol.* **6**, 233 (2005).
9. M. Boehm, J. S. Bonifacino, *Gene* **286**, 175 (2002).
10. D. J. Owen, B. M. Collins, P. R. Evans, *Annu. Rev. Cell Dev. Biol.* **20**, 153 (2004).
11. M. A. De Matteis, A. Godi, *Nat. Cell Biol.* **6**, 487 (2004).
12. C. P. Downes, A. Gray, J. M. Lucocq, *Trends Cell Biol.* **15**, 259 (2005).
13. J. C. Holthuis, G. van Meer, K. Huitema, *Mol. Membr. Biol.* **20**, 231 (2003).
14. R. Behnia, S. Munro, *Nature* **438**, 597 (2005).
15. S. Ellis, H. Mellor, *Trends Cell Biol.* **10**, 85 (2000).
16. J. S. Bonifacino, *Nat. Rev. Mol. Cell Biol.* **5**, 23 (2004).
17. I. Hinners, S. A. Tooze, *J. Cell Sci.* **116**, 763 (2003).
18. L. Liscum, N. J. Munn, *Biochim. Biophys. Acta* **1438**, 19 (1999).
19. G. van Meer, J. C. Holthuis, *Biochim. Biophys. Acta* **1486**, 145 (2000).
20. I. Gkantiragas *et al.*, *Mol. Biol. Cell* **12**, 1819 (2001).
21. J. B. Helms, C. Zurzolo, *Traffic* **5**, 247 (2004).
22. C. D'Souza-Schorey, P. Chavrier, *Nat. Rev. Mol. Cell Biol.* **7**, 347 (2006).
23. O. Paleotti *et al.*, *J. Biol. Chem.* **280**, 21661 (2005).
24. J. G. Donaldson, A. Honda, R. Weigert, *Biochim. Biophys. Acta* **1744**, 364 (2005).
25. L. Hicke, H. L. Schubert, C. P. Hill, *Nat. Rev. Mol. Cell Biol.* **6**, 610 (2005).
26. R. Puertollano, J. S. Bonifacino, *Nat. Cell Biol.* **6**, 244 (2004).
27. L. Hicke, R. Dunn, *Annu. Rev. Cell Dev. Biol.* **19**, 141 (2003).
28. D. J. Katzmann, G. Odorizzi, S. D. Emr, *Nat. Rev. Mol. Cell Biol.* **3**, 893 (2002).
29. K. Haglund, P. P. Di Fiore, I. Dikic, *Trends Biochem. Sci.* **28**, 598 (2003).
30. P. P. Di Fiore, S. Polo, K. Hofmann, *Nat. Rev. Mol. Cell Biol.* **4**, 491 (2003).
31. F. Fazioli, L. Minichiello, B. Matoskova, W. T. Wong, P. P. Di Fiore, *Mol. Cell. Biol.* **13**, 5814 (1993).
32. A. Benmerah, V. Poupon, N. Cerf-Bensussan, A. Dautry-Varsat, *J. Biol. Chem.* **275**, 3288 (2000).
33. H. Chen *et al.*, *Nature* **394**, 793 (1998).
34. G. Iannolo *et al.*, *Cancer Res.* **57**, 240 (1997).
35. A. Benmerah, B. Begue, A. Dautry-Varsat, N. Cerf-Bensussan, *J. Biol. Chem.* **271**, 12111 (1996).
36. H. M. Kent, H. T. McMahon, P. R. Evans, A. Benmerah, D. J. Owen, *Structure* **10**, 1139 (2002).
37. H. T. McMahon, J. L. Gallop, *Nature* **438**, 590 (2005).
38. M. A. De Matteis, A. Godi, *Biochim. Biophys. Acta* **1666**, 264 (2004).
39. J. Zimmerberg, M. M. Kozlov, *Nat. Rev. Mol. Cell Biol.* **7**, 9 (2006).
40. M. C. Duncan, G. S. Payne, *Trends Cell Biol.* **13**, 211 (2003).
41. P. De Camilli *et al.*, *FEBS Lett.* **513**, 11 (2002).
42. V. Legendre-Guillemin, S. Wasiak, N. K. Hussain, A. Angers, P. S. McPherson, *J. Cell Sci.* **117**, 9 (2004).
43. B. Habermann, *EMBO Rep.* **5**, 250 (2004).
44. B. J. Peter *et al.*, *Science* **303**, 495 (2004).
45. R. V. Stahelin *et al.*, *J. Biol. Chem.* **278**, 28993 (2003).
46. S. Carreno, A. E. Engqvist-Goldstein, C. X. Zhang, K. L. McDonald, D. G. Drubin, *J. Cell Biol.* **165**, 781 (2004).
47. A. E. Engqvist-Goldstein *et al.*, *Mol. Biol. Cell* **15**, 1666 (2004).
48. R. Lundmark, S. R. Carlsson, *J. Biol. Chem.* **278**, 46772 (2003).
49. F. Soulet, D. Yarar, M. Leonard, S. L. Schmid, *Mol. Biol. Cell* **16**, 2058 (2005).
50. R. Lundmark, S. R. Carlsson, *J. Biol. Chem.* **279**, 42694 (2004).
51. P. Sarret *et al.*, *J. Biol. Chem.* **279**, 8029 (2004).
52. K. Farsad *et al.*, *J. Cell Biol.* **155**, 193 (2001).
53. J. Modregger, A. A. Schmidt, B. Ritter, W. B. Huttner, M. Plomann, *J. Biol. Chem.* **278**, 4160 (2003).
54. R. Lundmark, S. R. Carlsson, *Biochem. J.* **362**, 597 (2002).
55. J. Hirst, A. Motley, K. Harasaki, S. Y. Peak Chew, M. S. Robinson, *Mol. Biol. Cell* **14**, 625 (2003).
56. K. Tsujita *et al.*, *J. Cell Biol.* **172**, 269 (2006).
57. T. Itoh *et al.*, *Dev. Cell* **9**, 791 (2005).
58. H. Cao *et al.*, *Mol. Cell. Biol.* **23**, 2162 (2003).
59. H. Cao *et al.*, *Nat. Cell Biol.* **7**, 483 (2005).
60. A. E. Engqvist-Goldstein, D. G. Drubin, *Annu. Rev. Cell Dev. Biol.* **19**, 287 (2003).
61. M. M. Kessels, J. Dong, W. Leibig, P. Westermann, B. Qualmann, *J. Cell Sci.* **119**, 1504 (2006).
62. M. M. Kessels, A. E. Engqvist-Goldstein, D. G. Drubin, B. Qualmann, *J. Cell Biol.* **153**, 351 (2001).
63. J. E. Hinshaw, *Annu. Rev. Cell Dev. Biol.* **16**, 483 (2000).
64. D. Danino, K. H. Moon, J. E. Hinshaw, *J. Struct. Biol.* **147**, 259 (2004).
65. A. Roux, K. Uyhazi, A. Frost, P. De Camilli, *Nature* **441**, 528 (2006).
66. M. A. McNiven, H. Cao, K. R. Pitts, Y. Yoon, *Trends Biochem. Sci.* **25**, 115 (2000).
67. M. Bonazzi *et al.*, *Nat. Cell Biol.* **7**, 570 (2005).
68. M. M. Kessels, B. Qualmann, *J. Cell Sci.* **117**, 3077 (2004).

69. The authors thank D. J. Katzmann (Mayo Clinic College of Medicine) and B. Wendland (Johns Hopkins University) for their thoughtful and helpful comments on this manuscript. Research in the laboratory of M.A.M. is supported by NIH/National Institute of Diabetes and Digestive and Kidney Diseases grant DK44650-15 and NIH/National Cancer Institute grant CA104125-02.

Supporting Online Material

www.sciencemag.org/cgi/content/full/313/5793/1591/DC1
Table S1
References

10.1126/science.1118133

Near-Field Microscopy Through a SiC Superlens

Thomas Taubner,[1]* Dmitriy Korobkin,[2] Yaroslav Urzhumov,[2]
Gennady Shvets,[2] Rainer Hillenbrand[1]†

Diffraction limits the spatial resolution of classical optical microscopy to about one-half of the illuminating wavelength. In scanning near-field optical microscopy (SNOM) (*1*), the use of a nanofocus generated by a tiny hole (aperture) in the metallic coating of a tapered glass fiber tip that is raster-scanned over the object of interest can overcome the diffraction limit. Alternately, in its apertureless (*2*) or scattering (*3*) version (s-SNOM), the nanofocus is defined by the presence of strongly confined electromagnetic fields at the apex of a metallic probe tip. In both cases, the probe must be very close to the investigated object, which limits SNOM applications to surface studies. We combine near-field microcopy with a phenomenon called "superlensing" that allows for subwavelength-scale resolved imaging of buried objects.

A superlens uses a thin slab of a material with a negative permittivity, ε, to form a high-resolution optical image at the opposing side of the slab (*4*–*6*). In our experiment, we placed a SiC superlens (*7*) between the scanning probe tip of an infrared s-SNOM and objects located 880 nm below the tip. The superlens (Fig. 1A) is a 440-nm-thick single-crystalline SiC membrane coated on both sides with 220-nm-thick SiO_2 layers (*7*). The two surfaces of the sandwich correspond to the object and the image planes of the lens, respectively. The object plane is covered by a Au film patterned with holes of different diameters and separations (Fig. 1B). In contrast to the first indirect demonstration of superlensing of a SiC slab concluded from enhanced transmission experiments (*7*), we directly map the image plane with a s-SNOM (*3*), recording both the amplitude and the phase of the optical field distribution (*8*). In our experiment, the superlens is operated in reflection mode where illumination and detection are carried out from the same side of the superlens. This extends its applicability to samples located on opaque substrates.

At mid-infrared wavelengths, λ close to 11 μm, where superlensing is expected (*7*), the infrared amplitude (Fig. 1C) and phase images (Fig. 1D) resolve the 1200-nm and 860-nm holes. Even the smaller 540-nm holes exhibit sufficient optical contrast to allow for the detection of λ/20-sized objects 880 nm away from the near-field probe. A control image is taken at a wavelength of λ = 9.25 μm, where the superlensing condition (*8*) is not satisfied. The image (Fig. 1E) does not exhibit optical contrast demonstrating that s-SNOM alone cannot resolve the objects 880 nm below the surface.

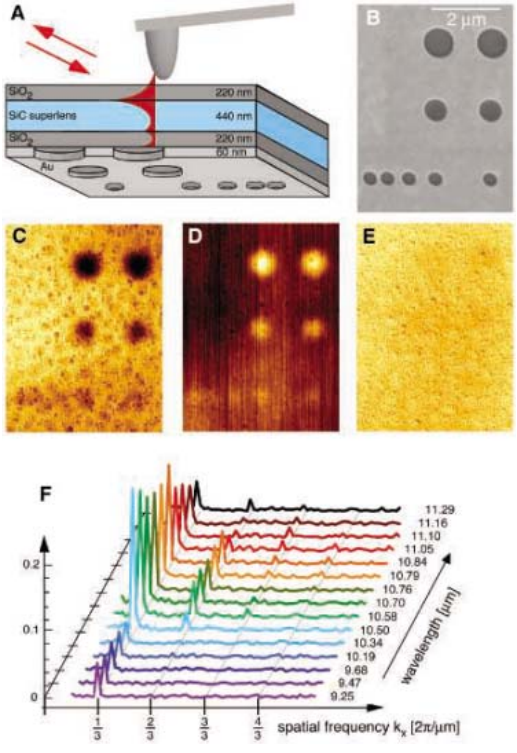

Fig. 1. Near-field microscopy through a 880-nm-thick superlens structure: (**A**) Experimental setup. (**B**) Scanning electron micrograph (mirrored) of the object plane, showing holes in a 60-nm-thick Au film. (**C**) Infrared amplitude in the image plane at λ = 10.85 μm where superlensing is expected. (**D**) Infrared phase contrast (λ = 11.03 μm). (**E**) Control image showing infrared amplitude at λ = 9.25 μm (no superlensing). (**F**) Fourier tranforms of line scans taken from amplitude images of a grating (≈3 μm period, averaged over 26 scan lines), normalized to unity for zero frequency. High spatial frequencies (up to the grating's fourth harmonic) are imaged by the superlens/s-SNOM system around λ ≈ 10.84 μm wavelength.

To quantify the resolution enhancement provided by the superlens, a grating with a ≈3-μm period and a 440-nm slit width was imaged. The Fourier transforms of line scans taken perpendicularly to the slits (Fig. 1F) show that high spatial frequencies, up to the grating's fourth harmonic, can be recovered only in a narrow spectral range (around λ ≈ 10.84 μm), demonstrating the resonant character of the imaging process by a superlens. In resonance the spatial resolution of the subsurface features is enhanced by a factor of four compared with near-field imaging without superlensing of the SiC slab (e.g., at λ = 9.47 μm).

Superlens-based near-field microscopy is neither restricted to SiC lenses nor to infrared wavelengths. It can be applied from visible to terahertz frequencies where superlensing can be provided by flat metal films, thin slabs of polar crystals, or even by artificial media (*9*) such as metamaterials and photonic crystals. It thus opens the door for high-resolution optical imaging of various manmade or biological nanostructures not directly accessible by a near-field probe.

References and Notes

1. A. Lewis *et al.*, *Nat. Biotechnol.* **21**, 1378 (2003).
2. F. Zenhausern, Y. Martin, H. K. Wickramasinghe, *Science* **269**, 1083 (1995).
3. R. Hillenbrand, T. Taubner, F. Keilmann, *Nature* **418**, 159 (2002).
4. J. B. Pendry, *Phys. Rev. Lett.* **85**, 3966 (2000).
5. N. Fang, H. Lee, C. Sun, X. Zhang, *Science* **308**, 534 (2005).
6. D. O. S. Melville, R. J. Blaikie, *Opt. Express* **13**, 2127 (2005).
7. D. Korobkin, Y. Urzhumov, G. Shvets, *J. Opt. Soc. Am. B* **23**, 468 (2006).
8. Materials and methods are available as supporting material on *Science* Online.
9. D. R. Smith, J. B. Pendry, M. C. K. Wiltshire, *Science* **305**, 788 (2004).
10. We thank C. Zorman for SiC epitaxy. This work was funded by Deutsches Bundesministerium für Bildung und Forschung (Nachwuchswettbewerb Nanotechnologie 2002), grant number 03N8705, and in part by the Multi-University Research Initiatives of the Army Research Office (grant no. W911NF-04-01-0203) and the Air Force Office of Research (grant no. FA 9550-06-01-0279).

Supporting Online Material

www.sciencemag.org/cgi/content/full/313/5793/1595/DC1
Materials and Methods
References

8 June 2006; accepted 14 July 2006
10.1126/science.1131025

[1]Nano-Photonics Group, Max-Planck-Institut für Biochemie, Am Klopferspitz 18, D-82152 Martinsried, Germany. [2]Department of Physics, University of Texas at Austin, Austin, TX 78712, USA.

*Present address: Department of Material Science, Stanford University, Stanford, CA 94305, USA.
†To whom correspondence should be addressed. E-mail: hillenbr@biochem.mpg.de

The Genome of Black Cottonwood, *Populus trichocarpa* (Torr. & Gray)

G. A. Tuskan,[1,3]* S. DiFazio,[1,4]† S. Jansson,[5]† J. Bohlmann,[6]† I. Grigoriev,[9]† U. Hellsten,[9]† N. Putnam,[9]† S. Ralph,[6]† S. Rombauts,[10]† A. Salamov,[9]† J. Schein,[11]† L. Sterck,[10]† A. Aerts,[9] R. R. Bhalerao,[5] R. P. Bhalerao,[12] D. Blaudez,[13] W. Boerjan,[10] A. Brun,[13] A. Brunner,[14] V. Busov,[15] M. Campbell,[16] J. Carlson,[17] M. Chalot,[13] J. Chapman,[9] G.-L. Chen,[2] D. Cooper,[6] P. M. Coutinho,[19] J. Couturier,[13] S. Covert,[20] Q. Cronk,[7] R. Cunningham,[1] J. Davis,[22] S. Degroeve,[10] A. Déjardin,[23] C. dePamphilis,[18] J. Detter,[9] B. Dirks,[24] I. Dubchak,[9,25] S. Duplessis,[13] J. Ehlting,[7] B. Ellis,[6] K. Gendler,[26] D. Goodstein,[9] M. Gribskov,[27] J. Grimwood,[28] A. Groover,[29] L. Gunter,[1] B. Hamberger,[7] B. Heinze,[30] Y. Helariutta,[12,31,33] B. Henrissat,[19] D. Holligan,[21] R. Holt,[11] W. Huang,[9] N. Islam-Faridi,[34] S. Jones,[11] M. Jones-Rhoades,[35] R. Jorgensen,[26] C. Joshi,[15] J. Kangasjärvi,[32] J. Karlsson,[5] C. Kelleher,[6] R. Kirkpatrick,[11] M. Kirst,[22] A. Kohler,[13] U. Kalluri,[1] F. Larimer,[2] J. Leebens-Mack,[21] J.-C. Leplé,[23] P. Locascio,[2] Y. Lou,[9] S. Lucas,[9] F. Martin,[13] B. Montanini,[13] C. Napoli,[26] D. R. Nelson,[36] C. Nelson,[37] K. Nieminen,[31] O. Nilsson,[12] V. Pereda,[13] G. Peter,[22] R. Philippe,[6] G. Pilate,[23] A. Poliakov,[25] J. Razumovskaya,[2] P. Richardson,[9] C. Rinaldi,[13] K. Ritland,[8] P. Rouzé,[10] D. Ryaboy,[25] J. Schmutz,[28] J. Schrader,[38] B. Segerman,[5] H. Shin,[11] A. Siddiqui,[11] F. Sterky,[39] A. Terry,[9] C.-J. Tsai,[15] E. Uberbacher,[2] P. Unneberg,[39] J. Vahala,[32] K. Wall,[18] S. Wessler,[21] G. Yang,[21] T. Yin,[1] C. Douglas,[7]‡ M. Marra,[11]‡ G. Sandberg,[12]‡ Y. Van de Peer,[10]‡ D. Rokhsar[9,24]‡

We report the draft genome of the black cottonwood tree, *Populus trichocarpa*. Integration of shotgun sequence assembly with genetic mapping enabled chromosome-scale reconstruction of the genome. More than 45,000 putative protein-coding genes were identified. Analysis of the assembled genome revealed a whole-genome duplication event; about 8000 pairs of duplicated genes from that event survived in the *Populus* genome. A second, older duplication event is indistinguishably coincident with the divergence of the *Populus* and *Arabidopsis* lineages. Nucleotide substitution, tandem gene duplication, and gross chromosomal rearrangement appear to proceed substantially more slowly in *Populus* than in *Arabidopsis*. *Populus* has more protein-coding genes than *Arabidopsis*, ranging on average from 1.4 to 1.6 putative *Populus* homologs for each *Arabidopsis* gene. However, the relative frequency of protein domains in the two genomes is similar. Overrepresented exceptions in *Populus* include genes associated with lignocellulosic wall biosynthesis, meristem development, disease resistance, and metabolite transport.

Forests cover 30% (about 3.8 billion ha) of Earth's terrestrial surface, harbor substantial biodiversity, and provide humanity with benefits such as clean air and water, lumber, fiber, and fuels. Worldwide, one-quarter of all industrial feedstocks have their origins in forest-based resources (*1*). Large and long-lived forest trees grow in extensive wild populations across continents, and they have evolved under selective pressures unlike those of annual herbaceous plants. Their growth and development involves extensive secondary growth, coordinated signaling and distribution of water and nutrients over great distances, and strategic storage and redistribution of metabolites in concordance with interannual climatic cycles. Their need to survive and thrive in fixed locations over centuries under continually changing physical and biotic stresses also sets them apart from short-lived plants. Many of the features that distinguish trees from other organisms, especially their large sizes and long-generation times, present challenges to the study of the cellular and molecular mechanisms that underlie their unique biology. To enable and facilitate such investigations in a relatively well-studied model tree, we describe here the draft genome of black cottonwood, *Populus trichocarpa* (Torr. & Gray), and compare it to other sequenced plant genomes.

P. trichocarpa was selected as the model forest species for genome sequencing not only because of its modest genome size but also because of its rapid growth, relative ease of experimental manipulation, and range of available genetic tools (*2*, *3*). The genus is phenotypically diverse, and interspecific hybrids facilitate the genetic mapping of economically important traits related to growth rate, stature, wood properties, and paper quality. Dozens of quantitative trait loci have already been mapped (*4*), and methods of genetic transformation have been developed (*5*). Under appropriate conditions, *Populus* can reach reproductive maturity in as few as 4 to 6 years, permitting selective breeding for large-scale sustainable plantation forestry. Finally, rapid growth of trees coupled with thermochemical or biochemical conversion of the lignocellulosic portion of the plant has the potential to provide a renewable energy resource with a concomitant reduction of greenhouse gases (*6*–*8*).

Sequencing and Assembly

A single female genotype, "Nisqually 1," was selected and used in a whole-genome shotgun

[1]Environmental Sciences Division, [2]Life Sciences Division, Oak Ridge National Laboratory, Oak Ridge, TN 37831, USA. [3]Plant Sciences Department, University of Tennessee, TN 37996, USA. [4]Department of Biology, West Virginia University, Morgantown, WV 26506, USA. [5]Umeå Plant Science Centre, Department of Plant Physiology, Umeå University, SE-901 87, Umeå, Sweden. [6]Michael Smith Laboratories, [7]Department of Botany, [8]Department of Forest Sciences, University of British Columbia, Vancouver, BC V6T 1Z4, Canada. [9]U.S. Department of Energy, Joint Genome Institute, Walnut Creek, CA 94598, USA. [10]Department of Plant Systems Biology, Flanders Interuniversity Institute for Biotechnology (VIB), Ghent University, B-9052 Ghent, Belgium. [11]Genome Sciences Centre, 100-570 West 7th Avenue, Vancouver, BC V5Z 4S6, Canada. [12]Umeå Plant Science Centre, Department of Forest Genetics and Plant Physiology, Swedish University of Agricultural Sciences, SE-901 83 Umeå, Sweden. [13]Tree-Microbe Interactions Unit, Institut National de la Recherche Agronomique (INRA)–Université Henri Poincaré, INRA-Nancy, 54280 Champenoux, France. [14]Department of Forestry, Virginia Polytechnic Institute and State University, Blacksburg, VA 24061, USA. [15]Biotechnology Research Center, School of Forest Resources and Environmental Science, Michigan Technological University, Houghton, MI 49931, USA. [16]Department of Cell and Systems Biology, University of Toronto, 25 Willcocks Street, Toronto, Ontario, M5S 3B2 Canada. [17]School of Forest Resources and Huck Institutes of the Life Sciences, [18]Department of Biology, Institute of Molecular Evolutionary Genetics, and Huck Institutes of Life Sciences, The Pennsylvania State University, University Park, PA 16802, USA. [19]Architecture et Fonction des Macromolécules Biologiques, UMR6098, CNRS and Universities of Aix-Marseille I and II, case 932, 163 avenue de Luminy, 13288 Marseille, France. [20]Warnell School of Forest Resources, [21]Department of Plant Biology, University of Georgia, Athens, GA 30602, USA. [22]School of Forest Resources and Conservation, Genetics Institute, and Plant Molecular and Cellular Biology Program, University of Florida, Gainesville, FL 32611, USA. [23]INRA-Orléans, Unit of Forest Improvement, Genetics and Physiology, 45166 Olivet Cedex, France. [24]Center for Integrative Genomics, University of California, Berkeley, CA 94720, USA. [25]Genomics Division, Lawrence Berkeley National Laboratory, Berkeley, CA 94720, USA. [26]Department of Plant Sciences, University of Arizona, Tucson, AZ 85721, USA. [27]Department of Biological Sciences, Purdue University, West Lafayette, IN 47907, USA. [28]The Stanford Human Genome Center and the Department of Genetics, Stanford University School of Medicine, Palo Alto, CA 94305, USA. [29]Institute of Forest Genetics, United States Department of Agriculture, Forest Service, Davis, CA 95616, USA. [30]Federal Research Centre for Forests, Hauptstrasse 7, A-1140 Vienna, Austria. [31]Plant Molecular Biology Laboratory, Institute of Biotechnology, [32]Department of Biological and Environmental Sciences, University of Helsinki, FI-00014 Helsinki, Finland. [33]Department of Biology, 200014, University of Turku, FI-20014 Turku, Finland. [34]Southern Institute of Forest Genetics, United States Department of Agriculture, Forest Service and Department of Forest Science, Texas A&M University, College Station, TX 77843, USA. [35]Whitehead Institute for Biomedical Research and Department of Biology, Massachusetts Institute of Technology, Cambridge, MA 02142, USA. [36]Department of Molecular Sciences and Center of Excellence in Genomics and Bioinformatics, University of Tennessee, Memphis, TN 38163, USA. [37]Southern Institute of Forest Genetics, United States Department of Agriculture, Forest Service, Saucier, MS 39574, USA. [38]Developmental Genetics, University of Tübingen, D-72076 Tübingen, Germany. [39]Department of Biotechnology, KTH, AlbaNova University Center, SE-106 91 Stockholm, Sweden.

*To whom correspondence should be addressed. E-mail: gtk@ornl.gov

†These authors contributed equally to this work as second authors.

‡These authors contributed equally to this work as senior authors.

sequence and assembly strategy (*9*). Roughly 7.6 million end-reads representing 4.2 billion high-quality (i.e., Q20 or higher) base pairs were assembled into 2447 major scaffolds containing an estimated 410 megabases (Mb) of genomic DNA (tables S1 and S2). On the basis of the depth of coverage of major scaffolds (~7.5 depth) and the total amount of nonorganellar shotgun sequence that was generated, the *Populus* genome size was estimated to be 485 ± 10 Mb (±SD), in rough agreement with previous cytogenetic estimates of about 550 Mb (*10*). The near completeness of the shotgun assembly in protein-coding regions is supported by the identification of more than 95% of known *Populus* cDNA in the assembly.

The ~75 Mb of unassembled genomic sequence is consistent with cytogenetic evidence that ~30% of the genome is heterochromatic (*9*). The amount of euchromatin contained within the *Populus* genome was estimated in parallel by subtraction on the basis of direct measurements of 4′,6′-diamidino-2-phenylindole–stained prophase and metaphase chromosomes (fig. S4). On average, 69.5 ± 0.3% of the genome consisted of euchromatin, with a significantly lower proportion of euchromatin in linkage group I (LGI) (66.4 ± 1.1%) compared with the other 18 chromosomes (69.7 ± 0.03%, $P \leq 0.05$). In contrast, *Arabidopsis* chromosomes contain roughly 93% euchromatin (*11*). The unassembled shotgun sequences were derived from variants of organellar DNA, including recent nuclear translocations; highly repetitive genomic DNA; haplotypic segments that were redundant with short subsegments of the major scaffolds (separated as a result of extensive sequence polymorphism and allelic variants); and contaminants of the template DNA, such as endophytic microbes inhabiting the leaf and root tissues used for template preparation (*12*) (fig. S1 and table S3). The end-reads corresponding to chloroplast (fig. S5) and mitochondrial genomes were assembled into circular genomes of 157 and 803 kb, respectively (*9*).

We anchored the 410 Mb of assembled scaffolds to a sequence-tagged genetic map (fig. S3). In total, 356 microsatellite markers were used to assign 155 scaffolds (335 Mb of sequence) to the 19 *P. trichocarpa* chromosome-scale linkage groups (*13*). The vast majority (91%) of the mapped microsatellite markers were colinear with the sequence assembly. At the extremes, the smallest chromosome, LGIX [79 centimorgans (cM)], is covered by two scaffolds containing 12.5 Mb of assembled sequence, whereas the largest chromosome, LGI (265 cM), contains 21 scaffolds representing 35.5 Mb (fig. S3). We also generated a physical map based on bacterial artificial chromosome (BAC) fingerprint contigs using a Nisqually-1 BAC library representing an estimated 9.5-fold genome coverage (fig. S2). Paired BAC-end sequences from most of the physical map were linked to the large-scale assembly, permitting 2460 of the physical map contigs to be positioned on the genome assembly. Combining the genetic and physical map, nearly 385 Mb of the 410 Mb of assembled sequence are placed on a linkage group.

Unlike *Arabidopsis*, where predominantly self-fertilizing ecotypes maintain low levels of allelic polymorphism, *Populus* species are predominantly dioecious, which results in obligate outcrossing. This compulsory outcrossing, along with wind pollination and wind-dispersed plumose seeds, results in high levels of gene flow and high levels of heterozygosity (that is, within individual genetic polymorphisms). Within the heterozygous Nisqually-1 genome, we identified 1,241,251 single-nucleotide polymorphisms (SNPs) or small insertion/deletion polymorphisms (indels) for an overall rate of approximately 2.6 polymorphisms per kilobase. Of these polymorphisms, the overwhelming majority (83%) occurred in noncoding portions of the genome (Table 1). Short indels and SNPs within exons resulted in frameshifts and nonsense stop codons within predicted exons, respectively, suggesting that null alleles of these genes exist in one of the haplotypes. Some of the polymorphisms may be artifacts from the assembly process, although these errors were minimized by using stringent criteria for SNP identification (*9*).

Table 1. Characterization of polymorphisms according to their positions relative to predicted coding sequences, introns, and untranslated regions (UTRs). Rate shows the percentage of potential sites of each class that were polymorphic. Most indels within exons resulted in frame shifts, but we could not quantify this due to difficulties with assembly and sequencing of regions containing indels. Nonsense mutations created stop codons within predicted exons.

Source	Number of loci	Rate (%)
Noncoding	1,027,322	0.32
INTRON	141,199	0.25
3′UTR	6,731	0.25
5′UTR	3,306	0.24
Exon	62,656	0.14
Within exons:		
Indels	2,722	0.01
Nonsense	926	0.02
Nonsynonymous	32,207	0.10

Gene Annotation

We tentatively identified a first-draft reference set of 45,555 protein-coding gene loci in the *Populus* nuclear genome (www.jgi.doe.gov/poplar) using a variety of ab initio, homology-based, and expressed sequence tag (EST)–based methods (*14*–*17*) (table S5). Similarly, 101 and 52 genes were annotated in the chloroplast and mitochondrial genomes, respectively (*9*). To aid the annotation process, 4664 full-length sequences, from full-length enriched cDNA libraries from Nisqually 1, were generated and used in training the gene-calling algorithms. Before gene prediction, repetitive sequences were characterized (fig. S15 and table S14) and masked; additional putative transposable elements were identified and subsequently removed from the reference gene set (*9*). Given the current draft nature of the genome, we expect that the gene set in *Populus* will continue to be refined.

About 89% of the predicted gene models had homology [expectation (E) value $\leq 1 \times 10^{-8}$] to the nonredundant (NR) set of proteins from the National Center for Biotechnology Information, including 60% with extensive homology that spans 75% of both model and NR protein lengths. Nearly 12% (5248) of the predicted *Populus* genes had no detectable similarity to *Arabidopsis* genes (E value $\leq 1 \times 10^{-3}$); conversely, in the more refined *Arabidopsis* set, only 9% (2321) of the predicted genes had no similarity to the *Populus* reference set. Of the 5248 *Populus* genes without *Arabidopsis* similarity, 1883 have expression evidence from the manually curated *Populus* EST data set, and of these, 274 have no hits (E value $\geq 1 \times 10^{-3}$) to the NR database (*9*). Whole-genome oligonucleotide microarray analysis provided evidence of tissue-based expression for 53% of the reference gene models (Fig. 1). In addition, a signal was detected from 20% of genes that were initially annotated and excluded from the reference set, suggesting that as many as 4000 additional genes (or gene fragments) may be present. Within the reference gene set, we identified 13,019 pairs of orthologs between

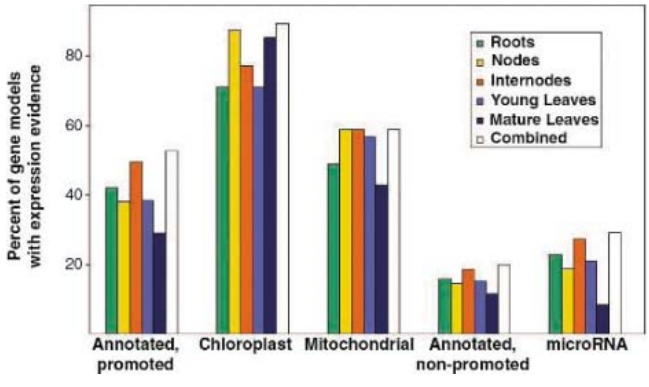

Fig. 1. Whole-genome oligonucleotide microarray expression data for all predicted gene models in *P. trichocarpa*. Values represent the proportion of genes expressed above negative controls at a 5% false discovery rate. The *x* axis represents the subsets of predicted genes that were analyzed for the annotated and promoted *P. trichocarpa* gene set (42,373 genes), chloroplast gene set (49 genes), mitochondria gene set (49 genes), annotated, nonpromoted gene set (10,875 genes), and microRNAs (48 miRNAs).

genes in *Populus* and *Arabidopsis* using the best bidirectional Basic Local Alignment Search Tool (BLAST) hits, with average mutual coverage of these alignments equal to 93%; 11,654 pairs of orthologs had greater than 90% alignment of gene lengths, whereas only 156 genes had less than 50% coverage. As of 1 June 2006, ~10% (4378) gene models have been manually validated and curated.

Genome Organization

Genome duplication in the Salicaceae. *Populus* and *Arabidopsis* lineages diverged about 100 to 120 million years ago (Ma). Analysis of the *Populus* genome provided evidence of a more recent duplication event that affected roughly 92% of the *Populus* genome. Nearly 8000 pairs of paralogous genes of similar age (excluding tandem or local duplications) were identified (Fig. 2). The relative age of the duplicate genes was estimated by the accumulated nucleotide divergence at fourfold synonymous third-codon transversion position (4DTV) values. A sharp peak in 4DTV values, corrected for multiple substitutions, representing a burst of gene duplication, is evident at 0.0916 ± 0.0004 (Fig. 3A). Comparison of 1825 *Populus* and *Salix* orthologous genes derived from *Salix* EST suggests that both genera share this whole-genome duplication event (Fig. 3B). Moreover, the parallel karyotypes and collinear genetic maps (*18*) of *Salix* and *Populus* also support the conclusion that both lineages share the same large-scale genome history.

If we naively calibrated the molecular clock using synonymous rates observed in the Brassicaceae (*19*) or derived from the *Arabidopsis-Oryza* divergence (*20*), we would conclude that the genome duplication in *Populus* is very recent [8 to 13 Ma, as reported by Sterk (*21*)]. Yet the fossil record shows that the *Populus* and *Salix* lineages diverged 60 to 65 Ma (*22–25*). Thus, the molecular clock in *Populus* must be ticking at only

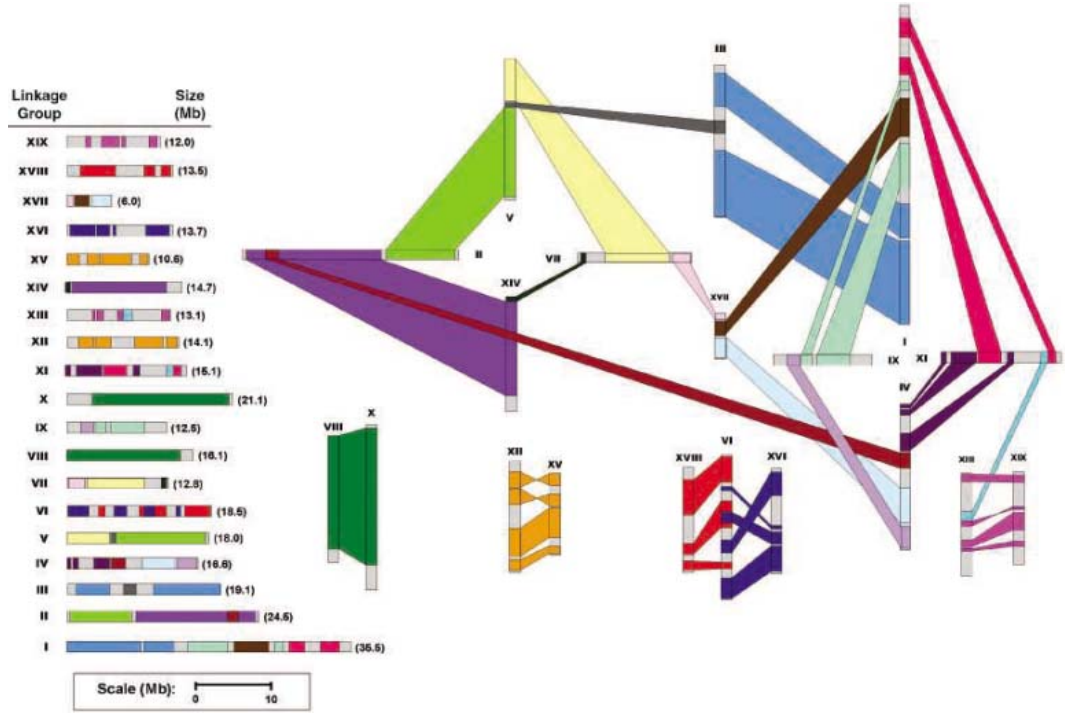

Fig. 2. Chromosome-level reorganization of the most recent genome-wide duplication event in *Populus*. Common colors refer to homologous genome blocks, presumed to have arisen from the salicoid-specific genome duplication 65 Ma, shared by two chromosomes. Chromosomes are indicated by their linkage group number (I to XIX). The diagram to the left uses the same color coding and further illustrates the chimeric nature of most linkage groups.

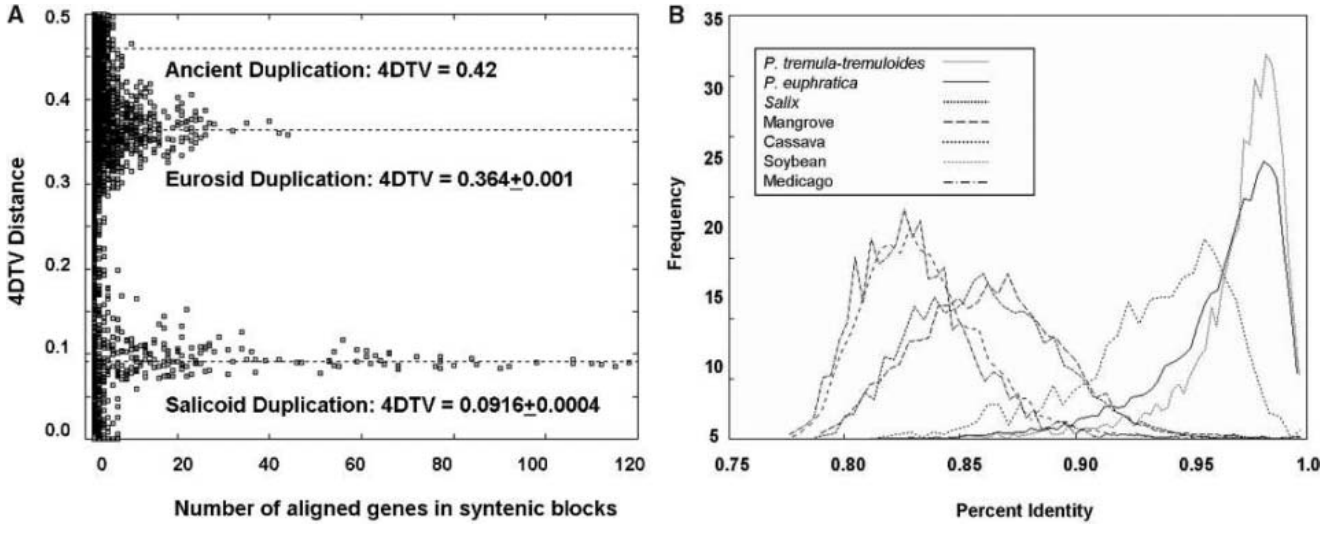

Fig. 3. (**A**) The 4DTV metrics for paralogous gene pairs in *Populus-Populus* and *Populus-Arabidopsis*. Three separate genome-wide duplications events are detectable, with the most recent event contained within the Salicaceae and the middle event apparently shared among the Eurosids. (**B**) Percent identity distributions for mutual best EST hit to *Populus trichocarpa* CDS.

one-sixth the estimated rate for *Arabidopsis* (that is, 8 to 13 Ma divided by 60 to 65 Ma). Qualitatively similar slowing of the molecular clock is found in the *Populus* chloroplast and mitochondrial genomes (*9*). Because *Populus* is a long-lived vegetatively propagated species, it has the potential to successfully contribute gametes to multiple generations. A single *Populus* genotype can persist as a clone on the landscape for millennia (*26*), and we propose that recurrent contributions of "ancient gametes" from very old individuals could account for the markedly reduced rate of sequence evolution. As a result of the slowing of the molecular clock, the *Populus* genome most likely resembles the ancestral eurosid genome.

To test whether the burst of gene creation 60 to 65 Ma was due to a single whole-genome event or to independent but near-synchronous gene duplication events, we used a variant of the algorithm of Hokamp *et al*. (*27*) to identify segments of conserved synteny within the *Populus* genome. The longest conserved syntenic block from the 4DTV ~0.09 epoch spanned 765 pairs of paralogous genes. In total, 32,577 genes were contained within syntenic blocks from the salicoid epoch; half of these genes were contained in segments longer than 142 paralogous pairs. The same algorithm, when applied to randomly shuffled genes, typically yields duplicate blocks with fewer than 8 to 9 genes, indicating that the *Populus* gene duplications occurred as a single genome-wide event. We refer to this duplication event as the "salicoid" duplication event.

Nearly every mapped segment of the *Populus* genome had a parallel "paralogous" segment elsewhere in the genome as a result of the salicoid event (Fig. 2). The pinwheel patterns can be understood as a whole-genome duplication followed by a series of reciprocal tandem terminal fusions between two separate sets of four chromosomes each—the first involving LGII, V, VII, and XIV and the second involving LGI, XI, IV, and IX. In addition, several chromosomes appear to have experienced minor reorganizational exchanges. Furthermore, LGI appears to be the result of multiple rearrangements involving three major tandem fusions. These results suggest that the progenitor of *Populus* had a base chromosome number of 10. After the whole-genome duplication event, this base chromosome number experienced a genome-wide reorganization and diploidization of the duplicated chromosomes into four pairs of complete paralogous chromosomes (LGVI, VIII, X, XII, XIII, XV, XVI, XVIII, and XIX); two sets of four chromosomes, each containing a terminal translocation (LGI, II, IV, V, VII, IX, and XI); and one chromosome containing three terminally joined chromosomes (LGIII with I or XVII with VII). The colinearity of genetic maps among multiple *Populus* species suggests that the genome reorganization occurred before the evolution of the modern taxa of *Populus*.

Genome duplication in a common ancestor of *Populus* and *Arabidopsis*. The distribution of 4DTV values for paralogous pairs of genes also shows that a large fraction of the *Populus* genome falls in a set of duplicated segments anchored by gene pairs with 4DTV at 0.364 ± 0.001, representing the residue of a more ancient, large-scale, apparently synchronous duplication event (Fig. 3A). This relatively older duplication event covers about 59% of the *Populus* genome with 16% of genes in these segments present in two copies. Because this duplication preceded and is therefore superimposed upon the salicoid event, each genomic region is potentially covered by four such segments. Similarly, the *Arabidopsis* genome experienced an older "beta" duplication that preceded the Brassicaceae-specific "alpha" event (*28*–*32*).

We next asked whether the *Arabidopsis* "beta" (*30*, *32*) and *Populus* 4DTV ~0.36 duplication events were (i) independent genome-wide duplications that occurred after the split from the last common eurosid ancestor (H_1) or (ii) a single shared duplication event that occurred in an ancestral lineage (i.e., before the divergence of eurosid lineages I and II) (H_2). These two hypotheses have very different implications for the interpretation of homology between *Populus* and *Arabidopsis*. Under H_1, each genomic segment in one species is homologous to four segments in the other; whereas under H_2, each segment is homologous to only two segments in the other species. These hypotheses were tested by comparing the relative distances between gene pairs sampled within and between *Populus* and *Arabidopsis*. H_2 was generally supported (*9*), but we could not reject H_1. We can only conclude that the *Populus* genome duplication occurred very close to the time of divergence of the eurosid I and II lineages (*9*), with slight support for a shared duplication. This coincident timing raises the possibility of a causal link between this duplication and rapid diversification early in eurosid (and perhaps core eudicot) history. We refer to this older *Populus*/*Arabidopsis* duplication event as the "eurosid" duplication event. We note that the salicoid duplication occurred independently of the eurosid duplication observed in the *Arabidopsis* genome.

Gene Content

Although *Populus* has substantially more protein-coding genes than *Arabidopsis*, the relative frequency of domains represented in protein databases (Prints, Prosite, Pfam, ProDom, and SMART) in the two genomes is similar (*9*). However, the most common domains occur in *Populus* compared with *Arabidopsis* in a ratio ranging from 1.4:1 to 1.8:1. Noteworthy outliers in *Populus* include genes and gene domains associated with disease and insect resistance (such as, in *Populus* versus *Arabidopsis*, respectively: leucine-rich repeats, 1271 versus 527; NB-ARC domain, 302 versus 141; and thaumatin, 55 versus 24), meristem development (such as NAC transcription factors, 157 versus 100, respectively), and metabolite and nutrient transport [such as oligopeptide transporter of the proton-dependent oligopeptide transporter (POT) and oligopeptide transporter (OPT) families, 129 versus 61, and potassium transporter, 30 versus 13, respectively].

Some domains were underrepresented in *Populus* compared with *Arabidopsis*. For example, the F-box domain was twice as prevalent in *Arabidopsis* as in *Populus* (624 versus 303, respectively). The F-box domain is involved in diverse and complex interactions involving protein degradation through the ubiquitin-26*S* proteosome pathway (*33*). Many of the ubiquitin-associated domains are underrepresented in *Populus* compared with *Arabidopsis* (for example, the *Ulp1* protease family and the C-terminal catalytic domain, 10 versus 63, respectively). Moreover, the RING-finger domains are nearly equally present in both genomes (503 versus 407, respectively), suggesting that protein degradation pathways in the two organisms are metabolically divergent.

The common eurosid gene set. The *Populus* and *Arabidopsis* gene sets were compared to infer the conserved gene complement of their common eurosid ancestor, integrating information from nucleotide divergence, synteny, and mutual best BLAST-hit analysis (*9*). The ancestral eurosid genome contained at least 11,666 protein-coding genes, along with an undetermined number that were either lost in one or both of the lineages or whose homology could not be detected. These ancestral genes were the progenitors of gene families of typically one to four descendents in each of the complete plant genomes and account for 28,257 *Populus* and 17,521 *Arabidopsis* genes. Gene family lists are accessible at www.phytozome.net. The gene predictions in these two genomes that could not be accounted for in the eurosid clusters were often fragmentary or difficult to categorize, and we could not confidently assign orthology to them. They may include previously unidentified or rapidly evolving genes in the *Populus* and/or *Arabidopsis* lineages, as well as poorly predicted genes.

Noncoding RNAs. Based on a series of publicly available RNA detection algorithms (*34*), including tRNAScan-SE, INFERNAL, and snoScan, we identified 817 putative tRNAs; 22 U1, 26 U2, 6 U4, 23 U5, and 11 U6 spliceosomal small nuclear RNAs (snRNAs); 339 putative C/D small nucleolar RNAs (snoRNAs); and 88 predicted H/ACA snoRNAs in the *Populus* assembly. All 57 possible anticodon tRNAs were found. One selenocysteine tRNA was detected and two possible suppressor tRNAs (anticodons that bind stop codons) were also identified. *Populus* has nearly 1.3 times as many tRNA genes as *Arabidopsis*. In contrast to *Arabidopsis* (fig. S7A), the copy number of tRNA in *Populus* was significantly and positively correlated with amino acid occurrence in predicted gene models (fig. S7B). The ratio of the number of snRNAs in *Populus* compared with the number in *Arabidopsis* is 1.3 to 1.0, yet U1, U2, and U5 are overrepresented in *Populus*, whereas U4 is underrepresented. Further-

more, U14 was not detected in *Arabidopsis*. The snRNAs and snoRNAs have not been experimentally verified in *Populus*.

There are 169 identified microRNA (miRNA) genes representing 21 families in *Populus* (table S7). In *Arabidopsis*, these 21 families contain 91 miRNA genes, representing a 1.9X expansion in *Populus*, primarily in miR169 and miR159/319. All 21 miRNA families have regulatory targets that appear to be conserved among *Arabidopsis* and *Populus* (table S8). Similar to the miRNA genes themselves, the number of predicted targets for these miRNA is expanded in *Populus* (147) compared with *Arabidopsis* (89). Similarly, the genes that mediate RNA interference (RNAi) are also overrepresented in *Populus* (21) compared to *Arabidopsis* (11) [e.g., AGO1 class, 7 versus 3; RNA helicase 2 versus 1; HEN, 2 versus 1; HYL1-like (double-stranded RNA binding proteins), 9 versus 5, respectively].

Tandem duplications. In *Populus* there were 1518 tandemly duplicated arrays of two or more genes based on a Smith-Waterman alignment E value $\leq 10^{-25}$ and a 100-kb window. The total number of genes in such arrays was 4839 and the total length of tandemly duplicated segments in *Populus* was 47.9 Mb, or 15.6% of the genome (fig. S8). By the same criteria, there are 1366 tandemly duplicated segments in *Arabidopsis*, covering 32.4 Mb, or 27% of the genome. By far the most common number of genes within a single array was two, with 958 such arrays in *Populus* and 805 in *Arabidopsis*. *Arabidopsis* had a larger number of arrays containing six or more genes than did *Populus*. Tandem duplications thus appear to be relatively more common in *Arabidopsis* than in *Populus*. This may in part be due to difficulties in assembling tandem repeats from a whole-genome shotgun sequencing approach, particularly when tandemly duplicated genes are highly conserved. Alternatively, the *Populus* genome may be undergoing rearrangements at a slower rate than the *Arabidopsis* genome, which is consistent with our observations of reduced chromosomal rearrangements and slower nucleotide substitution rates in *Populus*.

In some cases, genes were highly duplicated in both species, and some tandem duplications predated the *Populus*-*Arabidopsis* split (*9*). The largest number of tandem repeats in *Populus* in a single array was 24 and contained genes with high homology to S locus–specific glycoproteins. Genes of this class also occur as tandem repeats in *Arabidopsis*, with the largest segments containing 14 tandem duplicates on chromosome 1. One of the InterPro domains in this protein, IPR008271, a serine/threonine protein kinase active site, was the most frequent domain in tandemly repeated genes in both species (fig. S8). Other common domains in both species were the leucine-rich repeat (IPR007090, primarily from tandem repeats of disease resistance genes), the pentatricopeptide repeat RNA-binding proteins (IPR002885), and the uridine diphosphate (UDP)-glucuronosyl/UDP-glucosyltransferase domain (IPR002213) (table S9).

In contrast, some genes were highly expanded in tandem duplicates in one genome and not in the other (fig. S8). For example, one of the most frequent classes of tandemly duplicated genes in *Arabidopsis* was F-box genes, with a total of 342 involved in tandem duplications, the largest segment of which contained 24 F-box genes. *Populus* contains only 37 F-box genes in tandem duplications, with the largest segment containing only 3 genes.

Postduplication Gene Fate

Functional expression divergence. In *Populus*, 20 of the 66 salicoid-event duplicate gene pairs contained in 19 *Populus* EST libraries (2.3% of the total) showed differential expression (*9*) [displaying significant deviation in EST frequencies per library (Fig. 4)]. Out of 18 eurosid-event duplicate gene pairs (2.7% of the total), 11 also displayed significant deviation in EST frequencies per library. Many of the duplicate gene pairs that displayed significant overrepresentation in one or more of the 19 sampled libraries were involved in protein-protein interactions (such as annexin) or protein folding (such as cyclophilins). In the eurosid set, there was a greater divergence in the best BLAST hit among pairwise sets of genes. These results support the premise of functional expression divergence among some duplicated gene pairs in *Populus*.

To further test for variation in gene expression among duplicated genes, we examined whole-genome oligonucleotide microarray data containing the 45,555 promoted genes (*9*). There was significantly lower differential expression in the salicoid duplicated pairs of genes (mean = 5%) relative to eurosid duplications (mean = 11%), again suggesting that differential expression patterns for retained paralogous gene pairs is an ongoing process that has had more time to occur in eurosid pairs (Fig. 5). This difference could also be due to absolute expression level, which may vary systematically between the two duplication events. Moreover, differential expression was more evident in the wood-forming organs. Almost 14 and 13% (2632 pairs of genes) of eurosid duplicated genes in the nodes and internodes, respectively, displayed differential expression, compared with 8% or less in roots and young leaves (Fig. 5).

Single-nucleotide polymorphisms. *Populus* is a highly polymorphic taxon and substantial numbers of SNPs are present even within a single individual (Table 1). The ratio of nonsynonymous to synonymous substitution rate ($\omega = dN/dS$) was calculated as an index of selective constraints for alleles of individual genes (*9*). The overall average dN across all genes was 0.0014, whereas the dS value was 0.0035, for a total ω of 0.40, suggesting that the majority of coding regions in the *Populus* genome are subject to purifying selection. There was a significant, negative correlation between ω and the 4DTV distance to the most closely related paralog ($r = -0.034$, $P = 0.028$), which is consistent with the expectation of higher levels of nonsynonymous polymorphism in recently duplicated genes as a result of functional redundancy (*20*, *35*). Similarly, genes with recent tandem duplicates (4DTV ≤ 0.2) had significantly higher ω than did genes with no recent tandem duplicates (Wilcoxon rank sum $Z = 8.65$, $P \leq 0.0001$) (table S10).

The results for tandemly duplicated genes were consistent with expectations for accelerated evolution of duplicated genes (*20*). However, this expectation was not upheld for paralogous pairs of genes from the whole-genome duplication events. Relative rates of nonsynonymous substitution were actually lower for genes with paralogs from the salicoid and eurosid whole-genome duplication events than for genes with no paralogs (table S11). One possible explanation for this

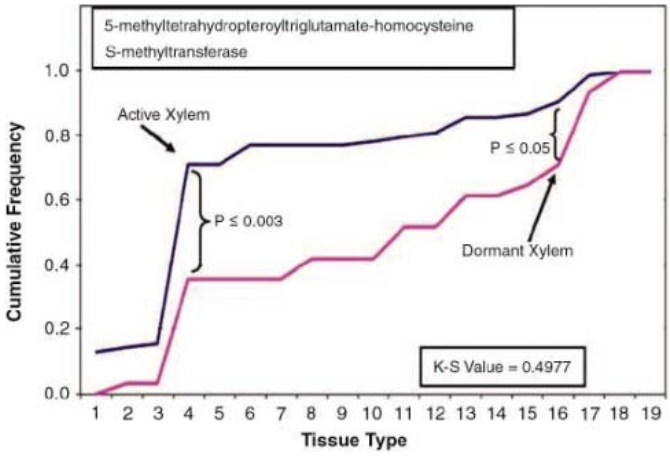

Fig. 4. Kolmogorov-Smirnov (K-S) test for differential expression for 5-methyltetrahydropteroyltriglutamate-homocysteine *S*-methyltransferase genes [for descriptions of the EST data set, see Sterky *et al.* (*79*)]. Results suggest that the duplicated genes in *Populus* are differentially expressed in alternate tissues. Tissue types include: cambial zone (1), young leaves (2), flower buds (3), tension wood (4), senescing leaves (5), apical shoot (6), dormant cambium (7), active cambium (8), cold stressed leaves (9), roots (10), bark (11), shoot meristem (12), male catkins (13), dormant buds (14), female catkins (15), petioles (16), wood cell death (17), imbibed seeds (18) and infected leaves (19).

discrepancy is that the apparent single-copy genes have a corresponding overrepresentation of rapidly evolving pseudogenes. However, this does not appear to be the case, as demonstrated by an analysis of gene size, synonymous substitution rate, and minimum genetic distance to the closest paralog as covariates in an analysis of variance with ω as the response variable (table S11). Therefore, genes with no paralogs from the salicoid and eurosid duplication events seem to be under lower selective constraints, and purifying selection is apparently stronger for genes with paralogs retained from the whole-genome duplications. Chapman *et al*. (*36*) have recently proposed the concept of functional buffering to account for similar reduction in detected mutations in paralogs from whole-genome duplications in *Arabidopsis* and *Oryza*. The vegetative propagation habit of *Populus* may also favor the conservation of nucleotide sequences among duplicated genes, in that complementation among duplicate pairs of genes would minimize loss of gene function associated with the accumulation of deleterious somatic mutations.

Gene family evolution. The expansion of several gene families has contributed to the evolution of *Populus* biology.

Lignocellulosic wall formation. Among the processes unique to tree biology, one of the most obvious is the yearly development of secondary xylem from the vascular cambium. We identified *Populus* orthologs of the approximately 20 *Arabidopsis* genes and gene families involved in or associated with cellulose biosynthesis. The *Populus* genome has 93 cellulose synthesis–related genes compared with 78 in *Arabidopsis*. The *Arabidopsis* genome encodes 10 *CesA* genes belonging to six classes known to participate in cellulose microfibril biosynthesis (*37*). *Populus* has 18 *CesA* genes (*38*), including duplicate copies of *CesA7* and *CesA8* homologs. *Populus* homologs of *Arabidopsis CesA4*, *CesA7*, and *CesA8* are coexpressed during xylem development and tension wood formation (*39*). Furthermore, one pair of *CesA* genes appears unique to *Populus*, with no homologs found in *Arabidopsis* (*40*). Many other types of genes associated with cellulose biosynthesis, such as *KOR*, *SuSY*, *COBRA*, and *FRA2*, occur in duplicate pairs in *Populus* relative to single-copy *Arabidopsis* genes (*39*). For example, *COBRA*, a regulator of cellulose biogenesis (*41*), is a single-copy gene in *Arabidopsis*, but in *Populus* there are four copies.

The repertoire of acknowledged hemicellulose biosynthetic genes in *Populus* is generally similar to that in *Arabidopsis*. However, *Populus* has more genes encoding α-L-fucosidases and fewer genes encoding α-L-fucosyltransferases than does *Arabidopsis*, which is consistent with the lower xyloglucan fucose content (*42*) in *Populus* relative to *Arabidopsis*.

Lignin, the second most abundant cell wall polymer after cellulose, is a complex polymer of monolignols (hydroxycinnamyl alcohols) that encrusts and interacts with the cellulose/hemicellulose matrix of the secondary cell wall (*43*). The full set of 34 *Populus* phenylpropanoid and lignin biosynthetic genes (table S13) was identified by sequence alignment to the known *Arabidopsis* phenylpropanoid and lignin genes (*44*, *45*). The size of the *Populus* gene families that encode these enzymes is generally larger than in *Arabidopsis* (34 versus 18, respectively). The only exception is cinnamyl alcohol dehydrogenase (CAD), which is encoded by a single gene in *Populus* and two genes in *Arabidopsis* (Fig. 6C); CAD is also encoded by only a single gene in *Pinus taeda* (*46*, *47*). Two lignin-related *Populus C4H* genes are strongly coexpressed in tissues related to wood formation, whereas the three *Populus C3H* genes show reciprocally exclusive expression patterns (*48*) (Fig. 6, A and B).

Secondary metabolism. Populus trees produce a broad array of nonstructural, carbon-rich secondary metabolites that exhibit wide variation in abundance, stress inducibility, and effects on tree growth and host-pest interactions (*49*–*53*). Shikimate-phenylpropanoid–derived phenolic esters, phenolic glycosides, and condensed tannins and their flavonoid precursors comprise the largest classes of these metabolites. Phenolic glycosides and condensed tannins alone can constitute up to 35% leaf dry weight and are abundant in buds, bark, and roots of *Populus* (*50*, *54*, *55*).

The flavonoid biosynthetic genes are well annotated in *Arabidopsis* (*56*) and almost all (with the exception of flavonol synthase) are encoded by single-copy genes. In contrast, all but three such enzymes (chalcone isomerase, flavonoid 3′-hydroxylase, and flavanone 3-hydroxylase) are encoded by multiple genes in *Populus* (*53*). For example, the chalcone synthase, controlling the committed step to flavonoid biosynthesis, has expanded to at least six genes in *Populus*. In addition, *Populus* contains two genes each for flavone synthase II (cytochrome accession number CYP98B) and flavonoid 3′,5′-hydroxylase (CYP75A12 and CYP75A13), both of which are absent in *Arabidopsis*. Furthermore, three *Populus* genes encode leucoanthocyanidin reductase, required for the synthesis of condensed tannin precursor 2,3-*trans*-flavan-3-ols, a stereochemical configuration also lacking in *Arabidopsis* (*57*). In contrast to the 32 terpenoid synthase (*TPS*) genes of secondary metabolism identified in the *Arabidopsis* genome (*58*), the *Populus* genome contains at least 47 *TPS* genes, suggesting a wide-ranging capacity for the formation of terpenoid secondary metabolites.

A number of phenylpropanoid-like enzymes have been annotated in the *Arabidopsis* genome (*44*, *45*, *59*–*61*). One example is the family encoding *CAD*. In addition to the single *Populus CAD* gene involved in lignin biosynthesis, several other clades of *CAD-like* (*CADL*) genes are present, most of which fall within larger subfamilies containing enzymes related to multifunctional alcohol dehydrogenases (Fig. 6). This comparative analysis makes it clear that there has been selective expansion and retention of *Populus CADL* gene families. For example, *Populus* contains seven *CADL* genes (*PoptrCADL1* to *PoptrCADL7*; Fig. 6C) encoding enzymes related to the *Arabidopsis* BAD1 and BAD2 enzymes with apparent benzyl alcohol dehydrogenase activities (*62*). BAD1 and BAD2 are known to be pathogen inducible, suggesting that this group of *Populus* genes, including the *Populus SAD* gene, previously characterized as encoding a sinapaldehyde-specific CAD enzyme (*63*), may be involved in chemical defense.

Disease resistance. The likelihood that a perennial plant will encounter a pathogen or herbivore before reproduction is near unity. The long-generation intervals for trees make it difficult for such plants to match the evolutionary rates of a microbial or insect pest. Aside from the formation of thickened cell walls and the synthesis of secondary metabolites that constitute a first line of defense against microbial and insect pests, plants use a variety of disease-resistance (*R*) genes.

The largest class of characterized *R* genes encodes intracellular proteins that contain a

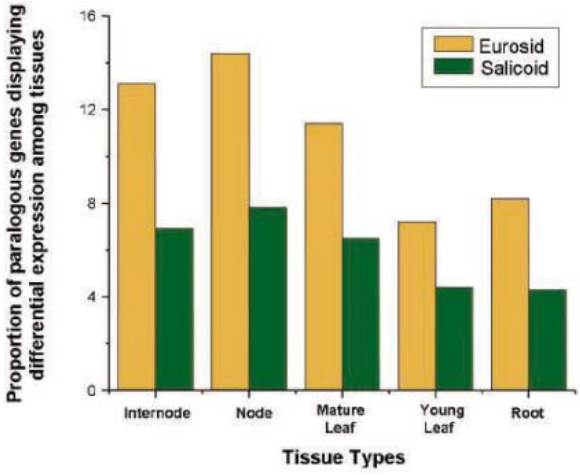

Fig. 5. Proportion of eurosid and salicoid duplicated gene sets differentially expressed in stems (nodes and internode), leaves (young and mature), and whole roots. Samples from four biological replicates collected from the reference genotype Nisqually 1 were individually hybridized to whole-genome oligonucleotide microarrays containing three 60-oligomer oligonucleotide probes for each gene. Differential expression between duplicated genes was evaluated in *t* tests and declared significant at a 5% false discovery rate (*9*).

nucleotide-binding site (NBS) and carboxy-terminal leucine-rich-repeats (LRR) (*64*). The NBS-coding *R* gene family is one of the largest in *Populus*, with 399 members, approximately twice as high as in *Arabidopsis*. The NBS family can be divided into multiple subfamilies with distinct domain organizations, including 64 TIR-NBS-LRR genes, 10 truncated TIR-NBS that lack an LRR, 233 non–TIR-NBS-LRR genes, and 17 unusual TIR-NBS–containing genes that have not been identified previously in *Arabidopsis* (TNLT, TNLN, or TCNL domains) (Table 2). Five gene models coding for TNL proteins contained a predicted N-terminal nuclear localization signal (*65*). The number of non–TIR-NBS-LRR genes in *Populus* is also much higher than that in *Arabidopsis* (209 versus 57, respectively). Notably, 40 non–TIR-NBS genes, not found in *Arabidopsis*, carry an N-terminal BED DNA-binding zinc finger domain that was also found in the *Oryza Xa1* gene. These findings suggest that domain cooption occurred in *Populus*. Most NBS-LRR (about 65%) in *Populus* occur as singletons or in tandem duplications, and the distribution of pairwise genetic distances among these genes suggests a recent expansion of this family. That is, only 10% of the NBS-LRR genes are associated with the eurosid and salicoid duplication events, compared with 55% of the extracellular LRR receptor-like kinase genes (for example, fig. S10).

Several conserved signaling components such as RAR1, EDS1, PAD4, and NPR1, known to be recruited by *R* genes, also contain multiple homologs in *Populus*. For example, two copies of the *PAD4* gene, which functions upstream of salicylic acid accumulation, and five copies of the *NPR1* gene, an important regulator of responses downstream of salicylic acid, are found in *Populus*. Nearly all genes known to control disease resistance signaling in *Arabidopsis* have putative orthologs in *Populus*. *Populus* has a larger number of β-1,3-glucanase and chitinase genes than does *Arabidopsis* (131 versus 73, respectively). In summary, the structural and genetic diversity that exists among *R* genes and their signaling components in *Populus* is remarkable and suggests that unlike the rest of the genome, contemporary diversifying selection has played an important role in the evolution of disease resistance genes in *Populus*. Such diversification suggests that enhanced ability to detect and respond to biotic challenges through *R* gene–mediated signaling may be critical over a decades-long life span of this genus.

Membrane transporters. Attributes of *Populus* biology such as massive interannual, seasonal, and diurnal metabolic shifts and redeployment of carbon and nitrogen may require an elaborate array of transporters. Investigation of gene families coding for transporter proteins (http://plantst.genomics.purdue.edu/) in the *Populus* genome revealed a general expansion relative to *Arabidopsis* (1722 versus 959, in *Populus* versus *Arabidopsis*, respectively) (table S12). Five gene families, coding for adenosine 5′-triphosphate–binding cassette proteins (ABC transporters, 226 gene models), major facilitator superfamily proteins (187 genes), drug/metabolite transporters (108 genes), amino acid/auxin permeases (95 genes), and POT transporters (90 genes), accounted for more than 40% of the total number of transporter gene models (fig. S14). Some large families such as those encoding POT (4.3X relative to *Arabidopsis*), glutamate-gated ion channels (3.7X), potassium uptake permeases (2.3X), and ABC transporters (1.9X) are expanded in *Populus*. We identified a subfamily of five putative aquaporins, lacking in the *Arabidopsis*. *Populus* also harbors seven transmembrane receptor genes that have previously only been found in fungi, and two genes, identified as mycorrhizal-specific phosphate transporters, that confirm that the mycorrhizal symbiosis may have an impact on the mineral nutrition of this long-lived species. This expanded inventory of transporters could conceivably play a role in adaptation to nutrient-limited forest soils, long-distance transport and storage of water and metabolites, secretion and movement of secondary metabolites, and/or mediation of resistance to pathogen-produced secondary metabolites or other toxic compounds.

Phytohormones. Both physiological and molecular studies have indicated the importance of

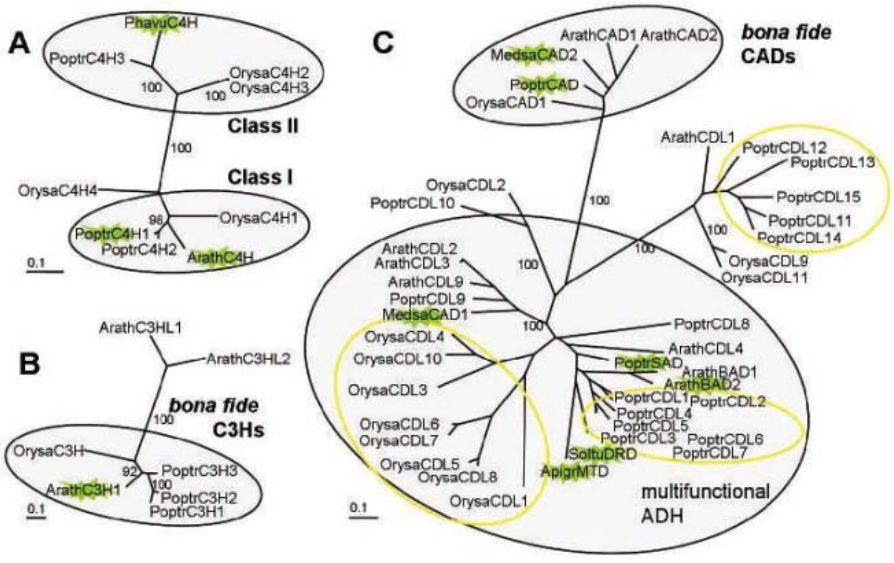

Fig. 6. Phylogenetic analysis of gene families in *Populus*, *Arabidopsis*, and *Oryza* encoding selected lignin biosynthetic and related enzymes. (**A**) Cinnamate-4-hydroxylase (*C4H*) gene family. (**B**) 4-coumaroyl-shikimate/quinate-3-hydroxlase (*C3H*) gene family. (**C**) Cinnamyl alcohol dehydrogenase (*CAD*) and related multifunctional alcohol dehydrogenase gene family. *Arabidopsis* gene names are the same as those in Ehlting *et al*. (*80*). *Populus* and *Oryza* gene names were arbitrarily assigned; corresponding gene models are listed in table S13. Genes encoding enzymes for which biochemical data are available are highlighted with a green flash. Yellow circles indicate monospecific clusters of gene family members.

Table 2. Numbers of genes that encode domains similar to plant *R* proteins in *Populus*, *Arabidopsis* (*81*), and *Oryza* (*82*). *, BED finger and/or DUF1544 domain; CC, coiled coil; –, not detected.

Predicted protein domains	Letter code	*Populus*	*Arabidopsis*	*Oryza*
TIR-NBS	TN	10	21	–
TIR-NBS-LRR	TNL	64	83	–
TIR-NBS-LRR-TIR	TNLT	13	–	–
TIR-NBS-LRR-NBS	TNLN	1	–	–
NBS-LRR-TIR	NLT	1	–	–
TIR-CC-NBS-LRR	TCNL	2	–	–
CC-NBS	CN	19	4	7
CC-NBS-LRR	CNL	119	51	159
BED/DUF1544*-NBS	BN	5	–	–
NBS-BED/DUF1544*	NB	1	–	–
BED/DUF1544*-NBS-LRR	BNL	24	–	–
NBS-LRR	NL	90	6	40
NBS	N	49	1	45
Others	–	–	41	284
Total NBS genes		398	207	535

hormonal regulation underlying plant development. Auxin, gibberellin, cytokinin, and ethylene responses are of particular interest in tree biology.

Many auxin responses (*66*–*71*) are controlled by auxin response factor (*ARF*) transcription factors, which work together with cognate AUX/IAA repressor proteins to regulate auxin-responsive target genes (*72*, *73*). A phylogenetic analysis using the known and predicted *ARF* protein sequences showed that *Populus* and *Arabidopsis ARF* gene families have expanded independently since they diverged from their common ancestor. Six duplicate *ARF* genes in *Populus* encode paralogs of *ARF* genes that are single-copy *Arabidopsis* genes, including *ARF5* (*MONOPTEROS*), an important gene required for auxin-mediated signal transduction and xylem development. Furthermore, five *Arabidopsis ARF* genes have four or more predicted *Populus ARF* gene paralogs. In contrast to *ARF* genes, *Populus* does not contain a notably expanded repertoire of *AUX/IAA* genes relative to *Arabidopsis* (35 versus 29, respectively) (*74*). Interestingly, there is a group of four *Arabidopsis AUX/IAA* genes with no apparent *Populus* orthologs, suggesting *Arabidopsis*-specific functions.

Gibberellins (GAs) are thought to regulate multiple processes during wood and root development, including xylem fiber length (*75*). Among all gibberellin biosynthesis and signaling genes, the *Populus* GA20-oxidase gene family is the only family with approximately two times the number of genes relative to *Arabidopsis*, indicating that most of the duplicated genes that arose from the salicoid duplication event have been lost. GA20-oxidase appears to control flux in the biosynthetic pathway leading to the bioactive gibberellins GA_1 and GA_4. The higher complement of GA20-oxidase genes may have biological importance in *Populus* with respect to secondary xylem and fiber cell development.

Cytokinins are thought to control the identity and proliferation of cell types relevant for wood formation as well as general cell division (*67*). The total number of members in gene families encoding cytokinin homeostasis related isopentenyl transferases (IPT) and cytokinin oxidases is roughly similar between *Populus* and *Arabidopsis*, although there appears to be lineage-specific expansion of IPT subfamilies. The cytokinin signal transduction pathway represents a two-component phosphorelay system, in which a two-component hybrid receptor initiates a phosphotransfer by means of histidine-containing phosphotransmitters (HPt) to phospho-accepting response regulators (RR). One family of genes, encoding the two-component receptors (such as CKI1), is notably expanded in *Populus* (four versus one in *Populus* and *Arabidopsis*, respectively) (*76*). Gene families coding for recently identified pseudo-*HPt* and atypical *RR* are overrepresented in *Populus* relative to *Arabidopsis* (2.5- and 4.0-fold increase in *Populus*, respectively). Both of these gene families have been implicated in the negative regulation of cytokinin signaling (*67*, *77*), which is consistent with the idea of increased complexity in regulation of cytokinin signal transduction in *Populus*.

Populus and *Arabidopsis* genomes contain almost identical numbers of genes for the three enzymes of ethylene biosynthesis, whereas the number of genes for proteins involved in ethylene perception and signaling is higher in *Populus*. For example, *Populus* has seven predicted genes for ethylene receptor proteins and *Arabidopsis* has five; the constitutive triple response kinase that acts just downstream of the receptor is encoded by four genes in *Populus* and only one in *Arabidopsis* (*78*). The number of ethylene-responsive element binding factor (ERF) proteins (a subfamily of the AP2/ERF family) is higher in *Populus* than in *Arabidopsis* (172 versus 122, respectively). The increased variation in the number of ERF transcription factors may be involved in the ethylene-dependent processes specific to trees, such as tension wood formation (*68*) and the establishment of dormancy (*71*).

Conclusions

Our initial analyses provide a flavor of the opportunities for comparative plant genomics made possible by the generation of the *Populus* genome sequence. A complex history of whole-genome duplications, chromosomal rearrangements and tandem duplications has shaped the genome that we observe today. The differences in gene content between *Populus* and *Arabidopsis* have provided some tantalizing insights into the possible molecular bases of their strongly contrasting life histories, although factors unrelated to gene content (such as regulatory elements, miRNAs, posttranslational modification, or epigenetic modifications) may ultimately be of equal or greater importance. With the sequence of *Populus*, researchers can now go beyond what could be learned from *Arabidopsis* alone and explore hypotheses to linking genome sequence features to wood development, nutrient and water movement, crown development, and disease resistance in perennial plants. The availability of the *Populus* genome sequence will enable continuing comparative genomics studies among species that will shed new light on genome reorganization and gene family evolution. Furthermore, the genetics and population biology of *Populus* make it an immense source of allelic variation. Because *Populus* is an obligate outcrossing species, recessive alleles tend to be maintained in a heterozygous state. Informatics tools enabled by the sequence, assembly, and annotation of the *Populus* genome will facilitate the characterization of allelic variation in wild *Populus* populations adapted to a wide range of environmental conditions and gradients over large portions of the Northern Hemisphere. Such variants represent a rich reservoir of molecular resources useful in biotechnological applications, development of alternative energy sources, and mitigation of anthropogenic environmental problems. Finally, the keystone role of *Populus* in many ecosystems provides the first opportunity for the application of genomics approaches to questions with ecosystem-scale implications.

References and Notes

1. Food and Agricultural Organization of the United Nations, *State of the World's Forests 2003* (FAO, Rome, 2003).
2. R. F. Stettler, H. D. Bradshaw Jr., in *Biology of* Populus *and Its Implications for Management and Conservation*, R. F. Stettler, H. D. Bradshaw Jr., P. E. Heilman, T. M. Hinckley, Eds. (NRC Research Press, Ottawa, 1996), pp. 1–7.
3. G. A. Tuskan, S. P. DiFazio, T. Teichmann, *Plant Biol.* **6**, 2 (2004).
4. T. M. Yin, S. P. DiFazio, L. E. Gunter, D. Riemenschneider, G. A. Tuskan, *Theor. Appl. Genet.* **109**, 451 (2004).
5. R. Meilan, C. Ma, in *Agrobacterium Protocols*, vol. 344 of *Methods in Molecular Biology*, K. Wang, Ed. (Humana Press, Totowa, NJ, 2006), pp. 143–151.
6. G. A. Tuskan, *Biomass Bioenerg.* **14**, 307 (1998).
7. G. A. Tuskan, M. Walsh, *For. Chron.* **77**, 259 (2001).
8. S. Wullschleger *et al.*, *Can. J. For. Res.* **35**, 1779 (2005).
9. Materials and methods are available as supporting material on *Science* Online.
10. H. D. Bradshaw, R. F. Stettler, *Theor. Appl. Genet.* **86**, 301 (1993).
11. M. Koornneef, P. Fransz, H. de Jong, *Chromosome Res.* **11**, 183 (2003).
12. O. Santamaria, J. J. Diez, *For. Pathol.* **35**, 95 (2005).
13. G. A. Tuskan *et al.*, *Can. J. For. Res.* **34**, 85 (2004).
14. A. A. Salamov, V. V. Solovyev, *Genome Res.* **10**, 516 (2000).
15. E. Birney, R. Durbin, *Genome Res.* **10**, 547 (2000).
16. T. Schiex, A. Moisan, P. Rouzé, in *Computational Biology: Selected Papers from JOBIM'2000, number 2066 in LNCS* (Springer-Verlag, Heidelberg, Germany, 2001), pp. 118–133.
17. Y. Xu, E. C. Uberbacher, *J. Comput. Biol.* **4**, 325 (1997).
18. S. J. Hanley, M. D. Mallott, A. Karp, *Tree Genet. Genomes*, in press.
19. M. A. Koch, B. Haubold, T. Mitchell-Olds, *Mol. Biol. Evol.* **17**, 1483 (2000).
20. M. Lynch, J. S. Conery, *Science* **290**, 1151 (2000).
21. L. Sterck *et al.*, *New Phytol.* **167**, 165 (2005).
22. L. A. Dode, *Bull. Soc. Hist. Nat. Autun* **18**, 161 (1905).
23. R. Regnier, in *Revue des Sociétés Savantes de Normandie* (Rouen, France, 1956), vol. 1, pp. 1–36.
24. M. E. Collinson, *Proc. R. Soc. Edinburgh B Bio. Sci.* **98**, 155 (1992).
25. J. E. Eckenwalder, in *Biology of Populus and Its Implications for Management and Conservation*, R. F. Stettler, H. D. Bradshaw Jr., P. E. Heilman, T. M. Hinckley, Eds. (NRC Research Press, Ottawa, 1996), chap. 1.
26. J. B. Mitton, M. C. Grant, *Bioscience* **46**, 25 (1996).
27. K. Hokamp, A. McLysaght, K. H. Wolfe, *J. Struct. Funct. Genomics* **3**, 95 (2003).
28. J. E. Bowers, B. A. Chapman, J. K. Rong, A. H. Paterson, *Nature* **422**, 433 (2003).
29. L. M. Zahn, J. Leebens-Mack, C. W. dePamphilis, H. Ma, G. Theissen, *J. Hered.* **96**, 225 (2005).
30. S. De Bodt, S. Maere, Y. Van de Peer, *Trends Ecol. Evol.* **20**, 591 (2005).
31. K. L. Adams, J. F. Wendel, *Trends Genet.* **21**, 539 (2005).
32. G. Blanc, K. Hokamp, K. H. Wolfe, *Genome Res.* **13**, 137 (2003).
33. B. A. Schulman *et al.*, *Nature* **408**, 381 (2000).
34. S. Griffiths-Jones *et al.*, *Nucleic Acids Res.* **33**, D121 (2005).
35. S. Lockton, B. S. Gaut, *Trends Genet.* **21**, 60 (2005).
36. B. A. Chapman, J. E. Bowers, F. A. Feltus, A. H. Paterson, *Proc. Natl. Acad. Sci. U.S.A.* **103**, 2730 (2006).
37. T. A. Richmond, C. R. Somerville, *Plant Physiol.* **124**, 495 (2000).
38. S. Djerbi, M. Lindskog, L. Arvestad, F. Sterky, T. T. Teeri, *Planta* **221**, 739 (2005).

39. C. P. Joshi *et al.*, *New Phytol.* **164**, 53 (2004).
40. A. Samuga, C. P. Joshi, *Gene* **334**, 73 (2004).
41. F. Roudier *et al.*, *Plant Cell* **17**, 1749 (2005).
42. R. M. Perrin *et al.*, *Science* **284**, 1976 (1999).
43. R. W. Whetten, J. J. Mackay, R. R. Sederoff, *Annu. Rev. Plant Physiol. Plant Mol. Biol.* **49**, 585 (1998).
44. J. Ehlting *et al.*, *Plant J.* **42**, 618 (2005).
45. J. Raes, A. Rohde, J. H. Christensen, Y. Van de Peer, W. Boerjan, *Plant Physiol.* **133**, 1051 (2003).
46. D. M. O'Malley, S. Porter, R. R. Sederoff, *Plant Physiol.* **98**, 1364 (1992).
47. J. J. Mackay, W. W. Liu, R. Whetten, R. R. Sederoff, D. M. Omalley, *Mol. Gen. Genet.* **247**, 537 (1995).
48. J. Schrader *et al.*, *Plant Cell* **16**, 2278 (2004).
49. S. Whitham, S. McCormick, B. Baker, *Proc. Natl. Acad. Sci. U.S.A.* **93**, 8776 (1996).
50. G. M. Gebre, T. J. Tschaplinski, G. A. Tuskan, D. E. Todd, *Tree Physiol.* **18**, 645 (1998).
51. G. Arimura, D. P. W. Huber, J. Bohlmann, *Plant J.* **37**, 603 (2004).
52. D. J. Peters, C. P. Constabel, *Plant J.* **32**, 701 (2002).
53. C.-J. Tsai, S. A. Harding, T. J. Tschaplinski, R. L. Lindroth, Y. Yuan, *New Phytol.* **172**, 47 (2006).
54. M. M. De Sá, R. Subramaniam, F. E. Williams, C. J. Douglas, *Plant Physiol.* **98**, 728 (1992).
55. R. L. Lindroth, S. Y. Hwang, *Biochem. Syst. Ecol.* **24**, 357 (1996).
56. B. Winkel-Shirley, *Curr. Opin. Plant Biol.* **5**, 218 (2002).
57. G. J. Tanner *et al.*, *J. Biol. Chem.* **278**, 31647 (2003).
58. S. Aubourg, A. Lecharny, J. Bohlmann, *Mol. Genet. Genomics* **267**, 730 (2002).
59. M. A. Costa *et al.*, *Phytochemistry* **64**, 1097 (2003).
60. D. Cukovic, J. Ehlting, J. A. VanZiffle, C. J. Douglas, *Biol. Chem.* **382**, 645 (2001).
61. J. M. Shockey, M. S. Fulda, J. Browse, *Plant Physiol.* **132**, 1065 (2003).
62. I. E. Somssich, P. Wernert, S. Kiedrowski, K. Hahlbrock, *Proc. Natl. Acad. Sci. U.S.A.* **93**, 14199 (1996).
63. L. Li *et al.*, *Plant Cell* **13**, 1567 (2001).
64. B. C. Meyers, S. Kaushik, R. S. Nandety, *Curr. Opin. Plant Biol.* **8**, 129 (2005).
65. L. Deslandes *et al.*, *Proc. Natl. Acad. Sci. U.S.A.* **99**, 2404 (2002).
66. E. J. Mellerowicz, M. Baucher, B. Sundberg, W. Boerjan, *Plant Mol. Biol.* **47**, 239 (2001).
67. A. P. Mähönen *et al.*, *Science* **311**, 94 (2006).
68. S. Andersson-Gunneras *et al.*, *Plant J.* **34**, 339 (2003).
69. J. M. Hellgren, K. Olofsson, B. Sundberg, *Plant Physiol.* **135**, 212 (2004).
70. M. G. Cline, K. Dong-Il, *Ann. Bot. (London)* **90**, 417 (2002).
71. R. Ruonala, P. Rinne, M. Baghour, H. Tuominen, J. Kangasjärvi, *Plant J.*, in press.
72. R. Moyle *et al.*, *Plant J.* **31**, 675 (2002).
73. D. Weijers *et al.*, *EMBO J.* **24**, 1874 (2005).
74. G. Hagen, T. Guilfoyle, *Plant Mol. Biol.* **49**, 373 (2002).
75. M. E. Eriksson, M. Israelsson, O. Olsson, T. Moritz, *Nat. Biotechnol.* **18**, 784 (2000).
76. T. Kakimoto, *Science* **274**, 982 (1996).
77. T. Kiba, K. Aoki, H. Sakakibara, T. Mizuno, *Plant Cell Physiol.* **45**, 1063 (2004).
78. T. Nakano, K. Suzuki, T. Fujimura, H. Shinshi, *Plant Physiol.* **140**, 411 (2006).
79. F. Sterky *et al.*, *Proc. Natl. Acad. Sci. U.S.A.* **101**, 13951 (2004).
80. J. Ehlting *et al.*, *Plant J.* **42**, 618 (2005).
81. B. C. Meyers, S. Kaushik, R. S. Nandety, *Curr. Opin. Plant Biol.* **8**, 129 (2005).
82. M. W. Jones-Rhoades, D. P. Bartel, *Mol. Cell* **14**, 787 (2004).

83. We thank the U.S. Department of Energy, Office of Science for supporting the sequencing and assembly portion of this study; Genome Canada and the Province of British Columbia for providing support for the BAC end, BAC genotyping, and full-length cDNA portions of this study; the Umeå University and the Royal Technological Institute (KTH) in Stockholm for supporting the EST assembly and annotation portion of this study; the membership of the International *Populus* Genome Consortium for supplying genetic and genomics resources used in the assembly and annotation of the genome; the NSF Plant Genome Program for supporting the development of Web-based tools; T. H. D. Bradshaw and R. Stettler for input and reviews on draft copies of the manuscript; J. M. Tuskan for guidance and input during the analysis and writing of the manuscript; and the anonymous reviewers who provided critical input and recommendations on the manuscript. GenBank Accession Number: AARH00000000.

Supporting Online Material

www.sciencemag.org/cgi/content/full/313/5793/1596/DC1
Materials and Methods
Figs. S1 to S15
Tables S1 to S14
References

13 April 2006; accepted 9 August 2006
10.1126/science.1128691

Opposing Activities Protect Against Age-Onset Proteotoxicity

Ehud Cohen,[1]* Jan Bieschke,[2]* Rhonda M. Perciavalle,[1] Jeffery W. Kelly,[2] Andrew Dillin[1]†

Aberrant protein aggregation is a common feature of late-onset neurodegenerative diseases, including Alzheimer's disease, which is associated with the misassembly of the $A\beta_{1-42}$ peptide. Aggregation-mediated $A\beta_{1-42}$ toxicity was reduced in *Caenorhabiditis elegans* when aging was slowed by decreased insulin/insulin growth factor–1–like signaling (IIS). The downstream transcription factors, heat shock factor 1, and DAF-16 regulate opposing disaggregation and aggregation activities to promote cellular survival in response to constitutive toxic protein aggregation. Because the IIS pathway is central to the regulation of longevity and youthfulness in worms, flies, and mammals, these results suggest a mechanistic link between the aging process and aggregation-mediated proteotoxicity.

Late-onset human neurodegenerative diseases including Alzheimer's (AD), Huntington's, and Parkinson's diseases are genetically and pathologically linked to aberrant protein aggregation (*1*, *2*). In AD, formation of aggregation-prone peptides, particularly $A\beta_{1-42}$, by endoproteolysis of the amyloid precursor protein (APP) is associated with the disease through an unknown mechanism (*3*, *4*). Whether intracellular accumulation or extracellular deposition of $A\beta_{1-42}$ initiates the pathological process is a key unanswered question (*5*). Typically, individuals who carry AD-linked mutations present with clinical symptoms during their fifth or sixth decade, whereas sporadic cases appear after the seventh decade. Why aggregation-mediated toxicity emerges late in life and whether it is mechanistically linked to the aging process remain unclear.

Perhaps the most prominent pathway that regulates life span and youthfulness in worms, flies, and mammals is the insulin/insulin growth factor (IGF)–1–like signaling (IIS) pathway (*6*). In the nematode *Caenorhabditis elegans*, the sole insulin/IGF-1 receptor, DAF-2 (*7*), initiates the transduction of a signal that causes the phosphorylation of the FOXO transcription factor, DAF-16 (*8*, *9*), preventing its translocation to the nucleus (*10*). This negative regulation of DAF-16 compromises expression of its target genes, decreases stress resistance, and shortens the worm's life span. Thus, inhibition of *daf-2* expression creates long-lived, youthful, stress-resistant worms (*11*). Similarly, suppression of the mouse DAF-2 ortholog, IGF1-R, creates long-lived mice (*12*). Recent studies indicate that, in worms, life-span extension due to reduced *daf-2* activity is also dependent upon heat shock factor 1 (HSF-1). Moreover, increased expression of *hsf-1* extends worm life span in a *daf-16*–dependent manner (*13*). That the DAF-16 and HSF-1 transcriptomes result in the expression of numerous chaperones (*13*, *14*) suggests that the integrity of protein folding could play a key role in life-span determination and the amelioration of aggregation-associated proteotoxicity. Indeed, amelioration of Huntington-associated proteotoxicity by slowing the aging process in worms has been reported (*13*, *15*, *16*).

Reduced IIS activity lowers $A\beta_{1-42}$ toxicity. One hypothesis to explain late-onset aggregation-associated toxicity posits that the deposition of toxic aggregates is a stochastic process, governed by a nucleated polymerization and requiring many years to initiate disease. Alternatively, aging could enable constitutive aggregation to become toxic as a result of declining detoxification activities. To distinguish between these two possibilities, we asked what role the aging process plays in $A\beta_{1-42}$ aggregation-mediated toxicity in a *C. elegans* model featuring intracellular $A\beta_{1-42}$ expression (*17*). If $A\beta_{1-42}$ toxicity results from a non-age-related nucleated polymerization, animals that express $A\beta_{1-42}$ and whose life span has been extended would be expected to succumb to $A\beta_{1-42}$ toxicity at the same rate as those with a natural life span. However, if the aging process plays a role in detoxifying an ongoing protein aggregation process, alteration of the aging program

[1]Molecular and Cell Biology Laboratory, Salk Institute for Biological Studies, 10010 North Torrey Pines Road, La Jolla, CA 92037, USA. [2]Department of Chemistry and Skaggs Institute of Chemical Biology, Scripps Research Institute, 10550 North Torrey Pines Road, La Jolla, CA 92037, USA.

*These authors contributed equally to this work.
†To whom correspondence should be addressed E-mail: dillin@salk.edu

would postpone the initiation of aggregation-mediated toxicity. To examine these hypotheses, we used worms that express the human $A\beta_{1-42}$ minigene driven by the *unc-54* promoter (strain CL2006), referred hereafter as $A\beta_{1-42}$ worms (*18*). Accordingly, $A\beta_{1-42}$ is solely expressed within the body wall muscles, resulting in their paralysis (*18*). The unaffected neighboring muscles serve as an intraorganismal control in the RNA interference (RNAi)–based experiments that alter aging (movie S1).

We first tested whether *daf-2* RNAi extends the life span of $A\beta_{1-42}$ worms. $A\beta_{1-42}$ animals grown on potent *daf-2* RNAi bacteria (*19*) exhibited increased life spans compared with control $A\beta_{1-42}$ worms grown on empty RNAi vector (EV) bacteria (Fig. 1A), similar to previous results with wild-type *C. elegans* (*11*). *daf-2* RNAi treatment also decreased the fraction of paralyzed worms compared with control animals over a 12-day time course (Fig. 1B and movies S1 and S2). At day 10 of adulthood, 50% of the control worms were paralyzed compared with 10% of the *daf-2* RNAi worms. *C. elegans* not expressing $A\beta_{1-42}$ showed no aging-related paralysis through 9 days and less than 7% showed paralysis after 12 days (fig. S1). Collectively, these data demonstrate that alteration of the aging program suppresses the pathological effect of $A\beta_{1-42}$ expression within the body wall muscles of *C. elegans*. Thus, $A\beta_{1-42}$ proteotoxicity does not appear to be a stochastic process, but it is highly dependent on the aging process.

***Daf-16* and *Hsf-1* are required for the protective effect of reduced IIS.** To understand the mechanism by which reduced IIS protected against $A\beta_{1-42}$ proteotoxicity, we asked whether *daf-16* and/or *hsf-1*, genes that encode transcription factors necessary, but not sufficient, for the full extended life span of *daf-2* mutant animals (*10*, *13*), were also required for amelioration of proteotoxicity by *daf-2* RNAi. Dilution of *daf-2* RNAi bacteria with equal amounts of either effective *hsf-1* (fig. S2) or *daf-16* (*19*) RNAi bacteria abolished the *daf-2* RNAi protective effect (Fig. 1C). A correspondingly equal dilution of *daf-2*, *daf-16*, or *hsf-1* with the EV bacteria did not influence the paralysis phenotype of each RNAi treatment (fig. S3). Therefore, analogous to the roles of *daf-16* and *hsf-1* in the regulation of aging by *daf-2*, both *daf-16* and *hsf-1* are necessary for the reduced IIS-mediated amelioration of $A\beta_{1-42}$ proteotoxicity in the *C. elegans* body wall muscles.

We also tested whether reduction of *daf-16* or *hsf-1* affected paralysis rates in animals with an intact *daf-2*. To avoid potential developmental disorders due to RNAi knockdown, we individually inactivated *daf-2*, *daf-16*, or *hsf-1* only during adulthood, the period required for the IIS pathway to regulate the aging process (*19*). As before, *daf-2* RNAi reduced the number of paralyzed worms (Fig. 1D). In contrast, either *daf-16* or *hsf-1* RNAi increased the number of paralyzed animals after 8 days. Reduction of *hsf-1* during development and adulthood increased the rate of paralysis relative to *hsf-1* reduction during adulthood only (Fig. 1E). In contrast, rates of paralysis of animals grown on *daf-16* RNAi bacteria during development and adulthood versus adulthood only were very similar.

We evaluated the possibility that RNAi utilization caused differential expression of $A\beta_{1-42}$. Quantitative reverse transcription polymerase chain reaction (RT-PCR) experiments indicated that the amounts of $A\beta_{1-42}$ messenger RNA (mRNA) transcripts within $A\beta_{1-42}$ worms grown on EV, *daf-2*, *daf-16*, or *hsf-1* RNAi bacteria were nearly identical (fig. S4A). In addition, Western blot (WB) analysis revealed that soluble $A\beta_{1-42}$ amounts were equivalent in all RNAi applications (fig. S4B). Thus, the different degrees of proteotoxicity cannot be explained by modulation of $A\beta_{1-42}$ expression.

Taken together, these results suggest that DAF-16 and HSF-1 target genes are jointly essential for the $A\beta_{1-42}$ detoxification mediated

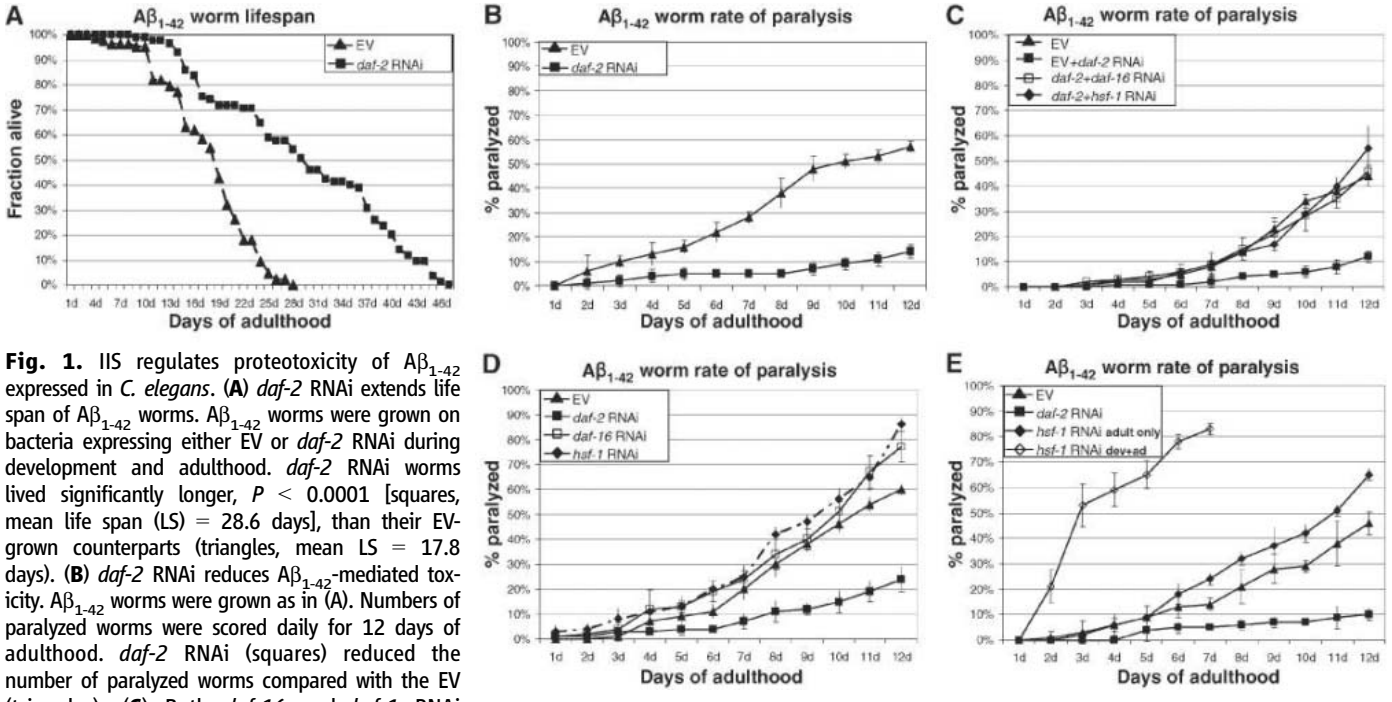

Fig. 1. IIS regulates proteotoxicity of $A\beta_{1-42}$ expressed in *C. elegans*. (**A**) *daf-2* RNAi extends life span of $A\beta_{1-42}$ worms. $A\beta_{1-42}$ worms were grown on bacteria expressing either EV or *daf-2* RNAi during development and adulthood. *daf-2* RNAi worms lived significantly longer, $P < 0.0001$ [squares, mean life span (LS) = 28.6 days], than their EV-grown counterparts (triangles, mean LS = 17.8 days). (**B**) *daf-2* RNAi reduces $A\beta_{1-42}$-mediated toxicity. $A\beta_{1-42}$ worms were grown as in (A). Numbers of paralyzed worms were scored daily for 12 days of adulthood. *daf-2* RNAi (squares) reduced the number of paralyzed worms compared with the EV (triangles). (**C**) Both *daf-16* and *hsf-1* RNAi abolished the protective effect of *daf-2* RNAi toward $A\beta_{1-42}$ toxicity. $A\beta_{1-42}$ worms were grown during development and adulthood on EV bacteria (triangles) or on dilutions of equal amounts of bacteria expressing the following RNAi species: *daf-2* and EV (solid squares), *daf-2* and *daf-16* (open squares), or *daf-2* and *hsf-1* (diamonds). (**D**) *daf-16* or *hsf-1*RNAi during adulthood results in an elevated rate of paralysis late in life. $A\beta_{1-42}$ worms were developed on EV and were transferred at day 1 of adulthood to bacteria expressing either EV (triangles), *daf-2* RNAi (solid squares), *daf-16* RNAi (open squares), or *hsf-1* RNAi (diamonds). *daf-2* RNAi reduced the number of paralyzed animals, whereas both *daf-16* and *hsf-1* RNAi increased the number of paralyzed worms late in life compared with the EV. (**E**) Reduced expression of *hsf-1* during development (dev) and adulthood (ad) further accelerates the rate of paralysis. $A\beta_{1-42}$ worms were grown during development and adulthood on bacteria expressing either EV (triangles), *daf-2* RNAi (squares) or *hsf-1* RNAi (open diamonds) or were developed on EV and transferred to *hsf-1* RNAi bacteria on day 1 of adulthood (solid diamonds). Error bars indicate standard deviations.

by inhibition of the IIS pathway. However, the HSF-1 transcriptome appears to play a more important role in suppressing $A\beta_{1-42}$-mediated toxicity, especially during development (Fig. 1E).

High molecular weight $A\beta_{1-42}$ aggregates do not correlate with toxicity. How could DAF-16 and HSF-1 transcriptomes protect worms from proteotoxicity? One possibility is that these transcriptomes prevent the formation of high molecular weight (high-MW) aggregates that are linked to toxicity. Alternatively, these transcriptomes could detoxify smaller oligomers that appear to mediate toxicity (*4*, *20*). To evaluate these possibilities, we asked whether *daf-2* RNAi mediated protection from $A\beta_{1-42}$ proteotoxicity and suppression of this protective effect by knockdown of either *daf-16* or *hsf-1* expression correlated with the amount of high-MW $A\beta_{1-42}$ aggregates. $A\beta_{1-42}$ worms were grown to day 1 of adulthood on EV or on *daf-2*, *daf-16*, or *hsf-1* RNAi bacteria. The worms were homogenized and centrifuged for 3 min at 3000 revolutions per min (rpm) to afford pellet and post debris supernatant (PDS) fractions (fig. S5A) that were evaluated separately (fig. S5, B and C). The PDS was subjected to ultracentrifugation, revealing the presence of high-MW $A\beta_{1-42}$ aggregates (Fig. 2A). If high-MW $A\beta_{1-42}$ aggregates were the toxic species, then *daf-2* RNAi animals would be expected to have less high-MW aggregates, and *daf-16* and *hsf-1* RNAi animals would be expected to accumulate more. PDS from *hsf-1* RNAi worms have the most high-MW aggregates, followed by *daf-2* and EV RNAi, whereas in *daf-16* RNAi worms the aggregates are hardly detectable. This observation is not consistent with high-MW $A\beta_{1-42}$ aggregates being the toxic species.

$A\beta_{1-42}$ aggregates in the PDS fraction were quantified with an in vitro kinetic aggregation assay, which is at least three orders of magnitude more sensitive than WB analysis (fig. S6). This assay enables the detection of small amounts of aggregates that can seed an $A\beta_{1-40}$ nucleated polymerization reaction in vitro. $A\beta_{1-42}$ worm PDS was sonicated to generate small fibrils (fig. S7). Addition of sonicated PDS to an in vitro $A\beta_{1-40}$ fibril formation assay would be expected to shorten the lag phase associated with the initiation of $A\beta_{1-40}$ aggregation in a fashion that is dependent on the concentration of fibrillar seeds (*21*). PDS from $A\beta_{1-42}$ worms grown to day 1 of adulthood on EV, *daf-2*, *daf-16*, or *hsf-1* RNAi bacteria were evaluated in vitro by assessing the time for half maximal aggregation of $A\beta_{1-40}$ (t_{50}) (Fig. 2B). Reactions seeded with PDS of *hsf-1* RNAi worms had significantly ($P < 0.0002$) faster $A\beta_{1-40}$ aggregation than did the control worms (EV). Similarly, homogenates from *daf-2* RNAi worms accelerated aggregation compared with the control worms ($P < 0.02$), but less than PDS from *hsf-1* RNAi worms. Lastly, *daf-16* RNAi worms harbored the least seeding competent aggregates. An in vitro kinetic aggregation assay using *hsf-1* RNAi worms not expressing $A\beta_{1-42}$ confirmed that the lag phase shortening is completely dependent on the presence of $A\beta_{1-42}$ (fig. S8).

Within the worm debris, less high-MW aggregates were found in the EV and *daf-2* RNAi-treated $A\beta_{1-42}$ worms compared with the increased amount found when *hsf-1* was reduced (Fig. 2, C and D). In contrast to *hsf-1* RNAi treatment, the least amount of high-MW $A\beta_{1-42}$ aggregates was found in the debris of *daf-16* RNAi worms. Strictly analogous results were observed by growing the $A\beta_{1-42}$ worms to day 3 of adulthood (Fig. 2E). Formic acid extraction of all of the $A\beta_{1-42}$ worm debris before analysis also indicated that *hsf-1* RNAi worms contained more high-MW $A\beta_{1-42}$ than did *daf-16* RNAi worms.

The relative amounts of $A\beta_{1-42}$ aggregates observed in the PDS and in the worm debris analyzed by WB rank order identically, with *hsf-1* RNAi worms having the most, followed by *daf-2* RNAi worms, then the $A\beta_{1-42}$ worms grown on EV bacteria, and lastly *daf-16* RNAi worms.

By using multiple ultracentrifugation steps with a final analysis by atomic force microscopy (AFM), we directly visualized high-density material purified from $A\beta_{1-42}$ worm PDS. Fibrillar structures were detected only in the *hsf-1* RNAi worms but not in PDS fractions of EV control (fig. S9), *daf-2*, or *daf-16* RNAi worms. To verify that the fibrillar structures observed by AFM contain $A\beta_{1-42}$, we used immunoelectron microscopy (immuno-EM) (fig. S10A). Quantification and distribution analysis of the gold particles labeling Aβ indicated that *hsf-1* RNAi treatment results in the most intense and specific signal. The PDS of $A\beta_{1-42}$ worms fed EV or *daf-2* RNAi bacteria had a weaker signal, whereas the *daf-16* RNAi worms had the least intense signal (Fig. 2F). Wild-type worms not expressing $A\beta_{1-42}$ that were fed *hsf-1* RNAi bacteria (negative control, fig. S10B) and in vitro aggregated $A\beta_{1-40}$ (positive control, fig. S10C) confirmed the immunogold particle signal specificity. Lastly, $A\beta_{1-42}$ worms were grown to day 2 of adulthood on the various RNAi species, and Aβ was visualized within the intact worm by using immunofluorescence (IF) microscopy. *daf-2* RNAi and EV worms had similar intermediate intensities, *hsf-1* RNAi-treated $A\beta_{1-42}$ worms exhibited the most intense signal, and *daf-16* RNAi treatment resulted in the weakest signal (Fig. 2G).

Collectively, results from five independent methods studying worm debris, PDS, and intact worms all indicate that *hsf-1* RNAi worms contain the largest amount of fibrils and high-MW $A\beta_{1-42}$ aggregates and that *daf-2* RNAi worms contain slightly more fibrils than their EV-treated counterparts, whereas *daf-16* RNAi worms contain the fewest fibrils and high-MW $A\beta_{1-42}$ aggregates. This points to a lack of correlation between high-MW $A\beta_{1-42}$ aggregates and $A\beta_{1-42}$-mediated toxicity, because (i) *daf-2* RNAi reduces toxicity but slightly enhances the amount of high-MW aggregates, (ii) *daf-16* RNAi increases toxicity but reduces the amount of high-MW aggregates, and (iii) *hsf-1* RNAi increases both toxicity and amount of high-MW $A\beta_{1-42}$ aggregates. The detection of aggregated $A\beta_{1-42}$ in early adulthood (days 1 to 2 of adulthood), before onset of paralysis (days 5 to 12), suggests that protein aggregation occurs early and throughout the life of the worm and is counteracted by aging-related processes to reduce toxicity.

HSF-1 but not DAF-16 controls disaggregation of $A\beta_{1-42}$ aggregates. Our findings suggest that two opposing mechanisms, regulated by the IIS pathway, protect worms from $A\beta_{1-42}$ mediated toxicity: The HSF-1 transcriptome regulates disaggregation, whereas the DAF-16 transcriptome mediates the formation of less-toxic high-MW aggregates. The latter is analogous to the aggregation-mediated neuroprotection invoked in Huntington's disease (*22*, *23*). Both activities appear to be required to protect the $A\beta_{1-42}$ worms from early-onset paralysis associated with proteotoxicity. Inhibiting the HSF-1 transcriptome during worm development is more deleterious than DAF-16 inhibition toward $A\beta_{1-42}$ toxicity, suggesting the former is the more important pathway (Fig. 1E). Thus, it is plausible that the HSF-1–controlled disaggregation and degradation pathway is the preferred pathway, whereas the DAF-16–controlled active aggregation is the backup pathway used mainly under severe stress conditions. We suppose that the HSF-1–controlled disaggregation pathway in the $A\beta_{1-42}$ worms is constantly overloaded. Thus, the DAF-16–regulated active aggregation machinery is continually assisting. Accordingly, *daf-2* RNAi worms have slightly more high-MW aggregates than EV animals because both the HSF-1–regulated and the DAF-16–regulated pathways are fully active.

To test the hypothesis that $A\beta_{1-42}$ disaggregation in the worm is regulated by HSF-1 but not DAF-16, we developed an in vitro assay to measure disaggregation of $A\beta_{1-40}$ fibrils by worm PDS. Time-dependent disaggregation of $A\beta_{1-40}$ fibrils in vitro, in the presence and absence of worm PDS, was quantified. To exclude the possibility of monitoring proteasomal and/or proteolytic degradation rather than disaggregation, we performed experiments in the presence of either (i) the proteasome inhibitor epoxomicin (10 μM) (fig. S11) or (ii) protease inhibitor cocktail. In buffer alone (Fig. 3A) and with added bovine serum albumin (BSA) (0.5 mg/ml), the fibrils were stable for at least 36 hours. In contrast, $A\beta_{1-40}$ fibrils underwent disaggregation when treated with PDS from $A\beta_{1-42}$ worms. Heat inactivation of PDS (95°C for 10 min) destroyed the disaggregation activity (Fig. 3A). The amount of $A\beta_{1-40}$ detected by WB after 17 and 96 hours of incubation with PDS in the absence of protease inhibitors was reduced, indicating that $A\beta_{1-40}$ was proteolyzed subsequent to disaggregation (Fig. 3B). In contrast, heat-inactivated PDS had

no detectable effect on the amount of $A\beta_{1-40}$. In the presence of a cocktail of protease inhibitors, $A\beta_{1-40}$ fibrils were disassembled but not degraded (Fig. 3C). Proteasome inhibitor alone did not prevent proteolysis, although more detailed experiments are needed before excluding proteasome involvement. $A\beta_{1-40}$ fibrils prepared in vitro were visible by AFM before treatment with worm PDS and after a 36-hour incubation with buffer, but not after incubation with PDS of EV-treated $A\beta_{1-42}$ worms (Fig. 3D). Collectively, the results confirm that the assay detects disaggregation activity of worm homogenates and demonstrate that worm PDS also proteolyses $A\beta_{1-40}$; yet, we can dissociate these activities with the appropriate use of protease inhibitors. In the presence of protease inhibitors, $A\beta_{1-40}$ fibrils will spontaneously reform if a longer time window (20 to 40 hours) is observed.

Does the disaggregation activity found within worm PDS reduce the toxicity of $A\beta_{1-40}$

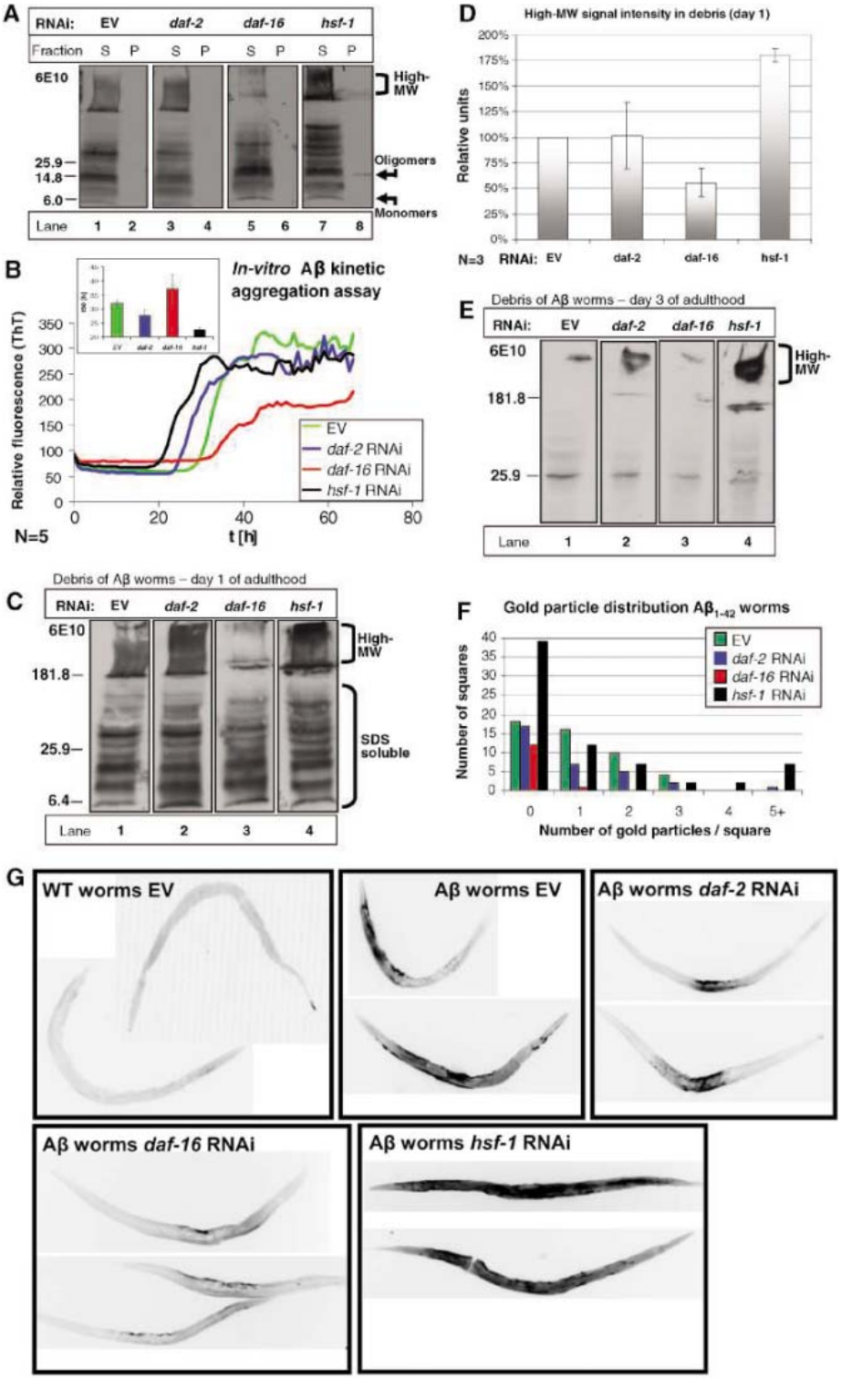

Fig. 2. Lack of correlation between $A\beta_{1-42}$ high-MW aggregates and toxicity. (**A**) $A\beta_{1-42}$ worms were fed bacteria expressing EV or double-stranded RNA of *daf-2*, *daf-16*, or *hsf-1* to day 1 of adulthood. The worms were homogenized, and equal amounts of PDS (fig. S5A) were incubated for 30 min on ice with 1% sarkosyl and spun for 1 hour in an ultracentrifuge (427,000 g). Supernatants and pellets were separated and loaded onto denaturing 12% polyacrylamide (PAA) gels and analyzed by WB using 6E10 monoclonal antibody (mAb). No Aβ signal was detected in pellets of EV, *daf-2*, and *daf-16* RNAi worm PDS (lanes 2, 4, and 6, respectively). A weak 16-kD Aβ band was detected in the pellet of PDS from *hsf-1* RNAi worms (lane 8, oligomers). (**B**) RNAi of $A\beta_{1-42}$ worms as in (A). PDS samples were prepared at day 1 of adulthood and were used to seed in vitro kinetic $A\beta_{1-40}$ aggregation reactions that were monitored by using thioflavin-T (ThT) fluorescence. PDS of *hsf-1* RNAi-treated animals (black) exhibited the most significant acceleration of the reaction, indicating the most seeding competent aggregates. *daf-2* RNAi (blue) accelerated the reaction compared with the EV (green), whereas *daf-16* RNAi (red) had the least seeding competent aggregates. (Inset) Statistical analysis of results obtained in (B). Error bars indicate standard deviations, $n = 5$. (**C**) $A\beta_{1-42}$ worms were grown and treated as in (A). Debris was analyzed by using 12% SDS PAA gel and WB. The largest amount of $A\beta_{1-42}$ high-MW aggregates was detected in animals with reduced *hsf-1* (lane 4); *daf-16* RNAi resulted in the least (lane 3), whereas *daf-2* RNAi (lane 2) had slightly more $A\beta_{1-42}$ high-MW aggregates. (**D**) Statistical analysis of the WB high-MW aggregate intensities in (C). Error bars indicate standard deviations, $n = 3$. (**E**) RNAi of $A\beta_{1-42}$ worms as in (A). Aβ contents of the worm debris were analyzed at day 3 of adulthood by using WB of a denaturing 4% PAA gel. The largest amount of high-MW $A\beta_{1-42}$ was detected in *hsf-1* RNAi worms (lane 4), followed by *daf-2* RNAi animals (lane 2); the least amount of $A\beta_{1-42}$ high-MW aggregates was found in *daf-16* RNAi animals (lane 3). (**F**) Quantification and distribution histogram analysis of gold particle labeling of the $A\beta_{1-42}$ worm preparations from immuno-EM analysis. EM images (fig. S10) were overlaid with a grid of 100 nm by 100 nm squares (Materials and Methods). Shown are distribution analyses of the number of immunogold particles found within squares that contained aggregate surfaces. The $A\beta_{1-42}$ immunogold staining signal of *hsf-1* RNAi worms is the most intense, whereas signal of $A\beta_{1-42}$ in *daf-16* RNAi treated worms is the weakest. (**G**) $A\beta_{1-42}$ worms were grown on RNAi bacteria as in (A) to day 2 of adulthood and were subjected to IF microscopy using the Aβ mAb 4G8. The signal intensity of *daf-2* RNAi worms was similar to that of EV worms. *daf-16* RNAi animals had the weakest signal, and *hsf-1* RNAi animals showed considerably stronger signal intensity. Wild-type animals not expressing $A\beta_{1-42}$ did not exhibit IF signal, demonstrating the specificity of the $A\beta_{1-42}$ mAb.

fibrils? Viability of rat adrenal pheochromocytoma (PC12) cells was discerned by the MTT assay (*24*) and normalized to cell survival when incubated in the absence of $A\beta_{1\text{-}40}$. Worm PDS dramatically reduced cytotoxicity of $A\beta_{1\text{-}40}$ aggregates prepared in vitro (Fig. 3E). Analogous results were obtained when resazurin (*25*) was used to measure $A\beta_{1\text{-}40}$ fibril toxicity on PC12 cells (fig. S12). Thus, disaggregation directly correlates with detoxification of $A\beta_{1\text{-}40}$ fibrils in these widely used cell-based assays.

Although HSF-1–regulated disaggregation activity could increase toxicity by releasing small toxic aggregates from larger less-toxic aggregates, our data point to the protective activity of HSF-1, suggesting a tight mechanistic link between disaggregation and degradation, possibly mediated by proteases such as the insulin-degrading enzyme (*26*) or neprilysin (*27*).

We measured the disaggregation activity of PDS from $A\beta_{1\text{-}42}$ worms grown on either EV, *daf-2*, *daf-16*, or *hsf-1* RNAi bacteria (Fig. 3F). Disaggregation curves were fit to an exponential decay function to quantify the results and to assess their statistical significance. No significant difference was observed among PDS of EV, *daf-2*, and *daf-16* RNAi worms. However, PDS of *hsf-1* RNAi worms exhibited a decreased disaggregation rate (35%, $N = 3$, $P < 0.03$), indicating that HSF-1 regulates the disaggregation activity (Fig. 3F inset). Nevertheless, the relatively small effect of *hsf-1* RNAi on disaggregation is unexpected given its robust physiological response on $A\beta_{1\text{-}42}$ toxicity. One possibility is that HSF-1 also regulates protective functions other than disaggregation. Alternatively, HSF-1 may be one component in a more complex mechanism that regulates disaggregation. It is also possible that the 35% decline in disaggregation results in exacerbated $A\beta_{1\text{-}42}$ proteotoxicity. In any case, reduced *hsf-1* slowed disaggregation whereas reduced *daf-16* did not, supporting the notion that HSF-1 regulates disaggregation.

Small $A\beta_{1\text{-}42}$ oligomers correlate with toxicity. The lack of correlation between proteotoxicity and large-MW aggregates suggests that small oligomers may be the key toxic species in the worm $A\beta_{1\text{-}42}$ aggregation model. Numerous lines of evidence implicate $A\beta_{1\text{-}42}$ oligomers in proteotoxicity (*28*–*30*). To determine whether small $A\beta_{1\text{-}42}$ aggregates correlate with toxicity, we grew worms to adulthood on EV, *daf-2*, *daf-16*, or *hsf-1* RNAi bacteria; subjected the PDS fractions to ultracentrifugation; and analyzed the soluble supernatants and insoluble pellets by WB (Fig. 2A). No Aβ was detected in the insoluble pellets of EV, *daf-2*, and *daf-16* RNAi-treated worms. However, a weak Aβ immunoreactive band of about 16 kD was detected in the insoluble pellet of *hsf-1* RNAi worms (Fig. 2A). This band size is consistent with a SDS-stabilized $A\beta_{1\text{-}42}$ trimer, possibly derived from a larger quaternary structure. When PDS incubation with 1% sarkosyl was shortened to 10 min, the 16-kD protein was

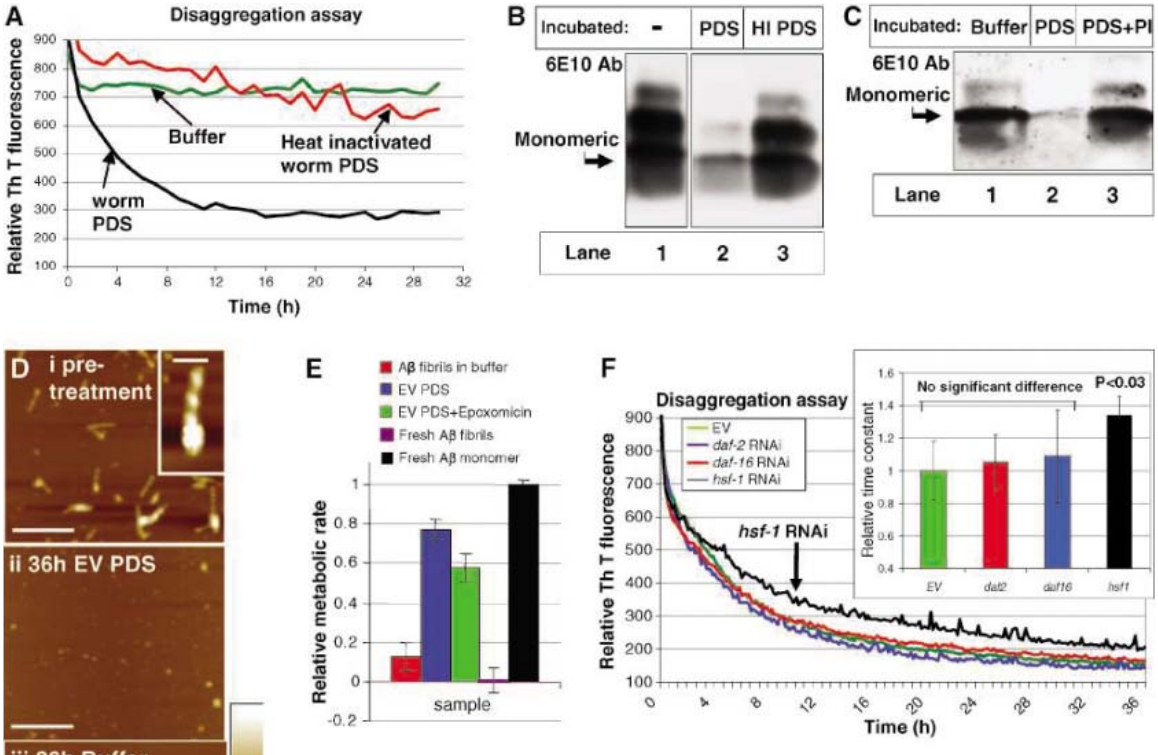

Fig. 3. *hsf-1* is required for efficient disaggregation of $A\beta_{1\text{-}42}$ aggregates. (**A**) Pre-aggregated, ThT-labeled $A\beta_{1\text{-}40}$ fibrils were incubated with either buffer (green), $A\beta_{1\text{-}42}$ worm PDS (black), or heat-inactivated PDS (red) in the presence of epoxomicin (10 μM). ThT fluorescence emission declined in the presence of worm PDS, indicating disaggregation activity. The $A\beta_{1\text{-}40}$ fibrils were stable in both buffer and heat-inactivated (HI) PDS. (**B**) Pre- and postdisaggregation samples were loaded onto 10% PAA gel. $A\beta_{1\text{-}40}$ was visualized by WB using 6E10 before the reaction (lane 1) and after 96 hours in the presence of worm PDS (lane 2) or in the presence of heat-inactivated PDS (lane 3). Less $A\beta_{1\text{-}40}$ was observed after incubation with worm PDS but not after incubation with heat-inactivated PDS. No proteasome inhibitors were used in this experiment. (**C**) Disaggregation reaction was performed in the absence and the presence of a protease inhibitor cocktail (PI) (lanes 2 and 3, respectively). WB analysis indicated that in the presence of PI, the total quantity of $A\beta_{1\text{-}40}$ did not change compared to the buffer-incubated fibrils, despite the disaggregation. (**D**) In vitro aggregated $A\beta_{1\text{-}40}$ fibrils were visualized by using AFM with no treatment (i), after a 36-hour incubation with EV-grown $A\beta_{1\text{-}42}$ worm PDS (ii), and after a 36-hour incubation with buffer only (iii). No large fibrils were detected after incubation with worm PDS. All large horizontal bars represent 1 μm; inset bar, 200 nm; and height scale bar, 20 nm. (**E**) Worm disaggregation activity reduces the $A\beta_{1\text{-}40}$ fibril-mediated cytotoxicity in cell-based assays. By using the disaggregation assay and conditions as in (B) and 72-hour incubation, we added $A\beta_{1\text{-}40}$ disaggregation samples (500 nM) to PC12 cell culture medium for 3 days. Cell viability was assayed by MTT metabolic activity (*24*). $A\beta_{1\text{-}40}$ toxicity was reduced in samples incubated with worm PDS in the presence (green) or absence (blue) of epoxomicin (10 μM). Samples incubated without worm PDS (red) showed similar toxicity to the starting material (purple). Monomeric $A\beta_{1\text{-}40}$ peptide did not exhibit toxicity under the assay conditions (black). Similar results were found with the use of a resazurin-based assay (fig. S12). (**F**) *hsf-1* is required for efficient disaggregation of pre-formed $A\beta_{1\text{-}40}$ fibrils. RNAi of $A\beta_{1\text{-}42}$ worms as in Fig. 2A. PDS of *hsf-1* RNAi worms (black) exhibited 20 to 50% decline in disaggregation activity compared with PDS of EV worms (green). There was no significant change in disaggregation activities in PDS of *daf-2* (blue) or *daf-16* (red) RNAi worms. (Inset) Statistical analysis of disaggregation results shown in (F) indicate that EV and *hsf-1* RNAi worms are significantly ($P < 0.03$) different ($n = 3$).

detected in all insoluble pellets (Fig. 4A). Notably, the amounts of the 16-kD species correlated with $A\beta_{1-42}$ toxicity; insoluble pellets from *daf-2* RNAi worms had the least intense signal, whereas *daf-16*, *hsf-1*, and EV RNAi worms had greater signal intensities. $A\beta_{1-42}$ monomers were detected in the supernatants of EV and *daf-2* RNAi worms but not in *daf-16* and *hsf-1* RNAi worms (Fig. 4A), suggesting that $A\beta_{1-42}$ monomers had formed trimers and/or larger assemblies thereof. In the absence of detergents, all of the $A\beta_{1-42}$ was retained in the insoluble pellet, suggesting that it may be associated with membranes. These observations are consistent with an $A\beta_{1-42}$ quaternary structure; apparently a trimer (16 kD) or an oligomer thereof mediating proteotoxicity, possibly in association with a membrane.

By using high resolution IF microscopy (Fig. 4B), we detected $A\beta_{1-42}$ aggregates along muscle fibers of $A\beta_{1-42}$ worms grown on either *hsf-1* or *daf-16* RNAi bacteria. Only a small amount of $A\beta_{1-42}$ aggregates was detected along muscular fibers of $A\beta_{1-42}$ worms grown on EV, and no such signal was detected in *daf-2* RNAi worms. These results support the hypothesis that small $A\beta_{1-42}$ oligomers in spatial proximity to the muscle fibers correlate with toxicity in this worm model and are consistent with recent studies showing that Aβ oligomers, potentially trimers, posses the highest toxicity toward hippocampal long-term potentiation of neural cells (*31*) and that Aβ trimer assemblies are involved in memory impairment of transgenic AD model mice (*32*).

Model of DAF-16– and HSF-1–mediated protection against $A\beta_{1-42}$ aggregate proteotoxicity. Our data suggests the following model for how *daf-2*–regulated pathways reduce aggregate mediated proteotoxicity (Fig. 5). First (stage 5-I), aggregation-prone peptides (such as $A\beta_{1-42}$) form small toxic aggregates constitutively. We suggest that cells have developed two mechanisms to detoxify these toxic misassemblies. The preferred detoxification route is to efficiently disaggregate the toxic oligomer and degrade the amyloidogenic peptide (stages 5-II and 5-V), a pathway that is positively regulated by HSF-1 (stage 5-A), perhaps via a subset of molecular chaperones (*33*). When this pathway is overtaxed, another activity transforms toxic low-MW oligomers into high-MW aggregates of lower toxicity. This mechanism (stage 5-III) is positively regulated by DAF-16 (stage 5-B) through its target genes. The cell ultimately has to get rid of these large aggregates by either degrading them using the HSF-1–controlled disaggregation and degradation machinery (stages 5-IV and 5-V) or possibly by their secretion (stage 5-VI). The opposing disaggregation (HSF-1) and aggregation (DAF-16) detoxification pathways both are negatively regulated by IIS signaling (stages 5-C and 5-D).

How does this model explain our results? (i) When *hsf-1* is reduced, disaggregation in stages 5-II and 5-IV is impaired. This leads to a reduction of disaggregation of small toxic aggregates and leaves the cell no alternative but to actively form less-toxic high-MW aggregates by using the DAF-16 regulated ma-

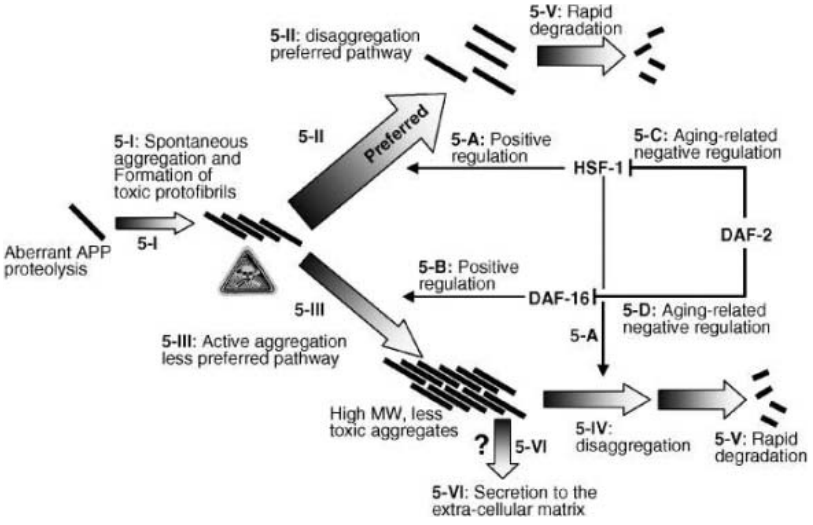

Fig. 5. Model of age-regulated HSF-1 and DAF-16 opposing anti-proteotoxicity activities. Aggregation-prone peptides spontaneously form small toxic aggregates (stage 5-I). Specialized cellular machinery identifies toxic aggregates and rapidly disaggregates and prepares them for degradation (stage 5-II). The products of this machinery are rapidly degraded (stage 5-V). This preferred mechanism is positively regulated by HSF-1 (stage 5-A) and negatively regulated by DAF-2 (stage 5-C). (Stage 5-III) When the HSF-1–regulated disaggregation machinery is overloaded, a secondary machinery that mediates aggregation is activated (stage 5-III), forming less-toxic high-MW aggregates. This machinery is positively regulated by DAF-16 (stage 5-B) and negatively by DAF-2 (stage 5-D). The high-MW aggregates, which accumulate as a result of the DAF-16–regulated mechanism, undergo either slow disaggregation and degradation by the HSF-1–regulated mechanism (stages 5-IV and 5V) or possibly secretion to the extracellular matrix (5-VI).

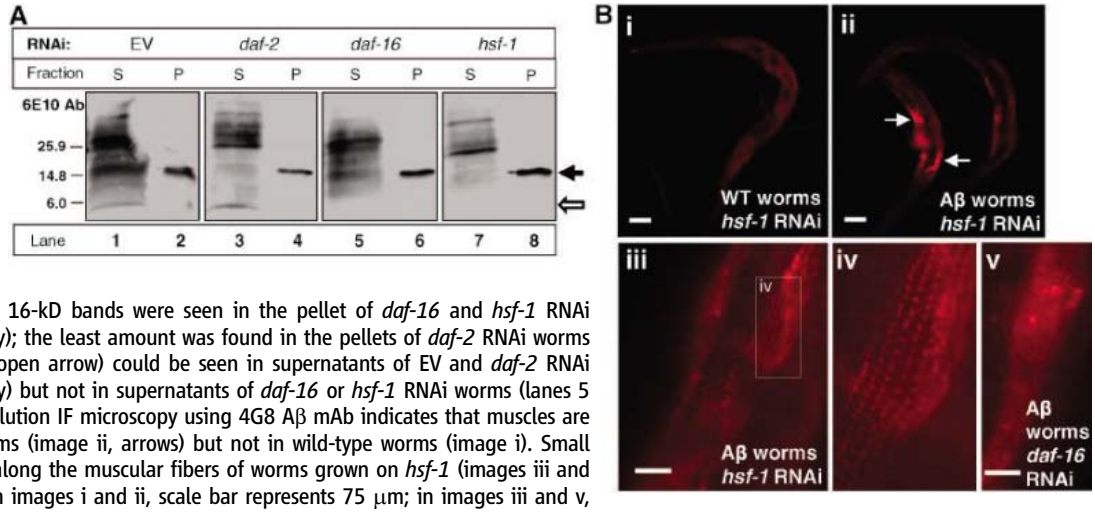

Fig. 4. Intensity of an Aβ immunoreactive 16-kD band correlates with toxicity. (**A**) Worm PDS supernatants and pellets were prepared as in Fig. 2A, except the PDS was incubated for 10 min on ice in 1% sarkosyl to maintain more proteins in their membrane-associated state. 16-kD Aβ bands were detected in all pellets (lanes 2, 4, 6 and 8, solid arrow). The most intense 16-kD bands were seen in the pellet of *daf-16* and *hsf-1* RNAi worms (lanes 6 and 8, respectively); the least amount was found in the pellets of *daf-2* RNAi worms (lane 4). Aβ monomers (~5-kD, open arrow) could be seen in supernatants of EV and *daf-2* RNAi worms (lanes 1 and 3, respectively) but not in supernatants of *daf-16* or *hsf-1* RNAi worms (lanes 5 and 7, respectively). (**B**) High resolution IF microscopy using 4G8 Aβ mAb indicates that muscles are labeled in *hsf-1* RNAi $A\beta_{1-42}$ worms (image ii, arrows) but not in wild-type worms (image i). Small $A\beta_{1-42}$ aggregates were detected along the muscular fibers of worms grown on *hsf-1* (images iii and iv) and *daf-16* RNAi (image v). (In images i and ii, scale bar represents 75 μm; in images iii and v, bar represents 15 μm).

chinery (stage 5-III). Moreover, the absence of HSF-1 also appears to slow the clearance of high-MW aggregates (stage 5-IV). Together, these activities lead to maximal accumulation of high-MW aggregates. (ii) When DAF-16 is reduced, cells lack the protective large-aggregate formation machinery, resulting in higher toxicity. Yet, the cells can disaggregate and degrade small aggregates (stage 5-II), resulting in fewer high-MW aggregates. The secondary importance of the DAF-16–regulated machinery explains why the toxicity of *daf-16* RNAi is lower than that of *hsf-1* RNAi. (iii) Inhibition of *daf-2*, a negative regulator of DAF-16 (stage 5-D) and perhaps of HSF-1 (stage 5-C) results in the up-regulation of both protective mechanisms: stages 5-II and 5-III. In this situation, both the clearance rate of small toxic aggregates and their detoxification by active aggregation are maximal, resulting in minimal toxicity. According to our model, the aging process actively reduces the cellular ability to detoxify small toxic aggregates by negative regulation of both detoxification mechanisms via the IIS pathway.

The IIS pathway plays a role in modulating other forms of toxic protein aggregation, such as in the aggregation of the huntingtin protein (*13*, *15*, *16*), suggesting that the activities identified here may be quite general. Additionally, small perturbations of proper protein-folding homeostasis have been demonstrated to have a profound impact on organismal integrity (*34*), suggesting that the protective mechanisms regulated by the IIS pathway may link longevity to protein homeostasis.

References and Notes

1. D. J. Selkoe, *Nature* **426**, 900 (2003).
2. R. R. Kopito, D. Ron, *Nat. Cell Biol.* **2**, E207 (2000).
3. E. Bossy-Wetzel, R. Schwarzenbacher, S. A. Lipton, *Nat. Med.* **10** (suppl.), S2 (2004).
4. B. Caughey, P. T. Lansbury, *Annu. Rev. Neurosci.* **26**, 267 (2003).
5. R. H. Takahashi *et al.*, *Am. J. Pathol.* **161**, 1869 (2002).
6. C. Kenyon, *Cell* **120**, 449 (2005).
7. K. D. Kimura, H. A. Tissenbaum, Y. Liu, G. Ruvkun, *Science* **277**, 942 (1997).
8. K. Lin, J. B. Dorman, A. Rodan, C. Kenyon, *Science* **278**, 1319 (1997).
9. S. Ogg *et al.*, *Nature* **389**, 994 (1997).
10. K. Lin, H. Hsin, N. Libina, C. Kenyon, *Nat. Genet.* **28**, 139 (2001).
11. C. Kenyon, J. Chang, E. Gensch, A. Rudner, R. Tabtiang, *Nature* **366**, 461 (1993).
12. M. Holzenberger *et al.*, *Nature* **421**, 182 (2003).
13. A.-L. Hsu, C. T. Murphy, C. Kenyon, *Science* **300**, 1142 (2003).
14. J. F. Morley, R. I. Morimoto, *Mol. Biol. Cell* **15**, 657 (2004).
15. J. F. Morley, H. R. Brignull, J. J. Weyers, R. I. Morimoto, *Proc. Natl. Acad. Sci. U.S.A.* **99**, 10417 (2002).
16. J. A. Parker *et al.*, *Nat. Genet.* **37**, 349 (2005).
17. C. D. Link *et al.*, *Neurobiol. Aging* **22**, 217 (2001).
18. C. Link, *Proc. Natl. Acad. Sci. U.S.A.* **92**, 9368 (1995).
19. A. Dillin, D. K. Crawford, C. Kenyon, *Science* **298**, 830 (2002).
20. C. A. Ross, M. A. Poirier, *Nat. Rev. Mol. Cell Biol.* **6**, 891 (2005).
21. K. Hasegawa, I. Yamaguchi, S. Omata, F. Gejyo, H. Naiki, *Biochemistry* **38**, 15514 (1999).
22. M. Arrasate, S. Mitra, E. S. Schweitzer, M. R. Segal, S. Finkbeiner, *Nature* **431**, 805 (2004).
23. F. Saudou, S. Finkbeiner, D. Devys, M. E. Greenberg, *Cell* **95**, 55 (1998).
24. M. Bucciantini *et al.*, *Nature* **416**, 507 (2002).
25. J. O'Brien, I. Wilson, T. Orton, F. Pognan, *Eur. J. Biochem.* **267**, 5421 (2000).
26. M. A. Leissring *et al.*, *Neuron* **40**, 1087 (2003).
27. N. Iwata *et al.*, *Science* **292**, 1550 (2001).
28. Y. Gong *et al.*, *Proc. Natl. Acad. Sci. U.S.A.* **100**, 10417 (2003).
29. D. M. Hartley *et al.*, *J. Neurosci.* **19**, 8876 (1999).
30. D. M. Walsh *et al.*, *Nature* **416**, 535 (2002).
31. M. Townsend, G. M. Shankar, T. Mehta, D. M. Walsh, D. J. Selkoe, *J. Physiol.* (2006).
32. S. Lesne *et al.*, *Nature* **440**, 352 (2006).
33. P. J. Muchowski, J. L. Wacker, *Nat. Rev. Neurosci.* **6**, 11 (2005).
34. T. Gidalevitz, A. Ben-Zvi, K. H. Ho, H. R. Brignull, R. I. Morimoto, *Science* **311**, 1471 (2006); published online 8 February 2006 (10.1126/science.1124514).

35. This study was generously supported by grants provided by the Backus and Ellison Medical Foundations (A.D.), NIH (DK 46335 and NS 50636), the Skaggs Institute of Chemical Biology, the Bundy Foundation, the Lita Annenberg Hazen Foundation, and the Max Planck Society (J.W.K. and J.B.). E.C. is supported by the John Douglas French Alzheimer's Foundation. We gratefully acknowledge M. Wood and the Microscopy Core Facility at the Scripps Research Institute for the preparation of immuno-EM samples and pictures, M. R. Ghadiri for use of AFM, G. Herradon for the gift of PC12 cells, the Caenorhabditis Genetics Center for CL2006 worms, and Dillin and Kelly lab members and D. Selkoe for critical comments during the course of this work.

Supporting Online Material

www.sciencemag.org/cgi/content/full/1124646/DC1
Materials and Methods
Figs. S1 to S12
References
Movies S1 and S2

5 January 2006; accepted 24 July 2006
Published online 10 August 2006;
10.1126/science.1124646
Include this information when citing this paper.

Oldest Writing in the New World

Ma. del Carmen Rodríguez Martínez,[1] Ponciano Ortíz Ceballos,[2] Michael D. Coe,[3] Richard A. Diehl,[4] Stephen D. Houston,[5]* Karl A. Taube,[6] Alfredo Delgado Calderón[1]

A block with a hitherto unknown system of writing has been found in the Olmec heartland of Veracruz, Mexico. Stylistic and other dating of the block places it in the early first millennium before the common era, the oldest writing in the New World, with features that firmly assign this pivotal development to the Olmec civilization of Mesoamerica.

Several writing systems are known from pre-Columbian Mesoamerica, most with dates after the first millennium before the common era (BCE). (*1*). Previously, no script has been associated unambiguously with the Olmec civilization, in many respects the progenitor of all later complex societies of Mexico and adjacent Central America (*2*). Recent proposals for late Olmec writing at La Venta, Tabasco, Mexico, rest on two categories of object, roller-seal iconography and isolated, discontinuous incisions, neither sure to be script (*3*). We report here on an Olmec

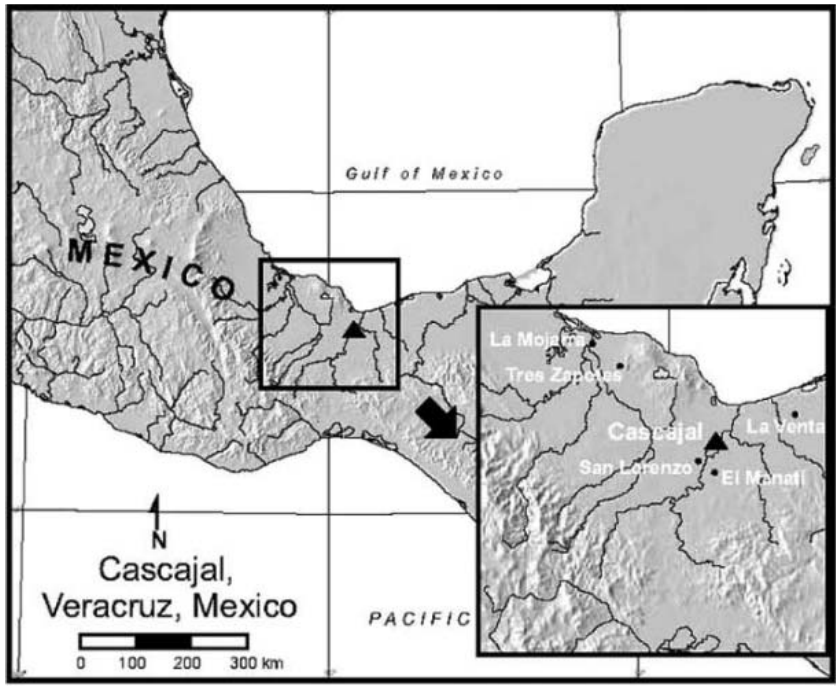

Fig. 1. Map showing location of Cascajal, Veracruz. Figure was prepared by Z. Nelson, Geography Department, Brigham Young University.

serpentine block incised with a previously unknown script, the earliest known thus far in Mesoamerica and, by extension, the Western Hemisphere. The Cascajal block and the script on it link the Olmec to literacy, document an unsuspected writing system, and reveal a new complexity to this civilization, including the possibility of information tools not hitherto known in this early period. The discovery of an ancient writing system is a rare event, so unusual as to deserve global attention (*4*–*6*).

Site description. The Cascajal block was first seen by M.C.R. and P.O.C. in April 1999, when local authorities requested that inspectors from the Instituto Nacional de Antropología e Historia (INAH) of Mexico come to the municipality of Jáltipan, Veracruz, to examine objects taken from a local gravel quarry in the ejido (communal lands) of Lomas de Tacamichapa (Fig. 1). This context is described in a paper by M.C.R. and P.O.C. (*7*). For some years, the quarry, an archaeological site that offered ready building material, had supplied fill for road construction. The site is labeled Cascajal and consisted of two parallel mounds, both defining an open area sealed off by two other mounds. A visit in May 2006 by M.C.R. and P.O.C. showed that the surface of the mounds was Classic period in date (late first millennium CE) but with earlier materials underneath. Cascajal was fully intervisible with the salt dome to the south that supports the large Olmec center of San Lorenzo (*8*).

The local authority for cultural materials, Cástulo Gabriel Cruz, who now cares for the block under INAH registration in the community of Lomas de Tacamichapa, reported that the block came from debris heaped to the side of a destroyed area, 40 m by 50 m in extent and 2.5 m deep, at the southwestern limits of the site. During the destruction of the mound from which the serpentine block came, a number of ceramic sherds, clay figurine fragments, and broken artifacts of ground stone were collected by the local workmen, and since that time have been safeguarded in the house of C. G. Cruz. These were examined and photographed in 1999 by M.C.R. and P.O.C. and again in 2006 by all of the present authors. About three-fourths of these materials are Formative in date, and of these, all but two or three sherds of the Formative period can be positively identified as belonging to the San Lorenzo phase (uncalibrated 1200 to 900 BCE). The anomalous sherds of the Formative period are of the Palangana phase, contemporary with the principal occupation of the Olmec site of La Venta, Tabasco (calibrated 800 to 400 BCE), but a very minor component at San Lorenzo, the largest site close to Cascajal. There appear to be no Late Formative ceramics. All of the remaining artifacts consist largely of Fine Orange ceramics as well as associated types that can be ascribed to the Terminal Classic Villa Alta phase (~CE 800 to 900), almost 1800 years after the date of ceramics recovered from Cascajal. Villa Alta occupation is widespread throughout the Coatzacoalcos drainage and covers some major Olmec sites, including San Lorenzo and Laguna de los Cerros. It seems probable, therefore, that the block, and its incising, can be dated to the San Lorenzo phase, perhaps toward the end of San Lorenzo B, that is to say, about 900 BCE. This dating is in agreement with the Olmec iconography that must have given rise to this script in the first place (*8*).

Fig. 2. Photograph of block, frontal view.

[1]Centro del Instituto Nacional de Antropología e Historia, Benito Juárez Número 425-431, Veracruz, Mexico. [2]Instituto de Antropología de La Universidad Veracruzana, Juárez Número 70, Xalapa, Veracruz, Mexico. [3]376 St. Ronan Street, New Haven, CT 06511, USA. [4]Department of Anthropology, University of Alabama, 24E ten Hoor Hall, Tuscaloosa, AL 35487, USA. [5]Department of Anthropology, Brown University, 128 Hope Street, Providence, RI 02912, USA. [6]Department of Anthropology, University of California Riverside, 334 Watkins Hall, Riverside, CA 92521, USA.

*To whom correspondence should be addressed. E-mail: Stephen_Houston@brown.edu

Features of the block. Carved of serpentine, the Cascajal block weighs about 12 kg and measures 36 cm in length, 21 cm in width, and 13 cm in thickness (Figs. 2 and 3). It displays five slightly convex sides. The remaining side shows the text, which consists of 62 signs. Scrutiny of this surface shows variable patina, vestiges of local orange clay, and the workings of two blades: one blunted and thus ideal for outlines, the other sharper to make incisions within signs. Unpatinated areas were highlighted by image processing in Adobe Photoshop CS (Adobe Systems Incorporated, San Jose, CA); other, unprocessed images are made available here as supporting online material. Enlargements of the high-resolution photos, taken with a Canon EOS 20D SLR (Canon, Tokyo, Japan) camera in raw format at 23.45 Mbytes per file, show unmistakable weathering, including pitting over incisions, with mineralization around the pits and inside the carved lines, a secure sign of ancient surface alteration. This was confirmed by 20× magnification and mineralogical analysis courtesy of Ricardo Sánchez Hernández and Jasinto Robles Camacho of the Laboratorio de Geología, INAH. In ancient times, the surface of the block had been carefully ground to prepare for the incised text, possibly as an erasable document that could be removed and revised.

Text analysis. The Cascajal block conforms to all expectations of writing (Figs. 4 and 5) (*9*). The text deploys (i) a signary of about 28 distinct elements, each an autonomous, codified glyphic entity; (ii) a few in repeated, short, isolable sequences within larger groupings; and (iii) a pattern of linear sequencing of variable length, with (iv) a consistent reading order. As products of a writing system, the sequences would by definition reflect patterns of language, with the probable presence of syntax and language-dependent word order (*10*).

Text orientation is clear. Olmec imagery consistently displays vegetal icons, which sprout to the top. The appearance of such signs in the text demonstrates that the inscription is horizontal. This orientation is further supported by the disposition of "sky-band" elements much like those on Olmec thrones and later regional iconography. Reading order is more difficult to establish. Most Mesoamerican scripts read left to right in unmarked conditions, i.e., when not arranged in unusual architectural settings. Left to right is likely to be present here, too. Yet, there is no strong evidence of overall organization. The sequences appear to be conceived as independent units of information, although to judge from shared details of carving they were recorded by the same hand.

The signary is likely to be incomplete. Three signs appear four times, six appear thrice, 12 occur twice, and seven occur once. The Cascajal block has three two-part sequences: sign 4 plus sign 1; sign 17 plus sign 8; and, perhaps, sign 3 plus sign 19. One sign, of an apparent insect

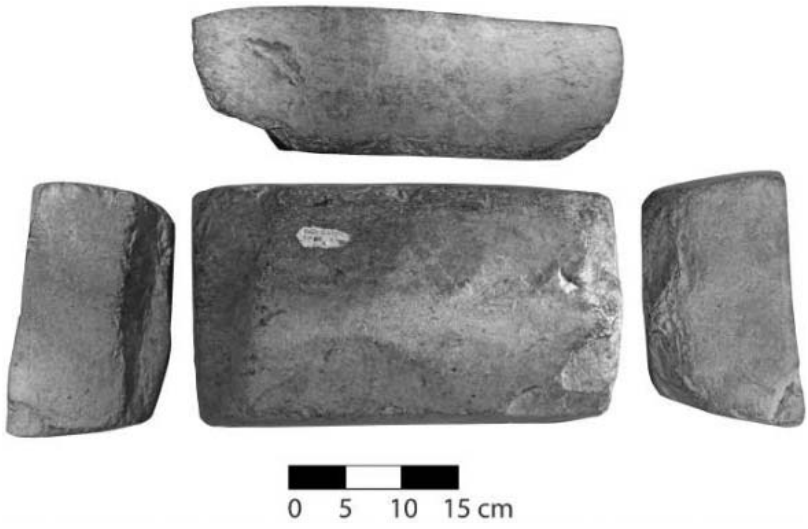

Fig. 3. Photographs of block, side and back views.

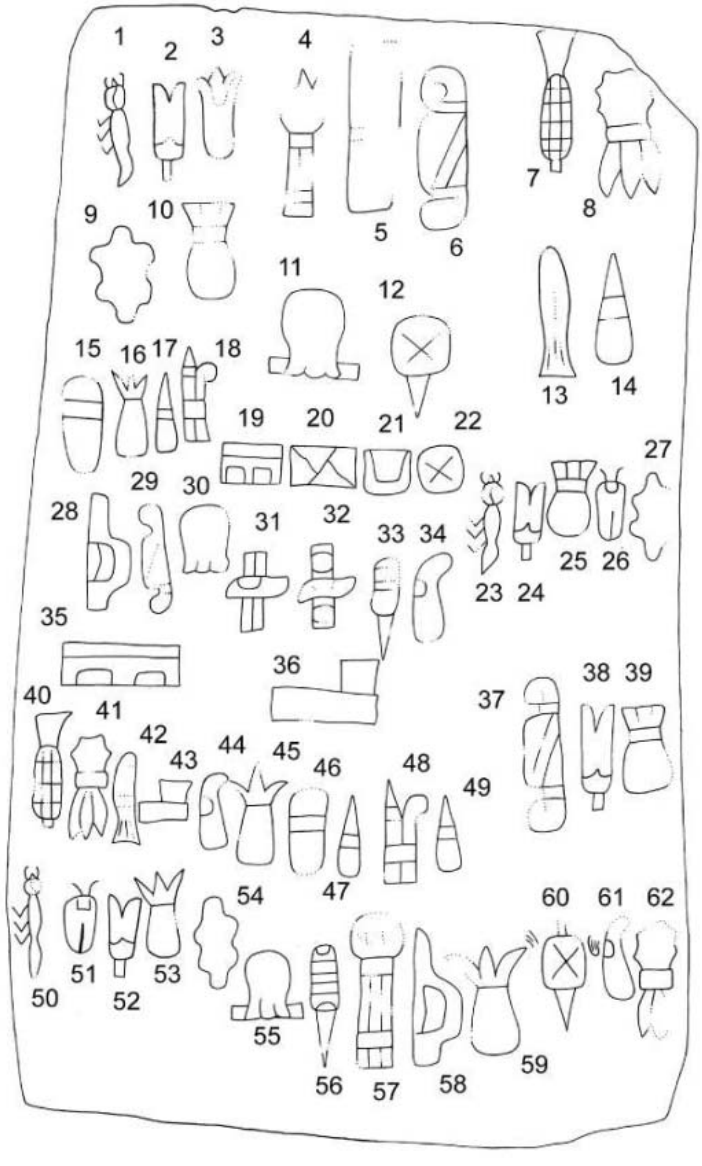

Fig. 4. Epigraphic drawing of block.

positioned as though scaling upward, faces its body to the direction of reading. It clearly opens sequences. In the shorter sequences, signs do not repeat. This is not the case with the two longest sequences at the base of the text. The chance of deciphering Olmec writing, that is, of linking it to language, is low. The sample is small, correlations to explanatory imagery are absent in the Cascajal block, and the restricted number of signs, although pointing by their small quantity to an alphabet, is potentially a meaningless statistic. With new finds there remains a strong chance of notable increments in the signary, as has proved true for the undeciphered Isthmian writing found not far from Cascajal (*11*). It is evident that some of the signs have an iconic origin, a few more transparent than others. The paired sets of eyes in signs 24 and 25 suggest the facial markings seen on some Olmec celts of the Middle Formative period [figure 44 in (*12*)]. Several paired sequences, such as the eyes or a throne sign paired with an evident mat sign, both common tropes for rulership in Mesoamerica, point to poetic couplets that are otherwise well attested in formal discourse of the region [figure 11 in (*13*), (*14*)]. If valid, the Cascajal examples would illustrate the earliest known couplets in Mesoamerica, a feature not yet seen in other Olmec icons. Signs 12, 17, and 27 show a thematic preoccupation with maize, or at least the ready use of such signs in the creation of a signary. Sign 6 may be a skin; sign 8, a strung bead or plaque; sign 10, a dart tip; sign 16, an object shown grasped in Olmec iconography; sign 18, a bivalve; sign 20, a possible perforator; and sign 21, a vertical fish. As for dating, iconographic parallels indicate that the Cascajal block is best assigned to the transition between the Early and Middle Formative period (~1000 to 800 BCE). Signs 12, 16, and 20 appear in Early Formative graphs of San Lorenzo, but sign 1, with cleft element and inverted V motif, serves as a diagnostic element of Middle Formative imagery [figure 12 in (*15*)]. Similar signs occur on figurines at Cantón Corralito, Chiapas, Mexico, but even earlier, at 1150 to 1000 BCE in uncalibrated dates [figure 3 in (*16*)]. The Corralito finds are especially relevant. They were excavated after the recovery of the Cascajal block, lending further weight to the general dating and validity of the text.

The significance of the find depends on whether more examples can be recovered and whether these can be salvaged by archaeologists rather than road builders, as regrettably occurred at Cascajal. It is probable that the Tlaltenco Celt and possibly the Humboldt Celt, both from Mexico, record the same script, also disposed in horizontal sequence [figures 32 and 34 in (*17*)]. The discovery of a rich inventory of wooden sculptures nearby, at El Manatí, of slightly earlier date, suggests that a dearth of texts today may be misleading (*18*). A tradition of coeval woodworking suggests an ancient reality of abundant wooden inscriptions, of which few would survive in tropical conditions. The small number of texts in Isthmian writing, found also in Veracruz as well as into Chiapas, Mexico, proves that a robust, widely spread script could exist without leaving many examples that last to the present.

The position of the Cascajal block in the development of New World writing, and particularly in Mesoamerica, is difficult to establish. The Cascajal script bears no secure links to later Isthmian writing, which has a quite distinct signary although also from Veracruz, nor to other writing systems of Middle Preclassic Mesoamerica. The dating of the block to the Early Formative–Middle Formative transition raises the possibility that its writing system is: (i) an isolate, devised locally, with no known successors or (ii) a widely spread script that disappeared before the advent of scripts across Mesoamerica in the middle of the first millennium BCE. The first view hints that the Cascajal block conforms to the domain of "shamanic" scripts devised by religious specialists, with tightly restricted, revelatory functions and limited use-span (*19*). Against this view is the clear linkage of the script to the widely diffused signs of Olmec iconography. The signs and sequences of the Cascajal block savor of widespread codification, not shamanic idiosyncrasy. The dating of the Cascajal block and its formal distinction from all later scripts mean that the trajectory of the Cascajal system recalls the obsolescence experienced by Indus script at about 1900 BCE, with scriptural silence until the far later introduction of a script from the Near East and intervening regions (*20*). These and other questions relating to content and function cannot be resolved until more examples of the Cascajal script are found.

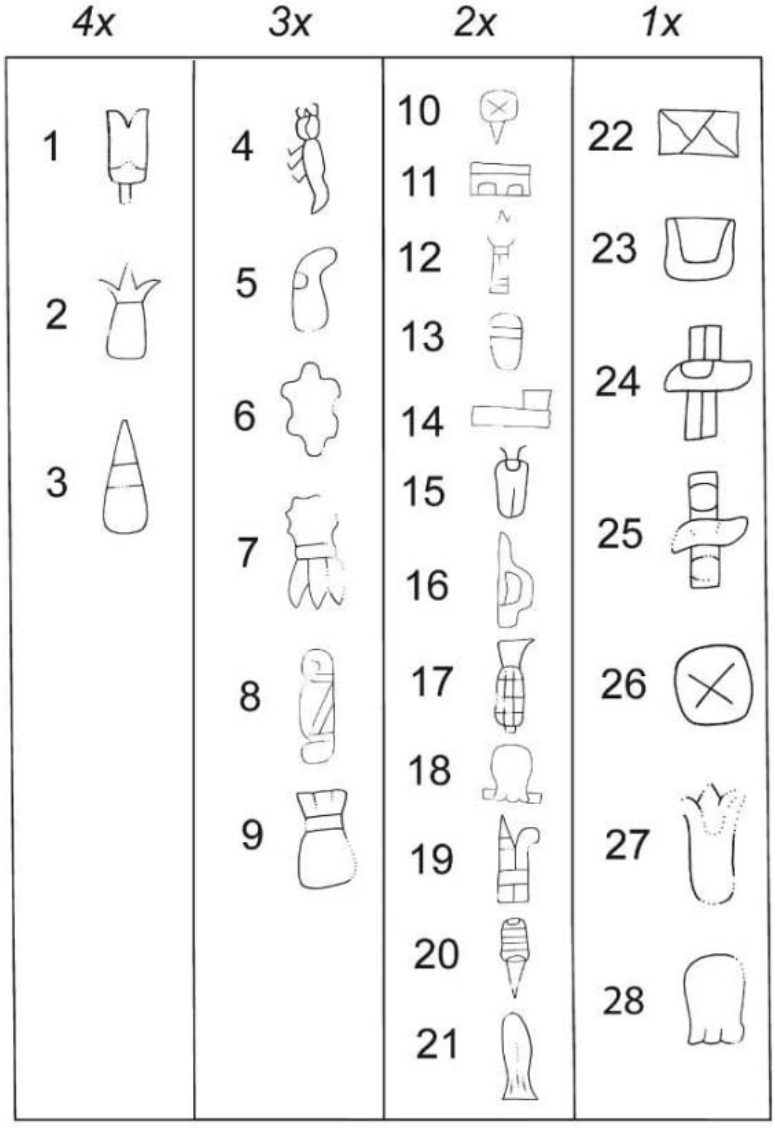

Fig. 5. Cascajal signary.

References and Notes

1. W. A. Saturno, D. Stuart, B. Beltrán, *Science* **311**, 1281 (2006); published online 4 January 2006 (10.1126/science.1121745).

2. R. A. Diehl, *The Olmecs: America's First Civilization* (Thames & Hudson, London, 2005).
3. M. E. D. Pohl, K. O. Pope, C. von Nagy, *Science* **298**, 1984 (2002).
4. V. Scheil, *Documents en Écriture Proto-Élamites* (Ernest Leroux, Paris, 1905).
5. J. Marshall, *Illus. Lond. News* **20**, 528 (1924).
6. H. Holmes, *Am. Anthropol.* **9**, 691 (1907).
7. P. Ortíz, C. Rodríguez, *Arqueología,* in press.
8. M. D. Coe, R. A. Diehl, *In the Land of the Olmec* (Univ. of Texas Press, Austin, TX, 1980).
9. S. Houston, in *The First Writing*, S. Houston, Ed. (Cambridge Univ. Press, Cambridge, 2004), p. 284.
10. M. D. Coe, *Breaking the Maya Code* (Thames & Hudson, London, rev. ed., 1999), p. 13.
11. S. D. Houston, M. D. Coe, *Mexicon* **25**, 151 (2004).
12. K. A. Taube, *Olmec Art at Dumbarton Oaks* (Dumbarton Oaks, Washington, DC, 2004).
13. K. A. Taube, in *The Olmec World: Ritual and Rulership*, J. Guthrie (Princeton Univ. Art Museum, Princeton, NJ, 1995).
14. T. D. Sullivan, *A Scattering of Jades: Stories, Poems, and Prayers of the Aztecs* (Univ. of Arizona Press, Tucson, AZ, 1994), pp. 229 and 258.
15. K. A. Taube, *Olmec Art at Dumbarton Oaks* (Dumbarton Oaks, Washington, DC, 2004).
16. D. Cheetham, J. E. Clark, in *XIX Simposio de Investigaciones Arqueológicas en Guatemala, 2005*, J. P. Laporte, B. Arroyo, H. E. Mejía, Eds. (Ministerio de Cultura y Deportes, Guatemala City, Guatemala, 2006).
17. P. D. Joralemon, *A Study of Olmec Iconography* (Dumbarton Oaks, Washington, DC, 1971).
18. P. Ortíz, C. Rodríguez, in *Olmec Art and Archaeology in Mesoamerica*, J. E. Clark, M. E. Pye, Eds. (Yale Univ. Press, New Haven, CT, 2000), pp. 75–93.
19. K. H. Basso, N. Anderson, *A Western Apache Writing System* (Peter de Ridder, Lisse, Netherlands, 1975), p. 5.
20. S. D. Houston, J. Baines, J. Cooper, *Comp. Stud. Soc. Hist.* **45**, 430 (2003).
21. Access to the Cascajal block was facilitated by members of the Patronato Prodefensa del Patrimonio Cultural Lomas de Tacamichapa, Cástulo Gabriel Cruz, President. The Centro Regional, Veracruz, of the INAH made the visit possible. J. Clark and D. Cheetham commented on the manuscript, as did several anonymous reviewers. Z. Nelson helped prepare figures.

Supporting Online Material

www.sciencemag.org/cgi/content/full/313/5793/1610/DC1
Materials and Methods
Figs. S1 to S3

19 June 2006; accepted 8 August 2006
10.1126/science.1131492

REPORTS

Probing Nanoscale Ferroelectricity by Ultraviolet Raman Spectroscopy

D. A. Tenne,[1]* A. Bruchhausen,[2] N. D. Lanzillotti-Kimura,[2] A. Fainstein,[2] R. S. Katiyar,[3] A. Cantarero,[4] A. Soukiassian,[5] V. Vaithyanathan,[5] J. H. Haeni,[5] W. Tian,[5] D. G. Schlom,[5] K. J. Choi,[6] D. M. Kim,[6] C. B. Eom,[6] H. P. Sun,[7] X. Q. Pan,[7] Y. L. Li,[5,8] L. Q. Chen,[5] Q. X. Jia,[8] S. M. Nakhmanson,[9] K. M. Rabe,[9] X. X. Xi[1,5]

We demonstrated that ultraviolet Raman spectroscopy is an effective technique to measure the transition temperature (T_c) in ferroelectric ultrathin films and superlattices. We showed that one-unit-cell-thick $BaTiO_3$ layers in $BaTiO_3/SrTiO_3$ superlattices are not only ferroelectric (with T_c as high as 250 kelvin) but also polarize the quantum paraelectric $SrTiO_3$ layers adjacent to them. T_c was tuned by ~500 kelvin by varying the thicknesses of the $BaTiO_3$ and $SrTiO_3$ layers, revealing the essential roles of electrical and mechanical boundary conditions for nanoscale ferroelectricity.

Ferroelectricity at the nanoscale has emerged as fertile ground for new physical phenomena and devices (*1*–*3*). Shrinking dimensions demand characterization techniques that are capable of probing the properties of ferroelectrics in, for example, ultrathin films and superlattices. In particular, it is difficult to measure the ferroelectric phase transition temperature T_c in such systems, and the T_c information is largely missing in reports of ferroelectricity in nanoscale ultrathin films and superlattices (*4*, *5*). One fundamental property of ferroelectrics that changes qualitatively during the phase transition is the dynamics of lattice vibrations (*6*). Thus, its temperature dependence allows the determination of T_c. Although lattice dynamics in ferroelectric films (*7*, *8*) and superlattices (*9*) from 150 nm to 2 μm in thickness have been investigated previously, such studies are very difficult on films thinner than ~100 nm. We report the use of ultraviolet (UV) Raman spectroscopy on $BaTiO_3/SrTiO_3$ superlattices with total thicknesses down to 24 nm, which enabled us to measure the T_c of the $BaTiO_3$ layers in the superlattices. We found that the $BaTiO_3$ layers are ferroelectric even when their thickness is only one unit cell (0.4 nm) and that they can induce polarization in the adjacent paraelectric $SrTiO_3$ layers that are much thicker. By varying the thickness of both the $BaTiO_3$ and $SrTiO_3$ layers, T_c was tuned from 250 K below to 235 K above the bulk value of $BaTiO_3$ (403 K). This result shows that under favorable electrical and mechanical boundary conditions, ferroelectricity is robust in nanoscale systems.

Conventional visible Raman spectroscopy works poorly for thin films of ferroelectrics and other wide–band-gap materials because the visible photon energy is much smaller than the band gap (*10*). Consequently, the absorption is extremely weak and the penetration depth is large, allowing light to travel through the film into the substrate, which generates overwhelming signals in the Raman spectra. For UV excitation, the photon energy is above the band gaps of ferroelectrics, leading to a much stronger absorption and a shorter penetration depth, preventing light from entering the substrate. UV excitation near the band gap also leads to strong resonance enhancement of Raman signals. This is demonstrated by Fig. 1, where Raman spectra of a $BaTiO_3/SrTiO_3$ superlattice

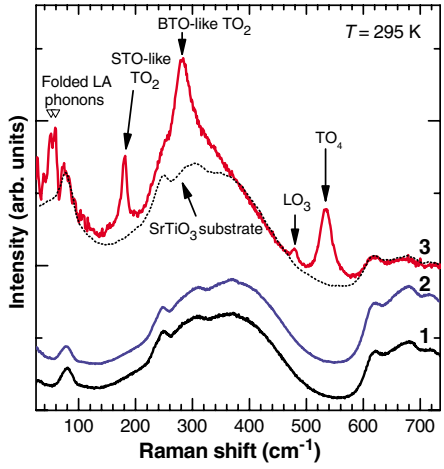

Fig. 1. Room-temperature Raman spectra of (1) a bare $SrTiO_3$ substrate (black curve); (2) a $(BTO_5/STO_4) \times 25$ superlattice (T_c = 530 K, blue curve) measured with visible excitation (514.5 nm); and (3) the same superlattice measured with 351.1-nm UV excitation (red curve). The dashed black line shows the bare $SrTiO_3$ substrate spectrum measured with 351.1-nm UV excitation. Triangles show the calculated frequencies of the first folded LA doublet. arb., arbitrary.

[1]Department of Physics, The Pennsylvania State University, University Park, PA 16802, USA. [2]Centro Atómico Bariloche y Instituto Balseiro, Comisión Nacional de Energía Atómica, 8400 San Carlos de Bariloche, Argentina. [3]Department of Physics, University of Puerto Rico, San Juan, Puerto Rico 00931–3343, USA. [4]Materials Science Institute, University of Valencia, Post Office Box 22085, E-46071 Valencia, Spain. [5]Department of Materials Science and Engineering, The Pennsylvania State University, University Park, PA 16802, USA. [6]Department of Materials Science and Engineering, University of Wisconsin, Madison, WI 53706, USA. [7]Department of Materials Science and Engineering, University of Michigan, Ann Arbor, MI 48109, USA. [8]Materials Science and Technology Division, Los Alamos National Laboratory, Los Alamos, NM 87545, USA. [9]Department of Physics and Astronomy, Rutgers, The State University of New Jersey, 136 Frelinghuysen Road, Piscataway, NJ 08854–8019, USA.

*To whom correspondence should be addressed: Department of Physics, Boise State University, 1910 University Drive, Boise, ID 83725–1570, USA. E-mail: dmitritenne@boisestate.edu

measured with visible (514.5 nm) and UV (351.1 nm) excitations are shown. The substrate features dominate the 514.5-nm spectrum, but they are greatly reduced in the UV spectrum, in which peaks of superlattice phonons are clearly observed.

UV Raman spectroscopy has not been widely used for measurements of ferroelectric films because of technical difficulties such as lower throughput efficiency, insufficient dispersion, and higher stray light level of UV Raman spectrometers as compared to those operating in the visible range. Recently, room-temperature measurement of $SrTiO_3$ films using 325-nm excitation has been reported (*11*). The recent progress in UV Raman instrumentation has made the measurement of ferroelectric films possible. In our experiment, a triple monochromator was used to provide high resolution and effective reduction of stray light (*12*). Powerful laser sources and optimized optical paths were used to improve the throughput. With these setups, we have measured Raman scattering in $BaTiO_3/SrTiO_3$ superlattices as thin as 24 nm and in $(Ba_{0.5}Sr_{0.5})TiO_3$ films that were 10 nm thick.

The $BaTiO_3/SrTiO_3$ superlattices are denoted by $(BTO_n/STO_m) \times$ number of periods, where n and m refer to the thickness, in unit cells, of the $BaTiO_3$ and $SrTiO_3$ layers, respectively. They were all grown on (001) $SrTiO_3$ substrates. Details of the sample preparation by reactive molecular-beam epitaxy (*13*) and structural characterization are presented in the supporting online material (*12*).

Curve 3 in Fig. 1 is typical of the UV Raman spectra of $BaTiO_3/SrTiO_3$ superlattices below T_c, exhibiting strong first-order (single-phonon) peaks as labeled in the figure. Weak second-order (two-phonon) features from the $SrTiO_3$ substrate can be seen between 600 and 700 cm^{-1} and as a background in the range from 200 to 500 cm^{-1}. The phonon mode assignment was made by comparison with the spectra of $SrTiO_3$ and $BaTiO_3$ single crystals (*12*) and with the help of first-principles calculations. The lines at about 290 cm^{-1} have similar positions and shapes to the TO_2 modes of A_1 symmetry of the tetragonal-phase $BaTiO_3$ (*14*, *15*); thus, they are assigned to the $BaTiO_3$ layers. The line at about 180 cm^{-1} corresponds closely to the TO_2 line in the electric field–induced Raman spectrum of $SrTiO_3$ crystals (*16*). It is not from the $SrTiO_3$ substrate, because the first-order Raman lines are symmetry-forbidden in bulk $SrTiO_3$ (*17*). Although the TO_1 mode of A_1 symmetry of $BaTiO_3$ is at about the same position (177 cm^{-1}), it has markedly different relative intensity and shape (*14*) from the 180-cm^{-1} line. Therefore, we attribute this line to the TO_2 phonon in the $SrTiO_3$ layers. The LO_3 and TO_4 modes involve both $SrTiO_3$ and $BaTiO_3$ layers and extend through the superlattice. A doublet of folded longitudinal acoustic (LA) phonons due to the superlattice periodicity (*18*) is also observed. The two triangles indicate the predicted first-doublet frequencies by an elastic continuum model (*19*). The observation of the LA phonon folding suggests that these superlattices possess the requisite structural quality for acoustic Bragg mirrors and cavities used for coherent phonon generation (*20*, *21*).

Bulk crystalline $BaTiO_3$ is cubic and paraelectric above T_c = 403 K, becomes tetragonal and ferroelectric below T_c, and goes through additional transitions to orthorhombic at 278 K and rhombohedral at 183 K (*22*). Bulk crystalline $SrTiO_3$ is paraelectric at all temperatures because of quantum fluctuations (*23*). The temperature evolution of Raman spectra for two superlattice samples is shown in Fig. 2A $(BTO_2/STO_{13}) \times 20$ and Fig. 2B $(BTO_8/STO_4) \times 10$. The shapes and positions of the $BaTiO_3$ lines at low temperatures are characteristic of $BaTiO_3$ in the tetragonal phase (*12*, *14*, *15*), indicating that the $BaTiO_3$ layers are tetragonal and ferroelectric below T_c. The presence of the first-order Raman lines of $SrTiO_3$ shows that the $SrTiO_3$ layers are polar because the first-order lines are symmetry-forbidden in nonpolar

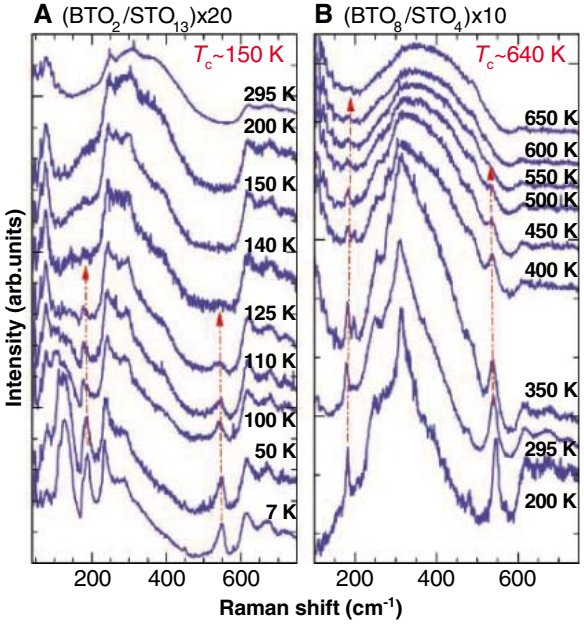

Fig. 2. Temperature evolution of UV Raman spectra of superlattices $(BTO_2/STO_{13}) \times 20$ (**A**) and $(BTO_8/STO_4) \times 10$ (**B**). The red arrows mark the $SrTiO_3$-like TO_2 mode at 180 cm^{-1} and the TO_4 mode at about 530 cm^{-1}, whose intensities decrease as the temperature increases and disappear at T_c.

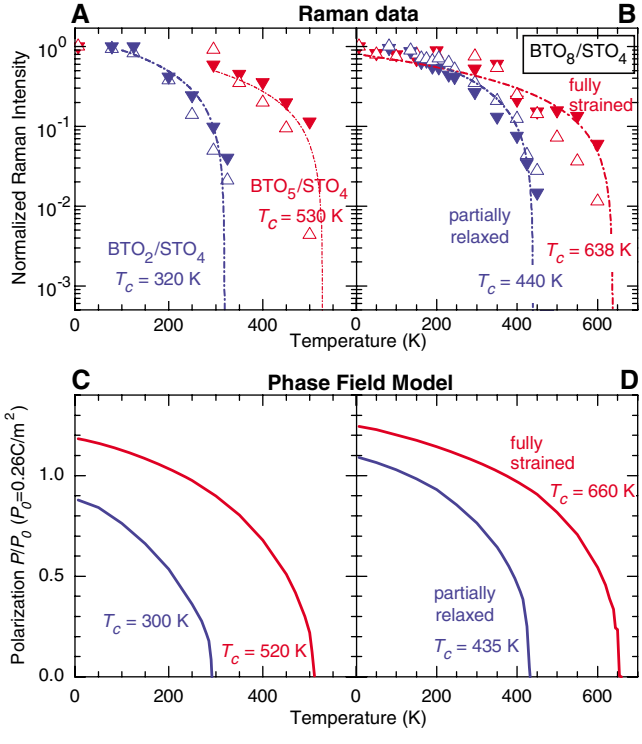

Fig. 3. Temperature dependencies of normalized Raman intensities of TO_2 (solid triangles) and TO_4 (open triangles) phonons for $(BTO_2/STO_4) \times 40$ and $(BTO_5/STO_4) \times 25$ (**A**) and $(BTO_8/STO_4) \times 10$ and $(BTO_8/STO_4) \times 40$ (**B**). Sample $(BTO_8/STO_4) \times 40$ is partially relaxed, whereas the other three samples are commensurate with the $SrTiO_3$ substrate. The dash-dotted lines are fits to a linear temperature dependence. (**C** and **D**) The 3D phase-field model calculations of polarization as a function of temperature in the same superlattice samples. Polarization (P) is given as a fraction of the polarization of bulk $BaTiO_3$ (P_0 = 0.26 C/m²).

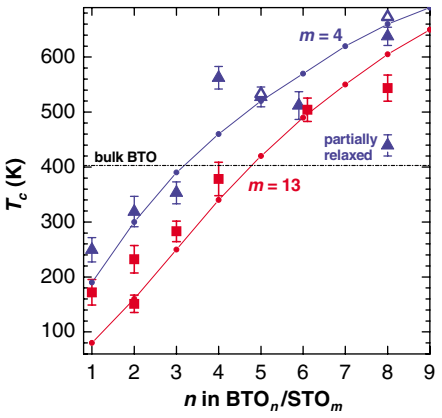

Fig. 4. Dependence of T_c on n and m in superlattices BTO$_n$/STO$_m$. Blue symbols are for $m = 4$ and red symbols are for $m = 13$. Open triangles are from temperature-dependent XRD measurements. Circles with lines are from the 3D phase-field model calculations. The black horizontal dash-dotted line shows the T_c in bulk $BaTiO_3$.

$SrTiO_3$ (*17*). The intensities of the first-order superlattice phonons decrease as the temperature increases and disappear at T_c. Above T_c, the spectra contain only the second-order features, as expected from the symmetry selection rules. When the $BaTiO_3$ layers are paraelectric, the induced polarization in the $SrTiO_3$ layers also disappears.

By plotting the first-order Raman intensity as a function of temperature, we can accurately determine T_c as the temperature where the intensity becomes zero. For this purpose, the TO_2 and TO_4 phonon lines are the most suitable because they do not overlap with the second-order features. The results, with the phonon intensities normalized by the Bose factor $n + 1 = \{1 - \exp[-(\hbar/2\pi)\omega/kT]\}^{-1}$ (where h is Planck's constant, ω is phonon frequency, k is Boltzmann's constant, and T is temperature) and by the intensities at 7 K, are presented for four superlattices: $(BTO_2/STO_4) \times 40$ and $(BTO_5/STO_4) \times 25$ in Fig. 3A and $(BTO_8/STO_4) \times 10$ and $(BTO_8/STO_4) \times 40$ (strain partially relaxed) in Fig. 3B. Both TO_2 and TO_4 phonons show similar behaviors, and the dashed-dotted lines are linear fits to the average of the two modes. The linear fit corresponds to a parabolic decrease of polarization with temperature, because Raman intensity is proportional to the square of atomic displacement. The intersection of a dash-dotted line with the horizontal axis is taken as the T_c of the sample.

The temperature dependence of polarization from a phase-field model calculation (*24*) is plotted in Fig. 3, C and D, for the same samples as in Fig. 3, A and B. The model assumes that the $BaTiO_3$ and $SrTiO_3$ layers in the superlattices have their respective bulk elastic and thermodynamic properties. The in-plane lattice constant is commensurately constrained to the $SrTiO_3$ substrate except for the partially relaxed case, and the top surface is stress-free. The surface depolarization field is ignored and a short-circuit electrostatic boundary condition is employed. A computational cell of 64 nm along the two in-plane directions and one unit cell along the growth direction was employed. The corresponding three-dimensional (3D) time-dependent Ginzburg-Landau equations are then numerically solved using the perturbation method with semi-implicit Fourier-spectral algorithms (*25*). The result reveals a spontaneous polarization along the growth direction with multiple 180° domains in the $BaTiO_3$ layers, which induces polarization in the adjacent $SrTiO_3$ layers, whose magnitude and distribution vary with the thickness and domain size of the $BaTiO_3$ layers. The spontaneous polarization in the $BaTiO_3$ layers becomes zero at T_c, and the predicted T_c values agree with those from the Raman data. This is remarkable considering that no fitting parameters from the Raman experiments are used in the calculations.

In Fig. 4, T_c determined by the Raman data, x-ray diffraction (XRD), and the phase-field model are shown as a function of the $BaTiO_3$ and $SrTiO_3$ layer thicknesses. The XRD measurement provides an additional confirmation of the Raman results, where a change in the temperature dependence of the out-of-plane lattice constant can be taken as an indication of T_c (*12*). The figure shows that the $BaTiO_3$ layers in the superlattices are ferroelectric even when their thickness is only one unit cell, with a T_c as high as 250 K. T_c increases with increasing n as the dipole-dipole interaction in $BaTiO_3$ layers becomes stronger, whereas large m suppresses T_c by reducing the coupling between the $BaTiO_3$ layers. By changing the values of n and m, we were able to tune T_c from 151 to 638 K; that is, from 250 K below to 235 K above the bulk value of $BaTiO_3$. The higher-than-bulk T_c is due to the strain in the $BaTiO_3$ layers, just as strain enhances T_c in single-layer ferroelectric films (*26*, *27*). When the strain is partially relaxed in sample $(BTO_8/STO_4) \times 40$, T_c drops almost to the bulk $BaTiO_3$ value. Although the 3D phase-field model allowing domain formation provides a good description of the Raman data, simulations assuming a single domain in the $BaTiO_3$ layers yield significantly lower T_c for $m = 13$, demonstrating the importance of domain formation in theoretical calculations (*28*).

We now can conclude that ferroelectricity can be very strong in one-unit-cell-thick $BaTiO_3$ layers ($T_c \sim 250$ K for $n/m = 1/4$). The electrical boundary condition plays a critical role. With the highly polarizable $SrTiO_3$ in contact with the $BaTiO_3$ layers, the critical thickness is reduced to a single unit cell. Meanwhile, the mechanical boundary condition imposed by the $SrTiO_3$ substrate leads to strain in the $BaTiO_3$ layers and thus to enhanced ferroelectricity. The interplay between the electrical and mechanical boundary conditions enables the tuning of T_c by nearly 500 K.

References and Notes

1. C. H. Ahn, K. M. Rabe, J.-M. Triscone, *Science* **303**, 488 (2004).
2. J. Junquera, P. Ghosez, *Nature* **422**, 506 (2003).
3. D. D. Fong *et al.*, *Science* **304**, 1650 (2004).
4. T. Tybell, C. H. Ahn, J.-M. Triscone, *Appl. Phys. Lett.* **75**, 856 (1999).
5. H. N. Lee, H. M. Christen, M. F. Chisholm, C. M. Rouleau, D. H. Lowndes, *Nature* **433**, 395 (2005).
6. M. E. Lines, A. M. Glass, *Principles and Applications of Ferroelectrics and Related Materials* (Clarendon, Oxford, 1977).
7. A. A. Sirenko *et al.*, *Nature* **404**, 373 (2000).
8. T. Ostapchuk *et al.*, *Phys. Rev. B* **66**, 235406 (2002).
9. R. S. Katiyar, Y. I. Yuzyuk, R. R. Das, P. Bhattacharya, V. Gupta, *Ferroelectrics* **329**, 907 (2005).
10. K. van Benthem, C. Elsässer, R. H. French, *J. Appl. Phys.* **90**, 6156 (2001).
11. L. H. Tisinger *et al.*, *J. Vac. Sci. Technol. B* **21**, 53 (2003).
12. See supporting material on *Science* Online for details.
13. D. G. Schlom *et al.*, *Mater. Sci. Eng. B* **87**, 282 (2001).
14. A. Scalabrin, A. S. Chaves, D. S. Shim, S. P. S. Porto, *Phys. Status Solidi B* **79**, 731 (1977).
15. D. A. Tenne *et al.*, *Phys. Rev. B* **69**, 174101 (2004).
16. P. A. Fleury, J. M. Worlock, *Phys. Rev.* **174**, 613 (1968).
17. W. G. Nilsen, J. G. Skinner, *J. Chem. Phys.* **48**, 2240 (1968).
18. B. Jusserand, M. Cardona, *Light Scattering in Solids V* (Springer, Heidelberg, Germany, 1989), pp. 49–152.
19. C. Colvard *et al.*, *Phys. Rev. B* **31**, 2080 (1985).
20. M. Trigo, A. Bruchhausen, A. Fainstein, B. Jusserand, V. Thierry-Mieg, *Phys. Rev. Lett.* **89**, 227402 (2002).
21. A. Bartels, T. Dekorsy, H. Kurz, K. Köhler, *Phys. Rev. Lett.* **82**, 1044 (1999).
22. L. E. Cross, in *Ferroelectric Ceramics*, N. Setter, E. L. Colla, Eds. (Birkhäuser Verlag, Basel, Switzerland, 1993), pp. 1–85.
23. K. A. Müller, H. Burkard, *Phys. Rev. B* **19**, 3593 (1979).
24. L.-Q. Chen, *Annu. Rev. Mater. Res.* **32**, 113 (2002).
25. L.-Q. Chen, J. Shen, *Comput. Phys. Commun.* **108**, 147 (1998).
26. K. J. Choi *et al.*, *Science* **306**, 1005 (2004).
27. J. H. Haeni *et al.*, *Nature* **430**, 758 (2004).
28. V. A. Stephanovich, I. A. Luk'yanchuk, M. G. Karkut, *Phys. Rev. Lett.* **94**, 047601 (2005).

29. We thank L. Bergman for her help in the early stage of this work. This work was partially supported by the U.S. Department of Energy (DOE) under grant no. DE-FG02-01ER45907 (X.X.X.); by the Office of Naval Research under grant nos. N00014-03-1-0721 (D.G.S.), N00014-04-1-0426 (D.G.S.), N00014-03-1-0534 P0005 (A.F.), N00014-05-1-0559 (C.B.E.), N00014-00-1-0261 (K.M.R.), and N00014-01-1-0365 (K.M.R.); by NASA under grant no. NASA3-NCC1034 (R.S.K.); by NSF under grant nos. DMR-0507146 (D.G.S., L.Q.C., X.Q.P., K.M.R., and X.X.X.), DMR-0122638 (L.Q.C.), DMR-0213623 (L.Q.C.), DMR-0313764 (C.B.E.), ECS-0210449 (C.B.E.), and DMR-0315633 (X.Q.P.); and by a Guggenheim fellowship (L.Q.C.). The work at Los Alamos National Laboratory was supported by the Laboratory-Directed Research and Development Program under DOE.

Supporting Online Material

www.sciencemag.org/cgi/content/full/313/5793/1614/DC1
Materials and Methods
Figs. S1 to S6
References

22 May 2006; accepted 31 July 2006
10.1126/science.1130306

Near-Threshold Inelastic Collisions Using Molecular Beams with a Tunable Velocity

Joop J. Gilijamse,[1] Steven Hoekstra,[1] Sebastiaan Y. T. van de Meerakker,[1]*
Gerrit C. Groenenboom,[2]* Gerard Meijer[1]

Molecular scattering behavior has generally proven difficult to study at low collision energies. We formed a molecular beam of OH radicals with a narrow velocity distribution and a tunable absolute velocity by passing the beam through a Stark decelerator. The transition probabilities for inelastic scattering of the OH radicals with Xe atoms were measured as a function of the collision energy in the range of 50 to 400 wavenumbers, with an overall energy resolution of about 13 wavenumbers. The behavior of the cross-sections for inelastic scattering near the energetic thresholds was accurately measured, and excellent agreement was obtained with cross-sections derived from coupled-channel calculations on ab initio computed potential energy surfaces.

The study of collisions between gas-phase atoms and molecules is a well-established method of gathering detailed information about their individual structures and mutual interaction (*1*). The level of detail obtained by these studies depends on the quality of preparation of the collision partners before the collision (*2*–*4*) and on how accurately the products are analyzed afterward (*5*–*7*). In recent years, it has become increasingly possible to control the internal and external degrees of freedom of the scattering partners, allowing the potential energy surfaces that govern the molecular collisions to be probed in ever greater detail. The most detailed information is obtained when crossed molecular beams are used to produce intense jets of molecules with a well-defined velocity, confined to only a few internal quantum states. Further state selection can be achieved by optical preparation of a single quantum state or by purification of the beam with the use of electrostatic or magnetic multipole fields (*2*, *3*). These methods allow the orientation of the molecules to be controlled before the collision (*8*, *9*) and the orientation of the scattered products to be measured (*10*).

One of the most important parameters describing a scattering event is the collision energy of the scatterers. However, control over the collision energy has been a difficult experimental task. Since the 1980s, ingenious crossed-beam machines have been engineered to vary the crossing angle of the intersecting beams, allowing variation of the collision energy while maintaining particle densities high enough for scattering (*11*). It was thereby possible to measure threshold behavior of rotational energy transfer (*12*, *13*) or to tune the collision energy over the reaction barrier for reactive scattering (*14*, *15*). These methods led to considerable improvement in the control over collision energy at high energies—for example, to probe short-range interactions. However, a similar level of control over collisions at low energies, which are sensitive probes for long-range interactions, is generally lacking. The angle of the intersecting beams cannot be varied to arbitrarily small values; and at low collision energies, the energy resolution, which is determined by the velocity spread of both beams, rapidly becomes comparable to the collision energy.

Low-energy collisions of atoms and molecules interrogate the part of the interaction potential energy surface that is relevant for the formation of long-lived complexes. From resonance phenomena in the scattering signal as a function of collision energy, accurate information on the interaction can be extracted (*16*–*18*). Near the energetic thresholds for inelastic scattering, resonant states can be formed when the colliding complex begins to rotate, leaving the constituents with insufficient translational energy to overcome their van der Waals attraction. Methods to experimentally extract information on these resonances are extremely limited. Thus far, low-energy collisions have only been studied in cryogenic cell environments (*19*) or in supersonic gas expansions that are specifically designed to maintain a thermal equilibrium at temperatures as low as 6 K (*20*). Recently, reports have appeared on the study of cold inelastic collisions between alkali atoms and dimers in an optically trapped gas (*21*, *22*).

An alternative experimental approach to studying collisions at a low and/or variable energy is to produce molecular beams with a low and/or variable velocity (*23*). Mechanical velocity selectors can be used to select molecules with a narrow velocity distribution out of molecular beams (*24*), but the particle densities and velocities that can be reached are set by the original velocity distribution of the beam. Exquisite control over the velocity of polar molecules in a molecular beam has only been possible since the development of the Stark deceleration technique. The Stark decelerator for neutral polar molecules is the equivalent of a linear accelerator for charged particles and exploits the interaction of a polar molecule with inhomogeneous time-varying electric fields (*25*, *26*). The deceleration (or acceleration) process can be seen as slicing a packet of molecules with a narrow velocity distribution out of the densest part of the molecular beam pulse. This packet can then be decelerated or accelerated to any velocity, maintaining the narrow velocity distribution and the particle density in the packet. In a crossed-beam configuration, this tool offers the revolutionary capability to study elastic or inelastic and reactive scattering as a function of the continuously variable collision energy, from low to high collision energies, and with a high intrinsic energy resolution. The computer-controlled velocity of the molecular beam allows scanning of the collision energy in an otherwise fixed experimental geometry. The deceleration process is highly quantum-state specific, and the state purity of the bunches of selected molecules that emerge from the decelerator can be close to 100%. Moreover, the decelerated molecules are all naturally spatially oriented, and steric effects can therefore in principle be studied as well.

Here, we report the use of a Stark-decelerated molecular beam with a tunable and narrow velocity distribution in a molecular beam scattering experiment. In a crossed-beam setup, rotationally inelastic scattering between state-selected OH radicals [$X^2\Pi_{3/2}$, $v = 0$, $J = 3/2$, f (*27*), referred to hereafter as $F_1(3/2f)$] and Xe atoms is studied throughout the 0.14 to 1.14 kcal/mol (50 to 400 cm^{-1}) region, with an overall energy resolution of ~0.03 kcal/mol (13 cm^{-1}). We chose the OH–rare gas system because at higher collision energies, rotationally inelastic collisions have been studied for this system in great detail, both experimentally and theoretically; state-to-state cross-sections and the effects of molecular orientation have been determined (*28*, *29*). The energy range covered in this study encompassed the energetic thresholds for inelastic scattering down to the lowest rotational levels of OH. The threshold behavior of the inelastic state-to-state cross-sections was accurately measured and was compared with the outcome of coupled-channels calculations on a computed OH-Xe potential energy surface.

A molecular beam of OH radicals in the low-field–seeking $F_1(3/2f)$ state was decelerated, guided, or accelerated with the use of a Stark decelerator (Fig. 1). The time-of-flight profile of the radicals that exit the decelerator is shown for a typical setting of the decelerator. The densest part of the OH beam, with an original velocity of 450 m/s, was selected and slowed down to a final velocity of 281 m/s. The

[1]Fritz-Haber-Institut der Max-Planck-Gesellschaft, Faradayweg 4-6, 14195 Berlin, Germany. [2]Theoretical Chemistry, Institute for Molecules and Materials, Radboud University Nijmegen, Toernooiveld 1, 6525 ED Nijmegen, Netherlands.

*To whom correspondence should be addressed. E-mail: basvdm@fhi-berlin.mpg.de (S.Y.T.M.); gerritg@theochem.ru.nl (G.C.G.)

decelerated packet of radicals arrived temporally delayed in the field-free interaction region and was scattered with a beam of pure Xe under an angle of 90°. In the experiments, the velocity of the OH radicals was varied from 33 to 700 m/s; the contribution of the OH radicals to the center-of-mass (CM) collision energy (E_{coll}) was thereby varied from less than 1 to ~310 cm^{-1}. The contribution of the width of the OH velocity distribution to the overall energy resolution was very small. The maximum rotational state purity of the packet of OH $F_1(3/2f)$ radicals before the collision was measured to be ≥99.7%. Contamination of the inelastic state-to-state scattering data by initial populations in different quantum states was negligible.

The xenon beam was produced by expansion of Xe at 2.5-atm backing pressure from a cooled pulsed valve (−70°C), resulting in a beam with a velocity of ~300 m/s. The exact velocity of the Xe atoms depends on the detailed settings of the pulsed valve as well as the timing of the collision event within the Xe gas pulse, and these settings were kept fixed during the measurements. Although the exact velocity of the Xe atoms was not measured, the constant contribution of the Xe atoms to the CM collision energy of ~60 cm^{-1} was sufficiently low that the total CM collision energy could be tuned over the energetic thresholds for scattering into both parity components of the $F_1(5/2)$ level (84 cm^{-1} excitation energy) and the $F_2(1/2)$ level (121 cm^{-1} excitation energy). The approximate 10% velocity spread in the Xe beam was by far the dominant contribution to the overall energy resolution in this experiment.

Saturated laser-induced fluorescence with tunable pulsed lasers was used to detect the OH radicals (*30*). For each setting of the OH velocity, the populations in the $F_1(3/2e)$, $F_1(3/2f)$, $F_1(5/2e)$, $F_1(5/2f)$, and $F_2(1/2e)$ levels were measured, both with and without collision of the Xe beam with the OH beam. The decrease of population in the $F_1(3/2f)$ level due to scattering with the Xe atoms was about 1%, indicating that single-collision conditions were fulfilled in the experiment. The signals associated with the scattering products were normalized by the signal of the incoming OH $F_1(3/2f)$ radical beam. Different excitation rates for the different branches of the optical transitions used to probe the different levels were taken into account to relate signal intensities to populations. Thus, transition probabilities for inelastic scattering to the $F_1(3/2e)$, $F_1(5/2e)$, $F_1(5/2f)$, and $F_2(1/2e)$ levels were obtained as a function of the OH contribution to the CM collision energy (Fig. 2). Collisions populating the $F_1(3/2e)$ level were most likely. Within the $F_1(5/2)$ level, collisions populating the lower Λ-doublet component of *e* parity were favored, consistent with findings of other $^2\Pi$–rare gas systems (*28*, *29*). For the $F_1(3/2e)$ and the $F_1(5/2e)$ and $F_1(5/2f)$ levels, the transition probabilities were almost constant at higher collision energies. Close to the $F_1(5/2)$ energetic threshold, collisions populating either one of the parity components of this level became less probable, and the transition probabilities for these levels dropped sharply. The only inelastic channel that was exoenergetic was scattering to the $F_1(3/2e)$ level, and its transition probability showed an increase at low collision energies. Excitation to the $F_2(1/2)$ level required a spin-orbit–changing collision, for which the cross-sections are generally lower than for a spin-orbit–conserving collision. The transition probability for this channel also showed a clear threshold behavior.

The theoretical framework to compute cross-sections for inelastic collisions of $^2\Pi$-state molecules such as OH with ^1S-state atoms such as Xe is well established (*31*). The electronic degeneracy of the Π state is lifted upon the approach of the atom, and two potential energy surfaces are required to describe the system. Contour plots of the potentials are shown in Fig. 3. We computed the potentials with the partially spin-restricted open-shell coupled-

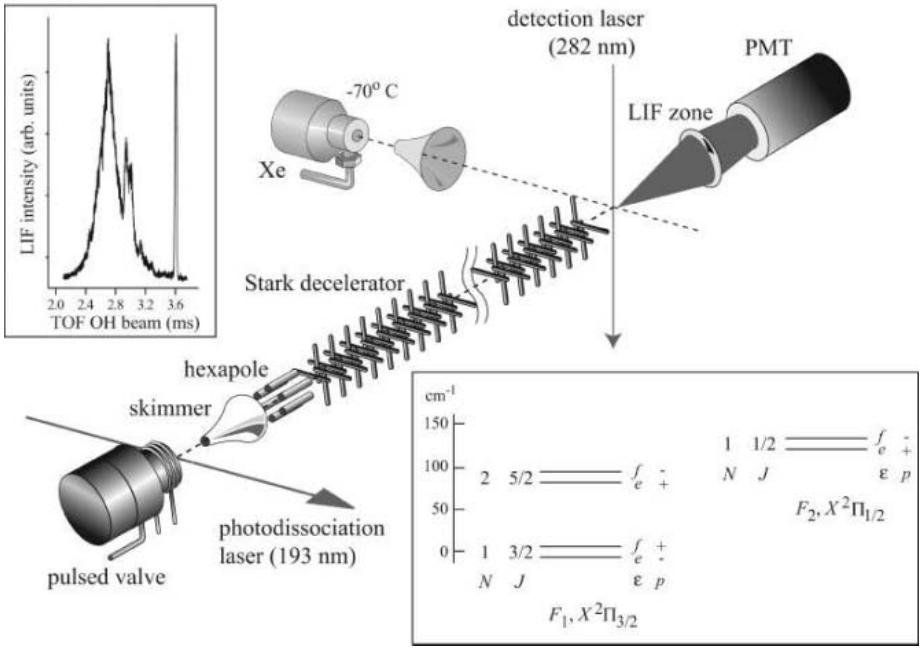

Fig. 1. Schematic representation of the experimental setup and the energy-level scheme of the OH radical. The OH radical beam is produced by photodissociation of gaseous HNO_3 that is coexpanded with a noble carrier gas (Ar, Kr, or Xe) into a vacuum. The beam is skimmed and radicals in the low-field–seeking $F_1(3/2f)$ state are focused with a hexapole into the Stark decelerator, where the beam is decelerated, guided, or accelerated to a velocity in the 33 to 700 m/s range. A typical time-of-flight (TOF) profile is shown in the left inset. The selected packet of radicals arrives temporally separated in the scattering region and is scattered with a beam of pure Xe at an angle of 90°, under single-collision conditions. The collision-induced populations in the $F_2(1/2)$, $F_1(3/2)$, and $F_1(5/2)$ rotational levels are probed before and after the collisions using a pulsed dye laser system in a saturated laser-induced fluorescence (LIF) scheme. The fluorescence is imaged onto a photomultiplier tube (PMT). In the energy-level scheme shown in the right inset, the splitting between both parity components of each rotational level is largely exaggerated for reasons of clarity.

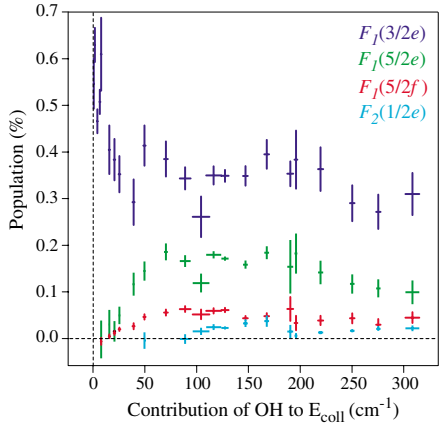

Fig. 2. Probabilities for inelastic scattering of OH $F_1(3/2f)$ radicals in collisions with Xe atoms to the $F_1(3/2e)$, $F_1(5/2e)$, $F_1(5/2f)$, and the $F_2(1/2e)$ levels as a function of $[1/2]\ [(m_{OH}m_{Xe})/(m_{OH} + m_{Xe})]\ v_{OH}^2$—i.e., as a function of the contribution of OH to the CM collision energy (where m_{OH} and m_{Xe} are the mass of OH and Xe, respectively, and v_{OH} is the velocity of the OH radicals in the laboratory frame). The horizontal error bars represent the uncertainty in collision energy that results from the velocity spread of the OH beam, which is different for every setting of the decelerator. The vertical error bars represent the statistical spread of the data as obtained from repeated runs of the experiment.

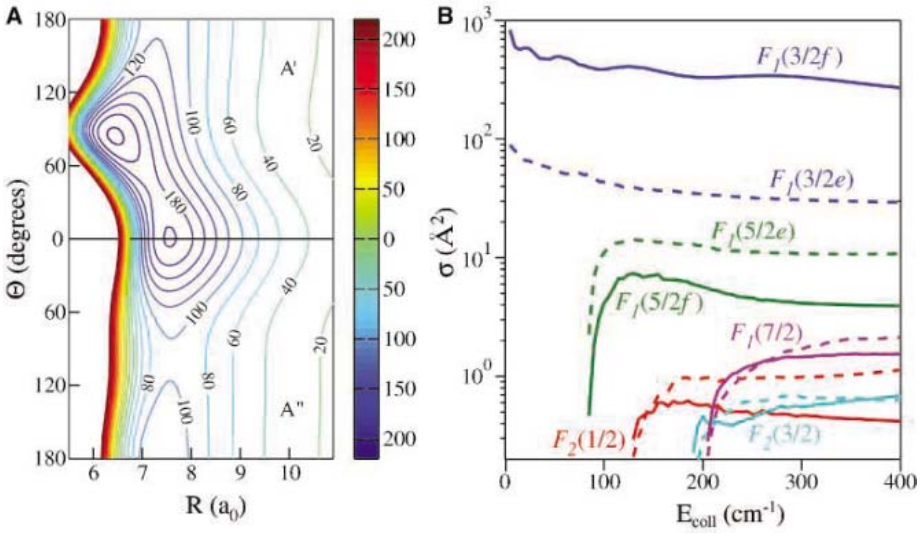

Fig. 3. (**A**) Contour plots of the A' (upper) and A'' (lower) potential surfaces in cm^{-1}. The potentials are computed with the RCCSD(T) method. A large one-electron basis consisting of the augmented-correlation consistent polarized valence quadruple zeta (aug-cc-pVQZ) set is used, extended with a set of (*3s*, *3p*, *2d*, *1f*, and *1g*) mid-bond orbitals with geometry-dependent exponents (*38*). The angular dependence of the sum of the potentials is represented by a Legendre polynomial expansion and the difference of the two potentials by associated Legendre functions, as required by theory (*31*). The proper R^{-n} analytic form is used for the radial dependence of the long-range expansion of the sum potential, and the reproducing kernel Hilbert space interpolation method (*39*) is used for the radial dependence of the short and intermediate range of the sum potential and for the difference potential. We tested the fit by performing additional ab initio calculations for 75 random geometries and found it to be very accurate: The errors at these points were on the order of a few tenths of a cm^{-1} or less. A fortran code of the potentials is available as supporting online material. (**B**) Computed cross sections for the first 10 channels, computed on a collision energy grid of E_{coll} = 5, 10, 15, …, 400 cm^{-1}. The solid and dashed lines correspond to channels of *f* and *e* spectroscopic labeling, respectively. The $F_1(3/2f)$ channel is the elastic channel. In the Hamiltonian we used the OH rotational constant B = 18.5487 cm^{-1}, the spin-orbit coupling constant A = −139.21 cm^{-1}, and Λ-doubling parameters p = 0.235 cm^{-1} and q = −0.0391 cm^{-1}. The channel basis included all OH rotational states with angular momentum $J \leq 21/2$. The highest total angular momentum in the basis has $F = 271/2$ and all $F \leq 201/2$ are present. The renormalized Numerov method was used to propagate the wave function from R = 4 to 35 a_0, where a_0 is the Bohr radius. Our computer code is verified by reproducing bound-state and scattering calculations on similar systems from the literature.

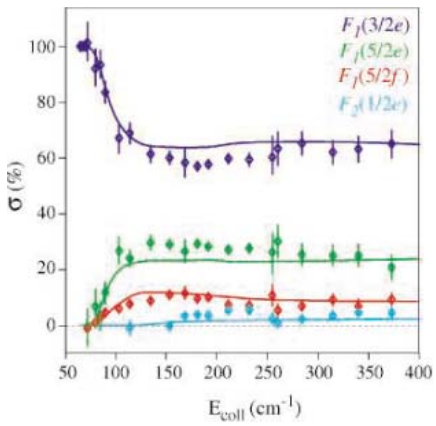

Fig. 4. Comparison of the collision energy dependence of the measured (data points with error bars) and calculated (solid curves) relative cross-sections—i.e., the fractional scattering of OH radicals into one of the $F_1(3/2e)$, $F_1(5/2e)$, $F_1(5/2f)$, or $F_2(1/2e)$ channels.

cluster method with single and double excitations and perturbative triples [RCCSD(T)] (*32*), as implemented in the MOLPRO 2002 program package (*33*). Interaction energies were obtained as the difference between the energy of the complex and the energies of the fragments. We computed the fragments in the same one-electron basis set as the complex to avoid the so-called basis set superposition error. This method is one of the best available to compute highly accurate potentials of weakly interacting systems. The Xe atom has 54 electrons; the 28 inner shell electrons are described by a relativistic pseudopotential (*34*). The interaction energies were computed for 300 geometries on a two-dimensional grid with 15 Gauss-Legendre points in the Jacobi-angle (θ) and atom-molecule separations up to R = 20 a_0. The OH bond length is kept fixed at r_0 = 1.8502 a_0. We used an analytical representation of the potentials (Fig. 3). The global minimum of −224 cm^{-1} occurs on the A' potential for a T-shaped geometry. This potential has a local minimum for a linear OH-Xe geometry (θ = 0°).

To compute the inelastic cross-sections, we performed fully converged coupled-channel calculations. The Hamiltonian includes the OH rotational, spin-orbit, and Λ-doubling terms. We used the *R*-embedded body-fixed channel basis for which the potential energy matrix elements are given in (*35*). Convergence of the cross-sections with respect to all parameters has been tested to be better than 1%. According to Wigner's threshold laws (*36*), the inelastic cross-sections at low energies are proportional to the square root of the excess energy. We found that in this case, a square root energy dependence holds approximately for several points above threshold on our 5 cm^{-1} interval grid as well.

Relating the measured energy-dependent transition probabilities (Fig. 2) to the calculated inelastic cross-sections (Fig. 3) requires detailed information on the relative velocity of the scatterers, the actual time interval during which scattering events are probed, and the detection probability of the scattered products (*12*). Systematic effects, such as the collision energy–dependent time interval for scattering and intensity and velocity of the incoming OH beam, cancel out when the relative inelastic transition probabilities are extracted from the measured absolute transition probabilities given in Fig. 2. If we assume an identical detection probability of the scattered products for the different inelastic channels for a given collision energy (*37*), the relative inelastic transition probabilities directly yield the relative cross-sections for inelastic scattering (Fig. 4). The horizontal axis is given an offset compared with the one in Fig. 2 to include the contribution of the Xe atoms to E_{coll}. The positions of the energetic thresholds are known with spectroscopic accuracy, and we obtained the best agreement when a velocity of the Xe atoms of 320 m/s was taken. The theoretical inelastic cross-sections (Fig. 3) were first convoluted with the experimental energy resolution, and we used the resultant values to calculate the relative cross-sections (solid curves in Fig. 4). Excellent agreement between theory and experiment was obtained throughout the range of collision energies probed. The ratio of scattering into the different channels, and, in particular, the shape of the inelastic cross-sections around threshold is perfectly reproduced.

Our measurements provide a very sensitive probe for the theoretical potential energy surfaces, from which a detailed understanding of the collision dynamics can be obtained. A next step will be to use two crossed velocity-tunable molecular beams or to collide the velocity-tunable beam with a stationary (i.e., trapped) sample of cold or ultracold atoms or molecules. In such systems, quantum state–selected atom-molecule and molecule-molecule collisions can be studied, down to collision energies less than 1 cm^{-1}, with a fraction of a wavenumber energy resolution.

References and Notes

1. R. D. Levine, R. B. Bernstein, *Molecular Reaction Dynamics and Chemical Reactivity,* (Oxford Univ. Press, New York, 1987).

2. G. Scoles, Ed., *Atomic and Molecular Beam Methods* (Oxford Univ. Press, New York, 1988), vol. 1.
3. G. Scoles, Ed., *Atomic and Molecular Beam Methods* (Oxford Univ. Press, New York, 1992), vol. 2.
4. T. P. Rakitzis, A. J. van den Brom, M. H. M. Janssen, *Science* **303**, 1852 (2004).
5. X. Liu, J. J. Lin, S. Harich, G. C. Schatz, X. Yang, *Science* **289**, 1536 (2000).
6. S. A. Harich *et al.*, *Nature* **419**, 281 (2002).
7. J. J. Lin, J. Zhou, W. Shiu, K. Liu, *Science* **300**, 966 (2003).
8. J. J. van Leuken, J. Bulthuis, S. Stolte, J. G. Snijders, *Chem. Phys. Lett.* **260**, 595 (1996).
9. R. N. Zare, *Science* **279**, 1875 (1998).
10. M. C. van Beek, G. Berden, H. L. Bethlem, J. J. ter Meulen, *Phys. Rev. Lett.* **86**, 4001 (2001).
11. G. Hall, K. Liu, M. J. McAuliffe, C. F. Giese, W. R. Gentry, *J. Chem. Phys.* **78**, 5260 (1983).
12. R. G. Macdonald, K. Liu, *J. Chem. Phys.* **91**, 821 (1989).
13. D. M. Sonnenfroh, R. G. Macdonald, K. Liu, *J. Chem. Phys.* **94**, 6508 (1991).
14. R. T. Skodje *et al.*, *Phys. Rev. Lett.* **85**, 1206 (2000).
15. D. Skouteris *et al.*, *Science* **286**, 1713 (1999).
16. W. Shiu, J. J. Lin, K. Liu, *Phys. Rev. Lett.* **92**, 103201 (2004).
17. R. C. Forrey, N. Balakrishnan, V. Kharchenko, A. Dalgarno, *Phys. Rev. A.* **58**, R2645 (1998).
18. N. Balakrishnan, A. Dalgarno, R. C. Forrey, *J. Chem. Phys.* **113**, 621 (2000).
19. C. D. Ball, F. C. De Lucia, *Phys. Rev. Lett.* **81**, 305 (1998).
20. I. R. Sims *et al.*, *J. Chem. Phys.* **97**, 8798 (1992).
21. P. Staanum, S. D. Kraft, J. Lange, R. Wester, M. Weidemüller, *Phys. Rev. Lett.* **96**, 023201 (2006).
22. N. Zahzam, T. Vogt, M. Mudrich, D. Comparat, P. Pillet, *Phys. Rev. Lett.* **96**, 023202 (2006).
23. C. E. Heiner, H. L. Bethlem, G. Meijer, *Phys. Chem. Chem. Phys.* **8**, 2666 (2006) and references therein.
24. L. T. Cowley, M. A. D. Fluendy, K. P. Lawley, *Rev. Sci. Instrum.* **41**, 666 (1970).
25. H. L. Bethlem, G. Berden, G. Meijer, *Phys. Rev. Lett.* **83**, 1558 (1999).
26. H. L. Bethlem, G. Meijer, *Int. Rev. Phys. Chem.* **22**, 73 (2003).
27. The labels $X^2\Pi_{3/2}$, v, and J indicate the electronic, vibrational, and rotational state of the OH radical, respectively. The spectroscopic symmetry labels *e* and *f* refer to the total parity of the electronic wavefunction, exclusive of rotation.
28. M. C. van Beek, J. J. ter Meulen, M. H. Alexander, *J. Chem. Phys.* **113**, 628 (2000).
29. M. C. van Beek, J. J. ter Meulen, M. H. Alexander, *J. Chem. Phys.* **113**, 637 (2000).
30. S. Y. T. van de Meerakker, N. Vanhaecke, G. Meijer, *Annu. Rev. Phys. Chem.* **57**, 159 (2006).
31. M. H. Alexander, *J. Chem. Phys.* **76**, 5974 (1982).
32. P. J. Knowles, C. Hampel, H.-J. Werner, *J. Chem. Phys.* **99**, 5219 (1993).
33. MOLPRO, version 2002.6, a package of ab initio programs, H. J. Werner, P. J. Knowles, R. Lindh, F. R. Manby, M. Schütz, and others, Cardiff, UK (www.molpro.net).
34. K. A. Peterson, D. Figgen, E. Goll, H. Stoll, M. Dolg, *J. Chem. Phys.* **119**, 11113 (2003).
35. G. Dhont, W. B. Zeimen, G. C. Groenenboom, A. van der Avoird, *J. Chem. Phys.* **120**, 103 (2004).
36. E. P. Wigner, *Phys. Rev.* **73**, 1002 (1948).
37. The validity of this assumption is verified by analytically modeling the detection probability in the limiting cases of forward, backward, and isotropic scattering. The difference is found to be within the error bars of our data.
38. G. C. Groenenboom, N. Balakrishnan, *J. Chem. Phys.* **118**, 7380 (2003).
39. T.-S. Ho, H. Rabitz, *J. Chem. Phys.* **104**, 2584 (1996).
40. This research is supported by the European Union Cold Molecules Network. We thank N. Vanhaecke for help preparing this experiment and D. W. Chandler for many fruitful discussions and for carefully reading the manuscript.

Supporting Online Material
www.sciencemag.org/cgi/content/full/313/5793/1617/DC1
Computer Codes

28 June 2006; accepted 7 August 2006
10.1126/science.1131867

Evidence for a Polar Ethane Cloud on Titan

C. A. Griffith,[1]* P. Penteado,[1] P. Rannou,[2] R. Brown,[1] V. Boudon,[3] K. H. Baines,[4] R. Clark,[5] P. Drossart,[6] B. Buratti,[4] P. Nicholson,[7] C. P. McKay,[8] A. Coustenis,[6] A. Negrao,[2,9] R. Jaumann[10]

Spectra from Cassini's Visual and Infrared Mapping Spectrometer reveal the presence of a vast tropospheric cloud on Titan at latitudes 51° to 68° north and all longitudes observed (10° to 190° west). The derived characteristics indicate that this cloud is composed of ethane and forms as a result of stratospheric subsidence and the particularly cool conditions near the moon's north pole. Preferential condensation of ethane, perhaps as ice, at Titan's poles during the winters may partially explain the lack of liquid ethane oceans on Titan's surface at middle and lower latitudes.

Past images of Saturn's largest moon, Titan, display large clouds only where solar heating is greatest, which presently occurs at high southern latitudes (*1*–*3*). The morphology of Titan's southern clouds indicates that they are convective, composed of methane, and result from the summer heating of Titan's surface and updrafts from Titan's summer Hadley cell (*1*, *4*–*6*). Similar processes instigate the formation of thunderstorms on Earth. The latent heat of Titan's major condensable constituent, methane, is large enough that, like water on Earth, adiabatic lifting and consequent cooling of air cause cloud formation (*7*). In contrast, at high northern latitudes, air circulates downward from the dry stratosphere (above an altitude of 40 km) and is heated through compression, which prevents the formation of methane clouds.

Spectral images of Titan's northern hemisphere, recorded by Cassini's Visual and Infrared Mapping Spectrometer (VIMS) (*8*), indicate a ubiquitous bright band at 51° to 68°N latitude, at the edge of Titan's arctic circle (Fig. 1). Its presence at higher latitudes cannot be determined because of a lack of illumination. The band appears at wavelengths that detect altitudes above 30 km (1.9, 2.13, and 2.7 to 2.9 μm) yet not at wavelengths that probe altitudes above 60 km (for example, at 1.67, 2.25, and 3.2 μm), indicating that particles near an altitude of 40 km are the cause (Fig. 2). Unlike Titan's southern clouds, this northern cloud shows no hourly variability and is diffusely spread over a large area, with only small continuous variations in optical depth between adjacent pixels (Fig. 1).

The cloud appears at latitudes where Titan's general circulation concentrates and transports photochemical products, principally ethane, to lower altitudes, where they condense and may form clouds (*6*). Methane (the second most abundant atmospheric constituent after nitrogen) is dissociated irreversibly by solar ultraviolet light, producing primarily ethane and, at one-sixth and one-10th of the ethane production rate, respectively, acetylene and haze, as well as other less abundant organic molecules (*9*, *10*). These photochemical by-products precipitate to Titan's surface. Titan's atmospheric composition and photochemical models indicate that ethane accumulates as a liquid (at the equatorial surface temperature of 93.5 K) at a rate of ~300 m (if global) over Titan's lifetime of 4.5 billion years, whereas solid sediments, including acetylene and haze particles, accumulate at roughly one-third of this rate (*10*). Thus, unless methane is a recent addition to Titan's atmosphere (*11*) or ethane incorporates itself into surface solids (*12*), it has been reasoned that a considerable fraction of the surface should be covered with liquid ethane (*13*). Titan's surface reveals dunes of solid sediments, probably including haze particles and acetylene ice (*14*). In addition, the surface is riddled with alluvial features (*15*–*17*), suggesting the occurrence of methane rain in the past. Craters are rare, indicating geological relaxation as well as their burial by photochemical sediments (*15*, *16*, *18*). Yet Titan appears depleted of its most abundant photochemical by-product. Except for the ethane-damp surface measured by Huygens (*19*), no condensed form of ethane has been detected (*20*), despite its rapid production in Titan's stratosphere and

[1]Lunar and Planetary Laboratory, University of Arizona, Tucson, AZ, 85721 USA. [2]Service d'Aéronomie, Université de Versailles-St-Quentin, BP3, 91371 Verriéres le Buisson, France. [3]Laboratoire de Physique de l'Université de Bourgogne, CNRS UMR 5027, Boîte Postale 47870, F-21078 Dijon, France. [4]Jet Propulsion Laboratory, California Institute of Technology, Pasadena, CA, 91109 USA. [5]U.S. Geological Survey, Denver, CO, 80225 USA. [6]Observatoire de Paris, 5 Place Jules Jannsen, Meudon, France. [7]Department of Astronomy, Cornell University, Ithaca, NY, USA. [8]National Aeronautics and Space Administration, Ames Research Center, Moffett Field, Mountain View, CA, USA. [9]Observatório Astronómico de Lisboa, 1349–018 Lisboa, Portugal. [10]Institute of Planetary Exploration, Deutsche Zentrum für Luft- und Raumfahrt, Germany.

the expectation of finding ethane-rich oceans before the Cassini encounter (*13*).

To determine the nature of Titan's northern cloud, whether it formed from methane or from the condensation of ethane and other photochemical by-products, we primarily analyzed the 2- to 2.5-μm, 2.8- to 3.2-μm, and 4.9- to 5.1-μm wavelength regions of VIMS' 0.88- to 5.11-μm spectra, which provide the clearest views down to the troposphere (*21*). The radiative transfer equation was solved with the discrete-ordinates approximation to simulate the absorption and scattering of Titan's atmosphere and surface (*22*). We first constrained the optical depths of the gases and haze above the clouds. We quantified methane absorption with line-by-line techniques (*5*) and new methane line parameters at 2.8 to 3.2 μm (*23*, *24*) and calculated pressure-induced H_2 and N_2 absorption using laboratory data (*25*). Real and imaginary indices of refraction of 1.35 and 0.0001, respectively, for ethane were assumed at both 2.1- and 2.9-μm wavelengths (*26*). We also assumed the presence of spherical haze particles having radii of 0.2 μm from altitudes of 180 to 90 km. Below 90 km, radii increase with atmospheric pressure to 0.8 μm at the altitude of 40 km (*5*). Analyses of the cloudless 2.1- to 2.2-μm spectra indicate a haze profile whose density decreases with altitude, with a scale height of 60 km above an altitude of 100 km; a particle density of 21 cm^{-3} at 130 km; and a constant density of 30 cm^{-3} from an altitude of 90 to 100 km, 9 cm^{-3} from 70 to 90 km, and 1 cm^{-3} from 30 to 70 km. Although other profiles also match the data, we can accurately estimate the haze optical depth above the cloud (0.16 at 2.1 μm), because it considerably exceeds the gas optical depth (0.05). A comparison of the calculations to the observed slope of Titan's 2.11- to 2.18-μm spectra provided the cloud heights (*5*). The 2.0-, 2.8-, and 5.0-μm albedos indicated the cloud optical depths. These values allowed us to estimate the size of the cloud particles (*5*) and their column mass, which provide clues to the formation and composition of Titan's northern cloud.

We analyzed the spectra lying within the 48° to 55°N latitude band that were farthest from the terminator and thus most directly illuminated by the Sun. The cloud was found to reside at altitudes of 30 to 50 km, with no trace of clouds above 60 km (Fig. 2), suggesting that we were not simply observing the low-altitude sedimentation of Titan's stratospheric hazes and condensates (*27*, *28*). At 55°N latitude, the cloud's optical depth was 0.06 ± 0.01 at both 2.1- and 2.9-μm wavelengths, assuming the optical constants of ethane. The error quoted above (0.01) refers to the 3σ standard deviation that results from noise. If the optical constants of haze are assumed, we derive optical depths

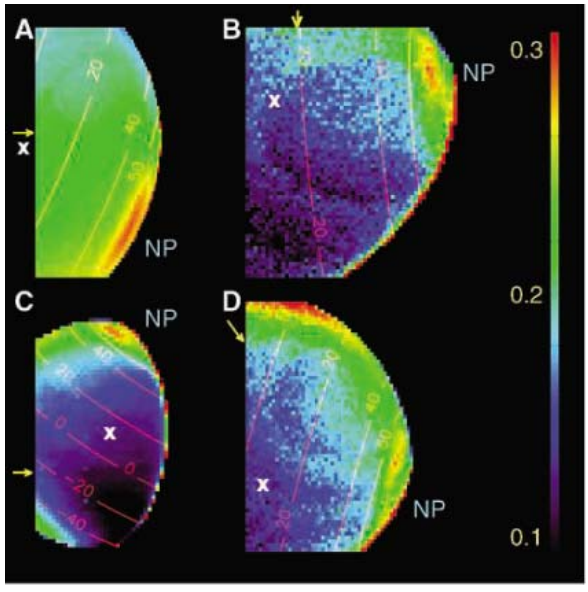

Fig. 1. Titan's 2.8-μm albedo, multiplied by the function $(\mu + \mu_o)/\mu_o^{0.3}$ (where μ_o and μ are the cosines of the illumination and emission angles), to lessen effects due to differences in illumination across the disk, indicates a cloud (red area) near 56°N. The cloud appears at all west longitudes observed: 115° to 190° (**A**), 10° to 118° [(**B**) and (**C**)], and 25° to 95° (**D**). Sunlight scattering off the limb (referred to as limb brightening) also appears red in (D). Titan's tilt prevents the illumination of latitudes exceeding 70°N. The pixel resolution (horizontal by vertical) is in the range from (50 to 95) by (50 to 150) km^2. Images were recorded at 6:26 universal time (UT) 13 December 2004 (A), 4:25 UT 22 August 2005 (B), 23:44 UT 21 August 2005 (C), and 2:55 UT 7 September 2005 (D). NP, direction of the north pole; x, subspacecraft point; yellow arrow, direction of solar illumination.

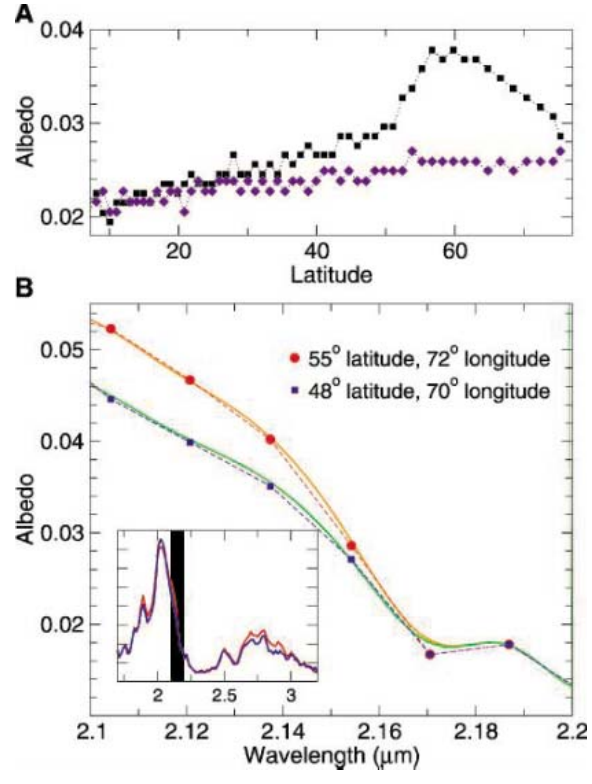

Fig. 2. (**A**) The change in Titan's albedo with latitude, made from a horizontal cut (at the 19th pixel row from the top) through the image in Fig. 1B at wavelengths of 2.11 μm (black squares) and 2.17 μm (purple diamonds), which probe the 30- to 50-km and 60- to 80-km altitude ranges, respectively. The cloud band appears north of 51°N latitude at 2.11 μm but not at 2.17 μm. (**B**) VIMS spectra recorded within (red circles) and outside of (blue squares) the bright cloud band (recorded at 23:04 UT 21 August 2005) are compared to calculated spectra that assume the absence of a cloud (green line) and the presence of a cloud at an altitude of 40 km of optical depth 0.02 (orange line). (**Inset**) The same observations shown over a larger wavelength region than that modeled in (B) (black rectangle) indicate increased brightness due to the cloud at wavelengths (1.9, 2.13, and 2.7 to 2.9 μm) that detect the tropopause. At 2 μm, the surface is visible and, for this pair of spectra, more highly reflective from cloudless terrain than cloudy terrain. The spectral resolution is 0.017 μm.

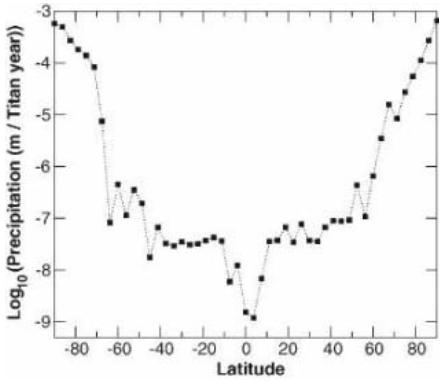

Fig. 3. The yearly average precipitation of ethane (dashed line) according to the GCM model of Rannou *et al.* (*6*). The downwelling circulation branch surrounding the poles during the winters causes ethane to descend from the stratosphere to the tropopause, where it condenses and precipitates to the surface. Consequently, ethane is predicted to accumulate in Titan's polar regions.

of 0.06 ± 0.01 at 2.1 μm and 0.12 ± 0.01 at 2.9 μm. Near 1.64 μm, VIMS spectra are corrupted because of a filter gap (*8*). The remaining spectral windows, 0.94, 1.08, and 1.28 μm, did not display albedo changes from the cloud, because the two-way optical depth to the cloud altitude exceeds unity, which is a result of the oblique solar illumination and the high scattering efficiency of the haze. We found that a cloud of optical depth 0.1 at 2.9 μm would be imperceptible at these lower wavelengths for particles larger than 1 μm. At 5 μm, Titan's haze scatters inefficiently, with an optical depth of less than 0.1. Yet no cloud signature was detected, indicating cloud optical depths smaller than 0.01. This constraint, taken together with the optical depths at 2.1 and 2.9 μm, indicates that the particle sizes were smaller than 3 μm. Thus, the effective radius of the cloud particles is 1 to 3 μm.

Titan's northern cloud consists of smaller particles than those composing the methane clouds in the south, whose radii exceed 10 μm. Particles with radii exceeding 50 μm are expected from methane condensation as a result of Titan's low density of nucleation sites, coupled with methane's high mixing ratio (*29*). The large southern particles suggest that in the north, where atmospheric conditions are similar, methane condensation similarly leads to particles with radii exceeding 50 μm. The small particle sizes thus suggest the condensation of a less abundant species.

Both the cloud's altitude and latitude agree with the predicted concentration of Titan's haze, which is expected to peak at an altitude of roughly 35 km poleward of ~60°N latitude, based on a recent general circulation model (GCM) (*6*). However, the optical constants of Titan's haze disagree with the cloud's spectral features. Haze particles are dark at 2.9 μm, unlike the observed cloud feature; consequently, two times more haze particles are needed to reproduce the cloud feature at 2.9 μm than at 2.1 μm, which is an unphysical result. The optical properties indicate that the cloud is not produced by a concentration of haze but rather by local condensation.

The characteristics of Titan's northern cloud are all consistent with the condensation of ethane. The cloud's 2.1- and 2.9-μm albedos can both be explained as resulting from a column of ~60,000 cm^{-2} of ethane particles having radii of 3 μm. The mass column abundance, $\sim 4 \times 10^{-6}$ g cm^{-2}, matches estimates at 60°N latitude from GCM models (*6*). The altitude of the cloud agrees with that expected for the winter subsidence of ethane, having a mixing ratio of $2.2 \pm 0.5 \times 10^{-5}$ at an altitude of ~150 km (*9*, *30*) and assuming the equatorial temperature profile (*6*, *31*). In addition, the particle sizes agree with those expected for high ethane condensates, given the abundance of ethane and the number density of nucleation sites (*6*, *32*). The unvarying nature of the cloud results from the slow vertical fall rate, which is 3 km per month for particles with radii of 2 μm (*32*).

The southern edge of Titan's cirrus cloud region occurs at the latitude north of which GCM models predict the descent of air from the stratosphere to the troposphere. Ethane, which is undersaturated at altitudes above ~65 km, descends to 30 to 50 km (where its mixing ratio exceeds saturation by a factor of several hundred) and condenses to form a cirrus cloud surrounding the pole. This explanation implies that we are observing the edge of a massive polar ethane cloud and the preferential condensation, sedimentation, and surface accumulation of ethane within 35° of Titan's poles (Fig. 3). Here, temperatures are expected to drop below the freezing point of pure ethane (90.3 K) during the winter and, depending on the haze opacity, possibly throughout most of Titan's year (*6*, *33*). If conditions remain cool enough throughout the year, Titan may accumulate ethane ice each winter at the poles and develop year-round polar caps.

An ethane cloud probably contains haze and other photochemically produced ices (such as acetylene), which condense mainly at altitudes of 65 to 90 km and mix downward to form part of the cirrus cloud (*27*, *28*). Additionally, methane and dissolved N_2 may condense on the ethane particles. Yet at the tropopause, methane is presently probably subsaturated because of the subsidence of air from the dry stratosphere (*6*). We detected no evidence for methane condensation resulting from meteorological methane fluctuations and temperature variations, which are spatially variable effects. The cloud is markedly uniform, without evident regions of methane-coated particles with radii exceeding 5 μm, which would have been detected in the 5-μm images, and without density variations resulting from the faster fall velocities of larger particles. Further investigations will better constrain the cloud composition, including Cassini VIMS measurements to be conducted during the close passes of the moon later in Titan's spring, when the north pole is better illuminated.

Presently, there is no direct evidence of polar caps composed of ethane. The northern pole has not been imaged. Cassini images of the southern pole do not indicate the morphology of 2 km of ethane ice, assuming current rates of ethane production over the past 4.5 billion years, accumulated within 35° of the poles. Yet south polar images suggest flow features, possibly associated with a smaller quantity of ethane ice accumulated on the young surface. The detection of surficial ethane ice is hindered by the correlation of ethane features and methane signatures, which obscure the visibility of Titan's surface. In addition, the polar surface is probably distinct and varied. Similarly, other hydrocarbons would precipitate preferentially at the poles and pollute the ethane ice, and any lowland methane lakes would dissolve and melt ethane, because the mixture's eutectic temperature is 72.5 K (*34*). Such lakes might condense out of Titan's humid lower troposphere during winter. The surface distribution of liquid or solid ethane, whether corralled into the polar regions by circulation or transported by surface flows to lower latitudes, will be determined with radar and near-infrared images of the geomorphology, radio determinations of the polar temperatures, and infrared measurements of the polar composition, which are scheduled for future Cassini encounters with Titan.

References and Notes

1. M. E. Brown, A. H. Bouchez, C. A. Griffith, *Nature* **420**, 795 (2002).
2. H. G. Roe, I. de Pater, B. A. Macintosh, C. P. McKay, *Astrophys. J.* **581**, 1399 (2002).
3. H. G. Roe, A. H. Bouchez, C. A. Trujillo, E. L. Schaller, M. E. Brown, *Astrophys. J.* **618**, L49 (2005).
4. C. A. Griffith, J. L. Hall, T. R. Geballe, *Science* **290**, 509 (2000).
5. C. A. Griffith *et al.*, *Science* **310**, 474 (2005).
6. P. Rannou, F. Montmessin, F. Hourdin, S. Lebonnois, *Science* **311**, 201 (2006).
7. J. E. McDonald, *J. Atmos. Sci.* **21**, 76 (1964).
8. R. Brown *et al.*, *Icarus* **164**, 461 (2003).
9. A. Coustenis, B. Bézard, *Icarus* **115**, 126 (1995).
10. Y. L. Yung, M. Allen, J. P. Pinto, *Astrophys. J. Suppl. Ser.* **55**, 465 (1984).
11. G. Tobie, J. I. Lunine, C. Sotin, *Nature* **440**, 61 (2006).
12. J. P. Osegovic, M. D. Max, *J. Geophys. Res.* **110**, 8004 (2005).
13. J. I. Lunine, D. J. Stevenson, Y. L. Yung, *Science* **222**, 1229 (1983).
14. R. Lorenz *et al.*, *Science* **312**, 724 (2006).
15. C. C. Porco *et al.*, *Nature* **434**, 159 (2005).
16. C. Elachi *et al.*, *Science* **308**, 970 (2005).
17. M. G. Tomasko *et al.*, *Nature* **438**, 765 (2005).
18. J. I. Lunine, N. Artemieva, R. Lorenz, E. Flamini, paper presented at the 36th Annual Lunar and Planetary Science Conference, League City, TX, 14 to 18 March 2005, abstract 1504.
19. H. B. Niemann *et al.*, *Nature* **438**, 779 (2005).
20. R. A. West, M. E. Brown, S. V. Salinas, A. H. Bouchez, H. G. Roe, *Nature* **436**, 670 (2005).
21. C. A. Griffith, T. Owen, T. R. Geballe, J. Rayner, P. Rannou, *Science* **300**, 628 (2003).
22. K. Stamnes, S. Tsay, K. Jayweera, W. Wiscombe, *Appl. Opt.* **27**, 2502 (1988).
23. V. Boudon, M. Rey, M. Loëte, *J. Quant. Spectrosc. Radiat. Transfer* **98**, 394 (2006).
24. L. S. Rothman *et al.*, *J. Quant. Spectrosc. Radiat. Transfer* **82**, 5 (2003).
25. A. R. W. McKellar, *Icarus* **80**, 361 (1989).
26. E. Quirico, B. Schmitt, *Icarus* **127**, 354 (1997).
27. R. D. Lorenz, E. F. Young, M. T. Lemmon, *Geophys. Res. Lett.* **28**, 4453 (2001).
28. L. A. Mayo, R. E. Samuelson, *Icarus* **176**, 316 (2005).
29. O. B. Toon, C. P. McKay, R. Courtin, T. P. Ackerman, *Icarus* **75**, 255 (1988).
30. F. M. Flasar *et al.*, *Science* **308**, 975 (2005).
31. M. Fulchignoni *et al.*, *Nature* **438**, 785 (2005).
32. E. L. Barth, O. B. Toon, *Icarus* **162**, 94 (2003).
33. T. Tokano, *Icarus* **173**, 222 (2005).
34. W. R. Thompson, J. C. G. Calado, J. A. Zollweg, in *Proceedings of the First International Conference on Laboratory Research for Planetary Atmospheres*, Bowie State University, Bowie, MD, 25 to 27 October 1989 (NASA Conference Publication 3077, 1990), pp. 303–326.

35. This research was funded by NASA's Planetary Atmosphere Program (C.A.G.), the Brazilian Government's Coordenação de Aperfeiçoamento de Pessoal de Nível Superior scholarship, the Cassini Mission (P.P.), and the Portuguese Fundação de Ciência e Tecnologia scholarship SFRH/BD/8006/2002 (A.N.).

3 April 2006; accepted 25 July 2006
10.1126/science.1128245

Early Reactivation of European Rivers During the Last Deglaciation

Guillemette Ménot,[1]* Edouard Bard,[1]* Frauke Rostek,[1] Johan W. H. Weijers,[2] Ellen C. Hopmans,[2] Stefan Schouten,[2] Jaap S. Sinninghe Damsté[2]

During the Last Glacial Maximum, the sea-level lowstand combined with the large extent of the Fennoscandian and British ice sheets led to the funneling of European continental runoff, resulting in the largest river system that ever drained the European continent. Here, we show an abrupt and early reactivation of the European hydrological cycle at the onset of the last deglaciation, leading to intense discharge of the Channel River into the Bay of Biscay. This freshwater influx, probably combined with inputs from proglacial or ice-dammed lakes, dramatically affected the hydrology of the region, both on land and in the ocean.

Despite the recognized sensitivity of oceanic circulation to changes in the freshwater budget at high latitudes (*1*–*4*), river runoff studies have so far mainly been focused on low-latitude paleorecords (*5*–*7*). Furthermore, except for a few continental archives such as speleothems and wetlands that reflect local conditions, little is known about hydrological and water drainage changes in Europe during the last deglaciation. During the Last Glacial Maximum (LGM), a large ice sheet (known as the Fennoscandian ice sheet) was established on the Eurasian continent. Both the sea-level lowstand and the extent of the ice sheet deeply influenced the drainage basins of European rivers that flowed into the Channel River, thus generating one of the largest rivers ever to have extended across the European continent (Fig. 1). Because this river transported much of the meltwaters coming from the European glaciers as well as from the Fennoscandian and British-Irish ice sheets (*8*, *9*), its runoff is expected to have reacted strongly to the retreat and growth of the Eurasian ice-sheets and of the alpine glaciers. Therefore, a record of the activity of this paleo-river could provide a detailed account of the effect of European deglaciation on the hydrological cycle.

Core MD952002 (47°27′N, 8°32′W, 2174-m water depth) was recovered on the northwestern slope of the Bay of Biscay in the direct axis of the English Channel during the IMAGES 101 cruise of the research vessel *Marion Dufresne* (Fig. 1). The chronology of this core is based on calibrated ^{14}C ages (*10*). This core covers a critical period including the last deglaciation, as well as abrupt climatic changes such as Heinrich events 1 and 2 (H1 and H2), which are clearly identified by two discrete peaks in the abundance of lithic grains and the magnetic susceptibility at 16 and 24 thousand years before the present (kyr B.P.) (Fig. 2B) (*11*). Total organic carbon (TOC) content varies between 0.2 and 1.2%, with minima during both H1 and H2 events (green circles in Fig. 2C). The $C_{37:4}$ alkenone, a biomarker derived from haptophyte algae and thought to be a proxy for low-salinity water associated with icebergs (*12*), is absent during the Holocene but exhibits high values between 11 and 18 kyr B.P., with a prominent maximum reached during H1, corresponding to 30% $C_{37:4}$ among the total of C_{37} alkenones (black diamonds in Fig. 2C). This is a characteristic feature for H1 in this area and has been related to the advection of low-salinity water associated with icebergs (*12*).

We applied the branched and isoprenoid tetraether (BIT) index to reconstruct terrestrial organic matter fluvially transported to the ocean (*13*). This proxy uses the relative abundance

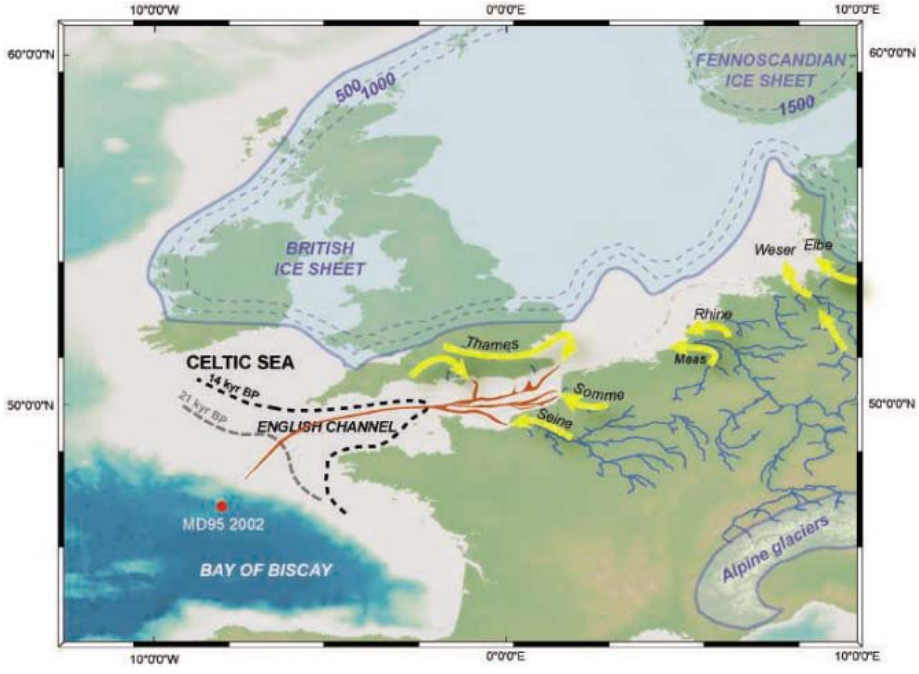

Fig. 1. The paleoenvironment of the LGM on the Eurasian continent was radically different from today. The Fennoscandian ice sheet was established on the northern part of Europe, extending west into the Norwegian Sea, south across the north German Plain into Poland, and eastward into North Poland and Russia (*27*, *28*). A smaller dome was installed on the British Isles (*27*). Recent geomorphological evidence indicates that the British-Irish ice sheet (BIS) and Fennoscandian ice sheet coalesced, and a huge ice dam extended over the present-day North Sea (*28*, *35*). The Alps were almost entirely covered by an ice dome formed by valley glaciers (*36*). The maximum extent of ice sheets at the LGM is illustrated by the blue contours. A final ice-age sea-level lowstand led to emersion of the channel between England and France, with the coastlines at 14 and 21 kyr B.P. illustrated by the dashed lines (after *31*). A paleo-river, known as the Channel River (in orange), extended across the emerged continental margin (*37*). It drained most of the major rivers in northwestern Europe, that is, the Rhine, Maas, Seine, Solent, and Thames (yellow arrows on the map). In addition to these rivers, the Irish Sea drained a large part of the BIS meltwaters (*32*). Furthermore, damming by the Fennoscandian ice sheet favored the development of southward-flowing meltwater valleys and ice-margin spillways running westward. These spillways collected proglacial waters from rivers even farther east than the Elbe basin and allowed drainage to the Channel River (*26*, *28*). Core MD952002 (red dot) was taken at a water depth of 2174 m in the axis of the English Channel, close to the LGM position of the Channel River outlet.

[1]CEREGE, Collège de France, UMR 6635, CNRS Université Aix-Marseille III, Europole de l'Arbois, BP 80, 13545 Aix-en-Provence, France. [2]Department of Marine Biogeochemistry and Toxicology, Royal Netherlands Institute for Sea Research (NIOZ), Post Office Box 59, 1790 AB Den Burg, Texel, Netherlands.

*To whom correspondence should be addressed. E-mail: gmenot@cerege.fr (G.M.); bard@cerege.fr (E.B.)

of membrane lipids (i.e., nonisoprenoid glycerol dialkyl glycerol tetraethers) (*14*) derived from anaerobic bacteria thriving in soils and peats (*15*), compared with crenarchaeol, a structurally related isoprenoid molecule characteristic of ubiquitous marine planktonic and lacustrine crenarchaeota (*16*). BIT values for suspended particulate matter in river waters are typically >0.9 (*17*). A survey of Holocene sediments showed that the BIT index can be directly correlated to the relative amount of fluvial terrestrial organic matter input. BIT-index values of <0.1 are typical for open marine settings receiving only small amounts of terrestrial organic matter, whereas values >0.4 are typical for river fans and fjord systems (*13*). The BIT-index values throughout the core MD952002 remain below 0.1, except for two well-defined peaks with values as high as 0.7 centered at 19.5 kyr B.P. and between 19 and 17 kyr B.P. (red circles in Fig. 2E). The two maxima in the BIT-index profile, therefore, reveal periods during which large amounts of terrestrial organic matter must have been transported to this site in the Bay of Biscay. These maxima are consistent with those obtained from the abundance of remains of freshwater algae (*Pediastrum sp.*) (blue curve on Fig. 2D) (*11*). The total organic carbon-to-nitrogen ratio (C/N) varies between 5 and 30, with minimum values typical of the marine environment end-member during H1 and H2 events, and higher values in the intervening period, also indicative of a larger terrestrial contribution (Fig. 2C).

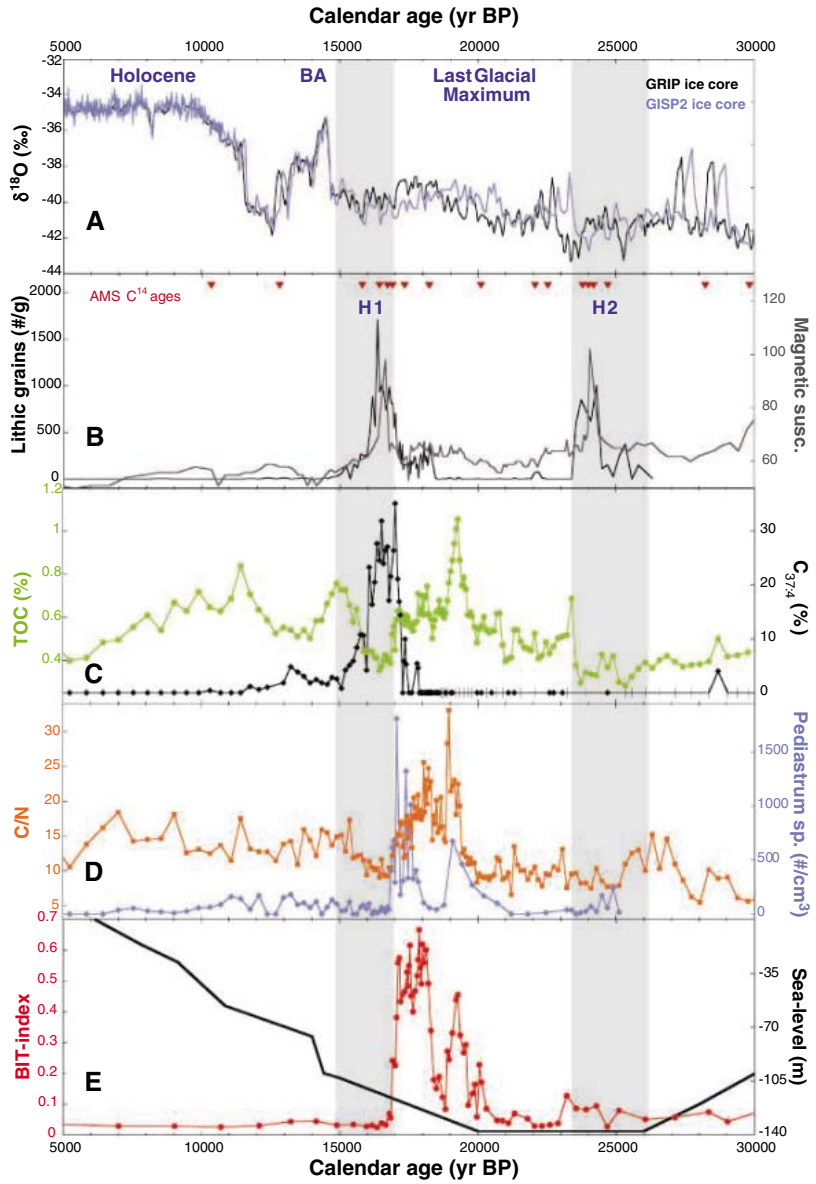

Fig. 2. Deglaciation-Holocene records of the past activity of the Channel River as a function of paleoclimatic changes. The chronology is based on calibrated ^{14}C ages measured on planktonic foraminifera [shown as triangles in (B)] (*10*). Climatic events are abbreviated as follows: B-A, Bølling-Allerød; H1, Heinrich 1; and H2, Heinrich 2. The gray areas underline the H1 and H2 events. (**A**) $\delta^{18}O$ GRIP (black line) (*38*) and $\delta^{18}O$ GISP2 (light blue line) (*39*) records reflecting Greenland air temperatures. (**B**) Black line shows the counting of grains identified as ice-rafted debris (IRD) per 10 g for the size fraction coarser than 150 μm, and the gray curve shows the magnetic susceptibility (MS) record measured on board *Marion Dufresne* (*40*). (**C**) Green circles represent the total organic carbon contents, and the black diamonds the percentage of $C_{37:4}$ among C_{37} alkenones, i.e., $\%C_{37:4} = 100 \times [C_{37:4}]/[C_{37:2} + C_{37:3} + C_{37:4}]$. Beyond 19 kyr B.P., the relative percentage of $C_{37:4}$ could not be quantified because alkenones are very scarce in the sediments corresponding to the last glacial period (black ticks in Fig. 2C and italics in table S1). (**D**) Orange squares indicate the total organic carbon-to-nitrogen ratios (C/N), and the blue symbols show the abundance of freshwater algae, *Pediastrum sp.* [counts from (*11*)]. (**E**) The BIT index, which is defined as follows: BIT = (I + II + III)/[(I + II + III) + (IV)] [the roman numbers refer to the glycerol dialkyl glycerol tetraethers in figure 1 of (*13*)], and is represented here by red dots. The black curve shows the sea-level curve (*41*). Analytical data for core MD952002 are given in table S1.

During H2 and the LGM, cold and dry conditions prevailed on the European continent (*18*). At that time, ice sheets reached their maximum extent (Fig. 1), and sedimentation at the Channel River outlet was typical of a marine environment with low values of the BIT index and TOC as well as low C/N ratios (Fig. 2, C to E). At the end of the LGM, between 21 and 17 kyr B.P., an early warming is observed in the Greenland air-temperature record (Fig. 2A). This temperature increase is also clearly detected in several North Atlantic records (e.g., *12*, *19*–*21*) as well as in continental reconstructions inferred from pollen in lacustrine and peat sequences over Europe (e.g., *22*, *23*). This warming was accompanied by enhanced precipitation, as is also evident from the pollen assemblages. Despite this climatic warming, soils remained partly frozen and hence impermeable (*24*). Furthermore, the vegetation cover was scarce and spatially discontinuous, mainly composed of peat with only few woody species (*25*). This situation led to the development of large fluvial systems, intense soil erosion, and enhanced river discharge. This transient period is coincident with an abrupt maximum in the BIT index in core MD952002 (Fig. 2), indicative of an early and drastic reactivation of European rivers.

Associated with this reactivation of the hydrological cycle, meltwaters might well have played a role in the runoff increase. In fact, when the Fennoscandian ice sheet started to retreat from its maximum position

at ~22 kyr B.P., a new series of short-lived glacial lakes formed at its southern margin, more particularly in the Polish basins and German lowlands (*26*, *27*). Because of the position of the ice margin, the meltwaters first drained through the southern Peribaltic area toward central Poland, to the Elbe River, and then to the Channel River (*28*). The retreat was not continuous, and readvances of the Fennoscandian ice sheet have been recognized based on geomorphological and lithostratigraphic evidences as well as by cosmonuclide and thermoluminescence dating (*26*, *27*). Two major deglaciation phases have been reported in Poland during the low sea-level stand: the Poznan and the Pomeranian phases at 22.0 and 18.6 kyr B.P., respectively (*26*). Similar pulsations have been described for the British-Irish ice sheet over the same period (*27*). On the southeastern sector, the Scandinavian ice sheet begins to retreat around 19 kyr B.P. after a phase of maximum extent at 20.9 kyr B.P. (*29*). A massive and early breakdown of the LGM system of ice domes in the Alps is reported to occur simultaneously (e.g., *30*).

A peculiar geographic setting reinforced the effect of this increased water runoff from the European continent, leading to increased discharge of the River Channel into the Bay of Biscay. In fact, the low sea level during the LGM (Fig. 2E) means that the river mouth was located very close to the core location [the dashed line in Fig. 1 represents the paleocoastline at 21 kyr B.P., reconstructed after (*31*)]. Moreover, due to the topography of the catchment basin, the Channel River drained a large area with inputs from the Rhine, Seine, Maas, and Thames basins (*9*). This topographic funneling effect was reinforced by the location of the British-Irish ice sheet, which reached its maximum extent at 16.7 kyr B.P. (*32*). A simultaneous readvance of the Scandinavian ice sheet is recorded on the southeastern sector (*29*).

The onset of the H1 event, at 17 kyr B.P., is characterized by the sudden drop in the BIT index (Fig. 2E). As already observed for Heinrich events (*19*), the biological productivity is low, but the BIT index indicates a predominant marine origin for the sedimentary organic matter (Fig. 2). Consistently, the C/N record exhibits a clear minimum over this time interval. Furthermore, a prominent $C_{37:4}$-alkenone peak is synchronous with the maximum abundance in lithic grains. A similar maximum of $C_{37:4}$ linked to H1 has already been described at other sites (*33*, *12*). The fall in BIT index is clearly simultaneous with the rise in lithic grain abundance and percentage of $C_{37:4}$ alkenone, indicating that this switch was probably due to the impact on marine hydrology of icebergs coming from the Fennoscandian and Laurentide ice sheets (*34*). In parallel, the return to dry and cold conditions on the continent during H1 probably led to a regime with less fluvial runoff.

There was no recurrence of high BIT-index values when warmer and wetter conditions returned during the Bølling-Allerød and the Holocene period (Fig. 2E). This is probably due to the sea-level rise of about 60 m compared with the LGM lowstand, which caused a northward displacement of the river mouth by about 300 km and thus a more attenuated influence of the Channel River at the core site (Fig. 1). Furthermore, due to the position of the Fennoscandian ice margins during the Bølling-Allerød, the meltwaters of the Peribaltic area drained into the southern part of the Baltic Basin and no longer through Poland and the Elbe Basin (*28*).

The abrupt runoff event that occurred at the onset of the last deglaciation on the European continent is unique in magnitude and timing and reflects an early reactivation of the European hydrological cycle leading to an intense discharge of terrestrial organic matter on the Celtic Margin and Bay of Biscay. The intensity of this event is due to a peculiar combination of topographic and paleoclimatic factors: The large extent of the Fennoscandian and British ice sheets, which coalesced over the North Sea, forced the drainage of rivers into the Channel River, thus creating one of the largest river systems ever existing on the European continent. The reactivation of European river runoff has also probably been fuelled by proglacial lakes developing at the southern margin of the ice sheets. Indeed, high abundances of remains of freshwater algae are found simultaneous with the large increase in BIT index (Fig. 2). Interestingly, although the freshening of the surface waters starting at 21.5 kyr B.P. is progressive and parallel to the temperature increase after the LGM, the return to fully marine conditions is sharp and occurs in about a century at the start of the H1 event. As a result of sea-level rise, after 17 kyr B.P., conditions never became suitable again for recording events of the Channel River of such a magnitude in the Bay of Biscay.

Our results reveal large changes in the magnitude of the discharge of cold freshwater into the North Atlantic during the last deglaciation. This situation is similar to that reconstructed for the Laurentide ice sheet, meltwater outflow which probably affected the meridional overturning circulation (*1*, *3*). Modeling experiments could help to evaluate the effect of the European river reactivation on the millennium-scale climatic events that punctuated the last deglaciation.

References and Notes

1. W. S. Broecker *et al.*, *Nature* **341**, 318 (1989).
2. T. F. Stocker, D. G. Wright, *Nature* **351**, 729 (1991).
3. S. Manabe, R. J. Stouffer, *Paleoceanography* **12**, 321 (1997).
4. A. Ganopolski, S. Rahmstorf, *Nature* **409**, 153 (2001).
5. A. T. Adegbie, R. R. Schneider, U. Rohl, G. Wefer, *Palaeogeogr. Palaeoclimatol. Palaeoecol.* **197**, 323 (2003).
6. T. C. Jennerjahn *et al.*, *Science* **306**, 2236 (2004).
7. E. Schefuß, S. Schouten, R. R. Schneider, *Nature* **437**, 1003 (2005).
8. J. D. Scourse, I. R. Hall, I. N. McCave, J. R. Young, C. Sugdon, *Earth Planet. Sci. Lett.* **182**, 187 (2000).
9. P. Antoine *et al.*, *J. Quat. Sci.* **18**, 227 (2003).
10. Methods are available as supporting material on *Science* Online.
11. S. Zaragosi *et al.*, *Earth Planet. Sci. Lett.* **188**, 493 (2001).
12. E. Bard, F. Rostek, J.-L. Turon, S. Gendreau, *Science* **289**, 1321 (2000).
13. E. C. Hopmans *et al.*, *Earth Planet. Sci. Lett.* **224**, 107 (2004).
14. J. S. Sinninghe Damsté, E. C. Hopmans, R. Pancost, S. Schouten, J. A. J. Geenevasen, *J. Chem. Soc. Chem. Commun.* **2000**, 1683 (2000).
15. J. W. H. Weijers *et al.*, *Environ. Microbiol.* **8**, 648 (2006).
16. J. S. Sinninghe Damsté, E. C. Hopmans, S. Schouten, A. C. T. van Duin, J. A. J. Geenevasen, *J. Lipid Res.* **43**, 1641 (2002).
17. L. Herfort *et al.*, *Limnol. Oceanogr.* **51**, 2196 (2006).
18. J. R. Allen *et al.*, *Nature* **400**, 740 (1999).
19. D. Pailler, E. Bard, *Palaeogeogr. Palaeoclimatol. Palaeoecol.* **181**, 431 (2002).
20. G. A. Jones, L. D. Keigwin, *Nature* **336**, 56 (1988).
21. R. B. Alley, E. J. Brook, S. Anandakrishnanc, *Quat. Sci. Rev.* **21**, 431 (2002).
22. M. F. Sanchez Goñi, J. L. Turon, F. Eynaud, S. Gendreau, *Quat. Res.* **54**, 394 (2000).
23. J. L. Combourieu Nebout *et al.*, *Geology* **30**, 863 (2002).
24. H. Renssen, J. Vandenberghe, *Quat. Sci. Rev.* **22**, 209 (2003).
25. P. C. Tzedakis, I. T. Lawson, M. R. Frogley, G. M. Hewitt, R. C. Preece, *Science* **297**, 2044 (2002).
26. L. Marks, *Quat. Sci. Rev.* **21**, 103 (2002).
27. D. Q. Bowen, F. M. Phillips, A. M. McCabe, P. C. Knutz, G. A. Sykes, *Quat. Sci. Rev.* **21**, 89 (2002).
28. J. Mangerud *et al.*, *Quat. Sci. Rev.* **23**, 1313 (2004).
29. V. R. Rinterknecht *et al.*, *Science* **311**, 1449 (2006).
30. S. Ivy-Ochs, H. Kerschner, P. W. Kubik, Ch. Schlüchter, *J. Quat. Sci* **21**, 115 (2006).
31. K. Lambeck, *Palaeogeogr. Palaeoclimatol. Palaeoecol.* **129**, 1 (1997).
32. A. M. McCabe, P. U. Clark, *Nature* **392**, 373 (1998).
33. A. Rosell-Melé, *Paleoceanography* **13**, 694 (1998).
34. F. E. Grousset, C. Pujol, L. Labeyrie, G. Auffret, A. Boelaert, *Geology* **28**, 123 (2000).
35. J. Svendsen *et al.*, *Quat. Sci. Rev.* **23**, 1229 (2004).
36. G. H. Denton, T. J. Hughes, Eds., The Last Great Ice Sheets (Wiley, New York, 1981).
37. J.-F. Bourillet, J.-Y. Reynaud, A. Baltzer, S. Zaragosi, *J. Quat. Sci.* **18**, 261 (2003).
38. S. J. Johnsen *et al.*, *J. Quat. Sci.* **16**, 299 (2001).
39. M. Stuiver, P. M. Grootes, *Quat. Res.* **53**, 277 (2000).
40. G. Auffret *et al.*, *Mar. Geol.* **188**, 79 (2002).
41. K. Lambeck, Y. Yokoyama, T. Purcell, *Quat. Sci. Rev.* **21**, 343 (2002).

42. We thank S. Zaragosi and F. Eynaud for useful discussions. Paleoclimate work at CEREGE is supported by grants to E.B. from the CNRS, the ANR, the Gary Comer Science and Education Foundation, and the European Community (project STOPFEN, HPRN-CT-2002-0221). The work at NIOZ was supported by grants to E.C.H. and J.S.S.D. from the Netherlands Organisation for Scientific Research (NWO).

Supporting Online Material

www.sciencemag.org/cgi/content/full/313/5793/1623/DC1
Methods
Table S1

26 May 2006; accepted 28 July 2006
10.1126/science.1130511

High Gamma Power Is Phase-Locked to Theta Oscillations in Human Neocortex

R. T. Canolty,[1*] E. Edwards,[1,2] S. S. Dalal,[3] M. Soltani,[1,2] S. S. Nagarajan,[3,4] H. E. Kirsch,[5] M. S. Berger,[6] N. M. Barbaro,[5,6] R. T. Knight[1,2,3,5,6]

We observed robust coupling between the high- and low-frequency bands of ongoing electrical activity in the human brain. In particular, the phase of the low-frequency theta (4 to 8 hertz) rhythm modulates power in the high gamma (80 to 150 hertz) band of the electrocorticogram, with stronger modulation occurring at higher theta amplitudes. Furthermore, different behavioral tasks evoke distinct patterns of theta/high gamma coupling across the cortex. The results indicate that transient coupling between low- and high-frequency brain rhythms coordinates activity in distributed cortical areas, providing a mechanism for effective communication during cognitive processing in humans.

Neuronal oscillations facilitate synaptic plasticity (*1*), influence reaction time (*2*), correlate with attention (*3*) and perceptual binding (*4*), and are proposed to play a role in transient, long-range coordination of distinct brain regions (*5*). Direct cortical recordings reveal that ongoing rhythms encompass a wide range of spatial and temporal scales—ultraslow rhythms less than 0.05 Hz coexist with fast transient oscillations 500 Hz or greater (*1*), with spatial coherence between these oscillations extending from several centimeters for the corticospinal tract (*6*) to the micrometer scale for subthreshold membrane oscillations in a single neuron (*7*). Exactly how these transient oscillations influence each other and coordinate processing at both the single-neuron and population levels remains unknown.

Evidence for cross-frequency coupling, where one frequency band modulates the activity of a different frequency band, is more abundant in animal than human data. For example, the theta rhythm can modulate the firing rate and spike timing of a single neuron (*8*–*11*) as well as the gamma power of the intracortical local field potential (*8*, *12*, *13*). Task-related changes in theta power have been observed in humans (*14*–*16*), and cross-frequency coupling at frequencies up to 40 Hz has been detected at the scalp (*17*, *18*). However, given the difficulty in localizing electrical sources from scalp recordings alone (*19*), subdural electrodes that record directly from the human cortex are needed to address this question. Furthermore, subdural electrodes are ideal for studying activity in the recently described human high gamma band (HG) at 80 to 150 Hz. HG activity is modulated by sensory, motor, and cognitive events (*20*), is functionally distinct from low gamma (30 to 80 Hz) with different physiological origins (*21*), and is correlated with the functional magnetic resonance imaging blood oxygen level–dependent (fMRI BOLD) signal (*22*–*24*). There have been no reports of coupling between any low-frequency rhythm and HG in signals recorded either at the scalp or directly from human sensory, motor, or association cortex. We therefore focus exclusively on theta/HG coupling in this report.

We analyzed multichannel subdural electrocorticogram (ECoG) data from five patients undergoing neurosurgical treatment for epilepsy. Typically, the events of interest in behavioral paradigms are the stimulus onsets and motor responses that evoke frequency-specific changes in the electrical activity of the brain. In contrast, the events of interest in cross-frequency coupling are features of the ongoing oscillatory activity itself. That is, cross-frequency coupling refers to statistical dependence between distinct frequency bands of the ongoing ECoG rather than dependence between the ECoG and external stimulus events. The dependence between two frequencies f_1 and f_2 can assume many forms, including coupling between the amplitude envelopes $A_1(t)$ and $A_2(t)$, the phase time series $\phi_1(t)$ and $\phi_2(t)$, or an amplitude-phase coupling between $A_1(t)$ and $\phi_2(t)$. We focus here on the last type of coupling and use an index of cross-frequency coupling that directly combines the amplitude envelope time series $A_1(t + \tau)$ of a high-frequency band with the phase time series $\phi_2(t)$ of a low-frequency band into one composite, complex-valued signal $z(t, \tau)$. The (normalized) temporal mean of this composite signal provides a sensitive measure of the coupling strength and preferred phase between the two frequencies (*25*).

Animal evidence for theta phase modulation of single-unit firing and the strong connection of theta to learning, attention, and memory (*26*, *27*) suggested to us that high-frequency oscillations in human neocortex may be modulated by the theta rhythm. Accordingly, we analyzed the ECoG across a range of behavior-

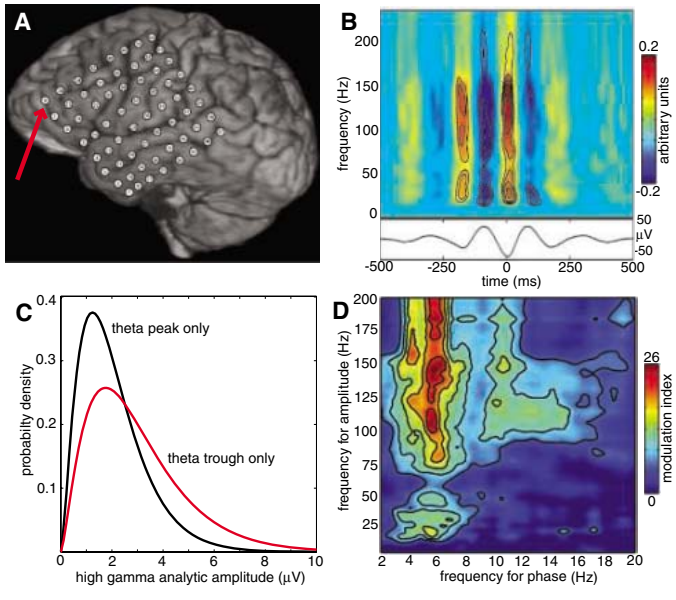

Fig. 1. High gamma (80 to 150 Hz) power is modulated by theta (4 to 8 Hz) phase. (**A**) Structural MRI showing position of 64-channel ECoG grid over frontal and temporal lobes in subject 1. (**B**) Example of phase-locked modulation of power in the ECoG signal from an electrode over the anterior portion of the middle frontal gyrus (arrow in Fig. 1A). (Top) Time-frequency plot of mean power modulation time-locked to the theta trough. Outermost contour indicates statistical significance ($P < 0.001$, corrected). Normalization permits comparison across frequencies; red and blue indicate a power increase or decrease, respectively, relative to the mean power. (Bottom) Theta trough–locked average of raw ECoG signal. (**C**) Best-fit gamma distributions for the high gamma analytic amplitude values that occurred at the peak (black, 0 radians) or the trough (red, π radians) of the theta waveform for the same electrode as in Fig. 1B. The difference in parameter values is significant ($P < 0.001$). (**D**) The modulation index (*25*) as a function of analytic amplitude (5 to 200 Hz) and analytic phase (2 to 20 Hz) for the same electrode as in Fig. 1B. Outermost contour indicates statistical significance ($P < 0.001$, corrected). Larger values indicate stronger cross-frequency coupling. Maximal coupling for this electrode is 146.2 Hz amplitude and 5.6 Hz phase (see also fig. S4).

[1]Helen Wills Neuroscience Institute, [2]Department of Psychology, University of California, Berkeley, CA 94720, USA. [3]Department of Bioengineering, [4]Department of Radiology, [5]Department of Neurology, [6]Department of Neurosurgery, University of California, San Francisco, CA 94143, USA.

*To whom correspondence should be addressed. E-mail: rcanolty@berkeley.edu

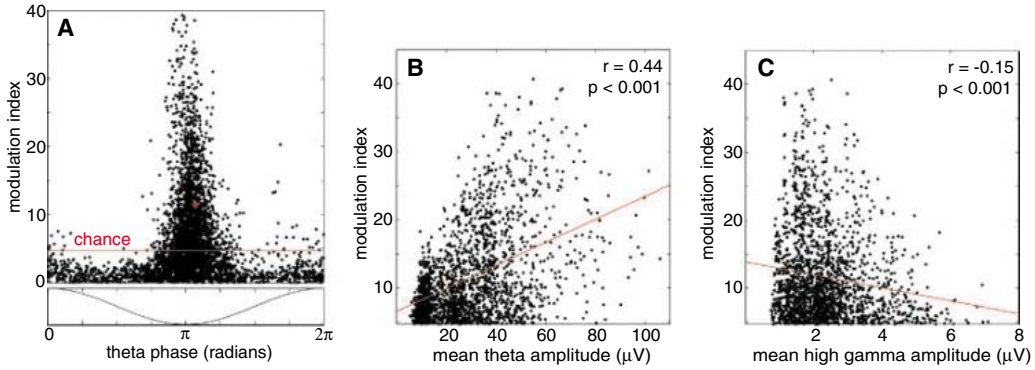

Fig. 2. Theta/HG coupling strength is a function of theta amplitude. (**A**) Theta/HG coupling strength and preferred theta phase. (Bottom) One theta cycle (schematic), from theta peak (0 radians) to trough (π radians) to peak (2π radians). (Top) Modulation index (*25*) computed separately for all electrodes in all subjects for each task. Larger magnitudes indicate stronger coupling (vertical axis), whereas the horizontal axis indicates the theta phase at which larger HG amplitudes tend to occur. Most electrodes with strong theta/HG coupling have a preferred theta phase of π, corresponding to the theta trough (see also Fig. 1C). The red dot indicates the electrode and recording block examined in Fig. 1. The red horizontal line corresponds to the significance threshold after correction for multiple comparisons. (**B**) Modulation index versus mean theta amplitude for all significant values from Fig. 2A (black dots) and best linear fit (red line), indicating their positive correlation. (**C**) Modulation index versus mean HG amplitude for all significant values from Fig. 2A (black dots) and best linear fit (red line), indicating their weak negative correlation (see also fig. S6).

al tasks (*25*). Figure 1B shows a time-frequency plot for data recorded from an electrode over the left middle frontal gyrus during an auditory language–related target detection task (Fig. 1A, arrow). Theta trough–locked averaging of the normalized time-frequency plane shows significant coupling ($P < 0.001$, corrected) between theta phase and high-frequency power, with an increase or decrease in power relative to baseline occurring at the theta trough or peak. Theta coupling was broadband from ~20 to 200 Hz, with the strongest modulation occurring in the HG band. Fig. 1D and fig. S4, using the modulation index discussed above, also show that coupling is strongest between theta phase and HG amplitude.

Across all tasks and subjects, 252 out of 299 tested electrodes (84.3%) showed significant theta/gamma coupling ($P < 0.001$ for each electrode, corrected). Excluding the 60 electrodes over resected tissue (which includes both epileptic and healthy tissue) increases this percentage to 88.7%, whereas only 66.7% of electrodes over resected tissue showed significant coupling. The largest HG amplitudes tended to occur at the trough of the theta waveform in electrodes with strong coupling (Figs. 1C and 2A). The coupling strength between the HG analytic amplitude time series $A_{HG}(t + \tau)$ and theta analytic phase $\phi_{TH}(t)$ should decrease to chance levels as the magnitude of the time lag τ increases. Figure 3A, displaying all ECoG electrodes for one subject, shows that this is indeed the case (see fig. S8 for all subjects).

The strength of theta/HG coupling depends on theta power as well as theta phase. We observed stronger coupling in electrodes with greater mean theta amplitude (Fig. 2B). That is, HG amplitudes have a stronger theta phase preference at greater theta power, indicating that theta/HG coupling strength can be modulated by adjusting theta power in a local cortical region. This contrasts with the weak negative correlation observed between theta/HG coupling strength and mean HG amplitude (Fig. 2C and fig. S6).

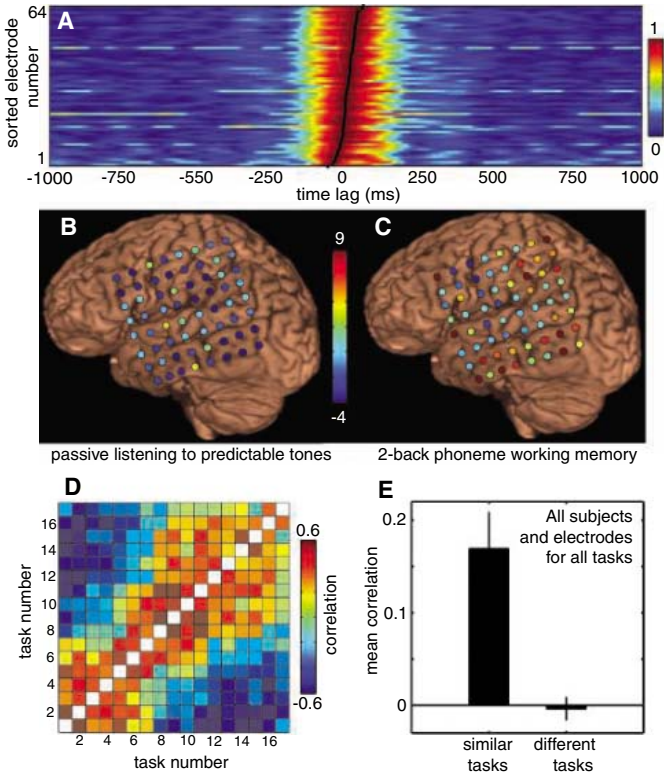

Fig. 3. Task-specific changes in the spatial pattern of theta/HG coupling strength. (**A**) Theta/HG coupling strength falls to chance at large time lags. Modulation index (*25*) as a function of lag for all electrodes over all tasks from subject 5. Electrodes are sorted by the time-lag τ_{max} associated with maximal coupling (black line). For ease of comparison, horizontal traces were renormalized so that the peak value for each channel is one (see also fig. S8). (**B**) The change in modulation index values from the mean for all electrodes in subject 2 during one task (passive listening to predictable tones). (**C**) As in (B), for a difficult working memory task. Subjects listened to a list of phonemes and responded when the current phoneme and the phoneme presented two items earlier were identical. (**D**) Similar tasks evoke similar spatial patterns of theta/HG coupling. Correlation matrix for all tasks in subject 2. Tasks: 1 to 4, passive listening to tones or phonemes; 5, mouth motor activation; 6, verb generation; 7, hand motor activation; 8 to 11 auditory working memory; 12 and 13, linguistic target detection; 14 to 17, auditory-vibrotactile target detection (see SOM text). (**E**) Mean correlation and standard error between similar tasks (positive, $P < 0.01$, corrected, 58 task pairs) as well as different tasks (not significant, 617 task pairs) for all electrodes in all subjects over all tasks.

Thus, mean HG power and the strength of theta/HG coupling appear to reflect independent dimensions of cortical activity.

Task-dependent modulation of theta power has been shown in humans (*26*), prompting the hypothesis that theta/HG coupling may be task-dependent. Two examples of task-specific changes in the spatial pattern of theta/HG coupling strength over all electrodes in one subject are shown in Fig. 3, B and C. Figure 3D shows that behavioral tasks evoke distinct and reproducible patterns of coupling in this subject, with similar tasks evoking similar coupling patterns whereas different tasks evoked alternate patterns. Spatial patterns associated with two runs of similar tasks were positively correlated, whereas runs

of different tasks exhibited a null or negative correlation. This trend held across all tasks and subjects, as shown by Fig. 3E. These results are consistent with the hypothesis that transient cross-frequency coupling modulates network engagement, enabling flexible control of cognitive processing.

Oscillations are rhythmic fluctuations in neuronal excitability that modulate both output spike timing and sensitivity to synaptic input (*5*). Therefore, effective communication between neuronal populations requires precise matching of the relative phase of distinct rhythms to axonal conduction delays. An oscillatory hierarchy operating across multiple spatial and temporal scales could regulate this proposed long-range communication (*13*). Basal forebrain cortical-projecting GABAergic (γ-aminobutyric acid–releasing) neurons are well positioned to control theta/HG coupling; these neurons preferentially synapse onto intracortical GABAergic neurons throughout the cortex, with disinhibitory spike bursts causing a brief increase in gamma power at the theta trough (*28*). Our observations that (i) HG power is modulated by theta phase, (ii) an increase in theta power strengthens theta/HG coupling, and (iii) the topography of theta/HG coupling is task-dependent support the hypothesis that cross-frequency coupling between distinct brain rhythms facilitates the transient coordination of cortical areas required for adaptive behavior in humans.

References and Notes

1. G. Buzsaki, A. Draguhn, *Science* **304**, 1926 (2004).
2. K. Linkenkaer-Hansen, V. V. Nikulin, S. Palva, R. J. Ilmoniemi, J. M. Palva, *J. Neurosci.* **24**, 10186 (2004).
3. T. Womelsdorf, P. Fries, P. P. Mitra, R. Desimone, *Nature* **439**, 733 (2006).
4. J. P. Lachaux *et al.*, *Neuroimage* **25**, 491 (2005).
5. P. Fries, *Trends Cogn. Sci.* **9**, 474 (2005).
6. J. M. Schoffelen, R. Oostenveld, P. Fries, *Science* **308**, 111 (2005).
7. E. M. Izhikevich, *Neural Netw.* **14**, 883 (2001).
8. A. Bragin *et al.*, *J. Neurosci.* **15**, 47 (1995).
9. G. Buzsaki *et al.*, *Neuroscience* **116**, 201 (2003).
10. A. G. Siapas, E. V. Lubenov, M. A. Wilson, *Neuron* **46**, 141 (2005).
11. H. Lee, G. V. Simpson, N. K. Logothetis, G. Rainer, *Neuron* **45**, 147 (2005).
12. J. J. Chrobak, G. Buzsaki, *J. Neurosci.* **18**, 388 (1998).
13. P. Lakatos *et al.*, *J. Neurophysiol.* **94**, 1904 (2005).
14. A. D. Ekstrom *et al.*, *Hippocampus* **15**, 881 (2005).
15. P. B. Sederberg, M. J. Kahana, M. W. Howard, E. J. Donner, J. R. Madsen, *J. Neurosci.* **23**, 10809 (2003).
16. J. Onton, A. Delorme, S. Makeig, *Neuroimage* **27**, 341 (2005).
17. B. Schack, N. Vath, H. Petsche, H. G. Geissler, E. Moller, *Int. J. Psychophysiol.* **44**, 143 (2002).
18. J. M. Palva, S. Palva, K. Kaila, *J. Neurosci.* **25**, 3962 (2005).
19. P. L. Nunez, R. S. Srinivasan, *Electric Fields of the Brain: The Neurophysics of EEG* (Oxford Univ. Press, Oxford, 2005).
20. N. E. Crone, D. L. Miglioretti, B. Gordon, R. P. Lesser, *Brain* **121**, 2301 (1998).
21. E. Edwards, M. Soltani, L. Y. Deouell, M. S. Berger, R. T. Knight, *J. Neurophysiol.* **94**, 4269 (2005).
22. N. K. Logothetis, J. Pauls, M. Augath, T. Trinath, A. Oeltermann, *Nature* **412**, 150 (2001).
23. R. Mukamel *et al.*, *Science* **309**, 951 (2005).
24. J. Niessing *et al.*, *Science* **309**, 948 (2005).
25. Materials and methods are available as supporting material on *Science* Online.
26. M. J. Kahana, D. Seelig, J. R. Madsen, *Curr. Opin. Neurobiol.* **11**, 739 (2001).
27. R. Miller, *Cortico-Hippocampal Interplay and the Representation of Contexts in the Brain* (Springer-Verlag, New York, 1991).
28. S. C. Lin, D. Gervasoni, M. A. L. Nicolelis, *J. Neurophysiol.* (2006); doi: 10.1152/jn.00524.2006.

29. This work was supported by the Rauch family, National Institute of Neurological Disorders and Stroke grant NS21135, NSF Fellowship 2004016118, and National Institute on Deafness and Other Communication Disorders grant F31DC006762. The authors thank P. Garcia and D. Filippi of the Department of Neurology, University of California San Francisco, for their help on electrical stimulation mapping and localizing epileptic tissue.

Supporting Online Material

www.sciencemag.org/cgi/content/full/313/5793/1626/DC1
Materials and Methods
SOM Text
Figs. S1 to S8

30 March 2006; accepted 20 July 2006
10.1126/science.1128115

Caveolin-1 Is Essential for Liver Regeneration

Manuel A. Fernández,[1,2]* Cecilia Albor,[1]* Mercedes Ingelmo-Torres,[1] Susan J. Nixon,[2] Charles Ferguson,[2] Teymuras Kurzchalia,[3] Francesc Tebar,[1] Carlos Enrich,[1] Robert G. Parton,[2]† Albert Pol[1]†

Liver regeneration is an orchestrated cellular response that coordinates cell activation, lipid metabolism, and cell division. We found that *caveolin-1* gene–disrupted mice (*cav1*$^{-/-}$ mice) exhibited impaired liver regeneration and low survival after a partial hepatectomy. Hepatocytes showed dramatically reduced lipid droplet accumulation and did not advance through the cell division cycle. Treatment of *cav1*$^{-/-}$ mice with glucose (which is a predominant energy substrate when compared to lipids) drastically increased survival and reestablished progression of the cell cycle. Thus, caveolin-1 plays a crucial role in the mechanisms that coordinate lipid metabolism with the proliferative response occurring in the liver after cellular injury.

The liver is pivotally positioned in the regulation of the body's metabolic homeostasis of lipids, carbohydrates, and vitamins. In addition, it produces essential serum proteins, lipoproteins, enzymes, and cofactors. Paradoxically, the liver is also the main detoxifying organ in the body, being continuously exposed to the threat of cellular injury. Consequently, the liver has evolved complex regenerative mechanisms to respond to chemical, traumatic, or infectious injuries (*1*–*3*). During regeneration, the liver continues to accomplish its critical functions, such as glucose homeostasis, protein synthesis, and bile secretion. Liver regeneration does not require stem cells but instead occurs when differentiated and largely quiescent hepatic cells reenter the cell cycle to replace the lost functional mass.

One of the most extensively characterized model systems to study liver regeneration is the partial hepatectomy in rodents. In this model, the left and medial lobes of the liver are excised, resulting in removal of 70% of the hepatic mass. Within minutes, hepatocytes then undergo a coordinated cellular activation termed the acute phase response. This highly regulated process is simultaneously mediated by different growth factors and cytokines that conduct the response signal into kinases and transcription factors. As a result of the acute response, the hepatocyte initiates the transcription of more than 100 early genes, accumulates triacylglycerol and cholesterol esters in intracellular lipid droplets (*4*), and progresses through the cell cycle. Lipid droplet formation is an essential part of the proliferative response during liver regeneration (*5*). Lipids stored in lipid droplets are delivered into the bile or used in the production of new lipoproteins and bile acids, for the synthesis of new membranes, or to supply the energy required for remnant hepatocytes to rebuild the liver. By compensatory hyperplasia, the regenerative process reestablishes the original liver mass in approximately 1 week, after which hepatocytes return to a quiescent state.

Caveolae are distinct domains of the plasma membrane of most cells, where cellular processes such as signaling and membrane sorting occur in a highly regulated lipid and protein environment (*6*). Caveolin, an essential component of caveolae, is a protein that has the distinct capability to create these highly ordered domains at the cell surface. In addition, caveolin and caveolae are key elements in the regulation of the intracellular homeostasis of lipids, cell activation, and cell

[1]Departament de Biologia Cellular, Facultat de Medicina, Institut d'Investigacions Biomèdiques August Pi i Sunyer, Universitat de Barcelona, Casanova 143, 08036 Barcelona, Spain. [2]Institute for Molecular Bioscience, Centre for Microscopy and Microanalysis and School of Biomedical Sciences, University of Queensland, Brisbane, Queensland 4072, Australia. [3]Max-Plank-Institute of Molecular Cell Biology and Genetics, Pfotenhauerstrasse 108, 01307 Dresden, Germany.

*These authors contributed equally to this work.
†To whom correspondence should be addressed. E-mail: R.Parton@imb.uq.edu.au (R.G.P.); apols@ub.edu (A.P.).

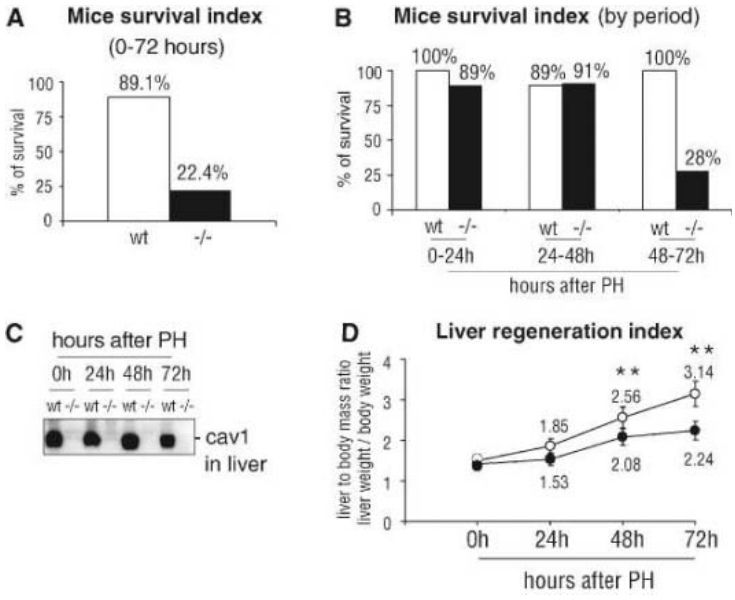

Fig. 1. Low survival and impaired liver regeneration of *cav1*$^{-/-}$ mice after partial hepatectomy. (**A**) Accumulated survival index 72 hours after partial hepatectomy of WT mice (white bars) and *cav1*$^{-/-}$ mice (black bars). (**B**) Survival index by period (0 to 24, 24 to 48, and 48 to 72 hours) of WT mice (white bars) and *cav1*$^{-/-}$ mice (black bars) for animals that, after partial hepatectomy (PH), reached and survived after each period. (**C**) Immunoblotting of caveolin-1 in liver homogenates corresponding to WT and *cav1*$^{-/-}$ mice after partial hepatectomy (40 μg of protein per lane). (**D**) Liver–to–body mass ratio in WT (white circles) and *cav1*$^{-/-}$ (black circles) animals. Immunoblots are representative of five independent experiments. The statistical significance of differences between WT and *cav1*$^{-/-}$ mice (asterisks) was determined with Student's *t* test, $^{**}P < 0.01$. Each point represents the average value and standard deviation of at least six independent measurements.

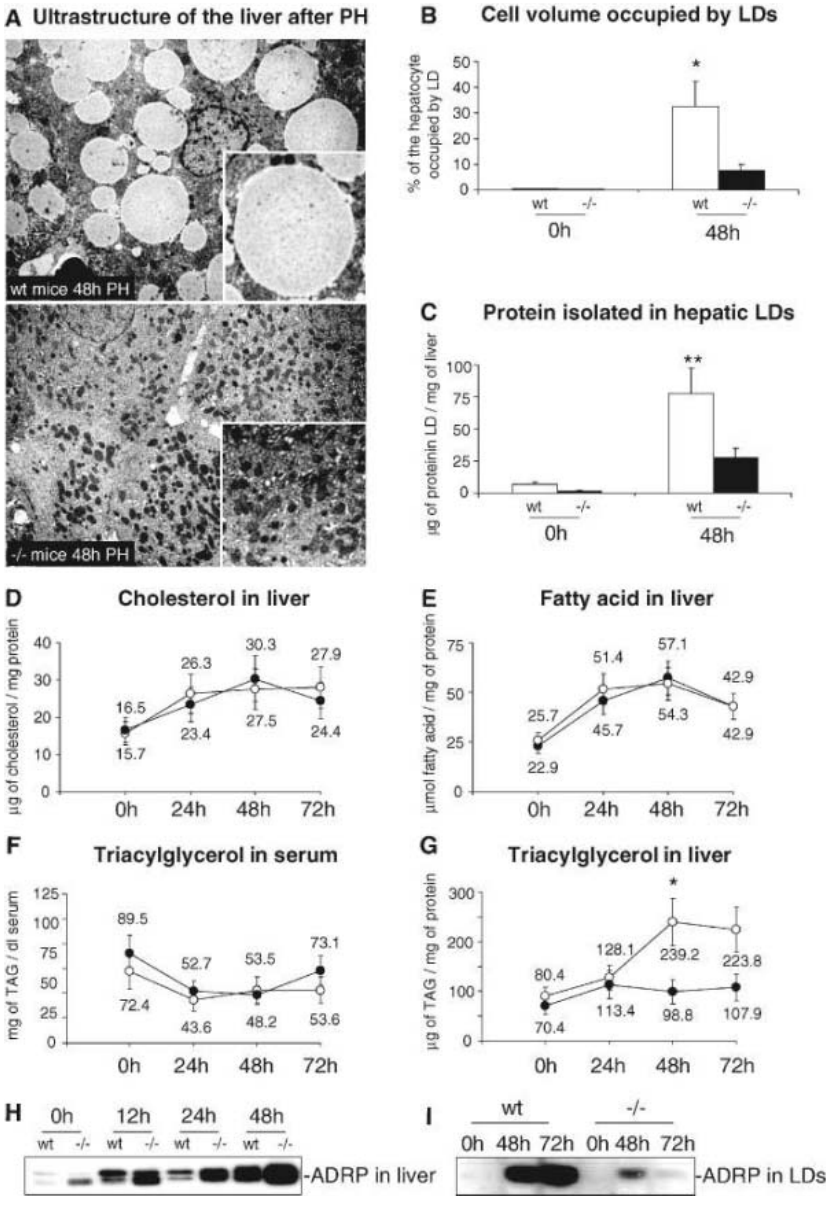

Fig. 2. Intracellular lipid imbalance in the liver of *cav1*$^{-/-}$ mice after partial hepatectomy. (**A**) Ultrastructure of the liver 48 hours after partial hepatectomy in WT mice (top panel) and *cav1*$^{-/-}$ mice (bottom panel). (**B**) Mean volume of the cell occupied by lipid droplets (LDs), calculated by quantitative EM, in WT mice (white bars) or *cav1*$^{-/-}$ mice (black bars) 48 hours after partial hepatectomy. (**C**) Amount of protein in a purified lipid droplet fraction from livers of WT mice (white bars) and *cav1*$^{-/-}$ mice (black bars). (**D** and **E**) Cholesterol and fatty acid levels in liver homogenates of WT mice (white circles) or *cav1*$^{-/-}$ mice (black circles) after partial hepatectomy. (**F** and **G**) Triacylglycerol levels in serum (F) and liver homogenates (G) of WT mice (white bars) and *cav1*$^{-/-}$ mice (black bars) after partial hepatectomy. (**H** and **I**) Expression of ADRP in liver homogenates (40 μg) (H) and lipid droplets purified from livers (30 μl) (G) of WT and *cav1*$^{-/-}$ mice. Immunoblots are representative of five (H) and two (I) independent experiments. The statistical significance of differences between WT and *cav1*$^{-/-}$ mice (asterisks) was determined with Student's *t* test, $^{*}P < 0.05$, $^{**}P < 0.01$. Each point represents the average value and standard deviation of at least four (B) or six [(C) to (G)] independent measurements.

proliferation. Recent work has linked caveolins to lipid droplet function (*7*). In addition, we have previously described the expression of caveolin and caveolae in hepatocytes and showed that caveolin associates with the lipid droplets formed after partial hepatectomy (*8*).

Liver regeneration results from the coordination of cell activation, lipid metabolism, and cell division. Although caveolin-1 has been connected with the regulation of each one of these processes, its precise role remains uncertain. Thus, the regeneration response triggered in the liver after partial hepatectomy offers an excellent integrated model system with which to evaluate in vivo the role of caveolin-1 in these processes occurring synchronously in a cell population. We studied the regeneration process triggered by partial hepatectomy in the liver of caveolin-1 gene–disrupted mice (*cav1*$^{-/-}$ mice) (*9*, *10*).

We analyzed 66 wild-type (WT) mice and 61 *cav1*$^{-/-}$ mice during the first 72 hours after partial hepatectomy. At the end of this period, WT mice showed an accumulated survival index of 89.1% (Fig. 1A). In contrast, *cav1*$^{-/-}$ mice showed a survival index of only 22.4%. Although the mortality of both groups was rather similar during the first 48 hours (100%/89% between 0 and 24 hours and 89%/91% between 24 and 48 hours for WT and *cav1*$^{-/-}$ mice, respectively), *cav1*$^{-/-}$ mice showed a marked mortality beyond this time point (72%) (Fig. 1B). In contrast, all of the WT mice that survived at 48 hours progressed to 72 hours. As expected, caveolin-1 was highly expressed in livers of WT mice but was not detected in *cav1*$^{-/-}$ mice at any point in the regeneration process (Fig. 1C). The liver–to–body mass ratio (equivalent to a regeneration index after partial hepatectomy), which was 5.9% in both untreated WT and *cav1*$^{-/-}$ mice, increased progressively in WT mice to reach 3.1% after 72 hours, which represents 52.5% of the original weight (Fig. 1D). Considering that only 22% of *cav1*$^{-/-}$ mice survived at this time point (Fig. 1A), the regeneration index of *cav1*$^{-/-}$ animals was 2.2% after 72 hours, which is only 38.0% of the original weight. *cav1*$^{-/-}$ mice that died during the period from 36 to 72 hours (78% of *cav1*$^{-/-}$ mice operated on) showed an extremely low regeneration index of approximately 1.7%.

After partial hepatectomy, the levels of fatty acids in the plasma increase severalfold, leading to intracellular accumulation of lipids and the formation of numerous cytosolic lipid droplets (*4*). We used quantitative electron microscopy (EM) to examine the ultrastructure of the liver after partial hepatectomy. No significant differences between WT and *cav1*$^{-/-}$ mice were observed in the serum (table S1) or liver before surgery; a small number of lipid droplets was observed in each case. Forty-eight hours after partial hepatectomy, the hepatocytes of WT mice accumulated enlarged lipid droplets in the cytosol (Fig. 2A). In contrast, lipid droplet accumulation was greatly reduced in the livers of *cav1*$^{-/-}$ mice. After 48 hours, the mean volume of lipid droplets was 32.6% (±9.8%) of cellular volume in WT mice as compared to 7.7% (±2.9%) in *cav1*$^{-/-}$ mice (Fig. 2B). When a purified fraction of lipid droplets was isolated from regenerating livers after 48 hours, a significant reduction in the total amount of purified protein from *cav1*$^{-/-}$ livers was observed (Fig. 2C). At this time, the levels of cholesterol and fatty acids in serum or in liver homogenates were not significantly different between WT or *cav1*$^{-/-}$ mice (Fig. 2, D and E), suggesting that a reduced level of serum lipids or reduced cellular uptake of lipids did not account for the lack of lipid droplets observed in the liver of *cav1*$^{-/-}$ mice. However, whereas the levels of triacylglycerol in serum were similar between WT and *cav1*$^{-/-}$ animals, the level of triacylglycerol in liver homogenates was clearly lower in *cav1*$^{-/-}$ animals after 48 hours (Fig. 2, F and G). At 24 hours after partial hepatectomy, both WT and *cav1*$^{-/-}$ livers showed a similar increment of their triacylglycerol content, but at later times, significant differences between the WT and *cav1*$^{-/-}$ mice were observed. Thus, although *cav1*$^{-/-}$ mice were able to synthesize triacylglycerol to some extent, they could not store these lipids efficiently in lipid droplets. In agreement with an intracellular lipid imbalance, the expression of adipophilin (ADRP, the major component of hepatic lipid droplets and highly expressed in response to fatty acids during liver regeneration) was slightly but consistently higher in *cav1*$^{-/-}$ mice when compared to WT mice (Fig. 2H), although it was not detected in the fraction corresponding to purified lipid droplets (Fig. 2I). Thus, caveolin is required for efficient lipid droplet formation in regenerating hepatocytes, and the absence of lipid droplets at 48 hours after partial hepatectomy coincides with the increased mortality of *cav1*$^{-/-}$ mice beyond this point.

To examine the effect of caveolin-1 deficiency at the cellular level, hepatocytes from

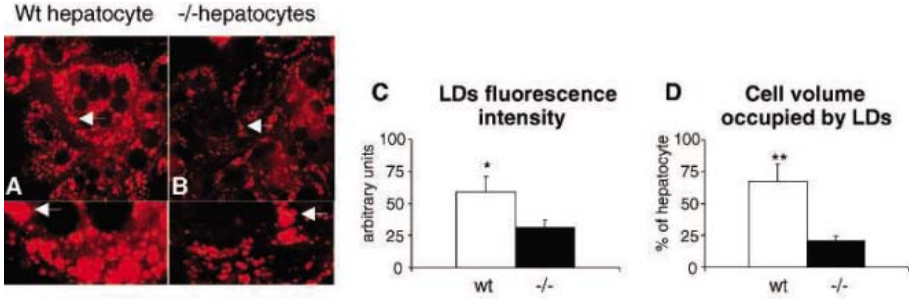

Fig. 3. Isolated *cav1*$^{-/-}$ hepatocytes show impaired lipid droplet accumulation. Hepatocytes were isolated from livers of WT mice (**A**) or *cav1*$^{-/-}$ mice (**B**) and allowed to attach on glass coverslips for 6 hours in a glucose-free medium supplemented with fatty acids. Cells were fixed and lipid droplet accumulation was analyzed by means of Nile Red fluorescence (**C**), and the percentage of the cytosol occupied by lipid droplets (**D**) was quantified in WT hepatocytes (white bars) and *cav1*$^{-/-}$ hepatocytes (black bars). Values are the result of three independent experiments. The statistical significance of differences between WT and *cav1*$^{-/-}$ mice (asterisks) was determined with Student's *t* test, $*P < 0.05$, $**P < 0.01$.

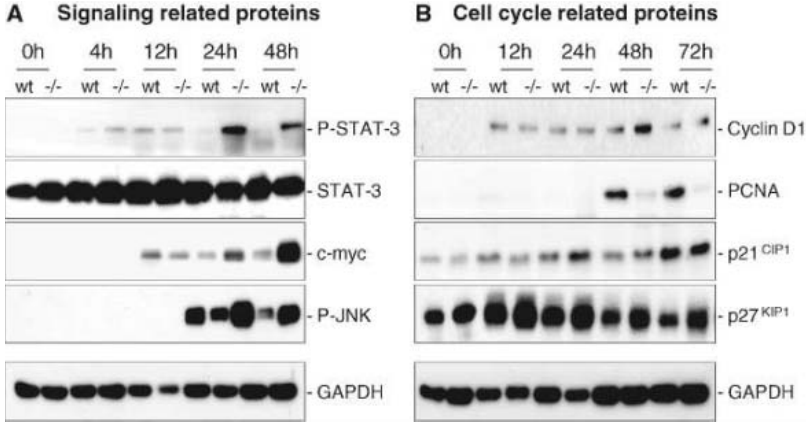

Fig. 4. Hyperactivation and cell cycle inhibition of *cav1*$^{-/-}$ hepatocytes after partial hepatectomy. The expression of markers corresponding to the acute phase response (**A**) or to the cell cycle machinery (**B**) in liver homogenates (40 μg) or for PCNA analyzed in isolated nuclei (20 μg) of WT and *cav1*$^{-/-}$ mice after partial hepatectomy is shown. Immunoblots are representative of at least three independent experiments. GAPDH, glyceraldehyde phosphate dehydrogenase.

WT and *cav1*$^{-/-}$ mice were isolated and treated with a combination of fatty acids for 6 hours. Hepatocytes growing on glass coverslips were stained with Nile Red (a neutral lipid probe) for detection of lipid droplets. As expected, fatty acids efficiently promoted the accumulation of enlarged lipid droplets in the cytosol of WT hepatocytes (Fig. 3A). In comparison, the intensity of Nile Red staining was significantly reduced in *cav1*$^{-/-}$ hepatocytes (Fig. 3, B and C). In addition, the mean volume of lipid droplets was 67.6% (±14.3%) of the cell cytosol in WT hepatocytes as compared to 20.5% (±4.9%) in *cav1*$^{-/-}$ cells (Fig. 3D). Hepatocytes isolated from WT and *cav1*$^{-/-}$ livers showed a similar uptake of fatty acids (fig. S1). When the expression of caveolin-1 was down-regulated by means of small interfering RNA in mouse embryonic fibroblasts obtained from WT mice, the accumulation of lipid droplets in cells expressing low levels of caveolin-1 was significantly reduced (fig. S2). In contrast, down-regulation of caveolin-2 in these cells did not affect the accumulation of lipid droplets (fig. S2). Thus, the inability of *cav1*$^{-/-}$ hepatocytes to accumulate lipid droplets during liver regeneration is caused by the lack of hepatic caveolin-1 rather than promoted by the absence of caveolin-1 in other tissues.

Hepatocytes without caveolin-1 do not efficiently accumulate triacylglycerol in lipid droplets and fail to regenerate. Caveolin is linked to numerous signaling processes, but the exact regulatory mechanisms are still unclear. We examined whether an impaired activation of the cells during the acute response may account for the lack of regeneration observed in *cav1*$^{-/-}$ mice. Hepatocyte activation after partial hepatectomy is promoted by two coordinated main signaling pathways: a cytokine-mediated pathway and a growth factor–mediated pathway. Binding of interleukin-6 (IL-6) to its receptor (IL-6 receptor) stimulates the Janus activated kinase (JAK-1), which in turn phosphorylates the signal transducer and activator of transcription 3 (STAT-3). Phosphorylated STAT-3 translocates to the nucleus to activate the transcription of target genes (such as c-*myc*). We examined the levels of phosphorylated STAT-3 and the expression of c-*myc* in liver homogenates. Twelve hours after partial hepatectomy, phosphorylation of STAT-3 was detected in both WT and *cav1*$^{-/-}$ mice (Fig. 4A). At later times, the levels of phospho–STAT-3 then decreased, as expected in WT mice livers, but STAT-3 remained phosphorylated in *cav1*$^{-/-}$ livers. Consistent with this finding, levels of c-*myc* were considerably higher in livers from *cav1*$^{-/-}$ mice. We also studied the growth factor–mediated signaling pathway. The hepatic growth factor (HGF) is considered to be an essential activator of the regeneration response of the liver. We evaluated HGF activity by visualizing the phosphorylation of its substrate, Jun N-terminal kinase (JNK). Phospho-JNK was detected in both WT and *cav1*$^{-/-}$ mice, but the levels of phosphorylated kinase were markedly higher in *cav1*$^{-/-}$ mice (Fig. 4A). Thus, although the acute phase response occurs as in WT mice, the signaling is more elevated and prolonged in *cav1*$^{-/-}$ livers.

We next evaluated the progression of hepatocytes through the cell cycle by studying specific proteins of the cell cycle machinery known to be regulated during liver regeneration (*11*). Expression of cyclin D, which is transcriptionally activated during the G_1 phase of the cell cycle, was observed in both WT and *cav1*$^{-/-}$ livers after 12 hours of partial hepatectomy (Fig. 4B). Although the proliferating cell nuclear antigen (PCNA, a marker for the S phase) was clearly observed at 48 to 72 hours in 95% of WT livers, its expression was not observed or was highly reduced in 80% of *cav1*$^{-/-}$ mice that survived at 72 hours. Although no differences were observed in the expression of the cell cycle inhibitor p21^{CIP1}, the amount of the inhibitor p27^{KIP1} detected in *cav1*$^{-/-}$ livers was slightly but consistently higher when compared to WT mice. Thus, the livers of *cav1*$^{-/-}$ mice do not seem to progress correctly through the cell cycle. The impaired liver regeneration observed in *cav1*$^{-/-}$ mice did not appear to result in an increased rate of apoptosis; no differences in the activity of caspases measured in regenerating livers were observed (fig. S3).

Glucose can be the predominant energy substrate during liver regeneration, when sufficient levels are available during the immediate post-hepatectomy phase (*12*, *13*). The continuous infusion of glucose into partially hepatectomized rats prevents both the loss of glycogen and the deposition of lipid (*14*). Because the livers of *cav1*$^{-/-}$ mice do not correctly metabolize lipids after partial hepatectomy (Fig. 2), we hypothesized that the impaired liver regeneration showed by these mice might be due to the perturbation of lipid handling. If so, the

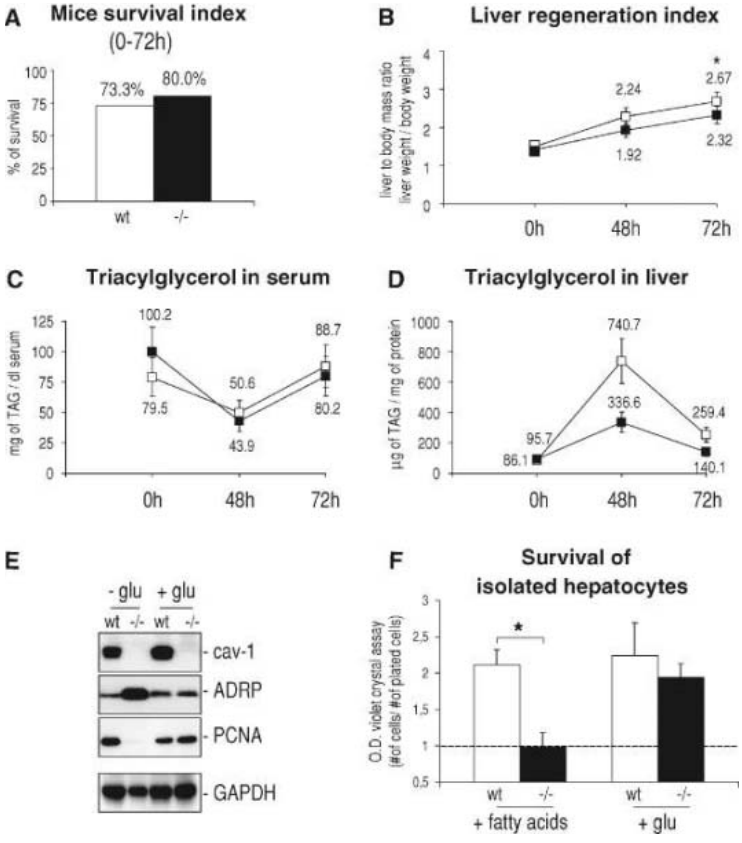

Fig. 5. The feeding of glucose reestablishes hepatocyte survival and cell cycle progression in *cav1*$^{-/-}$ mice. (**A**) Survival index after partial hepatectomy of glucose-treated *cav1*$^{-/-}$ mice (black bars) and WT mice (white bars). (**B**) Liver–to–body mass ratio corresponding to glucose-fed *cav1*$^{-/-}$ mice (black squares) and glucose-fed WT mice (white squares) after partial hepatectomy. (**C** and **D**) Triacylglycerol levels in serum (C) and liver homogenates (D) of glucose-fed WT mice (white squares) and glucose-fed *cav1*$^{-/-}$ mice (black squares) after partial hepatectomy. (**E**) The expression of caveolin-1 and ADRP in liver homogenates (40 µg) and of PCNA in isolated nuclei (20 µg). (**F**) Hepatocytes were isolated from livers of WT mice (white bars) and *cav1* $^{-/-}$ mice (black bars) and cultured for 48 hours in a medium supplemented with fatty acids or glucose. The number of living cells was determined by staining cell nuclei with crystal violet and is expressed with respect to the initial number of living hepatocytes. The statistical significance (asterisk) was determined with Student's *t* test, $*P < 0.05$. Each point and immunoblot represents the average value of at least four independent experiments. O.D., optical density.

treatment of animals with glucose before and during the regenerative process might allow liver regeneration in the *cav1*$^{-/-}$ mice. Thus, WT and *cav1*$^{-/-}$ mice were continuously supplied with 10% glucose in their drinking water for 60 hours before surgery and during the regeneration period afterward. Before partial hepatectomy, the ingestion of glucose-enriched water was approximately 10 ml per mouse per day (equivalent to 1 g of glucose per day). When *cav1*$^{-/-}$ mice were treated with glucose, the survival index at 72 hours after partial hepatectomy dramatically increased to reach values comparable to those of glucose-treated WT mice (80.0% for *cav1*$^{-/-}$ mice, $n = 26$ mice; 73.3% for WT, $n = 16$) (Fig. 5A). In WT mice treated with glucose, the liver regeneration index after 72 hours was 2.67% (±0.3), which, consistent with slightly delayed regeneration in glucose-fed rats (*15*, *16*), represents 45.3% (±5.1) of the original weight (Fig. 5B) (in contrast to 52.5% shown by WT mice that were not treated with glucose, Fig. 1D). Consistent with the decreased mortality of the *cav1*$^{-/-}$ mice, liver regeneration was rescued by glucose feeding. Glucose-fed *cav1*$^{-/-}$ mice showed a regeneration index of 2.32% (±0.4), which similarly to the WT glucose-fed mice represents 39.3% (±6.8) of the original liver weight. After partial hepatectomy, the levels of triacylglycerol in serum were similar to those shown by animals that were not treated with glucose. In contrast, in liver homogenate of glucose-fed animals, the level of triacylglycerol increased in both WT and *cav1*$^{-/-}$ mice (Fig. 5D). Although, as expected, no changes were observed in the expression of caveolin-1 (Fig. 5E), when treated with glucose, the expression of ADRP in *cav1*$^{-/-}$ animals was similar to that shown by WT mice (Fig. 5E). Treatment with glucose also rescued the inhibition of the cell cycle shown by *cav1*$^{-/-}$ mice (Fig. 4B). In that case, 87.5% of *cav1*$^{-/-}$ mice treated with glucose expressed high levels of PCNA 72 hours after partial hepatectomy (Fig. 5E). To examine the effect of glucose at the cellular level, hepatocytes from WT and *cav1*$^{-/-}$ mice were isolated and cultured in a glucose-free medium containing growth factors supplemented with a combination of fatty acids (0.5 mM palmitoleic acid and 0.5 mM oleic acid) or alternatively with glucose (4500 mg/l), and the number of cells was determined after 48 hours (number of living cells after 48 hours/number of living cells 6 hours after isolation) by staining of cell nuclei with a standard crystal violet measurement. In contrast to WT cells, *cav1*$^{-/-}$ hepatocytes did not survive in the presence of fatty acids, and a reduction in the number of cells was observed (Fig. 5F). In the presence of glucose, both WT and *cav1*$^{-/-}$ hepatocytes showed a similar index. Thus, the increased mortality and decreased liver regeneration in mice lacking caveolin-1 can be rescued by glucose addition, pinpointing the crucial role of caveolin-1 in lipid regulation during the regeneration process.

We have shown that caveolin is essential for liver regeneration. caveolin-1–deficient mice showed increased mortality and decreased liver regeneration after partial hepatectomy. In the absence of caveolin-1, hepatocytes did not accumulate lipid droplets, and this has important effects on other cellular processes such as cell signaling and cell division. As a result, regenerating *cav1*$^{-/-}$ hepatocytes showed atypical cell activation and did not entirely advance through the cell cycle. Because the treatment of *cav1*$^{-/-}$ mice with glucose increased mouse survival and reestablished progression of the cell cycle, we postulate that caveolin-1 has a crucial role in lipid regulation during the regeneration process. Thus, the S phase of the cell cycle may be metabolically regulated by the availability of lipid droplets or glucose. Although *cav1*$^{-/-}$ animals show a relatively mild phenotype, suggesting that other proteins may compensate for the lack of caveolins in certain cellular or functional contexts, caveolin-1 plays an essential role in the hepatocyte that becomes apparent only in response to liver injury.

References and Notes

1. N. Fausto, *Hepatology* **39**, 1477 (2004).
2. G. K. Michalopoulos, M. C. DeFrances, *Science* **276**, 60 (1997).
3. R. Taub, *Nat. Rev. Mol. Cell Biol.* **5**, 836 (2004).
4. E. A. Glende Jr., W. S. Morgan, *Exp. Mol. Pathol.* **8**, 190 (1968).
5. G. C. Farrell, *Hepatology* **40**, 1252 (2004).
6. T. V. Kurzchalia, R. G. Parton, *Curr. Opin. Cell Biol.* **11**, 424 (1999).
7. A. Pol *et al.*, *J. Cell Biol.* **152**, 1057 (2001).
8. A. Pol *et al.*, *Mol. Biol. Cell* **15**, 99 (2004).
9. M. Drab *et al.*, *Science* **293**, 2449 (2001).
10. S. Le Lay, T. V. Kurzchalia, *Biochim Biophys Acta* **1746**, 322 (2005).
11. J. H. Albrecht *et al.*, *Oncogene* **16**, 2141 (1998).
12. H. S. Lai, W. J. Chen, K. M. Chen, *J. Parenter. Enteral Nutr.* **16**, 152 (1992).
13. J. Simek, V. Chmelar, J. Melka, Z. Pazderka, Z. Charvat, *Nature* **213**, 910 (1967).
14. N. L. R. Bucher, R. A. Malt, *Regeneration of Liver and Kidney* (Little, Brown, Boston, 1971).
15. J. A. Caruana, D. A. Whalen Jr., W. P. Anthony, C. R. Sunby, M. P. Ciechoski, *Endocr. Res.* **12**, 147 (1986).
16. M. Holecek, J. Simek, *Exp. Pathol.* **33**, 257 (1988).

17. We thank A. Giménez, C. Claries, and O. Collazo from the Animal Facility (University of Barcelona) and the CORE facility (Hospital Clinic i Provincial de Barcelona). This work was supported by grants BMC2003-04754 and GEN2003-20662 to C.E. and BFU2005-01716 and GEN2003-20662 to A.P. [Ministerio de Educación y Ciencia (MEC), Spain] and a program grant from the National Health and Medical Research Council of Australia to R.G.P. A.P. and F.T. are supported by Ramón y Cajal Research Program (MEC). M.A.F. is supported by the postdoctoral fellowship program EX2005-0850 (MEC).

Supporting Online Material

www.sciencemag.org/cgi/content/full/313/5793/1628/DC1
Materials and Methods
Figs. S1 to S3
Table S1
References

2 June 2006; accepted 21 July 2006
10.1126/science.1130773

C-Terminal Signal Sequence Promotes Virulence Factor Secretion in *Mycobacterium tuberculosis*

Patricia A. DiGiuseppe Champion,[1,2] Sarah A. Stanley,[1,2] Matthew M. Champion,[3] Eric J. Brown,[2] Jeffery S. Cox[1,2]*

Mycobacterium tuberculosis uses the ESX-1/Snm system [early secreted antigen 6 kilodaltons (ESAT-6) system 1/secretion in mycobacteria] to deliver virulence factors into host macrophages during infection. Despite its essential role in virulence, the mechanism of ESX-1 secretion is unclear. We found that the unstructured C terminus of the CFP-10 substrate was recognized by Rv3871, a cytosolic component of the ESX-1 system that itself interacts with the membrane protein Rv3870. Point mutations in the signal that abolished binding of CFP-10 to Rv3871 prevented secretion of the CFP-10 (culture filtrate protein, 10 kilodaltons)/ESAT-6 virulence factor complex. Attachment of the signal to yeast ubiquitin was sufficient for secretion from *M. tuberculosis* cells, demonstrating that this ESX-1 signal is portable.

Proteins are sorted for translocation across cellular membranes through recognition of signal sequences (*1*, *2*). In prokaryotes, most proteins are secreted through the general secretion pathway, which recognizes N-terminal signal peptides (*3*). Additionally, Gram-negative pathogenic bacteria use specialized secretion machines to secrete virulence determinants during infection (*4*, *5*).

Mycobacterium tuberculosis does not have recognizable homologs of these specialized secretion systems. Instead, the ESX-1 system (ESAT-6 system-1) is required for controlling host-cell response to infection (*6*–*8*). ESX-1 is

[1]Department of Microbiology and Immunology, [2]Program in Microbial Pathogenesis and Host Defense, University of California, San Francisco, 600 16th Street, Campus Box 2200, San Francisco, CA 94143–2200, USA. [3]Applied Biosystems, 353 Hatch Drive, Foster City, CA 94404, USA.

*To whom correspondence should be addressed. E-mail: Jeffery.Cox@ucsf.edu

encoded by genes in the RD1 (region of difference 1) locus of the genome that is missing in the *M. bovis* Bacille Calmette-Guérin vaccine strain (*9*, *10*). This system includes a multitransmembrane protein, Rv3877 (Snm4), and two putative SpoIIIE/FtsK adenosine triphosphatase (ATPase) family members, Rv3870 (Snm 1) and Rv3871 (Snm2). These three proteins are required for secretion of two virulence factors, ESAT-6 and CFP-10 (*8*). ESAT-6 (product of the *esxA* gene) and CFP-10 (product of the *esxB* gene) interact to form a 1:1 dimer (*11*, *12*), and the stability of these proteins is interdependent in vivo. CFP-10, but not ESAT-6, interacts with the C-terminal domain of Rv3871, a cytosolic component of the ESX-1 system (*8*). Although the secretion of ESAT-6 and CFP-10 is critical for *M. tuberculosis* virulence, the molecular mechanisms of ESX-1 substrate selection and secretion are unclear.

To define targeting sequences responsible for directing secretion by ESX-1, we probed a series of N- and C-terminal deletions in *M. tuberculosis* CFP-10 for interaction with ESAT-6 and Rv3871 (*13*). Deletion of 25 amino acids from either the N or C terminus of CFP-10 abrogated the interaction of CFP-10 with ESAT-6 (Fig. 1A). In contrast, the last 25 amino acids of CFP-10 were necessary and sufficient for interaction with Rv3871 (Fig. 1B). Proteins containing deletions of the N-terminal 25 and 50 amino acids of CFP-10 retained Rv3871 binding activity, albeit at lower levels than full-length protein. These deletions interrupted domains of the folded protein (Fig. 1F), and the partial structures may have interfered with presentation of the interaction domain in the two-hybrid system.

Because the C-terminal domain of CFP-10 was required for interaction with both ESAT-6 and Rv3871, we identified individual residues required for the interaction of CFP-10 specifically with Rv3871 (Fig. 1C and fig. S1). Mutations in four of the seven C-terminal amino acids of CFP-10 (L94A, M98A, G99A, and F100A) abolished interaction with Rv3871 (Fig. 1C and fig. S1) but not with ESAT-6, demonstrating that these interactions are separable (Fig. 1C). Further deletion within the C-terminal tail of CFP-10 revealed that the last seven amino acids were sufficient for Rv3871 interaction (Fig. 1D). N-terminal deletions within the last seven amino acids of CFP-10 abrogated Rv3871 binding, demonstrating that L94 is critical for this interaction (Fig. 1D).

To independently test the interaction between CFP-10 and Rv3871, we performed in vitro pulldown experiments (Fig. 1E). HA-Rv3871 fusion protein bound to agarose beads was incubated with lysates from *Escherichia coli* cells expressing CFP-10 or CFP-10 lacking the C-terminal seven amino acids (CFP-10Δ7CT) in the presence of ESAT-6. Under these conditions, CFP-10 did not bind to Rv3871-coated beads. Indeed, interactions of secreted proteins with targeting proteins are typically weak and transient (*14*). Upon addition of protein cross-linker, however, the interaction was stabilized. Although low levels of CFP-10 were cross-linked nonspecifically to antibody-coated beads in the absence of Rv3871, CFP-10 interacted specifically with Rv3871 (Fig. 1E). In contrast, deletion of the C-terminal seven amino acids reduced binding to background levels (Fig. 1E). Thus, the last seven amino acids of CFP-10 are critical for interacting directly with Rv3871.

The published CFP-10/ESAT-6 solution structure shows that the C-terminal 14 amino acids of CFP-10 form an unstructured tail that does not interact with ESAT-6 (*11*) (Fig. 1F). Because most of the residues required for CFP-10 interaction with Rv3871 map to this unstructured C terminus (Fig. 1F), we hypothesized

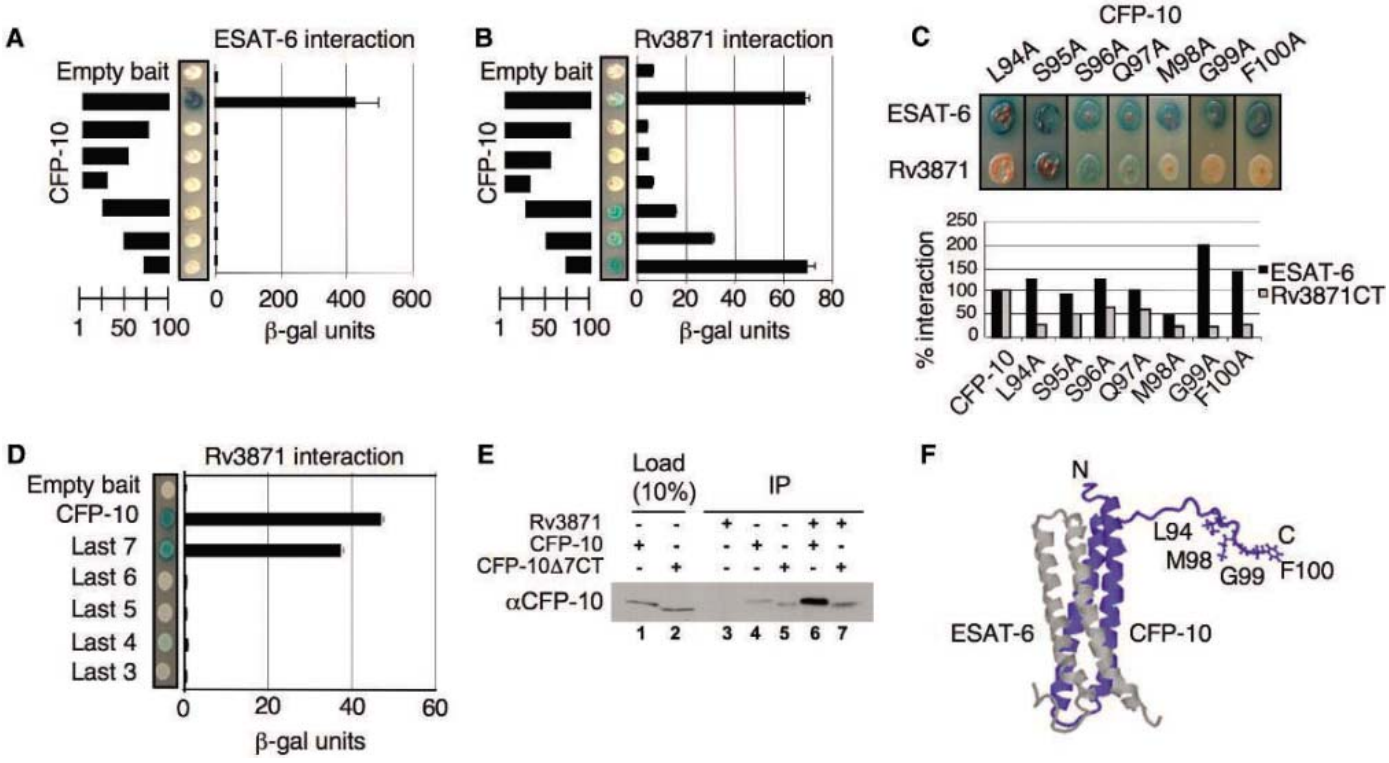

Fig. 1. The C terminus of CFP-10 is necessary and sufficient for Rv3871 interaction. Two-hybrid analysis of CFP-10 bait deletions with ESAT-6 (**A**) or Rv3871 (**B**) preys. (**C**) CFP-10 alanine scan mutants were tested for interaction with either ESAT-6 (top) or Rv3871 (bottom). (**D**) The last three to seven amino acids of CFP-10 were tested for interaction with Rv3871. For (A) to (D), β-galactosidase activity is shown; error bars represent standard deviation. (**E**) The interaction of HA-Rv3871 (amino acids 248 to 591) with CFP-10 by in vitro pulldown assays followed by CFP-10 immunoblot analysis. Equal amounts of CFP-10 and CFP-10Δ7CT were loaded into the pulldown (lanes 1 and 2), and CFP-10 and CFP-10Δ7CT were added to beads alone (lanes 4 and 5) or to Rv3871-bound beads (lanes 6 and 7). (**F**) ESAT-6 (gray) and CFP-10 (blue) solution structure (*11*) modeled by Protein Explorer (*24*) with the N and C termini of CFP-10 labeled.

that targeting information for both ESAT-6 and CFP-10 could lie in the last seven amino acids of CFP-10.

To test the role of the CFP-10/Rv3871 interaction in secretion in vivo, we introduced mutant forms of *esxB* into the *ΔesxB M. tuberculosis* strain. Despite bearing an in-frame deletion in the *esxB* gene, neither CFP-10 nor ESAT-6 was detectable in the cell lysate (Fig. 2A), consistent with previous results (*8*, *15*). Expression of wild-type CFP-10 and ESAT-6 in the *ΔesxB* strain restored production and secretion of these proteins into the culture supernatant (Fig. 2A), whereas expression of CFP-10 lacking the terminal 25 amino acids (CFP-10Δ25CT) did not, presumably because of a lack of interaction with ESAT-6 (Figs. 1A and 2A). In contrast, expression of CFP-10 lacking the seven terminal amino acids (CFP-10Δ7CT) resulted in stable production of both ESAT-6 and CFP-10. Thus, the carboxy-terminal seven amino acids of CFP-10 are not required for protein stability or for interaction of CFP-10 with ESAT-6. The CFP-10Δ7CT and ESAT-6 proteins, although stable, were not secreted into the culture supernatant (Fig. 2A), establishing that these residues target both CFP-10 and ESAT-6 for secretion in vivo.

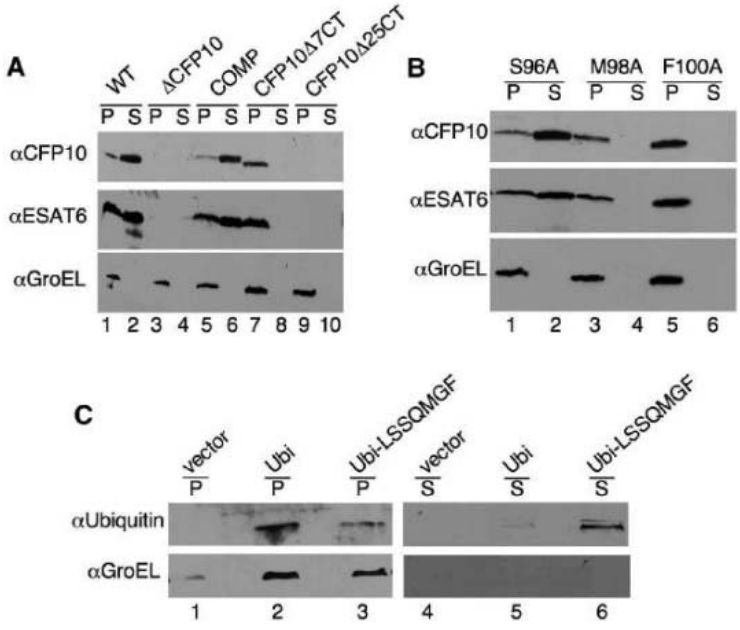

Fig. 2. The last seven amino acids of CFP-10 are necessary and sufficient for secretion from *M. tuberculosis* in vivo. (**A**) Immunoblot analysis of cell pellets (P) and supernatants (S) from wild-type (WT) *M. tuberculosis* (lanes 1 and 2), or *ΔesxB* strains bearing either the pMH406 complementation plasmid (COMP) (lanes 5 and 6), or plasmids expressing ESAT-6 and CFP-10Δ7CT (lanes 7 and 8) or CFP-10Δ25CT (lanes 9 and 10). GroEL was a control for autolysis. (**B**) Immunoblot analysis from *ΔesxB M. tuberculosis* harboring plasmids expressing ESAT-6 and either CFP-10 S96A (lanes 1 and 2), CFP-10 M98A (lanes 3 and 4), or CFP-10 F100A (lanes 5 and 6). (**C**) Immunoblot analysis of pellets and supernatants from *ΔesxB M. tuberculosis* strains harboring either pMH406 (vector) (lanes 1 and 4), or plasmids expressing yeast ubiquitin (Ubi) (lanes 2 and 5), or yeast ubiquitin tagged at its C terminus with LSSQMGF (Ubi-LSSQMGF) (lanes 3 and 6).

Table 1. ESAT-6 and CFP-10 paralogs identified in the culture filtrate by quantitative liquid chromatography–tandem mass spectrometry (LC-MS/MS).

Protein name	Rv No.	Confidence of ID	% Sequence coverage >99% conf. peptides*	Ratio 116/114 *ΔesxB*/ WT†	Ratio 117/114 *Δ*Rv3877/ WT†	C-terminal peptide present?
EsxA	Rv3874	>99.9%	93.70%	≈0	≈0	yes
EsxB	Rv3875	>99.9%	92.00%	≈0	≈0	yes
EsxN	Rv1793	>99.9%	98.90%	1.02:1	1.1:1	yes
EsxL	Rv1198	>99.9%	98.90%	0.92:1	0.92:1	yes
EsxO	Rv2346c	>99.9%	98.90%	0.99:1	1.01:1	yes
EsxP‡	Rv2347c	>99.9%	93.90%	1.00:1	1.00:1	yes
EsxK‡	Rv1197	>99.9%	93.90%	1.00:1	1.00:1	yes
EsxJ§	Rv1038c	>99.9%	93.90%	1.1:1	0.99:1	yes
EsxW§	Rv3620c	>99.9%	93.90%	1.1:1	0.99:1	yes
EsxG	Rv0287	>99.9%	73.20%	1.00:1	1.00:1	yes

*Sequence coverage = total amino acids identified/total in database, including signal sequences and N-terminal methionine. Only reported for those peptides with MS/MS confidence scores >99%. †Ratio normalized for lysis and mixing error. 95% confidence interval was <±0.2 for each Esx peptide. ‡,§Insufficient MS/MS or protein sequence evidence exists to differentiate these isoforms.

We generated single-point mutations in the last seven amino acids of CFP-10 and tested these mutant proteins for stability and secretion. Stable expression of the CFP-10 S96A, CFP-10 M98A, or CFP-10 F100A mutant protein was detectable in *ΔesxB* cell lysates, consistent with the dispensability of these residues for interaction with ESAT-6 in vivo. CFP-10 S96A, which could interact with Rv3871 (Fig. 1C), also allowed secretion of ESAT-6 into the culture supernatant from *ΔesxB M. tuberculosis* cells (Fig. 2B). In contrast, neither CFP-10 M98A nor CFP-10 F100A was secreted into the culture supernatant (Fig. 2B). Like CFP-10Δ7CT, these mutant CFP-10 proteins could not promote the secretion of ESAT-6 into the culture filtrate (Fig. 2B), demonstrating that these two residues are required for targeting both CFP-10 and ESAT-6 for secretion in vivo.

Because the last seven amino acids of CFP-10 were necessary for CFP-10/ESAT-6 secretion, we tested whether these residues are sufficient for secretion. We expressed yeast ubiquitin or the last seven amino acids of CFP-10 fused to the C terminus of ubiquitin in the *ΔesxB M. tuberculosis* strain and monitored secretion into the culture supernatant by immunoblot analysis. Native ubiquitin was found exclusively in the cell pellets (Fig. 2C). In contrast, addition of the CFP-10 signal sequence led to secretion of ubiquitin from the cells (Fig. 2C). Quantitative immunoblot analysis revealed that the ratio of secreted to cell-associated protein was lower by a factor of about 10 for the ubiquitin fusion protein than for CFP-10/ESAT-6, indicating that other features of CFP-10 or the CFP-10/ESAT-6 complex probably facilitate transport of these substrates by ESX-1. However, the last seven amino acids of CFP-10 can constitute a portable signal sequence sufficient to direct the secretion of a heterologous protein.

Ten CFP-10 paralogs are encoded by the *M. tuberculosis* genome as a result of numerous duplications of the *esxA/esxB* operon (fig. S3A). At least three CFP-10 paralogs (EsxG, EsxW, and EsxJ, K, or M) and five ESAT-6 paralogs (EsxH, EsxL, EsxN, EsxO, and EsxR) have been identified in the culture supernatants of *M. tuberculosis* (*16*–*18*) and are candidate virulence factors. It is unclear whether these paralogs are secreted by the ESX-1 system or by distinct secretory systems (*19*). Alignment of the amino acid sequences of these proteins (Fig. 3A) revealed

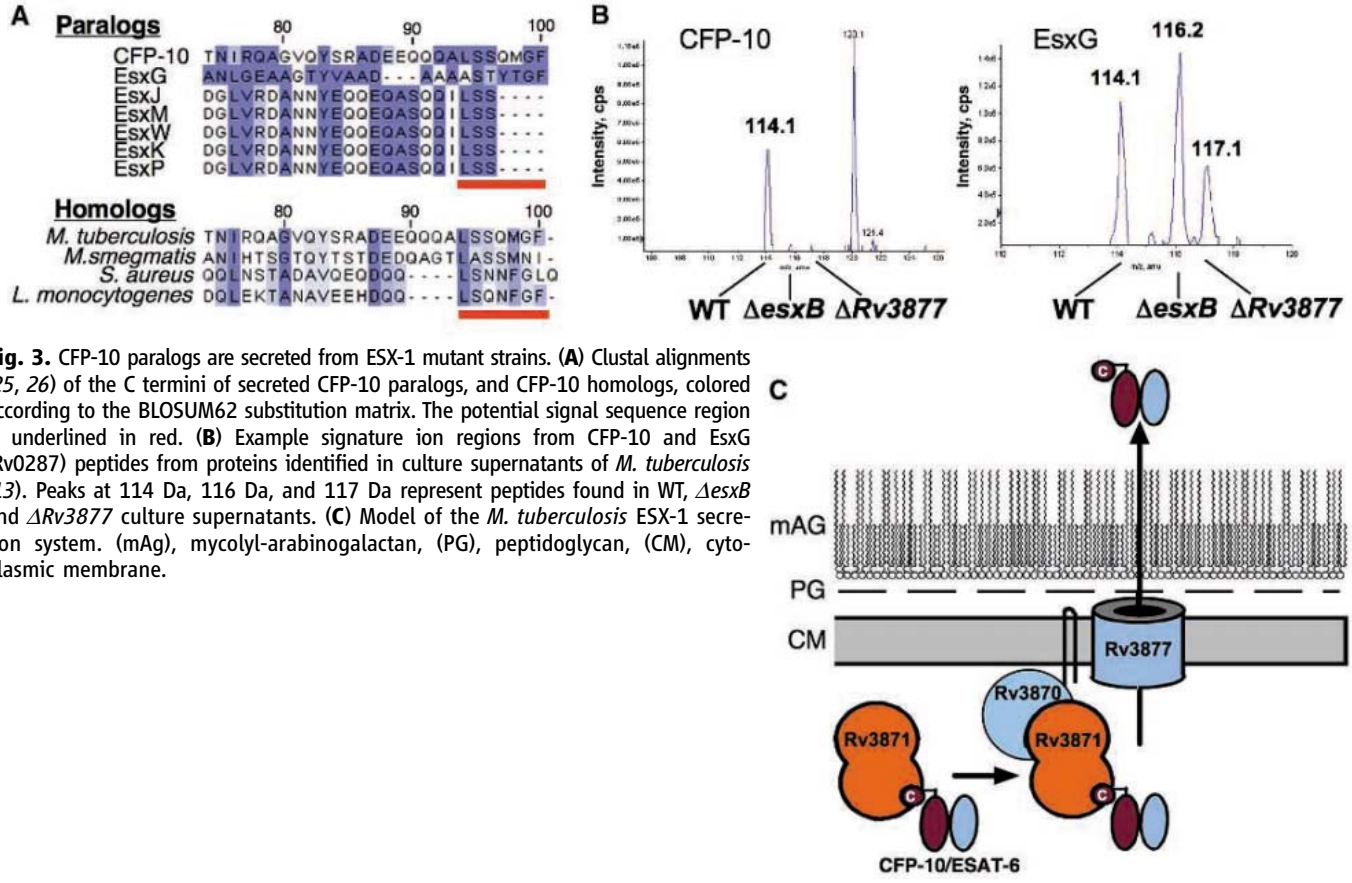

Fig. 3. CFP-10 paralogs are secreted from ESX-1 mutant strains. (**A**) Clustal alignments (*25*, *26*) of the C termini of secreted CFP-10 paralogs, and CFP-10 homologs, colored according to the BLOSUM62 substitution matrix. The potential signal sequence region is underlined in red. (**B**) Example signature ion regions from CFP-10 and EsxG (Rv0287) peptides from proteins identified in culture supernatants of *M. tuberculosis* (*13*). Peaks at 114 Da, 116 Da, and 117 Da represent peptides found in WT, *ΔesxB* and *ΔRv3877* culture supernatants. (**C**) Model of the *M. tuberculosis* ESX-1 secretion system. (mAg), mycolyl-arabinogalactan, (PG), peptidoglycan, (CM), cytoplasmic membrane.

that five CFP-10 paralogs (EsxJ, EsxK, EsxP, EsxM, and EsxW) end in "QILSS," which is similar to the "QALSS" found near the C terminus of CFP-10, but lack the terminal "MGF" required for CFP-10 secretion. EsxG ends in "ASTYTGF," substituting the critical L94 and M98 residues of CFP-10 with alanine and threonine, respectively. We would predict that these paralogs and their associated ESAT-6 paralogs would be secreted independently of ESX-1.

To determine this, we measured the levels of these proteins in culture supernatants from wild-type, *ΔRv3877*, and *ΔesxB M. tuberculosis* strains using quantitative mass spectrometry (*13*, *20*). Peptides from CFP-10 and ESAT-6, three ESAT-6 paralogs (EsxN, EsxL, and EsxO), and at least three CFP-10 paralogs (EsxG, EsxP or K, and EsxJ or W) (Fig. 3B, Table 1, and fig. S2) were present in wild-type supernatants, consistent with previous findings (*16*–*18*). Although peptides from CFP-10 and ESAT-6 were absent from supernatants from *ΔesxB* and *ΔRv3877* deletion *M. tuberculosis* strains (Fig. 3B), each of the other Esx proteins was secreted to wild-type levels (Fig. 3B, Table 1, and fig. S2). Thus, the C-terminal signal sequence possibly allows the ESX-1 system to discriminate between CFP-10 and its paralogs. Interestingly, five of these paralog pairs are embedded within loci with synteny to the ESX-1 region (*21*), raising the possibility that other ESX-1–like secretion systems function to secrete these Esx paralogs.

Alignment of CFP-10 protein sequences from other bacterial species that are secreted by homologous ESX-1 systems (*6*–*8*, *15*, *22*, *23*) reveals a notable stretch of conservation at the C terminus (Fig. 3A and fig. S3B). Because these residues do not play a structural role in the folded CFP-10/ESAT-6 dimer, the conservation at the C terminus suggests strongly that the mechanism of ESX-1 C-terminal signal sequence recognition has been conserved during bacterial evolution.

We propose the following model for the targeting and secretion of substrates by the ESX-1 secretion system in *M. tuberculosis* (Fig. 3C). ESAT-6 and CFP-10 fold and form a stable dimer in the cytoplasm before targeting. The C-terminal domain of CFP-10 is recognized by Rv3871, targeting both ESAT-6 and CFP-10. Substrate-bound Rv3871 interacts with Rv3870, a membrane-bound component of ESX-1, thus linking the cytosolic component of the system with membrane components. Because Rv3870 and Rv3871 are both members of the SpoIIIE/FtsK ATPase family, these proteins probably perform the work necessary to secrete ESX-1 substrates. This is reminiscent of Type IV secretion systems in Gram-negative bacteria, in which a membrane-bound SpoIIIE/FtsK–like ATPase functions to recognize an unstructured C-terminal signal sequence and direct the secreted substrate to the cytoplasmic membrane (*4*).

References and Notes

1. G. Blobel, B. Dobberstein, *J. Cell Biol.* **67**, 835 (1975).
2. W. Wickner, R. Schekman, *Science* **310**, 1452 (2005).
3. S. D. Emr, T. J. Silhavy, *Prog. Clin. Biol. Res.* **91**, 3 (1982).
4. P. J. Christie, K. Atmakuri, V. Krishnamoorthy, S. Jakubowski, E. Cascales, *Annu. Rev. Microbiol.* **59**, 451 (2005).
5. K. S. Ramamurthi, O. Schneewind, *Annu. Rev. Cell Dev. Biol.* **18**, 107 (2002).
6. K. M. Guinn *et al.*, *Mol. Microbiol.* **51**, 359 (2004).
7. T. Hsu *et al.*, *Proc. Natl. Acad. Sci. U.S.A.* **100**, 12420 (2003).
8. S. A. Stanley, S. Raghavan, W. W. Hwang, J. S. Cox, *Proc. Natl. Acad. Sci. U.S.A.* **100**, 13001 (2003).
9. G. G. Mahairas, P. J. Sabo, M. J. Hickey, D. C. Singh, C. K. Stover, *J. Bacteriol.* **178**, 1274 (1996).
10. M. A. Behr *et al.*, *Science* **284**, 1520 (1999).
11. P. S. Renshaw *et al.*, *EMBO J.* **24**, 2491 (2005).
12. P. S. Renshaw *et al.*, *J. Biol. Chem.* **277**, 21598 (2002).
13. Materials and methods are available as supporting material on *Science* Online.
14. J. J. Flanagan *et al.*, *J. Biol. Chem.* **278**, 18628 (2003).
15. S. E. Converse, J. S. Cox, *J. Bacteriol.* **187**, 1238 (2005).
16. J. Mattow *et al.*, *Electrophoresis* **24**, 3405 (2003).
17. I. Rosenkrands *et al.*, *Electrophoresis* **21**, 935 (2000).
18. R. L. Skjot *et al.*, *Infect. Immun.* **70**, 5446 (2002).
19. P. Brodin, I. Rosenkrands, P. Andersen, S. T. Cole, R. Brosch, *Trends Microbiol.* **12**, 500 (2004).

20. L. R. Zieske, *J. Exp. Bot.* **57**, 1501 (2006).
21. S. T. Cole *et al.*, *Nature* **393**, 537 (1998).
22. M. L. Burts, W. A. Williams, K. DeBord, D. M. Missiakas, *Proc. Natl. Acad. Sci. U.S.A.* **102**, 1169 (2005).
23. L. Y. Gao *et al.*, *Mol. Microbiol.* **53**, 1677 (2004).
24. E. Martz, *Trends Biochem. Sci.* **27**, 107 (2002).
25. W. R. Pearson, D. J. Lipman, *Proc. Natl. Acad. Sci. U.S.A.* **85**, 2444 (1988).
26. W. R. Pearson, *Methods Enzymol.* **183**, 63 (1990).

27. We thank H. Madhani and the Cox laboratory for the critical reading of this manuscript, and members of the Cox, A. Sil, and E. Brown laboratories for helpful discussion. This investigation was supported by NIH under Ruth L. Kirschstein National Research Service Award A105155 to P.A.C. This work was supported by NIH grants AI63302 and AI51667. J.S.C gratefully acknowledges the support of the Sandler Family Supporting Foundation and the W. M. Keck Foundation.

Supporting Online Material
www.sciencemag.org/cgi/content/full/313/5793/1632/DC1
Materials and Methods
SOM Text
Figs. S1 to S3
Tables S1 and S2

12 June 2006; accepted 13 July 2006
10.1126/science.1131167

An Alternative Bactericidal Mechanism of Action for Lantibiotic Peptides That Target Lipid II

Hester E. Hasper,[1] Naomi E. Kramer,[1,2] James L. Smith,[3] J. D. Hillman,[4] Cherian Zachariah,[5] Oscar P. Kuipers,[2] Ben de Kruijff,[1] Eefjan Breukink[1]*

Lantibiotics are polycyclic peptides containing unusual amino acids, which have binding specificity for bacterial cells, targeting the bacterial cell wall component lipid II to form pores and thereby lyse the cells. Yet several members of these lipid II–targeted lantibiotics are too short to be able to span the lipid bilayer and cannot form pores, but somehow they maintain their antibacterial efficacy. We describe an alternative mechanism by which members of the lantibiotic family kill Gram-positive bacteria by removing lipid II from the cell division site (or septum) and thus block cell wall synthesis.

In less than eight decades, Alexander Fleming's discovery of penicillin in 1928 catalyzed a multibillion-dollar pharmaceutical industry, spawned a plethora of antibiotics, and saved countless lives. However, human deaths stemming from infectious diseases have steadily reemerged in parallel with the rise of antibiotic-resistant pathogens, and medical researchers urgently need to develop new classes of antibiotics. Here, we report our findings on an alternative mechanism for bactericidal activity in members of the lantibiotic family of small peptides. No protein receptor is required for the bactericidal activity of this class of antibiotics. These molecules kill bacteria by sequestering the essential cell wall biosynthetic molecule lipid II from the sites where bacterial cell wall synthesis occurs.

The cell wall of bacteria forms a large scaffold of linear polymers of alternating amino sugars that are cross-linked via peptide bridges (the peptidoglycan layer). This layer is essential for survival. Its composition is quite uniform throughout the eubacteria, and consequently cell wall biosynthesis is an important target for antibiotics (*1*, *2*). One of the key molecules in bacterial peptidoglycan synthesis is lipid II, because it is essential for the transport of cell wall subunits across the bacterial cytoplasmic membrane (fig. S1A). This highly dynamic molecule is present in all eubacteria in relatively small amounts (*3*). Lipid II is assembled on the cytoplasmic side of the bacterial membrane and is composed of one peptidoglycan subunit linked via a pyrophosphate on a polyisoprenoid membrane anchor [GlcNAc-MurNAc-pentapeptide (fig. S1B)]. Subsequently, lipid II is transported across the plasma membrane, where it delivers its cargo to a multienzyme complex for polymerization and insertion into the preexisting cell wall (*4*).

The glycopeptide vancomycin binds specifically to the C-terminal D-Ala-D-Ala sequence of the pentapeptide of lipid II, thereby (i) preventing the binding of penicillin-binding proteins (PBPs) that are responsible for the polymerization and integration of the peptidoglycan subunits into the cell wall and (ii) consequently inhibiting cell wall synthesis, ultimately leading to cell death. The group of small molecules known as lantibiotics also targets lipid II but acts by distinct mechanisms (*5*). Members of this family of antimicrobial peptides are characterized by the posttranslational addition of lanthionine rings (*6*–*8*). The best-known lantibiotic, nisin (fig. S1C), contains five lanthionine rings and kills bacteria by targeted pore formation (*9*, *10*). Recent structural studies show that the lanthionine rings A and B form a baseball glove–like structure (the pyrophosphate cage) that binds the pyrophosphate of lipid II (*11*). This formation is followed by the assembly of nisin into a pore complex, together with lipid II, that has a stochiometry of eight nisins and four lipid IIs (*12*). Yet there are nisin mutants (in the hinge region comprising residues 20 to 22) that do not have the ability to form pores but are still potent antibiotics (*12*, *13*). Likewise, other related lantibiotics with similar A/B ring structures [for instance, mutacin 1140 (fig. S1D)] also do not form pores (fig. S2). However, these lantibiotics are very efficient bactericides as well (*14*). We have discovered that lantibiotics with an N-terminal pyrophosphate cage have an alternative lipid II–dependent bactericidal mechanism.

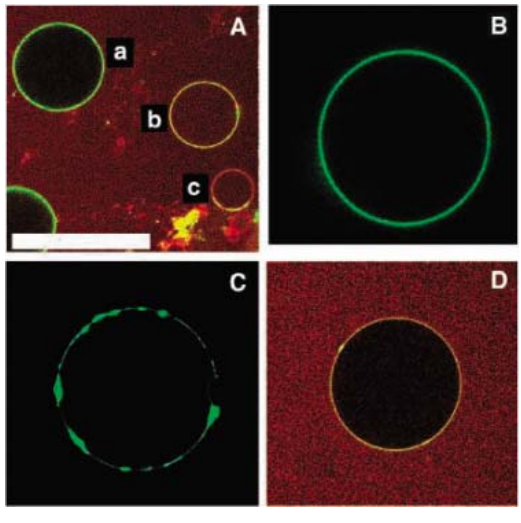

Fig. 1. Lipid II segregation caused by lantibiotics visualized by fluorescence microscopy. (**A**) Nisin in action. After the addition of 2 to 4 μl of a 2 mM nisin solution, the peptide started to diffuse into the field of view from the bottom right corner. This image is a snapshot of three vesicles that have either not yet encountered nisin (vesicle a), just encountered nisin (vesicle b), or already been exposed to nisin for some time (vesicle c). Scale bar, 60 μm. (**B**) GUV doped with NBD-labeled lipid II before treatment with mutacin 1140. (**C**) Mutacin 1140–induced segregation of NBD-labeled lipid II. (**D**) Snapshot of a GUV treated with mutacin 1140 just at the onset of the lipid II segregation; the interior remains black. The green fluorescence of the NBD-labeled lipid II and the red fluorescence of Texas Red were sequentially detected with the use of two lasers.

[1]Department of Biochemistry of Membranes, Bijvoet Center for Biomolecular Research, Institute of Biomembranes, Utrecht University, Padualaan 8, 3584 CH, Utrecht, Netherlands. [2]Department of Genetics, Groningen Biomolecular Sciences and Biotechnology Institute, University of Groningen, Post Office Box 14, 9750 AA, Haren, Netherlands. [3]Department of Biological Sciences, Post Office Box GY, Mississippi State University, Mississippi State, MS 39762, USA. [4]Oragenics Incorporated, 13700 Progress Boulevard, Alachua, FL 32615, USA. [5]Banyon Biomarkers, 12085 Research Drive, Alachua, FL 32615, USA.

*To whom correspondence should be addressed. E-mail: e.j.breukink@chem.uu.nl

We visualized the effect of nisin on giant unilamellar vesicles (GUVs) doped with fluorescently labeled lipid II. The fluorescence of the 7-nitrobenz-2-oxa-1,3-diazol-4-yl (NBD)–labeled lipid II was initially spread homogeneously over the GUV surface, and the fluorescence of the soluble marker Texas Red remained extracellular (Fig. 1A). After the addition of nisin, the GUVs first filled up with red fluorescence as a result of pore formation (Fig. 1), and the green fluorescence originating from NBD-labeled lipid II then clearly segregated in the membrane (Fig. 1). Thus, wild-type nisin caused the segregation of lipid II in model membranes after the formation of pores.

The addition of mutacin 1140 to NBD-labeled lipid II–doped GUVs (Fig. 1B) resulted in hot spots of lipid II fluorescence appearing within the membranes (Fig. 1C). Mutacin 1140 did not increase the permeability of the membrane, because red fluorescence was not seen inside the GUVs (Fig. 1D and fig. S2). A hinge-region mutant of nisin [(N20PM21P)-nisin] that is a potent bacterial killer but is unable to form pores (*12*, *13*) gave results similar to those of mutacin 1140 (fig. S3). Comparable fluorescent patches were observed on the GUVs (fig. S4), when fluorescently labeled nisin [fluorescein was attached to the C terminus, where it does not affect the activity of the lantibiotic (fig. S5)] was added to GUVs doped with unlabeled lipid II. Hence, the patches contained both the lantibiotics and lipid II. These results suggest that the sequestration of lipid II is involved in the mode of action of these lantibiotics.

Peptidoglycan synthesis of bacteria has been shown to take place at defined positions on the bacterial membrane. During cell division, large amounts of peptidoglycan are synthesized at the septum and, during cell elongation (in the case of a rod-shaped cell), peptidoglycan synthesis is organized in helical threads along the longitudal axis of the cell (*15*). This synthesis coincides with the localization of lipid II in vivo to the septum of *Bacillus subtilis* and in helical threads along the long axis of this bacterium, as visualized with fluorescently labeled vancomycin (*15*). If lipid II cannot colocalize with peptidoglycan synthesis, then cell wall formation is inhibited, and bacteria are killed.

We tested whether the lantibiotic-induced lipid II segregation seen in GUVs occurs in bacteria. As a marker for the location of lipid II in vivo, we used fluorescently labeled vancomycin as described in (*15*). Labeled vancomycin bound to GUVs only when they contained wild-type lipid II, and it did not cause any segregation (Fig. 2A), demonstrating that it did not change the localization of the randomly dispersed lipid II. Like the results described by Daniel and Errington (*15*), the vancomycin label clearly revealed pools of lipid II in the septum (Fig. 2, B and C), as well as in helical threads along the long axis of *Bacillus* cells. After the addition of fluorescently labeled nisin to these bacteria, a different lipid II distribution pattern was observed (Fig. 2, D and E). The fluorescence was absent from the septum (Fig. 2D), and the helical threads were not seen. Instead, the fluorescence originating from the nisin molecules appeared to be clustered in patches on the bacterial membranes, as in the observations in the GUVs. The effects were observed for more than 80% of the bacteria (fig. S6). Similar results were obtained with fluorescently labeled (N20PM21P)-nisin (fig. S7), and control experiments showed that, under the conditions used, the fluorescently labeled nisins bound only to lipid II (fig. S8). Similar patches could be observed upon treatment of *Lactococcus lactis* IL1403 with fluorescently labeled nisin, demonstrating that the lipid II sequestration by nisin was not limited to rod-shaped bacteria (fig. S9). These results demonstrate that nisin segregates lipid II into abnormal domains not only in vitro but also in vivo.

Our results provide an explanation for previously observed effects of staphylococcin T (a lantibiotic similar to mutacin 1140) on *Micrococcus* sp. (*16*), which may now be explained by an uncoupling between cell wall synthesis and membrane synthesis during cell division. Recently, it has been shown that lantibiotics similar to mutacin 1140 (such as gallidermin and epidermin) are able to form pores only in model membranes composed of short-chain phospholipids that form thin membranes (*17*). Their high level of antibacterial activity can now be explained by the sequestration mechanism described here.

Based on these experiments, we propose that nisin and a broad range of at least 10 other lantibiotics (*18*–*20*) having similar A/B ring structures displace lipid II from its functional location in Gram-positive bacteria. The lantibiotics bind to the pyrophosphate of lipid II, and their effect depends on the combination of the length of the peptide and the thickness of the lipid bilayer. Lantibiotics resembling nisin kill the bacteria primarily by forming pores together with lipid II. Those that bear the pyrophosphate cage, but are short and cannot span a bacterial bilayer to form pores, still remove lipid II from its functional location. This sequestering effect is a distinct mode of bactericidal activity that is currently known only in the lantibiotics which does not appear to have any known candidate resistance mechanisms.

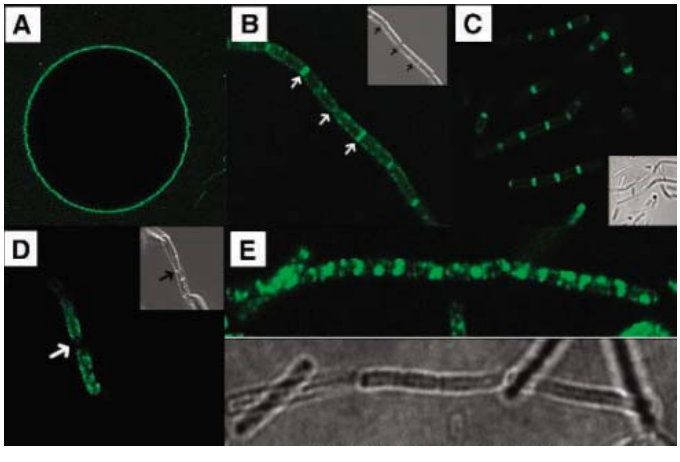

Fig. 2. Nisin segregates lipid II into nonphysiological domains in vivo. (**A**) GUV containing 0.5 mole percent wild-type lipid II 15 min after the addition of fluorescently labeled vancomycin. (**B**) *B. megaterium* cells that were incubated for 10 min with labeled vancomycin (2 μg/ml). The arrows point at newly formed division sites or older exemplars. (**C**) *B. subtilis* stained with fluorescent vancomycin (4 μg/ml). (**D**) *B. megaterium* cells after incubation for 10 min with fluorescein-labeled nisin (0.5 μg/ml). The arrow marks where the bacterium has already divided. (**E**) *B. subtilis* cells after incubation with fluorescein-labeled nisin (4 μg/ml). The bottom image in (E) and the insets in (B) to (D) show Nomarski images.

References and Notes

1. A. L. Koch, *Clin. Microbiol. Rev.* **16**, 673 (2003).
2. C. H. Walsh, *Nat. Rev. Microbiol.* **1**, 65 (2003).
3. Y. van Heijenoort, M. Gomez, M. Derrien, J. Ayala, J. van Heijenoort, *J. Bacteriol.* **174**, 3549 (1992).
4. W. Vollmer, J. V. Holtje, *Curr. Opin. Microbiol.* **4**, 625 (2001).
5. E. Breukink, B. de Kruijff, *Nat. Rev. Drug Discovery* **5**, 321 (2006).
6. B. Li *et al.*, *Science* **311**, 1464 (2006).
7. L. Xie *et al.*, *Science* **303**, 679 (2004).
8. C. Chatterjee, M. Paul, L. L. Xie, W. A. van der Donk, *Chem. Rev.* **105**, 633 (2005).
9. E. Breukink *et al.*, *Science* **286**, 2361 (1999).
10. H. Brotz *et al.*, *Mol. Microbiol.* **30**, 317 (1998).
11. S. T. D. Hsu *et al.*, *Nat. Struct. Mol. Biol.* **11**, 963 (2004).
12. H. E. Hasper, B. de Kruijff, E. Breukink, *Biochemistry* **43**, 11567 (2004).
13. I. Wiedemann *et al.*, *J. Biol. Chem.* **276**, 1772 (2001).
14. H. Morency, M. Mota-Meira, G. LaPointe, C. Lacroix, M. C. Lavoie, *Can. J. Microbiol.* **47**, 322 (2001).
15. R. A. Daniel, J. Errington, *Cell* **113**, 767 (2003).
16. B. Furmanek *et al.*, *J. Appl. Microbiol.* **87**, 856 (1999).
17. R. R. Bonelli, T. Schneider, H. G. Sahl, I. Wiedemann, *Antimicrob. Agents Chemother.* **50**, 1449 (2006).
18. P. A. Wescombe, J. R. Tagg, *Appl. Environ. Microbiol.* **69**, 2737 (2003).
19. T. Stein *et al.*, *J. Bacteriol.* **184**, 1703 (2002).
20. O. McAuliffe, R. P. Ross, C. Hill, *FEMS Microbiol. Rev.* **25**, 285 (2001).

21. H.E.H. and N.E.K. were supported by the Nederlandse Organisatie voor Wetenschappelijk and the Onderzoek Stichting voor de Technische Wetenschappen (grant 349-5257). We thank P. van den Bogaard and D. Sakharov for their help with the confocal fluorescence experiments.

Supporting Online Material

www.sciencemag.org/cgi/content/full/313/5793/1636/DC1
Materials and Methods
Figs. S1 to S9
References

11 May 2006; accepted 26 July 2006
10.1126/science.1129818

The Dynamic Energy Landscape of Dihydrofolate Reductase Catalysis

David D. Boehr, Dan McElheny,* H. Jane Dyson, Peter E. Wright†

We used nuclear magnetic resonance relaxation dispersion to characterize higher energy conformational substates of *Escherichia coli* dihydrofolate reductase. Each intermediate in the catalytic cycle samples low-lying excited states whose conformations resemble the ground-state structures of preceding and following intermediates. Substrate and cofactor exchange occurs through these excited substates. The maximum hydride transfer and steady-state turnover rates are governed by the dynamics of transitions between ground and excited states of the intermediates. Thus, the modulation of the energy landscape by the bound ligands funnels the enzyme through its reaction cycle along a preferred kinetic path.

It has long been recognized that dynamic fluctuations in protein conformation play a central role in enzyme catalysis (*1*–*3*). Protein dynamics are implicated in events such as substrate or cofactor binding and product release, and the chemical event itself involves an inherently dynamic process, with changes in atomic coordinates required along the reaction coordinate (*4*). Although there is considerable evidence from both theory and experiment that many enzymes are inherently flexible, the fundamental mechanisms by which protein fluctuations couple to catalytic function remain poorly understood.

Escherichia coli dihydrofolate reductase (DHFR) has been used extensively as a model enzyme for investigating the relations between structure, dynamics, and function. Theoretical and experimental investigations suggest that protein fluctuations play a direct role in catalysis by DHFR [see (*5*) for a recent review]. The enzyme catalyzes the reduction of 7,8-dihydrofolate (DHF) to 5,6,7,8-tetrahydrofolate (THF) by using reduced nicotinamide adenine dinucleotide phosphate (NADPH) as a cofactor. The kinetic mechanism involves rebinding of NADPH to assist the release of the THF product. The enzyme (E) cycles through five major intermediates: E:NADPH, E:NADPH:DHF, E:NADP$^+$:THF, E:THF, and E:NADPH:THF (*6*) (Fig. 1A). The structures of all of the kinetic intermediates, or models of the intermediates, have been determined by x-ray crystallography, and the conformational changes that occur during the catalytic cycle have been delineated (*7*, *8*). The major sites of conformational change include the active-site loop (residues 9 to 24, termed the Met^{20} loop) and the substrate-binding pocket (*7*) (Fig. 1B). In the holoenzyme E:NADPH and the Michaelis complex E:NADPH:DHF (modeled by the ternary E:NADP$^+$:folate complex), the Met^{20} loop adopts a closed conformation, where it packs against the nicotinamide ring of the cofactor bound within the active site. In the three product complexes, the Met^{20} loop adopts an occluded conformation, where it sterically hinders the nicotinamide ring from binding in the active site; therefore, the nicotinamide ring is outside the pocket in these complexes. The substrate-binding pocket undergoes a similar transition, closing more tightly when both substrate and cofactor are present and opening to release products (*7*).

Protein dynamics can be evaluated experimentally by nuclear magnetic resonance (NMR) spin relaxation techniques (*9*). Carr-Purcell-Meiboom-Gill (CPMG)–based R_2 relaxation dispersion experiments monitor motion on the μs to ms time scale that is generally the most relevant for protein conformational change (*10*). Through these methods, the transverse relaxation rate, R_2, can be decomposed into R_{ex}, the contribution from exchange between different conformations, and R_0, all other contributions (*9*). For two-site chemical exchange between a ground state (A) and an excited state (B), R_2 relaxation dispersion is a function of the exchange rate constant k_{ex} ($k_{ex} = k_{A\rightarrow B} + k_{B\rightarrow A}$), the populations of states A and B (p_A and p_B, respectively), and the chemical shift difference between states A and B ($\Delta\omega$) (*11*), thus giving information regarding the kinetics and thermodynamics of protein motion (*12*–*15*) and providing insight into the structure of the higher energy state (*13*, *15*, *16*).

The ^{15}N R_2 relaxation dispersion measurements for the Michaelis complex model E:NADP$^+$:folate (*15*) indicated that many of the residues that exhibit exchange contributions to relaxation are directly or indirectly associated with the Met^{20} loop (Fig. 2A). These residues show characteristic chemical shift differences between closed and occluded complexes, and their resonances have been previously categorized as active site loop conformation markers (*17*). Likewise, chemical shift perturbation studies identified cofactor-binding and substrate- or

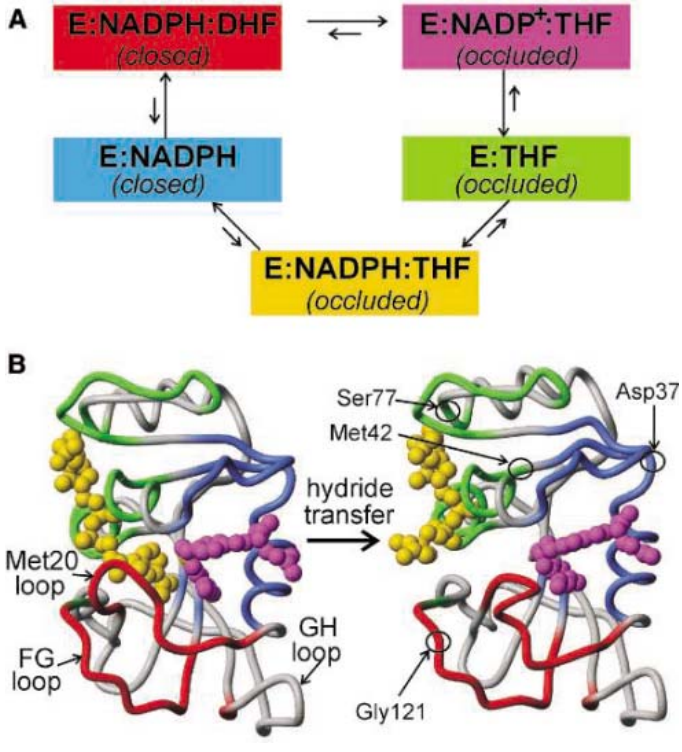

Fig. 1. Conformational changes during the DHFR catalytic cycle. (**A**) Met^{20} loop conformations for each complex in the catalytic cycle (*8*). The complexes are shown in distinctive colors that are used in Fig. 4. (**B**) Structures of E:NADP$^+$:folate [left, Protein Data Bank (PDB) 1RX2 (*7*)] and E:NADPH:5,10-dideazaTHF (ddTHF) [right, PDB 1RX6 (*7*)], illustrating the conformational changes that occur upon hydride transfer. In E:NADP$^+$:folate, a model for the Michaelis complex E:NADPH:DHF, the Met^{20} loop is in a closed conformation, and the folate-cleft width, measured between the van der Waals contact surfaces of Ile^{50} and Leu^{28}, is 17.9 Å. In E:NADPH:ddTHF, a model for the product ternary complex E:NADP$^+$:THF, the folate cleft opens by 0.8 Å, and the Met^{20} loop is in an occluded conformation, restricting cofactor access to the active site. Residues that define the active site loop conformation, substrate-/product-binding, and cofactor-binding markers (*17*) are colored red, blue, and green, respectively. The bound cofactor is colored gold, and folate and ddTHF are shown in magenta. The residues for which dispersion data are shown in Fig. 2 are identified by open circles.

Department of Molecular Biology and Skaggs Institute for Chemical Biology, Scripps Research Institute, 10550 North Torrey Pines Road, La Jolla, CA 92037, USA.

*Present address: Division of Biological Sciences, University of Chicago, Chicago, IL 60637, USA.

†To whom correspondence should be addressed. E-mail: wright@scripps.edu

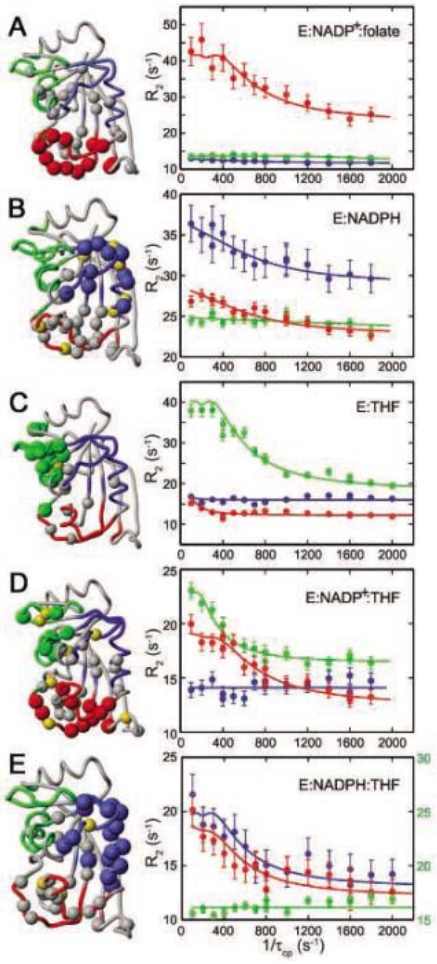

Fig. 2. Relaxation dispersion data for each intermediate in the catalytic cycle of DHFR. (Left) Model structures for various intermediates of the DHFR catalytic cycle (*7*). The backbone is colored red, green, or blue as in Fig. 1B. Residues for which conformational exchange is observed are indicated with spheres, which are colored red, green, and blue for resonances that report on active site loop conformation, cofactor binding, and substrate/product binding, respectively, and gray for resonances that are not identified with any of these categories. Yellow indicates resonances that show broadening, but for which data quality was insufficient to obtain reliable R_2 relaxation dispersion results. (Right) Representative ^{15}N R_2 relaxation dispersion curves for each complex. A full set of data for all residues that show detectable relaxation dispersion is included (figs. S1 to S5). Error bars indicate estimated uncertainties in R_2 (*15*). (**A**) E:NADP$^+$:folate (PDB 1RX2) and NMR data at 303 K. (**B**) E:NADPH (PDB 1RX1) and NMR data at 284 K. (**C**) E:THF (PDB 1RX5) and NMR data at 300 K. (**D**) E:NADP$^+$:THF (PDB 1RX4) and NMR data at 300 K. (**E**) E:NADPH:THF (PDB 1RX6) and NMR data at 300 K. Relaxation dispersion data were collected and analyzed at two external magnetic field strengths (^1H 500 MHz and 800 MHz), but only 800 MHz data are shown for clarity. Red curves report on the active site loop conformation marker Gly^{121}; blue curves, on the substrate-/product-binding marker Asp^{37}; and green curves, on the cofactor-binding marker Ser^{77} [(A) to (C) and (E)] or Met^{42} (D). The green curve for Ser^{77} in (E) (green) has been offset for clarity (right axis). This figure was generated in part by using MOLMOL (*27*).

product-binding (substrate-/product-binding) marker resonances associated with residues that cluster around the cofactor- and substrate-binding pockets, respectively (*17*) (Fig. 1B). A comparison of the dynamic chemical shift differences ($\Delta\omega$ values) determined from fits of the R_2 relaxation dispersion data to the equilibrium chemical shift differences ($\Delta\delta$ values) between the closed complex E:NADP$^+$:folate and the occluded complex E:DHNADPH:folate showed a remarkable linear correlation (*15*). Thus, the higher energy state contributing to R_2 relaxation in the closed E:NADP$^+$:folate complex represents an occluded conformation similar to that found in the E:NADP$^+$:THF product ternary complex.

A complete set of ^{15}N and ^1H R_2 relaxation dispersion data have now been obtained for DHFR complexes that represent all of the kinetic intermediates populated in the steady-state catalytic cycle. Dispersion data measured at two frequencies were fitted to the general two-site exchange equations; the methods, dispersion curves, and fitted parameters for all complexes are provided (tables S1 to S4 and figs. S1 to S5). Some of these data are shown in Figs. 2 and 3.

Analysis of amide ^{15}N and ^1H R_2 relaxation dispersion measurements for the holoenzyme E:NADPH revealed exchange processes for many residues located in or around the substrate binding site (Fig. 2B). Dispersive behavior was also observed for several residues in the active site loop and the loop (residues 116 to 132) between β strands F and G (the FG loop), but no relaxation dispersion was seen for residues in the cofactor-binding site. The localization of the residues showing exchange contributions to relaxation around the substrate-binding pocket suggests that the higher energy conformation sampled by E:NADPH plays an important role in capturing the substrate. Indeed, there is a strong linear correlation between the $\Delta\omega$ values derived from the relaxation dispersion curves and the $\Delta\delta$ values derived from the chemical shift differences between E:NADPH and E:NADPH:THF, or between E:NADPH and E:NADP$^+$:folate, representing the previous step or the next step in the cycle, respectively (Fig. 3A). This result implies that the E:NADPH complex samples a higher energy substate in which the empty substrate-/product-binding pocket adopts a conformation similar to that of the ligand-bound state. A similar observation has been reported for ribonuclease A (RNaseA): As a result of conformational fluctuations, the free enzyme samples a higher energy state whose structure resembles the ligand-bound form (*18*). Although many residues in the Met^{20} and FG loops experience exchange contributions, the derived $\Delta\omega$ values do not correlate with the $\Delta\delta$ values between the closed and the occluded conformations (fig. S6); the active site loop conformation in the excited state is currently unknown.

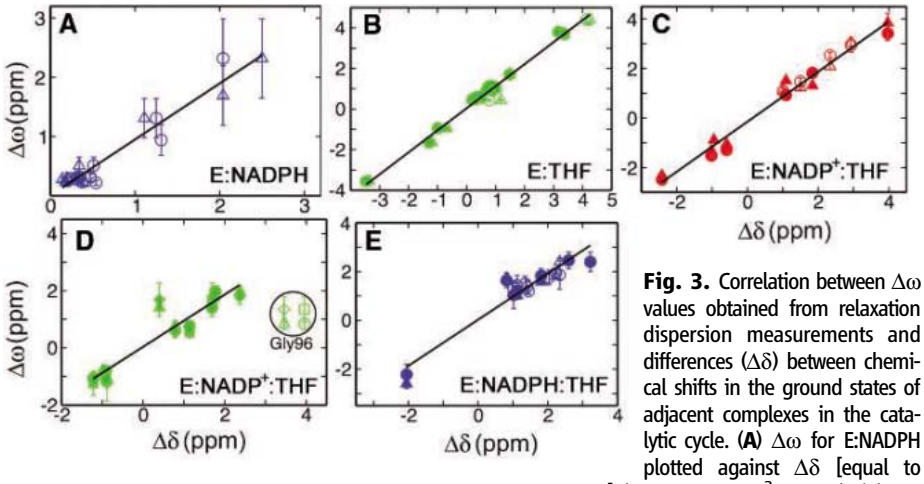

Fig. 3. Correlation between $\Delta\omega$ values obtained from relaxation dispersion measurements and differences ($\Delta\delta$) between chemical shifts in the ground states of adjacent complexes in the catalytic cycle. (**A**) $\Delta\omega$ for E:NADPH plotted against $\Delta\delta$ [equal to $\delta_{(E:NADPH)} - \delta_{(E:NADPH:THF)}$, circles; or $\delta_{(E:NADPH)} - \delta_{(E:NADP^+:folate)}$, triangles] (slope = 0.95, $R^2 = 0.97$); (**B**) $\Delta\omega$ for E:THF plotted against $\Delta\delta$ [equal to $\delta_{(E:THF)} - \delta_{(E:NADP^+:THF)}$, circles; or $\delta_{(E:THF)} - \delta_{(E:NADPH:THF)}$, triangles] (slope = 1.1, $R^2 = 0.99$); (**C**) $\Delta\omega$ for E:NADP$^+$:THF plotted against $\Delta\delta$ [$\delta_{(E:NADP^+:THF)} - \delta_{(NADP^+:folate)}$] by using 10 mM (circles) and 50 mM (triangles) NADP$^+$ (slope = 1.0, $R^2 = 0.99$); and (**D**) $\Delta\omega$ for E:NADP$^+$:THF plotted against $\Delta\delta$ [$\delta_{(E:NADP^+:THF)} - \delta_{(E:THF)}$] by using 10 mM (circles) or 50 mM (squares) NADP$^+$, or plotted against $\Delta\delta$ [$\delta_{(E:NADP^+:THF)} - \delta_{(E:folate)}$] by using 10 mM (triangles) or 50 mM (diamonds) NADP$^+$ (slope = 0.91, $R^2 = 0.94$). The data points for the Gly^{96} amide, which hydrogen-bonds directly to the cofactor, are enclosed in a circle and were not included when determining the line of best fit. (**E**) $\Delta\omega$ for E:NADPH:THF plotted against $\Delta\delta$ [$\delta_{(E:NADPH:THF)} - \delta_{(E:NADPH)}$] (slope = 0.97, $R^2 = 0.98$). Residues are colored red, green, and blue to indicate residues reporting on the active site loop conformation, cofactor binding, and substrate/product binding, respectively. Solid symbols indicate that the sign of $\Delta\omega$ could be determined from a comparison of HSQC and heteronuclear multiple-quantum coherence spectra at an external magnetic field strength of ^1H 500 MHz (*28*), and open symbols indicate residues where only the absolute values for $\Delta\omega$ and $\Delta\delta$ are reported. Error bars indicate uncertainties in $\Delta\omega$ estimated by Monte Carlo simulation (*15*).

In direct contrast to the E:NADPH complex, residues surrounding the cofactor-binding cleft display exchange contributions to relaxation in the E:THF complex (Fig. 2C). A linear correlation is observed between $\Delta\omega$ and $\Delta\delta_{(E:THF\ -\ E:NADP^+:THF)}$ or $\Delta\delta_{(E:THF\ -\ E:NADPH:THF)}$ values (Fig. 3B), suggesting that the higher energy conformation contributing to ^{15}N R_2 relaxation in E:THF resembles the product ternary complexes. Any relaxation dispersion observed for residues lining the substrate-binding pocket or in the FG loop can generally be traced to local differences in conformation between E:THF and product ternary complexes (table S2 and fig. S7).

In the E:$NADP^+$:THF complex, conformational changes are observed in the active site loops and the ligand-binding pockets (Fig. 2D). The $\Delta\omega$ values for residues surrounding the cofactor-binding cleft and the active site loops correlate with different $\Delta\delta$ values (Fig. 3, C and D). The $\Delta\omega$ values for residues in the active site loops correlate to $\Delta\delta_{(E:NADP^+:THF\ -\ E:NADP^+:folate)}$ (Fig. 3C), showing that the occluded E:$NADP^+$:THF complex samples a higher energy state in which the active site loops are in a closed conformation, resembling the conformation of the E:DHF:NADPH Michaelis complex (modeled by E:$NADP^+$:folate) that immediately precedes it in the catalytic cycle. For many of the residues surrounding the cofactor-binding cleft, a linear correlation is observed between $\Delta\omega$ and $\Delta\delta_{(E:NADP^+:THF\ -\ E:folate)}$ and/or $\Delta\delta_{(E:NADP^+:THF\ -\ E:THF)}$ (Fig. 3D), revealing the presence of an additional excited state in which the conformation of the adenosine-binding site is similar to that in the binary E:THF product complex. The excited protein substates do not reflect physical dissociation of cofactor or chemical changes. The population of E:THF in equilibrium with the ternary product complex E:$NADP^+$:THF is estimated to be 0.4% on the basis of rate constants determined from pre–steady-state analysis (*6*), whereas the excited state population from relaxation dispersion experiments is much larger (p_B > 2.3%). Repeat experiments at fivefold higher $NADP^+$ concentration, where the population of the E:THF complex is estimated to be ~0.08%, showed identical R_2 relaxation dispersion for the residues surrounding the adenosine-binding site (table S3), which rules out cofactor dissociation as the origin of the exchange contributions to the R_2 relaxation rates. In addition, the x-ray structures (*7*) show that the Gly^{96} amide forms a hydrogen bond to the phosphate group of the cofactor, which leads to a large change in the ^{15}N chemical shift [3.5 to 4.0 parts per million (ppm)] upon binding of $NADP^+$ to the E:THF or E:folate complexes. However, the $\Delta\omega$ for Gly^{96} is much smaller (<1.35 ppm) (Fig. 3D), implying that the hydrogen bond remains largely intact and that conformational exchange is not modulated by cofactor dissociation. The closed excited-state conformation of the active site loops also cannot be a consequence of hydride transfer, because the rate constant of the back reaction is too slow at this pH (~0.03 s^{-1}) for this process to contribute measurably to R_2 relaxation dispersion (*6*).

The ground-state conformations of E:NADPH:THF and E:$NADP^+$:THF are very similar, as evidenced by their nearly identical ^{15}N heteronuclear single-quantum coherence (HSQC) spectra, yet the two complexes exhibit very different R_2 relaxation dispersion. The E:NADPH:THF complex (Fig. 2E) exhibits more pronounced dispersive behavior for residues surrounding the substrate-/product-binding

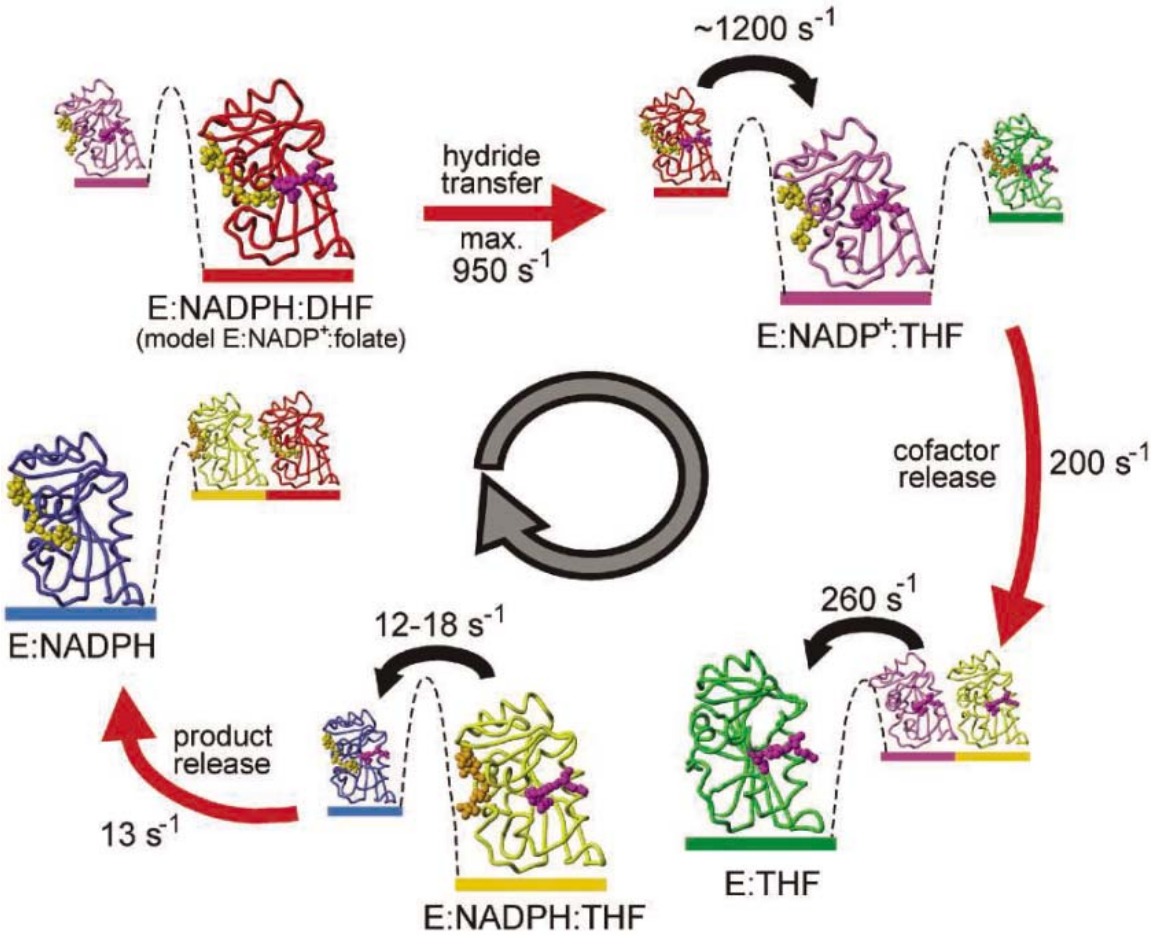

Fig. 4. The dynamic energy landscape of DHFR catalysis. Ground state (larger) and higher energy (smaller) structures of each intermediate in the cycle, modeled on the published x-ray structures (*7*), are shown color-coded according to the scheme in Fig. 1A, with NADPH and $NADP^+$ shown in gold and substrate, product, and analogs shown in magenta. For each intermediate in the catalytic cycle, the higher energy conformations detected in the relaxation dispersion experiments resemble the ground-state conformations of adjacent intermediates; their interconversion rates, also obtained from the relaxation dispersion experiments, are shown with black arrows. Rate constants for the interconversion between the complexes, measured by pre–steady-state enzyme kinetics at 298 K, pH = 6 (*6*) are indicated with red arrows. R_2 relaxation dispersion measurements were made at pH = 6.8 (E:$NADP^+$:folate) or pH = 7.6 (E:NADPH:THF, E:$NADP^+$:THF, E:NADPH, and E:THF) at 281 K (E:NADPH), 300 K (E:NADPH:THF, E:$NADP^+$:THF, and E:THF), or 303 K (E:$NADP^+$:folate).

pocket and no conformational exchange for residues in the cofactor-binding cleft. The Δω values for most residues surrounding the substrate-/product-binding pocket correlate strongly with $\Delta\delta_{(E:NADPH:THF\ -\ E:NADPH)}$ (Fig. 3E). Again, this cannot be due to the physical dissociation of THF from the complex, because the population of the excited-state ($p_B > 1.9\%$) is substantially greater than the population of the binary E:NADPH complex in equilibrium with E:NADPH:THF (population ~ 0.12%). Moreover, repeating the experiment at a THF concentration three times higher (estimated population of E:NADPH ~ 0.04%) yielded nearly identical results (table S4). Many residues associated with the active site loops also display conformational exchange, yet the derived Δω values for most of these do not correlate with an occluded-to-closed conformational change. This result provides further evidence that we are not observing physical dissociation of product THF to form the closed E:NADPH complex but are monitoring fluctuations into a higher energy conformation of E:NADPH:THF that resembles one without product bound. The higher energy substates sampled by E:NADPH and E:NADPH:THF may be similar, because Δω values for resonances showing dispersion in both the binary and the ternary complex display a linear correlation (fig. S11).

These results can be placed in the context of the catalytic cycle (Fig. 4). The higher energy conformations that we observe in the R_2 relaxation dispersion experiments appear to play a direct role in catalysis. In all five intermediates, there is conformational exchange on a μs-ms time scale between the ground-state structure and one or two excited states that resemble the ground state of the preceding and/or the following intermediate in the catalytic cycle. The binary complexes E:NADPH and E:THF sample excited-state conformations that facilitate binding of substrate/product and cofactor, respectively. Thus, binding of ligands to the enzyme appears to occur by a conformational selection (*19*, *20*) or selected-fit (*21*) mechanism, rather than by the induced-fit mechanism (*22*) that has been traditionally invoked to explain substrate-induced conformational change. An underlying tenet of the induced-fit model is conformational homogeneity, with binding occurring by a sequential mechanism; the ligand binds to the enzyme and induces a conformational change that increases the complementarity between ligand and protein. However, most proteins are structurally heterogeneous; their energy landscapes are rugged, and a number of conformational substates lie close in energy to the ground state and are populated through thermal fluctuations (*23*). In the conformational selection model, a small population of a minor conformational substate resembling the ligand-bound or induced conformation is already present in solution, in a preexisting equilibrium with the major ligand-free state. Ligand binds to the minor substate, causing a shift in the equilibrium such that the ligand-bound conformation becomes the new major substate (*19*, *20*). The experimentally determined bimolecular rate constant for binding of substrate to E:NADPH ($4 \times 10^7\ M^{-1}\ s^{-1}$) (*6*) is consistent with a mechanism that invokes the diffusion-controlled association ($\sim 10^9\ M^{-1}\ s^{-1}$) of substrate with a small population ($p_B = 2\%$) of a binding-competent excited state of the E:NADPH holoenzyme.

Our results suggest that ligand release also occurs through higher energy substates. The excited state structures of E:$NADP^+$:THF and E:NADPH:THF resemble conformations in which the cofactor- or product-binding pocket is empty, even though ligand dissociation has not occurred. Fluctuations that populate these higher energy substates effectively prepare the enzyme for ligand dissociation; this process can be viewed as the opposite to conformational selection and ligand binding. Indeed, Δω values for amides in the substrate-/product- and cofactor-binding pockets of the complementary binary and ternary complexes E:NADPH/E:NADPH:THF and E:(THF or folate)/E:$NADP^+$:THF, respectively, are correlated (fig. S11), suggesting that exchange contributions to relaxation arise from similar, but opposing, processes.

Transitions between the conformational substates occur at rates, determined from the R_2 relaxation dispersion experiments, that are directly relevant to DHFR catalysis. Comparison with the rate constants determined from pre–steady-state kinetics (*6*) provides strong evidence that the rate of progression through the various steps of the reaction cycle is governed by the dynamics of the conformational fluctuations between the ground and the excited states of the kinetic intermediates (Fig. 4). Thus, the first-order rate constant for release of THF from the E:NADPH:THF complex ($12.5\ s^{-1}$ at 298 K), which is the rate-determining step at physiological pH, is very similar to the ground-to-excited state conformational exchange rate constant (12 to $18\ s^{-1}$ at 300 K) that we measure for the residues surrounding the substrate-/product-binding pocket. This argues strongly that product dissociation occurs from the excited state. Maximum substrate turnover can also be rationalized in the context of this model. Subsequent to hydride transfer, which is effectively instantaneous relative to the rate of protein conformational change (*24*), the enzyme is converted from the closed E:NADPH:DHF Michaelis complex to a closed E:$NADP^+$:THF complex. The kinetic rate constant for the conformational change from the higher energy closed state to the occluded ground state of E:$NADP^+$:THF ($k \sim 1200\ s^{-1}$ at 300 K) is very similar to the pH-independent rate constant for hydride transfer ($k_{hyd} = 950\ s^{-1}$ at 298 K) (*6*). Thus, both the product release and the chemical transformation rate constants are largely determined by the exchange rate constants between substates that are thermally populated within the conformational ensemble; that is, the maximum hydride transfer rate and the steady-state turnover rate are dictated by physical changes within the energy landscape of the enzyme. A correlation between the overall turnover rate and protein motions has also been described for the enzyme cyclophilin (*25*).

Because R_2 relaxation dispersion experiments can generally only characterize higher energy conformations that make up at least 1 to 2% of the ensemble, there may be additional excited states that are inaccessible to the technique. However, the excited-state conformations that we observe, together with the ground-state conformation, will constitute the lowest-energy members of the conformational ensemble of each intermediate. These results imply that the most functionally relevant conformations also possess the lowest energy of all potential conformations. In this view, ligands dictate not only the ground-state conformation but also the most accessible higher energy substates. As ligands change, through binding or dissociation processes or through chemistry, the energy landscape and the populations of the accessible states change in response. Thus, the dynamic energy landscape (*26*) efficiently funnels the enzyme through its catalytically competent conformations along a preferred kinetic path, where the number and heights of the energetic barriers between consecutive conformations have been minimized.

References and Notes

1. G. G. Hammes, *Nature* **204**, 342 (1964).
2. G. Careri, P. Fasella, E. Gratton, *Annu. Rev. Biophys. Bioeng.* **8**, 69 (1979).
3. B. Gavish, M. M. Werber, *Biochemistry* **18**, 1269 (1979).
4. W. R. Cannon, S. F. Singleton, S. J. Benkovic, *Nat. Struct. Biol.* **3**, 821 (1996).
5. J. R. Schnell, H. J. Dyson, P. E. Wright, *Annu. Rev. Biophys. Biomol. Struct.* **33**, 119 (2004).
6. C. A. Fierke, K. A. Johnson, S. J. Benkovic, *Biochemistry* **26**, 4085 (1987).
7. M. R. Sawaya, J. Kraut, *Biochemistry* **36**, 586 (1997).
8. R. P. Venkitakrishnan *et al.*, *Biochemistry* **43**, 16046 (2004).
9. A. G. Palmer III, *Chem. Rev.* **104**, 3623 (2004).
10. J. P. Loria, M. Rance, A. G. Palmer, *J. Am. Chem. Soc.* **121**, 2331 (1999).
11. M. Tollinger, N. R. Skrynnikov, F. A. Mulder, J. D. Forman-Kay, L. E. Kay, *J. Am. Chem. Soc.* **123**, 11341 (2001).
12. F. A. Mulder, A. Mittermaier, B. Hon, F. W. Dahlquist, L. E. Kay, *Nat. Struct. Biol.* **8**, 932 (2001).
13. D. M. Korzhnev *et al.*, *Nature* **430**, 586 (2004).
14. M. Wolf-Watz *et al.*, *Nat. Struct. Mol. Biol.* **11**, 945 (2004).
15. D. McElheny, J. R. Schnell, J. C. Lansing, H. J. Dyson, P. E. Wright, *Proc. Natl. Acad. Sci. U.S.A.* **102**, 5032 (2005).
16. J. Evenas, A. Malmendal, M. Akke, *Structure* **9**, 185 (2001).
17. M. J. Osborne, R. P. Venkitakrishnan, H. J. Dyson, P. E. Wright, *Protein Sci.* **12**, 2230 (2003).
18. H. Beach, R. Cole, M. L. Gill, J. P. Loria, *J. Am. Chem. Soc.* **127**, 9167 (2005).
19. C. J. Tsai, S. Kumar, B. Y. Ma, R. Nussinov, *Protein Sci.* **8**, 1181 (1999).
20. H. R. Bosshard, *News Physiol. Sci.* **16**, 171 (2001).
21. C. Wang, N. Karpowich, J. F. Hunt, M. Rance, A. G. Palmer, *J. Mol. Biol.* **342**, 525 (2004).
22. D. E. Koshland, *Proc. Natl. Acad. Sci. U.S.A.* **44**, 98 (1958).
23. H. Frauenfelder, F. Parak, R. D. Young, *Annu. Rev. Biophys. Biophys. Chem.* **17**, 451 (1988).

24. S. Hammes-Schiffer, S. J. Benkovic, *Annu. Rev. Biochem.* **75**, 519 (2006).
25. E. Z. Eisenmesser *et al.*, *Nature* **438**, 117 (2005).
26. S. Kumar, B. Y. Ma, C. J. Tsai, N. Sinha, R. Nussinov, *Protein Sci.* **9**, 10 (2000).
27. R. Koradi, M. Billeter, K. Wüthrich, *J. Mol. Graph.* **14**, 51 (1996).
28. N. R. Skrynnikov, F. W. Dahlquist, L. E. Kay, *J. Am. Chem. Soc.* **124**, 12352 (2002).

29. We thank J. Chung and G. Kroon for assistance with the NMR experiments, L. Tennant for technical assistance, and S. Benkovic for valuable discussions. This work was supported by NIH grants GM56879 and GM75995 and by the Skaggs Institute for Chemical Biology. D.D.B. was a recipient of a Canadian Institutes of Health Research postdoctoral fellowship. D.M. was supported by a postdoctoral fellowship from NIH.

Supporting Online Material
www.sciencemag.org/cgi/content/full/313/5793/1638/DC1
Materials and Methods
Figs. S1 to S11
Tables S1 to S4

22 May 2006; accepted 25 July 2006
10.1126/science.1130258

Imaging Intracellular Fluorescent Proteins at Nanometer Resolution

Eric Betzig,[1,2]*† George H. Patterson,[3] Rachid Sougrat,[3] O. Wolf Lindwasser,[3] Scott Olenych,[4] Juan S. Bonifacino,[3] Michael W. Davidson,[4] Jennifer Lippincott-Schwartz,[3] Harald F. Hess[5]*

We introduce a method for optically imaging intracellular proteins at nanometer spatial resolution. Numerous sparse subsets of photoactivatable fluorescent protein molecules were activated, localized (to ~2 to 25 nanometers), and then bleached. The aggregate position information from all subsets was then assembled into a superresolution image. We used this method—termed photoactivated localization microscopy—to image specific target proteins in thin sections of lysosomes and mitochondria; in fixed whole cells, we imaged vinculin at focal adhesions, actin within a lamellipodium, and the distribution of the retroviral protein Gag at the plasma membrane.

Transfected cells expressing fluorescent proteins (*1*) contain information that is accurate at the molecular level about the spatial organization of the target proteins to which they are bound. However, the best resolution that can be obtained by diffraction-limited conventional optical techniques is coarser than the molecular level by two orders of magnitude. Great progress has been made with superresolution methods that penetrate beyond this limit, such as near field (*2*), stimulated emission depletion (*3*), structured illumination (*4*, *5*), and reversible saturable optical fluorescence transitions microscopy (*6*), but the goal remains a fluorescence technique capable of achieving resolution closer to the molecular scale.

Early results (*7*) in single-molecule microscopy (*8*) and the spatiospectral isolation of individual exciton recombination sites in a semiconductor quantum well (*9*) led to a proposal for a means of molecular resolution fluorescence microscopy a decade ago (*10*). In brief, individual molecules densely packed within the resolution limit of a given instrument [as defined by its point-spread function (PSF)] are first isolated from one another on the basis of one or more distinguishing optical characteristics. Each molecule is then localized to much higher precision by determining its center of fluorescence emission through a statistical fit of the ideal PSF to its measured photon distribution (Fig. 1). When the background noise is negligible compared with the molecular signal, the error in the fitted position is $\sigma_{x,y} \approx s/(N^{1/2})$, where s is the standard deviation of a Gaussian approximating the true PSF (≈200 nm for light of wavelength λ = 500 nm) and N is the total number of detected photons (*11*, *12*). Given that it is possible to detect many more than 10^4 photons from a single fluorophore before it bleaches, single-molecule localization to nearly 1-nm precision has already been demonstrated (*13*–*15*) and applied to studies of molecular motor dynamics (*13*).

Multiple emitters within a single diffraction-limited region (DLR) have been isolated from one another by either spectral (*15*, *16*) or temporal means, the latter exploiting the photobleaching (*14*, *17*) or blinking (*18*) of the emitters. However, the number of emitters isolated per DLR (typically 2 to 5) has been too small to give resolution within the DLR that is comparable to existing superresolution techniques, and it is far from the molecular level. Here, we developed a method for isolation of single molecules at high densities (up to ~$10^5/\mu m^2$) based on the serial photoactivation and subsequent bleaching of numerous sparse subsets of photoactivatable fluorescent protein (PA-FP) molecules (*19*–*24*) within a sample. We then applied the method to image specific target proteins in thin (~50- to 80-nm) sections and near the surfaces of fixed cultured cells, resolving the most precisely localized molecules therein at separations (~10 nm) approaching the molecular level.

The method and typical data subsets are shown in Fig. 1. Cultured mammalian cells expressing PA-FP–tagged target proteins were prepared by transient transfection, fixed, and processed on cover slips either as whole cells or in cryosections cut from a centrifuged pellet of cells (*25*). Such cover slips were then placed in a custom microscope chamber (fig. S1) designed to minimize thermal and mechanical drift (fig. S2) (*25*). They were continuously excited by a laser at a wavelength (λ_{exc} = 561 nm) near the excitation maximum of the activated form of the expressed PA-FPs. Finally, to minimize both autofluorescence and detector noise, they were imaged by total internal reflection fluorescence (TIRF) microscopy (*13*, *26*) onto an electron-multiplying charge coupled device (EMCCD) camera that can detect single photons.

Initial image frames typically consisted of sparse fields of individually resolvable single molecules on a weaker background presumably dominated by the much larger population of PA-FP molecules still in the inactivated state. When necessary, excitation and thus bleaching was maintained until such sparse fields were obtained. Additional image frames were then captured until single-molecule bleaching resulted in a mean molecular separation considerably larger than that required for isolation (Fig. 1, A and C). At that point, we applied a light pulse from a second laser at a wavelength (λ_{act} = 405 nm) capable of activating the remaining inactive PA-FPs, at a duration and intensity chosen so that the overall density of activated PA-FPs was increased back to a higher, but still resolvable, level (Fig. 1, B and D). This process of photoactivation, measurement, and bleaching was then repeated (movie S1) for many cycles over ~10^4 to >10^5 image frames (depending on the expression level and spatial distribution of the PA-FPs) until the population of inactivated, unbleached molecules was depleted. At typical frame rates of ~0.5 to 1.0 s, between 2 and 12 hours were required to acquire a complete image stack that could be distilled to a single superresolution image containing ~10^5 to >10^6 localized molecules. We continued to explore methods (such as brighter molecules, higher excitation power, and higher activation density) to speed this process.

When the *xy* frames from any such image stack are summed across time *t*, the molecular signals overlap to produce a diffraction-limited image (Fig. 1, E and F) similar to that obtained by conventional TIRF, in which all molecules emit simultaneously (fig. S3). However, when the data are plotted in a multidimensional volume *xyt* (Fig. 1, center), the signal from each molecule *m* is uniquely isolated and can be summed at each pixel and across all of

[1]Howard Hughes Medical Institute, Janelia Farm Research Campus, Ashburn, VA 20147, USA. [2]New Millennium Research, LLC, Okemos, MI 48864, USA. [3]Cell Biology and Metabolism Branch, National Institute of Child Health and Human Development (NICHD), Bethesda, MD 20892, USA. [4]National High Magnetic Field Laboratory, Florida State University, Tallahassee, FL 32310, USA. [5]NuQuest Research, LLC, La Jolla, CA 92037, USA.

*These authors contributed equally to this work.
†To whom correspondence should be addressed. E-mail: betzige@janelia.hhmi.org.

the frames in which it appears. This result (Fig. 1G, left) is then fitted using a robust nonlinear least squares algorithm to an assumed Gaussian PSF of free center coordinates x_o, y_o (Fig. 1G, center) (*25*), yielding coordinates x_m, y_m for the location of the molecule, with a position uncertainty $(\sigma_{x,y})_m$. Finally, each molecule is rendered in a new *xy* frame as a Gaussian of standard deviation $(\sigma_{x,y})_m$ (rather than the much larger standard deviation *s* of the original PSF), centered at x_m, y_m (Fig. 1, G, right, and A′ to D′) and normalized to unit strength when integrated over all *xy* space. Thus, the super-resolution image obtained by summing the rendered Gaussians associated with all localized molecules in the original image stack (Fig. 1, E′ and F′) provides a probability density map where brightness is proportional to the likelihood that a PA-FP molecule can be found at a given location.

This technique, termed photoactivated localization microscopy (PALM), is capable of resolving the most precisely localized molecules at separations of a few nanometers. These represent the very brightest emitters (the much larger population of all isolated molecules exhibits a much broader range of photon counts; fig. S4). Thus, when rendering PALM images, a fundamental trade-off exists: Including fewer, but brighter, molecules results in higher localization and crisper images, but at a reduced molecular density giving less complete information about the spatial distribution of the target protein (fig. S5). Both parameters—localization precision and the density of rendered molecules—are key to defining performance in PALM. Their specific values for the images in Figs. 2 to 4 are given in table S1.

This performance is largely dictated by the photophysical characteristics of the PA-FPs. Longer photobleaching half-life leads to more photons per molecule, but for a given excitation intensity, it also requires longer data acquisition times between activation pulses to maintain an appropriate density of individually resolvable molecules. Higher excitation cross-sectional σ and fluorescence quantum efficiency Φ can speed this process of signal extraction and bleaching, with the added benefit of increasing the molecular contrast relative to the autofluorescence background. Also vital is the contrast $C(\lambda_{exc}) = (\sigma\Phi)_{act}/(\sigma\Phi)_{inact}$ between the PA-FP in its activated and inactivated state at λ_{exc}, because this dictates the maximum molecular density beyond which the background from many weakly emitting inactivated molecules in a DLR dominates the signal from a single activated one. PA-FPs that remain activated until bleached ensure that all possible photons are extracted. Finally, PA-FPs less prone to blinking are desirable, given that it can be difficult to distinguish a single blinking molecule from multiple molecules that are serially activated and bleached in the same DLR (*25*).

Although we have demonstrated isolation and localization with both green [photoactivatable green fluorescent protein (PA-GFP) and Dronpa]

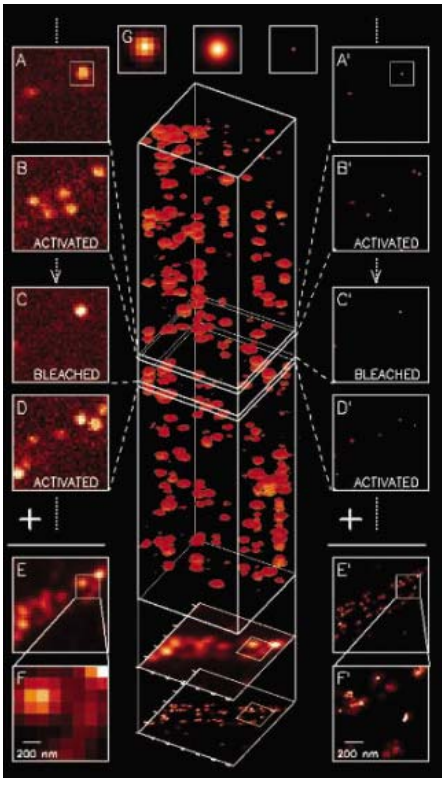

Fig. 1. The principle behind PALM. A sparse subset of PA-FP molecules that are attached to proteins of interest and then fixed within a cell are activated (**A** and **B**) with a brief laser pulse at λ_{act} = 405 mm and then imaged at λ_{exc} = 561 mm until most are bleached (C). This process is repeated many times (**C** and **D**) until the population of inactivated, unbleached molecules is depleted. Summing the molecular images across all frames results in a diffraction-limited image (**E** and **F**). However, if the location of each molecule is first determined by fitting the expected molecular image given by the PSF of the microscope [(**G**), center] to the actual molecular image [(G), left], the molecule can be plotted [(G), right] as a Gaussian that has a standard deviation equal to the uncertainty $\sigma_{x,y}$ in the fitted position. Repeating with all molecules across all frames (**A**′ through **D**′) and summing the results yields a superresolution image (**E**′ and **F**′) in which resolution is dictated by the uncertainties $\sigma_{x,y}$ as well as by the density of localized molecules. Scale: 1 × 1 μm in (F) and (F′), 4 × 4 μm elsewhere.

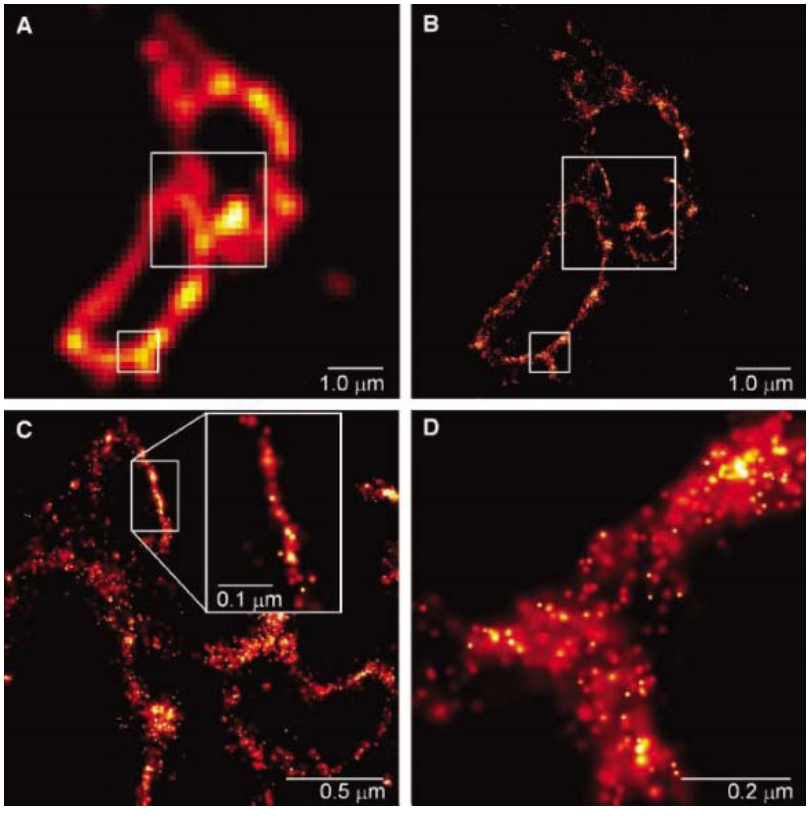

Fig. 2. Comparative summed-molecule TIRF (**A**) and PALM (**B**) images of the same region within a cryoprepared thin section from a COS-7 cell expressing the lysosomal transmembrane protein CD63 tagged with the PA-FP Kaede. The larger boxed region in (B), when viewed at higher magnification (**C**) reveals smaller associated membranes that may represent interacting lysosomes or late endosomes that are not resolvable by TIRF. In a region where the section is nearly orthogonal to the lysosomal membrane, the most highly localized molecules fall on a line of width ~10 nm (inset). In an obliquely cut region [(**D**), from the smaller boxed region in (B)], the distribution of CD63 within the membrane plane can be discerned.

and yellow [Kaede, Kikume Green-Red (KikGR), and Eos Fluorescent Protein (EosFP)] excitable PA-FPs, for imaging cellular structures we focused on tetrameric Kaede and the various oligomers of EosFP—the former for its somewhat higher brightness and the latter for their less perturbative effect on cellular structure and function. Each also exhibits high contrast relative to both the inactivated state and autofluorescence background at λ_{exc} = 561 nm.

We used PALM imaging to view intracellular structures in thin cryosections (*25*), akin to those used in transmission electron microscopy (TEM) but imaged under ambient conditions (Figs. 2 and 3). In Fig. 2, lysosomes in a COS-7 cell are visualized through expression of the lysosomal transmembrane protein CD63 fused to Kaede. Localization to the lysosome membrane was confirmed by comparative immunofluorescence labeling in similarly prepared samples (fig. S6). A TIRF image shows the outlines of the limiting membrane (Fig. 2A) but only hints at the intricate structure that is resolved by PALM, such as smaller associated membranes that may represent interacting lysosomes or late endosomes (Fig. 2, B and C). Indeed, in regions where the section plane is nearly orthogonal to the membrane, the most highly localized molecules fall on a line with an apparent width of ~10 nm (inset, Fig. 2C), demonstrating that they are indeed fixed and that sample drift has been successfully mitigated (*25*). In other regions of the cryosection where the cut is more oblique to the lysosome, a wider, yet still sharply defined, swath of membrane is projected onto the image plane (Fig. 2D), permitting detailed investigation of the distribution of CD63 within the membrane plane.

In Fig. 3, PALM images of dEosFP-tagged cytochrome-C oxidase import sequence localized within the matrix of mitochondria in a COS-7 cell are compared with TEM images of the same mitochondria. The high degree of correlation between the two data sets validates the PALM imaging principle, and the sharpness of the mitochondrial edges (Fig. 3H) as viewed by PALM is far closer to that seen by TEM than that observed by diffraction-limited TIRF (Fig. 3A). Such comparative PALM/TEM imaging permits the nanometer-scale distribution of a specified protein to be determined in relation to the rest of the cellular ultrastructure at much higher molecular density than in immunolabeled TEM—more than 5500 molecules are localized in Fig. 3E, compared with the 20 or so particles typical in immunogold labeling of the mitochondrial matrix. Superposition of the PALM and TEM images (Fig. 3, D and G) also reveals that the matrix reporter molecules extend up to, but not into, the ~20-nm outer mitochondrial membrane, underscoring the resolution capability of the technique. Correlated PALM/TEM does not have the added preparation steps and specificity issues associated with exogenous labels for combined fluorescence/EM such as fluorescein or resorufin arsenical helix binder (*27*). Finally, efforts are underway to establish dual-labeled PALM or PALM fluorescence resonance energy transfer, which would permit the relative distribution or regions of interaction between multiple proteins to be discerned at the nanometer level.

Thin sections are advantageous for PALM because they exhibit less autofluorescence than bulk samples, ensure that the PA-FPs are immobile, and permit the study of intracellular organelles that are inaccessible under TIRF excitation. However, demonstration of PALM on fixed cultured cells in phosphate-buffered saline (Fig. 4) is also notable both as a means to study proteins at or near the plasma membrane under minimally invasive conditions and as a precursor to eventual three-dimensional (3D) PALM imaging.

Confirmation that the nanometer-level resolution of PALM is retained under such conditions is given by the comparison of TIRF (Fig. 4A) and PALM (Fig. 4B) images of dEos-fused vinculin at focal adhesion regions (fig. S7) of a fox lung fibroblast (FoLu) cell to a cover slip. PALM reveals the heterogeneity within a selected attachment (box, Fig. 4A) and, in one subregion, suggests the partial assembly of a vinculin network (arrows, Fig. 4B). Similarly, a TIRF image (Fig. 4C) of tandem-dimer EosFP-fused actin in a cultured FoLu cell (fig. S8) shows both large cytoskeletal stress fibers and a lamellipodium, whereas PALM within the latter (Fig. 4D) reveals an increased concentration of actin at the leading

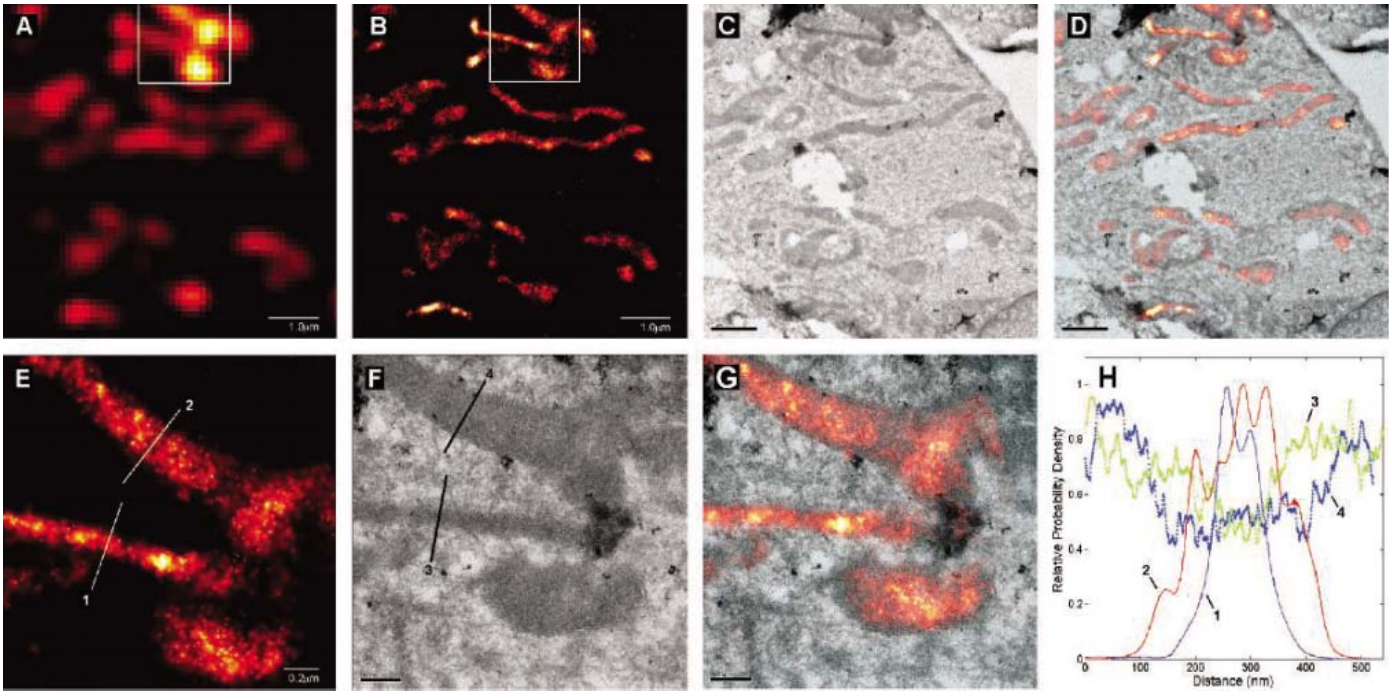

Fig. 3. Comparative summed-molecule TIRF (**A**), PALM (**B**), TEM (**C**), and PALM/TEM overlay (**D**) images of mitochondria in a cryo-prepared thin section from a COS-7 cell expressing dEosFP-tagged cytochrome-C oxidase import sequence. Higher magnification PALM (**E**), TEM (**F**), and overlay (**G**) images within the box in (B) reveal that these matrix reporter molecules extend up to, but not into, the ~20-nm outer mitochondrial membrane. The molecular distribution across two mitochondria along lines 1 and 2 in PALM image (E) are compared in (**H**) to the TEM signal along lines 3 and 4 in (F) across the same mitochondria. Scale bars: 1.0 μm in (A) to (D); 0.2 μm in (E) to (G).

edge. Under even higher magnification (inset, Fig. 4D), numerous short filaments are observed. These may be independent structures fixed in the process of assembly, or they may be part of a larger, continuous 3D network only partially revealed by the short extent of the evanescent excitation field.

In whole cells, PALM with TIRF excitation is well suited to studies of proteins bound to the plasma membrane, such as the dEosFP-fused Gag protein of human immunodeficiency virus 1 imaged by TIRF and PALM in Fig. 4, E and F, respectively. Gag, a retroviral protein that mediates the assembly of virus-like particles (VLPs), is revealed by PALM in various stages of organization: voids (arrows marked V), one high-density region (arrow R), and several tight clusters probably indicative of budding VLPs (arrows marked P, and magnified inset of Fig. 4F).

In the future, PALM should benefit from improvements in and additions to the palette of available PA-FPs, as well as from the discovery of means to modify the PA-FP environment to enhance photostability (*13*) and suppress blinking. Recently, we demonstrated photoactivation in PALM through ultraviolet-induced uncaging (*28*) of fluorophores (fig. S10) which, when combined with immunolabeling or other developing methods to achieve high-specificity intracellular protein labeling (*27*, *29*), might offer a different avenue to improved localization precision and faster frame rates, given that a broad spectrum of high-brightness caged fluorophores is potentially available.

Algorithmically, additional well-localized molecules might be mined from the data if better means are found to unambiguously collate the multiple photon bursts from blinking molecules. Possible improvements to the fitting algorithm to achieve higher localization accuracy should also be explored. Although most of the observed molecules are well represented by a circularly symmetric Gaussian PSF, possible systematic position errors due to chromophore orientation, pixel nonuniformity, and chromatic aberration deserve closer attention. Perhaps most importantly, position error due to background nonuniformity within the molecular fitting window needs to be addressed, particularly when the number of inactivated molecules contributing to this background is high.

Experimentally, multiple angles and polarizations of TIRF excitation may eventually permit the precise determination of the *xyz* position and dipole orientation for fixed PA-FP molecules within the evanescent field. Standing wave TIRF could provide an excitation PSF of width $\sim \lambda_{exc}/6$, improving localization precision for a given photon count. Bulk cellular autofluorescence complicates the extension of PALM to 3D, but the improved single-molecule sensitivity predicted for a proposed optical lattice microscope (*30*) may help. However, the most promising path to 3D may involve cryogenic PALM of vitrified cells, due to the narrow molecular line widths, large cross-sections, and improved stability expected (*8*). On the other hand, the ambient, TIRF-based PALM system demonstrated here has the advantage of simplicity, requiring only a TIRF-capable microscope with appropriate lasers, filters, and EMCCD camera, as well as basic acquisition, localization, and image rendering software. As such, it could be widely adopted in short order for the near-molecular resolution imaging of specified proteins for in vitro preparations and fixed cells.

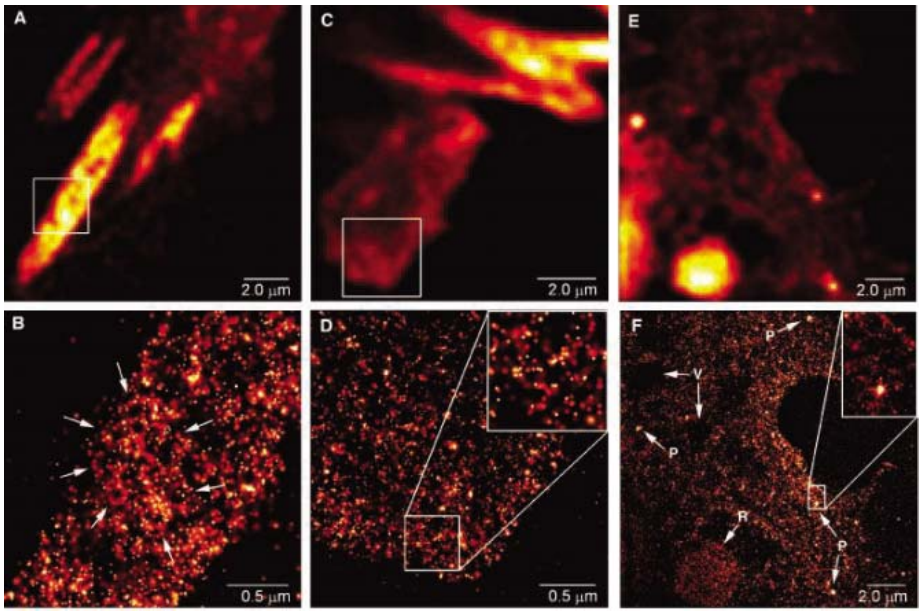

Fig. 4. Examples of PALM imaging near the surfaces of whole, fixed cells. (**A**) A summed-molecule TIRF image of focal adhesions for a FoLu cell expressing dEos-tagged vinculin. (**B**) A magnified PALM view of the structure within a single adhesion over the region indicated by the box in (A), including apparent assembly of vinculin in a partial network (arrows). (**C**) A summed-molecule TIRF image near the periphery of a FoLu cell expressing tdEos-tagged actin. (**D**) A magnified PALM view of the actin distribution within the portion of the lamellipodium outlined by the box in (C). Inset, a further magnified view near the leading edge over the region indicated by the smaller box. (**E** and **F**) Summed-molecule TIRF and PALM images, respectively, of a COS-7 cell expressing the retroviral protein Gag tagged with dEos. The PALM image highlights voids (arrows labeled V), a higher density region (arrow R), and probable condensation at several points (arrows labeled P) into VLPs of ~100- to 150-nm size (inset).

References and Notes

1. J. Lippincott-Schwartz, G. H. Patterson, *Science* **300**, 87 (2003).
2. E. Betzig, J. K. Trautman, *Science* **257**, 189 (1992).
3. K. I. Willig, S. O. Rizzoli, V. Westphal, R. Jahn, S. W. Hell, *Nature* **440**, 935 (2006).
4. M. G. L. Gustafsson, *J. Microsc.* **198**, 82 (2000).
5. M. G. L. Gustafsson, *Proc. Natl. Acad. Sci. U.S.A.* **102**, 13081 (2005).
6. M. Hofmann, C. Eggeling, S. Jakobs, S. W. Hell, *Proc. Natl. Acad. Sci. U.S.A.* **102**, 17565 (2005).
7. E. Betzig, R. J. Chichester, *Science* **262**, 1422 (1993).
8. W. E. Moerner, *J. Phys. Chem. B* **106**, 910 (2002).
9. H. F. Hess, E. Betzig, T. D. Harris, L. N. Pfeiffer, K. W. West, *Science* **264**, 1740 (1994).
10. E. Betzig, *Opt. Lett.* **20**, 237 (1995).
11. M. K. Cheezum, W. F. Walker, W. H. Guilford, *Biophys. J.* **81**, 2378 (2001).
12. R. E. Thompson, D. R. Larson, W. W. Webb, *Biophys. J.* **82**, 2775 (2002).
13. A. Yildiz *et al.*, *Science* **300**, 2061 (2003); published online 5 June 2003 (10.1126/science.1084398).
14. X. Qu, D. Wu, L. Mets, N. F. Scherer, *Proc. Natl. Acad. Sci. U.S.A.* **101**, 11298 (2004).
15. L. S. Churchman, Z. Ökten, R. S. Rock, J. F. Dawson, J. A. Spudich, *Proc. Natl. Acad. Sci. U.S.A.* **102**, 1419 (2005).
16. A. M. van Oijen, J. Köhler, J. Schmidt, M. Müller, G. J. Brackenhoff, *J. Opt. Soc. Am. A* **16**, 909 (1999).
17. M. P. Gordon, T. Ha, P. R. Selvin, *Proc. Natl. Acad. Sci. U.S.A.* **101**, 6462 (2004).
18. K. A. Lidke, B. Rieger, T. M. Jovin, R. Heintzmann, *Opt. Express* **13**, 7052 (2005).
19. G. H. Patterson, J. Lippincott-Schwartz, *Science* **297**, 1873 (2002).
20. R. Ando, H. Hama, M. Yamamoto-Hino, H. Mizuno, A. Miyawaki, *Proc. Natl. Acad. Sci. U.S.A.* **99**, 12651 (2002).
21. J. Wiedenmann *et al.*, *Proc. Natl. Acad. Sci. U.S.A.* **101**, 15905 (2004).
22. R. Ando, H. Mizuno, A. Miyawaki, *Science* **306**, 1370 (2004).
23. H. Tsutsui, S. Karasawa, H. Shimizu, N. Nukina, A. Miyawaki, *EMBO Rep.* **6**, 233 (2005).
24. K. A. Lukyanov, D. M. Chudakov, S. Lukyanov, V. V. Verkhusha, *Nat. Rev. Mol. Cell Biol.* **6**, 885 (2005).
25. Materials and methods are available as supporting material on *Science* Online.
26. D. Axelrod, *Methods Cell Biol.* **30**, 245 (1989).
27. G. Gaietta *et al.*, *Science* **296**, 503 (2002).
28. J. C. Politz, *Trends Cell Biol.* **9**, 284 (1999).
29. I. Chen, A. Y. Ting, *Curr. Opin. Biotechnol.* **16**, 35 (2005).
30. E. Betzig, *Opt. Express* **13**, 3021 (2005).

31. This project was supported in part by the Intramural Program of NICHD and the NIH Intramural AIDS Targeted Antiviral Program (IATAP). We thank J. Wiedenmann and U. Nienhaus of the University of Ulm for the gift of a cDNA encoding the EosFP.

Supporting Online Material

www.sciencemag.org/cgi/content/full/1127344/DC1
Materials and Methods
Figs. S1 to S10
Table S1
Movie S1
References

13 March 2006; accepted 2 August 2006
Published online 10 August 2006;
10.1126/science.1127344
Include this information when citing this paper.

For news and research with impact, turn to *Science*

There's only one source for news and research with the greatest impact – *Science*. With over 700,000 weekly print readers, and millions more online, *Science* ranks as one of the most highly read multidisciplinary journals in the world. And for impact, *Science* can't be beat. According to the recently released Thomson ISI Journal Citation Report 2005, *Science* ranked as the No. 1 most-cited multidisciplinary journal with a citation factor of 31. Founded in 1880 by inventor Thomas Edison, and published by the nonprofit AAAS, *Science*'s reputation as the leading source for news, research, and leading edge presentation of content continues to grow. Looking for news and research that will impact the world tomorrow? Then look in *Science*.

www.sciencemag.org

To join AAAS and receive your own personal copy of *Science* every week go to **www.aaas.org/join**

Science
AAAS

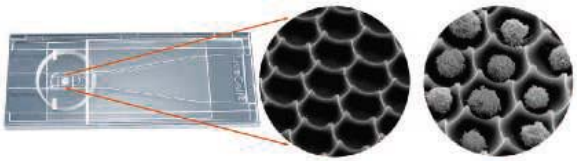

Living Cell Imaging

The NUNC LiveCell Array is a microscope slide–based high-content analysis (HCA) tool that enables multi-parametric, imaging-based assays on thousands of intact individual cells, including non-adhering blood and bone marrow cells. It allows scientists to observe each cell at its own identified location, tracking its individual, real-time responses to intervention. Scientists can now observe each cell at its own identified location, tracking its individual, real-time responses to intervention. Multiple functional assays can be performed on a living cell, followed by post-fixation studies on the same cell to maximize usage of cell samples. The disposable NUNC LiveCell Array microscope slide contains an embedded, transparent array of pico-wells available in sizes of 15, 20, 100, or 250 μm in diameter.

NUNC For information 800-446-2543 www.nalgenunc.com

High-Pressure Freezer

The EM PACT2 High-Pressure Freezer with EM Rapid Transfer System (RTS) is designed to help researchers achieve reproducible results for localization and characterization of organelles and subcellular components. The high-pressure system allows high-quality specimen freezing up to 200 μm into the specimen for subsequent sectioning and observation in an electron microscope. This fully mobile instrument needs only to be connected to a standard power supply and comes with its own compressor located on the same trolley. Any fluid can be used as a hydraulic fluid, and specimen pods are maintenance-free. A cell can be viewed under a confocal microscope, quickly frozen with the EM PACT2/EM RTS, then viewed in an electron microscope. The EM RTS can also be used to enhance the speed of taking a biopsy.

Leica For information 800-248-0123 www.leica-microsystems.com

Protein Kinase Array

The Panorama Human Kinase v1 Array contains 152 commonly studied kinases. This array makes use of a unique fusion tag attached to each kinase that serves to tether and uniformly orient proteins on the array surface, and has been show to confer kinase functionality. This technology offers a unique advantage that allows proteins to behave in a sterically unencumbered manner on the array and potentially result in more physiologically relevant data.

Sigma-Aldrich For information 800-521-8956 www.sigma-aldrich.com

Insertion Kits

EZ-Tn5 and HyperMu Insertion Kits are used to randomly insert a short fragment of DNA (a transposon) into the DNA of any type of clone the user wants to sequence. The transposon contains unique primer binding sites near each end. The user or a core facility can rapidly generate the clone's complete sequence simply by sequencing bidirectionally from a set of randomly chosen insertion clones. These kits avoid the inconsistencies associated with continually designing new primers and are also suitable for closing gaps due to repetitive DNA or AT-rich and GC-rich regions.

Epicentre Biotechnologies For information 800-284-8474 www.EpiBio.com

Peptide Synthesis Service

Activotec offers custom production of a wide range of high quality peptides that are difficult to make. The company provides fast delivery times of milligrams to grams of peptides at all required purity levels with any modifications required. It has particular expertise in difficult-to-synthesize sequences, non-natural modifications, and peptide therapeutics. Examples of peptide modifications recently undertaken include N terminal acylation, C terminal acylation, site-specific peptide modifications, biotinylated peptides, conjugation to carrier proteins, fluorescent-tagged peptides, incorporation of unusual amino acids, and phosphorylated peptides.

Activotec For information +44 1223-260008 www.activotec.com

Kinase Assays

Omnia Kinase Assays are for the rapid, homogenous, and sensitive detection of enzymatic activity under physiological adenosine triphosphate concentrations. A simple mix-and-read procedure means users can mix reagents, read real-time fluorescent signals, and get results in under an hour.

Invitrogen For information 800-955-6288 www.invitrogen.com

Literature

The *Sigma-RBI Handbook of Receptor Classification and Signal Transduction* is available both online and in print. The handbook has been updated to keep pace with the growing number of key receptors and signaling enzymes that are the focus of cell signaling research. It also highlights the development and availability of new and improved pharmacological tools used to investigate their function and regulation. Designed for a broad spectrum of life science researchers, the handbook presents concise and peer-reviewed information on the characterization and classification of a wide range of receptors, ion channels, transporters, neurotransmitter synthesis/metabolism pathways, and intracellular signaling enzymes. More than 80 existing entries were updated, and 26 new entries were added with a focus on kinases and ion channels.

Sigma-Aldrich For information 314-286-7616 www.sigma-aldrich.com/ehandbook

Newly offered instrumentation, apparatus, and laboratory materials of interest to researchers in all disciplines in academic, industrial, and government organizations are featured in this space. Emphasis is given to purpose, chief characteristics, and availability of products and materials. Endorsement by *Science* or AAAS of any products or materials mentioned is not implied. Additional information may be obtained from the manufacturer or supplier by visiting www.science.labvelocity.com on the Web, where you can request that the information be sent to you by e-mail, fax, mail, or telephone.

POSITIONS OPEN

INSTITUT PASTEUR

POSTDOCTORAL FELLOWSHIPS
Institut Pasteur, Paris, France

Founded in 1887 by Louis Pasteur and located in the heart of Paris, the Institut Pasteur is a world-renowned private research organization. The Pasteur Foundation is seeking outstanding Fellowship Applicants. Candidates may apply to any laboratory within 10 departments: cell biology and infection; developmental biology; genomes and genetics; immunology; infection and epidemiology; microbiology; neuroscience; parasitology and mycology; structural biology and chemistry; and virology. See website for details.

Fellowships are $60,000 per year for three years ($45,000 stipend plus $15,000). *U.S. citizenship required.* Deadline: February 2, 2007.

E-mail: pasteurus@aol.com.

Website: http://www.pasteurfoundation.org.

POSTDOCTORAL POSITIONS

NIH-funded positions available immediately to study the role of lung-specific innate immune defense mechanisms, such as surfactant proteins that belong to the collectin family of proteins, in defense against specific pathogens. The studies will include inducible transgenic mice expressing surfactant proteins in the lungs for these investigations. Modulation of dendritic cell function as well as T helper and T regulatory cell responses in the transgenic mice subjected to infection models will be investigated. Technical approaches utilized in the laboratory include transgenic and gene knockout mice, microarray, proteomics, flow cytometry, siRNA, and standard immunological, biochemical, and molecular biology techniques (see **website: http://immunology.medicine.pitt.edu/** and *J. Clin. Investig.* **116:**996, 2006; *Proc. Natl. Acad. Sci. USA* **103:** 7777, 2006; *Journal of Immunology* **174:**854, 2005; *J. Clin. Invest.* **114:**28, 2004; *Journal of Experimental Medicine* **197:**1689, 2003. Strong background in molecular biology is essential. Experience in animal work highly desirable. Please send a brief cover letter, curriculum vitae, and the names and telephone numbers of two to three references to: **Dr. Anuradha Ray, Department of Medicine/Pulmonary Division, University of Pittsburgh School of Medicine, MUH 628 N.W., 3459 Fifth Avenue, Pittsburgh, PA 15213. E-mail: raya@pitt.edu.**

Two **POSTDOCTORAL POSITIONS** are available to study Nrf2 and INrf2 (Keap1) signaling in oxidative stress. It involves studying modifications of Nrf2 and INrf2 by serine and tyrosine kinases and redox factors and generation of knockout/transgenic mice models to study in vivo role of Nrf2 and INrf2 in prevention of oxidative stress and related diseases. Experience in biochemical and molecular biology techniques is required. Applicants should submit curriculum vitae, names, addresses, telephone numbers, and e-mail addresses of three references. Contact: **Dr. Anil K. Jaiswal, Ph.D., Professor, Department of Pharmacology, Baylor College of Medicine, One Baylor Plaza, Houston, TX 77030, U.S.A.** or **e-mail: ajaiswal@bcm.tmc.edu.**

POSTDOCTORAL POSITION is available to study mechanisms and tissue interactions in breast carcinogenesis. Qualified individuals should have a Ph.D. or an M.D./Ph.D. as well as experience in molecular biology and developmental or cell biology. Please send a cover letter, resume or curriculum vitae, and a summary of research interests to **Carlos Sonnenschein, M.D.** at **e-mail: cschaeberle@gmail.com,** or **fax: 617-636-3971.**

POSITIONS OPEN

POSTDOCTORAL OR RESEARCH ASSOCIATE POSITION
University of Minnesota, Department of Neurology

Postdoctoral or Research Associate Position in biochemical protein analysis is available immediately in the laboratories of **Karen H. Ashe, M.D., Ph.D.** (Department of Neurology) and **Carrie M. Wilmot, Ph.D.** (Department of Biochemistry, Molecular Biology, and Biophysics) to determine the biochemical characteristics of molecular assemblies linked to the progression of Alzheimer's disease **(website: http://www.neurology.umn.edu/neurology/faculty/hsiaoashe/home.html).**

The candidate must possess a Ph.D. in biochemistry or molecular biology. Candidates with a rigorous background in protein purification from source material, particularly involving antibody affinity chromatography, are encouraged to apply.

Apply online and attach curriculum vitae, and the names of at least two references at **website: http://employment.umn.edu (requisition 140580)** or send by e-mail to **e-mail: dr. karen ashe: hsiao005@umn.edu.**

The University of Minnesota is an Equal Opportunity Educator and Employer.

MULTIPLE SCLEROSIS / NEUROIMMUNOLOGY RESEARCH

Seeking **POSTDOCTORAL FELLOWS** for research in neuroimmunology and multiple sclerosis. Requirements include background in immunology / T cell biology, experience in experimental allergic encephalomyelitis models and neuroimmunology, as well as technical proficiency in conducting in vivo experiments, cell culture, fluorescence activiated cell sorter, and enzyme-linked immunosorbent assay. Contact:

A. M. Rostami, M.D., Ph.D.,
Department of Neurology
Thomas Jefferson University
Philadelphia, PA

Interested candidates should send curriculum vitae to **e-mail: bxc170@jefferson.edu.**

Seeking **POSTDOCTORAL FELLOW or RESEARCH ASSOCIATE** to work in field of growth factors in embryonic and adult kidney. Range of possible work includes identification of new growth factors, creation of transgenic animals, and evaluation of iron dependent growth activities. Applicant must have outstanding skills in cloning and use of transgenic and knockout models. Alternatively, skill in adenovirus creation needed. Send curriculum vitae to **Jonathan Barasch, M.D., e-mail:jmb4@columbia.edu.** *Columbia University is an Affirmative Action/Equal Opportunity Employer.*

A **POSTDOCTORAL** position is available immediately to study the host immune response to enteric pathogens in the Division of Infectious Diseases at the Department of Biomedical Sciences, Tufts University Cummings School of Veterinary Medicine. Candidates with a Ph.D. degree or equivalent with experience in cellular and molecular biology are encouraged to apply. Please send curriculum vitae and a list of three references to: **Dr. Saul Tzipori (e-mail: saul.tzipori@tufts.edu)** or **Dr. Hanping Feng (e-mail: hanping.feng@tufts.edu).** *Tufts University is an Affirmative Action/Equal Opportunity Employer.*

RESEARCH POSITION. RESEARCH ASSISTANT (B.S./M.S.) and postdoctoral research projects: (1) DNA damage in lung and liver carcinogenesis. (2) Mutations in lung cancer. (3) Repair of ultraviolet damage in mammalian cells. Experience in molecular biology, biochemistry, and genetics. Laboratories are located in a beautiful rural setting in Sterling Forest, Tuxedo, New York. Curriculum vitae and references by **e-mail: tang@env.med.nyu.edu** or by mail to: **Dr. Moon-shong Tang, Department of Environmental Medicine, New York University, Tuxedo, NY 10987.**

Success Factors for Postdocs

Be Prepared!

Ensuring a successful postdoctoral appointment and using the experience to launch a solid career require careful preparation. Scientists who responded to this year's postdoctoral survey, sponsored by *Science* Careers, outline strategies based on their personal histories. BY PETER GWYNNE

KEVIN CIVEROLO

Ensuring a successful postdoctoral appointment and using it as a springboard to an equally effective scientific career demand careful preparation. That's the main lesson provided by respondents to the third annual survey of postdocs sponsored by *Science* Careers. The idea that a Ph.D. scientist can drift into a postdoctoral appointment because one is available and then rely on reputation and natural talent to obtain the first job in academe, government, or industry simply doesn't apply to the 21st century workplace.

"The survey results confirm what we have been saying: Enter a postdoctoral position with a strategic plan regarding your long-term objectives and how you will get from point A to point B," asserts Alyson Reed, executive director of the National Postdoctoral Association. "We have also been encouraging people to consider plan B. If their objective is to secure a tenure-track position, they should consider the likelihood – probably low – for getting one. So they should have an acceptable second choice and ensure that training is available to help expose them to issues other than the tenure-track."

Participants in the survey also rated the factors that had the most influence on their choice of a postdoctoral position. The principal investigator, the direction and vision of the PI's team, and the availability of mentoring, the opportunity to network, and funding and grants for the would-be postdocs' research scored the highest rankings.

Influential Factors

The survey, conducted by Cell Associates, aimed to identify the main factors that influence the success of a postdoctoral experience. Over several weeks starting in early June, 1,661 qualified survey takers in the United States and Europe responded online to a series of questions about their postdoctoral supervisors, themselves, and issues related to their careers. A large majority of 84 percent of surveys came from scientists in the United States. The remainder came from individuals in continental Europe, Ireland, and the United Kingdom. About two-thirds of the respondents had held a single postdoctoral position or were currently involved in their first postdoc. Of those who had held multiple positions, 69 percent did so to receive additional training, while 37 percent con- CONTINUED »

AAAS
http://www.aaas.org

Duke University
http://www.duke.edu

National Postdoctoral Association
http://www.nationalpostdoc.org

New York State Department of Environmental Conservation
http://www.dec.state.ny.us

Trinity College, Dublin
http://www.tcd.ie

University of California, San Diego
http://www.ucsd.edu

University of California, San Francisco
http://www.ucsf.edu

University of Colorado
http://www.colorado.edu

University of Paris 7
http://www.univ-paris.fr

Xoma LLC
http://www.xoma.com

Success Factors for Postdocs


ALISON DONNELLY

tinued their postdoctoral research because of poor job prospects; some respondents quoted both reasons and some of those sought additional training more than once. Three-quarters of the respondents held or had held postdoctoral positions in academic institutions. Three-quarters also cited life or medical sciences as the discipline in which they carried out their postdoctoral work.

Three factors had the most influence on respondents' choice of specific postdoctoral positions: the research topic (mentioned by 86 percent of respondents); their principal investigator (76 percent); and good publication prospects (70 percent). And what attributes did potential postdocs seek in their PIs? Scientific quality, revealed in such factors as publishing in leading journals, being a recognized leader in the field, and attracting talented scientists to the group and keeping them happy featured in answers from 65 percent of respondents.

Slightly fewer survey takers – 59 percent – mentioned issues related to the direction and vision of the PI's team, such as giving postdocs the autonomy necessary to develop independent research, having a clear vision of where the group is heading, showing willingness to take risks to compete effectively, making continuous improvements, and making changes when necessary to keep moving in the right direction.


JOSEPH GRABER

Mentoring and Other Issues

Similar percentages regarded effective mentoring, via ready availability to give advice, help in resolving problems, and career guidance; encouragement of networking, through opportunities to attend scientific conferences and to meet influential researchers; and easy access to help in obtaining funding and grants as very important factors in the choice of a PI. Surprisingly, perhaps, only 41 percent of respondents rated a fair salary and compensation and job security as major attributes. And just 16 percent noted help for spouses or partners to find jobs as a key factor. While respondents on different continents agreed on most attributes, Americans regarded mentoring and funding as more important than did Europeans, while the Europeans put more stress on help for partners.

Scientists plainly don't start their postdocs in the pursuit of financial riches. Last year's median annual salary for the American respondents still working as postdocs was $38,000. (The sample size was too small to provide meaningful salary numbers for European postdocs.) Only 11 percent of participants reported receiving compensation other than a salary. For just over half of those, that took the form of travel costs.

Postdoctoral positions represent way stations to the academy for a majority of survey takers. On completion of their postdoctoral studies, 62 percent of former postdocs and 55 percent of current ones hoped to land a tenure-track academic position. An additional 15 percent of former postdocs and 20 percent of current postdocs sought to start their careers in industry. And 14 percent and 12 percent of former and current postdocs looked for nontenure-track positions as research scientists.

However, respondents who have finished their postdoctoral work reported clashes with workplace realities. Only 54 percent of those who sought tenure-track academic posts actually found such positions, while the number who became nontenure-track research scientists exceeded by 50 percent those who originally wanted such work.


LORI HUDSON

Positives and Negatives

Postdoctoral research inevitably has positives and negatives. In general, survey participants most appreciated the opportunity to work with colleagues who could help them in their research, the independence and freedom to choose research projects that a postdoctoral appointment provides, and the chance to learn new techniques. On the down side, many respondents cited low salaries and job insecurity as unfavorable parts of the postdoctoral experience. Others complained that they lacked independence and/or had poor relationships with their supervisors.

To explore those feelings further, we talked to a small number of respondents. They recounted their own experiences before, during, and – in the cases of former postdocs – after their postdoctoral research. They provided advice on how wannabe postdocs should prepare for their experience, in terms of finding a suitable position and organizing their expectations for it. And they recommended actions that current postdocs should take as they ready themselves for the remainder of their careers.

One key to that advice is the issue of what makes a good postdoctoral experience. "A successful postdoc would be when you can develop your own skill set and become more independent and find your niche," says Rachel Wain, a British life scientist in the third year of her postdoctoral fellowship at the University of California, San CONTINUED »

Number of Postdoc Positions Held

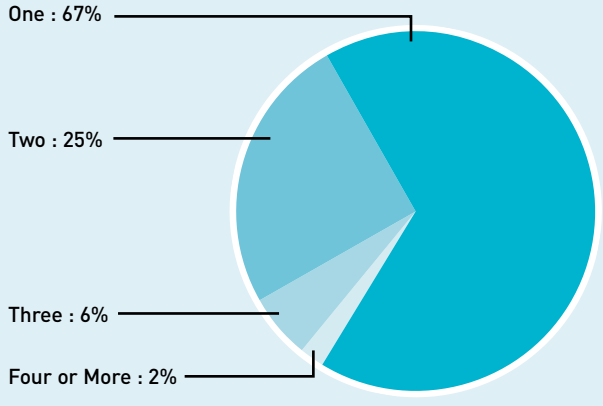

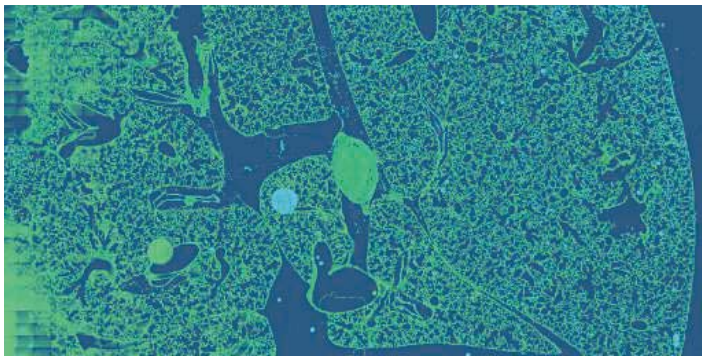

Carley, Pulmozyme® Patient

BECAUSE

We are dedicated to finding cures for cancer and other serious diseases.

For 30 years, Genentech has been at the forefront of the biotechnology industry, using human genetic information to develop novel medicines for serious and life-threatening diseases. Today, Genentech is among the world's leading biotech companies, with multiple therapies on the market for cancer and other serious medical conditions. The company is the leading provider of anti-tumor therapeutics in the United States.

Our founders believed that hiring highly talented, enthusiastic people would make Genentech a success. Today, we still believe our employees are our most important asset.

Genentech is dedicated to fostering an environment that is inclusive and encourages diversity of thought, style, skills and perspective. Genentech offers an array of family-friendly programs, highly competitive health care benefits and a variety of onsite services for busy people with busy lives. To learn more about all of our current opportunities, please visit **www.gene.com/careers**. Please use "Ad - Science" when a "source" is requested. Genentech is an equal opportunity employer.

The following Postdoctoral Research Fellow opportunities exist in our South San Francisco headquarters.

Postdoctoral Research Fellow – Immunology, Req. #1000010229
The candidate will study the role of macrophages in innate immunity.

Postdoctoral Research Fellow – Immunology, Req. #1000013299
The candidate will study development and functional maturation of T cells and/or dendritic cells.

Postdoctoral Research Fellow – Molecular Biology, Req. #1000014803
The candidate will study Ras signaling in mammalian cells.

Postdoctoral Research Fellow – Molecular Biology, Req. #1000014157
The candidate will study genetically engineered murine models (GEMMs) of lung cancer.

Postdoctoral Research Fellow – Molecular Oncology, Req. #1000014519
The candidate will join Dr. Dixit's laboratory to study cellular signaling in inflammation and cancer.

Postdoctoral Research Fellow – Protein Chemistry, Req. #1000013972
The candidate will join the Gonzalez Lab to develop new technologies and methodologies for receptor interaction screening.

Postdoctoral Research Fellow – Protein Chemistry, Req. #1000014182
The candidate will develop innovative proteomic techniques and apply them to important biological problems with relevance to disease.

Postdoctoral Research Fellow – Protein Engineering, Req. #1000014242
The candidate will analyze protein structure and function, as well as decipher intracellular signaling pathways.

Postdoctoral Research Fellow – Protein Engineering, Req. #1000013867
The candidate will study the function and regulation of cell surface-expressed serine proteases (type II transmembrane serine proteases) in cancer.

Genentech was named #1 on FORTUNE's 2006 "100 Best Companies to Work For" list.

Genentech
IN BUSINESS FOR LIFE

Success Factors for Postdocs

Francisco. "And if you want to become a PI, you should also learn more about the academic field, so that you have more understanding of grant writing and items you don't get exposed to as a Ph.D. student."

Joseph Graber, a microbiologist who has just started work as a AAAS science policy fellow after completing his postdoctoral fellowship, takes a similar view. "I would define a successful postdoctoral experience as one that moves the fellow forward to the next stage of his or her career, whatever that may be, and provides the fellow with opportunities to acquire skills and experience that will be necessary for that career," he says.

ALEXANDER OWYANG

Three Success Factors

Alexander Owyang, a scientist at Xoma (US) LLC who completed a single postdoctoral appointment at pharmaceutical firm Schering-Plough Biopharma (formerly the DNAX Research Institute), enumerates the success factors. "Number one, you're able to move on to the next stage – to get a scientist position that you would enjoy," he says. "Number two, you are able to increase and expand your expertise. And thirdly it's great to have good peer-reviewed publications, because they validate your contribution to the body of knowledge." Alexey Wolfson, an assistant research professor at the University of Colorado who completed two postdocs, puts the issue more pithily. "It's doing really good science, publishing it, and being satisfied with what you are doing," he says.

The postdoctoral experience doesn't focus entirely on the research. "Postdocs give a very good opportunity to hone your communications skills, such as presenting before an audience and writing papers," says Kevin Civerolo, a scientist at the New York State Department of Environmental Conservation.

For many scientists nowadays, the original postdoctoral appointment represents merely the curtain raiser to a second postdoc, at which point the individual will begin the tough task of finding the first job. "It's common now in France that you do two postdocs," explains Jonathan Weitzman, a British life scientist just appointed professor at the University of Paris 7, after completing postdoctoral appointments in the United States and France and working as a senior research scientist at the Pasteur Institute. "In a second postdoc it's a matter of choosing a mentor who can help you find a job. No one would take a second postdoc in a French lab that doesn't have the political connections to offer you the chance of a job."

ALYSON REED

Some individuals see each postdoctoral appointment as the stepping stone to more of the same. "A successful postdoctoral experience is one in which you further your skills and secure your next postdoc," says Alison Donnelly, a postdoc at Trinity College, Dublin, who has had eight postdoctoral appointments – some lasting just three to four months – since 1998, when she finished her Ph.D. in environmental science. "In Ireland," she explains, "we have very few research institutes. The majority of the research is carried out in universities." That fact leaves very few tenure-track positions available to postdocs, and leads to a system in which multiple postdocs are a fact of life.

That situation isn't restricted to European countries. Civerolo, for example, undertook two postdoctoral appointments, both in atmospheric science, before he took his present job. Many other American scientists now feel unable to resist that particular career track.

RACHEL WAIN

High Points and Low

Inevitably, postdoctoral scholars go through highs and lows in terms of their work and their lives outside the laboratory. "The most positive factor for me is being in an environment where we are very well funded," says Lori Hudson, a first year postdoc at Duke University. "And the collegial atmosphere: All the people in my group are very open to sharing their expertise. The only negative thing would be the pressure to work nights and weekends. I think the issue of work-family balance is typical for scientists."

Jessica Ward, a coral specialist also in the first year of her first postdoc at the Scripps Institution of Oceanography, affiliated with the University of California, San Diego, tells a similar tale. "My most positive factor is the environment I work in," she says. "I have a very supportive mentor, and all the other postdocs in the lab have been very helpful. For Ward, the negative side is more personal. "My partner is on the East coast and about to move to Kentucky as a faculty member," she notes. But even that problem has a potential solution. "I had a long talk with my PI about a grant proposal; I hope we'll find a way to share my time between San Diego and Kentucky," she says. "I also discussed with him our plan to start a family. He was incredibly supportive."

Other postdocs have experienced more negatives than positives. Wain, who took her skills in protein folding to a CONTINUED »

Reasons for Holding More Than One Postdoc Position

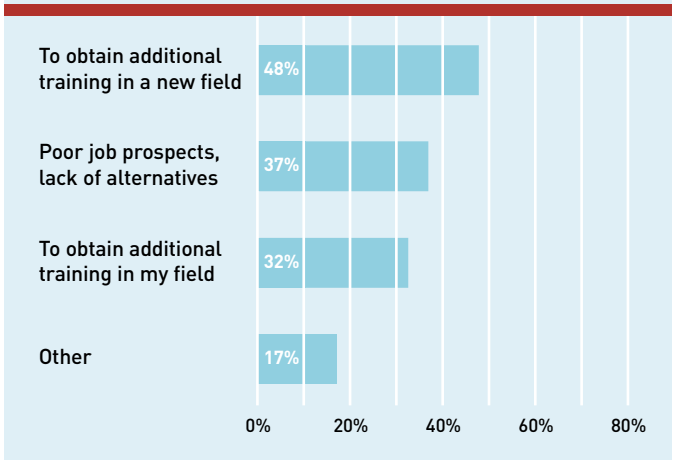

Winning 7 out of 12 Life Science Industry Awards in 2006 was a resounding confirmation of our achievements from the scientific community. Forbes named us to their list of America's best biggest companies and Business 2.0 ranked us in the 100 Fastest Growing Tech Companies. And the list of achievements and accolades goes on.

Proud? You bet! Because behind it all you will find our passionate people collaborating closely to devise the next product or service innovation that will generate scientific breakthroughs around the world. The work is challenging, the rewards are exhilarating and the people are inspiring.

At Invitrogen you will find exceptional career opportunities worldwide in a fast-paced collegial environment, where the potential to learn and grow is virtually unlimited. Our labs and offices are infused with entrepreneurial energy. Yet amidst this dynamic atmosphere all Invitrogen employees share a commitment to integrity and hold fast to the belief that in everything they do, they are making a contribution to a better world. We invite you to join our dedicated team as we continue our quest to improve the human condition.

We are proud to be an equal opportunity employer dedicated to hiring a diverse work team.

A variety of opportunities are available in our **Maryland** facilities:

Senior Director, Research & Development (Rockville)

Senior Director, Toxicology (Rockville)

Scientist, Process Development (Frederick)

Scientist, Cell Culture (Frederick)

Veterinary Pathologist (Rockville)

Apply online at **www.invitrogen.com/careers**

The Life Science LSIA 2006 Industry Awards

B2 100 Fastest-Growing Tech Companies

Forbes 2006 THE PLATINUM LIST

invitrogen™

Success Factors for Postdocs

prion laboratory at the University of California, San Francisco, soon found her expectations dashed. "My lab doesn't have any graduate students, so opportunities to improve my supervisory skills haven't been available," she points out. "And with the prion field being as political as it is, it's difficult to gain independence." Wolfson, meanwhile, found his first postdoctoral appointment to be "a disaster" for a strictly scientific reason: "The project didn't work," he recalls. "It gave me negative feelings about myself."


JESSICA WARD

Taking a Proactive Stance

In response to the negatives, some respondents have taken a proactive stance by helping to form postdoctoral associations intended to improve their lot. "I've been involved with the postdoctoral association at UCSF," Wain says. "There have been improvements made. There's a big drive towards mentoring." In Ireland, Donnelly helped to set up the Trinity Research Staff Association, which aims to support the growing number of postdocs who have faint prospects of tenure-track jobs by encouraging the university to provide courses in such issues as research management and policy development.

Postdoctoral associations play obvious roles in furthering the goals of their members. But the essence of ensuring a successful postdoctoral experience is advance preparation by the individual. "I did very little preparation," Donnelly recalls, regretfully. "I finished my Ph.D. with the thinking that I would do a postdoc or two and get an academic position." Eight years and eight postdocs on, the academic position remains a dream. So Donnelly advises scientists seeking postdoctoral appointments to undertake thorough due diligence. "Think very carefully about what you want to do," she says. "Visit the university where you want to go and ask: What are you going to do for me? Are you going to provide professional opportunities? Are you going to mentor me? Will you help me to decide how to get out if I want to, by providing short courses?"

Postdocs regard face-to-face meeting with potential PIs and their team members as almost mandatory elements of preparation. "To learn about the working environment of the lab that I'd be joining, I had numerous conversations with my prospective mentor, with other researchers who'd had previous interactions with him, and with current and former graduate students and postdocs who were working or had worked in his lab," AAAS science policy fellow Graber remembers.

Thorough Preparation

Owyang of Xoma undertook his own thorough preparation for his industrial postdoctoral research project. "I started the process more than nine months before I left graduate school," he recalls. "I sent letters to a couple of dozen laboratories in California, including DNAX. That was the only industry I contacted, because it has a rich history of academically oriented research. The company had very rigorous interviews, which included all the PIs. I knew they were interested because near the end of the day, the PI of the group I was interested in handed me a folder containing all his recent papers – most of which I had already read. I chose to accept their offer because it seemed like a great opportunity to do basic research while also gaining exposure to the biotech industry."

Weitzman of the University of Paris 7 points out that prospective postdocs should consider the background of their potential PIs. "You face a choice: Do you go with a young rising star or someone more established?" he says. "My second postdoc, with a scientist towards the end of his career, allowed me to be completely independent."

Postdoctoral independence means making provision for the career beyond the postdoctoral appointment. "If you just treat the postdoc as a holding pattern, it's probably a recipe for failure," the National Postdoctoral Association's Reed asserts. So any scientist should think about a variety of job possibilities as soon as possible. "Don't feel that you're on a narrow track," Civerolo of New York's Department of Environmental Conservation advises. "There are industry, government, nonprofit, and other opportunities out there as well as academic ones. Understand that postdoctoral appointments are generally short – one or two years – so you're on a steep learning curve. And don't be afraid to try new things or go in another direction entirely; be flexible."


JONATHAN WEITZMAN

Skills for a Wider World

Part of that flexibility involves developing skills that will benefit the individual scientist in the wider world. "Try to write your own grant applications or to go for independent funding," Wolfson advises. "You should do so not so much to get the grants, but to get the experience." Graber agrees. "Apply for independent funding early and often, regardless of whether or not your mentors have money available to pay your salary," he counsels. "Having a successfully funded grant application on your CV opens doors to any career that you might move to." Weitzman's experience illustrates that fact. "By the time I had finished my second postdoc, I had an independent grant on which I was the leader," he says. "And I had established a network of colleagues."

Hudson at Duke University summarizes the issue of preparing for one's career after the postdoctoral experience. "Have clear goals," she advises. "Don't get too sidetracked with, say, assay development. Make sure that your individual projects are benefiting you as well as the lab. After all, you have to be a little selfish." Ward of the Scripps Institution has her own upbeat view of how postdocs should get ready for their scientific careers: "You need to stay focused and have a plan," she recommends. "You need to have fun. It's not the end of the world if you don't get your dream job. You can justify it if you're enjoying your work."

A former science editor of Newsweek, *Peter Gwynne (pgwynne767@aol.com) covers science and technology from his base on Cape Cod, Massachusetts, U.S.A.*

MEDICAL COLLEGE OF WISCONSIN

Postdoctoral Position

Federally funded postdoctoral position immediately available to study the role of neural stem cell (NSC) and mesenchymal stem cell (MSC) transplantation in spinal cord injury (SCI). The project/s will focus on combinatorial approaches to treat SCI using NSC (human and rodent derived), MSC and metalloproteinases. The ideal candidate will have experience in at least three of the following: cell culture, gene transfection, small animal surgery, confocal microscopy and image analysis.

Please e-mail resume and references to:

Dr. Shekar N. Kurpad, MD, PhD
Department of Neurosurgery,
Medical College of Wisconsin
9200 W. Wisconsin Ave.
Milwaukee, WI 53226

skurpad@mcw.edu

THE UNIVERSITY OF IOWA

Getting Neuroscience Postdoctoral Scholar Award
$50,000/year

The Department of Molecular Physiology and Biophysics at The University of Iowa announces a 3-year Postdoctoral award in honor of Dr. Peter A. Getting's contributions to the department and the neuroscience field. This competitive award will be granted to an outstanding candidate, recently completing their Ph.D. or M.D.-Ph.D. degree for studies in various disciplines (neurophysiology, membrane trafficking and ion channel biophysics).

Applicants should access the research programs of individual faculty at **www.physiology.uiowa.edu** select an appropriate supervisor, submit a letter of application, C.V. and names of references to that faculty member for nomination to the selection committee.

The University of Iowa is an AA/EO Employer. Women and minorities are encouraged to apply.

STONY BROOK

POSTDOCTORAL POSITIONS

The Research Foundation of Stony Brook University/ SUNY anticipates the following postdoctoral positions being available between September 2006 and Spring 2007.

- **APPLIED MATH AND STATISTICS**
  Computational Biology: Development and application for structure-based drug design. Robert C. Rizzo, WC-R-3470-06-09-S
- **BIOCHEMISTRY AND CELL BIOLOGY**
  Glycosylation and cell wall biogenesis in yeast and pathogenic fungi. Neta Dean, WC-R-3452-06-08-S
  Role of RNA-protein interactions in bacterial pathogenesis. A. Wali Karzai, WC-R-3366-06-09-F
  Biosynthesis and catabolism of glycoproteins. William J. Lennarz, WC-R-3453-06-09-S
  Developmental regulation of the secretory pathway during sporulation in yeast. Aaron Neiman, WC-R-3451-06-09-S
- **BIOMEDICAL ENGINEERING**
  Structure and phase behavior of aqueous self-assembled nanostructured materials. Helmut Strey, WC-R-3488-06-09-S
- **CHEMISTRY**
  Polymer synthesis, colloids, fibers, polymer inorganic hybrids, polyoxometalates. Ben Chu, WC-R-3483-06-09-S
  Flow-induced polymer crystallization, spinning processes, bio-related polymers and nanocomposites. Benjamin Hsiao, WC-R-3484-06-09-S
  Relativistic Heavy Ion reaction studies. Roy Lacey, WC-R-3478-06-09-S
  Chemical Biology: Specific recognition of cell-surfaced nanopatterns. Nicole S. Sampson, WC-R-3476-06-09-S
  Mechanistic studies of natural product biosynthetic enzymes in pathogens. Peter Tonge, WC-R-3475-06-09-S
  Synthesis and evaluation of enzyme inhibitors for antibacterial drug discovery. Peter Tonge, WC-R-3474-06-09-S
  Vibrational, NMR, and fluorescence spectroscopy of fluorescent proteins and enzymes. Peter Tonge, WC-R-3473-06-09-S
- **ENVIRONMENTAL MOLECULAR**
  Environmental molecular science research–sequestration of contaminants by natural materials. (two positions) Richard J. Reeder, WC-R-2962-06-04-F and WC-R-3457-06-09-S
- **MARINE SCIENCES**
  Analysis of endocrine-disrupting contaminants in environmental samples by LC-MS. (two positions) Bruce Brownawell, WC-R-3468-06-09-S and WC-R-3374-06-07-S
- **ORAL BIOLOGY AND PATHOLOGY**
  Host immune responses in epidermal stem cell-based gene therapy. Soosan Ghazizadeh, HS-S-3442-06-09-S
- **PATHOLOGY/BIODEFENSE**
  Interactions of francisella tularensis with host cells of innate immunity. Martha B. Furie, WC-R-3458-06-09-S
- **PHARMACOLOGY**
  Molecular carcinogenesis and toxicogenomics. Arthur Grollman, HS-R-3469-06-09-S
  Temporal/spatial analysis of AKAP scaffolds by biosensors and proteomics. Craig C. Malbon, HS-R-3416-06-07-S
- **PSYCHIATRY**
  Patient-reported outcomes, electronic diary data, behavioral medicine. Arthur Stone, WC-S-3400-06-07
- **UROLOGY**
  Preclinical studies for Prostrate, Bladder, Kidney Cancer and Cancer Vaccines. Christopher S. Lee, HS-S-3441-06-09-S

To apply online and for information, see *www.postdocs.stonybrook.edu* or mail résumés to: Murray Lamond, Office of the President, Stony Brook University, Stony Brook, NY 11794-0701.

Equal Opportunity/Affirmative Action Employer.

POSITIONS OPEN

POSTDOCTORAL RESEARCH ASSOCIATE
Membrane Protein Structure and Folding

A Research Associate position in molecular physiology and biological physics at the University of Virginia is currently available for a highly motivated individual to work on the structure and folding of membrane proteins using nuclear magnetic resonance (NMR) and other spectroscopic techniques. The successful candidate has experience in cloning and expression of membrane proteins and/or NMR spectroscopy and biophysical techniques characterizing membrane proteins. The University of Virginia is a top-ranked public university located in Charlottesville, one of the best places to live in the United States. This position will remain open until filled. Candidates holding a Ph.D. degree in an applicable science field should send curriculum vitae and contact information for three references to: **Professor Lukas Tamm, Molecular Physiology and Biological Physics, University of Virginia, P.O. Box 800736, Charlottesville, VA 22908, U.S.A., e-mail: lkt2e@virginia.edu.**

The University of Virginia is an Equal Opportunity Employer.

UNIVERSITY OF PITTSBURGH CANCER INSTITUTE

Two **POSTDOCTORAL FELLOWSHIPS** are available to work with **Z. Sheng Guo, Ph.D.** and **David L. Bartlett, M.D.** The Fellows will work in exciting field of cancer biology and therapy incorporating epigenetic therapy, immunotherapy, and oncolytic virotherapy. One Fellow should possess a Ph.D. in immunology. Expertise in T cell and dendritic cell biology is a plus. The second Fellow should have a Ph.D. in virology or related field and will work on oncolytic virotherapy. We offer a competitive benefit package and a great work environment for you to succeed in. Interested candidates should send cover letter, curriculum vitae, and names of three references to **Z. Sheng Guo, Ph.D.,** via **e-mail: guozs@upmc.edu.**

POSTDOCTORAL RESEARCH OPPORTUNITY
University of Texas, M.D. Anderson Cancer Center Houston, Texas

A Postdoctoral Fellowship is available in the Ovarian Cancer Research Laboratory directed by **Robert C. Bast Jr.,** to conduct research focused on exploring imprinted tumor suppressor genes, signal transduction, and autophagy in ovarian and breast cancer. Applicants should possess a Ph.D., or equivalent, and have had experience with molecular and cellular biology and animal models. Send e-mail with cover letter, curriculum vitae, and three references to **Robert C. Bast Jr., M.D., e-mail:rbast@mdanderson.org.**

All positions at the University of Texas, M.D. Anderson Cancer Center are sensitive and subject to examination of criminal history record information. Smokefree and drugfree environment. M.D. Anderson Cancer Center is an Equal Opportunity Employer and does not discriminate on the basis of race, color, national origin, gender, sexual orientation, age, religion, disability, or veteran status except where such distinction is required by law.

POSTDOCTORAL POSITIONS are available to study the role of homeobox genes in development and cancer. Qualified individuals should have a Ph.D. and/or M.D., as well as prior experience in molecular biology, mouse genetics and/or developmental biology. Please send curriculum vitae, summary of research interests, and three confidential letters of reference to: **Cory Abate-Shen, Ph.D., Center for Advanced Biotechnology and Medicine; University of Medicine and Dentistry of New Jersey - Robert Wood Johnson Medical School, 679 Hoes Lane, Piscataway, NJ 08854. Fax: 732-235-5789, e-mail: abate@cabm.rutgers.edu.**

POSITIONS OPEN

POSTDOCTORAL RESEARCH ASSOCIATE
Molecular Mechanisms of Exocytosis

A Research Associate position in cell biology at the University of Virginia is currently available for a highly motivated individual to work in a joint project between two well-established cell biology and biophysics laboratories to elucidate molecular mechanisms of exocytosis in neuroendocrine cells using advanced fluorescence microcopy and single molecule approaches. The successful applicant will have experience in molecular cloning and transfection, cell culturing, and microscopy. The University of Virginia is a top-ranked public university located in Charlottesville, one of the best places to live in the United States. This position will remain open until filled. Candidates holding a Ph.D. degree in an applicable science field should send curriculum vitae and contact information for three references to: **Professor David Castle, Cell Biology, e-mail: jdc4r@virginia.edu,** or **Professor Lukas Tamm, Molecular Physiology and Biological Physics, e-mail: lkt2e@virginia.edu, University of Virginia, P.O. Box 800736, Charlottesville, VA 22908, U.S.A.**

The University of Virginia is an Equal Opportunity Employer.

BIOFILMS-MICROBIAL FUEL CELLS

POSTDOCTORAL POSITIONS available to study the structure and function of biofilms responsible for electricity production in microbial fuel cells harvesting energy from waste organic matter and renewable biomass. Previous experience in the study of microbial biofilms is highly desirable. Minimum qualifications are a Ph.D. in microbiology or a related field. Salary is commensurate with experience. For research program details please visit **website: http://www.geobacter.org.** Please e-mail curriculum vitae and names of three references to: **Dr. Derek Lovley, Department of Microbiology, University of Massachusetts, Amherst, MA. E-mail: dlovley@microbio.umass.edu,** or send application materials to: **Search Committee R27005 Microbiology, 203N Morrill IVN, Umass Amherst, MA 01003.** Review of applications will begin on September 12, 2006, and continue until the positions are filled. *University of Massachusetts is an Affirmative Action/Equal Opportunity Employer. Women and members of minority groups are encouraged to apply.*

POSTDOCTORAL POSITIONS
Heart Failure

Two NIH-funded Postdoctoral positions available immediately to study gene regulation and molecular pathways relevant to pathogenesis of heart failure (see *J. Biol. Chem.* **280:**43121, 2005 and *J. Biol. Chem.* **278:**20047, 2003). Ph. D. required. Experience in basic physiology, cell culture, and molecular biology techniques will be helpful, but not essential. A senior position of **RESEARCH ASSISTANT PROFESSOR** is also available for a trained person. Send resume and three names of references to: **Mahesh P. Gupta, Ph.D. Department of Surgery (Cardiac, MC 5040), University of Chicago, 5841 S. Maryland Avenue, Chicago, IL 60637. E-mail: mgupta@surgery.bsd.uchicago.edu.** *University of Chicago is an Equal Opportunity/Affirmative Action Employer.*

POSTDOCTORAL/RESEARCH ASSOCIATE/RESEARCH SPECIALIST are available in the Lung Biology and Toxicology Laboratory at Oklahoma State University (OSU) to study exocytosis, cell differentiation, and fluid transport from molecular level to whole animal using various modern techniques including DNA microarray and RNA interference. Highly motivated candidates are encouraged to apply. A background in molecular and cellular biology, electrophysiology, lung biology, and/or animal physiology is a plus. Send curriculum vitae to: **Dr. Lin Liu, Department of Physiological Science, Oklahoma State University, Stillwater, OK 74078; e-mail: liulin@okstate.edu.** Applications will be accepted through October 15, 2005, or until suitable candidates are identified. *OSU is an Affirmative Action/Equal Opportunity Employer.*

POSITIONS OPEN

A **POSTDOCTORAL POSITION** in microbial genetics is available to investigate gene regulation in *Haemophilus ducreyi*, the etiologic agent of chancroid. Emphasis will be placed on the elucidation of the regulatory mechanism(s) by which *H. ducreyi* controls the differential expression of the LspA1 and LspA2 proteins; these exoproteins are major virulence determinants. Position requires a Ph.D. in microbiology, biochemistry, genetics, or a related biological science and experience with recombinant DNA techniques. Position includes salary, fringe benefits, and the opportunity to work in a dynamic research environment. Send curriculum vitae and the names and telephone numbers of three references to: **Dr. Eric J. Hansen, Department of Microbiology, The University of Texas Southwestern Medical Center at Dallas, 5323 Harry Hines Boulevard, Dallas, TX 75390-9048. Fax: 214-648-5905. E-mail: eric.hansen@utsouthwestern.edu.** *University of Texas Southwestern is an Equal Opportunity/Affirmative Action Employer.*

POSTDOCTORAL POSITIONS IN BIOCHEMISTRY AND MOLECULAR BIOPHYSICS
Washington University, St. Louis

Postdoctoral positions are available for studies of DNA motor proteins (helicases and translocases) involved in DNA replication, recombination and repair and single-strand binding protein-DNA interactions using biochemical and biophysical approaches. Candidates should have interests in mechanistic studies using transient kinetic methods (fluorescence, stopped-flow, quenched-flow) and thermodynamics. Send curriculum vitae to: **Professor Timothy M. Lohman, Biochemistry and Molecular Biophysics, P.O. Box 8231, Washington University School of Medicine, 660 South Euclid Avenue, St. Louis, MO 63110 (e-mail: lohman@biochem.wustl.edu).**

A **POSTDOCTORAL FELLOW POSITION** is available immediately at University of California, Los Angeles, to study cellular mechanisms of hippocampal synaptic dysfunction in Alzheimer models. The position requires strong background in cellular neurobiology and experience in the following areas: electrophysiological recordings in neuronal cultures or brain slices, immunohistochemistry, Western blotting, gene construct and transfection in neurons. Salary is commensurate with experience and competitive benefits package available. Send curriculum vitae and names of three references to: **Dr. Cui-Wei Xie, University of California, Los Angeles UCLA-NPI, 760 Westwood Plaza, Los Angeles, CA 90024. E-mail: cxie@mednet.ucla.edu.**

POSTDOCTORAL POSITIONS
University of California, Berkeley

Postdoctoral Positions available to study bacterial pathogenesis and the cellular biology of microbial infection. Fellows have the opportunity to acquire research skills using bioinformatics, microarray, and molecular genetic techniques, and to utilize modern technology in experimental designs applied to infectious agents. Recent Ph. D. graduates with productive research background in microbiology, cell biology, and/or immunology are encouraged to apply. Send curriculum vitae and names of references by mail to: **Dr. R. S. Stephens, 140 Warren Hall, University of California, Berkeley, CA 94720.**

POSTDOCTORAL POSITION is available immediately to study the virulence functions of GPI-proteins during *Candida albicans* infection. Research involves targeted gene disruption and overexpression in *C. albicans*, identification of host cell receptors, and assessment of virulence in murine models. Experience in molecular and cellular biology desired. Please submit curriculum vitae, summary of research experience, and three references to**: Dr. Yue Fu, Harbor-University of California at Los Angeles Medical Center, 1124 W. Carson Street, Torrance, CA 90502. E-mail: yuefu@ucla.edu.**

National Cancer Institute

U.S. DEPARTMENT OF HEALTH AND HUMAN SERVICES

National Institutes of Health

SALLIE ROSEN KAPLAN FELLOWSHIP
FOR WOMEN IN BASIC, CLINICAL, EPIDEMIOLOGICAL OR PREVENTION SCIENCE

The Sallie Rosen Kaplan Fellowship for Women Scientists in Cancer Research is made possible by a generous bequest to the Foundation for NIH (FNIH). This is a competitive program for postdoctoral fellows applying to train in any of the National Cancer Institute's intramural research settings, including basic, clinical, epidemiological, and prevention science.

The postdoctoral fellowship experience at the NCI can serve as a first postdoctoral training assignment, or offer more experienced postdoctoral scientists an opportunity to further their training in more advanced methods, to acquire new research capabilities, to make changes in the direction of their research, or to receive training in fundamental sciences and clinical disciplines for the purpose of enhancing the transfer of biotechnology to cancer clinical programs.

Program duration is normally 2 to 5 years. Fellows will be supported by a Cancer Research Training Award (CRTA), with an augmented stipend in the first year provided by the FNIH. The CRTA Fellowship stipend range is $39,800 to $73,500 commensurate with level of experience. Standard self and family health insurance is provided and high option coverage is available.

Candidates for the Sallie Rosen Kaplan Fellowship must be female, must possess a doctoral degree, and have less than 5 years postdoctoral research experience. U.S. citizenship or U.S. permanent residency (green card) is required. Candidates selected for the fellowship will be notified by March 2007 and the starting date will be no earlier than May 2007. Applicants are required to apply online at **http://generalemployment.nci.nih.gov** by December 15, 2006.

DHHS, NIH and NCI Are Equal Opportunity Employers

---

*InVivo*Scribe Technologies
www.invivoscribe.com

Postdoctoral Positions

*InVivo*Scribe Technologies has postdoctoral positions available in our San Diego laboratories to develop applications for our proprietary in vivo cDNA synthesis technologies.

Successful candidates will have a Ph.D. in molecular virology or molecular biology with a solid background in retroviral replication and extensive experience in several of the following areas: construction/expression of modified proviral genomes; retroviral vector construction; expression of modified tRNAs; gene transfection, cDNA synthesis, and quantitative gene expression analysis; in vitro RNA transcription; introduction of protein/nucleic acid complexes into eukaryotic cells to direct exogenous gene expression.

Please send a cover letter including your c.v. by email to the attention of **Jeffrey Miller, Ph.D.** at: **hr@invivoscribe.com**.

*InVivo*Scribe Technologies is a profitable, privately held biotechnology company with headquarters in San Diego, California, and a sales and distribution office in La Ciotat, France. We are the world's leading provider of PCR-based tests, reagents and controls used to identify and monitor leukemias, lymphomas, and other lymphoproliferative disease.

We are an equal opportunity employer and offer a competitive benefits package that includes comprehensive healthcare, vision, dental insurance, and a 401k retirement plan.

University of California
LAWRENCE LIVERMORE NATIONAL LABORATORY
Science in the National Interest

LAWRENCE POSTDOCTORAL FELLOWSHIP

The Lawrence Livermore National Laboratory (LLNL) has openings available under its Lawrence Fellowship Program. This is a highly desirable, prestigious postdoctoral position with ample resources and freedom to conduct cutting-edge research in a field of the candidate's choice. The duration of the Fellowship is up to three years. Typically two to four openings are available each year. Fellowships are awarded only to candidates with exceptional talent, credentials and a track record of research accomplishments.

Candidates will do original research in one or more aspects of science relevant to the mission and goals of LLNL which include: Physics, Applied Mathematics, Computer Science, Chemistry, Material Science, Engineering, Environmental Science, Atmospheric Science, Geology, Energy, Lasers and Biology. Successful candidates may participate in experimental or theoretical work at LLNL, and will have access to LLNL's extensive computing facilities, specialized laboratory facilities and field equipment. A senior scientist will serve as a mentor to each of the Fellows. The candidates will receive full management and administrative support. The salary is $7,933/mo.

Please refer to our web page **http://fellowship.llnl.gov** for eligibility requirements and instructions on how to apply. When applying and prompted, please mention where you saw this ad. The deadline for application is November 1, 2006. LLNL is operated by the University of California for the National Nuclear Security Administration/Department of Energy. We are an Equal Opportunity Employer with a commitment to workforce diversity.

Lawrence Livermore National Laboratory

http://fellowship.llnl.gov

NATIONAL RESEARCH COUNCIL

OF THE NATIONAL ACADEMIES

Research Associateship Program

Postdoctoral Research Awards
Senior Research Awards
Summer Faculty Fellowships
Davies Teaching Fellowships

offered for research at

US government laboratories and affilited centers

Opportunities for postdoctoral and senior research in all areas of science and engineering

- Awards for independent research at over 120 participating laboratory locations
- 12-month awards renewable for up to 3 years
- Annual stipend $38,000 to $65,000 - higher for senior researchers
- Relocation, professional travel, health insurance
- Annual application deadlines Feb. 1, May 1, Aug. 1, Nov. 1

Detailed program information, including instructions on how to apply, is available on the NRC Web site at :

www.national-academies.org/rap

Questions should be directed to :

National Research Council
TEL: (202) 334-2760
E-MAIL: rap@nas.edu

Qualified applicants will be reviewed without regard to race, religion, color, age, sex or national origin.

THE NATIONAL ACADEMIES
Advisers to the Nation on Science, Engineering, and Medicine

THE UNIVERSITY OF TEXAS MD ANDERSON CANCER CENTER
Making Cancer History™

POSTDOCTORAL FELLOWSHIPS IN CANCER RESEARCH

The University of Texas M.D. Anderson Odyssey Program encourages the newest generation of cancer researchers to explore novel areas of clinical or basic cancer research in preparation for successful, independent careers in this field while taking advantage of the resources offered by The University of Texas M.D. Anderson Cancer Center in Houston, Texas. The Odyssey Program supports the training and research efforts of dedicated scientists at the beginning of their careers by sponsoring outstanding junior and senior postdoctoral fellows who wish to pursue innovative cancer research. Odyssey Scholarships and Fellowships are awarded based on level of experience, strength of credentials, and potential of proposal. Odyssey Fellows and Scholars receive up to three years of support for their salaries and a yearly research allowance for supplies, small equipment and meeting expenses.

2007 Application Deadlines:

Spring Deadlines: letter of intent due Monday, February 5, 2007
Application due Monday, March 5, 2007

Odyssey Scholarship
No fixed deadline (notice of intent due 3 weeks prior to submitting application)

For further information, consult our website: **http://www.mdanderson.org/odyssey**

M.D. Anderson Cancer Center is an Equal Opportunity Employer and does not discriminate on the basis of race, color, national origin, gender, sexual orientation, age, religion, disability or veteran status, except where such distinction is required by law. All positions at M.D. Anderson are considered security sensitive; drug screening and thorough background checks will be conducted. The University of Texas M.D. Anderson Cancer Center values diversity in its broadest sense. Diversity works at M.D. Anderson. Smoke-free environment.

U.S. MILITARY HIV RESEARCH PROGRAM
IN PARTNERSHIP WITH DAIDS/NIAID/NIH/HHS

Postdoctoral Positions
HIV Research in Viral and Host Genetics

The U.S. Military HIV Research Program supports the global effort to develop HIV vaccines and is seeking 2 postdoctoral fellows to assist the Molecular Virology component, which plays a vital role in HIV vaccine development. These exciting new research opportunities focus on HIV variation and host-pathogen relationships in HIV infection and disease.

Postdoctoral in Viral Genetics

Incumbent will study HIV genetic variation in relation to vaccine development, and develop and apply innovative molecular biology approaches for the study of viral variation in human populations where HIV vaccines will be evaluated. Must have a Ph.D. in Molecular Biology or related discipline, emphasis in Virology, Genetics, or Evolutionary Biology preferred. Please apply on-line at: **www.hjf.org/careers**, Job Req: **202086** or email your resume to: **careers@hjf.org**, specify 202086 in subject line.

Postdoctoral in Human Genetics

Incumbent will study human genetic factors of importance to HIV infection and disease in the context of vaccine development. Will develop and apply innovative molecular biology approaches for the study of polymorphic human genes in populations, including HLA and host restriction factors, in populations where HIV vaccines will be evaluated. Must have a Ph.D. in Molecular Biology or related discipline, emphasis in Genetics or Immunology preferred. Please apply on-line at: **www.hjf.org/careers**, Job Req: **201639** or email your resume to: **careers@hjf.org**, specify 201639 in subject line.

All applicants should have strong laboratory skills in Molecular Biology, including DNA sequencing, conventional and real-time PCR, and molecular cloning. Experience with project planning, implementation, and data analysis.

The Henry M. Jackson Foundation for the Advancement of Military Medicine offers a competitive salary and generous benefits package. Affirmative Action/Equal Employment Opportunity.

POSTDOCTORAL FELLOWSHIP OPPORTUNITIES

The **Santa Fe Institute** (SFI) anticipates offering several Postdoctoral Fellowships to begin in September 2007.

The Postdoctoral Fellowship program provides up to three years of support for independent research at SFI. Postdoctoral Fellows are encouraged to engage research questions of their own design, and to form collaborations with members of the faculty, other SFI postdocs, and researchers from around the world. Fellows pursue research that lies at the boundaries of the traditional academic disciplines, and that creates new fields of inquiry.

In addition to salary, health benefits, and retirement contributions, Fellows have access to funds to support travel to meetings, to visit collaborators at other institutions, and to bring collaborators to visit SFI. Fellows are encouraged to participate in all SFI activities, to invite speakers for the colloquium series, and to organize workshops and working groups.

Research at SFI is integrative, and there are no formal programs or departments. Individual research projects draw input from a variety of fields, including biology, chemistry, computer science, physics, mathematics, economics, sociology, anthropology, and political science. We welcome applications from any of these fields, as well as others not listed here. Descriptions of the research interests of the faculty and current Postdoctoral Fellows can be found at http://www.santafe.edu/research/researchers.php. Most research at SFI focuses on theoretical and computational approaches, although applicants whose research includes an experimental or data-collection component in collaboration with off-site colleagues are also encouraged to apply.

Candidates should have a Ph.D. (or expect to receive one by September 2007), a strong academic record, and a proven ability to work independently. We are particularly favorable toward applicants with an interest in trans-disciplinary interactions and collaboration, and who have demonstrated the potential to think outside traditional paradigms.

Applications are welcome from candidates in any country. Women and minorities are especially encouraged to apply. Successful foreign applicants must acquire an acceptable visa (usually a J-1) as a condition of employment.

TO APPLY: Please view the full position announcement and application instructions at **http://www.santafe.edu/education/postdocinst07.php**. For full consideration, please submit all application materials, including three letters of recommendation, by **November 15, 2006**. For further information, please e-mail **postdocinfo@santafe.edu**.

SFI is an equal opportunity employer.

National Cancer Institute

U.S. DEPARTMENT OF HEALTH AND HUMAN SERVICES

National Institutes of Health

POSTDOCTORAL FELLOWSHIP (Ph.D./M.D.) OPPORTUNITIES

The National Cancer Institute offers numerous postdoctoral fellowship opportunities in a large variety of science disciplines (chemistry, biochemistry, bioinformatics, biology, biostatistics, cancer biology, cell biology, epidemiology, genetics, HIV research, immunology, microbiology, molecular biology, nuclear radiochemistry, nutrition, optical probe chemistry, pathology, pharmacology, virology, etc.).

Fellowship opportunities can be viewed on our training and employment Web site "StarCatcher" **http://generalemployment.nci.nih.gov**. We recommend that you post your resume in either job category "Postdoctoral Fellowship (U.S. citizens and permanent residents)" or "Postdoctoral Fellowship (foreign visiting fellows)" for viewing by our principal investigators. Then use the links to our research divisions to apply for current positions and communicate directly with the principal investigators. The **Center for Cancer Research** (NCI's largest clinical and basic science research division) lists multiple fellowship opportunities on their link and provides the opportunity to search their index of branches/labs/programs to find areas of research of particular interest to you. The **Division of Cancer Epidemiology and Genetics** provides an online application for fellowships in molecular, nutrition, radiation and genetic epidemiology. The **Division of Cancer Prevention** offers an online application process for fellowship opportunities in cancer prevention.

NCI facilities located in Bethesda, Rockville, Gaithersburg and Frederick Maryland, present a professional environment and possess the best-funded and equipped laboratories in the United States. As the largest institute within the National Institutes of Health, NCI provides postdoctoral fellows the opportunity to interact with scientists from a wide range of life/medical sciences, and to attend lectures given by international renowned scientists. Stipend range $39,800 to $73,500 commensurate with experience. Standard self and family health insurance is provided and high-option coverage is available. Program duration is 2 to 5 years.

Open to graduating doctorate degree (Ph.D. and/or M.D.) students and current postdoctoral fellows with less than 5 years postdoctoral experience. U.S. citizenship, permanent residency (green card), or current authorization (F-1 or J-1 visa) for training in the United States is required.

Apply online at **http://generalemployment.nci.nih.gov**

DHHS, NIH and NCI are EQUAL OPPORTUNITY EMPLOYERS

ANNOUNCEMENTS

The Cystinosis Research Foundation 2006 Autumn Call for Funding Proposals

$1.2 Million Available

The Cystinosis Research Foundation's (CRF) ultimate goal is a cure for this disease. Research awards will be given for up to two years. The CRF has over $1.2 million dollars in research funds available. The number of awards and their value will depend on the number of outstanding proposals and the funds available at the time.

- Research Proposal — The CRF is pleased to announce its second 2006 call for research proposals. The CRF is prepared to fund proposals to improve the immediate care of children and young adults with cystinosis and to develop new understanding and treatment of cystinosis to help these children.
- Post-Doctoral Fellowships — The CRF plans to establish the first post-doctoral research fellowship program in the United States to encourage young investigators to establish careers in cystinosis research. Fellows will be funded for 2-3 years to a maximum of $75,000/year.

For the current funding cycle, proposals and fellowship applications must be received by November 6, 2006. Decisions for funding will be made by the end of the year. **For instructions on how to prepare proposals, visit www.natalieswish.org and click on research/grant guidelines.**

Review Process — Proposals are reviewed by a Scientific Review Board comprised of experts on Cystinosis who then advise the CRF on the scientific merit of each proposal. The CRF will balance the eventual funding to support clinical and bench research, and fellowships.

GEORGIA CAMPUS PCOM

Faculty Positions - Assistant Professor

(Associate considered)

Georgia Campus – PCOM is seeking candidates for the following full-time faculty positions for its Division of Basic Sciences. GA-PCOM teaches an integrated medical curriculum to osteopathic medical students and has an evolving graduate program in biomedical sciences; candidates for these positions will be expected to make contributions to the teaching of master's level candidates in our biomedical sciences graduate program. Candidates will be expected to engage in scholarly activity by engaging in research activities that will support graduate program development including mentoring of students, publication of works and the pursuit of extramural funding to support an independent research program. Candidates for each position must have an earned PhD degree in the respective field or closely related area; three (3) years of postdoctoral experience is required.

Biochemistry and Molecular Biology

Candidates must have ability to teach in the area of medical biochemistry and/or molecular biology. Preference will be given to candidates in the areas of molecular biology/genetics and nutritional biochemistry.

Physiology

Candidates should be broadly trained with emphasis in GI or neurophysiology. Must have interest in developing viable research program.

Microbiology

Prefer training in bacteriology but will consider other areas. Major teaching areas will be in bacteriology and mycology. Broad experience in other areas a plus.

The Georgia Campus of PCOM is Georgia's newest medical college with a total enrollment of 170 students in its first and second year DO classes and 54 biomedical sciences graduate students. The campus is located in beautiful Suwanee, Georgia, just 38 miles from the airport and 33 miles to downtown Atlanta.

Candidates should send letter of interest and curriculum vitae to:
Philadelphia College of Osteopathic Medicine, Human Resources Department,
4190 City Avenue, Philadelphia, PA 19131, Fax 215-871-6505 or email: hr@pcom.edu EOE

www.pcom.edu

UMDNJ NEW JERSEY MEDICAL SCHOOL
University of Medicine & Dentistry of New Jersey

Vice Chair of Research Associate/Full Professor Department of Anesthesiology

We are looking for a highly motivated and committed faculty member to take a leading role, as Vice Chair for Research, in strengthening our research program in the Department of Anesthesiology at UMDNJ New Jersey Medical School. We are seeking either an MD or PhD who is actively engaged in research and is interested in directing the further development of basic, translational, and clinical research in our department as well as maintaining his/her own research program. This individual will be provided with substantial resources for his/her own research and also for building a strong research group within the department. The individual will also be expected to integrate departmental research activity with that of New Jersey Medical School. Quality of research is of particular importance as is relevance to anesthesiology.

Interested candidates should forward cover letter and CV to: **Ellise Delphin, MD, MPH, Professor and Chair, Department of Anesthesiology, UMDNJ-New Jersey Medical School, 185 So. Orange Avenue, Newark, NJ 07103** or by email to **moynahan@umdnj.edu**.

POSTDOCTORAL OPPORTUNITIES

Max-Planck-Institut

für Wissenschaftsgeschichte

Postdoctoral Fellowship

The **Max Planck Institute for the History of Science in Berlin** announces five postdoctoral fellowships for up to two years, beginning in fall 2007.

1. One fellowship, beginning 1 October 2007, in Department III (headed by Hans-Jörg Rheinberger). Projects related to the history and epistemology of the life sciences are particularly welcome.
2. Four fellowships, beginning 1 September 2007, in Department II (headed by Lorraine Daston). Projects should relate to the history and/or philosophy of scientific observation, in either the natural or human sciences.

Outstanding junior scholars (Ph.D. awarded no earlier than 2002) are invited to apply. Fellowships are endowed with a monthly stipend between 1.900 and 2300 € (fellows from abroad). Women are especially encouraged to apply. The Max Planck Society is committed to employing more handicapped individuals. Qualified candidates with relevant projects may submit applications to both departments. The fellowships are open to candidates of all nationalities. The colloquium language is English.

Applications may be submitted in French, German, or English. Candidates are requested to send a curriculum vitae, publication list, research prospectus (maximum 1000 words), a sample text, and two letters of recommendation no later than **December 1, 2006** to:

Max Planck Institute for the History of Science
Administration, PD-II-III
Boltzmannstraße 22
D-14195 Berlin, Germany

Department of Chemistry
Inorganic Chemistry Laboratory

UNIVERSITY OF OXFORD

Technical Manager at the Multidisciplinary Research Centre for Advanced EPR

Academic-Related Research Staff Grade 8

Salary in the range of £31,525 - £37,643 p.a.

Applications are invited for the position of an EPR Technical Manager at the newly established Multidisciplinary Research Centre for Advanced EPR at the University of Oxford. You will organise and overlook the smooth technical day-to-day running of this facility. You will support the centre's technical, computational and experimental developments and research programme through strong interactions with all research groups (with interest ranging from quantum computing to biomedical applications). The post is available from November 2006. The starting salary is dependent on experience.

Further particulars are available from the below address or by e-mail from rita.higgs@chem.ox.ac.uk Informal enquiries may be made to Dr C R Timmel, e-mail: christiane.timmel@chem.ox.ac.uk.

Four copies of applications in the form of a letter, showing how you fulfil the selection criteria, CV and the names and addresses of two academic referees, should be sent (hard copy only) to: The Administrator, (quoting reference DH06020/CRT), University of Oxford, Inorganic Chemistry Laboratory, South Parks Road, Oxford, OX1 3QR, by the closing date of 9th October, 2006. At least one of these referees should be your current 'line manager' or supervisor, who may be contacted prior to interview.

The University is an Equal Opportunities Employer.

www.ox.ac.uk/jobs

National Institute of General Medical Sciences (NIGMS)

DIRECTOR, CENTER FOR BIOINFORMATICS AND COMPUTATIONAL BIOLOGY

The Person: The ideal candidate will have considerable research experience demonstrating a strong understanding of both computation and biological issues. In addition, candidates should possess recognized research management and leadership abilities. Candidates with primary training in computation/informatics and experience in biological research or with primary training in a biological/health related area and experience in computation/informatics will be considered. This individual will report to the Director, NIGMS, but will also have access to the Director, NIH, in coordinating activities across NIH and among Federal agencies.

The Challenge: A significant challenge for the biomedical research community is the integration of the vast amount of accumulating scientific data in order to develop predictive understanding of basic biological processes. The ability to meet this challenge will be critically dependent on advances in bioinformatics and computational biology. The Center for Bioinformatics and Computational Biology is responsible for stimulating and funding research in these areas of importance for NIGMS. The Center supports research on bioinformatics, databases, and data mining; on modeling of complex biological systems; on algorithmic development and software engineering; and on mathematical biology, among other areas. In addition, the Center is responsible for managing the NIH Biomedical Information Science and Technology Initiative (BISTI), an agency-wide effort to stimulate and coordinate use of computer science and technology to address problems in biology and medicine. Finally, the Center plays a major role in coordinating and directing the Bioinformatics and Computational Biology component of the NIH Roadmap for Medical Research. The institute is seeking a leader in this field to direct the Center and the BISTI efforts, and to coordinate the work of both with other interested federal agencies and the broader scientific community. Information about the Center and BISTI is available at: **http://www.nigms.nih.gov/About/Overview/cbcb.htm and http://www.bisti.nih.gov/**

Position Requirements: Candidates must have an M.D., Ph.D., or equivalent degree in a field relevant to the position. Please see the official vacancy announcement for qualification requirements and what to submit. The position will be filled under a Title 42 excepted service appointment, offering a competitive salary commensurate with qualifications and experience, within the range of $125,304 to $183,500. A recruitment or relocation bonus may be available. Relocation expenses will be paid.

How to Apply: The official vacancy announcement is available at: **http://www.nigms.nih.gov/About/Job_Vacancies/**

Applications must be received by the closing date: **Friday, September 29, 2006**.

You may contact Erin Bandak, Human Resources Specialist, with questions about this vacancy on 301-594-2035.

Positions @ NIH

The National Institutes of Health

Director, Division of Cardiovascular Diseases
National Heart, Lung, and Blood Institute

The National Heart Lung and Blood Institute (NHLBI) at the National Institutes of Health (NIH) seeks a dynamic physician-scientist to provide strategic leadership for its newly organized Division of Cardiovascular Diseases (DCVD). The Director will assume responsibility for creating and nurturing internationally-renowned programs which will participate actively in international research in cardiovascular diseases across the spectrum of basic science and clinical research including translational research and the conduct of a wide variety of clinical trials. The Director will recruit scientists and scientific administrators, develop and nurture a strong workforce, and build depth in disease-specific branches. Key challenges include establishment of priorities, integration of basic and clinical science, building teams, and interaction with scientific colleagues in many settings. Functioning as a key member of the senior leadership team of the Institute, the incumbent will collaborate with closely aligned programs in the Institute. The DCVD Director will have a profound impact upon the national investment in research, and the quality of service to the international research community. The Director of DCVD will have the opportunity to advocate for areas of critical importance to the national and global populace, to establish and implement programs congruent with NHLBI's strategic plan, and to improve the health of the public. Applicants must possess an MD or equivalent degree as well as senior level research experience, interpersonal and communications expertise and ability. The successful candidate will be a respected, accomplished researcher with maturity, integrity and outstanding communication skills.

Application Process: Please submit your CV, bibliography, and two letters of recommendation to: **Joanna Fesler, Program Manager, STG International, Inc, 4900 Seminary Rd., Suite 1100, Alexandria, VA 22311**. For further information, please call **877-784-6452 or email jfesler@stginternational.com**. Your application package should be received by **October 15, 2006**. All information provided by candidates will remain strictly confidential and will not be released outside the NHLBI search process without a signed release from candidates.

Salary is commensurate with experience and a full package of Civil Service benefits is available including retirement, health and life insurance, leave and savings plan (401K equivalent).

The National Heart, Lung, and Blood Institute (NHLBI) provides leadership for a national program in diseases of the heart, blood vessels, lung, and blood; blood resources; and sleep disorders. With nationwide responsibility for improving the health and well-being of all Americans, the Department of Health and Human Services oversees the biomedical research programs of the NIH. The NIH encourages the application and nomination of qualified women, minorities and individuals with disabilities.

Director, Division of Prevention and Population Sciences
National Heart, Lung, and Blood Institute

The National Heart Lung and Blood Institute (NHLBI) at the National Institutes of Health (NIH) seeks a dynamic scientist to provide strategic leadership for its newly reorganized Division of Prevention and Population Sciences (DPPS). The Director will assume primary responsibility for creating, nurturing and supporting internationally-renowned programs in population sciences and prevention in the areas of cardiovascular disease, and collaborating with closely aligned programs in the Division of Cardiovascular Diseases, Division of Lung Diseases, the Division of Blood Diseases and Resources, and the Division of Extramural Research Activities. The NHLBI also manages a strong program in biostatistics and resources for the conduct of clinical research. The NHLBI is engaged in a strategic planning process which will guide its scientific agenda for the next decade. The DPPS Director will advocate for areas of profound importance to the national and global populace, to establish and implement programs congruent with NHLBI's strategic plan and which will impact the health of the public. Functioning as a key member of the senior leadership team of the Institute, the incumbent will have a profound impact upon the national investment in research and the quality of service to the international research community. Applicants must possess an M.D., Ph.D. or equivalent degree as well as senior level research experience and ability to interact successfully with a broad range of individuals. The successful candidate will be a respected, accomplished scientist with maturity, integrity and outstanding communication skills.

Application Process: Please submit your CV, bibliography, and two letters of recommendation to: **Joanna Fesler, Program Manager, STG International, Inc, 4900 Seminary Rd., Suite 1100, Alexandria, VA 22311**. For further information, please call **877-784-6452 or email jfesler@stginternational.com**. Your application package should be received by **October 15, 2006**. All information provided by candidates will remain strictly confidential and will not be released outside the NHLBI search process without a signed release from candidates.

Salary is commensurate with experience and a full package of Civil Service benefits is available including retirement, health and life insurance, leave and savings plan (401K equivalent).

The National Heart, Lung, and Blood Institute (NHLBI) provides leadership for a national program in diseases of the heart, blood vessels, lung, and blood; blood resources; and sleep disorders. With nationwide responsibility for improving the health and well-being of all Americans, the Department of Health and Human Services oversees the biomedical research programs of the NIH. The NIH encourages the application and nomination of qualified women, minorities and individuals with disabilities.

WWW.NIH.GOV

Chief, Laboratory of Human Bacterial Pathogenesis
National Institute of Allergy and Infectious Diseases
National Institutes of Health

The National Institute of Allergy & Infectious Diseases (NIAID), Division of Intramural Research (DIR) is seeking an outstanding individual to head the Laboratory of Human Bacterial Pathogenesis (LHBP) in Hamilton, Montana.

The mission of the LHBP is to study human bacterial diseases related to emerging and re-emerging pathogens. The research to be conducted in the LHBP is to include; 1) the molecular basis of host-pathogen interactions, 2) the genetic basis of bacterial virulence and pathogenesis, 3) the use of animal modeling to define host defense mechanisms and biology and immunology of host-pathogen interactions, and 4) development of novel and improved intervention strategies to control bacterial infectious diseases. The ultimate goal is to develop diagnostics, vaccines, and therapeutics for emerging and re-emerging infectious diseases.

This position requires a Ph.D. and/or M.D. or equivalent with proven leadership abilities and a strong independent research program. Preference will be given to candidates with a documented record of accomplishment in bacterial disease research, and especially to those whose program(s) are consistent with the mission of the NIAID to study emerging and re-emerging bacterial pathogens.

The Laboratory Chief will have independent resources to lead and conduct laboratory research and translational/clinical research, as appropriate. Mechanisms are available to conduct clinical studies at the Bethesda campus and/or to obtain clinical samples through contract mechanisms at non-NIH institutions. The individual will supervise other Principal Investigators with independent research programs investigating the pathogenicity of Staphylococcus and Streptococcus species. Committed resources include space, support personnel, animal resources and an allocated annual budget to cover service, supplies and salaries. A Laboratory Chief in the DIR is equivalent to a Department Chair in a University or Medical School. Salary is dependent on experience and qualifications.

Interested candidates may contact **Dr. Karyl Barron, Deputy Director, DIR, NIAID at (301) 402-2208 or email (kbarron@niaid.nih.gov)** for additional information about the position. To apply for the position, candidates must submit a curriculum vitae, bibliography, a detailed statement of research interests, and reprints of up to three selected publications preferably via email to: **Felicia Braunstein at braunsteinf@niaid.nih.gov or by US Mail to: Ms. Felicia Braunstein, DIR Committee Manager, 10 Center Drive MSC 1349, Building 10, Rm. 4A-30, Bethesda, Maryland 20892-1349**. In addition, the names of three referees must be sent to **Dr. Tom Schwan, Chairperson, NIAID Search Committee, c/o Ms. Felicia Braunstein, DIR Committee Manager, 10 Center Drive MSC 1349, Building 10, Rm. 4A-30, Bethesda, Maryland 20892-1349**. Please note search **#005** when sending materials. Completed applications **MUST** be received by **October 6, 2006**. Further guidance on submitting your application is available on our website at: **http://healthresearch.niaid.nih.gov**.

The National Institute of Allergy and Infectious Diseases, a major research component of the NIH and the Department of Health and Human Services, is recruiting for a Staff Scientist. The position will be available in the Respiratory Viruses Section of the Laboratory of Infectious Diseases, and scientists with a M.D. or Ph.D. are eligible. The research activity involves (1) the development of live attenuated flavivirus vaccine candidates and their evaluation in rodents and non-human primates as well as in the clinical trials in humans; (2) the use of novel approaches for construction of chimeric viruses to examine basic questions of viral pathogenesis and the molecular basis of attenuation of highly neurovirulent flaviviruses; (3) the evaluation of the immunologic determinants of resistance to infection and illness caused by these flaviviruses. This full-time research position offers a unique opportunity to work on investigations that range from basic molecular biology to applied vaccinology. Staff Scientist applicants should have at least six years of laboratory work experience in molecular virology and immunology; the salary range is $73,178 - $165,195. Preference will be given to candidates who have experience working with neurotropic viruses. Applicants should submit their curriculum vitae, a letter of research interests, and names and addresses of three references to:

Alexander Pletnev, NIAID, NIH, 12735 Twinbrook Parkway, Twinbrook 3, Room 3W13, MSC 8133, Bethesda, MD 20892-8133, FAX: (301) 480-4873, email: apletnev@niaid.nih.gov. Review of applicants will begin **October 1, 2006** and continue until a successful candidate is identified.

TENURE-TRACK INVESTIGATOR, NICHD

The Program on Cell Regulation and Metabolism (PCRM), National Institute of Child Health and Human Development, invites applicants for a Tenure-track Principal Investigator studying gene expression, cell cycle control, signal transduction, or development using yeast, fruit fly, or nematode as a model system and emphasizing a genetic approach. The PCRM is an interactive environment featuring studies on transcriptional and translational control of gene expression, signal transduction, chromosome structure, nucleocytoplasmic transport, cell cycle control, transposable elements, DNA repair, hormone regulation of development, and development of the visual system using bacteria, yeast, fruit fly, frog, and mammalian cells as experimental systems. Applicants should have a Ph.D. or M.D. and a proven ability to conduct innovative research. Send a c.v., 2-page statement of research plans, and 3 recommendation letters by **November 15, 2006** to: **Alan Hinnebusch, Ph.D., NIH, Bldg 18T, Rm 106, Bethesda, MD 20892.**

Chief, Laboratory of Virology
National Institute of Allergy and Infectious Diseases
National Institutes of Health

The National Institute of Allergy & Infectious Diseases (NIAID), Division of Intramural Research (DIR) is seeking an outstanding individual to head the newly established Laboratory of Virology (LV) located at the Rocky Mountain Laboratories in Hamilton, Montana. LV will interact with four other Intramural Research Laboratories at this location presently studying infectious diseases involving viruses, bacteria, rickettsia, chlamydia and prions.

The mission of the LV is to study high containment BSL-3 and BSL-4 viral pathogens with the goal of developing diagnostics, vaccines, and therapeutics. The research to be conducted in the LV is to include studies of vector/reservoir transmission, pathogenesis, pathophysiology and host immune response of high containment viral pathogens. In addition, the LV must maintain a flexible infrastructure to permit rapid analysis of newly emerging high containment viral pathogens of special interest.

The selected candidate will supervise research in a newly constructed Integrated Research Facility which houses three BSL-4 lab suites, three BSL-3 lab suites and multiple BSL-2 lab suites, as well as extensive associated BSL-2, 3, and 4 animal facilities.

This position requires a Ph.D., M.D., D.V.M. or equivalent with proven ability to carry out a strong independent research program. Preference will be given to candidates with a record of leadership and accomplishment in BSL-4 or Select Agent BSL-3 viral pathogen research, with program(s) consistent with the mission of the NIAID. The selected person will also be expected to recruit and supervise other Principal Investigators with independent research programs.

The Laboratory Chief will have independent resources to conduct laboratory research and translational/clinical research, as appropriate. Committed resources include space, support personnel and an allocated annual budget to cover service, supplies and salaries. A Laboratory Chief in the DIR is equivalent to a Department Chair in a University or Medical School. Applicants must be eligible for the appropriate security clearance under the CDC Select Agent Program. Salary is dependent on experience and qualifications. Interested candidates may contact **Dr. Karyl Barron, Deputy Director, DIR, NIAID at 301/402-2208 or email (kbarron@niaid.nih.gov)** for additional information about the position.

To apply for the position, candidates must submit a curriculum vitae, bibliography, a detailed statement of research interests, the names of three references, and reprints of three selected publications, preferably via email to: **Felicia Braunstein at braunsteinf@niaid.nih.gov or by US Mail to: Ms. Felicia Braunstein, DIR Committee Manager, 10 Center Drive MSC 1349, Building 10, Rm. 4A-30, Bethesda, Maryland 20892-1349**. Please note search **#006** when sending materials. Completed applications **MUST** be received by **Friday, November 3, 2006**. Further information on working at NIAID is available on our website at: **http://healthresearch.niaid.nih.gov**

Chief, Laboratory of Human Bacterial Pathogenesis
National Institute of Allergy and Infectious Diseases
National Institutes of Health

The National Institute of Allergy & Infectious Diseases (NIAID), Division of Intramural Research (DIR) is seeking an outstanding individual to head the Laboratory of Human Bacterial Pathogenesis (LHBP) in Hamilton, Montana.

The mission of the LHBP is to study human bacterial diseases related to emerging and re-emerging pathogens. The research to be conducted in the LHBP is to include; 1) the molecular basis of host-pathogen interactions, 2) the genetic basis of bacterial virulence and pathogenesis, 3) the use of animal modeling to define host defense mechanisms and biology and immunology of host-pathogen interactions, and 4) development of novel and improved intervention strategies to control bacterial infectious diseases. The ultimate goal is to develop diagnostics, vaccines, and therapeutics for emerging and re-emerging infectious diseases.

This position requires a Ph.D. and/or M.D. or equivalent with proven leadership abilities and a strong independent research program. Preference will be given to candidates with a documented record of accomplishment in bacterial disease research, and especially to those whose program(s) are consistent with the mission of the NIAID to study emerging and re-emerging bacterial pathogens.

The Laboratory Chief will have independent resources to lead and conduct laboratory research and translational/clinical research, as appropriate. Mechanisms are available to conduct clinical studies at the Bethesda campus and/or to obtain clinical samples through contract mechanisms at non-NIH institutions. The individual will supervise other Principal Investigators with independent research programs investigating the pathogenicity of Staphylococcus and Streptococcus species. Committed resources include space, support personnel, animal resources and an allocated annual budget to cover service, supplies and salaries. A Laboratory Chief in the DIR is equivalent to a Department Chair in a University or Medical School. Salary is dependent on experience and qualifications.

Interested candidates may contact **Dr. Karyl Barron, Deputy Director, DIR, NIAID at (301) 402-2208 or email (kbarron@niaid.nih.gov)** for additional information about the position. To apply for the position, candidates must submit a curriculum vitae, bibliography, a detailed statement of research interests, and reprints of up to three selected publications preferably via email to: **Felicia Braunstein at braunsteinf@niaid.nih.gov or by US Mail to: Ms. Felicia Braunstein, DIR Committee Manager, 10 Center Drive MSC 1349, Building 10, Rm. 4A-30, Bethesda, Maryland 20892-1349**. In addition, the names of three referees must be sent to **Dr. Tom Schwan, Chairperson, NIAID Search Committee, c/o Ms. Felicia Braunstein, DIR Committee Manager, 10 Center Drive MSC 1349, Building 10, Rm. 4A-30, Bethesda, Maryland 20892-1349**. Please note search **#005** when sending materials. Completed applications **MUST** be received by **October 6, 2006**. Further guidance on submitting your application is available on our website at: **http://healthresearch.niaid.nih.gov**.

WWW.NIH.GOV

Department of Health and Human Services
National Institutes of Health
National Institute of Allergy and Infectious Diseases

With nation-wide responsibility for improving the health and well being of all Americans, the Department of Health and Human Services oversees the biomedical research programs of the National Institutes of Health (NIH) and those of NIH's research Institutes.

The National Institute of Allergy and Infectious Diseases (NIAID), a major research component of the NIH and the Department of Health and Human Services, is recruiting for a Tenure/Tenure Track position in the Laboratory of Host Defenses (LHD). The LHD studies immune functions essential for host defense against infection (inherited immune deficiencies) and those required for immune homeostasis (autoimmunity associated with excessive inflammation). The LHD seeks an M.D. or M.D., Ph.D. physician scientist to develop an independent translational research program related to the genetic basis, pathophysiology, diagnosis and treatment of autoimmune diseases associated with excessive inflammation. An emphasis on clinical aspects of innate immunity including phagocytic cells, natural killer cells, dendritic cells and other antigen presenting cells, toll-like receptors or other pattern recognition receptors in its interface with acquired immunity is desirable. The applicant should have a strong track record of basic research of the genetic basis of disease and alterations in signaling pathways responsible for immune dysregulation. The applicant must possess expertise and experience in the design and conduct of diagnostic and therapeutic clinical trials studying and treating autoimmune diseases. Strong clinical credentials in a specialty area relevant to the proposed translational research program (relevant specialties include but are not limited to rheumatology, pulmonary diseases, hematology, immunology or infectious diseases) are required. The program of study proposed by the applicant must include both laboratory components and the conduct of clinical protocols to assess new diagnostic and therapeutic modalities to diagnose and treat autoimmunity associated with excessive inflammation. Applicants particularly suitable for this program are those who have knowledge and experience in the development and clinical application of novel biological agents including chemokines, soluble chemokine receptors, adenosine receptor agonists, monoclonal antibodies, cellular therapies including transplantation or gene therapy to correct the abnormalities in immunity, that achieve immune tolerance or to reduce abnormal inflammation.

The applicant must provide evidence in the submitted materials that the applicant has a current license to practice medicine in one of the states of the United States or must have the all the credentials required by the State of Maryland for licensing to allow the practice of medicine. These credentials must include but are not limited to having a Doctor of Medicine or Doctor of Osteopathy degree from an accredited school in the U.S. or Canada, or a Doctor of Medicine or equivalent degree from a foreign medical school that provided education and medical knowledge substantially equivalent to accredited schools in the U.S. as demonstrated by permanent certification by the Educational Commission for Foreign Medical Graduates (ECFMG).

To be considered for this position, you will need to submit a curriculum vitae, bibliography, three (3) letters of reference, a detailed statement of research interests, and a hardcopy of selected publications to **Thomas A. Fleisher, MD, Chairperson, NIAID Search Committee, c/o Ms. Anissa N. Hunter, DIR Committee Coordinator, Reference Ad #009, 10 Center Drive MSC 1356, Building 10, Rm. 4A26, Bethesda, Maryland 20892-1356**. Completed applications **MUST** be received by **Thursday, November 15, 2006**. For additional information on this position, and for instructions on submitting your application, please see our website at: **www.niaid.nih.gov**.

Multiple Faculty Openings in Nanoscience (tenure-track / full professor)

TU Delft

Kavli Institute of Nanoscience Delft, Faculty of Applied Sciences
Delft University of Technology, The Netherlands

Introduction
The Kavli Institute of Nanoscience Delft is strengthening and expanding its current activities. As a result, applications are welcome from new potential colleagues for a variety of positions (Assistant Professor, Associate Professor & Full Professor). The profiles for these new positions are broad. We are seeking to attract candidates now active in those research areas of nanoscience which will compliment and strengthen our department.

Organisation
The Nanoscience department at TU Delft was recently established as Kavli Institute of Nanoscience, joining a global league with Caltech and Cornell.

With a strong international orientation, its members pursue cutting-edge research at the forefront of a variety of research fields within nanoscience. Current activities comprise quantum transport, molecular electronics, theory, nanoelectronics & -photonics, single-molecule biophysics, and electron microscopy. The availability of excellent, state-of-the-art nanofabrication and research infrastructure contribute to its success.

This department, together with its sister departments within the Faculty of Applied Sciences, represent the physics, chemistry and biotechnology activities of Delft University of Technology and share responsibility for the associated undergraduate and postgraduate programmes.

Profile
We plan to expand our research fields to complement existing activities. Therefore, persons with a strong track record in areas related (but not restricted) to molecular chemistry, nanoscale materials, molecular biosciences, nanomedicine, and nanophotonics are invited to apply for the existing openings. Successful candidates will be expected to establish an active research programme and contribute to teaching at both the undergraduate and graduate level.

Please send applications to the chairman of the search committee:
Prof. H.W.M. Salemink (**nanoscience@tnw.tudelft.nl**), chairman Department of Nanoscience.
For questions, details and procedures contact Roel Kamerling (**r.kamerling@tudelft.nl**) or visit our website at **www.ns.tudelft.nl**. We will continue our search until the positions are filled and no strict application deadline has been set. We will commence reviewing candidates in October 2006.

Prof.dr. H.W.M. Salemink, Delft University of Technology, Kavli Institute of Nanoscience Delft, Lorentzweg 1, 2628 CJ Delft, The Netherlands, Telephone: +31 - (0)15 – 278 3310.

STANFORD UNIVERSITY DEPARTMENT OF MOLECULAR PHARMACOLOGY

The Department of Molecular Pharmacology at Stanford University School of Medicine invites applications for a tenure-track or tenured position at the ASSISTANT or ASSOCIATE PROFESSOR level. Candidates whose research interests lie at the interface of biomedical and physical sciences (e.g., chemical biology, quantitative biology, or systems biology) are particularly encouraged to apply. Stanford offers an outstanding environment for creative interdisciplinary biomedical research. Rank and salary are dependent on the candidate's qualifications. The predominant criterion for appointment in the University Tenure Line is a major commitment to research and teaching.

Candidates should have a Ph.D. and/or M.D. degree and postdoctoral research experience. Selection will begin immediately. Candidates should send curriculum vitae, a description of future research plans and the names of three references by **October 1, 2006**, to:

James E. Ferrell, Jr., M.D. Ph.D.
c/o Jean Kavanagh, FAA
Department of Molecular Pharmacology
269 Campus Drive
CCSR Bldg Room 3145A
Stanford University School of Medicine
Stanford CA 94305-5174

Stanford University is an Equal Opportunity, Affirmative Action Employer.

Training Program in Cell and Molecular Dermatology

Postdoctoral fellowships available in NIH-funded Training Program in Cell and Molecular Dermatology at the University of Michigan. Training opportunities are available in basic science and translational research. Areas of focus include cancer biology (melanoma and non-melanoma skin cancer), psoriasis (genetics, genomics, and immunology), wound repair, chronological aging, and photoaging. Due to NIH restrictions, trainees must be U.S. citizens or permanent residents.

For further information about research activities in the Department of Dermatology, visit **http://www.med.umich.edu/derm/index.shtml**.

Send CV and references to:

Dr. James T. Elder
3312 CCGC
University of Michigan
Ann Arbor, MI 48109-0932
Email: jelder@umich.edu
Fax: (734) 763-4575

An Equal Opportunity/Affirmative Action Employer.

CytRx® CORPORATION

CytRx Corporation in Worcester, MA is a biopharmaceutial company that is developing the next generation of molecular medicines against proprietary drug targets for the treatment of metabolic diseases and their complications. Having built a powerful integrated RNAi-based target validation platform, CytRx is now actively using this platform to develop small molecule and RNAi-based therapeutics against novel drug targets. Located at the Worcester Biotech Park adjacent to the University of Massachusetts Medical School, our company offers challenging opportunities for highly motivated individuals seeking a fast-paced entrepreneurial environment. We are currently recruiting to fill the following positions:

VICE PRESIDENT, R&D

A newly created position, the Vice President, R&D will be a key member of the senior executive team and will be responsible for the vision, strategy, and day-to-day R&D activities of the Worcester site. Position requires an M.D. or Ph.D. in Life Sciences with demonstrated outstanding accomplishments in successful discovery programs within industry or academia. Extensive experience in leading a first class research group and a proven track record of product development is desirable.

DIRECTOR Biology/Metabolic Diseases

We are seeking an experienced scientist/leader to direct a group of 10 scientists to identify targets and advance lead candidates in the area of diabetes, obesity and atherosclerosis. Requires experience in the development and application of in vitro and in vivo model systems to advance drug candidates. Qualified candidates will have a Ph.D. in biological sciences, experience managing Ph.D. scientists and several years relevant experience in metabolic diseases research. Excellent communication skills and the aptitude to work in a highly collaborative environment are essential.

PRINCIPAL INVESTIGATOR/ SR. PI– Biology/Metabolic Diseases

We are seeking outstanding biologists to work as part of our target discovery and validation group. Candidates will use CytRx's proprietary RNAi based discovery platform to advance novel drug targets. Requires experience in utilizing molecular approaches to address biological questions of relevance to metabolic diseases. Research accomplishment using muscle, fat, liver or other relevant cells for assessing metabolic parameters is preferred. Qualified candidates will have a Ph.D. in biological sciences and 1-3 years relevant experience in metabolic diseases research. Excellent written and oral communication skills are critical.

CytRx Laboratories offers a highly enriching start-up environment with competitive compensation, benefits and stock options.

Contact:
hr@cytrx.com
508-767-3861
508-767-3862 (Fax)

cnïc

MINISTERIO DE SANIDAD Y CONSUMO

Instituto de Salud Carlos III

The CNIC (Spanish National Center for Cardiovascular Research) is a public Foundation established by the Spanish Ministry of Health and Consumer Affairs through the Carlos III Institute of Health. The Center's innovative financing structure includes a significant contribution from the private sector.

Following its recent restructuring into six new research departments, the CNIC is now seeking to recruit

BIOMEDICAL INVESTIGATORS

Post-doctoral Investigators – Junior Investigators – Senior Investigators

The CNIC is dedicated to excellence in cardiovascular research and to translating new knowledge into real improvements in clinical practice. The Center is located in a recently constructed building in the center of Madrid. The building has a total floor space of 23,000 m^2 and is equipped with the latest scientific equipment and research-support infrastructure. When fully occupied, this facility will house more than 300 investigators.

As part of its program of expansion and reorganization, the CNIC is seeking research staff for five of its new Research Departments to work in the following areas:

- Vascular Biology and Inflammation (REF: VBI)
- Atherothrombosis and Cardiovascular Imaging (REF: ACI)
- Regenerative Cardiology (REF: RC)
- Cardiovascular Developmental Biology (REF: CDB)
- Cardiovascular Epidemiology and Population Genetics (REF: CEPG)

Candidates for the category of **Post-doctoral Investigator** should have a PhD in a discipline related to biomedicine, as well as research experience in at least one of the areas identified above, with articles published in international journals.

Candidates for the category of **Junior Investigator** should possess an outstanding scientific track record, with publications of high impact at an international level.

Candidates for the category of **Senior Investigator** should, in addition to the above, demonstrate proven abilities and experience in strategic planning, resource management, and leadership and training.

The CNIC offers:

1) salaries competitive with those at leading biomedical research centers in Europe and the USA

2) an opportunity to join a growing center at a crucial stage of its development, and to rise to the challenge of creating an excellent scientific and technical working environment

3) significant start-up research funding commensurate with experience and track record

Applications, including a curriculum vitae, publications list, concise statement of research interests, and the **DEPARTMENTAL REFERENCE/S** of interest, should be sent by email to

investigacion@cnic.es

The CNIC treats all applicants and employees equally irrespective of nationality, ethnic origin, gender, marital or parental status, sexual orientation, creed, disability, age or political belief.

The CNIC is a bilingual institution, with Spanish and English as its official languages. Successful candidates must be fluent in at least one of these, and will be expected to become fluent in both within a reasonable period after their incorporation.

Details of our employment policy and further information about the CNIC can be obtained at **http://www.cnic.es**

University of Michigan Medical School

Center for Genetics in Health and Medicine

The University of Michigan is recruiting to fill an **ENDOWED CHAIR** with an established physician-scientist active in patient care and research who will serve as the **DIRECTOR** of the newly established, interdepartmental **Center for Genetics in Health and Medicine.** The Director will hold a basic science faculty appointment in the Department of Human Genetics and a joint appointment in the appropriate clinical department. The Center's mission is to develop and support an interactive community of faculty in the basic and clinical sciences that will develop new research opportunities that integrate modern genetics research with clinical and public health activities.

A curriculum vitae, description of current and future research, and three letters of recommendation should be submitted electronically to: hgsearch@umich.edu.

Dr. Sally Camper, Chair
Department of Human Genetics
Interim Director, CGHM
University of Michigan Medical School
4909 Buhl Bldg., 1241 Catherine St.
Ann Arbor, MI 48109-0618

For fullest consideration, applications should be complete by November 15, 2006.

The University of Michigan is an Equal Opportunity Employer and encourages applications from women and minorities.

http://www.cghm.med.umich.edu/

University of Michigan Medical School

Department of Human Genetics

The University of Michigan Department of Human Genetics is recruiting **SEVERAL FACULTY** at the rank of **ASSISTANT PROFESSOR** with research interests in genetics and genomics. New faculty will join an active and growing program that includes molecular, developmental, population and statistical geneticists working with model organisms, patients, and populations.

A curriculum vitae, description of current and future research, and three letters of recommendation should be submitted electronically to: hgsearch@umich.edu.

Dr. Sally Camper, Chair
Department of Human Genetics
University of Michigan Medical School
4909 Buhl Bldg., 1241 Catherine St.
Ann Arbor, MI 48109-0618

For fullest consideration, applications should be complete by November 15, 2006.

The University of Michigan is an Equal Opportunity Employer and encourages applications from women and minorities.

http://www.med.umich.edu/hg/

Department of Physiology
Tenure Track Faculty Positions

The Department of Physiology at The University of Texas Health Science Center at San Antonio (UTHSCSA) is continuing its major expansion. This year we seek to hire two tenure track faculty positions to begin by August 2007. The intention is to hire Assistant Professors, but exceptional candidates at more senior levels will be considered. At present, the Department of Physiology has clusters of research strength in neuroscience, cardiovascular function, ion channel biophysics, and the molecular biology of aging. Although candidates that can extend or bridge these areas are encouraged to apply, we are most interested in talented investigators using cutting edge techniques and/or model systems to elucidate fundamental physiological mechanisms at the molecular, cellular, or integrative levels. Candidates will be expected to contribute to the teaching mission that includes training medical, dental, and graduate students.

UTHSCSA is a Tier I Research Institution and the Department of Physiology nationally ranked 17th out of 98 in the most recent NIH funding. Plans and resources are in place to continue to grow both the University as a whole and the Department of Physiology in particular. Competitive start-up packages and ample resources will be offered to those selected to be a part of this exciting endeavor. UTHSCSA is located in the Northwest section of San Antonio and sits as a gateway to the picturesque Texas Hill Country. San Antonio is a vibrant, dynamic, and multicultural city with much to offer including an attractive cost-of-living.

Candidates should submit a Curriculum Vitae, and research accomplishments/goals (not to exceed two pages) as a single PDF to:

David S. Weiss, Ph.D., Professor and Chair
Department of Physiology
E-Mail: PhysioSearch@uthscsa.edu
Website: www.physiology.uthscsa.edu

Also, arrange for three letters of recommendation to be forwarded to the above e-mail address. Candidates who wish to be considered for this position should ensure that their applications are complete by **November 30, 2006**.

All faculty appointments are designated as security sensitive positions. The University of Texas Health Science Center at San Antonio is an Equal Employment Opportunity/Affirmative Action Employer.

香港城市大學 City University of Hong Kong

City University of Hong Kong invites applications for the following posts.

Associate Professorship/Assistant Professorship
Department of Biology and Chemistry *[Ref. A/471/32]*
Department of Computer Science *[Ref. A/472/32]*
Department of Electronic Engineering *[Ref. A/473/32]*
Department of Physics and Materials Science *[Ref. A/474/32]*
in
Bioinformatics, Nano-bio-science, New Materials, Computational Chemistry/Biology, and Application of Innovative Technologies in Novel Devices

Duties: Teach undergraduate/postgraduate courses and conduct research in the abovementioned areas. **Special emphasis will be given to teaching and research across boundaries of academic departments/disciplines.**

Requirements: A PhD degree with strong research background and publications in high-impact and peer-reviewed international journals. Candidates with applied research achievements and a successful record for winning competitive grants will receive very positive consideration. Relevant experience in business and industry will be a definite asset.

Salary and Conditions of Service
Salary offered will be highly competitive and commensurate with qualifications and experience. Appointment will be on a fixed-term gratuity-bearing contract. Fringe benefits include annual leave, medical and dental schemes, and housing benefits where applicable.

Information and Application
Information concerning the posts and the University is available at http://www.cityu.edu.hk or from the Human Resources Office, City University of Hong Kong, Tat Chee Avenue, Kowloon, Hong Kong [Fax : (852) 2788 1154 or (852) 2788 9334/E-mail : hrojob@cityu.edu.hk]. Please send an application letter enclosing a current curriculum vitae to the Human Resources Office by **30 November 2006**. Please quote the reference of the post in the application and on the envelope. The University reserves the right to consider late applications and nominations, and to fill or not to fill the positions.

OPEN TO

CHINA

Great research is born of open, agile minds. We invite you to share your unique abilities with us in support of our research efforts at our facility in China.

The Novartis Institutes for BioMedical Research is looking for biologists (PhD/MD) with at least five years of independent research experience, and chemists (PhD) with three or more years of biotech or pharmaceutical experience, for the following permanent positions in China:

BIOLOGY

Director, Drug Discovery
— PhD and/or MD (18518BR)

Director, Research Project Management
— PhD and/or MD (19824BR)

Director, External Collaboration
— PhD and/or MD, +/–MBA (19825BR)
Fluency in Chinese, familiarity with China's academic institutions and biotech industry preferred.

Group Leader (Associate Director level),
Molecular Virology — PhD and/or MD (19826BR)
HBV, HCV, and EBV specialists preferred.

Research Investigator, Virology
— PhD (19828BR)
HBV, HCV, and EBV specialists preferred.

Group Leader (Associate Director level),
Cancer Biology — PhD and/or MD (19830BR)

Group Leader (Associate Director level),
Liver Diseases — PhD and/or MD (19832BR)

CHEMISTRY

Group Leader (Associate Director level),
Medicinal Chemistry (18513BR)

Research Investigator, Medicinal Chemistry
— PhD (19834BR)

Research Investigator, Analytical Chemistry
— PhD (19836BR)

Research Investigator, Pharmacokinetics
— PhD (19837BR)

Comprehensive relocation packages and competitive compensation are available for these positions.

To view full descriptions of all open positions and to apply, visit www.nibr.novartis.com and follow the links to Careers and Job Opportunities. Please be sure to reference the corresponding Job ID number, as listed above, when applying.

Novartis is committed to embracing and leveraging diverse backgrounds, cultures, and talents to achieve competitive advantage.
Novartis is an equal opportunity employer. M/F/D/V

NOVARTIS
INSTITUTES FOR
BIOMEDICAL RESEARCH

www.nibr.novartis.com

Population Council

POPULATION COUNCIL SEEKS DIRECTOR FOR NEW HIV and AIDS PROGRAM

The Population Council, an international research organization, is seeking a program director for its new program in HIV and AIDS.

This program is being created as part of a major strategic reorganization at the Council. Its goal is to arrest the spread of HIV and AIDS in developing countries and to mitigate the impact on individual and community health. Activities include basic research in immunology; development and introduction of biomedical products; social science and health research; formulation of evidence-based policies; and development, evaluation, and scale-up of effective service-delivery models.

The program director will play the leading role in setting agendas and priorities for future program development and implementation; analysis and implementation of ongoing projects; allocation of unrestricted funds; fundraising; and representation of the Council to governments, non-governmental organizations, industry partners, donor agencies, and professional organizations worldwide. We seek an experienced individual with an international reputation for excellence in designing and implementing research programs; promoting the use of research results to improve programs and policies; strong publication record; superior leadership and team-building skills; MD or doctoral degree in relevant field; and experience working in the developing world. Knowledge of the pharmaceutical industry is preferred.

The program director will be headquartered in New York and will work closely with staff members in 17 regional and country offices in Latin America and the Caribbean, Southeast Asia, Sub-Saharan Africa, and West Asia and North Africa. Send CV and cover letter to the attention of **Ms. Vivien Rabin, Director of Human Resources; Population Council, One Dag Hammarskjold Plaza, New York, NY 10017; jobs@popcouncil.org; fax # (646) 277-8243**. For full job description, go to: **http://www.popcouncil.org/opportunities/07-06.html**.

AA/EOE M-F.

Columbia University
IN THE CITY OF NEW YORK

Tenure-Track Faculty in Developmental Neuroscience

The Columbia University Center for Neuroscience Initiatives, in conjunction with the Department of Psychiatry at Columbia and the Department of Developmental Psychobiology at the New York State Psychiatric Institute, is seeking applications for a new tenure-track faculty position in the area of Developmental Neuroscience. Candidates must have an M.D., Ph.D., or equivalent degree. The appointment is open to individuals at the level of Assistant or Associate Professor.

Applicants should have a demonstrated ability to conduct innovative, basic research that has the potential to contribute to translational investigations. Expertise in a broad range of neuroscience methodologies is highly desirable. These can include, but are not limited to, molecular neurobiology, neurogenetics, neuroanatomy, neuropharmacology, and electrophysiology. Areas of particular interest include developmental studies of neural circuits that underlie higher-level brain functions, and the regulation of emotional and/or cognitive states. Interest in genetic and environmental determinants of plasticity in neural systems will also be a useful area of emphasis.

Applicants should send their CV, a statement of research interests, and names of three referees to:

Bradley S. Peterson, M.D.
Columbia University Department of Psychiatry
1051 Riverside Drive, Unit 74, Room 2301
New York, NY 10032

E-mail: PetersoB@childpsych.columbia.edu

Columbia University takes affirmative action to ensure equal employment opportunity.

University of Central Florida

Transgenic Animal Facility Manager

Burnett College of Biomedical Sciences is building a 28,300 sq.ft. transgenic facility in the new 200,000 sq.ft. research building. The transgenic facility will serve about 40 research teams. Further major expansion of animal facilities is expected with the establishment of the new medical school that will be located adjacent to the Burnett Biomedical Sciences building in the new UCF Medical campus.

Applicants must have AALAS accreditation and experience with care for transgenic/knockout mice. Ability to work independently is preferred.

Please apply on-line at:
www.jobswithucf.com
Position #42239

The University of Central Florida is an Equal Opportunity, Equal Access, and Affirmative Action Employer. As a member of the Florida State University System, all application materials and selection procedures are available for public review.

CHAIR
Department of Biomedical Engineering
Vanderbilt University
Nashville, TN

Applications are invited for the Chair of the Department of Biomedical Engineering at Vanderbilt University. The department has 18 full time primary faculty, an enrollment of 400 undergraduate and 70 graduate students, and active research programs in many aspects of biomedical engineering including cellular and tissue engineering, imaging science, optics, biomaterials, nanotechnology, image guided therapies, and physiological modeling and measurements. Detailed information about the department is available at **http://www.bme.vanderbilt.edu**. Candidates should have an international reputation for outstanding scientific research accomplishments in a recognized field of biomedical engineering and a strong commitment to teaching. They should also have demonstrated leadership abilities and management skills, and a proven capacity to work effectively with faculty, students, staff, administrators, industry and others, and to attract external funding.

Interested candidates should submit a statement of interest and CV, or make informal enquiries to: **Professor John C. Gore, Ph.D., Chair, Search Committee for BME, Vanderbilt University Institute of Imaging Science, R-1302 Medical Center North, 1161 21st Ave South, Nashville, TN 37232-2675.**

Vanderbilt University is an Equal Employment Opportunity/Affirmative Action Employer.

Faculty Positions
Microbial Pathogenesis

The Department of Microbiology and Molecular Genetics of UMDNJ - New Jersey Medical School invites applicants for two tenure-track faculty positions at or above the level of Assistant Professor. We seek outstanding scientists who will develop externally funded research programs in molecular and/or genetic studies on the pathogenesis of viruses, bacteria, fungi or parasites. The new appointees will become part of a growing group of molecular biologists with common research interests in infectious diseases. In addition, they will participate in teaching graduate, medical and dental students. The department is housed in the new International Center for Public Health (ICPH) which it shares with the PHRI Center and the Global Tuberculosis Center. These entities form a cohesive group of scientists sharing common interests that create an exciting and productive environment. The ICPH is located in the pleasant University Heights section of Newark and is within 20 minutes of both New York City and more rural suburbs. Applicants must have a Ph.D., MD or equivalent degree and at least 2 years of postdoctoral research experience.

Please submit curriculum vitae including a statement of research interests and future plans. Applicants should also have three letters of reference transmitted to the department to complete their application. Materials should be sent to the **Chair of the Microbiology and Molecular Genetics Search Committee, Department of Microbiology and Molecular Genetics, UMDNJ - New Jersey Medical School, PO Box 1709, Newark NJ 07101-1709** or email a Word document, a Rich Text File, or a PDF attachment to **microsearch@umdnj.edu.** Review of applicants will commence upon receipt and will continue until the positions are filled. Further information on the department is available at **http://njmsmicro.umdnj.edu/.** UMDNJ is an Affirmative Action/Equal Opportunity Employer.

UMDNJ
NEW JERSEY MEDICAL SCHOOL
University of Medicine & Dentistry of New Jersey

Plant Molecular Biologist: Metabolomics

The new Department of Cell and Systems Biology at the University of Toronto invites applications for a tenure track faculty position to be appointed at the Assistant Professor level in the area of Plant Molecular Sciences to begin July 1, 2007.

Our vision is to advance systems biology in the area of Plant Metabolomics. Consequently, candidates must have demonstrated excellence in addressing fundamental questions in plant biology (particularly plant biochemistry, plant development or plant microbe interactions) using a metabolomics approach. Individuals with experience in high-throughput metabolomics analysis, method development for metabolite profiling, integration of metabolomics data into systems level analysis and/or computational analysis of complex metabolomics data are particularly encouraged to apply.

Candidates should have at least two years of research experience beyond their doctoral degree. In addition to pursuing a vigorous research program, the successful candidate will be expected to contribute to undergraduate and graduate teaching in molecular life sciences including the newly formed Cell and Systems Biology undergraduate program. She or he would also be expected to interact with faculty across campus working in related fields. There will be a generous start-up package and salary will be commensurate with qualifications and experience.

Applicants should arrange to have at least three letters of recommendation sent directly to the address below. In addition, applicants should forward their curriculum vitae, copies of significant publications, and statements of research and teaching interests to the **Chair, Plant Metabolomics Search Committee, Department of Cell and Systems Biology, University of Toronto, 25 Harbord Street, Toronto, ON M5S 3G5 Canada** by **November 1, 2006**. Inquiries should be directed to Professor Peter McCourt at **mccourt@botany. utoronto.ca**.

The University of Toronto offers the opportunity to teach, conduct research and live in one of the most diverse cities in the world, and is responsive to the needs of dual career couples. The University of Toronto is strongly committed to diversity within its community and especially welcomes applications from visible minority group members, women, Aboriginal persons, persons with disabilities, members of sexual minority groups, and others who may contribute to the further diversification of ideas. All qualified candidates are encouraged to apply; however, Canadians and permanent residents will be given priority.

Federal Ministry
of Education
and Research

Junior Research Groups for Nutrition Research

The German Federal Ministry of Education and Research (BMBF) provides the opportunity to build up an independent research group in molecular nutrition for outstanding scientists, not older than 39 years, from Germany or abroad. The main objective is to contribute towards understanding the effect of individual foodstuffs and their constituents on human health. Functional Food of the future should add an individual benefit to human health.

Besides a strategically convincing scientific concept for new approaches to molecular nutrition research, applicants need a German research institution to host their independent research group. Officially the grant has to be awarded to a German institution. Depending on the proposed scientific concept the group may consist of 1 group leader, 1 – 2 postdoctoral scientists, 1 – 2 PhD students, technical assistants. Successful candidates will be grant-funded for 5 years. Proposals will be selected by a jury.

The closing date for applications is 30 November, 2006

Contact:
Dr. Henrike Boermans, e-mail: h.boermans@fz-juelich.de

www.fz-juelich.de/ptj/nachwuchswettbewerbernaehrung

Tenure-Track Faculty Positions in Developmental Biology

Sloan-Kettering Institute, Memorial Sloan-Kettering Cancer Center invites applications for junior tenure-track faculty positions in the Program in Developmental Biology. Successful candidates will carry out independent research programs addressing problems in any aspect of Developmental Biology. Topics of particular interest include neural development, stem cell biology, gametogenesis and genetic mechanisms in development. Sloan-Kettering Institute offers a highly interactive and exciting research environment with outstanding infrastructure and resources to support research (www.ski.edu). New faculty will be eligible for appointment in the new Gerstner Sloan-Kettering Graduate School of Biomedical Sciences as well as the Weill Graduate School of Biomedical Sciences of Cornell University, a graduate program conducted jointly between Sloan-Kettering Institute and Weill Medical College.

Candidates should e-mail their application in PDF format to **devbio@mskcc.org** by November 15, 2006. The application should include a Curriculum Vitae, a description of past research, a description of proposed research, and copies of three representative publications. Candidates should arrange to have three letters of reference sent by e-mail to **devbio@mskcc.org** and by regular mail to **Developmental Biology Search, c/o Mr. Steven Cappiello, Memorial Sloan-Kettering Cancer Center, 1275 York Avenue, Box 193, New York, New York 10021.** The letters should arrive by November 15, 2006. Inquiries may be sent to Mr. Cappiello at **devbio@mskcc.org** or to Dr. Kathryn Anderson, Chair, Developmental Biology Program, Sloan-Kettering Institute. Memorial Sloan-Kettering Cancer Center is an Equal Opportunity Employer. Smoke-free environment.

Memorial Sloan-Kettering Cancer Center
The Best Cancer Care. Anywhere.
www.mskcc.org

THE UNIVERSITY OF HONG KONG

香 港 大 學

The University of Hong Kong is at the international forefront of higher learning and research, with more than 100 teaching departments and sub-divisions of studies, and more than 60 research institutes and centres. It has over 20,000 undergraduate and postgraduate students from 48 countries. English is the medium of instruction. The University is committed to international standards for excellence in scholarship and research.

School of Biological Sciences

Applications are invited for appointments as: **(1) Director of the School of Biological Sciences (at Chair level) (Ref.: RF-2006/2007-15); and (2) Professor/Chair of Biological Sciences (Ref.: RF-2006/2007-16)**, tenable from January 1, 2007 or as soon as possible thereafter. The appointments will initially be made on a three-year fixed-term basis. Candidates with exceptional qualifications may be considered for tenured appointment.

The newly formed School of Biological Sciences aspires to become a top research school in Asia with world-class research and teaching. The School has excellent research facilities and resources, and is supported by a dedicated team of experienced academic and research staff. The areas of expertise include biotechnology, molecular and cell biology, comparative endocrinology, human nutrition, food technology, ecology and biodiversity, marine biology and environmental toxicology.

Applicants should have a distinguished international reputation with a substantial research record. The appointees are expected to provide academic leadership in research and teaching. Research start-up funds will be available. For the position of Director, experience in management would be an advantage.

Starting annual salary for a Chair is within the non-clinical professorial range, the minimum of which is circa HK$1.1M, and that for a Professorship is around HK$803,700 (approximately US$1 = HK$7.8) (subject to review from time to time at the entire discretion of the University). The appointments also attract a contract-end gratuity and University contribution to a retirement benefits scheme, totalling up to 15% of basic salary.

At current rates, salaries tax does not exceed 16% of gross income. The appointments carry leave, housing benefits and medical and dental benefits.

Further particulars and application forms (272/302 amended) can be obtained at https://extranet.hku.hk/apptunit/; or from the Appointments Unit (Senior), Human Resource Section, Registry, The University of Hong Kong, Hong Kong (**Fax**: (852) 2540 6735 or 2559 2058; **E-mail**: apptunit@hkucc.hku.hk). Queries about the posts should be addressed to Professor S. Kwok, Dean, Faculty of Science (**Fax**: (852) 2858 4620); **E-mail**: sunkwok@hku.hk). **Closes October 31, 2006**.

The University is an equal opportunity employer and is committed to a No-Smoking Policy

Ecological/Evolutionary Genetics
Department of Biology
Indiana University, Bloomington

The Department of Biology invites applications for an open-rank position in Ecological and Evolutionary Genetics. We are especially interested in candidates investigating genetic variation in natural systems for any type of organism(s), individuals conducting experimental evolution on model organisms, or who creatively bridge traditional boundaries in evolutionary biology. For information about the Biology Department and for links to the campus and the Bloomington community, see **http://www.bio.indiana.edu**. For the graduate program in Evolution, Ecology and Behavior see **http://www.bio.indiana.edu/gradprograms/EEB/index.html**.

Candidates should send a curriculum vita, a statement of research and teaching interests, and representative reprints to:

Curt Lively
Ecological Genetics Search
Department of Biology
Indiana University
1001 E. Third Street
Bloomington, IN 47405-3700

Un-tenured candidates should also arrange to have three letters of recommendation sent to the same address, or by email to **jebennet@indiana.edu**. Review of applications will begin **1 November 2006**.

Indiana University is an Affirmative Action/Equal Opportunity Employer. Women and minority candidates are encouraged to apply.

St. Jude Children's Research Hospital
ALSAC • Danny Thomas, Founder
Finding cures. Saving children.

ASSISTANT MEMBER DEVELOPMENTAL NEUROBIOLOGY

An Assistant Member position is available in our Department of Developmental Neurobiology at St. Jude Children's Research Hospital (www.stjude.org/developmental-neurobiology) to establish a research program in contemporary developmental or cellular neurobiology. We are particularly interested in applicants using mouse models to investigate cell lineage specification, stem cell biology or protein trafficking in the nervous system. It is anticipated that successful applicants will have graduated within the past five years and have already achieved recognition through high profile publications.

There are currently seven faculty members in Developmental Neurobiology with the following research interests:

James Morgan (Chair): Molecular basis of neurodevelopment
Richard Smeyne: Cell biology of neurodegenerative disease
Suzanne Baker: Normal and neoplastic growth regulation in brain
Jian Zuo: Genetics of hearing and vision
Richard Gilbertson: Genomics and stem cells of brain tumors
Michael Dyer: Regulation of proliferation during retinal development
Stanislav Zakharenko: Mechanisms of synaptic plasticity

St. Jude offers a very competitive package for incoming junior faculty including salaries for the investigator and their personnel; generous laboratory space, startup and continuing support for equipment and consumables. Appointees have access to a wide range of institutional core facilities for protein and nucleic acid chemistry, microarray facilities, gene knockout and transgenic technologies and in vivo and ex vivo imaging capabilities that include a state-of-the-art multiphoton microscope. The Department is well equipped for most aspects of anatomy and histology, image analysis, cell and molecular biology, transgenics, behavioral analysis and electrophysiology.

Those interested in joining this multidisciplinary department should arrange to have their CV, a brief research proposal and three letters of recommendation sent to: The Developmental Neurobiology Search Committee/Job Code F4262, Attn: Ms. Carol Jacks, Department of Developmental Neurobiology, St. Jude Children's Research Hospital, 332 N. Lauderdale St., Memphis, TN 38105-2794.

www.stjude.org

St. Jude is an Equal Opportunity Employer and a Drug Free Workplace.
Candidates receiving offers of employment will be subject to preemployment drug testing and background checks.

ROPES & GRAY

Patent Agent/ Technical Advisor Program Boston and New York City

FISH & NEAVE IP GROUP OF ROPES & GRAY

The Fish & Neave Intellectual Property Group of Ropes & Gray LLP is an internationally known intellectual property law practice of over 200 lawyers. We are seeking Ph.D. candidates, nearing the completion of their studies and thesis defense, or recent Ph.D. graduates, working in academia or industry to join our Patent Agent/Technical Advisor Program. The candidates' Ph.D. degrees should be in the areas of synthetic organic chemistry, cellular biology, immunology, molecular biology, neurobiology, pharmaceutical sciences, bioinformatics, genomics, proteomics, polymer chemistry, or biochemistry.

The positions are full-time. We train the Patent Agent/Technical Advisor to prepare and to prosecute patent applications and to perform other tasks relating to our practice, including litigation, transactions, counseling and licensing. After one year with the firm, the Patent Agent/Technical Advisor also attends law school, either days or nights. During the last 15 years, more than 60 Ph.D's have joined our program and more than 40 have graduated from law school and are now working as intellectual property lawyers in biopharmaceuticals. The remainder are continuing their law school studies. Benefits: competitive salary; full law school tuition (with book allowance); medical benefits; 20-days paid vacation.

E-mail resumes with complete undergraduate and graduate transcripts to: **hiringprogram@ropesgray.com**.

Students may also mail their materials to:

Ms. Heather C. Fennell
Legal Recruitment Manager
Ropes & Gray LLP
Fish & Neave Intellectual Property Group
1251 Avenue of the Americas
New York, NY 10020

SYSTEMS BIOLOGY/PROTEOMICS CHAIR
The University of British Columbia, Vancouver, BC

The University of British Columbia recently launched a major initiative to fill five new faculty positions in the area of Systems Biology and Proteomics. Physically contiguous space has been provided at the centre of the campus, adjacent to the new Michael Smith Laboratories (http://www.msl.ubc.ca), offering an exceptional collaborative and interdisciplinary environment.

After highly successful first rounds of hiring, three full-time tenure-track faculty positions in Proteomics have been filled at the Assistant Professor level (http://www.proteomics.ubc.ca). We are now searching for exceptional candidates at a more senior level who are interested in providing leadership for this initiative. Candidates should have an outstanding record of accomplishments in fields relevant to Systems Biology and/or Proteomics including but not limited to mass spectrometry, bioinformatics, protein interaction networks, protein arrays, structural biology, HTS assays, protein chemistry, cell biology, signal transduction and physiology. The successful candidate will provide leadership in the operation and development of the UBC Systems Biology/Proteomics initiative. Academic appointment could be within or between departments in the Faculties of Medicine, Science and/or Pharmaceutical Sciences.

UBC has deep research strength across the Life Sciences, Physical Sciences and Computation, including its research hospitals and its formal associations with the British Columbia Cancer Agency, Genome British Columbia, the Genome Sciences Centre and the Institute for Systems Biology in Seattle. Researchers thus enjoy numerous opportunities for stimulating and productive collaborations. Opportunities exist to attract substantial research funding from government (e.g. Canadian Institutes for Health Research, Natural Sciences and Engineering Research Council of Canada, Canadian Foundation for Innovation), foundations (e.g. Michael Smith Foundation, Genome Canada) and industry.

Applications are being accepted on-line at **http://www.msl.ubc.ca/employment/faculty/**

Closing date for applications is November 15, 2006 but review of files will start prior to that date. Expected start date is July 1, 2007. Please direct any inquiries to proteomics@msl.ubc.ca

UBC hires on the basis of merit and is committed to employment equity. All positions are subject to final budgetary approval.

EMORY

Department of Chemistry
Emory University
Multiple Faculty Positions – Open Rank

A major financial commitment to Chemistry and a University-wide initiative in Computational and Life Sciences have uniquely positioned the Department of Chemistry for significant growth. Currently with 20 tenure track faculty, the Department graduates about 50 undergraduate BS majors annually and supports 150 graduate research students. We now plan to expand our research and teaching space to accommodate up to 10 new research faculty appointments, significantly enriching the commitment to chemical research. Accordingly, we seek:

Faculty applicants are encouraged **at all levels** across all areas of Chemistry from individuals with a proven record of accomplishment in research and scholarship. A Ph.D. in chemistry or a related field and a proven record of scholarship are required.

We aim to strengthen our core chemistry disciplines as well as broaden the impact of molecular sciences across our campus. Several aligned initiatives in materials and biomedical sciences, including the expanding resources available at the nationally recognized Woodruff Health Sciences Center, provide extensive opportunities for interdisciplinary and collaborative research.

Please submit a curriculum vitae, a cover letter, and a summary of research interests (candidates at the Assistant Professor level, specific research plans), and arrange for three letters of recommendation to be sent via **chemsearch@emory.edu** to **Search Committee Chair, Department of Chemistry, 1515 Dickey Drive, Emory University, Atlanta, GA 30322**. Reference posting **#207294**. Application review will begin on **October 1, 2006**.

Emory University is an Affirmative Action/Equal Opportunity Employer and welcomes applications from women and members of minority groups.

The University of Texas at Austin

Endowed Chair Positions
The Institute for Cellular and Molecular Biology

The Institute for Cellular and Molecular Biology invites applications for Endowed Chair positions. Academic appointments at the level of tenured Professor will be held in an appropriate academic unit in the College of Natural Sciences. Candidates should have an outstanding research program that applies molecular biological and/or biochemical approaches to important biological problems. The positions carry exceptional salaries and start-up packages.

Building on a strong existing faculty, the Institute has recruited more than 40 new faculty members in the past eight years. Faculty roster can be viewed at: http://www.icmb.utexas.edu. In addition to it's highly interactive and interdisciplinary research environment, the Institute is the home base for the University-wide Graduate Program in Cell and Molecular Biology and supports the state-of-the-art core facilities for DNA and protein analysis, mass spectrometry, electron and confocal microscopy, DNA microarrays, robotics, and mouse genetic engineering. A recently instituted MD-PhD program with the UT Medical Branch and the forthcoming Dell Pediatrics Research Institute will further enhance the environment for Biomedical Research.

Austin is located in the Texas hill country and is widely recognized as one of America's most beautiful and livable cities.

Please send curriculum vitae, summary of research interests, and names of five references to:

Dr. Alan M. Lambowitz, Director
Institute for Cellular and Molecular Biology
The University of Texas at Austin
1 University Station A4800
Austin TX 78712-0159

Homepage • http://www.icmb.utexas.edu

The University of Texas at Austin is an Equal Opportunity Employer. Qualified women and minorities are encouraged to apply; a background check will be conducted on applicant selected.

POSTDOC OPPORTUNITIES

BLOOD COAGULATION AND FIBRINOLYSIS RESEARCH

POSTDOCTORAL POSITIONS are available to investigate the mechanisms and regulation of blood coagulation and fibrinolysis with molecular biology, protein chemistry, enzyme kinetics, and fluorescence spectroscopy techniques. Interested individuals who are recent Ph.D. degree graduates in biochemistry, biophysics, chemistry, or biology should send a copy of their curriculum vitae and arrange for two letters of recommendation to be sent to: **Dr. Paul E. Bock, Vanderbilt University School of Medicine, Department of Pathology, C-3322 MCN, 1161 21st Avenue S., Nashville, TN 37232-2561. E-mail: paul.bock@vanderbilt.edu.**

Vanderbilt University is an Equal Opportunity/Affirmative Action Employer.

POSTDOCTORAL POSITION
Harvard Medical School

Postdoctoral positions are available to study the mechanisms of translational control in neurons, and the role of dendritic protein synthesis in synaptic plasticity, cognition and neuropsychiatric disease (*Cell* **116:**467, 2004, *Neuron* **44:**59, 2004).

Candidates should be highly motivated and have expertise in molecular biology, biochemistry, or electrophysiology. Please send curriculum vitae and names of three references to: **Dr. Ray Kelleher, Center for Human Genetic Research, Massachsetts General Hospital, 185 Cambridge Street, Boston, MA 02114, e-mail: kelleher@helix.mgh.harvard.edu.**

POSTDOCTORAL POSITION

A Postdoctoral position is available to study cell/molecular and biology of complications of diabetes mellitus and kidney development. Potential candidates must have documented experience in this area of research and in cell and molecular biology techniques. Please send curriculum vitae with references to: **Yashpal S. Kanwar, M.D., Ph.D., Northwestern University Medical School, 303 E. Chicago Avenue, Chicago, IL 60611, U.S.A. E-mail: y-kanwar@northwestern.edu.**

POSITIONS OPEN

CONSERVATION BIOLOGY FACULTY POSITIONS
Fordham University

The Department of Biological Sciences of Fordham University invites applicants for two separate tenure-track faculty positions in conservation biology at the **ASSISTANT PROFESSOR** level for fall 2007. For the first position, we seek an **ANIMAL ECOLOGIST** interested in establishing research collaborations with the Wildlife Conservation Society. The second position will be filled by a **PLANT CONSERVATION BIOLOGIST** interested in establishing research collaborations with the New York Botanical Garden. There are also research opportunities at Fordham's biological field station, the Louis Calder Center, and other scientific institutions in the region. We seek individuals who will establish a vigorous, extramurally funded research program. The successful candidates must have a Ph.D. and postdoctoral experience and are expected to teach at both the undergraduate and graduate levels. Applicants should indicate which position they seek (Animal or Plant Conservation Ecologist) and submit curriculum vitae, research statement, teaching philosophy, and the names and contact information of three references by November 1, 2006, to: **Dr. Robert Ross, Chair, Department of Biological Sciences, Fordham University, 441 E. Fordham Road, Larkin Hall 160, Bronx, NY 10458.**

Fordham University is an independent, Catholic university in the Jesuit tradition that welcomes applications from men and women of all backgrounds. Fordham is an Equal Opportunity/Affirmative Action Employer.

POSITIONS OPEN

FACULTY POSITION
Plant Metabolism/Biotechnology
Washington State University, Pullman, Washington

The School of Biological Sciences at Washington State University (WSU) in Pullman, Washington, invites applications for a full-time tenure-track position at the **ASSISTANT/ASSOCIATE PROFESSOR** level in plant metabolism/biotechnology (details at **website: http://www.sci.wsu.edu/sbs/index.php3**). Experience in applying rapidly developing techniques (e.g. genomics, proteomics, and metabolomics) to the study of plant metabolism is desirable. Examples of areas of research include coordination of chloroplast, mitochondrial and nuclear gene expression, primary metabolism (C, N, S, P), compartmentation and flux, and hormonal regulation. Potential applications of genetic modification include analysis of gene function and plant performance (e.g. water use efficiency, nutritional quality, partitioning, growth dynamics, and senescence). The successful candidate will be expected to establish an internationally recognized, externally funded research program and teach undergraduate and graduate courses. Applicants must have a Ph.D., one year of postdoctoral experience, and evidence of success, or potential, in grantsmanship and teaching. Applicants should submit a letter of application, curriculum vitae, selected reprints, statements on research and teaching interests, and have three letters of reference sent to: **Dr. Gerald Edwards, c/o Linda Larrabee, Plant Metabolism Search Committee, School of Biological Sciences, Washington State University, Pullman, WA, 99164-4236,** or via **e-mail: larrabee@wsu.edu.** Review of applications will begin on November 15, 2006. *WSU is an Equal Opportunity Educator and Employer. Members of protected groups are encouraged to apply.*

RESEARCH ASSISTANT PROFESSOR

This position is a full-time, nontenure-track position in the Department of Molecular and Cellular Biochemistry. The individual should hold a Ph.D. or equivalent degree in biochemistry or a related field and have at least three years of postdoctoral experience with peer-reviewed publications in respectable scientific journals. The successful candidate should have experience in conducting studies on the mammalian signal transduction pathways and the regulation of neural survival. He/she should be familiar with cell culture techniques, cell transfection techniques, and molecular biological techniques. The successful candidate will be expected to obtain extramural funding to support their salary and their research.

Interested individual should send their curriculum vitae and three references to:

Research Assistant Professor Search Committee
Department of Molecular and Cellular Biochemistry
278 Biomedical Biological Sciences Research Building
741 South Limestone
Lexington, KY 40536-0509

If offered this position, you will be required to pass a pre-employment drug screen and national background check as required by University of Kentucky Human Resources. The University of Kentucky is an Equal Opportunity Employer and encourages applications from women and qualified minorities.

TENURE-TRACK POSITION
LaGrange College

LaGrange College seeks a **BIOCHEMIST** for a tenure-track position. Research involving undergraduates and an interest in participating in interdisciplinary teaching are extremely desirable. An earned Ph.D. is required for a tenure-track appointment. Send letter, curriculum vitae, three letters of recommendation, statement of teaching philosophy, and transcripts to: **Dr. Bill McCoy, Chair, Department of Chemistry and Physics, LaGrange College, 601 Broad Street, LaGrange, GA 30240** or to **e-mail: wmccoy@lagrange.edu.** Review of candidates begins November 1, 2006, and will continue until the position is filled. For more information about the College and this position, please refer to our **website: http://www.lagrange.edu.**

POSITIONS OPEN

TENURE-TRACK ASSISTANT PROFESSOR

The Department of Biological Sciences at Mount Holyoke College invites applicants for a tenure-track position in cell biology at the Assistant Professor level, beginning fall 2007. Applicants are expected to have a Ph.D., and postdoctoral experience is preferred. The college is well equipped with cell and molecular biology facilities, including a newly staffed interdepartmental Microscopy Center, housing transmission electron microscope, scanning electron microscopy, atomic force microscopy, fluorescence and confocal microscopes with image processing software. The applicant should have a strong commitment to undergraduate teaching and research; a research program that can easily accommodate and encourage undergraduates is crucial. The candidate will have the opportunity to teach cell biology at different levels of the curriculum, with participation in the Program in Biochemistry encouraged.

Mount Holyoke is an undergraduate liberal arts college for women with 2,000 students and 200 faculty. The college is located about 80 miles west of Boston in the Connecticut River Valley and is a member of the Five College Consortium consisting of Amherst, Hampshire, Mount Holyoke and Smith Colleges, and the University of Massachusetts. The campus has grown increasingly diverse over the past fifteen years; half of the faculty are women and one quarter are persons of color. Among our students, approximately 40 percent are students of color and 17 percent are international. We in the Department of Biological Sciences appreciate the complexities of living and working in a diverse world and strive to find ways to redress inequities. We particularly encourage people who share these commitments to submit their application.

Applicants should submit their curriculum vitae, brief statements of teaching and research interests, a list of relevant course work and reprints of two publications. We ask that applicants incorporate relevant background experience or proposed strategies for mentoring a diverse student body into their materials. Applications and three letters of recommendation should be sent to:

Cell Biology Search Committee
Department of Biological Sciences
Mount Holyoke College
South Hadley, MA 01075

Review of applications is expected to begin by October 16, 2006. For more information, go to **website: http://www.mtholyoke.edu/acad/biol/.**

Mount Holyoke is committed to fostering multicultural diversity and awareness in its faculty, staff, and student body and is an Affirmative Action, Equal Opportunity Employer. Women and persons of color are especially encouraged to apply.

SCIENTIFIC PROGRAM DIRECTOR (SPD)

JDRF, Juvenile Diabetes Research Foundation International, the world's leading charitable funder of diabetes research, has a dynamic research opportunity available at the Foundation's New York City headquarters for a Scientific Program Director (SPD) with the Complications team.

The SPD is responsible for JDRF's Diabetic Complications Research Program portfolio. S/he will develop research strategy and project/program portfolio for the area and proactively manage the academic and industry-based projects/programs. The SPD also collaborates with staff to manage, facilitate, and integrate this research program.

Requirements include: Ph.D. or M.D.; five to ten years of progressively responsible and related experience and experience managing research portfolios, especially in industry/pharmaceuticals; minimum of three years in a supervisory capacity; and be a team player, with knowledge of diabetes desirable.

Please send curriculum vitae with salary requirements to **e-mail: jobs@JDRF.org** with /SPDC in the subject line (e-mail preferred) or to: **S. Del Valle, Ref: SPDC, Juvenile Diabetes Research Foundation, 120 Wall Street, New York, NY 10005.**

Equal Opportunity Employer.

New York University

DEAN

NYU College of Dentistry

New York University invites applications and nominations for a Dean of the NYU College of Dentistry. The committee seeks a seasoned, talented, ambitious academic leader who can guide the NYU College of Dentistry (NYUCD) on a continuing upward trajectory to a position of research, teaching and clinical preeminence among elite academic centers nationally and internationally.

The NYUCD, established in 1865, is the third oldest dental school in the United States and the largest private institution of its kind. Over the past 8 years the NYUCD has undergone the most dramatic changes in its history, including significant improvements in admissions, academic programs, faculty recruitment, research, physical plant and fundraising. In research, the NYUCD is ranked 6th in NIDCR funding. In education, the College is twice the size of its nearest competitor, and has experienced a 30% increase in applications in the last 2 years. The NYUCD has a historical commitment to providing health care to the people of New York. The College's clinics provide nearly 300,000 visits each year, including services to over 30,000 new patients, many from underserved populations. The College is also strongly committed to global health, with a large program for international dentists and the expansion of pre-doctoral clinical outreach programs in developing countries.

True to its recent meteoric rise, one of the most dramatic moves in the history of the College was to have the NYU College of Nursing join the College of Dentistry in the fall of 2005. The College of Nursing is one of the top nursing programs in the country with over 800 students. This merger is the first of its kind in the country and reflects the uniqueness and pioneering spirit of New York University. In bringing these two colleges together, the University hopes to create a new paradigm for health care delivery, research and education as we move forward into the 21st century.

NYU is an emerging great university, the dominant academic dental center in New York City, the largest and densest health care marketplace in America. The University, Board and NYUCD leadership believe it is positioned for continuing success.

The Search Committee seeks an entrepreneurial, sophisticated leader who can capitalize on the New York location and the collaborative strength of the Nursing and Dental communities, and lead the College through the next phase of its strategic vision for its research, teaching and clinical missions. Further information can be found at **http://www.nyu.edu/dental**.

Nominations, inquiries or applications may be sent in confidence to

3277@imsearch.com *(electronic submissions strongly preferred)*, or to:

Michael Baer or Barbara Stevens, Isaacson, Miller

1875 Connecticut Avenue, NW, Suite 710, Washington, DC 20009

NYU is an Equal Opportunity/Affirmative Action Employer.

University of Central Florida

Faculty Positions in Biochemistry

The Chemistry Department invites applications for both a tenure-track faculty position and non-tenure track positions (Visiting Lecturer or Lecturer) to begin in Fall 2007; rank is open for the tenure-track position. Candidates with research interests in forensic science and forensic biochemistry are especially encouraged to apply. A Ph.D. in Chemistry, or closely related field, is required for the tenure-track position and nontenure-track Visiting Lecturer and Lecturer positions, and postdoctoral experience is required for the tenure-track position. Candidates at the higher ranks must have a demonstrated record of accomplishments in extramural funding, publication, and teaching. In addition to contributing to teaching at both the graduate and undergraduate levels, applicants for the tenure-track position are expected to develop an externally-funded, nationally-recognized research program. The faculty member will contribute to the BS Chemistry, BS/MS Forensic Science, Ph.D. Chemistry, and Ph.D. Biomolecular Science programs. Depending upon the faculty member's interests and background, opportunities exist to interact with the National Center for Forensic Science (NCFS), CREOL, Biomolecular Science Center, Nanoscience Technology Center, and other departments within the university. The University of Central Florida is located in Orlando, Florida and has become one of the nation's largest universities with 46,000 students and is continuing to build nationally-recognized research programs.

Applicants should clearly indicate to which position they are applying and submit a curriculum vitae, description of their research plans (tenure-track only), graduate/undergraduate course teaching interests, teaching philosophy, and have three letters of recommendation sent on their behalf to: **Biochemistry Search Committee, Department of Chemistry, University of Central Florida, Orlando, FL 32816-2366** or send via email to: **chemstaf@mail.ucf.edu**. Review of applications will begin **November 15th 2006** and continue until the position is filled.

The University of Central Florida is an Equal Opportunity Employer and welcomes nominations and applications from women and minority group candidates. UCF makes all application materials (including transcripts) available for public review upon request.

ACADEMIC PHYSICIAN SCIENTISTS

The Saul R. Korey Dept of Neurology, Albert Einstein College of Medicine and the Dept of Neurology, Montefiore Medical Center

The University Dept of Neurology is undergoing major program expansion in multiple areas of clinical, translational and basic science research. We seek new faculty members interested in the areas of molecular genetics, stem cell biology and regenerative neurology, aging and dementia, movement disorders, neuromuscular disorders, cerebrovascular diseases neurooncology, neuroimmunology, autism and neurodevelopmental disorders and the neurobiology of disease. Applicants should have MD, MD/PhD or Ph.D. degrees with evidence of significant scholarly activities in clinical, translational or basic science research.

The University Dept of Neurology is one of the oldest, largest (120 faculty members) and most prestigious in the nation. It has a outstanding record of innovative multidisciplinary comprehensive clinical care, research and training programs with extensive collaborations with AECOM-associated comprehensive clinical care and clinical, translational and basic science research centers and institutes. The Department serves a unique, ethnically diverse patient population of over 5 million individuals from the Bronx, Southern Westchester, Northern New Jersey and Long Island.

We offer competitive salary, benefits and resource packages and academic rank at the Assistant, Associate or Full Professor level on the University tenure-track system depending on the level of academic accomplishments and experience. Interested applicants should forward a CV, a statement of academic interests, goals and accomplishments and three letters of reference to **Mark F. Mehler, MD, Alpern Professor and University Chair, Dept of Neurology, c/o Ms. Ana Cioffi, Administrator, email: cioffi@aecom.yu.edu, ALBERT EINSTEIN COLLEGE OF MEDICINE, Jack and Pearl Resnick Campus, K220, 1410 Pelham Parkway South, Bronx, N.Y. 10461.** EOE

ALBERT EINSTEIN COLLEGE OF MEDICINE

Advancing science, building careers

POSITIONS OPEN

AQUATIC BIOLOGIST AND EXECUTIVE DIRECTOR
Missouri River Institute

The University of South Dakota invites applications and nominations for Executive Director of the Missouri River Institute (MRI). The MRI is a developing entity with a multifaceted mission, addressing ecological and water quality issues associated with large floodplain river systems. The MRI Director will develop a vision for the future of the Institute to foster its growth and development. The successful candidate will direct a research program, currently supported with external funds, with a focus on large floodplain river systems; and contribute to teaching and mentoring of graduate and undergraduate students within his or her area of expertise. Effort will be 50 percent in the MRI (administration and directing research) and 50 percent in the Department of Biology (to include teaching up to one course per year). Academic credentials qualifying for appointment of Associate or Full Professor (tenure-track) are required, and administrative experience as Director or Chair is highly desired. Demonstrated experience in obtaining and administering large research programs (including budgeting and assessment) is essential. The Director will display excellent interpersonal skills, proficiency with written and oral communications, and research productivity.

The attractive startup package includes competitive salary and benefits and, contingent upon satisfactory performance, three years of administrative and research support and an MRI operating budget. After this period, the Director will be expected to generate external funding for growth of the Institute, and have a self-sustaining research program. Research and administrative space will be provided at both Ponca State Park and the Vermillion campus.

Applications should include a cover letter specifying qualifications for the position, a statement of research interests, names and contact information for four professional references, and curriculum vitae. Applications must be submitted online at **website: http://yourfuture.sdbor.edu.** Questions should be directed to the Department of Biology (**telephone: 605-677-5211**) or Office of Research and Sponsored Programs **(telephone: 605-677-5370).** Information about the University of South Dakota can be found at **website: http://www.usd.edu.** *The University of South Dakota is an Equal Opportunity/Affirmative Action Employer committed to increasing the diversity of its faculty, staff, and students.*

TENURE-TRACK FACULTY POSITION IN THE AREAS OF PAIN, STRESS, OR INFLAMMATION

The Department of Biomedical Sciences at the University of Maryland, Baltimore, is seeking candidates for a tenure-track faculty appointment. We encourage applications for positions at the **ASSISTANT PROFESSOR** level but will also consider applications from more senior investigators. The applicant should have a Ph.D., postdoctoral experience, and an active research program. Preference will be given to a **NEUROSCIENTIST** interested in the molecular, genetic, cellular electrophysiological, and/or imaging approaches to studying the neurobiological response to somatic and visceral tissue injury. The individual filling this position will also be expected to participate in professional and graduate student educational programs. The successful applicant will have research space in a new state-of-the-art facility, to be occupied in October 2006. The University of Maryland has a world-renowned program in neuroscience, providing for interactions among the various basic and clinical neuroscience divisions, and linking neurosciences to other scientific disciplines within the University. We strongly encourage applications from qualified women and minority candidates. Send curriculum vitae, statement of career objectives, and the names of at least three references to: **Dr. Joel Greenspan, Chair, Search Committee, Department of Biomedical Sciences, University of Maryland, Baltimore, 666 W. Baltimore Street, Baltimore, MD 21201. Website: http://bms.dental.umaryland.edu.**

THE UNIVERSITY OF KANSAS
Department of Chemistry
Room 2010 Malott Hall, 1251 Wescoe Hall Drive
Lawrence, Kansas 66045

ASSISTANT PROFESSOR position in experimental physical chemistry. The Chemistry Department invites applications for a tenure-track Assistant Professor faculty position beginning August 16, 2007. A Ph.D. in physical chemistry or related field and evidence of potential to build a vigorous research program in experimental physical chemistry or closely related field are required. Postdoctoral experience and multidisciplinary research plans are desirable. Duties include teaching at the undergraduate and graduate levels and development and direction of a vigorous research program in experimental physical chemistry. Salary will be commensurate with qualifications and experience. Applicants should submit a letter of interest, curriculum vitae, research plan, and description of teaching interests. In addition, applicants should arrange for the submission of at least three letters of recommendation to: **Professor Carey Johnson, Physical Search Committee Chair, e-mail: ckjohnson@ku.edu, telephone: 785-864-4219.** Initial review of applications will begin November 1, 2006, and will continue until the position is filled.

Equal Opportunity/Affirmative Action Employer.

ASSISTANT PROFESSOR
The University of Chicago
Department of Chemistry

The Department of Chemistry of the University of Chicago invites applications from outstanding individuals for the position of Assistant Professor of chemistry. This search is in the areas broadly defined as inorganic, organic, and physical chemistry. Applicants must mail hardcopies of curriculum vitae, a list of publications, and a succinct outline of their research plans, and arrange for three letters of recommendation to be sent by mail to: **Michael D. Hopkins, Chairman, Department of Chemistry, The University of Chicago, 5735 S. Ellis Avenue, Chicago, IL 60637.** Review of completed applications will begin October 1, 2006; to ensure full consideration, all material should be submitted by that date.

An Equal Opportunity/Affirmative Action Employer.

FRED HUTCHINSON CANCER RESEARCH CENTER

RESEARCH ASSOCIATE G-21074. Perform clinical laboratory research on graft versus host disease, steroid therapy resistance, and tolerance in patients after hematopoietic stem cell transplantation. Requires a Master's degree in medical or biological science, or foreign degree equivalent; three yearrs of clinical laboratory research experience in hematopoietic stem cell transplantation, including technical experience and proficiency in isolating, purifying, and maintaining specific lymphocyte subsets; performing flow cytometry and analyzing immunophenotype and cell death; performing in vitro functional assays to measure immune activation and effector functions; analyze and interpret precursor frequency assays; and prepare dendritic cell cultures. Full-time, Seattle, Washington. For more information send resumes to **website: http://www.fhcrc.org.**

FACULTY POSITION: VERTEBRATE BIOLOGIST

Spring Hill College, a Jesuit, Catholic College. **ASSISTANT PROFESSOR** (tenure track) for August 2007. Principles of biology, human anatomy and physiology, vertebrate zoology, upper division courses in area of specialty. Expertise in developmental biology and/or neurobiology desirable. Ph.D. and documented teaching excellence required. Those interested in developing research program with undergraduates encouraged to apply. Send cover letter, curriculum vitae, statements on teaching/research, unofficial academic transcripts, and three letters of reference to: **Dr. David F. Dean, Chair, Spring Hill College, 4000 Dauphin Street, Mobile, AL 36608 (e-mail: ddean@shc.edu).** See **website: http://www.shc.edu/jobs.** *Equal Opportunity Employer.*

CONSERVATION BIOLOGY

The Department of Biology at the College of William and Mary seeks applications for a tenure-track position at the **ASSISTANT PROFESSOR** level in conservation biology. The position is open to applicants conducting research in any field or scale of conservation biology that contributes to existing Departmental strengths in molecular and ecology/evolutionary biology. The ideal candidate will have strong quantitative skills, a sustained research focus in conservation biology, and the ability to integrate approaches across diverse levels of biological organization. The successful candidate is expected to maintain an externally funded research program involving both undergraduate and Master's degree students. Teaching expectation is an upper-level conservation biology course with laboratory, and an introductory biology lecture course (genetics, organisms, ecology, and evolution) to alternate with another course in the candidate's area of expertise (one course per semester). Postdoctoral research experience is required, and previous experience teaching undergraduate courses will be viewed favorably. Review begins October 12, 2006, and will continue until an appointment is made. Submit a letter of application, curriculum vitae, statements of research plans and teaching philosophy, a list of courses taken/taught relevant to conservation biology, and three letters of reference to: **Conservation Biology Search Committee, Department of Biology, The College of William and Mary, P.O. Box 8795, Williamsburg, VA 23187-8795.** Information on the Biology Department and this position may be obtained at **website: http:// www.wm.edu/biology.** *The College is an Equal Employment Opportunity/Affirmative Action Employer.*

FACULTY POSITION

Applications are invited for a tenure-track position at the **ASSISTANT or ASSOCIATE PROFESSOR** level in the Department of Physiology and Biophysics, University of Miami Miller School of Medicine. (In exceptional cases, an appointment at tenured **FULL PROFESSOR** will be considered). We seek outstanding candidates with demonstrated research interests in the neurosciences and/or physiology and biophysics that complement the existing research focuses in the Department **(website: http://chroma.med.miami.edu/physiol/faculty.htm).** Candidates should have a Ph.D. and/or M.D. degree in a relevant field as well as postdoctoral training and publications in highly rated journals. The successful candidate will be expected to conduct an active, independent, funded research program, and to contribute teaching with excellence in medical and graduate courses in neuroscience and physiology. Send paper copies of: letter of application, curriculum vitae, statements of research and teaching interests, and copies of three publications to: **Dr. Gerhard Dahl, Department of Physiology and Biophysics, R-430, University of Miami Miller School of Medicine, 1600 N.W. 10th Avenue, Miami, FL 33136.** Letters of recommendation from three references should be sent directly to the same address. Review of applications will commence when received and will continue until the position is filled. *The University of Miami is an Equal Opportunity/Affirmative Action Employer.*

EVOLUTIONARY BIOLOGY

The Department of Ecology and Evolutionary Biology at the University of Colorado seeks to fill two positions at the **ASSISTANT PROFESSOR** level in evolutionary biology. Individuals working in any area of the discipline are encouraged to apply and will be expected to pursue active research programs as well as to teach in their areas of expertise. Applicants should submit current curriculum vitae, statements of research and teaching interests, and the names and addresses of four references to: **Evolutionary Biology Search Committee, 334 UCB, University of Colorado, Boulder CO 80309.** Review of applications will begin on October 13, 2006. *The University of Colorado at Boulder is committed to diversity and equality in education and employment.*

UIC University of Illinois at Chicago

Dean of the College of Liberal Arts and Sciences

Nominations and applications are invited for the position of Dean of the College of Liberal Arts and Sciences (LAS) at the University of Illinois at Chicago (UIC).

UIC is the largest public research university in the metropolitan Chicago area and has assumed a leading role in defining the mission of urban universities in contemporary American life. Located just west of downtown Chicago, UIC serves as a significant contributor to the cultural, social and economic richness of the city. The campus includes 15 colleges and schools, serving one of the nation's most diverse student populations, with a total student body of approximately 25,000, and a faculty and staff of 12,500.

The UIC College of Liberal Arts and Sciences has experienced a substantial increase in its research profile, reflecting the distinction of its faculty and programs, with research grant expenditures totaling over $22 million annually. LAS is the largest college on campus, with more than 400 faculty and a staff of over 200. The College offers 46 undergraduate major fields of specialization, 44 minors, and approximately 41 graduate degrees at masters and doctoral levels. Its 21 departments and programs include African-American Studies, Asian Studies, Gender and Women's Studies, Latin American and Latino Studies, and Jewish and Religious Studies. LAS vigorously supports interdisciplinary research and teaching efforts with other colleges through its nationally renowned Institute for the Humanities as well as by expanding relationships with Chicago area institutions such as the Botanical Gardens, the Field Museum, the Mexican Fine Arts Museum and the Newberry Library. The UIC Honors College attracts exceptional undergraduates, many of whom are LAS students. In addition, a guaranteed professional admissions program, to such colleges as Medicine and Public Health, draws many of the state's most gifted undergraduate students to LAS.

The College of Liberal Arts and Sciences provides foundational learning that opens career opportunities for students at many levels. LAS faculty and students pursue research across the disciplines of the natural sciences, social sciences, and the arts and the humanities. This breadth of interest allows the College to offer core educational experiences for undergraduates and graduate students and a high level of service to other campus colleges. LAS plays the central role in providing the general education curriculum for all of UIC's 16,000 undergraduate students, and grants approximately 80 doctoral degrees each year.

Candidates for the position must have the following qualifications: an outstanding record of scholarly and educational achievement commensurate with an appointment as a tenured full professor in one of the departments or programs of the College; a history of administrative experience; a demonstrated commitment to diversity, student learning, and shared faculty governance; and experience with and a commitment to fundraising. Equally important is the ability to manage a complex organization while articulating a vision for the future in terms of concrete goals and resources organized to achieve strategic ends.

For full consideration, please send a cover letter, curriculum vitae, and the names and contact information for a minimum of three references by **November 10, 2006**, *preferably electronically*, to **lassearch@uic.edu**, addressed to:

Mary Case, Co-Chair, or Eric Gislason, Co-Chair
Search Committee for Dean of the
College of Liberal Arts and Sciences
Office of the Provost (m/c 105)
University of Illinois at Chicago
601 South Morgan Street
Chicago, Illinois 60607-7128
http://www.uic.edu/depts/oaa/search

The University of Illinois at Chicago is an Affirmative Action/ Equal Opportunity Employer. Women, minorities, and people with disabilities are strongly encouraged to apply.

Southern Illinois University Carbondale

The College of Science at Southern Illinois University Carbondale seeks outstanding scientists in the general areas of microbial pathogenesis and parasitology. The appointments at the Assistant Professor level will be in the Department of Microbiology and the Department of Zoology. Applicants must hold a Ph.D. or other appropriate doctoral degree and have a record of relevant postdoctoral research training by the time of appointment. The applicants must also have an externally funded research program or the potential for developing one, as well as a significant record of peer-reviewed publications. This research cluster in pathogenesis/ parasitology/ epidemiology is an ongoing part of SIUC's commitment to enhance interdisciplinary research and become a leading public research university (**http://news.siu.edu/s150/**).

Microbial Pathogenesis: The Department of Microbiology at Southern Illinois University Carbondale invites applications for a tenure-track position as an Assistant Professor with a start date of August 16, 2007. The successful candidate will contribute to an area of existing strength in microbiology with a concentration in a basic research aspect of microbial pathogenesis including host-pathogen interactions. The successful applicant is expected to help teach introductory microbiology or molecular biology, and teach an advanced undergraduate or graduate course in an area of expertise, or other courses as the program requires.

Parasitology: The Department of Zoology at Southern Illinois University Carbondale invites applications for a tenure-track position as an Assistant Professor with a start date of August 16, 2007. The successful candidate will enhance and complement existing programmatic strengths in the areas of ecology, environmental biology, conservation, biodiversity, and evolutionary biology with a basic research program in some aspect of parasite biology such as host-pathogen interactions or co-evolution, host defense mechanisms, host specificity, epidemiology, biogeography, population dynamics, responses to environmental factors, or development of methods and agents to combat parasites. The successful applicant is expected to teach an introductory parasitology course, help teach animal diversity, and teach an advanced graduate course in an area of expertise, or other courses as the program requires.

Applications: Review of applications for both positions will begin **October 15, 2006** and continue until the positions are filled. Applicants should submit a curriculum vitae, a statement of teaching and research interests, and the names and addresses of at least three references, respectively, to: **Microbial Pathogenesis Search Committee Chair, Department of Microbiology, Mailcode 6508, Southern Illinois University Carbondale, 1125 Lincoln Dr., Carbondale, IL 62901. E-mail: microbiology@micro.siu.edu** or **Parasitology Search Committee Chair, Department of Zoology, Mailcode 6501, 1125 Lincoln Dr., Southern Illinois University Carbondale, Carbondale, IL 62901. E-mail: zoology@zoology.siu.edu**.

Southern Illinois University Carbondale is a large, public, comprehensive research-intensive university situated in a pleasant small-town setting southeast of St. Louis. The Department of Microbiology, with a faculty of seven, offers an undergraduate Microbiology degree as well as M.S. and Ph.D. degrees through the interdisciplinary Molecular Biology, Microbiology, and Biochemistry Graduate Program (**http://www.science.siu.edu/microbiology/**). The Department of Zoology, with a faculty of 25, offers B.S., M.S. and Ph.D. degrees in Zoology (**http://www.science.siu.edu/zoology/**).

SIUC is an Affirmative Action/Equal Opportunity Employer that strives to develop a diverse faculty and staff and to increase its potential to serve a diverse student population. All applications are encouraged and will receive consideration.

POSITIONS OPEN

BIOLOGICAL CHEMISTRY FACULTY POSITION
Wayne State University

The Department of Chemistry at Wayne State University seeks applications for a tenure-track position in the Division of Biological Chemistry. Preference will be given toward candidates at the **ASSISTANT PROFESSOR** level. Candidates must have a Ph.D. and the potential to develop a nationally recognized, externally funded research program of outstanding quality in any area of biological chemistry. The Department offers exciting opportunities for candidates with research interests complementing a large group of faculty working in the areas of DNA, RNA, and protein biochemistry, enzymology, carcinogenesis, biophysical, bioorganic, and bioinorganic chemistry, as well as molecular and cellular biology (see Departmental **website: http://chem.wayne.edu** for further information).

The Department of Chemistry has a supportive academic environment and a strong graduate program. Excellent opportunities exist for collaborative research with individuals in the Department of Biological Sciences, the basic science departments in the highly ranked School of Medicine, the College of Pharmacy and Health Sciences, as well as in the Center for Molecular Medicine and Genetics, the Institute for Environmental Health Sciences, and the Barbara Ann Karmanos Cancer Institute. The Department of Chemistry offers an excellent research environment that includes ample, newly renovated research laboratories and a fully staffed Central Instrument Facility that manages state-of the art equipment for: electrospray ionization, and MALDI-TOF mass spectrometry, circular dichroism, electron paramagnetic resonance, surface plasmon resonance, transmission electron microscopy, and nuclear magnetic resonance (NMR), including a 700 megahertz NMR with cryoprobe. The Wayne State faculty also have access to the resources of the Michigan Core Technology Alliance **(website: http://www.ctaalliance.org/),** which includes facilities for bioinformatics, proteomics, genomics, animal models and structural biology, including 900 megahertz NMR and a dedicated synchrotron beamline for X-ray crystallography.

Applicants should submit a complete resume and description of future research plans, as well as three letters of recommendation addressing both research and teaching potential. All materials should be sent to: **Professor Charles H. Winter, Associate Chair, 141 Chemistry, Wayne State University, 5101 Cass Avenue, Detroit, MI 48202-3489.** Review of applications will begin in October 2006. *Women and minority candidates are encouraged to apply. Wayne State University is an Equal Opportunity and Affirmative Action Employer.*

ASSISTANT/ASSOCIATE PROFESSOR
Anatomical Sciences/Neurobiology
University of Louisville

The Department of Anatomical Sciences and Neurobiology is seeking applications for two tenure-track positions at the rank of either Assistant or Associate Professor. The successful candidates must have a Ph.D. and/or M.D. degree, an outstanding publication record, and an externally funded research program in neurosciences. Current strengths in the Department include molecular and developmental neurobiology, neural plasticity, and sensory systems. There are excellent opportunities for collaboration. The successful candidates will be teaching in either the medical, dental, or graduate programs. Review of applications will begin immediately. Information about the Department can be found at **website: http://www.louisville.edu/medschool/anatomy.**

Please send curriculum vitae, statement of research interests/plans, and names of three references to: **Dr. Mengsheng Qiu, ASNB Faculty Search Committee, Department of Anatomical Sciences and Neurobiology, University of Louisville School of Medicine, Health Sciences Center, Louisville, KY 40292.**

The University of Louisville is an Affirmative Action/Equal Opportunity Employer. The University of Louisville encourages women and minorities to apply.

ASSISTANT/ASSOCIATE PROFESSOR
Department of Biomedical Engineering
The University of Michigan

The Department of Biomedical Engineering at the University of Michigan College of Engineering is searching for new faculty positions in neural engineering, tissue engineering, biosolid mechanics, biocomputation, and biomedical optics. Applications in these areas are of particular interest but applications in all areas within biomedical engineering will be considered. Successful candidates will join a vibrant bioengineering community with strengths in biomaterials, biosensors, tissue engineering, biofluid mechanics, microfluidics, biomolecular engineering, biomolecular devices, bioprocess technology, biomedical imaging and optics, neural engineering, biomicroelectromechanical systems, and micro/nano technology. Qualifications include an earned Ph.D. in engineering or a physical science-related discipline and demonstrated excellence in, and commitment to, teaching, research, and scholarship. Women and minority candidates are encouraged to apply.

Applicants should send a letter of interest with curriculum vitae and a list of references to:

Biomedical Engineering Search Committee
Biomedical Engineering
The University of Michigan
1107 Carl A. Gerstacker Building
2200 Bonisteel Boulevard
Ann Arbor, MI 48109-2099

An Equal Opportunity Affirmative Action Employer.

STRUCTURE BIOLOGY AND BIOCHEMISTRY
The University of South Carolina

The Department of Chemistry and Biochemistry in the College of Arts and Sciences invites applications for a tenure-track position in structural biology and biochemistry at the **ASSISTANT PROFESSOR** level. The successful applicant will be expected to develop and maintain a productive, extramurally funded research program in the broad area of structural biology including X-ray and electron crystallography, electron microscopy (high resolution transmission electron microscopy) and M.S. proteomics. New faculty would be expected to actively interact with the established groups working in plant virology, nanobiotechnology, plant signal transduction, and protein/nucleic acid interactions at the University of South Carolina. The candidate is also expected to have a strong commitment to teaching at the undergraduate and graduate levels. Applicants should submit a letter of application, curriculum vitae, three letters of recommendation, and a description of research plans to: **Structural Biology Faculty Search Committee, Department of Chemistry and Biochemistry, University of South Carolina, Columbia, SC 29208.** The Committee will begin reviewing applications November 15, 2006. Homepage at **website: http://www.chem.sc.edu/.** *The University of South Carolina is an Affirmative Action, Equal Opportunity Employer. Minorities and women are encouraged to apply. The University of South Carolina does not discriminate in educational or employment opportunities or decisions for qualified persons on the basis of race, color, religion, sex, national origin, age, disability, sexual orientation, or veteran status.*

CAREER OPPORTUNITY

This unique program offers the candidate with an earned doctorate in the life sciences the opportunity to obtain the Doctor of Optometry (O.D.) degree in 27 months (beginning in March of each year). Employment opportunities exist in research, education, industry, and private practice. Contact the **Admissions Office, telephone: 800-824-5526** at **The New England College of Optometry, 424 Beacon Street, Boston, MA 02115.** Additional information at **website: http://www.neco.edu, e-mail: admissions@neco.edu.**

TENURE-TRACK FACULTY POSITION
in Molecular Microbiology

The Division of Cell Biology and Biophysics, School of Biological Sciences, University of Missouri-Kansas City, invites applications for a full-time tenure-track faculty position at the **ASSISTANT PROFESSOR** or **ASSOCIATE PROFESSOR** level. Preference will be given to individuals with research and teaching expertise in molecular microbiology. The successful candidate will be required to establish a strong research program compatible with one of the School's focus areas of molecular cell biology or structural biology. We seek an outstanding scholar with demonstrable achievements in research, teaching experience in an English-language institution, and exemplary communication and supervisory skills. Teaching will be in at least two of the following subject areas: bacteriology, molecular biology, cell biology, virology, biochemistry. State-of-the-art core facilities are maintained by the School, and competitive salary, startup funds, and laboratory space will be provided. Review of applications will begin immediately and continue until the position is filled. Applications, including curriculum vitae, reprints of publications, summary of present and future research plans and three letters of recommendation (to be solicited by the applicant), should be forwarded to: **CBB Search Committee, Division of Cell Biology and Biophysics - BSB 403, University of Missouri-Kansas City, 5100 Rockhill Road, Kansas City, MO 64110-2499.**

Equal Opportunity/Affirmative Action Employer

FACULTY POSITIONS IN MOLECULAR BIOLOGY
The University of Texas Southwestern Medical Center

The Department of Molecular Biology at the University of Texas Southwestern (UTSW) Medical Center invites applications for tenure-track faculty positions. We are interested primarily in applications for **ASSISTANT PROFESSOR** positions, but applicants for other ranks will also be considered. We are seeking individuals with innovative research programs in the areas of cell signaling, development, and gene regulation. Successful applicants should be capable of establishing a vigorous independent research program and teaching in one of several active graduate programs. Attractive startup packages, state-of-the-art core facilities, and new laboratory space are available.

Applicants should submit curriculum vitae containing a summary of past research accomplishments, a statement of future objectives, and names of three references to:

Eric N. Olson
Chairman
Department of Molecular Biology
University of Texas
Southwestern Medical Center at Dallas
5323 Harry Hines Boulevard
Dallas, TX 75390-9148

UTSW is an Equal Opportunity Employer.

ASSISTANT PROFESSORSHIP IN CHEMISTRY
Harvard University
Department of Chemistry and Chemical Biology

Applicants are invited to apply for tenure-track Assistant professorships in all fields of chemistry. Applicants should arrange to have three letters of recommendation sent independently and should provide curriculum vitae, a list of publications, and an outline of their future research plans. Applications and supporting materials should be sent to: **Chair, c/o Ms. Carol Gonzaga, Department of Chemistry and Chemical Biology, Harvard University, 12 Oxford Street, Cambridge, MA 02138-2902.** Reference position: JFCCB133B. The deadline date for receipt of applications and supporting materials is October 15, 2006. *Harvard University is an Affirmative Action, Equal Opportunity Employer. Applications from and nominations of women and minority candidates are strongly encouraged.*

Asuragen™

Exciting Career Opportunities for Research Scientists

Recruiting Senior Scientists, Post Docs, and other R&D level positions for our Diagnostics and Research & Development divisions. These creative individuals will join interdisciplinary teams developing products and technologies in the areas of sample preparation, RNA quantification, RT-PCR, siRNA, miRNA, functional genomics and microarray expression analysis. Applicants with either molecular biology, biochemistry / chemistry backgrounds will be considered. Most importantly, we are searching for outstanding, productive, entrepreneurial scientists who are stimulated by practicing science in a unique product-focused environment that rewards creative thinking and making things happen.

Qualifications:
Scientists with a Ph.D. in molecular biology, biochemistry or related field with at least two years postdoctoral and a strong publication record.

Asuragen is proud of its "science centric" culture, which focuses on providing an exciting and challenging work environment where individuals are part of a team, recognized for their creativity and diligence in seeking to meet company goals. Our diverse work force is encouraged to take on new responsibilities at all levels, fostering an entrepreneurial feeling across the company. We offer a competitive salary, medical, dental, disability and life insurance, a 401(k) plan with company matching, an employee bonus plan, stock options, and a tuition reimbursement plan.

On March 1, 2006, Ambion completed the sale of its Research Products division to Applied Biosystems Group (NYSE: ABI) resulting in the simultaneous spin-off and creation of Asuragen, Inc. Ambion's CEO and founder, Matt Winkler and a number of Ambion's senior managers have taken Ambion's Diagnostic and Service divisions, along with about 15 members of the Research Product division's researchers to form Asuragen, a new company with about 115 employees. The new company's focus is cutting-edge molecular diagnostic products particularly around the early detection of cancer. Although operating under the name Asuragen is new, these efforts are not new to this team. Ambion Diagnostics started developing its first product in 1999, and began operations as an independent Ambion business unit a year later.

To apply, please send CV's to: hduncan@asuragen.com and reference job "Senior Scientist."

To view all open positions at Asuragen, please visit:www.asuragen.com
EOE

Max-Planck-Institut
für Wissenschaftsgeschichte

The **Max Planck Institute for the History of Science, Berlin** (Department II; Director: Prof. Lorraine Daston) seeks an outstanding junior scholar (Ph.D. no earlier than 2001, postdoc desirable but not necessary) for a

three-year position (Research fellowship)

to begin 1 August 2007 in conjunction with the research project "History of Scientific Observation" (for more details concerning the project and the Institute, see www.mpiwg-berlin.mpg.de/projects/department2). Applications (which may be submitted in French, German, or English) from qualified candidates of all nationalities and disciplinary bakkgrounds are welcome; the colloquium language is English. It is expected that candidates will be able to present their own work and discuss that of others fluently in that language. Research projects may focus on either the natural or human sciences.

The position is primarily devoted to research, with no teaching duties. It is ranked at the BAT IIA level (TVÖD E13) in the German system, which roughly corresponds to that of Lecturer in Britain, Assistant Professor in North America, and Maître de conférences in France. Salary is set by both the position's rank and individual factors; please address specific questions to Ms. Claudia Paass (paass@mpiwg-berlin.mpg.de).

Applications consisting of a curriculum vitae (including list of publications), a research project (maximum 1000 words), and two letters of recommendation should be sent by **15 December 2006** to

Max-Planck-Institut für Wissenschaftsgeschichte
Abt. Personal/WiMi Obs
Boltzmannstraße 22
14195 Berlin, Germany

For questions concerning the research project and Department II, please contact Prof. Lorraine Daston (ldaston@mpiwg-berlin.mpg.de) or Dr. Fernando Vidal (vidal@mpiwg-berlin.mpg.de); for administrative questions concerning the position and the Institute, please contact Mr. Jochen Schneider (jsr@mpiwg-berlin.mpg.de). Applications from women are especially welcomed. The Max Planck Society is committed to employing more handicapped individuals and especially encourages them to apply.

CALIFORNIA STATE UNIVERSITY, EAST BAY
DEPARTMENT OF BIOLOGICAL SCIENCES

TWO TENURE-TRACK POSITIONS at the level of Assistant Professor beginning Fall 2007. We encourage applications from individuals committed to excellence in teaching and research at an institution that is intent on fostering a culturally diverse intellectual community. We seek a **PHYSIOLOGIST** who uses modern approaches to study physiological problems of vertebrates or invertebrates at any level of organization, from cellular/molecular to the whole organism. Teaching duties will include courses in Human Anatomy and Physiology for non-majors, Animal Physiology for majors or other undergraduate/Master's level courses within the applicant's area of expertise. We also seek a **EUKARYOTIC GENETICIST** with research emphasis in molecular genetics. Teaching duties will include courses in Genetics and other undergraduate/Master's level cellular/molecular courses within the applicant's area of expertise. For either position, the Ph.D. and postdoctoral research experience are required.

Apply by hard copy with a letter of application, CV, statement of research interests and goals, statement of teaching experience and philosophy, selected reprints, and three letters of recommendation to: **Physiologist Search Committee or Eukaryotic Geneticist Search Committee, Department of Biological Sciences, California State University, East Bay, Hayward, CA 94542**. Review of applications will begin **November 1, 2006**; the searches will remain open until the positions are filled.

Equal Opportunity Employer.

Biostatistics Faculty Position in Savannah

A biostatistics faculty member is needed immediately in the Department of Laboratory Oncology Research at the Curtis and Elizabeth Anderson Cancer Institute at Memorial Health University Medical Center in Savannah, GA.

Memorial Health's new state-of-the-art biomedical research facility is dedicated to translational research of human cancer, with major focus on molecular genetics. The position is available at the Assistant, Associate or Full Member level, with faculty appointment at the Mercer University School of Medicine. The successful candidate will collaborate with laboratory scientists and disease-oriented subspecialty physicians and will have–or develop–an independent research program. Experience in classical statistics and biostatistics preferred. A generous start-up package, space, and IT resources are available.

To apply, send c.v. and contact information for three references to:

Jeff Boyd, Ph.D., Vice President for Laboratory Science, Anderson Cancer Institute at Memorial Health University Medical Center
4700 Waters Avenue
Savannah, Ga. 31404
boydje1@memorialhealth.com

Curtis & Elizabeth Anderson Cancer Institute
at Memorial Health University Medical Center

*The Curtis and Elizabeth Anderson Cancer Institute at Memorial Health University Medical Center is not affiliated with the University of Texas M.D. Anderson Cancer Center.

POSITIONS OPEN

PHYSICAL CHEMISTRY FACULTY POSITION
University of California, Los Angeles (UCLA)

The Department of Chemistry and Biochemistry of the University of California, Los Angeles (UCLA), intends to make a tenure-track faculty appointment in physical chemistry (either experimental or theoretical). Candidates at all ranks will be considered. Candidates must give evidence of exceptional promise (for a junior appointment) or great distinction (for a senior appointment) in research and teaching. Applications should include curriculum vitae, a statement of research accomplishments and description of proposed research (not exceeding four pages), reprints of representative publications, and a list of professional references. Junior faculty applicants should arrange to have three letters of recommendation sent at the time of application. To assure consideration, all application materials should be received by October 31, 2006, and directed to:

Chair
Physical Chemistry Search Committee
Department of Chemistry and Biochemistry
University of California, Los Angeles
P.O. Box 951569
Los Angeles, CA 90095-1569
Fax: 310-206-8010

UCLA is an Equal Opportunity/Affirmative Action Employer. Women and minorities are encouraged to apply.

POSITION IN CHEMISTRY

Full-time, tenure-track position in the Department of Physical Sciences, Eastern Connecticut State University (ECSU). Ph.D. in biochemistry, bio-analytical chemistry, chemistry, or environmental chemistry required. Postdoctoral experience preferred with strong evidence of quality teaching. Applicants with expertise in environmental or forensic chemistry are especially encouraged to apply. Teaching expectations include advanced biochemistry and chemistry courses as well as introductory chemistry courses designed in support of the integrative liberal arts core curriculum. The successful candidate will support the Department's growing Biochemistry Program through course development, program assessment, and involving undergraduates in research. Send curriculum vitae, transcript of all graduate work, a statement of teaching philosophy and research interests, documentation of teaching ability, and three current letters of recommendation to: **Tim Swanson, Department of Physical Sciences, Goddard Hall, Eastern Connecticut State University, Willimantic, CT 06226.** Search will continue until position is filled. *ECSU is an Affirmative Action/Equal Opportunity Employer.*

ASSISTANT PROFESSOR
Biomolecular Chemistry
University of Wisconsin, Madison
School of Medicine and Public Health

We invite applications for a tenure-track position, beginning fall 2007. We seek colleagues eager to establish a vigorous biochemical or molecular biological research program of medical significance, and to teach at several levels. A doctorate and significant postdoctoral experience is required. Physician scientists addressing problems at the molecular level are encouraged to apply. The University of Wisconsin, Madison has a long storied tradition of research excellence, and is located in the heart of one of the country's most livable cities.

Deadline to ensure consideration is October 16, 2006. Send curriculum vitae, a two-page research plan, and three letters of reference to: **Search Committee, Biomolecular Chemistry, 587 MSC, Univeristy of Wisconsin School of Medicine and Public Health, 1300 University Avenue, Madison, WI 53706-1532. E-mail: cayers@wisc.edu. Website: http://www.bmolchem.wisc.edu.** *Equal Opportunity/Affirmative Action Employer. Minorities and women are encouraged to apply.*

Chicago's Jesuit University
LOYOLA UNIVERSITY CHICAGO
Stritch School of Medicine

TENURE-TRACK ASSISTANT/ ASSOCIATE PROFESSORS

The Department of Pharmacology at Loyola University Chicago, Stritch School of Medicine is recruiting tenure-track Assistant/Associate Professors to establish their own independent research as well as interact with existing faculty within the Department and the Cardiovascular, Neuroscience, and Oncology Institutes. Candidates whose research focuses on the dissection of fundamental mechanisms for clinical/therapeutic applications are highly encouraged to apply. Generous startup funds and laboratory space are available. For more information about the Department visit **website: http://www.luhs.org/depts/pharmacology/index.html.** Applicants should have a Ph.D. and/or M.D. degree, and be committed to excellence in research and teaching of pharmacology. Applications should include curriculum vitae and a research interest statement. Three letters of reference to support the candidacy should be sent separately. Address all correspondence to: **Dr. Tarun B. Patel, Chair, Department of Pharmacology, Loyola University Chicago, Stritch School of Medicine, 2160 S. First Avenue, Maywood, IL 60153.** (No electronic applications accepted.) *Equal Employment Opportunity/Affirmative Action Employer.*

UNIVERSITY OF VIRGINIA
Department of Chemistry

We invite applications for a tenure-track faculty position at the **ASSISTANT or ASSOCIATE PROFESSOR** level in spectroscopy. Selection criteria will include a Ph.D. in a related field, a strong record of innovative research, the potential for establishing an active and highly visible research program, and an interest and commitment to teaching excellence. This faculty search especially encourages research proposals exploring emerging spectroscopic opportunities and applications in biological, materials, physical, or interdisciplinary chemistry. Search Committee review of applications will begin October 31, 2006, but applications will continue to be accepted for consideration until the position is filled. Applicants should send curriculum vitae, a brief description of future research plans, and arrange for three letters of recommendation to be sent to: **Chair, Faculty Search Committee, Department of Chemistry, University of Virginia, P.O. Box 400319, Charlottesville, VA 22904-4319.** *The University of Virginia is an Equal Opportunity/Affirmative Action Employer and is strongly committed to building diversity within its community.*

ASSISTANT PROFESSOR
Genomics: Quantitative, Population, or Comparative

The Biology Department at University of Kentucky seeks a tenure-track Assistant Professor with expertise in genomics. Candidates that integrate experimental and computational approaches to study populations, complex traits, or genomes are especially encouraged to apply. The Department will consider applications from a wide range of specializations, including but not limited to bioinformatics, development, neurobiology, evolution, genetics, and ecology. Applicants must provide evidence that they will develop an active, independently funded research program. A commitment to teaching and student training is expected. Applicants should submit curriculum vitae and a statement detailing their current and future research plans, and arrange for submission of three letters of recommendation. Please address applications to: **Randal Voss, Chair, Genomics Search Committee, Department of Biology, University of Kentucky, 101 TH Morgan Building, Lexington, KY 40506.** Applications must be received by November 1, 2006, to ensure full consideration.

FACULTY POSITION
Department of Chemical Engineering
Columbia University

The Department of Chemical Engineering announces a faculty position to be filled at the rank of **ASSISTANT PROFESSOR, ASSOCIATE PROFESSOR, or PROFESSOR.** The Department seeks outstanding individuals with the motivation to excel in research, teaching, and service. Candidates at the Associate or Full Professor level should have a record of continued strong leadership in research. A doctorate in chemical engineering or a related field is required. Columbia University offers an attractive, highly intellectual, and collaborative environment, and the Chemical Engineering Department leads an NIH Center of Excellence in Genomic Sciences and a NSF Integrative Graduate Education and Research Traineeship program on soft materials. Assistance with faculty housing is available. Starting date: September 2007. Candidates should submit a brief research plan, statement of teaching objectives that demonstrates a commitment to chemical engineering education, the names and contact information of three references, curriculum vitae, and reprints of recent key research publications. E-mail submission is preferred. Reply by November 30, 2006, to:

Search Committee
Department of Chemical Engineering
Columbia University
500 West 120th Street, Room 801, MC 4721
New York, NY 10027
E-mail: facultyposition@cheme.columbia.edu

Columbia University is an Equal Opportunity/Affirmative Action Employer. We encourage women and minorities to apply.

FACULTY POSITION in PHARMACOLOGY
University of South Carolina
School of Medicine

The Department of Pharmacology, Physiology and Neuroscience at the University of South Carolina (USC) School of Medicine invites applications for a faculty position, rank open. A major responsibility of this position will be teaching medical and graduate pharmacology. Applicants must have a doctoral degree and teaching experience in pharmacology. Laboratory space and startup funds will be made available for individuals with funded research programs; opportunities for collaborative research with current Departmental faculty members are also available.

Applicants should submit a single Adobe Acrobat or Microsoft Word file that includes a cover letter summarizing qualifications, curriculum vitae and publication list, a statement of professional goals, summary of teaching evaluations, and contact information for four references. The file should be attached to an e-mail message sent to **e-mail: ppn.search@med.sc.edu** and containing Pharmacology Search as the subject. For more information about the Department please visit our **website: http://ppn.med.sc.edu/.**

USC is an Affirmative Action/Equal Opportunity Employer.

Florida Institute of Technology **(website: http://www.fit.edu),** a premier, independent, technological university located on Florida's East Coast, invites applications for **HEAD** of the Department of Biological Sciences. The University seeks an outstanding individual with skills and resources to advance one of the most productive and well-funded departments on campus. The new Head must be poised to advance the Department's academic reputation and expand the M.S. and Ph.D. programs. Successful applicants must have a doctorate, an international reputation in research with a distinguished publication record, an active research program, and outstanding leadership qualities. Interested candidates are invited to submit detailed curriculum vitae, a letter of application, and contact information for five references. Applications will be treated confidentially and should be submitted electronically to **e-mail: bioheadsearch@fit.edu.** Review of applications will begin October 15, 2006. *Florida Institute of Technology is an Equal Opportunity/Affirmative Action Employer. Women and minorities are encouraged to apply.*

Assistant, Associate or Full Professor of Nutritional Biochemistry (11-mo, tenure track). Salary dependent on qualifications and experience; start-up package. *Required:* PhD and/or DVM or equivalent and advanced training in nutrition, biochemistry or related field; successful research program w/state-of-the-art methods in molecular biology, metabolomics, genomics, and/or proteomics to investigate the interface of intermediary metabolism, nutrition and disease; documented research record/high potential to develop an independent research program related to nutritional biochemistry w/ applications to human and animal diseases; demonstrated teaching experience/aptitude in physiological chemistry, nutritional biochemistry, or nutrition; outstanding ability/potential to acquire extramural research support; excellent interpersonal and communication skills and demonstrated ability to work with others in a collegial, team atmosphere. *Preferred:* Experience in multi-disciplinary approaches and collaborations to study metabolic and chronic disease; metabolic regulation; molecular nutrition; nutritional genetics, or microarray/proteomic studies of effects of diet on gene/protein regulation.

To receive fullest consideration, apply by **January 3, 2007**; position open until filled. Electronically submitted applications encouraged. Submit (1) a letter of intent outlining special interest in the position, overall related qualifications and experience and career goals; (2) cv, and (3) the names and addresses of 3 professional references to:

Dr. Isaac N. Pessah, Chair
c/o Ms. Joan Learned
Dept of Molecular Biosciences
School of Veterinary Medicine
University of California
1 Shields Avenue
Davis, CA 95616-8741
Email: jlearned@ucdavis.edu

UCD is an AA/EOE

Two Faculty Positions in Immunology Department of Microbiology and Molecular Genetics Michigan State University

Immunology has recently been identified as an area of growth for the biological and medical sciences at Michigan State University. Two positions will be filled as soon as possible and three more will be filled in the next year. The Department of Microbiology and Molecular Genetics and the program in immunology seek applications for **two tenure-track assistant or associate professor positions in immunology**. Particular areas of interest include mucosal immunity, innate immunity, antiviral immunity, host responses to infection, and immunologic or inflammatory diseases. A doctoral degree (PhD, DVM or MD) and a minimum of two years of postdoctoral research experience are required.

The successful candidate will join a department with strong basic research programs in microbial biology, virology, immunology, pathogenesis, eukaryotic cell biology and molecular genetics. He or she will be expected to establish an extramurally funded research program, mentor graduate students, and interact with other faculty in the Department and University. The laboratory is in a new building that offers state of the art research, library and teaching facilities. Further information on the department of Microbiology is available at **www.mmg.msu.edu**.

Salary will be commensurate with experience. Applicants should submit a letter of application, curriculum vitae, statement of research goals, copies of pertinent reprints and contact information (address, e-mail and phone) for three referees to: **Immunology Search Committee Chairperson, Department of Microbiology and Molecular Genetics, 2209 Biomedical Physical Sciences, Michigan State University, East Lansing, MI 48824-4320; Tel: (517) 355-6463 x 1510; Email: mmgchair@msu.edu**. Applications should be submitted electronically to the email above, or they may be submitted by mail. Review of applications will begin about **October 15, 2006**, but will be accepted until the position is filled.

Michigan State University is an Affirmative Action/Equal Opportunity Employer. Women and minority candidates are particularly encouraged to apply.

AWARDS

EURYI Call for Proposals

The Foundation for Polish Science is pleased to announce that in 2006, it joined the prestigious **EURYI (European Young Investigator Award) programme.**

The **EURYI programme**, coordinated in Poland by the Foundation for Polish Science, is addressed to outstanding young researchers from anywhere in the world who have between 2-8 years of postdoctoral experience at the closing date of the call and **who wish to conduct their independent research in Poland.**

THE TOTAL VALUE of an award shall not exceed **1 250 000** € over 5 years.

The selection criteria for the **EURYI Award** are:

- the research quality and potential of the applicant,
- the originality as well as the groundbreaking character of the research proposal and its feasibility,
- the potential of the candidate and the proposed research programme to improve the position of European research at the world level.

The applications should be submitted to the FNP by **November 30, 2006.**

For further information visit:
www.fnp.eu
www.esf.org
www.eurohorcs.org

The application forms are accessible at:
www.fnp.eu

COURSE

COURSE ANNOUNCEMENT

22nd Annual Offering of Critical Issues in Tumor Microcirculation, Angiogenesis and Metastasis: Biological Significance and Clinical Relevance

A Continuing Education Course of Harvard Medical School and Massachusetts General Hospital
Boston, MA, USA - June 5 – 8, 2007

Dr. Rakesh K. Jain of Harvard Medical School and Massachusetts General Hospital is offering a Continuing Medical Education summer course entitled "Critical Issues in Tumor Microcirculation, Angiogenesis and Metastasis: Biological Significance and Clinical Relevance." The purpose of the course is to present the latest findings in systems biology of cancer.

Faculty Includes: **Peter Carmeliet, M.D., Ph.D. • Harold F. Dvorak, M.D. • Isaiah J. Fidler D.V.M., Ph.D. • Judah Folkman, M.D. •Herbert I. Hurwitz, M.D. • Rakesh K. Jain, Ph.D. • Robert S. Kerbel, Ph.D. • Marsha Moses, Ph.D.**

This course meets the criteria for 22 credit hours in category I of the Physician's Recognition Award of the American Medical Association.

To register or view course information online, please visit the HMS-CME home page:
http://cme.med.harvard.edu

For more information, please access our Website: **http://steele.mgh.harvard.edu/TumorCourse.html**.

PRIZES

The Linus Pauling Institute Prize for Health Research Call for Nominations

The Linus Pauling Institute Prize for Health Research is a prize sponsored by the Linus Pauling Institute at Oregon State University (**http://lpi.oregonstate.edu**). The Prize consists of $50,000 and a medal, and is awarded biennially. The LPI functions from the basic premise that an optimum diet and a healthy lifestyle are the keys to optimum health. The mission of the LPI is to determine the function and role of vitamins, essential minerals, and phytochemicals in promoting optimum health and preventing and treating disease; to determine the role of oxidative/nitrative stress and antioxidants in human health and disease; and to help people everywhere achieve a healthy and productive life, full of vitality, with minimal suffering, and free of cancer and other debilitating diseases. The Prize recognizes innovation and excellence in research relating to LPI's mission, with the goal to stimulate innovative research that enhances our knowledge of the role of diet and lifestyle in the primary and secondary prevention of disease and the role of oxidative/nitrative stress in disease pathology. **Procedure:** The nominator should submit a nomination letter, two supporting letters, and the candidate's curriculum vitae. The candidate's research accomplishments in light of the purpose of the Prize should be amply described in the letters. The recipient must be present to accept the Prize and deliver a talk at LPI's "Diet and Optimum Health" conference held in Portland, Oregon, May 16-19, 2007. Nomination packages should be sent to: **Linus Pauling Institute, Attn: Barbara McVicar, Oregon State University, 571 Weniger Hall, Corvallis, OR 97331-6512**. Complete nomination materials must be received by **November 1, 2006**.

POSITIONS OPEN

UNIVERSITY OF KANSAS
Department of Chemistry
2010 Malott Hall
1251 Wescoe Hall Drive
Lawrence, KS 66045

FACULTY POSITION in inorganic chemistry. The Chemistry Department invites applications for a tenure-track faculty position in inorganic chemistry at any rank **(ASSISTANT, ASSOCIATE, or FULL PROFESSOR)** consistent with the candidate's experience and qualifications, beginning August 18, 2007, or thereafter, contingent upon final budgetary approval. A Ph. D. in inorganic chemistry or closely related field is required. For candidates at the Assistant Professor level, postdoctoral experience is desirable. Duties include teaching at the undergraduate and graduate levels and the direction of a vigorous research program in inorganic chemistry. Candidates at the junior level must show evidence of well-defined research plans, and candidates at the senior levels must show evidence of an internationally recognized and well-funded research program. Applicants in all areas of inorganic chemistry are encouraged to apply, but we are especially interested in applications in inorganic mechanisms, catalysis, bioinorganic, and materials chemistry fields. All applicants should submit a letter of interest, resume, and a statement of teaching interests. Junior applicants should submit a brief summary of two to three research proposals and arrange for at least three letters of recommendation to be sent. Senior candidates should submit a brief description of research goals over the next five years, a listing of current funding, and the names of at least three references. Applications should be sent to: **Inorganic Search Committee, c/o Department of Chemistry, Room 2010 Malott Hall, 1251 Wescoe Hall Drive, University of Kansas, Lawrence, KS 66045.** Initial review of applications will begin October 20, 2006, and will continue until the position is filled.

Equal Opportunity/Affirmative Action Employer.

ASSISTANT PROFESSOR

The Department of Biology at Denison University invites applications for a tenure-track position with emphasis in physiology to begin August 2007. Research system and specialization within physiology are open. A strong potential for excellence in teaching and a productive research program involving undergraduates as evidenced by recent peer-reviewed publications and meeting presentations are essential. A Ph.D. and demonstrated teaching experience are required; postdoctoral experience is an asset. Teaching responsibilities include junior/senior level courses in animal physiology and human physiology (taught in alternate years), majors introductory courses (Biology 201 and 150), as well as occasional nonmajors offerings.

Denison offers competitive startup funds, summer support for student and faculty research, and the new Talbot Hall of Biological Science. See our **website: http://www.denison.edu/biology** for more detailed descriptions of the evaluation criteria for the Biology Program, and the position. Please note that Talbot Hall does not provide facilities for the housing of mammals or birds. Candidates should send a cover letter addressing their interest in liberal arts education; curriculum vitae; separate statements of teaching philosophy and experience, a statement of research interests and future plans within the context of a small liberal arts college; a statement of their ability to contribute to the mentoring of an increasingly diverse student body; copies of transcripts (graduate and undergraduate); and the names, e-mail addresses, and telephone numbers of three references to: **Chair, Physiologist Search Committee, Biology Department, Denison University, Granville, OH 43023.** We are especially interested in hiring a candidate who will help our University adapt to the increasing diversity of the American population. Review of applications will begin October 6, 2006. *Denison is an Affirmative Action/Equal Opportunity Employer.*

The Department of Biology at Colgate University seeks a tenure-track **ASSISTANT PROFESSOR** to start August 2007. Ph.D. or expectation of completion this academic year required; teaching and postdoctoral research experience desirable. The successful candidate will contribute to a foundation course called Molecules, Cells, and Genes, teach elective courses including behavioral genetics, and participate in University-wide programs. The appointee will join a biology faculty deeply committed to a strong, research-oriented program involving undergraduate students and will add to this effort by offering a research tutorial in their area of interest; opportunities also exist to lead a semester-long program at the NIH. Applications are especially encouraged from candidates whose research is focused in the area of behavioral genetics of model organisms. Please forward a letter of application with curriculum vitae, transcripts, and separate statements of teaching philosophy and research interests to: **Dr. Ken Belanger, Department of Biology, Colgate University, Hamilton, NY 13346-1398** and also arrange to have three letters of recommendation sent to this address. Review of applications will begin October 16, 2006, and continue until the position is filled. We intend to begin interviewing candidates by the beginning of November 2006. *Colgate University is an Equal Opportunity/Affirmative Action Employer. Developing and maintaining a diverse faculty and staff further the University's academic mission. Women and minorities are especially encouraged to apply.*

The Department of Biology at Colgate University seeks a tenure-track **ASSISTANT PROFESSOR** to start August 2007. Ph.D. or expectation of completion this academic year required; teaching and postdoctoral research experience desirable. The successful candidate will: contribute to a foundation course in evolution, ecology, and diversity; teach elective courses in botany/phycology and in their area of specialty; and contribute to interdisciplinary and University-wide programs (including environmental studies). The appointee will join a biology faculty deeply committed to a strong, research-oriented program involving undergraduate students and will add to this effort by offering a research tutorial in their area of interest. Please forward a letter of application with curriculum vitae, transcripts, and separate statements of teaching philosophy and research interests to: **Dr. Timothy McCay, Department of Biology, Colgate University, Hamilton, NY 13346-1398** and also arrange to have three letters of recommendation sent to this address. Review of applications will begin October 16, 2006, and continue until the position is filled. We intend to begin interviewing candidates by the beginning of November 2006. *Colgate University is an Equal Opportunity/Affirmative Action Employer. Developing and maintaining a diverse faculty and staff further the University's academic mission. Women and minorities are especially encouraged to apply.*

THE ENDOWMENT FOR SCHOLARS
in Biomedical Research at
The University of Texas Southwestern
Medical Center

University of Texas (UT), Southwestern, is pleased to announce the continuation of the Endowed Program for Scholars in Biomedical Research. The Program, which is fully funded from private endowment, will provide $1,000,000 over four years to support the research activities of each new **ASSISTANT PROFESSOR** (tenure track) appointed to the Program; five will be appointed annually. Academic appointments and research space will be provided by individual medical school departments or research centers. Positions in both basic science and clinical departments are available. The goal of the program is to assure a successful beginning of the research careers of an ever-growing cadre of outstanding young investigators at UT Southwestern.

For detailed information about currently available faculty positions, please access our webpage **website: http://www8.utsouthwestern.edu/utsw/home/scholars/index.html.**

UT Southwestern is an Equal Opportunity Institution.

TENURE-TRACK FACULTY POSITIONS
Biochemistry / All Ranks
Indiana University, Bloomington, Indiana

The Department of Chemistry at Indiana University has a distinguished record of scientific achievement and is in the midst of significant additions to its faculty. Several new initiatives are underway in Bloomington, Indiana, including the construction of a new center for interdisciplinary research. We invite applications for tenure-track faculty in biochemistry beginning August 2007. Successful candidates will possess outstanding credentials and be expected to develop a vigorous, independent research program. All faculty members contribute to teaching and curricular development. Candidates with interests in all aspects of biochemistry but especially areas such as chemical biology, structural biology, and proteomics will be considered in a new human biology program. Individuals of advanced stature with proven performance in research and teaching are encouraged to apply and will be considered at the **ASSOCIATE or FULL PROFESSOR** level.

Applicants must specify the area or areas in which they have special competence and include curriculum vitae. Assistant Professor candidates should include a summary of future research plans and arrange to have four letters of recommendation forwarded to the Department. Review of applications will begin upon receipt and will continue until the positions are filled. Send applications to: **Professor Richard D. DiMarchi, Chairman, Biochemistry Search Committee, Department of Chemistry, 800 E. Kirkwood Avenue, Indiana University, Bloomington, IN 47405. Fax: 812-856-5050, e-mail: chemchair@indiana.edu.** *Indiana University is an Affirmative Action/Equal Opportunity Employer and especially encourages applications from women and members of minority groups.*

Texas Christian University (TCU) invites nominations/applications for its prestigious **ROBERT A. WELCH CHAIR IN CHEMISTRY.** While the area of research is open, we seek a scholar with an internationally recognized research program that will complement existing faculty strengths. Previous Welch Chairs at TCU include **Paul D. Bartlett** and **C. David Gutsche.**

Located in the Fort Worth/ Dallas area, TCU is an independent, coeducational institution of approximately 7,200 undergraduate students and 1,500 graduate students, offering 98 undergraduate majors and 20 graduate degrees in 59 areas, including six doctoral fields of study, with a commitment to both teaching and research. The Chemistry Department offers the Ph.D., M.S., and B.S. degrees and is well equipped, particularly with excellent X-ray diffraction, mass spectroscopy, and nuclear magnetic resonance facilities. Please send curriculum vitae, detailed research plans, and a list of references to: **Professor Jeffery L. Coffer, Department of Chemistry, P.O. Box 298860, Texas Christian University, Fort Worth, TX 76129.** E-mail inquiries may be sent to **e-mail: j. coffer@tcu.edu.** The search is ongoing until the position is filled. *TCU is an Equal Employment Opportunity/Affirmative Action Employer.*

BIOLOGY ASSISTANT PROFESSOR. Hamline University invites applications for a tenure-track position to begin September 2007. We seek candidates with research interests in developmental biology or neurobiology. Applicants must be committed to teaching and developing an active undergraduate research program. Postdoctoral experience and ability to contribute to a scientific computing emphasis in the Science Division desired. Ph.D. required. For complete information see **website: http://science.hamline.edu.** Send cover letter, curriculum vitae, teaching philosophy, research plans, and three reference letters to: **Bonnie Ploger, Biology Department, Hamline University, 1536 Hewitt Avenue, St. Paul, MN 55104,** or **e-mail: bploger@hamline.edu.** Application review begins October 9, 2006. *Members of underrepresented groups are strongly encouraged to apply. Hamline University is an Equal Educational/Employment Institution.*

AWARDS

Call for Proposals

The Alzheimer's Drug Discovery Foundation (ADDF), an affiliated public charity of the Institute for the Study of Aging (ISOA), invites scientists from the biotech industry and academia to apply for a research grant program entitled *Novel Approaches to Drug Discovery for Alzheimer's Disease*. The goal of the program is to facilitate the discovery and development of effective therapies for Alzheimer's disease. This program is made possible by a generous donation from Elan Pharmaceuticals, Inc. and funds from ADDF.

The deadline for **grant submission is October 13, 2006**, and funding will be awarded in January 2007. Former recipients of ADDF and ISOA funding are eligible to apply.

Grant applications and a full program description are available at **http://www.alzdiscovery.org**

For more information contact **Wendy Ramos** at **212-901-8005** or **wramos@alzdiscovery.org**

Alzheimer's Drug Discovery Foundation

élan

SYMPOSIA

Institute of Molecular Biology (IMB)

Academia Sinica announces an INTERNATIONAL SYMPOSIUM "Molecular Biology in the 21st Century: Interface, Integration, and Perspectives" November 12-14, 2006

To celebrate the 20th anniversary of the establishment of IMB. Speakers from local institutions in Taiwan and from abroad will gather and discuss the future development of molecular biology in relation to the fields of biology, medicine and biotechnology. Poster session will also be held to facilitate interaction between the speakers and the symposium participants.

CURRENTLY SCHEDULED SPEAKERS:

International Speakers

David Baltimore, Sydney Brenner, Linda Buck, Winslow Briggs, Mark Davis, Walter Gehring, Leroy Hood, Andrew Murray, Allan Spradling, Joan Steitz, Tom Steitz, Richard Tsien, Irving Weissman,

Local Speakers

Zhi-Feng Chang, Rey-Huei Chen, Ann-Shyn Chiang, Cheng-Ting Chien, Bon-chu Chung, Chwan-Deng Hsiao, Yi-Ping Hsueh, John Kung, Hou-min Li, Sue Lin-Chao, Woan-Yuh Tarn, Ting-Fang Wang

For registration information, please go to: http://www.imb.sinica.edu.tw/20th

CONFERENCE

HOWARD HUGHES MEDICAL INSTITUTE

JANELIA CONFERENCES

SPRING 2007

The Janelia Farm Research Campus is pleased to announce its first season of conferences. These small, intense conferences are intended to foster rapid scientific advances and collaborative interactions. All participants are expected to contribute to the intellectual content of the meetings. The Howard Hughes Medical Institute fully supports the Janelia Conferences—there are no registration, accommodation, or dining fees for participants. The conference organizers invite all participants, selecting some from an open pool of applicants.

Neuron Identities ■ March 4–7, 2007
Organizers: Sydney Brenner, Salk Institute & Janelia Farm/HHMI; Linda B. Buck, Fred Hutchinson Cancer Research Center/HHMI; Constance L. Cepko, Harvard Medical School/HHMI; Terrence J. Sejnowski, Salk Institute/HHMI

Neuroanatomy and Stereotypy of the Adult *Drosophila* Nervous System ■ March 11–13, 2007
Organizers: Julie Simpson, Janelia Farm/HHMI; Nicholas J. Strausfeld, Arizona Research Laboratories Division of Neurobiology

Insect Behavior: Small Brains, Big Functions ■ March 13–15, 2007
Organizers: Ulrike Heberlein, University of California, San Francisco; Martin Heisenberg, University of Würzburg; Roland Strauss, University of Würzburg

Expanding the Genetic Toolkit in Mouse ■ March 18–21, 2007
Organizers: Alan Bradley, Wellcome Trust Sanger Institute; Kevin Moses, Janelia Farm/HHMI; Janet Rossant, Hospital for Sick Children, Toronto; Joseph S. Takahashi, Northwestern University/HHMI

Neural Circuits and Behavior in *C. elegans* ■ March 25–28, 2007
Organizers: Cornelia I. Bargmann, Rockefeller University/HHMI; Sydney Brenner, Salk Institute & Janelia Farm/HHMI; Dmitri Chklovskii, Cold Spring Harbor Laboratory & Janelia Farm/HHMI; Sean Eddy, Janelia Farm/HHMI

Visual Processing in Insects: From Anatomy to Behavior ■ April 29–May 2, 2007
Organizers: Claude Desplan, New York University; Ulrike Gaul, Rockefeller University; Kevin Moses, Janelia Farm/HHMI

Information: www.hhmi.org/janelia

Application deadline: November 15, 2006

HHMI janelia farm research campus

POSITIONS OPEN

FACULTY POSITION
Department of Chemistry
Georgia State University

The Department of Chemistry at Georgia State University anticipates a faculty position opening at the **ASSISTANT PROFESSOR** level. The Department seeks outstanding candidates capable of achieving excellence in research and teaching. Applicants must have a Ph.D. or equivalent degree with postdoctoral training. Although outstanding scientists in all areas of chemistry are encouraged to apply, preference will be given to those candidates with a research focus in biochemistry, biological, bioanalytical, or biophysical chemistry. There is an option for a joint appointment in the Biology Department. Georgia State University offers an attractive, highly intellectual, collaborative, and continually growing environment, with 20 full-time, tenured or tenure-track faculty and more than 60 Ph.D. and 30 M.S. students. Candidates should submit a research plan, a statement of teaching objectives that demonstrates a commitment to education, curriculum vitae, reprints of at most three recent research publications, a two-page summary of research accomplishments, and arrange to have three letters of recommendation sent to: **Professor D. W. Dixon, Faculty Search Committee Chair, Department of Chemistry, Georgia State University, P.O. Box 4098, Atlanta, GA 30302-4098.** Reviewing of applications will start on October 16, 2006, and will be open until the position is filled, for an employment start date of summer 2007.

Georgia State University is an Equal Opportunity/Affirmative Action Employer. Applications from women and ethnic minorities are strongly encouraged.

FACULTY POSITIONS (TWO) IN BIOLOGY

York College of the City University of New York invites applications for two tenure-track positions at the **ASSISTANT PROFESSOR** level in genetics/bioinformatics and in plant physiology/evolution to begin September 1, 2007. Qualifications include a Ph.D. with postdoctoral experience and evidence of excellence in teaching. Instructional responsibilities include lecture and laboratory courses in area of expertise as well as other major or nonmajor courses as needed. Candidates must demonstrate a strong interest and commitment to undergraduate teaching and the capability of developing and maintaining an active research program supported by external funding. The academic program and instructional and research equipment available at York College can be found at **website: http://natsci.york.cuny.edu.** Applicants should submit a cover letter, curriculum vitae, statements of research and teaching experience, and the name and contact information of three professional references to: **Dr. Margaret MacNeil, Biology, York College/CUNY, 94-20 Guy R. Brewer Boulevard, Jamaica, NY 11451.** The application deadline is October 23, 2006. *Equal Employment Opportunity/Affirmative Action/ADA/IRCA.*

ASSISTANT PROFESSORS, ORGANIC AND BIOLOGICAL CHEMISTRY
Boston University

The Department of Chemistry invites applications for two tenure-track positions at the rank of Assistant Professor, representing the areas of organic chemistry and biological chemistry. The successful candidates will be expected to establish recognized, innovative research programs having to do with compelling topics that tend to crosscut among subdisciplines and complement the activities of current faculty. Candidates should submit curriculum vitae, along with research proposals, and arrange for three letters of recommendation to be sent to: **Dr. Guilford Jones, Chair, Department of Chemistry, Boston University, 590 Commonwealth Avenue, Boston, MA 02215.** The deadline for receipt of applications is October 31, 2006. *Boston University is an Affirmative Action/Equal Opportunity Employer.*

NEUROSCIENTIST
University of Wyoming

The Department of Zoology and Physiology in conjunction with the Graduate Neuroscience Program at the University of Wyoming invites applications for a full-time, nine-month, tenure-track faculty position at the rank of **ASSISTANT PROFESSOR,** starting August 2007. We are seeking an individual who has a strong background in neuroscience with an emphasis in neural plasticity. The successful candidate must have a Ph.D. or equivalent, evidence of research productivity, and teaching ability; a minimum of two years of postdoctoral experience is preferred. Teaching responsibilities will include a graduate level functional neuroanatomy course. S/he will be expected to have or to develop an externally funded research program and to participate in the University's Graduate Neuroscience program and the NIH-funded Neuroscience Center of Biomedical Research Excellence. The Department has access to outstanding microcopy and macromolecular facilities. A competitive startup package is available. Additional Departmental research strengths include animal and cell physiology, ecology, and wildlife biology.

Interested applicants should send curriculum vitae, a statement of research and teaching experience, three publications that represent their best work, and three letters of recommendation to: **Neuroscience Search Committee, Department of Zoology and Physiology, Department 3166, 1000 E. University Avenue, Laramie, WY 82071. Fax: 307-766-5625. Website: http://uwadmnweb.uwyo.edu/Zoology.** Review of applications will begin in December 2006. *The University is a Carnegie Foundation Research/Doctoral Extensive Institution, and is an Affirmative Action/Equal Employment Opportunity Employer.*

FACULTY POSITION
Department of Applied Science
College of William and Mary

The Department of Applied Science at the College of William and Mary, an interdisciplinary Ph.D.-focused Department established in 1995, invites applications for a tenure-track position at the **ASSISTANT PROFESSOR** level in biophysics, neurophysiology, biomedical engineering, biomaterials, or a related field, emphasizing either computational or experimental approaches. The new faculty member will be expected to establish a vigorous, independent, and well-funded graduate research program at the interface of the physical, mathematical, and biological sciences. Excellence and high commitment to the teaching of graduate and undergraduate students is expected of all faculty at the College. Located two hours south of Washington, D.C. in Williamsburg, Virginia, the College of William and Mary is the second oldest university in the United States and was recently named by the editors of Newsweek as the "hottest small state school" in the nation. Candidates should submit complete curriculum vitae, research statement, and copies of no more than five refereed publications to: **Faculty Search Committee, Department of Applied Science, The College of William and Mary, P.O. Box 8795, Williamsburg, VA 23187-8795,** and arrange to have three letters of recommendation mailed to the same address. Review of materials is expected to begin January 1, 2007, and continue until the position is filled. The College is an Equal Employment Opportunity/Affirmative Employer. For more information see **website: http://as.wm.edu.**

The Department of Biological Sciences at Salisbury University (SU) is accepting applications for a tenure-track position in physiology/pathophysiology at the rank of **ASSISTANT PROFESSOR,** starting fall 2007. A Ph.D. and evidence of the potential for excellence in teaching and research will be required. For further information please see the SU **website: http://www.salisbury.edu/hr/Jobs/default.asp?asearch=faculty**.

RESEARCH ASSISTANT III
University of Iowa
Department of Neurosurgery

The Department of Neurosurgery is recruiting a Research Assistant III to join the Human Brain Research Laboratory (HBRL) to support and participate in its ongoing research on the basic mechanisms in the human brain that underlie hearing, speech, language, and emotion. He/she will provide technical support for all phases of the research, and will function as a technical expert and have overall responsibility for the development, management, and maintenance of laboratory instrumentation, including computer hardware and software. The successful candidate will have a Master's degree and academic knowledge in the fields of electrical and/or computer engineering or an equivalent combination of education and experience. A strong background in computer programming (especially MatLab), database management, and networking is essential. Experience in the use of modern electrophysiological instrumentation, including the latest Tucker Davis Technology data acquisition and stimulus generation systems and Hewlett Packard VX-1 data acquisition system is desirable.

Interested candidates should apply for this position by visiting our **website: http://jobs.uiowa.edu** and refer to requisition 53125. *The University is an Affirmative Action/Equal Opportunity Employer. Women and minorities are strongly encouraged to apply.*

MICROBIOLOGIST

St. Ambrose University seeks a tenure-track, **ASSISTANT PROFESSOR;** beginning August 2007. Primary teaching responsibilities include microbiology and nonmajors' undergraduate courses in biology. We particularly welcome candidates who are dedicated to teaching excellence and interested in pursuing research with undergraduates. Ph.D. is required. St. Ambrose University is a private, liberal arts Catholic institution of 3,600 undergraduate and graduate students, and is located in the Quad Cities of Iowa and Illinois. Review of applications will begin on October 20, 2006, and continue until the position is filled. Please send curriculum vitae, a statement of teaching philosophy, and three letters of reference to: **Director of Human Resources, Street Ambrose University, 518 W. Locust Street, Davenport, IA 52803.** *Affirmative Action/Equal Opportunity Employer.*

MARKETPLACE

Simplify Gene Silencing Experiments with *Silencer*® Pre-designed siRNA

Fast. Easy. Guaranteed.

- Ready to use siRNAs provided in as little as 4 days
- Searchable database makes it simple to find siRNAs for human, mouse, and rat genes
- Efficient gene knockdown guaranteed
- Now save 18% when you purchase 3 siRNAs per gene

Tired of wasting time with poorly designed siRNAs? *Silencer*® Pre-designed siRNAs—highly effective, ready-to-use siRNAs available for all human, mouse and rat genes—provide guaranteed gene silencing. Each one has been designed using a carefully optimized algorithm and then manufactured to exacting quality standards to provide potent and specific gene silencing.

Verify Gene Silencing Results and Save 18%

Journal article reviewers generally require that you verify gene silencing results with a second siRNA. *Silencer* Pre-designed siRNAs make it easy to comply. Ambion guarantees that at least two *Silencer* Pre-designed siRNAs will knockdown target mRNA levels by ≥70% when three are purchased for the same gene.

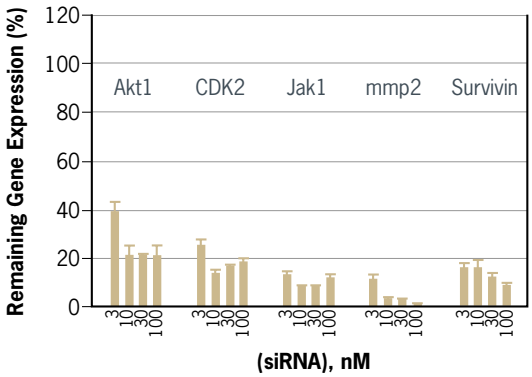

Potency of *Silencer*® siRNAs at Low Concentrations. The algorithm Ambion uses to design *Silencer* Pre-designed siRNAs results in efficient gene silencing. Most *Silencer* siRNAs are effective at 3-10 nM.

Ambion RNAi Resources

On the Web: RNA Interference Resource
Protocols, data, references, and more
www.ambion.com/RNAi

Via Mail: RNA Interference Research Guide
New tools and techniques for performing RNAi
Request a free copy at **www.ambion.com/contact/litreq**

Via e-mail: Silencer E-Newsletter
Experimental tips, new tools for RNAi, and exclusive special offers
Sign up at **www.ambion.com/contact/litreq**

Via phone: RNAi Specialists
Assistance with experimental setup, design, and troubleshooting
See **www.ambion.com/contact**
for our full list of toll free phone numbers

Learn how you can get fast, easy and guaranteed siRNAs at
www.ambion.com/info/siRNA

Ambion®
THE RNA COMPANY®
An Applied Biosystems Business

Ambion, Inc.
U.S. 800-888-8804 • Canada 800-445-1161
U.S. tel +1-512-651-0200 • fax +1-512-651-0201

Ambion (Europe) Ltd
tel +44 (0)1480-373-020
fax +44 (0)1480-373-010

Ambion K.K. (Japan)
tel +81 (0)3-5638-2181
fax +81 (0)3-5638-2182

Direct free phone numbers, distributors:
www.ambion.com/contact